Ocean Engineering Studies

Compiled 1990

Volume III: Acrylic Windows

Short-Term Pressurization

J. D. Stachiw

NAVAL OCEAN SYSTEMS CENTER

Ocean Engineering Studies

Compiled 1990

Volume III: Acrylic Windows—
Short-Term Pressurization

J. D. Stachiw

PUBLISHED BY
NAVAL OCEAN SYSTEMS CENTER
SAN DIEGO, CALIFORNIA

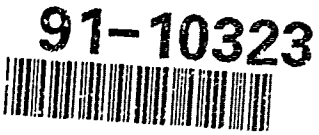

R 512

Technical Report

WINDOWS FOR EXTERNAL OR INTERNAL HYDROSTATIC PRESSURE VESSELS

Part I — Conical Acrylic Windows Under Short-Term Pressure Application

January 1967

NAVAL FACILITIES ENGINEERING COMMAND

U. S. NAVAL CIVIL ENGINEERING LABORATORY

Port Hueneme, California

WINDOWS FOR EXTERNAL OR INTERNAL HYDROSTATIC PRESSURE VESSELS
PART I - CONICAL ACRYLIC WINDOWS UNDER SHORT-TERM PRESSURE APPLICATION

Technical Report R-512

Y-F015-01-07-001

by

J. D. Stachiw and K. O. Gray

ABSTRACT

Conical acrylic windows for fixed ocean-floor structures were placed under short-term loading (pressurization from zero to failure at a fixed rate). The windows, of different thicknesses and different included conical angles, were subjected to various applied pressures, and their subsequent behavior was studied.

Acrylic windows, in the form of truncated cones with included angles of 30°, 60°, 90°, 120°, and 150°, were tested to destruction at ambient room temperature by applying hydrostatic pressure to the base of the truncated cone at a continuous rate of 650 psi/min. The pressure at which the windows failed and the magnitude of displacement through the window mounting at different pressure levels were recorded. The ultimate strength of the conical windows (denoted by the critical pressure at which actual failure occurred) was found to be related both to thickness and included conical angle.

Graphs are presented defining the relationships of critical pressure versus thickness-to-diameter ratio, and pressure versus magnitude of displacement for the windows.

Nondimensional scaling factors for critical pressure and displacement applicable to large-diameter windows are discussed and presented in graphic form.

This initial study produced design criteria for conical acrylic windows for any ocean depth under conditions of short-term loading. These criteria may be applied to windows in either an internal pressure vessel used to contain high pressures, and thus simulate the ocean environment, or an external one used to resist high pressures, such as deep submergence structures in the ocean.

TABLE OF CONTENTS: VOLUME III

CONTENTS

INTRODUCTION

The Naval Facilities Engineering Command* is responsible for the construction and maintenance of underwater structures attached to the ocean floor. Such structures may include instrumented or manned underwater surveillance or observation posts that will rely, at least in part, on visual observation and the transmitting and receiving of electromagnetic radiation through "non-opaque" hull areas for the performance of their mission. Windows of certain types have been employed for these purposes on research submarines, and have been found to be of practical value especially for visual and sonic (sonar) observation in hydrospace. Similar windows will be utilized on permanent ocean floor installations. The published data on the strength of underwater optical-viewing windows used on submarines is very meager,[1,2,3] and formulas for its calculation are lacking. Furthermore, the operational requirements of permanent underwater installations are sufficiently different from those of submarines to make most of the existing data inapplicable to the deep submergence structures. For these reasons, a study has been undertaken at the Deep Ocean Laboratory of the Naval Civil Engineering Laboratory (NCEL) to generate information for the design of feasible underwater windows. This information, besides satisfying the primary underwater window design requirements, will also prove valuable in the design and operation of windows in internal pressure vessels used for simulation of deep ocean environments.

The performance of underwater windows is influenced by such major factors as the duration of loading or application of pressure; temperature; the thickness, shape, and type of the window material; and the number of pressure cycles involved. Since all these variables must be considered in combination, the whole investigation must proceed in phases, with the factors evaluated in one combination at a time. The phase of study described in this report was planned to determine the relationship between the shape, thickness, and critical pressure of truncated-cone-shaped acrylic plastic windows under short-term loading at room temperature.

BACKGROUND INFORMATION

Windows for underwater applications where high pressures are encountered have been of conical shape since the beginning of deep submergence research. The first scientist to explore this field, Auguste Piccard,[1] not only introduced the conical window shape but also the use of acrylic plastic for windows in deep submergence structures. The conical shape was chosen because of its wide field of vision, as well as its wedging and self-sealing behavior under high pressure. Acrylic plastic, introduced for the underwater application by Professor Piccard in 1939, is still the primary material used for underwater high-pressure windows because of its low cost, wide availability, and excellent optical properties. It is readily bonded, permitting windows of any thickness to be built up by lamination of sheets, and is impact-resistant enough to render unnecessary additional protective covers except for windows employed on combat missions. The long, excellent performance record of acrylic plastic for underwater windows prompted the decision to investigate it first, ahead of other, recently developed optically transparent materials.

Acrylic plastic, like most plastics, deforms with time under sustained loading. For this reason, an acrylic window subjected to sustained pressure loading will ultimately fail at a much lower pressure than if it were pressurized rapidly till failure occurs. Thus, the pressure rating of a window is affected by the duration of load application. In addition, if the window is subjected to more than one pressure cycle of a given duration, its pressure rating will change accordingly. Therefore, to obtain complete design information for acrylic windows, it is necessary to subject them to different types of loadings. However, a standard must be established to which strengths can be compared. Since this has not been done in the course of underwater window investigation to date, a fundamental purpose of the initial phase

*Formerly Bureau of Yards and Docks.

of the present study was to set such a standard. The one selected around which to compile basic data was the failure of windows under short-term pressure application at an ambient temperature in the approximate range of 60° to 70°F. The short-term loading, which denotes not a specific time but pressurization from zero to failure (or critical pressure) at a fixed rate, here was to be applied at the rate of 650 psi/min.

Since the compressive and tensile strength of acrylic material decreases with an increase in temperature, it was considered wise to conduct experiments at prevailing room temperature of 60° to 70°F, for this would be a more severe test than if the pressurizing medium, water, were around 40°F, the temperature of most ocean depths. Also, this temperature range would facilitate the use of conical acrylic windows in internal pressure vessels, where the water employed is likely to be at room temperature.

DESIGN OF EXPERIMENT

The experimental study had two objectives: to determine the short-term pressure strength of a series of windows of different conical angles and thicknesses, and to provide experimental data for future analytical studies dealing with the strength of such windows. To implement the latter objective, the windows were designed not only with a 90° included conical angle, the one customarily used in all present underwater deep submergence windows, but also with 30°, 60°, 120° and 150° included angles. It was felt that by varying the angle from 30° to 150°, sufficient perturbation of the angle parameter was introduced into the experiment to permit the evaluation of its influence on window strength. The thickness-to-diameter (t/D) ratio was varied for the same reason. This ratio is a single, computationally useful nondimensional term combining the two other parameters besides cone angle which determine the critical pressure of conical windows: the thickness, t, of the truncated cone, and the minor diameter, D, of the cone. Sufficient perturbation was assured for the thickness-to-diameter ratio by varying it from 0.125 to 1.0. (Although the t/D ratios are herein expressed in decimal form, sometimes to three places, these values are actually the decimal equivalents of nominal fractional values.)

To obtain true experimental response from the windows whose t/D ratios and conical angles were varied, special effort was made to hold both the temperature and the rate of pressurization constant. Furthermore, the window material and metallic flanges for mounting test specimens were kept the same for each series of experiments, in order to prevent excessive variations in both window material strength and flange rigidity.

A summary of the experiment, reflecting the various categories of the complete test data found in Appendix G, is presented in Table 1.

Table 1. Summary of Experimental Work

Window Diameter 1/ (in.)	Mounting Flange Type	Included Conical Angle (deg)	t/D Ratio (Nominal)	Remarks
1	I	30, 60, 90, 120, 150	0.125, 0.25, 0.375, 0.5, 0.625, 0.75, 0.875, 1.0	Short-term critical pressure and displacement tests
1	I	30	0.5	Low-temperature-effect tests
1	II	30	1.0	Type II flange effect tests
2	I	30	0.125, 0.25, 0.5	Window t/D ratio scaling factor validation tests
4-1/2	I	60	0.125, 0.25, 0.5	Window t/D ratio scaling factor validation tests
8	I	90	0.5	Window t/D ratio scaling factor validation tests

1/ Minor diameter of the truncated acrylic cone.

Window Test Specimens

The conical window test specimens (Figure 1) were machined from acrylic plates and sheets only. The material used was commercial quality Grade G Plexiglas, the physical properties of which are described in Appendix A. This off-the-shelf acrylic material was chosen with the designer in mind, permitting him to specify and easily procure fairly inexpensive stock for his own experimentation or use based on data presented herein.

Since the windows were machined from commercially available sheets and plates of acrylic material, small variations were anticipated in their mechanical properties. Preliminary experiments indicated this variation in strength, together with variations in conical angle and thickness resulting from the necessary machining tolerances, caused considerable scatter of experimental values. Although such a scatter increased the experimental task, certain advantages result for the potential designer. From the range of scatter of experimentally derived critical pressures, the designer can determine what deviations of window strength may be expected when ordinary machine shop tolerances are used on Grade G Plexiglas material received from various manufacturers. Knowing what deviations to expect from the average window strengths given in this report, he will then be able to introduce an appropriate factor of safety.

Since it may often be difficult or economically impractical to provide future submarines, permanent underwater installations, or pressure vessels requiring cone-shaped acrylic windows with custom-fitted, lapped-in-place originals or replacements, this study has relied exclusively on mass-produced, interchangeable specimens. None of the windows received any further shaping or lapping in place following fabrication in the NCEL machine shop. Spot checks of the as-machined windows indicated dimensions were less than ±30 minutes off from specified nominal angle, and ±0.020 inch from the specified nominal thickness. The sealing surfaces of the windows were machined to a 32 rms finish, while the parallel viewing surfaces were polished to an optical finish.

Window Specimen Holders

The test specimens were mounted in metallic flanges designed to fit into the end closure of the pressure vessel (Figure 2). The pressure vessel employed for this study was the Mk-I modification of 16-inch Naval gun shells,[4] a convenient, medium-size vessel with a useful inside diameter of 9 inches. (This diameter determined the choice of the minor diameter of 1 inch for the basic series of window test specimens, since the major diameter of the acrylic window specimens tested could reach 6-1/4 inches, and in the case of validation tests with larger diameter windows, 8 inches.)

The mounting flanges, machined from mild steel, were of sufficient thickness to withstand all but minor deformation during application of hydrostatic pressure to the window specimens. In addition to the dimensional stability offered by the rigidity of the comparatively massive flange construction, the hydrostatic loading caused by surrounding fluid under pressure also acted on the flange to minimize its expansion from the wedging action of the conical window. It can, therefore, be postulated that for all practical purposes the window flanges were rigid, and only the acrylic windows were deformed during the tests.

Mounting flanges with conical cavities of different angle sizes were employed to accommodate the range of 30° to 150° included angles of the conical window specimens. A cylindrical cavity of varying length extended beyond the conical cavity of the mounting flange, to accommodate the displaced (extruded or deflected) portion of the window resulting from pressure action. (See Figure 3.) Flanges were of two types, DOL (Deep Ocean Laboratory) Type I and DOL Type II, with a difference in configuration related chiefly to the radial restraint provided by the cavity receiving the displaced portion of the window and explained in the paragraphs which follow. In this study, the DOL Type II configuration flange was used only in a small number of tests, for exploratory purposes.

To standardize the displacement aspect of testing, all windows were machined to position the low-pressure (minor-diameter) surface flush with the small end of the conical cavity in the mounting flange. Thus, as the thickness of the windows tested varied, the high-pressure face (the one exposed to the hydrostatic pressure) extended to different elevations in the flange conical cavity. As the window moved axially under hydrostatic pressure, portions of it would protrude into the adjoining cylindrical cavity, and would not be further subjected to wedging action by the flange.

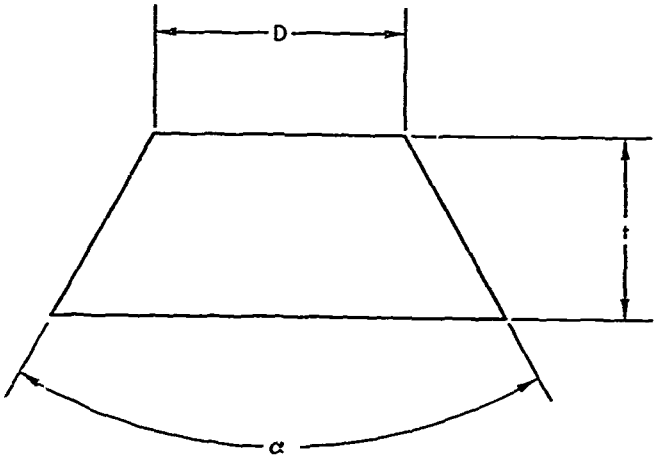

Included Conical Angle, α [1] (deg)	Window Diam, D [2] (in.)	t/D Ratio (Nominal)							
		0.125	0.25	0.375	0.5	0.625	0.75	0.875	1.0
		Nominal Thickness, t (in.) [3]							
30	1	1/8	1/4	3/8	1/2	5/8	3/4	7/8	1.0
60	1	1/8	1/4	3/8	1/2	5/8	-	-	-
90	1	1/8	1/4	3/8	1/2	5/8	-	-	-
120	1	1/8	1/4	3/8	1/2	5/8	-	-	-
150	1	1/8	1/4	3/8	1/2	5/8	-	-	-
30	2	1/4	1/2	-	1	-	-	-	-
60	4-1/2	9/16	1-1/8	-	2-1/4	-	-	-	-
90	8	-	-	-	4	-	-	-	-

[1] Dimensional tolerance of ±30 minutes.

[2] Diameter of low-pressure face (minor diameter), with tolerance of ± 0.005 inch.

[3] Commercial stock size, with tolerance of ±10%.

Figure 1. Types of conical acrylic window test specimens.

Foreword

For successful operation, all manned diving systems, submersibles, and hyperbaric chambers require pressure-resistant viewports. These viewports allow the personnel inside the diving bells and submersibles to observe the environment outside the pressure-resistant hulls. In addition, on land, operators of hyperbaric chambers can observe the behavior of patients or divers undergoing hyperbaric treatment inside the chambers.

Since the viewports form a part of the pressure-resistant envelope, they must meet or surpass the safety criteria used for designing either the metallic or plastic composite pressure envelope. The ASME Boiler and Pressure Vessel Code Section 8 provides such design criteria, and the chambers' pressure hulls designed on their basis have generated an unexcelled safety record.

The viewports, because of the unique structural properties of the acrylic plastic used in constructing the windows, could not be designed according to the same criteria as for the pressure envelopes fabricated of metallic or plastic composite materials. To preclude potential catastrophic failures of windows designed on the basis of inadequate data, in 1965, the U.S. Navy initiated a window testing program at the Naval Civil Engineering Laboratory and the Naval Ocean Systems Center. Under this program, window testing was conducted until 1975.

The objective of the window testing program was to generate test data concerning the structural performance of acrylic-plastic windows fabricated in different shapes, sizes, and thicknesses. Candidates for investigation included the effect of major design parameters, like the thickness to diameter ratio, bevel angle of bearing surfaces, and the ratio of window diameter to seat-opening diameter on the structural performance of the windows, and empirical relationships were to be formulated between these variables and the critical pressures at which windows fail. To make the test results realistic, the test conditions were varied to simulate the in-service environment that the windows were to be subjected. Thus, during testing, the windows were subjected not only to short-term pressurization at room temperature, but also to long-term sustained and repeated pressurization at different ambient temperatures.

On the basis of these data, empirical relationships were formulated between design parameters and test conditions. Committees in the Pressure Technology Codes of the American Society of Mechanical Engineers subsequently incorporated these relationships into the Safety Standard for Pressure Vessels for Human Occupancy (ASME PVHO-1 Safety Standard). Since that time, this ASME Safety Standard has formed the basis — worldwide — for designing acrylic windows in pressure chambers for human occupancy. Their performance record is excellent, since the publication of the Safety Standard in 1977, no catastrophic failures have been recorded that resulted in personal injury.

The data generated by the Navy's window testing program were originally disseminated in technical reports of the Naval Civil Engineering Laboratory and the Naval Ocean Systems Center, and were made available to the general public through the Defense Technical Information Center. To facilitate distribution of these data to users inside and outside of the Department of Defense, the technical reports have been collected and are being reissued as volumes of the U.S. Navy Ocean Engineering Studies.

These volumes, containing the collected technical reports on pressure-resistant plastic windows, will be deposited in technical libraries of Naval Laboratories and universities with ocean engineering programs. This dissemination of collected data should significantly reduce the effort currently being expended by students, engineers, and scientists in their search for data dispersed among the many reports published over a 10-year period by several Naval activities.

Volume III of the Ocean Engineering Series is a compilation of four technical reports that focus exclusively on the critical pressures of acrylic windows under short-term pressurization. Three different window shapes are discussed in these reports: flat disc, conical frustum, and spherical shell. Since the structural properties of acrylic plastic are not a function of material thickness, the critical pressures of scale-model acrylic windows described in these reports apply to windows of any size.

J. D. Stachiw
Marine Materials Office
Ocean Engineering Division

(25) * Acrylic windows,
* Conical bodies,
* Hemispherical shells

Figure 2. Steel mounting flange for conical acrylic windows attached to end closure of Mk-I pressure vessel.

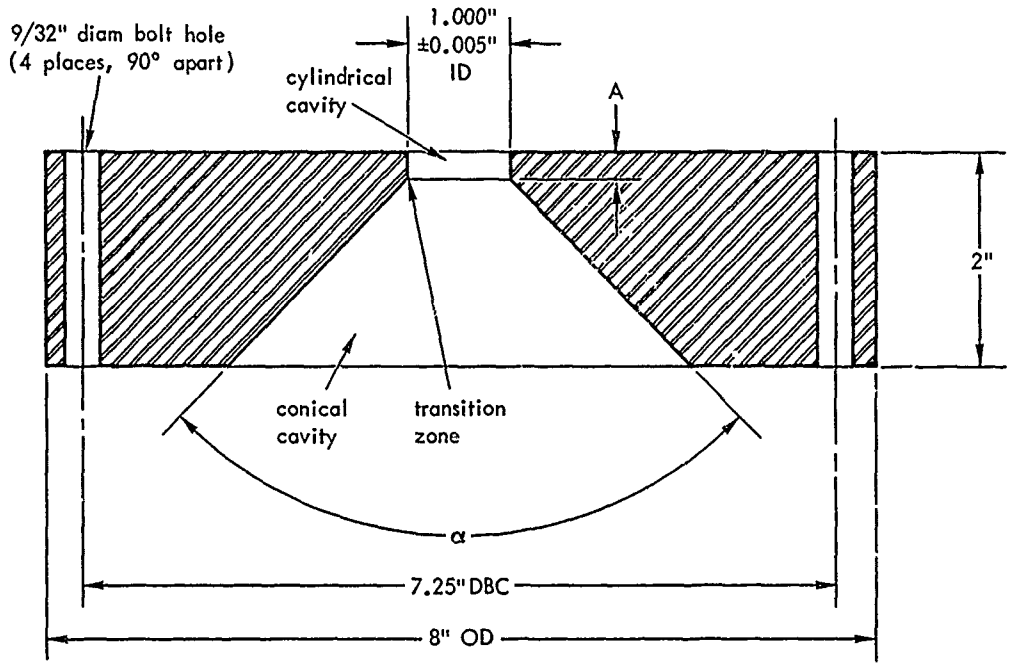

Included Conical Angle, α [1/] (deg)	Cylindrical Cavity Length, A (in.)
30	1/4
60	1/4
90	1/4
120	1/2
150	1-1/4

[1/] Dimensional tolerance of ±30 minutes.

Figure 3. Steel mounting flanges, DOL Type I configuration, for 1-inch-diameter conical acrylic window test specimens.

Exploratory work (Table G-11, Appendix G) indicated that continued radial support for the displaced portion of the window has a definite relationship to the window critical pressure. Therefore, each test mounting flange, though its cylindrical cavity in many cases had a length of only 0.25 inch, was backed by a flange adapter (Figure 4) with a cylindrical cavity always matching the minor diameter of the mounting flange cavity. In this way, regardless of how much a window extruded, its extruded portion was always radially restrained by a cylindrical wall, either of the flange or of the adapter. Such arrangement standardized the test conditions for window specimens whatever their thickness, conical angle, diameter, or amount of displacement under testing. The type of flange configuration assuring the displaced portion of support, whatever its length, was designated DOL Type I, and the one not providing such support, DOL Type II. (See Appendix F.) In the latter configuration, the cavity for receiving the displaced portion of the window was not cylindrical but flared sharply, and was not extended by use of a flange adapter.

Instrumentation

The instrumentation consisted of a thermometer, a pressure gage, and a displacement measuring device. The thermometer was used to measure the temperature of the water in contact with the window in the vessel; the pressure gage, the pressure of the water in the vessel; and the displacement measuring device, within 0.001 inch, the displacement of the center of the window low-pressure face as it extruded or deflected into the cylindrical cavity of the mounting. Since the displacement measuring device (Figures 5 and 6) was mechanical, no problems were encountered in zeroing or balancing it. Although more sophisticated instrumentation employing electric resistance strain gages[2] or photoelastic techniques[3] could have been used, its potential contribution in the determination of ultimate short-term window strength was deemed insufficient to warrant consideration.

TEST PROCEDURE

The window mounting flange with the appropriate conical opening was placed on the flange adapter (Figure 4) and bolted in position. The window, to which the displacement indicator wire was already fastened by means of a small acrylic anchor piece cemented onto its low-pressure face, was liberally coated with silicone grease and inserted into the mounting flange. No retaining device was necessary, as the grease exerted enough adhesion to keep the window from falling out. Next, the mounting assembly was inserted into the end closure of the pressure vessel and locked in place. The 0.010-inch-thick steel wire connected to the window low-pressure face was then fastened to a 1-pound weight. With the wire positioned over pulleys that centered one wire end over the window and the other over a dial indicator, the weight was placed on the dial indicator rod, depressing it slightly (Figure 5). During the experiment, the weight was kept from shifting on the dial indicator rod by a plastic weight guide tube and a recess on the bottom of the weight into which the indicator rod fitted. The test setup with the displacement measuring device in position is shown in Figure 6.

To permit pressurization of the vessel, three entries were provided in the top of the vessel end closure. One was used to admit the pressurizing fluid to the vessel, one for sensing the pressure, and one to remove entrapped air and to relieve the pressure in the vessel on completion of the test. The pressure inside the vessel was monitored at all times with a 16-inch-diameter Bourdon tube-type pressure gage connected to a fitting in the end closure with 1/16-inch-outside-diameter tubing. The use of such small tubing was instrumental in reducing the severity of the hydraulic shock to the mechanism of the gage at the moment of window failure, when the pressure in the vessel was reduced from as high as 30,000 psi to 0 psi in less than 1 second. The pressurization of the vessel was accomplished by means of two air-driven pumps with a maximum pressurization capability of 30,000 psi (Figure 7).

Although different rates of pressurization were feasible, a pumping rate of 650 ±100 psi/min was selected as a standard. The temperature of the pressurizing medium (fresh water) and of the vessel was maintained in the general range of 60° to 70°F, although for some selected tests it was reduced to a range of 35° to 40°F. The temperature readings were recorded before and after window failure to obtain an average.

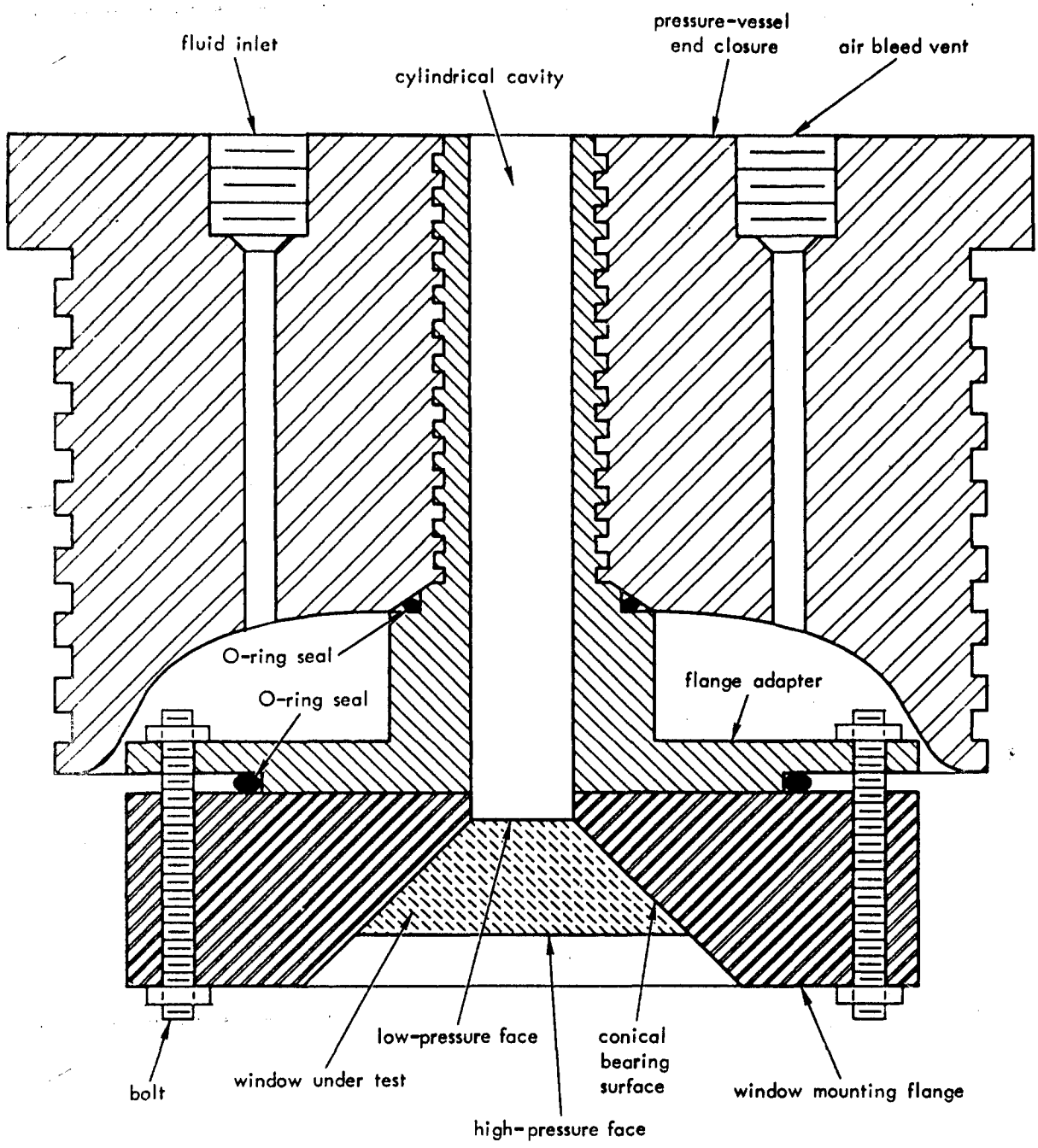

Figure 4. Flange adapter attached to DOL Type I mounting flange, with mounting assembly positioned in end closure of pressure vessel.

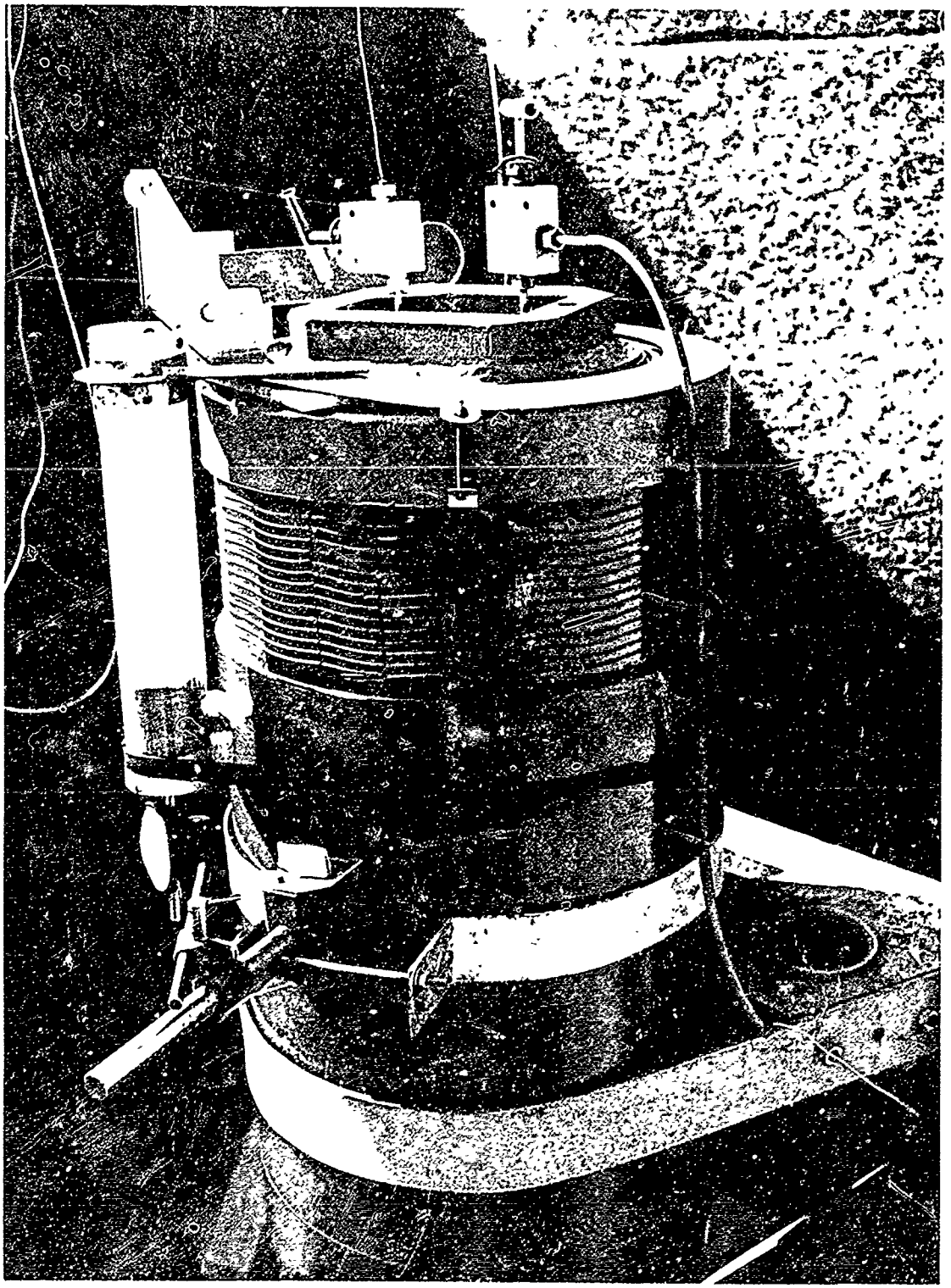

Figure 5. Window displacement measuring device.

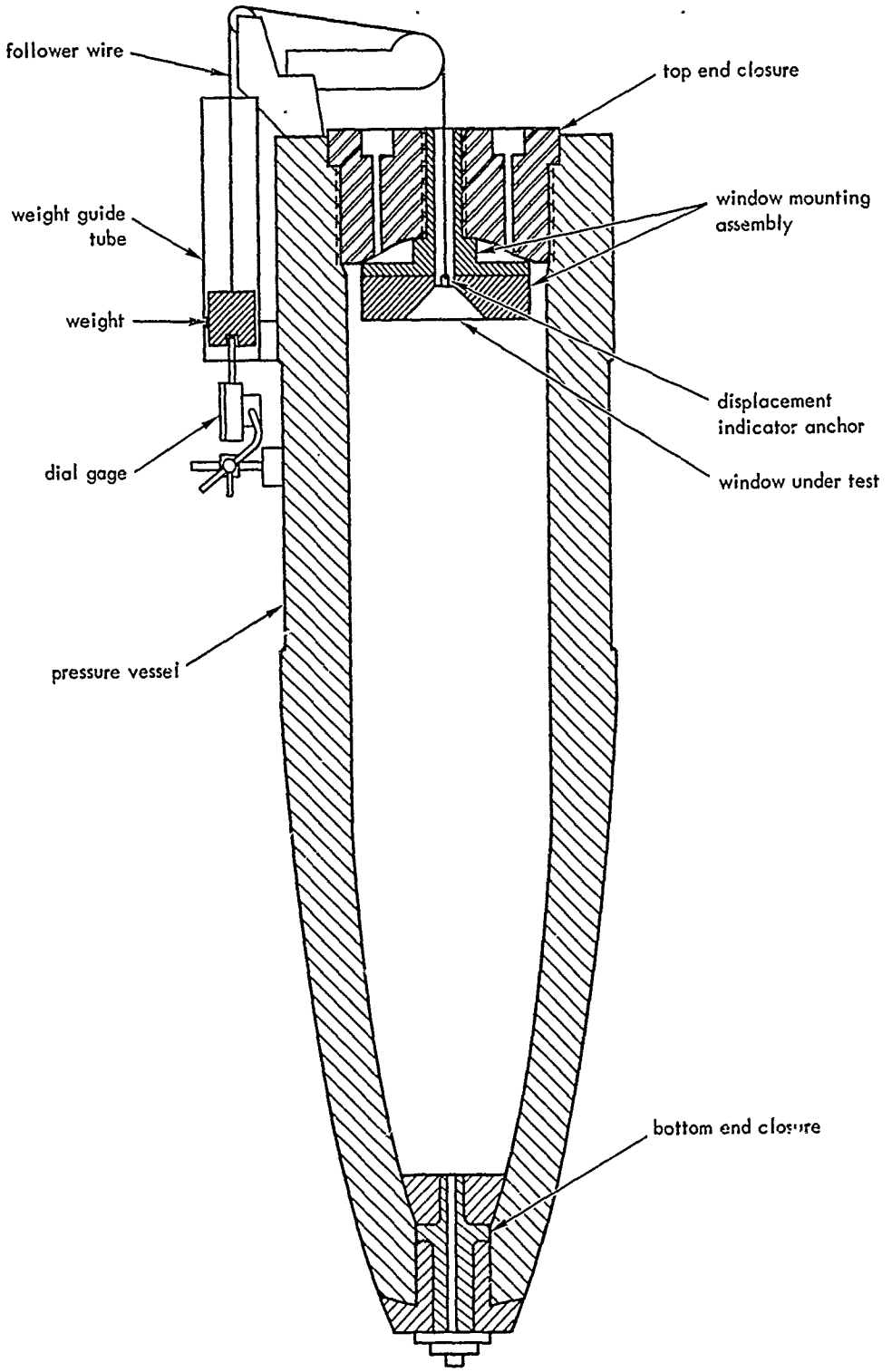

Figure 6. Schematic of window test assembly, with window displacement measuring device in position.

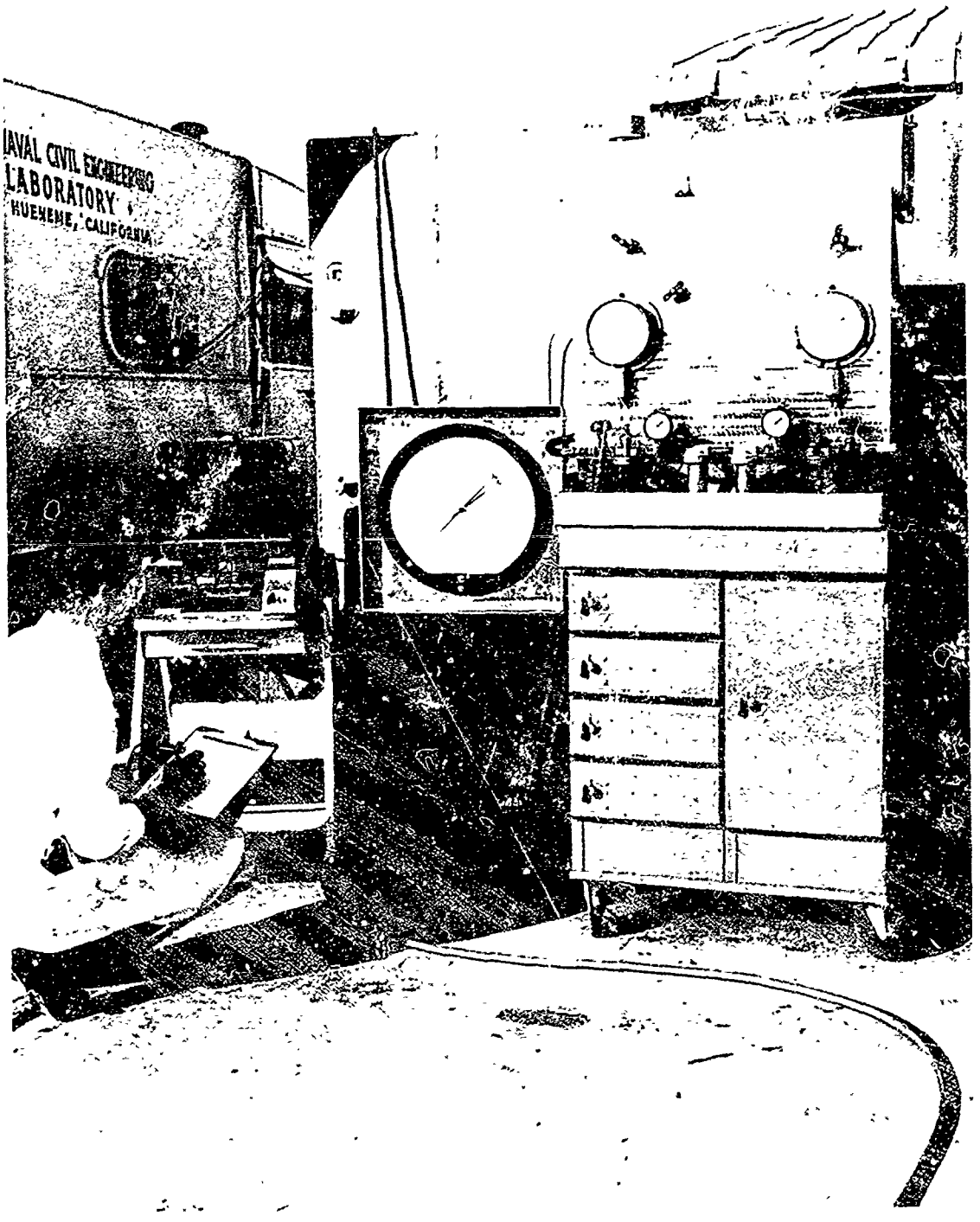

Figure 7. High-pressure pumping unit, precision pressure gage (center), and television monitor used in test procedure.

Once the pressurization process was begun, it was continued until the window failed. Displacement readings were recorded at 1,000-psi intervals without interruption of the pressurizing. Both the pressurization and the recording of displacement data were continuous until window failure occurred with an explosive release of compressed water and fragments of window. Water and fragments were ejected high into the air through the opening in the end closure. To protect the operator of the pressurizing system from possible failure of the vessel, he as well as the monitoring equipment were separated from the test area by a massive concrete block (Figure 8). The dial indicator readings were observed by means of a closed-circuit television system (Figure 9).

EXPERIMENTAL DATA

All the windows which were tested to destruction failed explosively. There was, however, a distinct difference in the mode of failure among the windows, depending on their t/D ratio and included angle. Discussion of the modes of failure is presented in Appendix B.

Scatter of Data

Experimental data consisting of critical pressures at which window failures occurred and magnitudes of displacement at different pressures varied from window to window, even though the windows were of the same nominal dimensions. To obtain a representative value of the experimental parameters, five or more windows of each nominal thickness used were tested for each t/D ratio, and their critical pressures and displacements averaged. This procedure was repeated for each conical angle considered. Since eight nominal t/D ratios and five conical angles were investigated, around 200 experiments were performed and the data from them recorded.

Because the average of any number of experimental readings at a given t/D ratio does not convey adequately the scatter of individual readings, both the minimum and the maximum of each experimental parameter range were also recorded for each t/D ratio. In general, it can be stated that the range of scatter of individual experimental points is less than plus-or-minus 10% of the average value computed for a given t/D ratio and conical angle. Such a magnitude of scatter range is small when one considers that the variation in temperature was of the same magnitude, the thickness of the window varied within plus-or-minus 0.020 inch of nominal thickness, and that the angular dimension varied within ±30 minutes of the nominal value.

Size of Sample Group. The size of the sample group was varied and statistical methods were used to verify that five experimental values provided an adequate representation of the experimentally determined variables. The discussion of this study is presented in Appendix C.

Effects of Temperature. Groups of similar specimens were tested at both 35° to 40°F and 67° to 75°F; it was determined that the lower temperature produced a measurable increase in the critical pressure. The discussion of this study is presented in Appendix D.

Subsidiary Experiments

Applicability of 1-Inch-Diameter Window Test Data to Windows of Larger Sizes. Several experiments were conducted with larger windows to determine if the data obtained from tested 1-inch-diameter windows was applicable to larger sizes. It was determined that the t/D ratio (with certain limiting conditions) is a direct scaling factor for critical pressure and that displacement, while not directly scalable, can be estimated reasonably accurately with an appropriate scaling factor. The data and discussion are presented in Appendix E.

Evaluation of Other Window Mounting Flange Configurations. Exploratory experiments were conducted which demonstrated that the configuration of the transition zone between the adjoining cavities of the mounting flange, the conical cavity and the one for accommodating the acrylic displacement, has considerable influence on the short-term critical pressure of the window.

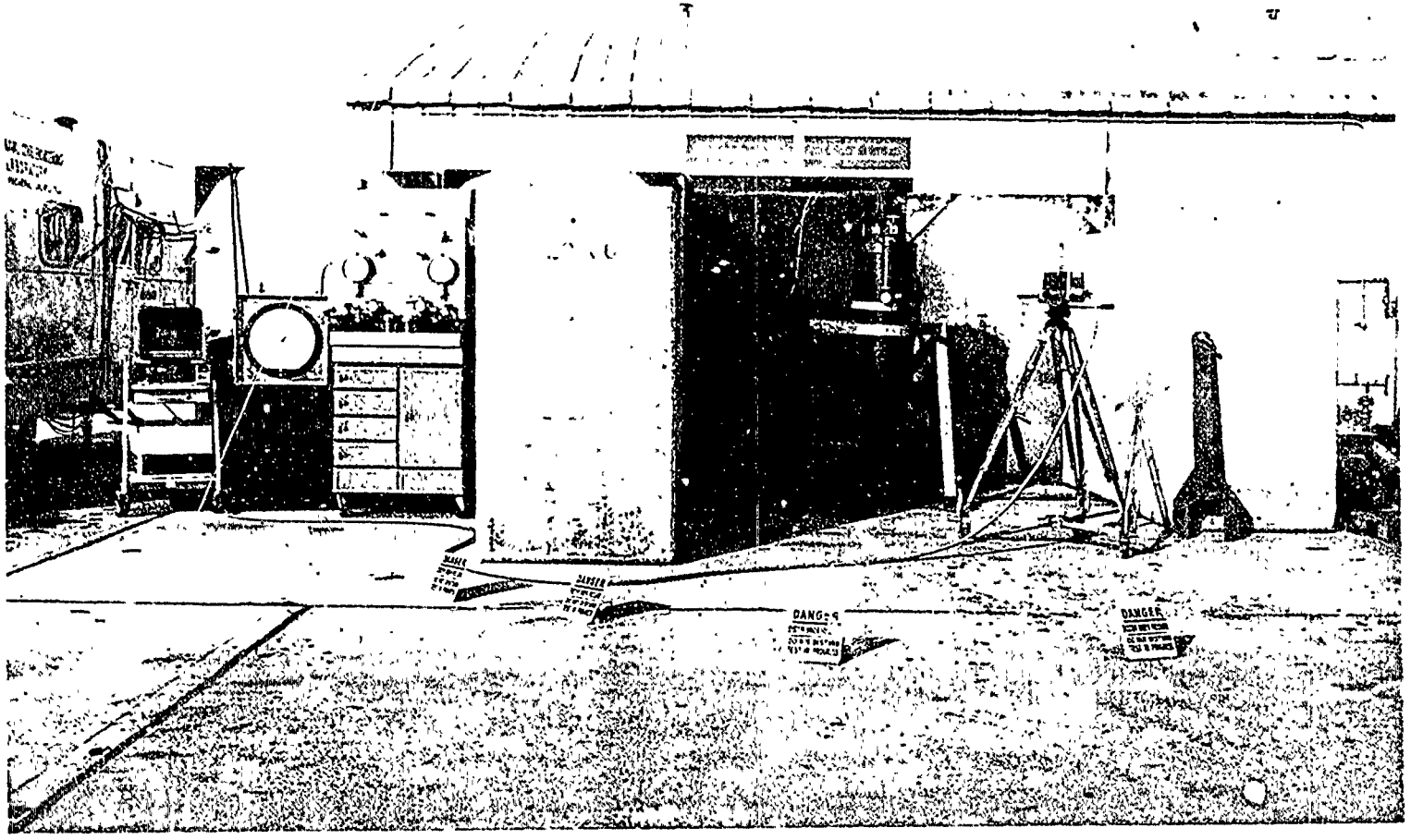

Figure 8. Complete setup for window test program.

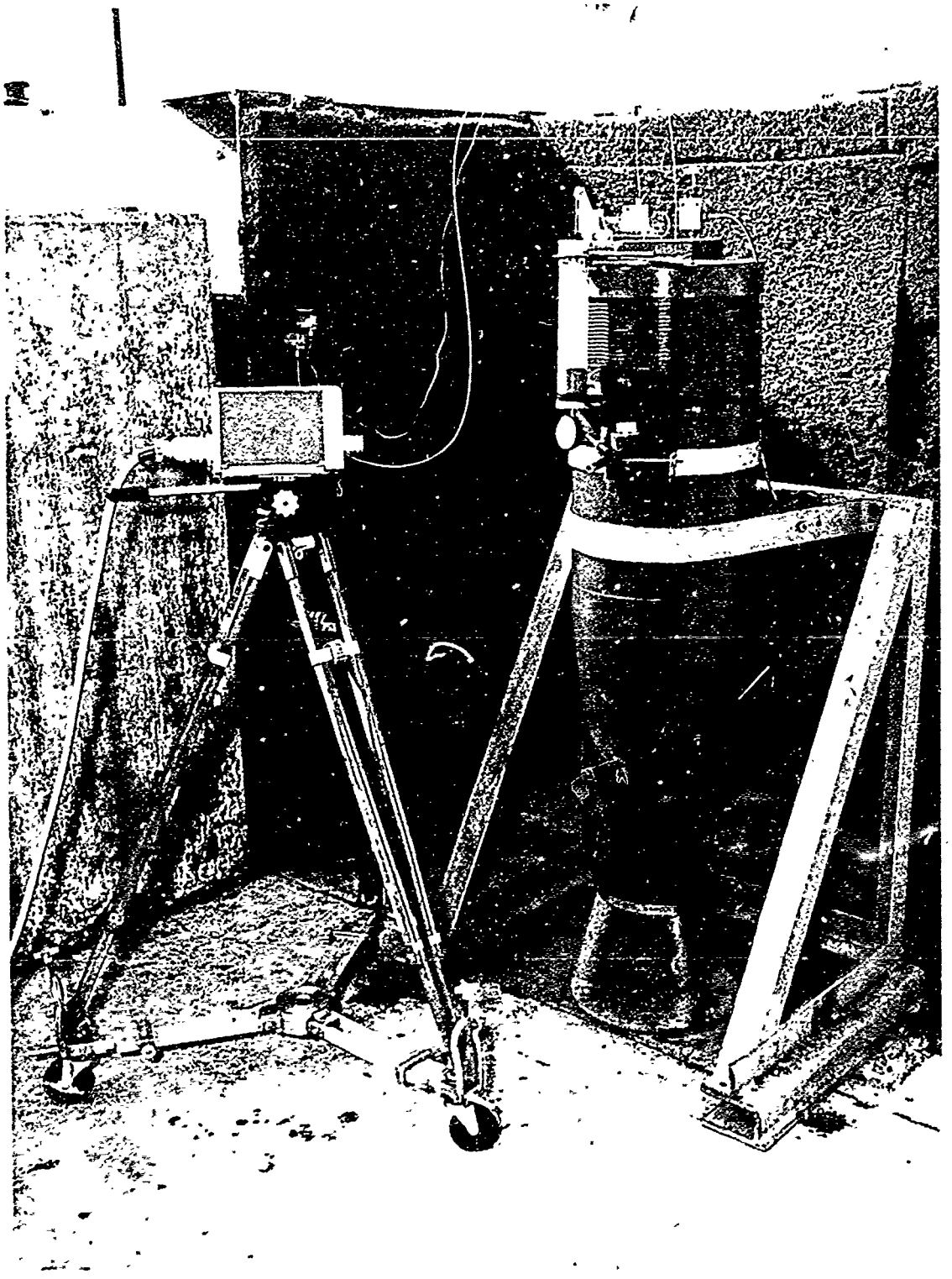

Figure 9. Window displacement measuring system with television camera used to monitor dial gage readings.

One-Inch-Diameter, 30° Conical Windows

Complete data from the testing of 1-inch-diameter, 30° conical windows are presented in Tables G-1 through G-11, Appendix G.

All these windows failed by being ejected from the vessel. In every case the whole window disintegrated into small particles that were carried outside the vessel by the high-velocity stream of water. Inspection of the mounting flange failed to show any pieces of the fractured window adhering to it.

The critical pressure recorded during the testing of the 30° window specimens (Figure 10), when plotted, appear to vary exponentially with t/D ratios, with small variations in the ratio producing large differences in pressure. The displacements of the windows (Figure 11) were large and decidedly nonlinear for all t/D ratios.

One-Inch-Diameter, 60° Conical Windows

Complete data from the testing of 1-inch-diameter, 60° conical windows are presented in Tables G-12 through G-16, Appendix G.

In comparing the critical pressures of the 60° windows (Figure 12) with those of the 30° windows, it became apparent that the 60° type of window was the more pressure-resistant. The differences in critical pressure between windows of the same t/D ratio but different included angle varied with the t/D ratio. The difference was quite small at low t/D ratios, but extremely large at intermediate and high t/D ratios. The high critical pressures of 60° windows were accompanied by smaller displacements (Figure 13) when comparison was made at the same pressure to 30° windows of the same t/D ratio.

One-Inch-Diameter, 90° Conical Windows

Complete data from the testing of 1-inch-diameter, 90° conical windows are presented in Tables G-17 through G-22, Appendix G.

The critical pressures of the 90° windows (Figure 14) were not markedly higher than those of the 60° windows with the same t/D ratio. This showed that the increase in short-term pressure resistance of conical windows, with increase of included angle, was reaching a plateau with the 90° windows, and probably no further gain in pressure resistance was to be achieved by enlarging the included conical angle to 120° or 150°. The displacements of the 90° windows (Figure 15) were observed to be significantly less than those of the 60° windows.

One-Inch-Diameter, 120° Conical Windows

Complete data from the testing of 1-inch-diameter, 120° conical windows are presented in Tables G-23 through G-27, Appendix G.

The critical pressures of these windows (Figure 16) were found to be essentially the same as those of the 90° windows. This seemed to indicate that no further advantage was to be gained in terms of pressure capability by increasing the angle of the windows past 90°.

The displacements of the 120° windows (Figure 17) were observed to be approximately the same as those of 90° windows. Since the displacements were generally smaller than those for the 90° windows, and since the cold-flow cratering (pressure-induced plastic deformation, here a depression, occurring at room temperature) on the high-pressure face of the 120° windows appeared to be less pronounced at the same pressure than for 90° windows, the 120° windows would probably perform better optically at higher pressures than the 90° windows.

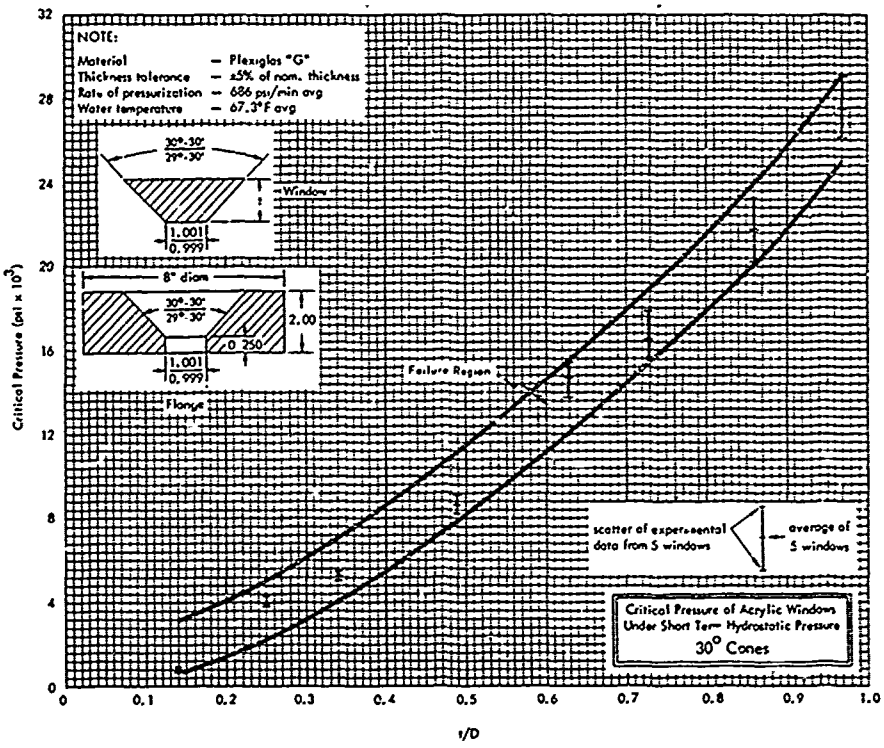

Figure 10. Critical pressures of 1-inch-diameter, 30° conical acrylic windows under short-term hydrostatic pressure.

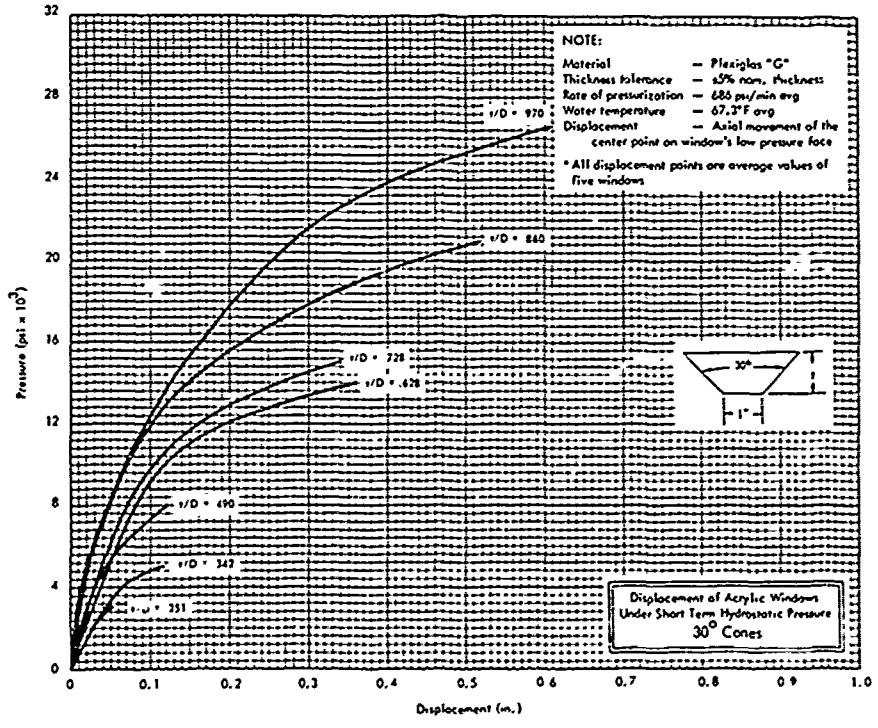

Figure 11. Displacements of 1-inch-diameter, 30° conical acrylic windows under short-term hydrostatic pressure.

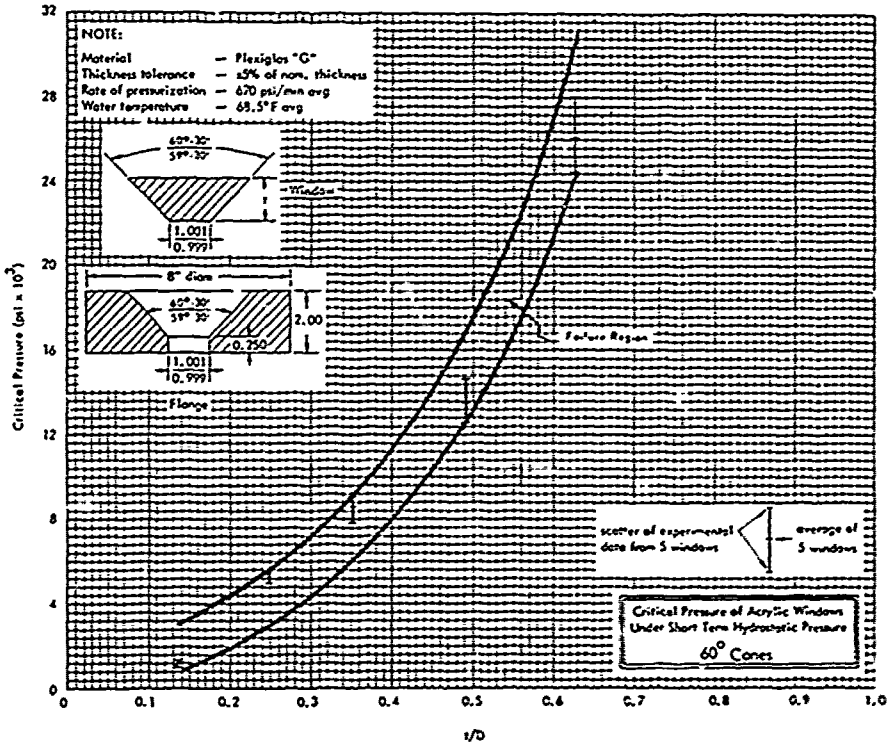

Figure 12. Critical pressures of 1-inch-diameter, 60° conical acrylic windows under short-term hydrostatic pressure.

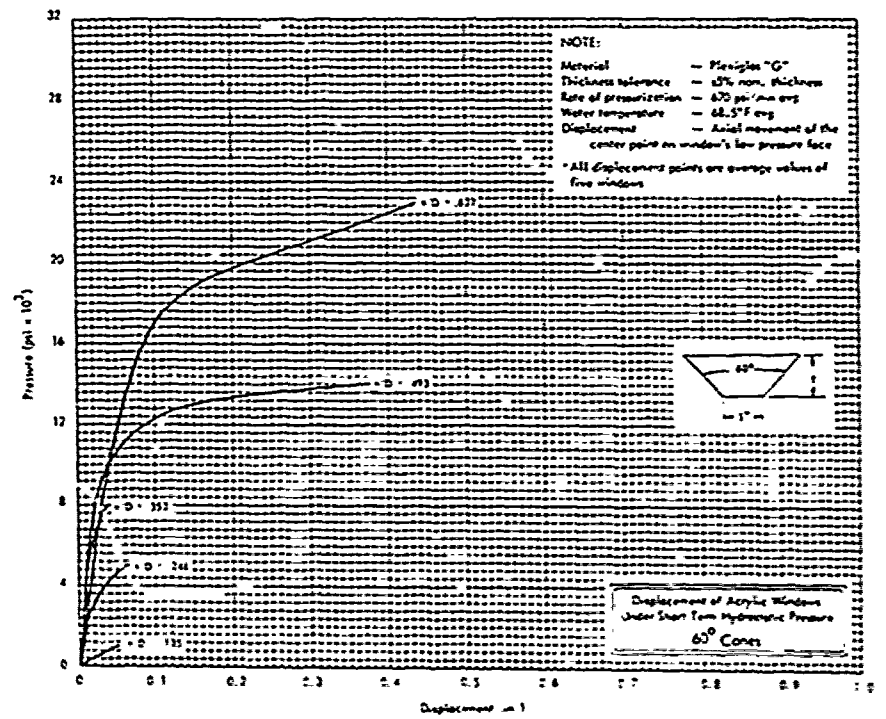

Figure 13. Displacements of 1-inch-diameter, 60° conical acrylic windows under short-term hydrostatic pressure.

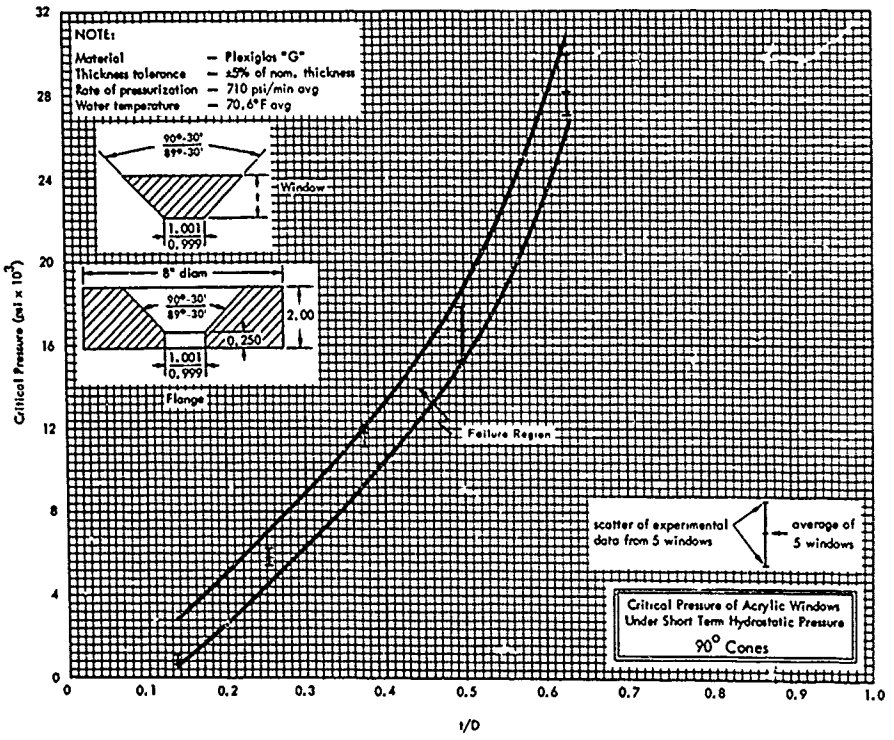

Figure 14. Critical pressures of 1-inch-diameter, 90° conical acrylic windows under short-term hydrostatic pressure.

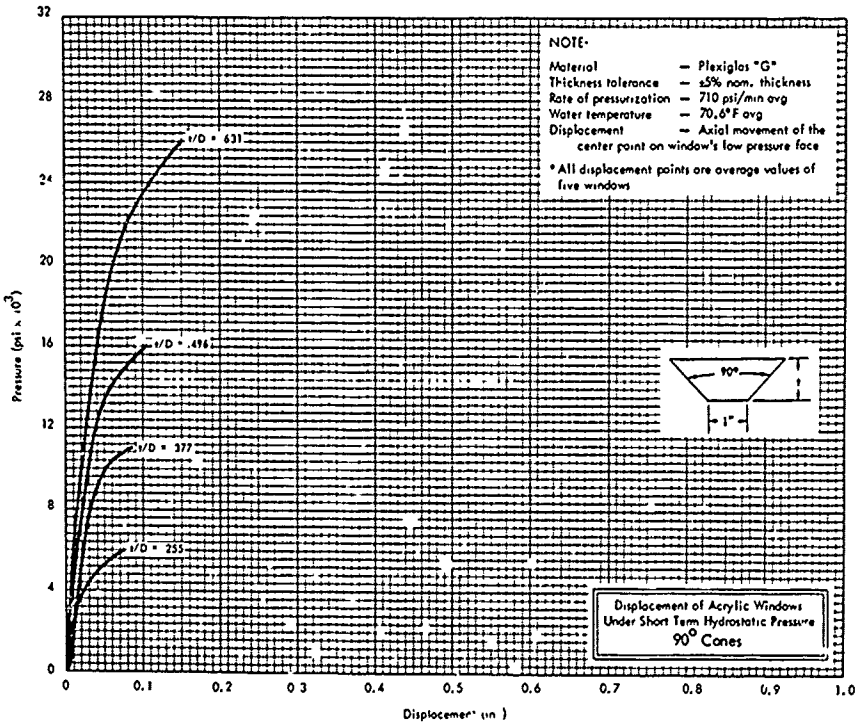

Figure 15. Displacements of 1-inch-diameter, 90° conical acrylic windows under short-term hydrostatic pressure.

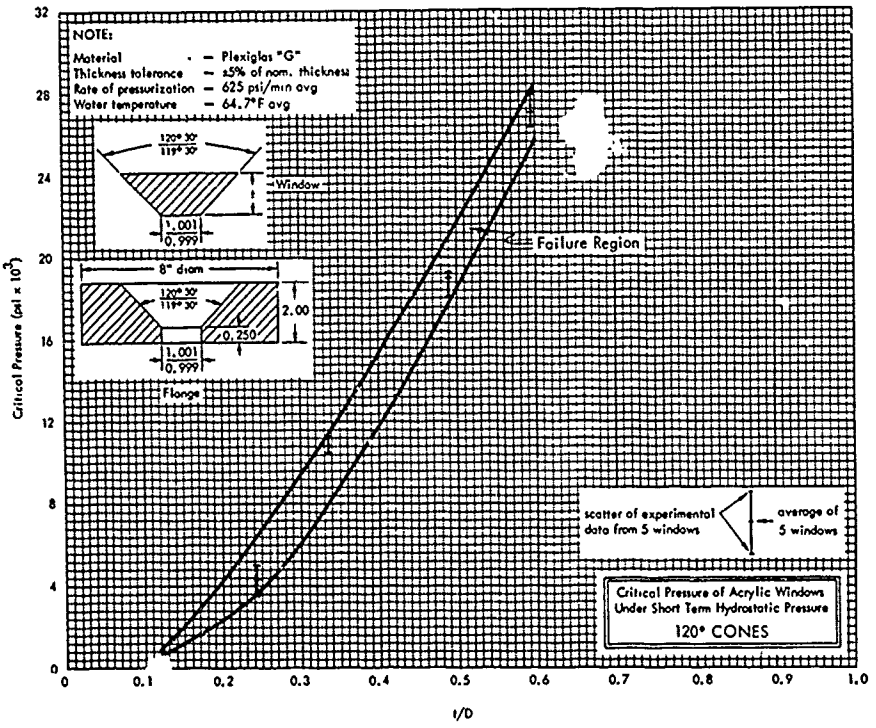

Figure 16. Critical pressures of 1-inch-diameter, 120° conical acrylic windows under short-term hydrostatic pressure.

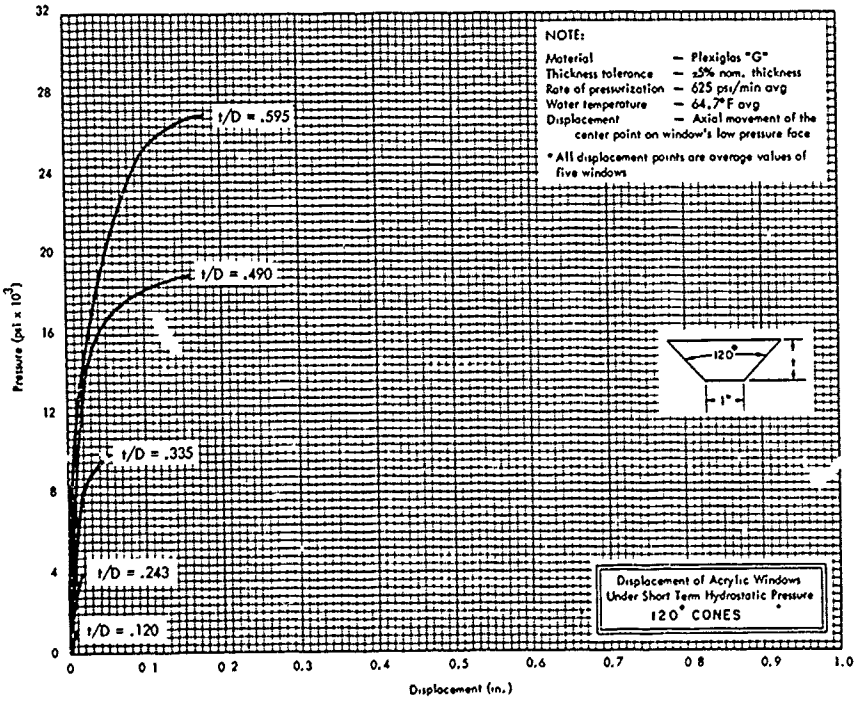

Figure 17. Displacements of 1-inch-diameter, 120° conical acrylic windows under short-term hydrostatic pressure.

One-Inch-Diameter, 150° Conical Windows

Complete data from the testing of 1-inch-diameter, 150° conical windows are presented in Tables G-28 through G-33, Appendix G.

The critical pressures of the 150° conical windows (Figure 18) were in general the same as those of 120° windows, except for 0.375 t/D ratio windows, whose critical pressures were slightly higher. This indicated that, for the most part, no benefit in critical pressure was to be derived by increasing the included angle of the windows above 90° or 120°.

The displacements of the 150° conical windows (Figure 19) were, in general, the same as those of the 120° windows, but noticeably smaller than those of the 90° windows. The shape of the displacement curves shows that very little plastic flow took place in the 150° conical windows prior to their failure at critical pressure, much the same as in the case of the 120° windows.

Two-Inch-Diameter, 30° Conical Windows

Complete data from the testing of 2-inch-diameter, 30° conical windows are presented in Tables G-34 through G-37, Appendix G.

These windows failed at pressures (Figure 20) approximately the same as those of 1-inch-diameter, 30° windows with the same t/D ratio.

The displacements of the 2-inch-diameter windows (Figure 21) were found to be considerably larger than those of the 1-inch-diameter windows with the same t/D ratios. A definite ratio between the magnitudes of displacement for windows of these two diameters could not be derived which would be accurate regardless of t/D ratio. Nevertheless, a 1:2 ratio, representing the ratio between the 1-inch- and 2-inch-diameter windows, can prove useful in estimating the displacement of 2-inch-diameter windows of various t/D ratios from known displacements of 1-inch-diameter windows.

Four-and-One-Half-Inch-Diameter, 60° Conical Windows

Complete data from the testing of 4.5-inch-diameter, 60° conical windows are presented in Tables G-38 through G-40, Appendix G.

The window specimens tested of this type, with t/D ratios of 0.125, 0.25, and 0.5, failed at essentially the same pressures (Figure 22) as the 1-inch-diameter windows with the same t/D ratios. The displacements of the 4.5-inch-diameter windows, however, differed considerably from those of the 1-inch-diameter, 60° windows. When the magnitude of displacement of the 4.5-inch-diameter windows (Figure 23) was compared to that of the 1-inch-diameter windows, it was found to be considerably higher. Although a definite ratio between the magnitudes of displacement for windows with these two diameters could not be derived which would be accurate regardless of the t/D ratio, it appears that a t/D ratio of 1:4.5 is a good approximation. This figure would indicate that the ratio of displacement magnitude for 1-inch- and 4.5-inch-diameter windows is probably the same as that of the two window diameters.

Eight-Inch-Diameter, 90° Conical Windows

The short-term hydrostatic testing with an 8-inch-diameter, 90° conical window (Figures 24 and 25) was conducted under the same experimental conditions as those for 1-inch-diameter, 90° windows, except that an 18-inch-inside-diameter pressure vessel (Figure 25) was used for pressurization. Only the 0.5 t/D ratio was investigated, and its critical pressure compared to that of the 1-inch-diameter conical windows with a 0.5 t/D ratio.

The critical pressure (Figure 26) of the 8-inch-diameter, 90° window was found to be essentially the same as the critical pressure of the 1-inch-diameter, 90° window with corresponding t/D ratio.

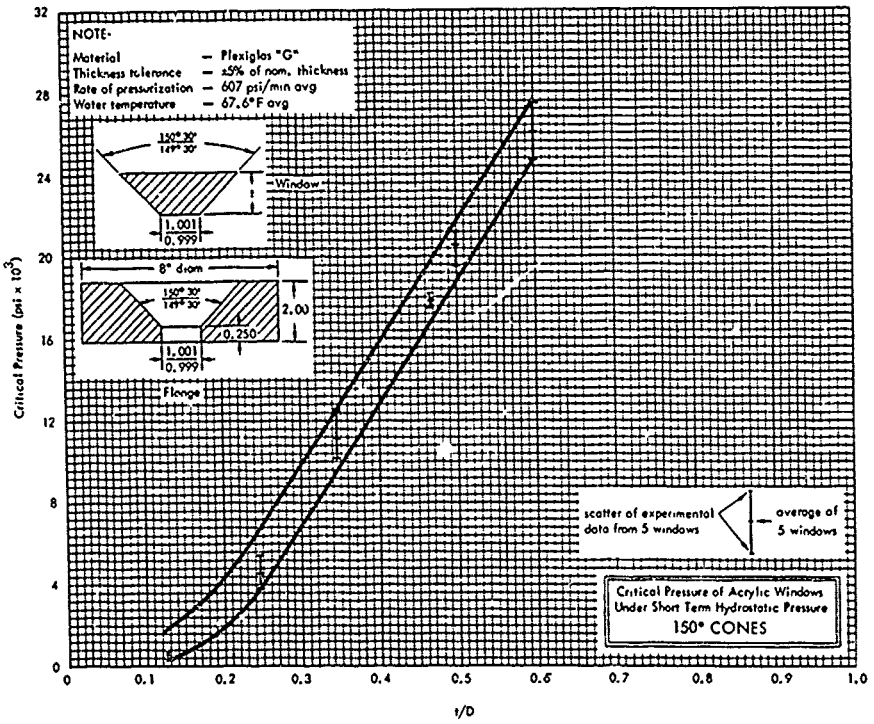

Figure 18. Critical pressures of 1-inch-diameter, 150° conical acrylic windows under short-term hydrostatic pressure.

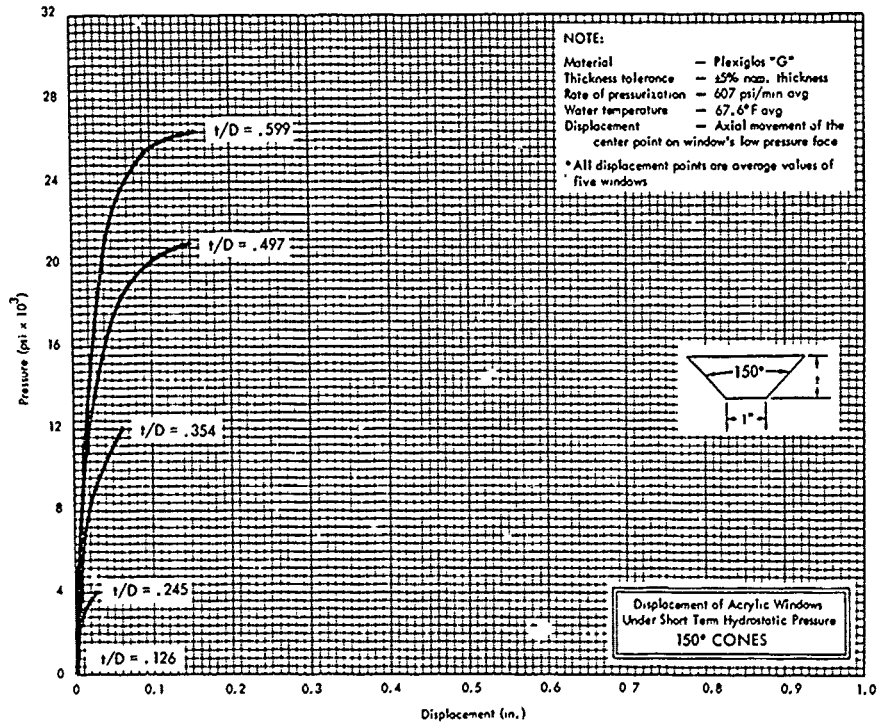

Figure 19. Displacements of 1-inch-diameter, 150° conical acrylic windows under short-term hydrostatic pressure.

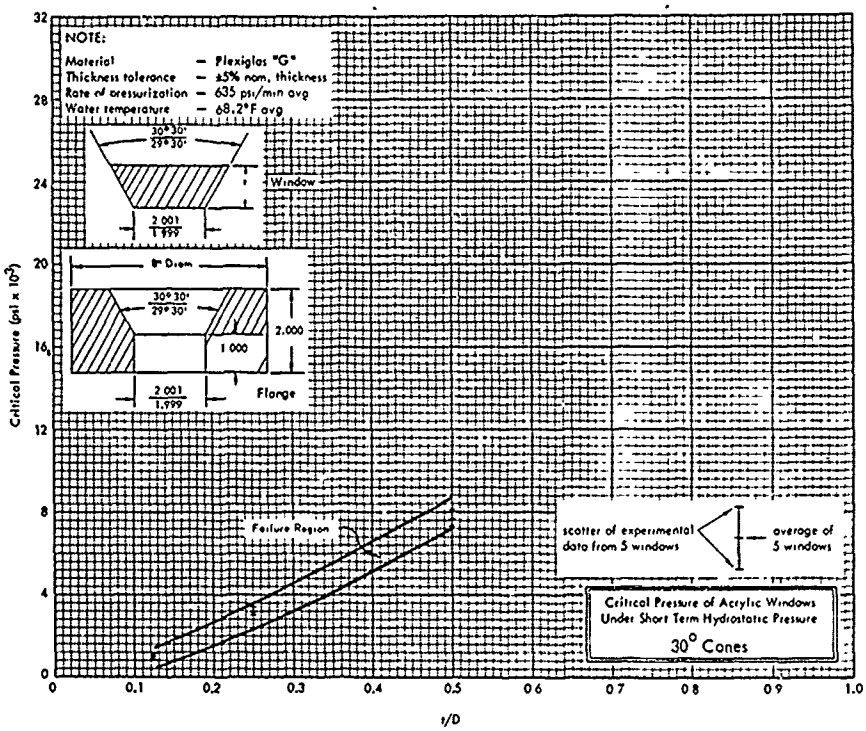

Figure 20. Critical pressures of 2-inch-diameter, 30° conical acrylic windows under short-term hydrostatic pressure.

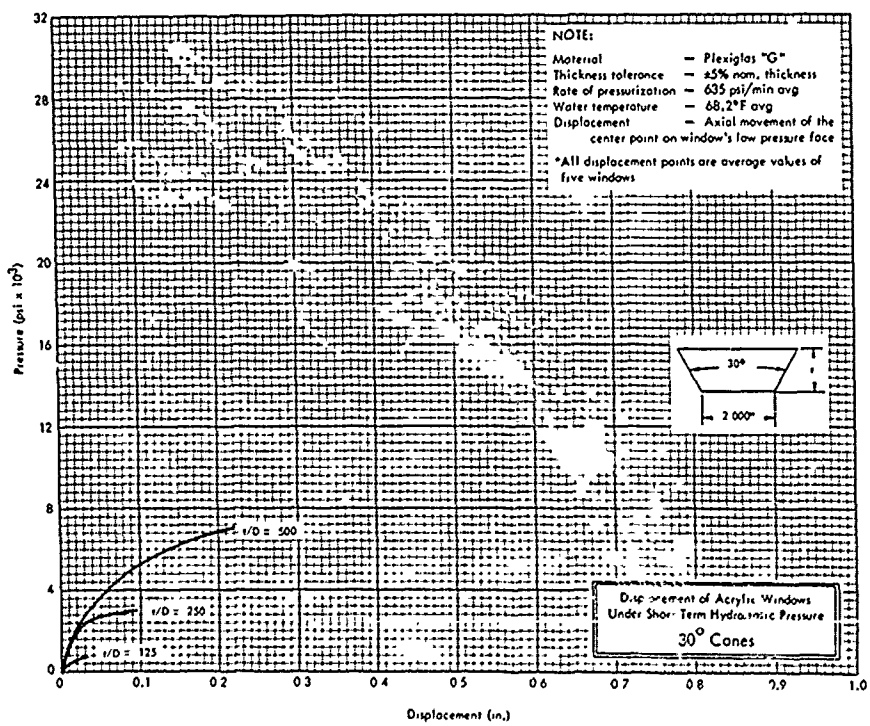

Figure 21. Displacements of 2-inch-diameter, 30° conical acrylic windows under short-term hydrostatic pressure.

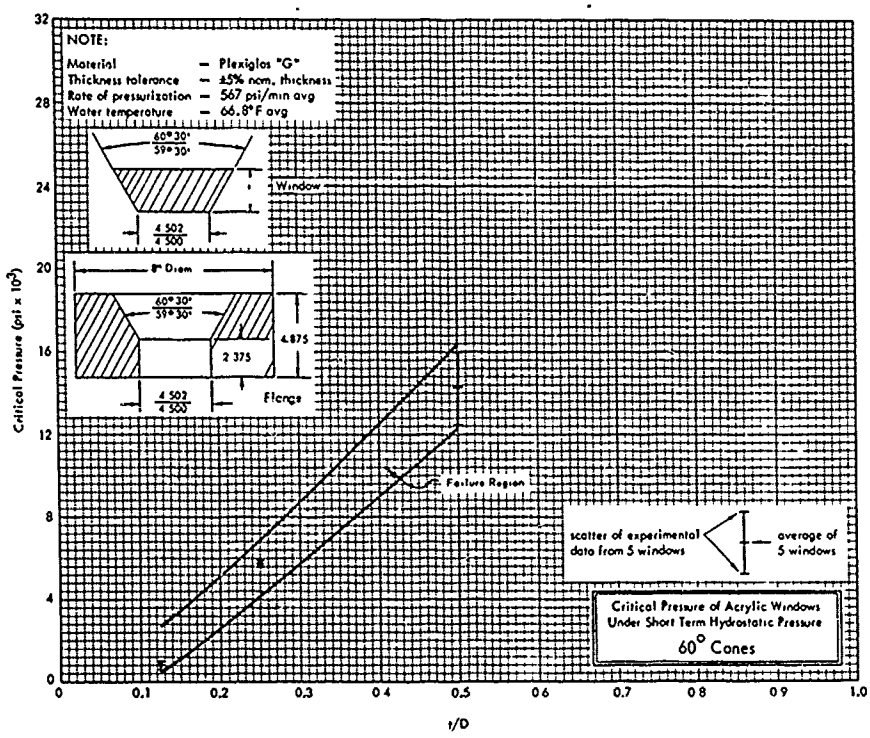

Figure 22. Critical pressures of 4.5-inch-diameter, 60° conical acrylic windows under short-term hydrostatic pressure.

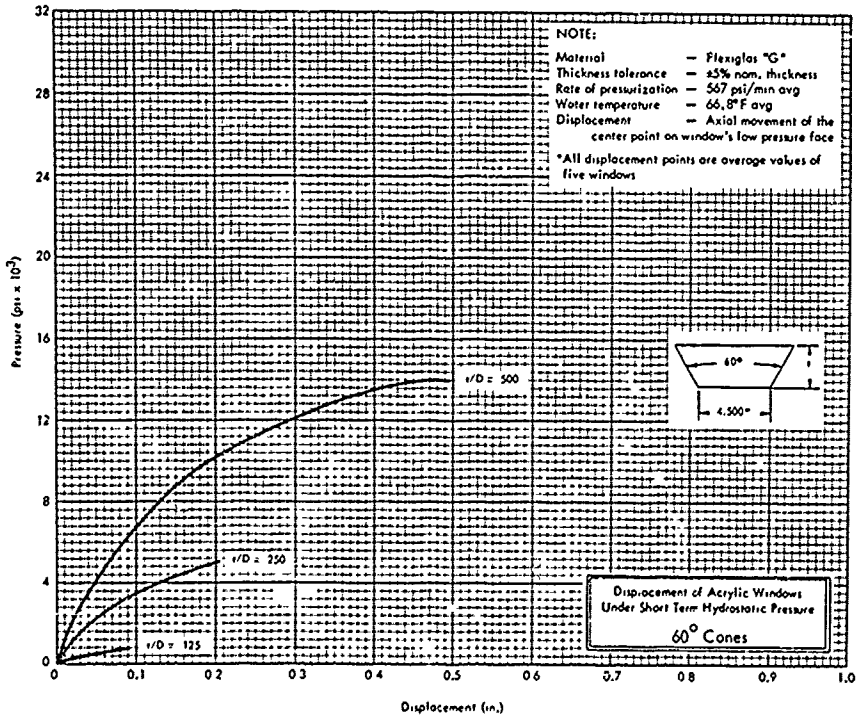

Figure 23. Displacements of 4.5-inch-diameter, 60° conical acrylic windows under short-term hydrostatic pressure.

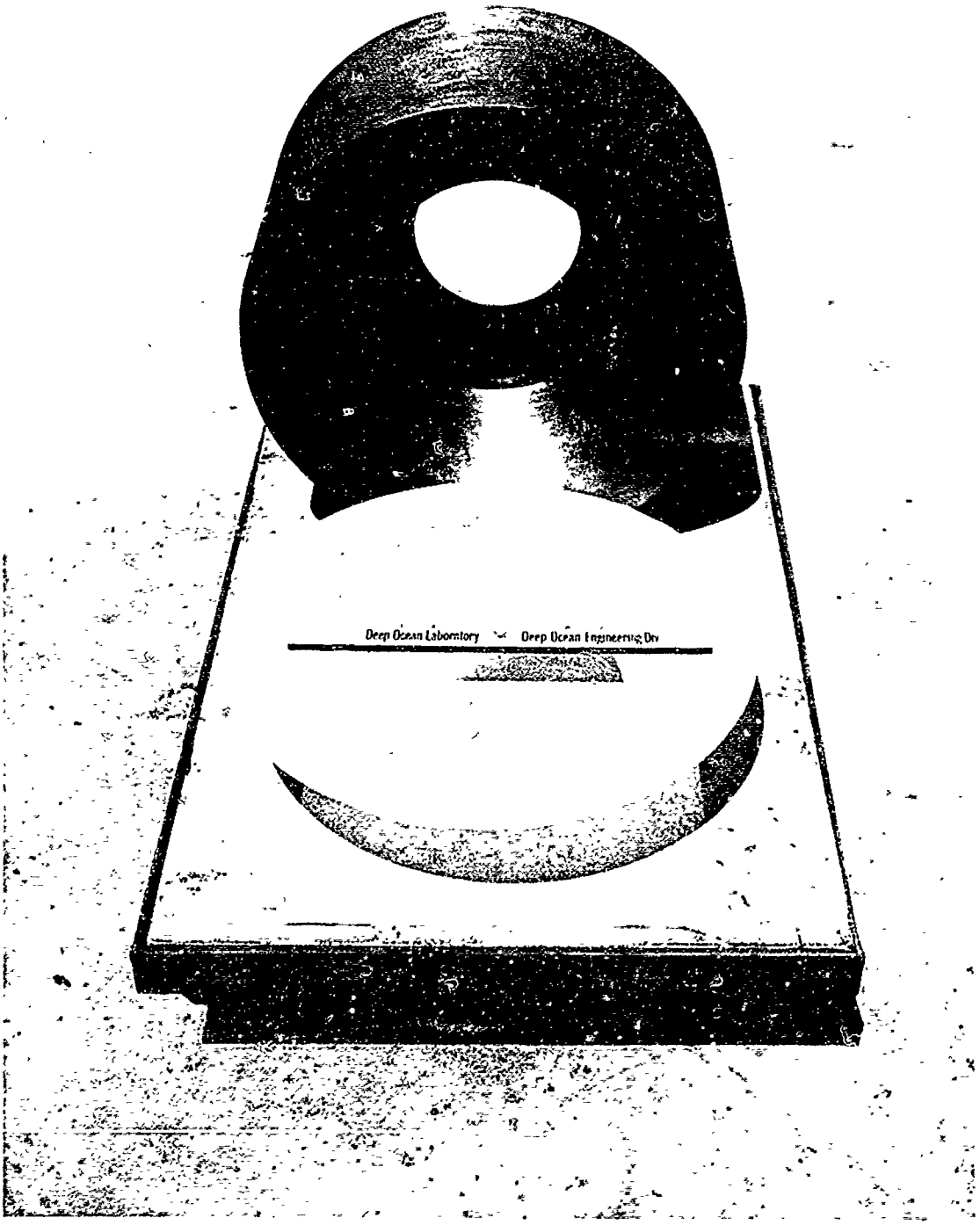

Figure 24. Eight-inch-diameter, 90° conical acrylic window and mounting flange.

Figure 25. End closure assembly for 18-inch-inside-diameter pressure vessel, with 8-inch-diameter, 90° conical acrylic window being secured in mounting flange.

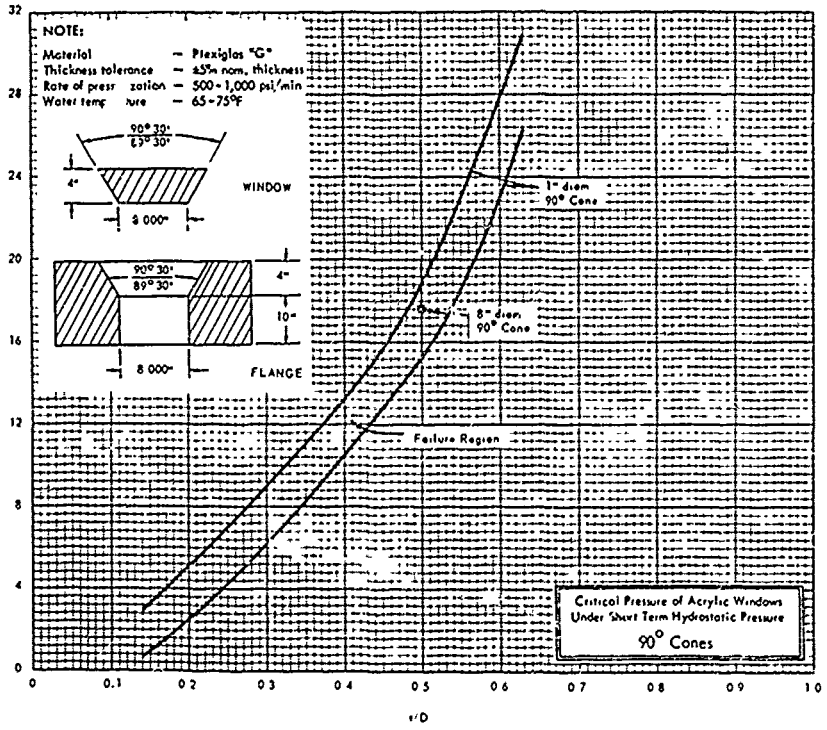

Figure 26. Critical pressure of 8-inch-diameter, 90° conical acrylic window under short-term hydrostatic pressure.

FINDINGS

1. The analysis of experimental data derived from the testing of 1-inch-diameter windows has shown that the displacements of conical acrylic windows larger than 1 inch in diameter, while not directly scalable, can be estimated by application of the proper scaling relationship.

2. The critical pressures of conical acrylic windows in DOL Type I configuration flanges have been found to vary with t/D ratio, as well as the conical angle of the windows. An increase in the t/D ratio is invariably followed by an increase in the window critical pressure, but an increase in the conical angle is not always followed by a critical pressure increase (Figures 27 through 31).

3. The critical pressure of conical acrylic windows under short-term hydrostatic loading increases with a decrease in the temperature of the pressurizing medium. Although sufficient data does not exist to determine accurately how much higher the critical pressure is in the approximately 35° to 40°F than in the approximately 60° to 70°F temperature range, it can be estimated that in all probability it is 10% to 20% higher.

4. The critical pressures of conical acrylic windows with a diameter larger than 1 inch have been found to be the same as those of 1-inch-diameter windows with identical conical angle and t/D ratio.

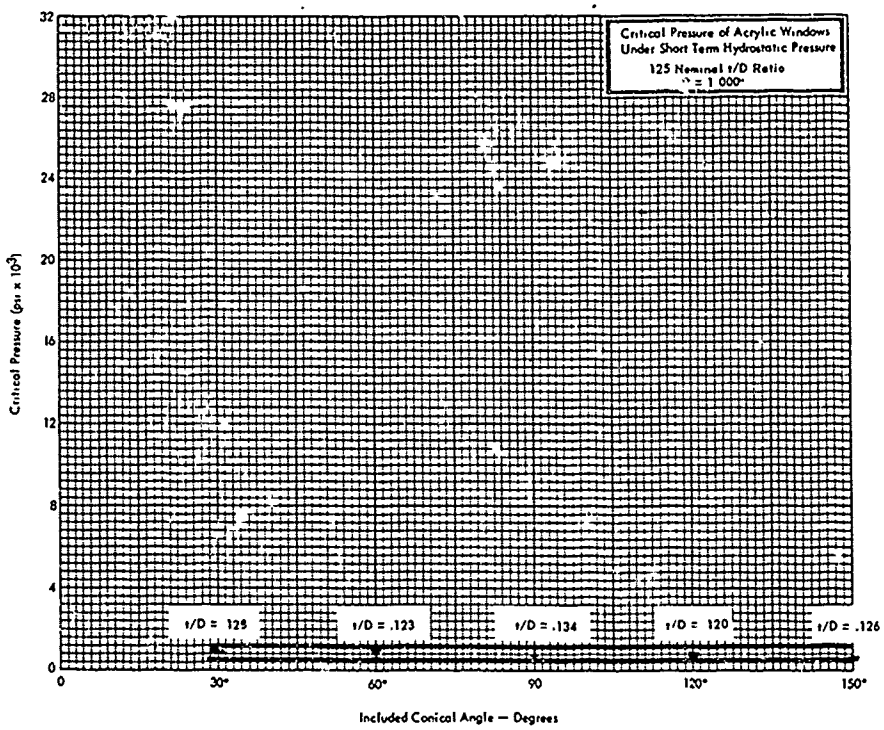

Figure 27. Critical pressures of conical acrylic windows under short-term hydrostatic pressure, 0.125 nominal t/D ratio.

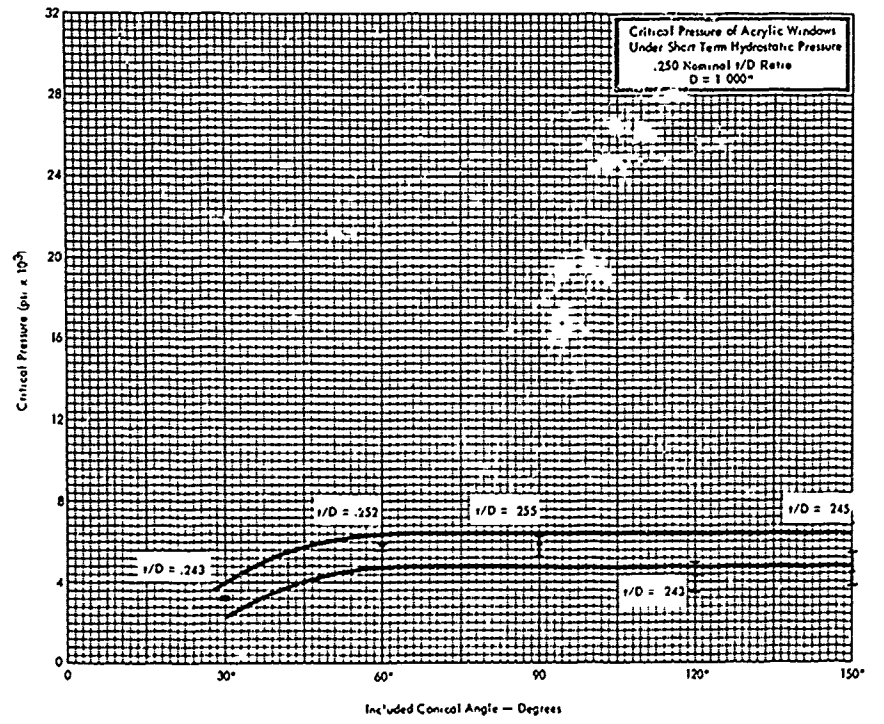

Figure 28. Critical pressures of conical acrylic windows under short-term hydrostatic pressure, 0.25 nominal t/D ratio.

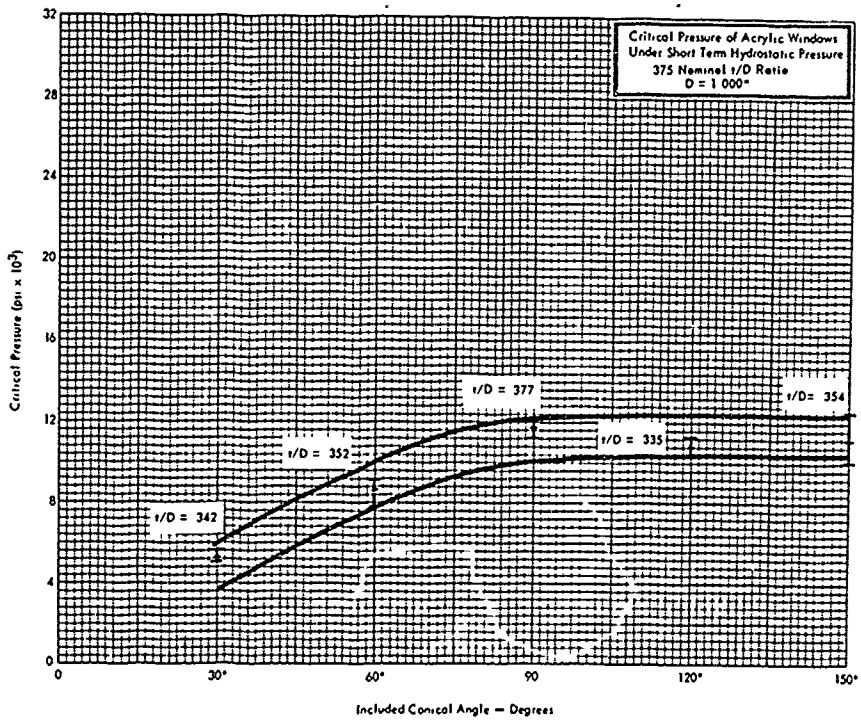

Figure 29. Critical pressures of conical acrylic windows under short-term hydrostatic pressure, 0.375 nominal t/D ratio.

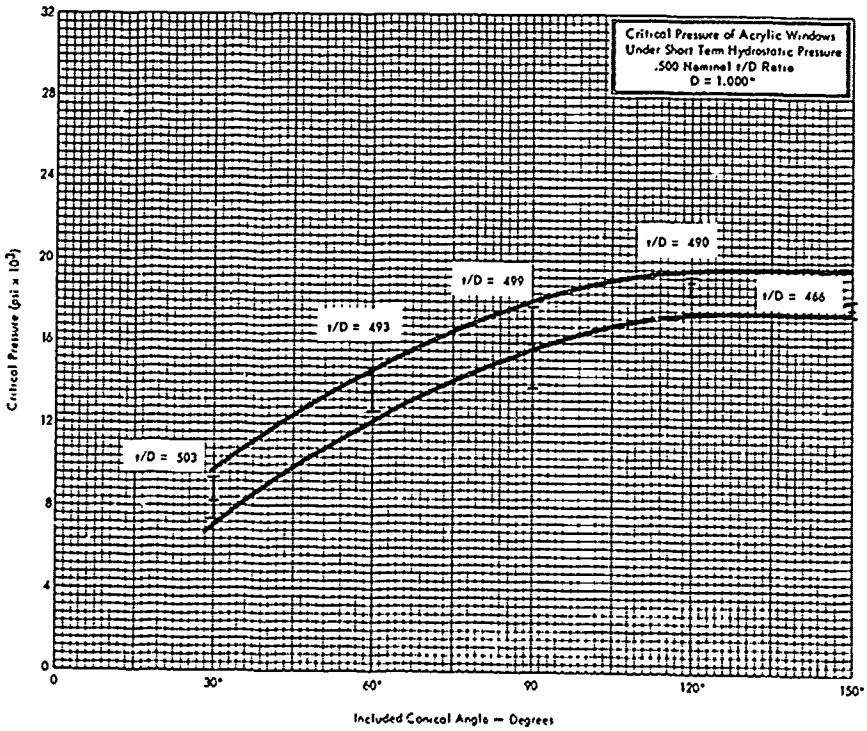

Figure 30. Critical pressures of conical acrylic windows under short-term hydrostatic pressure, 0.5 nominal t/D ratio.

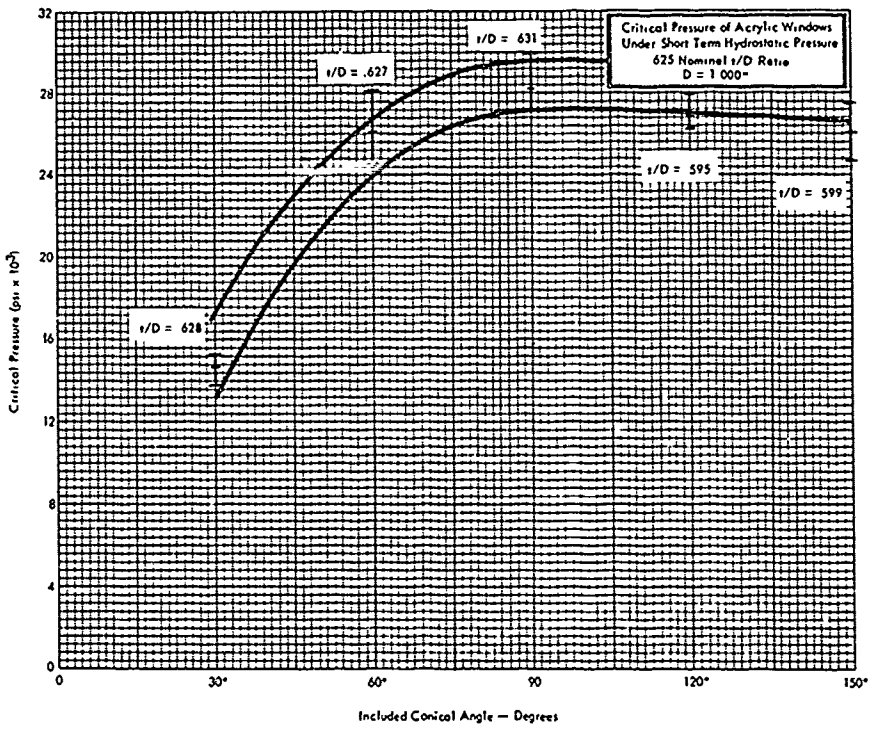

Figure 31. Critical pressures of conical acrylic windows under short-term hydrostatic pressure, 0.625 nominal t/D ratio.

CONCLUSIONS

1. The critical pressures and displacements of the conical acrylic windows presented in this report are valid only for windows mounted in the DOL Type I steel flange. (In this configuration, the pressure-displaced portion of the window has radial support, whatever its extent.) If the DOL Type II steel flange is used to retain the window, much lower critical pressure will result. (The DOL Type II configuration does not provide radial support for the displaced portion.)

2. The critical pressure of large-diameter conical acrylic windows can be predicted directly, with reasonable accuracy, from curves derived from experimental data obtained in the testing of 1-inch-diameter windows provided the larger windows (1) are composed of the same material, (2) have the same t/D ratio and conical angle as the 1-inch-diameter window and, (3) are mounted in a DOL Type I flange.

3. Observation of the material cold flow in the windows tested leads to the conclusion that the optical properties of windows are impaired at pressures considerably below their individual critical pressure. Since optical distortion measurements were not performed with the windows in this study, it is not possible to state quantitatively when the optical distortion of a window progresses to the point where the window loses its value for accurate observation of the hydrospace or the interior of a pressure vessel. Qualitative observations of windows whose testing has been interrupted prior to failure indicate, however, a reasonable assumption to be that the optical properties of windows are not seriously impaired at pressures less than 50% of their critical pressure.

FUTURE STUDIES

Various other studies in the continuing program for investigation of factors which influence the performance of acrylic underwater windows are either in progress or being planned. Studies in progress include the following:

1. Conical acrylic windows under long-term loading (500 to 1,000 hours) at 20,000 psi
2. Short-term critical pressure of flat acrylic windows
3. Short-term critical pressure of spherical acrylic windows

Studies in the planning stage cover:

1. Conical acrylic windows under long-term loading (500 to 1,000 hours) at 10,000 psi
2. Conical acrylic windows under cyclical pressure loading from 0 to 10,000 psi
3. Flat acrylic windows under long-term pressure loading at 20,000 psi
4. Flat acrylic windows under cyclical pressure loading from 0 to 10,000 psi

Appendix A

PHYSICAL PROPERTIES OF GRADE G PLEXIGLAS*

Maximum tensile strength	10, 500 psi
Maximum flexure strength	16, 000 psi
Maximum compressive strength	18, 000 psi
Maximum shear strength	9, 000 psi
Modulus of elasticity in tension (at strain less than 1%)	450, 000 psi
Modulus of elasticity in compression (at strain less than 1%)	450, 000 psi
Maximum elongation at rupture in tension	4.9%
Impact strength (Izod milled notch)	0. 4 ft-lb/in. (per inch of notch)
Rockwell hardness	M-93

*Staff Report, Plexiglas Design and Fabrication Data. Bulletin 229g, Rohm and Haas Co., August 1961.

Appendix B

MODES OF FAILURE OF CONICAL ACRYLIC WINDOWS

In the following descriptions of failure modes for conical acrylic windows, certain terms have special definitions. Cold flow is the plastic deformation of the acrylic window material at room temperature resulting from application of high hydrostatic pressure to the window high-pressure face while the low-pressure face remains at atmospheric pressure. Cratering denotes the formation of a roughly circular depression in the center of the window high-pressure face as a result of cold flow. A fracture cone is a cone-shaped fracture surface inside the body of a window observed at the termination of the test.

In the photographs supplementing the descriptions of the failure modes, the grid pattern seen on many of the high-pressure window faces is the reflection of a grid cast there at the time the photographs were made. This reflection is a device intended to reveal any cratering or other irregularity on the high-pressure face, as a result of cold flow or partial mechanical failure. Any irregularity in the mirrorlike window surface is made apparent by a distorted reflection of the regular square pattern of the grid.

One-Inch-Diameter, 30° Conical Windows

All the 1-inch-diameter, 30° conical windows failed explosively, with all fragments ejected from the pressure vessel. An interesting feature was the lack of deformation on the high-pressure faces of these windows. Examination of a test specimen removed from the fixture after being pressurized to approximately 85% of its critical pressure revealed almost no cold-flow cratering on the high-pressure face (Figure B-1) but a considerable amount on the low-pressure face, as evidenced by the moderately long, cylindrical extrusion (Figure B-2). The low-pressure face also exhibited the circumferential cracks typical of low-pressure faces of all conical acrylic windows regardless of their included angle size. Since the deformation was noted at a pressure very close to the critical pressure of the window, it is reasonable to assume that the failure of the 30° window does not result from any deep cratering of the high-pressure face, but propagation of cracks from the bearing surfaces to the interior of the window. When these cracks, already apparent in the specimen examined, penetrate to the window center, fracturing of the window occurs followed by ejection of the fragments from the mounting flange.

One-Inch-Diameter, 60° Conical Windows

The mode of failure of the 1-inch-diameter, 60° conical windows was not as uniform as that of the 30° windows, but varied with the t/D ratio. Windows with low t/D ratios, 0.125 and 0.25, failed by fracturing in such a manner that only the center portion was ejected, with the rest of the window staying in the mounting flange in the form of a continuous ring. The low-pressure face of these windows (Figure B-3) exhibited a conical fracture surface, while the high-pressure face remained flat without trace of cold flow, showing only a round hole with ragged edges in the center (Figure B-4).

The 60° windows with an intermediate t/D ratio (0.375 to 0.625) also fractured in the center, so that only the center portion of the window was ejected, while the other fragments remained in the flange in most cases. The windows with the intermediate t/D ratios had very severe cold-flow symptoms on the high-pressure face (Figures B-5 and B-6). This extensive cold flow was a bona fide indication that the proportions of the window were such that the failure of the material had to occur in the plastic range of its properties. The low-pressure face of the windows with intermediate t/D ratios had the same type of conical fracture cavity as the low t/D ratio, 60° windows (Figure B-7). The cold flow on the high-pressure face, when considered together with the conical fracture cavity on the low-pressure face, indicated that, although the amount of cold flow increased with the increase of t/D ratio, the actual mechanism of fracture was the same.

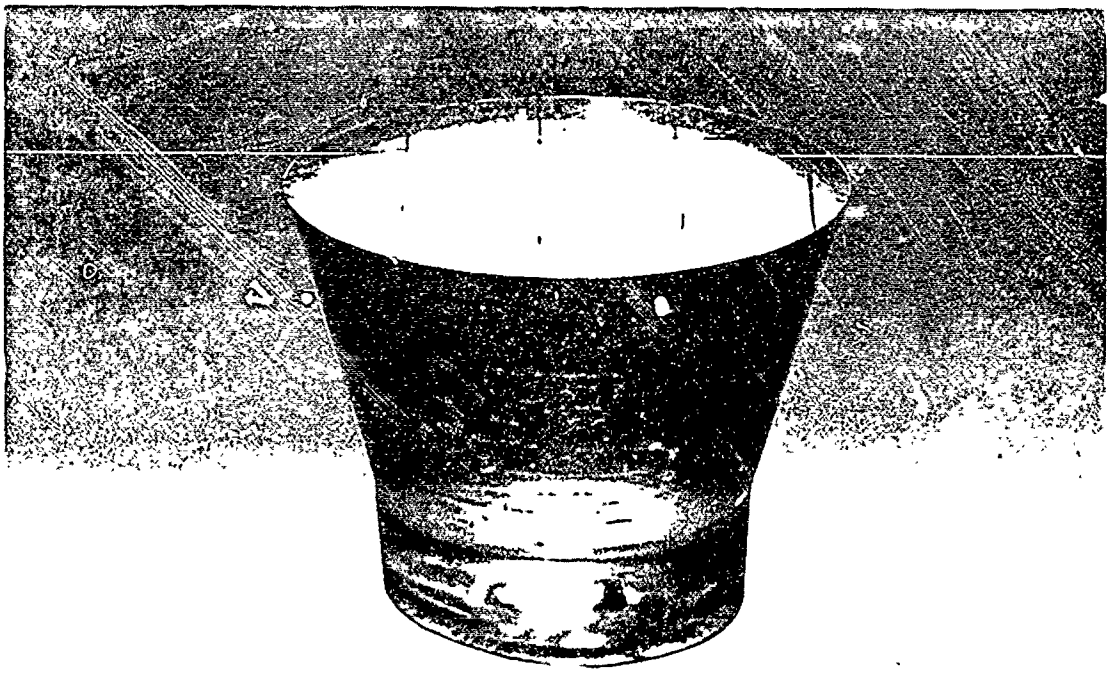

Figure B-1. Arrested failure of 1-inch-diameter, 30°, 1.0 t/D ratio window at 24, 000 psi, high-pressure face.

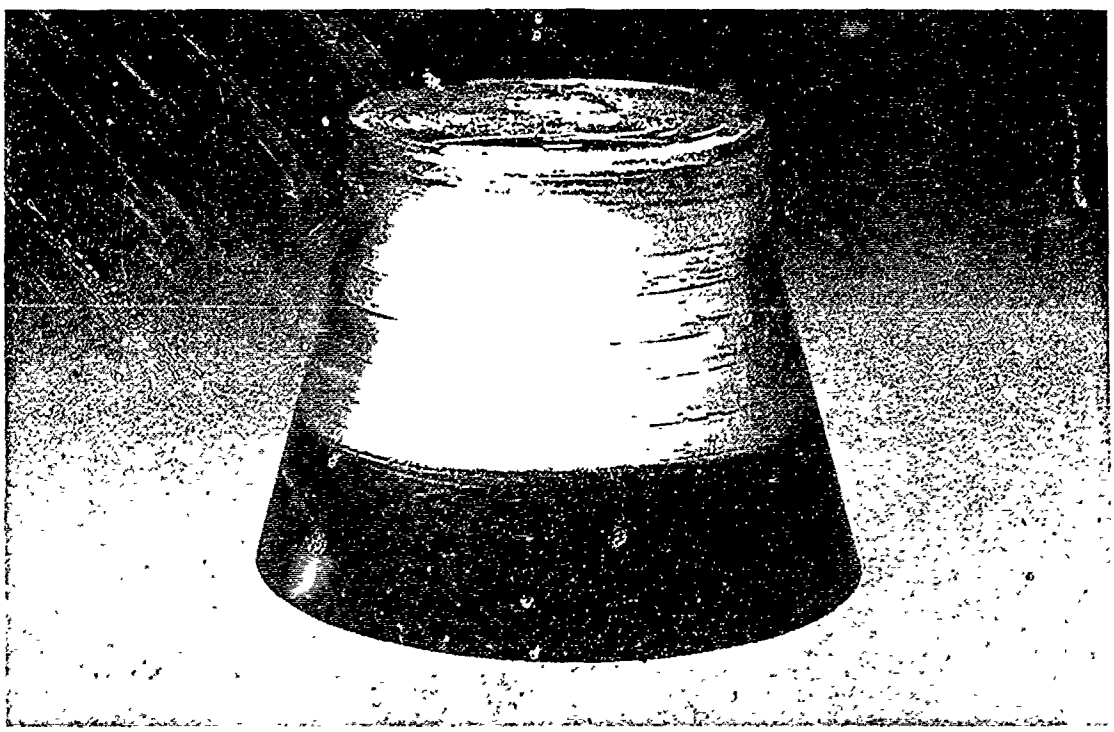

Figure B-2. Arrested failure of 1-inch-diameter, 30°, 1.0 t/D ratio window at 24, 000 psi, low-pressure face.

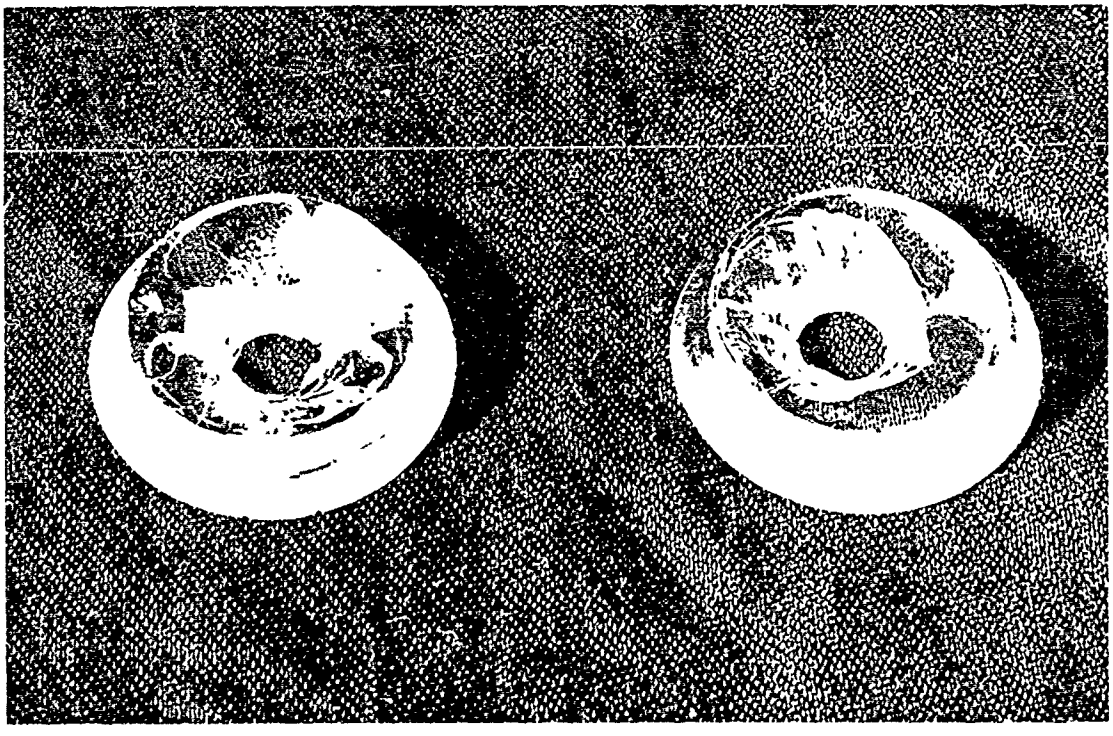

Figure B-3. Failed 1-inch-diameter, 60°, 0.25 t/D ratio windows, low-pressure faces.

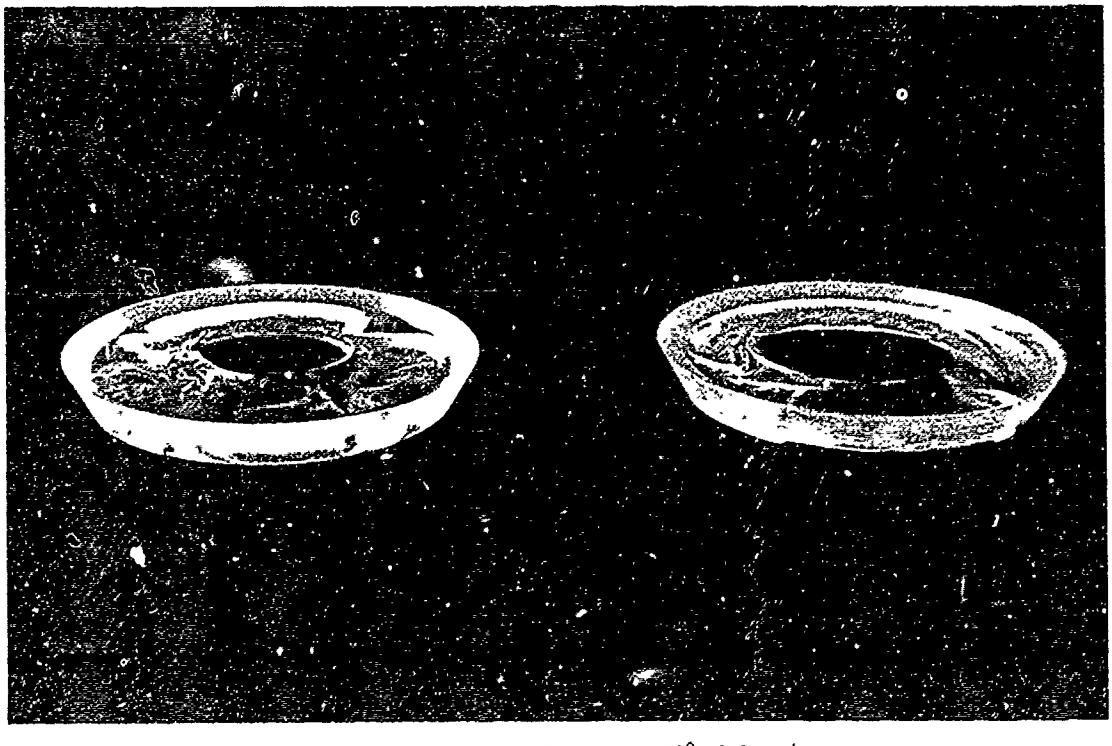

Figure B-4. Failed 1-inch-diameter, 60°, 0.25 t/D ratio windows, high-pressure faces.

Figure B-5. Failed 1-inch-diameter, 60°, 0.35 t/D ratio window, high-pressure face.

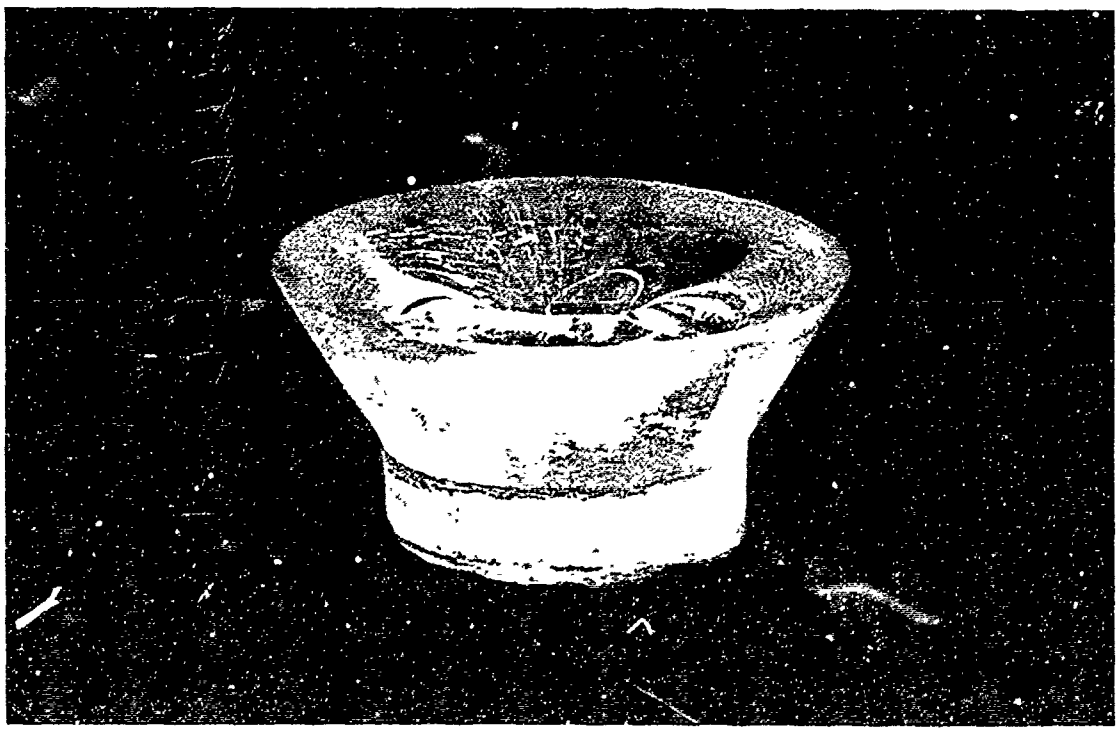

Figure B-6. Arrested failure of 1-inch-diameter, 60°, 0.625 t/D ratio window at 26, 600 psi, high-pressure face.

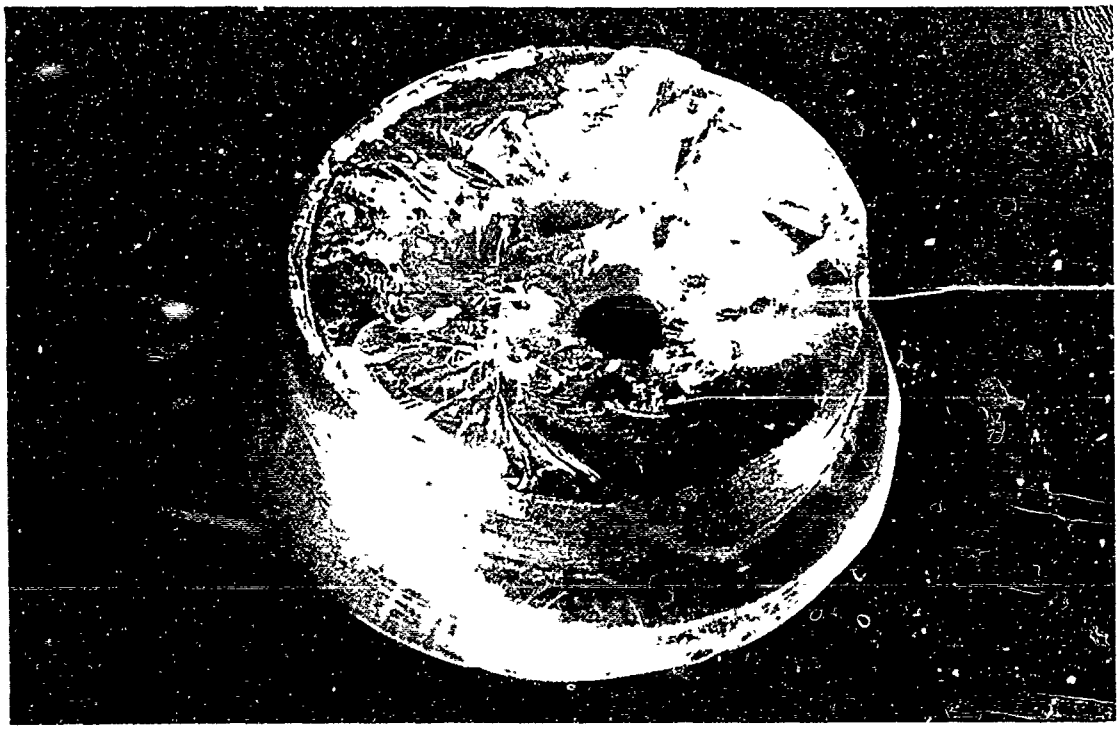

Figure B-7. Failed 1-inch-diameter, 60°, 0.35 t/D ratio window, low-pressure face.

When the 60° windows with high t/D ratios were observed during tests, it was found they behaved in a manner similar to the low and intermediate t/D ratio windows except that no pieces of window remained in the flange after testing. The cold flow, of course, would be more pronounced than in either the low or intermediate ratio windows, as the proportions of the window were such that a cold flow had to occur before a conical fracture on the low-pressure face could be initiated. Even windows pressurized to 30% to 50% below the critical pressure showed considerable extrusion into the cylindrical cavity of the mounting flange (Figure B-8). When the large amount of cold flow on the low-pressure face of the high t/D ratio (1.0) window (Figure B-8) was compared with the small amount of cold flow on the high-pressure face (Figure B-9), the tentative conclusion was reached that the high t/D ratio, 60° window underwent three phases of deformation. The first phase was characterized by the uniform radial compression of the window caused by hydrostatic pressure forcing the acrylic plastic into the cylindrical cavity, resulting in the large amount of extrusion there. Very little, or no cold flow occurred on the high-pressure face of the window during that phase, as the face still remained essentially flat without noticeable crater. The duration of the first phase was probably to 50% of the critical pressure of the window.

The second phase, lasting from approximately 50% of critical pressure to just below the critical pressure, was characterized by extensive cold flow on the low-pressure face (Figure B-10), while the crater on the high-pressure face became noticeable (Figure B-11). Considerable cracking of the window body occurred in the transition zone between the conical and cylindrical sections of the window, as well as on the low-pressure face. The cracks in the transition zone (Figure B-10) extended at an angle from the bearing surface of the window into its interior, forming the incipient conical fracture surface. The cracks on the low-pressure face, on the other hand, extended along the circumference of the face, forming several continuous-crack circles.

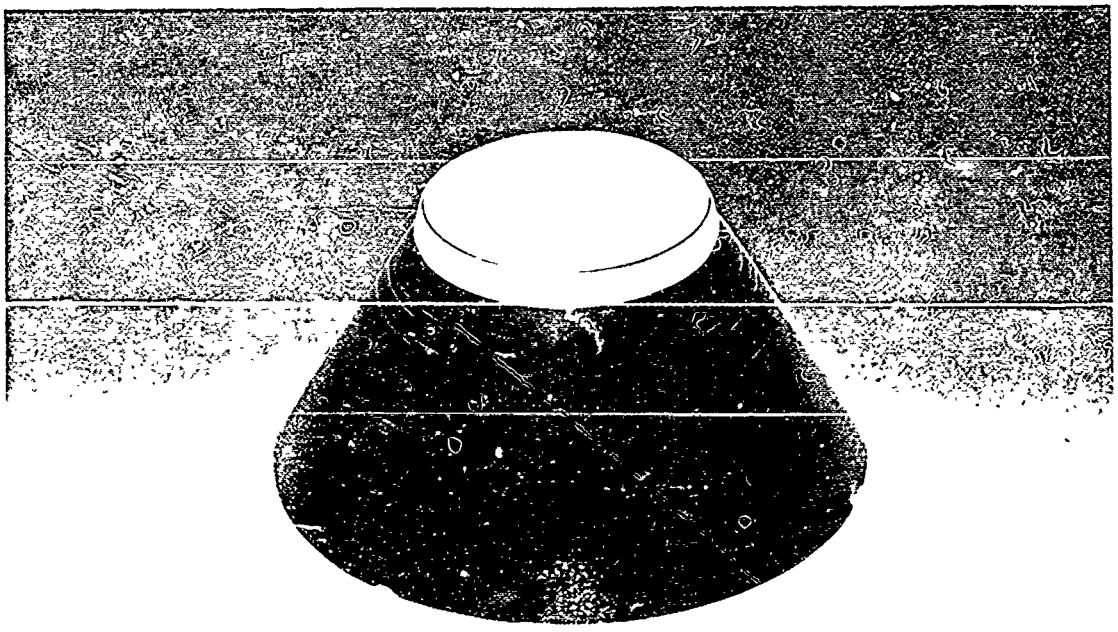

Figure B-8. Arrested failure of 1-inch-diameter, 60°, 1.0 t/D ratio window at 22,000 psi, low-pressure face. (Phase 1 of deformation.)

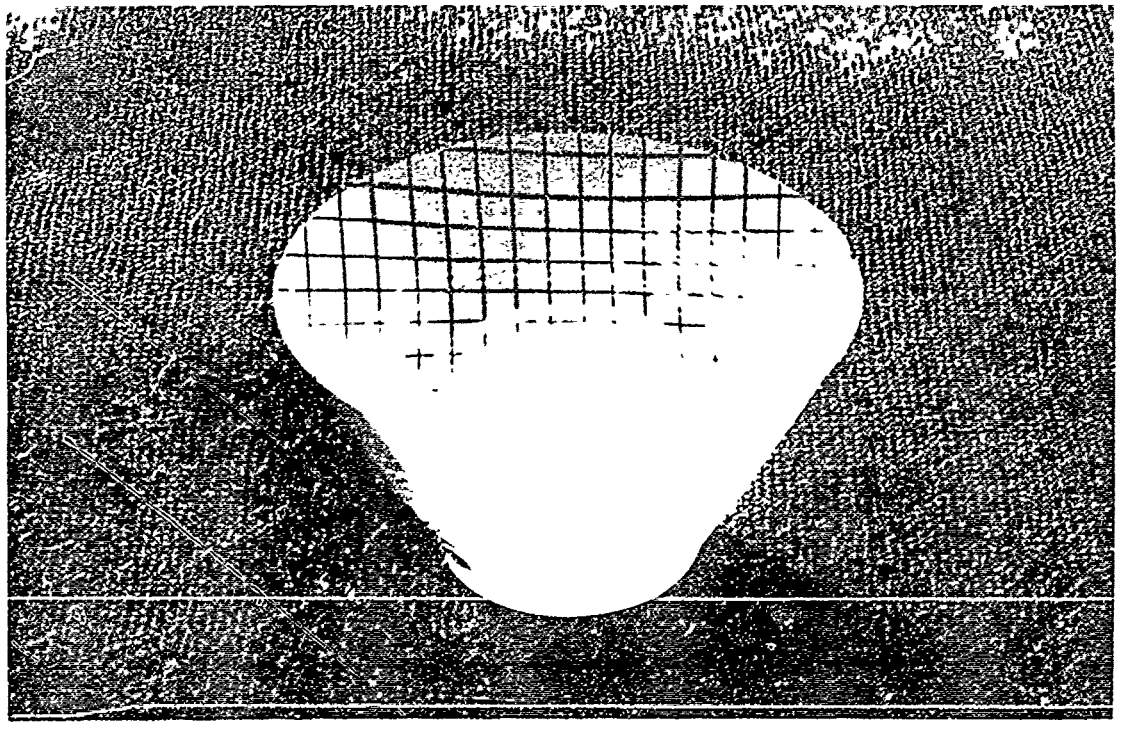

Figure B-9. Arrested failure of 1-inch-diameter, 60°, 1.0 t/D ratio window at 22,000 psi, high-pressure face. (Phase 1 of deformation.)

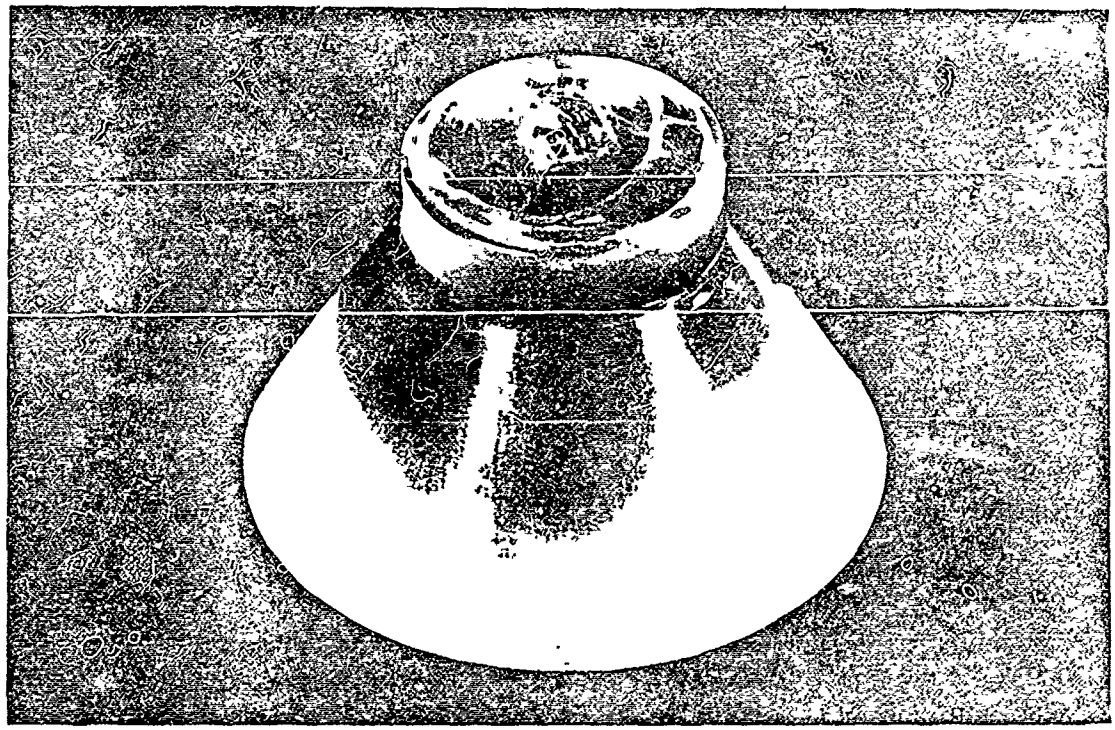

Figure B-10. Arrested failure of 1-inch-diameter, 60°, 1.0 t/D ratio window at 28,000 psi, low-pressure face. (Phase 2 of deformation.)

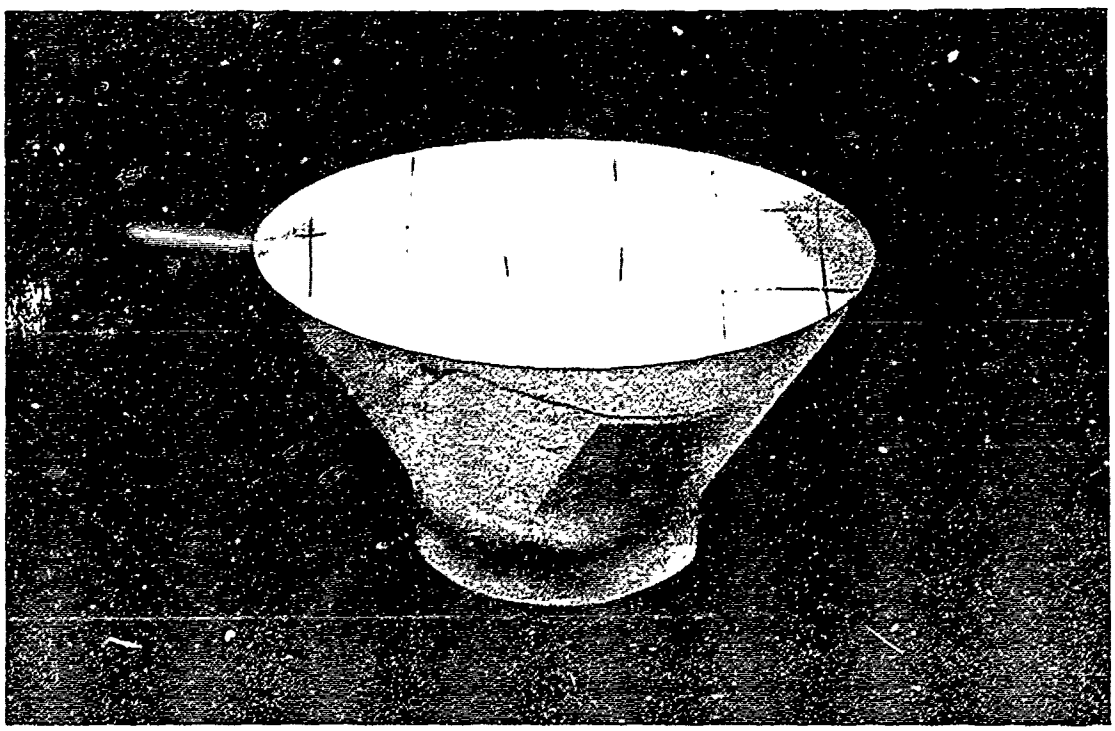

Figure B-11. Arrested failure of 1-inch-diameter, 60°, 1.0 t/D ratio window at 28,000 psi, high-pressure face. (Phase 2 of deformation.)

The third phase of deformation of the high t/D ratio, 60° windows took place at the point of critical pressure. At that time, the cold-flow crater in the high-pressure face had progressed to such a depth of the window body that the small cracks at the bottom of the crater united with the cracks progressing from the window bearing surface at the cone-to-cylinder transition zone, and a conical fracture surface was created. When the conical fracture surface was generated, the center portion of the window was ejected first, followed immediately by the remainder propelled by the high-velocity stream of water.

One-Inch-Diameter, 90° Conical Windows

The 1-inch-diameter, 90° conical windows failed in a manner similar to the 60° windows. The low t/D ratio windows failed by ejection of the center portion of the window with the rest remaining in the flange. The intermediate and high t/D ratio windows in most cases failed by complete fragmentation. The low t/D ratio windows failed without cold flow (Figures B-12 and B-13), while those with intermediate and high t/D ratios exhibited cold flow. The phases of window deformation were the same as in the 60° windows, except that the magnitudes of deformation were different for the same t/D ratios. Again, as in the 60° windows, one could see the minute cold flow on the high- and low-pressure faces in Phase 1 (Figures B-14 and B-15) and the fair amount of cold flow in Phase 2 (Figures B-16 and B-17). The basic difference in Phases 1 and 2 of the 90° windows from the corresponding phases of the 60° windows lay in the amount of cold flow at the same pressure. While the cold flow was extensive for the 60° windows, for the 90° windows only slight indication of it was evident. Thus, when a comparison was made between a 60° and a 90° window from interrupted failure tests, one could see that although both windows had the same t/D ratio (0.625) and both had been pressurized to 26,600 psi prior to removal from the vessel, only the 60° window exhibited cold flow extensively on both the high-pressure and low-pressure faces (Figures B-6 and B-18).

One-Inch-Diameter, 120° Conical Windows

In the $0.125 \leq t/D \leq 0.625$ range of ratios, conical windows failed consistently by fracturing in the middle, so that the center portion was ejected (Figures B-19 through B-24) while the remainder of the window was retained by the mounting flange. This was quite different from the failure of 60° and 90° windows, where the center portion of the window was ejected only in the low and intermediate $0.125 \leq t/D \leq 0.375$ range of ratios, while at the high t/D ratios the whole window was invariably ejected.

During some of the testing (arrested failures) it was possible to retrieve the center portion. Close inspection of this portion revealed that the mechanism of failure of the 120° windows was quite complex, as the center portion exhibited, in addition to the cold-flow crater on the high-pressure face, a conical fracture cavity on the low-pressure face which also showed signs of cold-flow displacement into the cylindrical opening in the mounting flange.

Thus, a typical 120° window, as exemplified by the 0.5 t/D ratio window in Figures B-25 and B-26, had two fracture cones, an inner one and an outer one. The latter surrounded the whole center portion of the window generally ejected from the flange in small fragments. In the example shown of a typical 120° window failure, the center portion, including the inner fracture cone, was not ejected from the flange, but retrieved from a basket hung immediately below it on the high-pressure side of the window. The reason in this case for the center portion of the window not being ejected was probably the fact that the apex of the inner fracture cone on the low-pressure face met the apex of the cold-flow crater on the high-pressure face, creating a passage for the fluid and thus permitting the pressure in the vessel to be relieved a split second before the center portion of the specimen was extruded sufficiently to be ejected through the cylindrical opening in the flange.

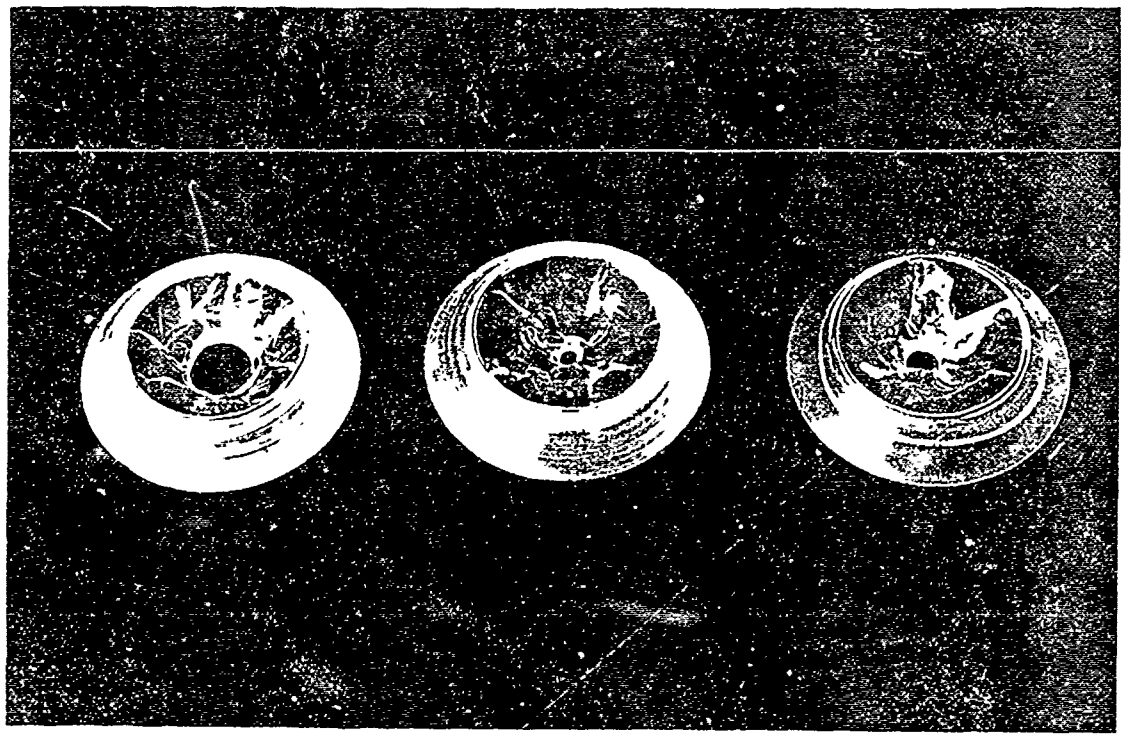

Figure B-12. Failed 1-inch-diameter, 90°, 0.25 t/D ratio windows, low-pressure faces.

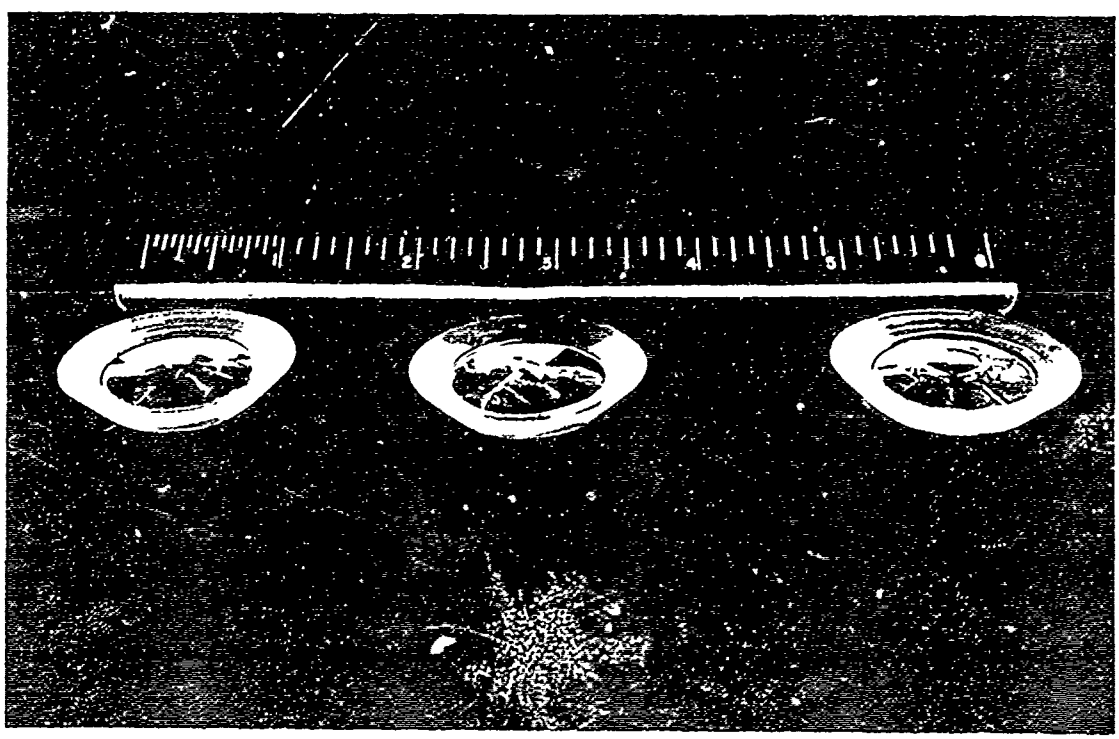

Figure B-13. Failed 1-inch-diameter, 90°, 0.25 t/D ratio windows, high-pressure faces.

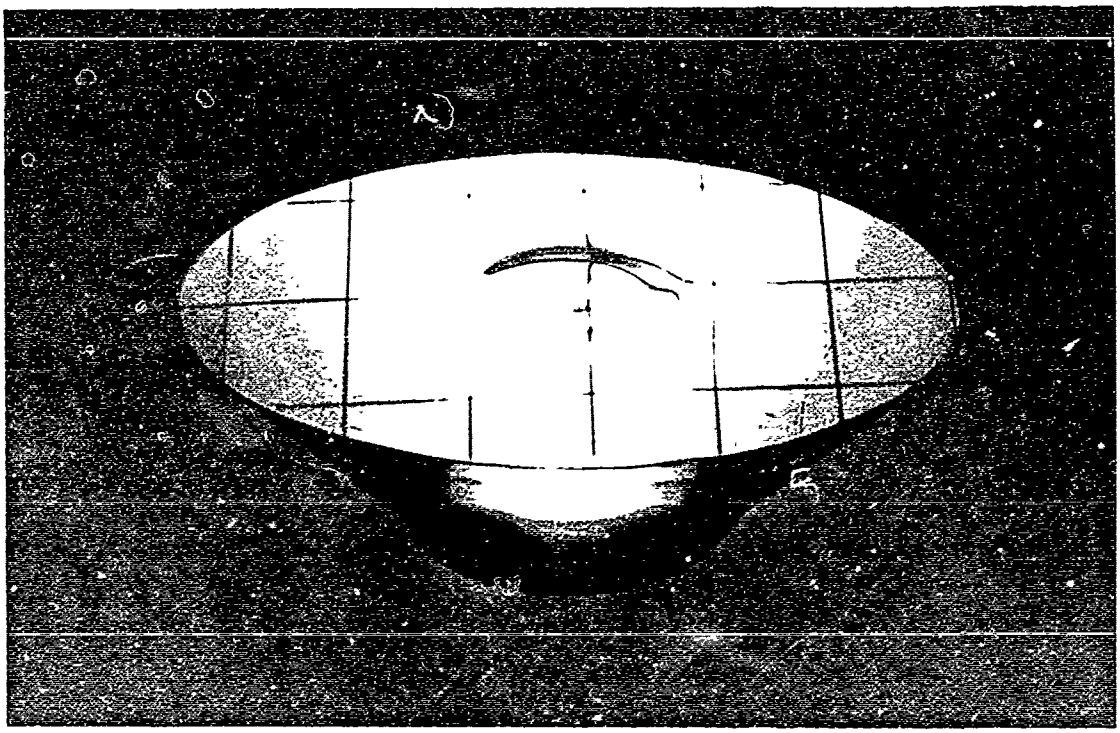

Figure B-14. Arrested failure of 1-inch-diameter, 90°, 0.625 t/D ratio window at 26, 500 psi, high-pressure face. (Phase 1 of deformation.)

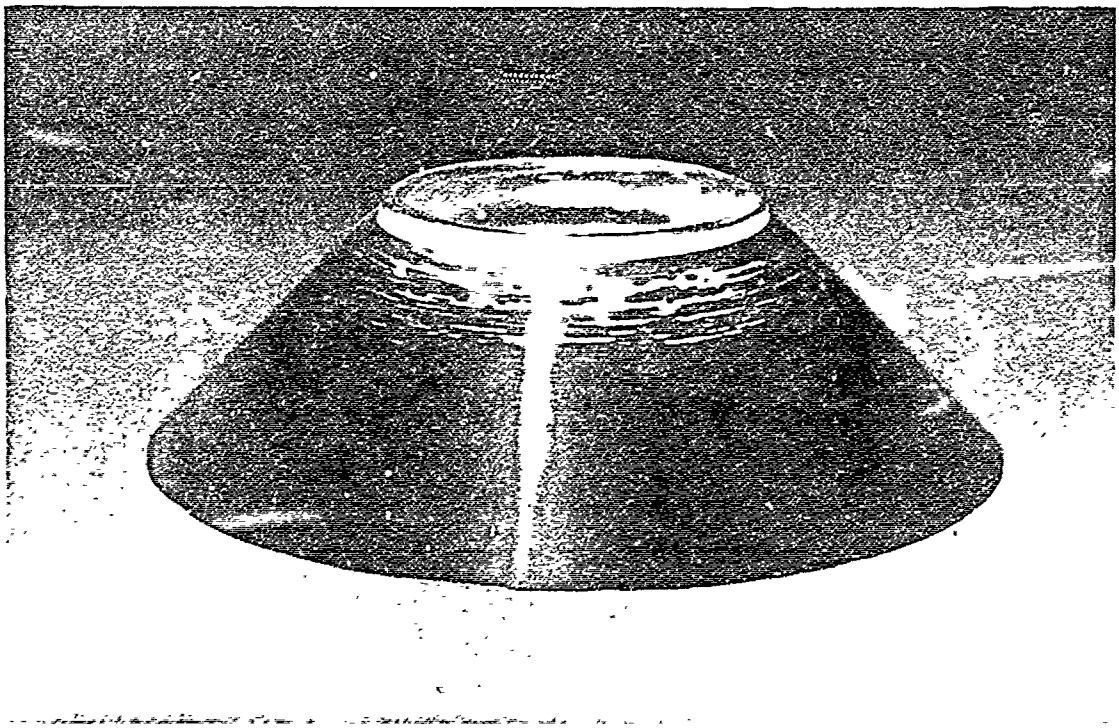

Figure B-15. Arrested failure of 1-inch-diameter, 90°, 0.625 t/D ratio window at 26, 500 psi, low-pressure face. (Phase 1 of deformation.)

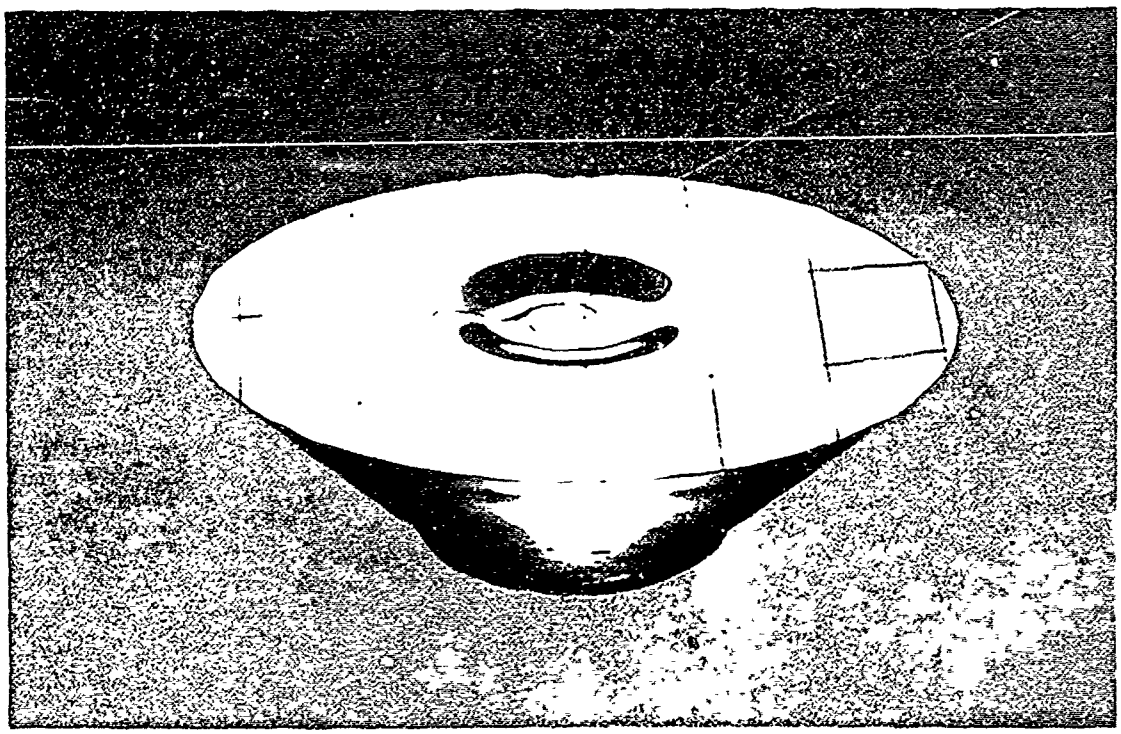

Figure B-16. Arrested failure of 1-inch-diameter 90°, 0.625 t/D ratio window at 28,600 psi, high-pressure face. (Phase 2 of deformation.)

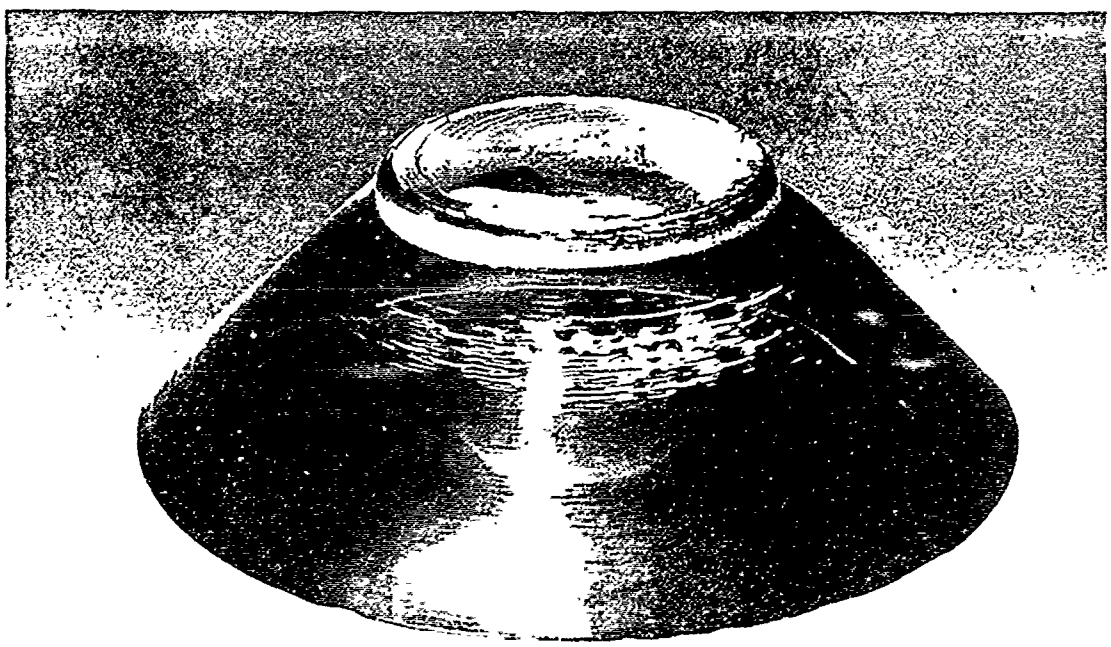

Figure B-17. Arrested failure of 1-inch-diameter, 90°, 0.625 t/D ratio window at 28,600 psi, low-pressure face. (Phase 2 of deformation.)

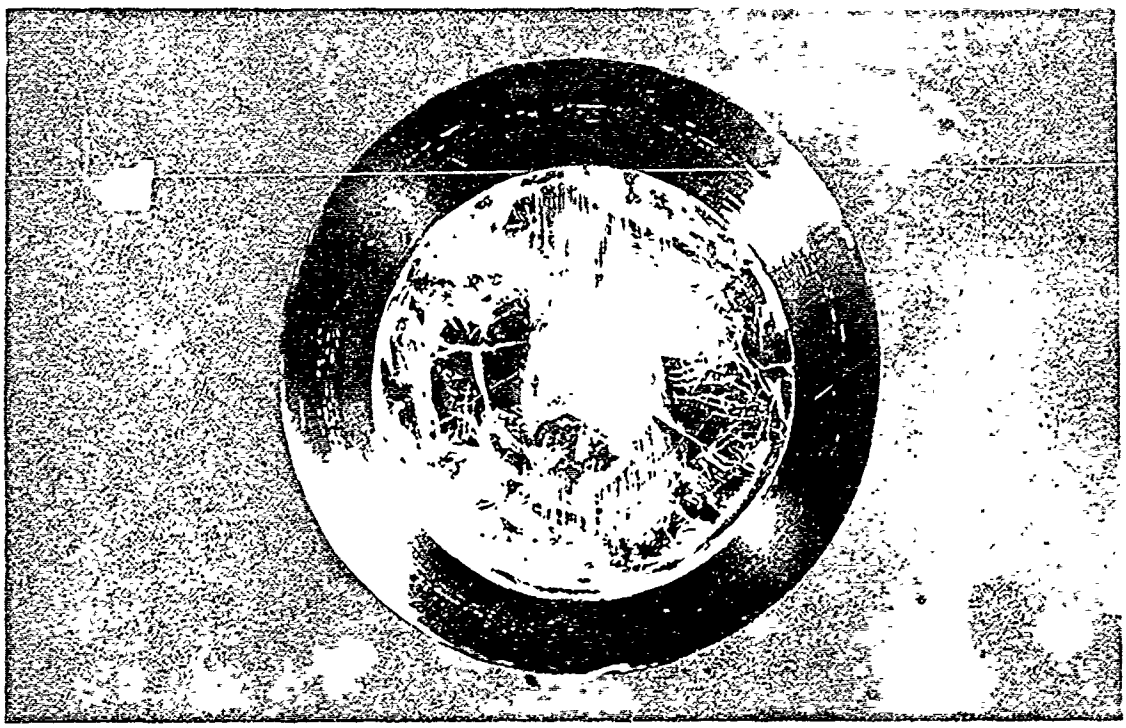

Figure B-18. Arrested failure of 1-inch-diameter, 60°, 0.625 t/D ratio window at 26, 600 psi, low-pressure face.

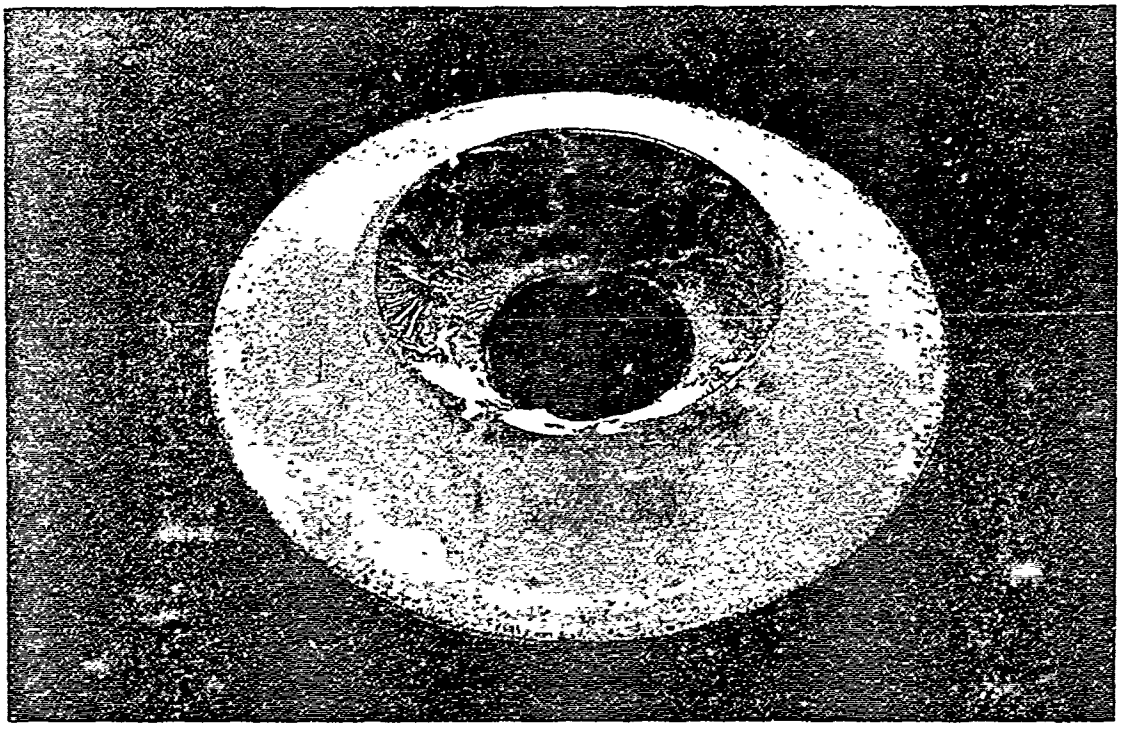

Figure B-19. Failed 1-inch-diameter, 120 , 0.25 t D ratio window, low-pressure face.

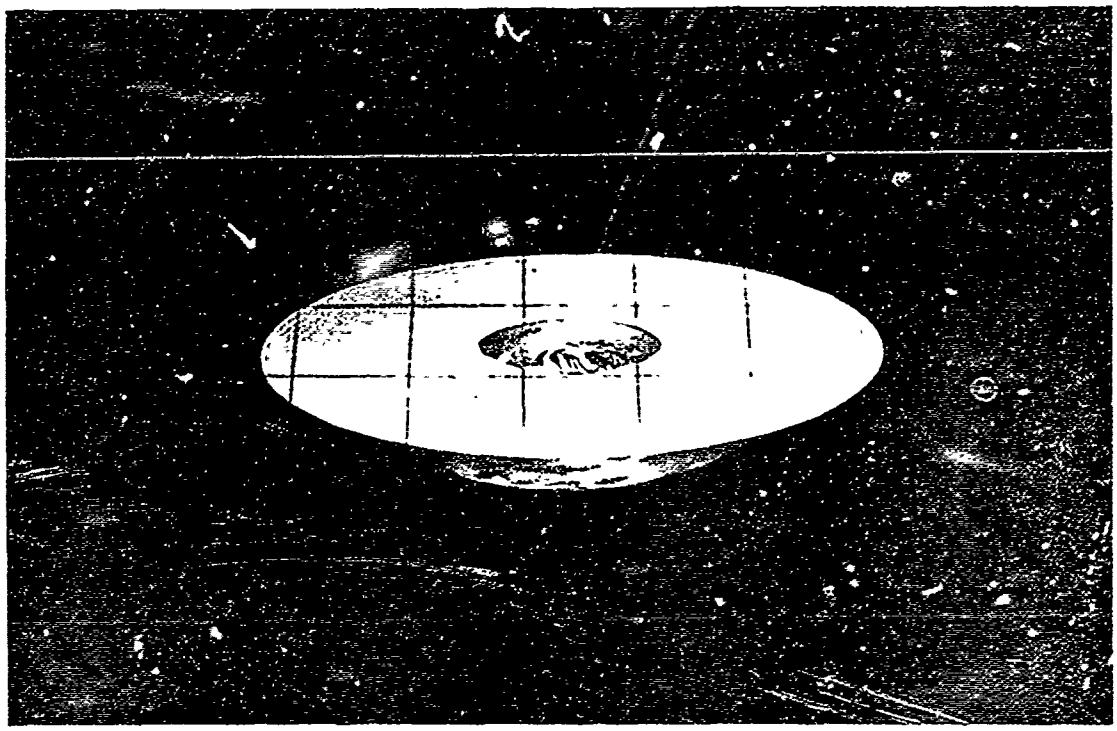

Figure B-20. Failed 1-inch-diameter, 120°, 0.25 t/D ratio window, high-pressure face.

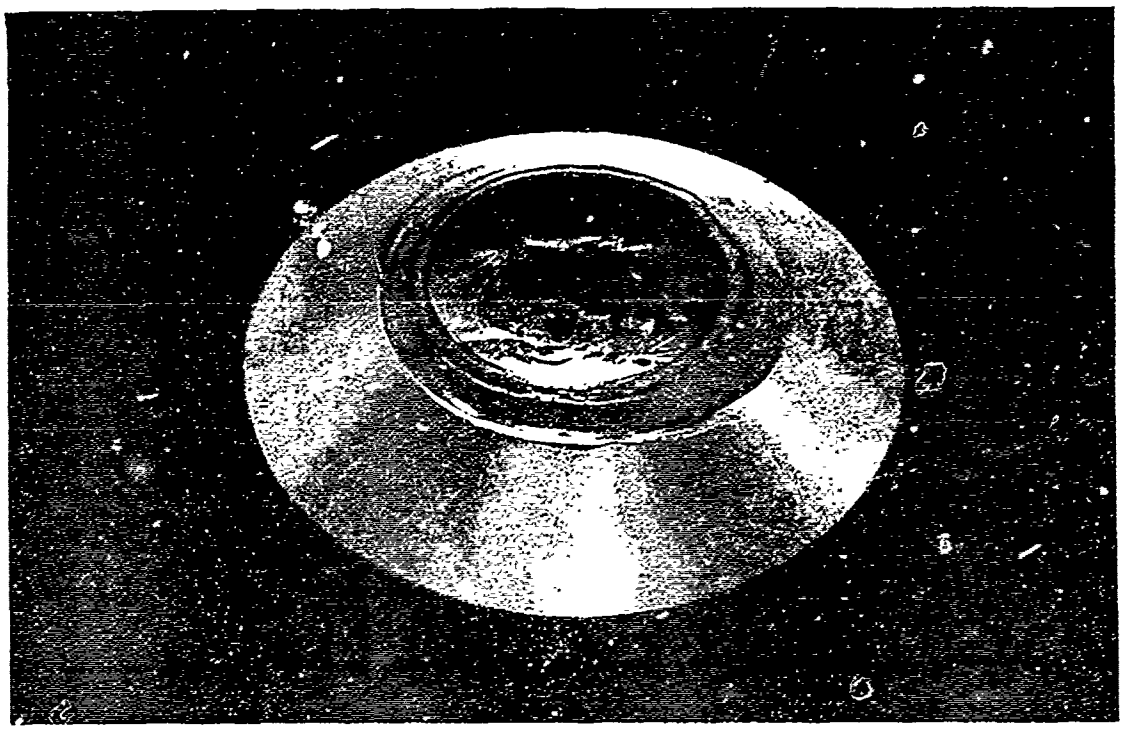

Figure B-21. Failed 1-inch-diameter, 120°, 0.375 t/D ratio window, low-pressure face.

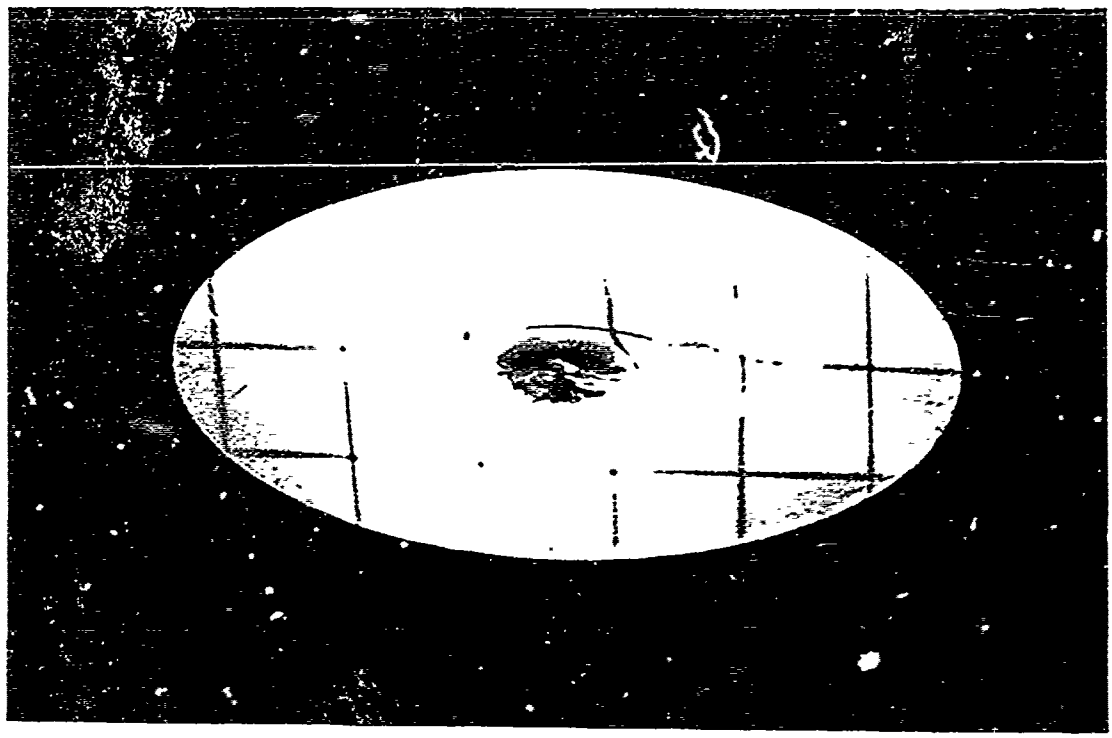

Figure B-22. Failed 1-inch-diameter, 120°, 0.375 t D ratio window, high-pressure face.

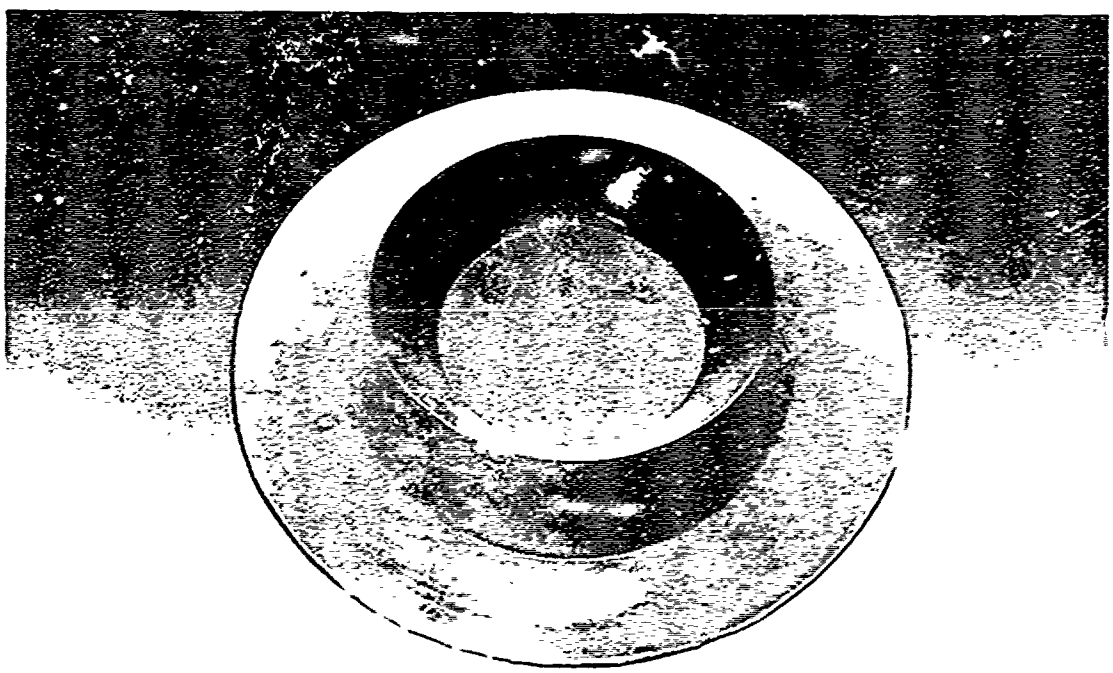

Figure B-23. Failed 1-inch-diameter, 120°, 0.625 t D ratio window, low-pressure face.

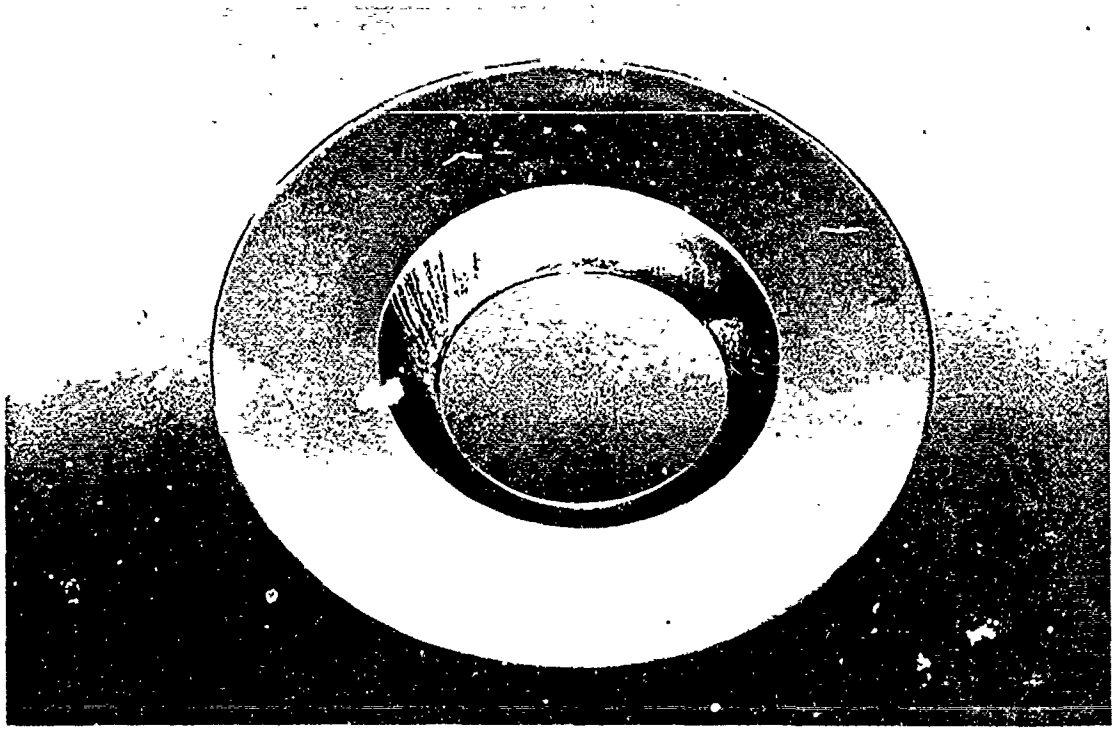

Figure B-24. Failed 1-inch-diameter, 120°, 0.625 t/D ratio window, high-pressure face.

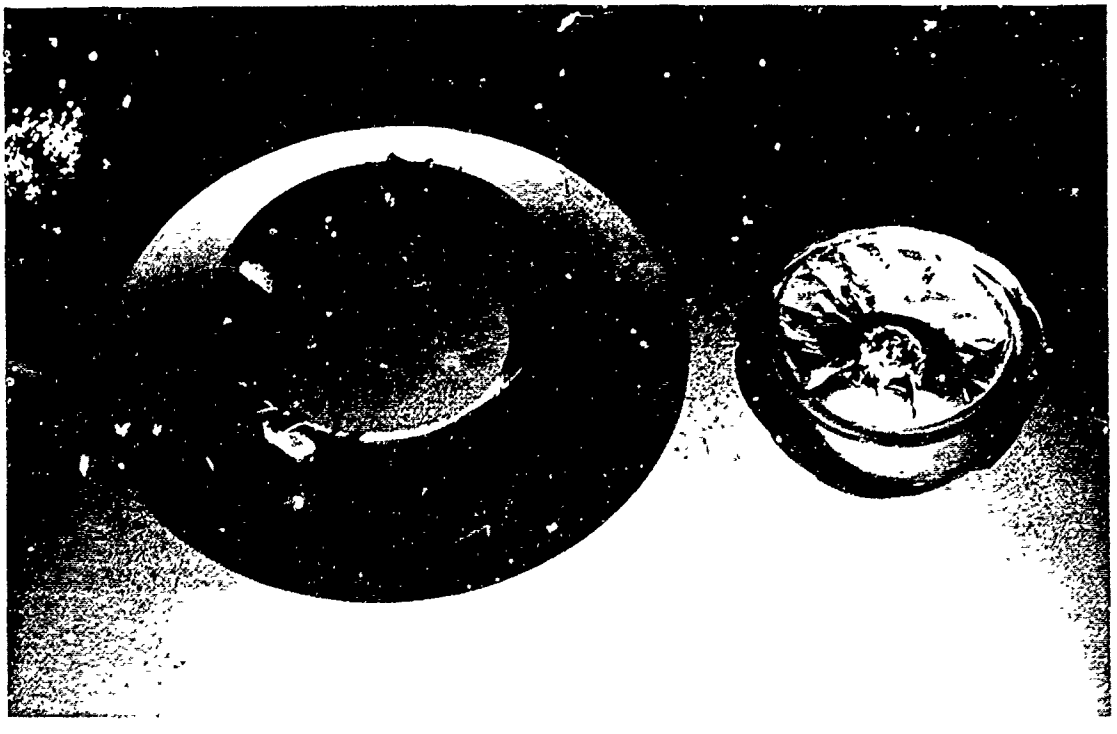

Figure B-25. Failed 1-inch-diameter, 120°, 0.5 t/D ratio window, low-pressure face, with center portion alongside.

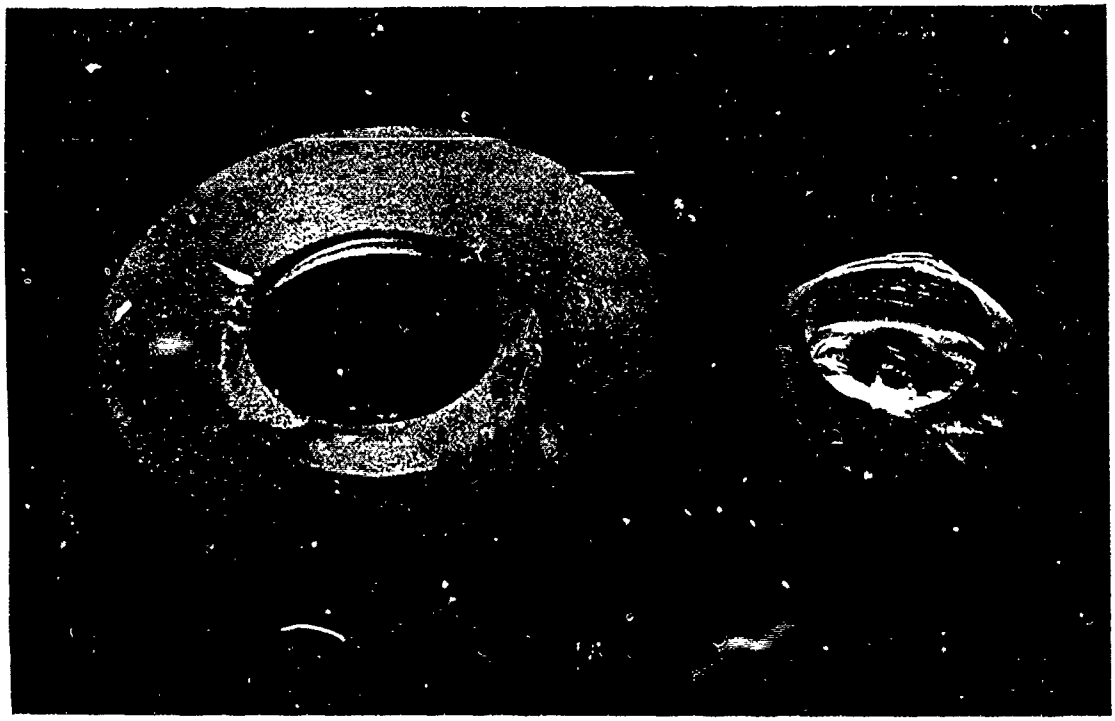

Figure B-26. Failed 1-inch-diameter, 120°, 0.5 t/D ratio window, high-pressure face, with center portion alongside.

From inspection of the retrieved window center portion, and of the outer ring-shaped fragment, as well as other windows whose testing was terminated before ejection, it can be postulated that cracks in the 120° windows were initiated at three locations. The one where cracks first appeared, at approximately 70% of critical pressure, was below the shape-transition zone on the bearing surface of the window (Figures B-27 and B-28). The cracks initiated here were continuous around the circumference of the window, and propagated themselves into the interior of the window body at approximately right angles to the conical surface.

The second location of crack initiation lay on the high-pressure face of the window. The cracks appeared here later than at the shape-transition zone and were not as continuous as those in the first location. The cracks on the high-pressure face were generated on the periphery of the cold-flow crater, which became noticeable in the 120° conical windows only at hydrostatic pressures in excess of 70% of the window critical pressure (Figure B-29).

The third location where cracks were generated was around the circumference of the low-pressure face. These cracks appear only after those in the other locations have grown to considerable proportions. It can be shown that the cracks on the low-pressure face had not yet developed (Figures B-30 and B-31) in windows with $0.5 \leq t/D \leq 0.625$ ratios at approximately 90% of the window critical pressure. Therefore, they must appear at pressures higher than 90% of critical pressure.

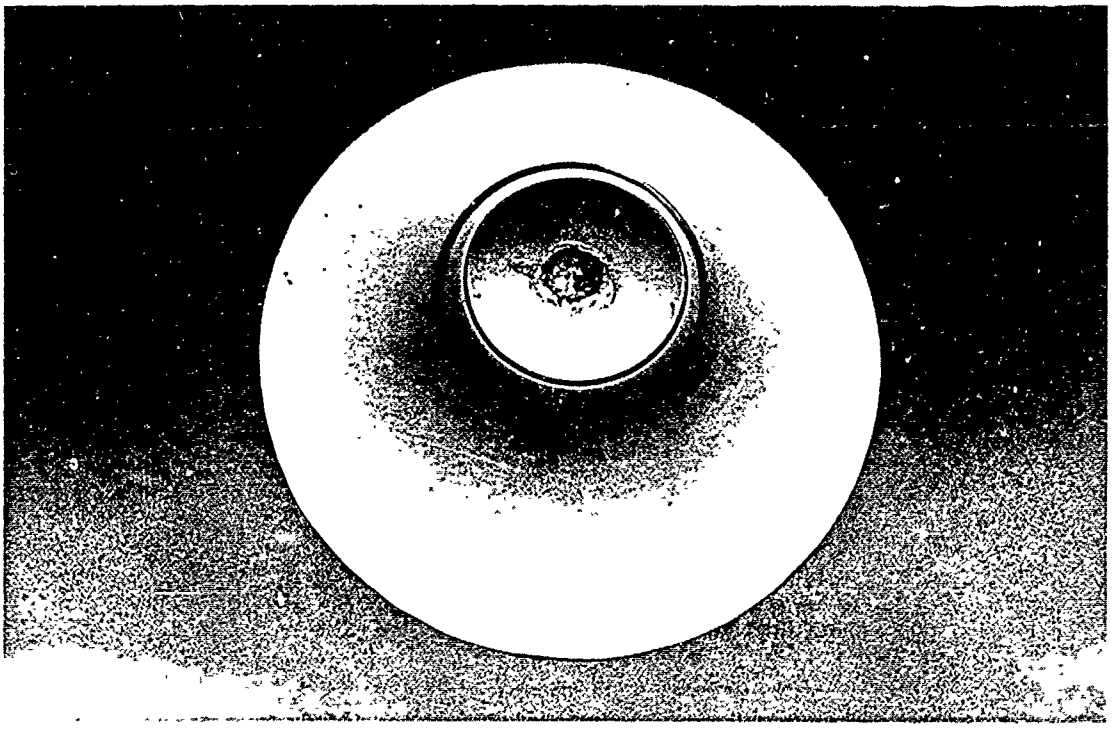

Figure B-27. Arrested failure of 1-inch-diameter, 120°, 0.625 t/D ratio window at 22, 500 psi, low-pressure face.

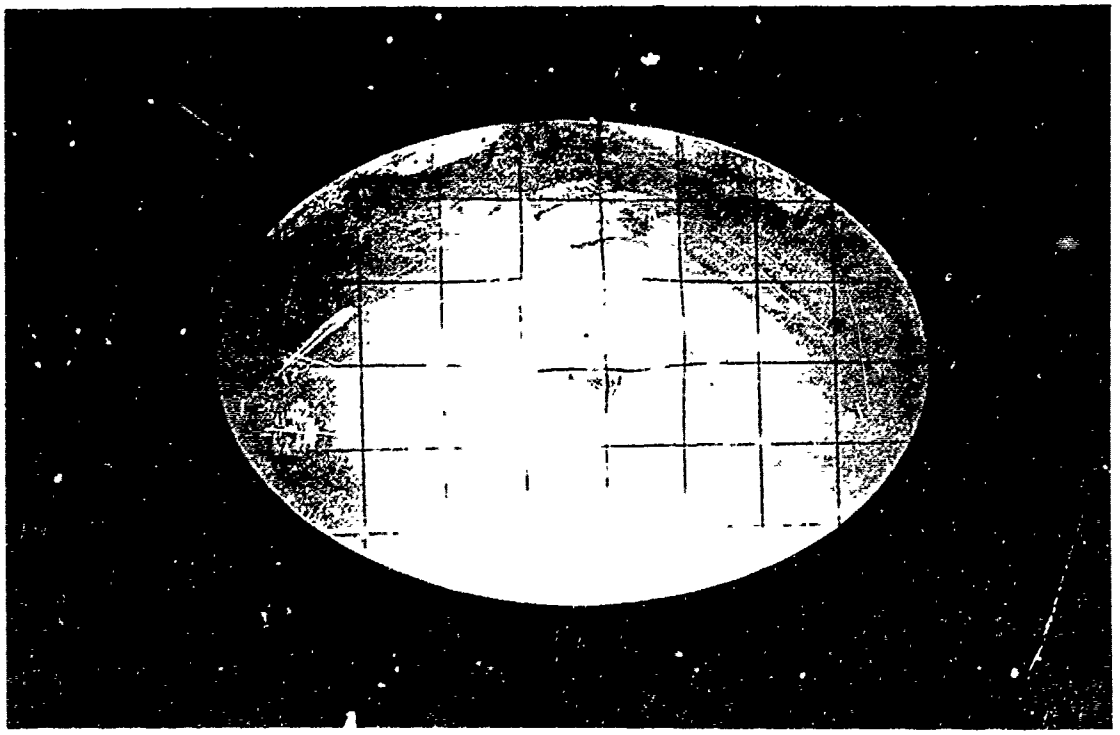

Figure B-28. Arrested failure of 1-inch-diameter, 120°, 0.625 t/D ratio window at 22, 500 psi, high-pressure face.

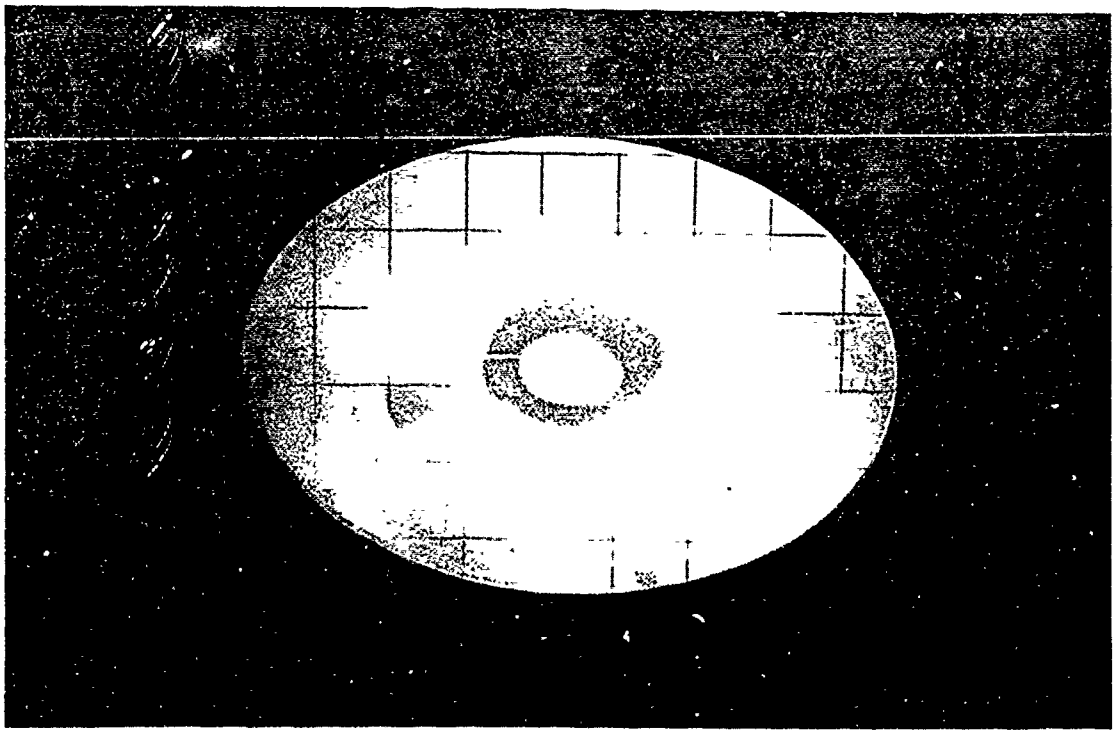

Figure B-29. Arrested failure of 1-inch-diameter, 120°, 0.625 t/D ratio window at 26, 000 psi, high-pressure face.

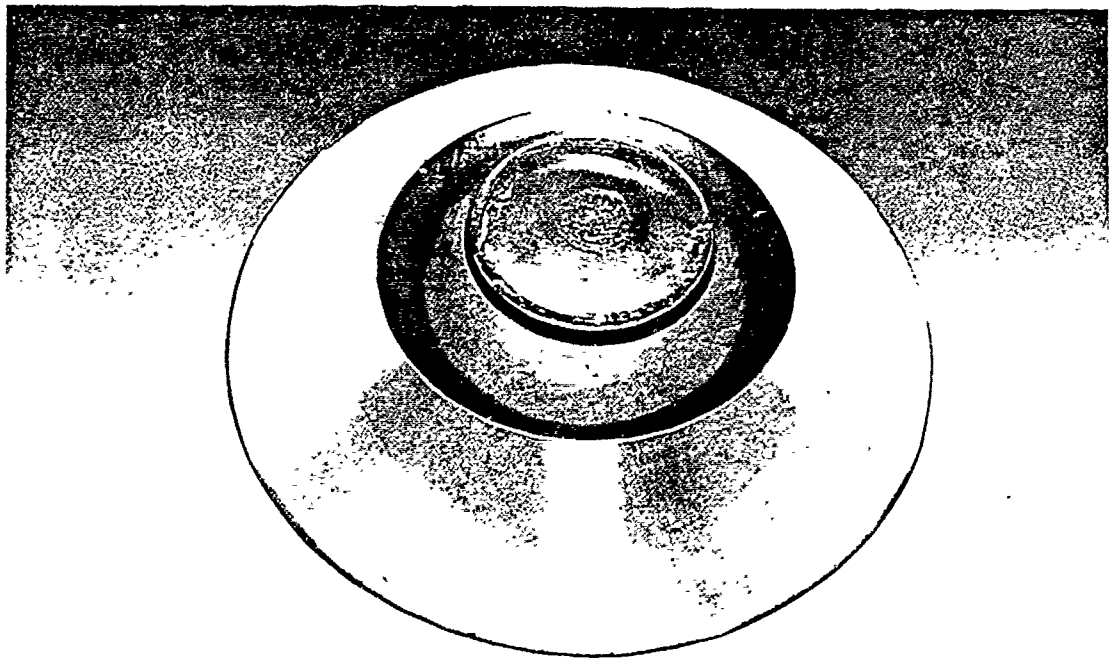

Figure B-30. Arrested failure of 1-inch-diameter, 120°, 0.625 t/D ratio window at 26, 000 psi, low-pressure face.

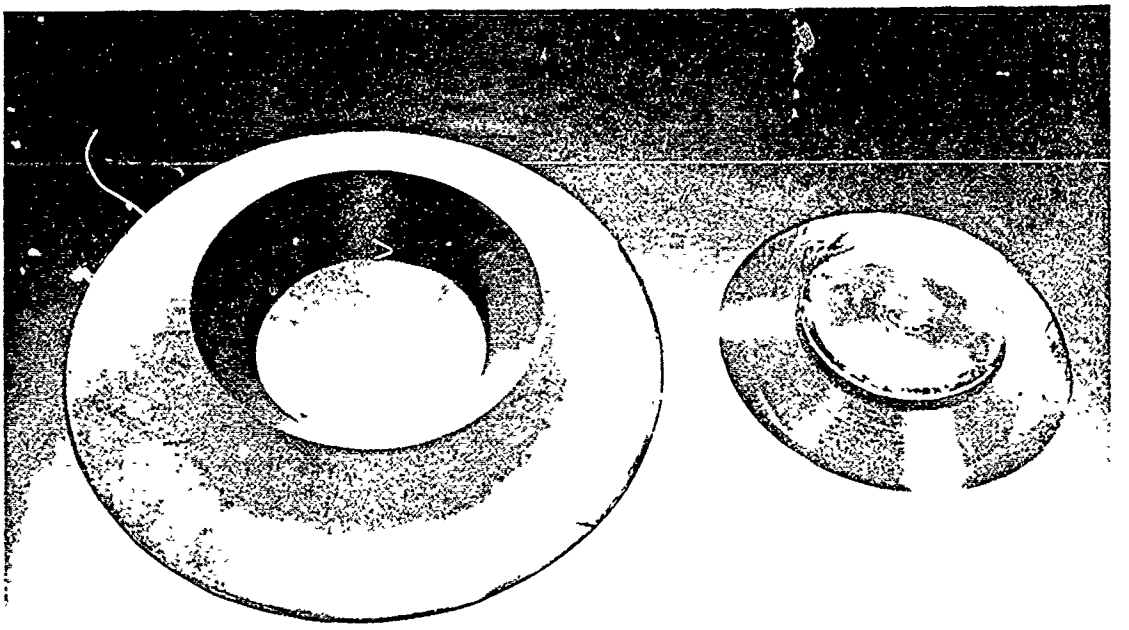

Figure B-31. Arrested failure of 1-inch-diameter, 120°, 0.625 t/D ratio window at 26,000 psi, low-pressure face, with center portion alongside.

The 1-inch-diameter, 150° conical windows failed essentially in the same manner as the 120° windows, by ejection of the center portion, except that the center portions of the 0.125 t/D ratio windows were not ejected when the window critical pressure was reached. The reason for this failure to eject was that upon propagation of cracks in the window (Figures B-32 and B-33) at critical pressure, the center of the window deflected into the flange cylindrical opening to such an extent that the seal between the conical surface of the window and that of the flange cavity was broken, thus relieving the hydrostatic pressure in the vessel. (If the vessel had been of very large capacity, or the window in a structure submerged in the ocean, where infinite hydrostatic energy exists, the center of the 0.125 t/D window would also have ejected, though some leakage around the conical window surface would have occurred just prior to the ejection.)

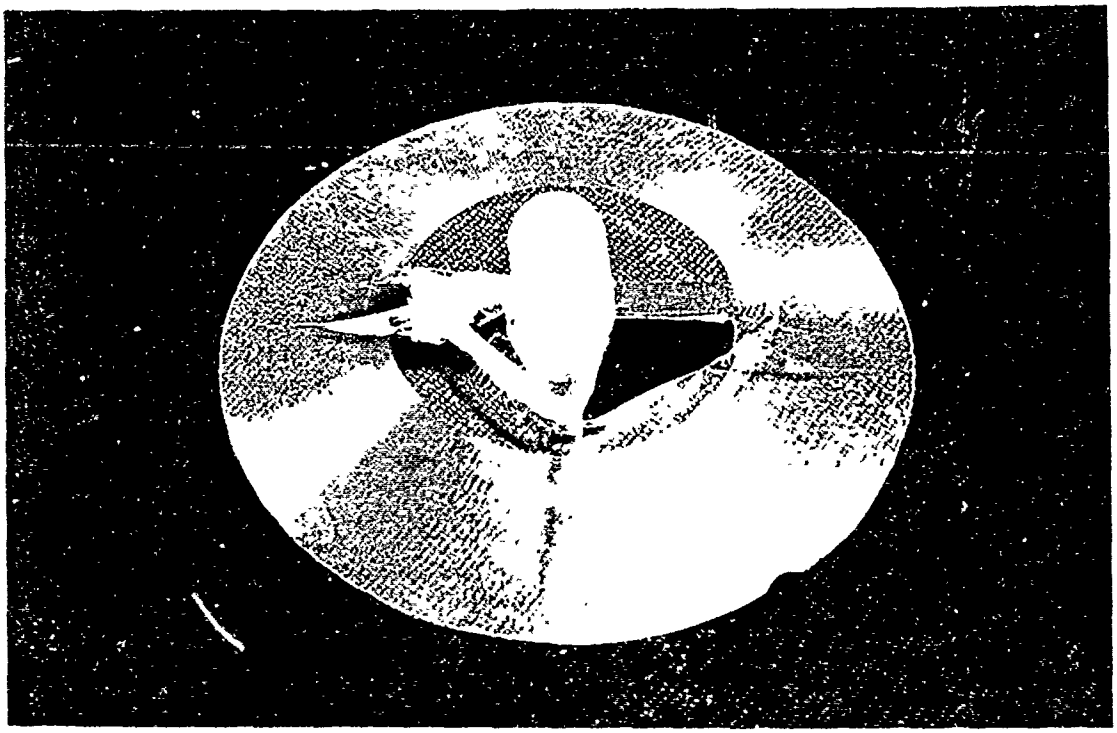

Figure B-32. Failed 1-inch-diameter, 150°, 0.125 t/D ratio window, low-pressure face, with displacement indicator anchor attached.

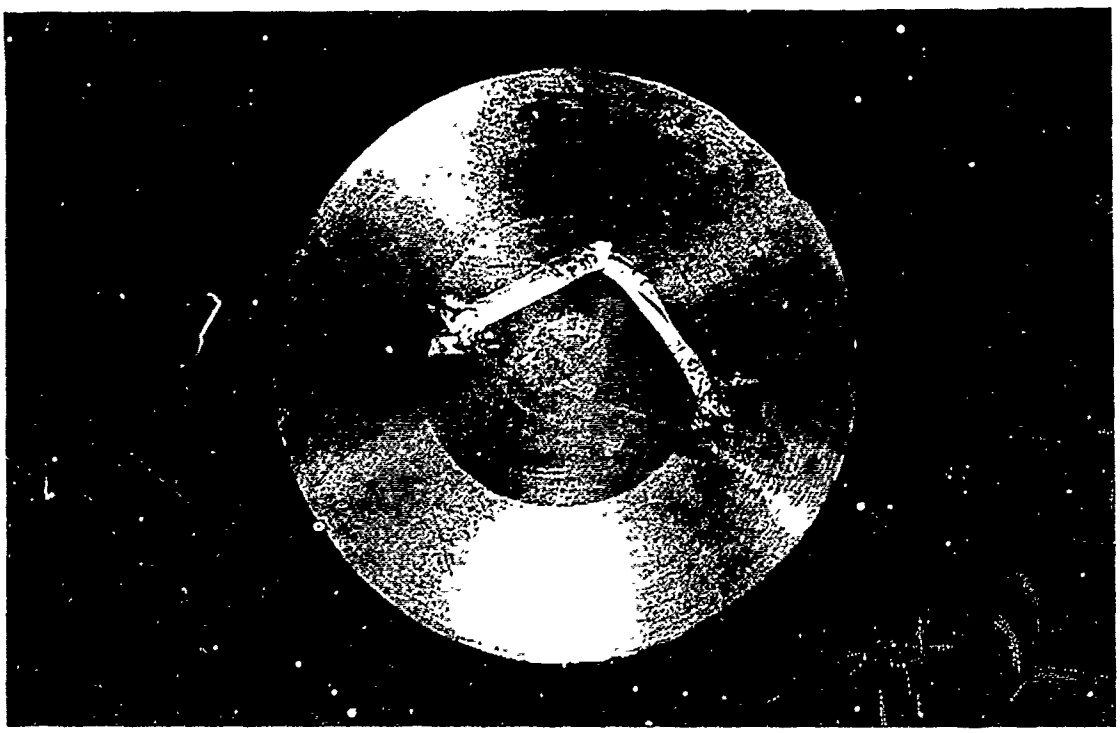

Figure B-33. Failed 1-inch-diameter, 150°, 0.125 t/D ratio window, high-pressure face.

That this was the mechanism of failure for the 0.125 t/D windows was evidenced on 0.25 t/D windows in the transition t/D range between windows whose center was ejected every time in the test, and windows whose center was not ejected because of prior leakage around the conical sealing surfaces. Thus, in 0.25 t/D windows, three different types of failure occurred. One type (Figures B-34 and B-35) was the same as for the 0.125 t/D ratio windows, where the presence of radial cracks in the center of the window permitted it to deflect to such an extent that the seal was lost between window and flange. The second type of failure for the 0.25 t/D ratio windows was a central fracture cone which originated from circumferential cracks on the window low-pressure face. This fracture cone, also previously found in 0.25 t/D windows with 60°, 90° and 120° angles, was characterized by ragged fracture surfaces, and the fact that its outside diameter was approximately 1 inch (the diameter of the window low-pressure face). The third type of failure of 0.25 t/D ratio windows was the presence of two fracture cones in the center portion of the window. The inner one was initiated by the circumferential cracks on the window low-pressure face, while the outer fracture cone started from a circumferential crack on the window bearing surface below (on the conical side) the shape-transition zone. The outer fracture cone, so typical of previously tested 120° conical windows, had a smooth cleavage surface, and its major diameter was invariably larger than the diameter of the low-pressure face.

The 150° windows with t/D ratios larger than 0.25 invariably failed by ejection of the window center portion bounded by the outer fracture cone (Figures B-36 through B-39). The inner fracture cone that started at the low-pressure face was also present in all these windows, except that it generally was not found after window failure, since it lay within the body of material ejected at critical pressure. Close inspection of a 0.625 t/D window which was loaded to only approximately 80% of its critical pressure confirmed this. In this arrested-failure specimen, three fracture cones could actually be seen (Figure B-40). The outer cone fracture had already penetrated the whole thickness of the window body, while the two inner cone fractures had penetrated only partially. The high-pressure face of the window exhibited a well-defined cold-flow crater bounded by the outer fracture cone (Figure B-41). Beyond the boundary of the outer fracture cone the high-pressure face of the window showed no traces of cold-flow cratering (Figure B-42).

Two-Inch-Diameter, 30° Conical Windows

All 2-inch-diameter, 30° conical windows failed by being ejected from the vessel. Their critical pressures were in the same pressure range as the critical pressures of 1-inch-diameter, 30° windows. The displacements for the two types of windows were different. The ratio between the displacements of the 2-inch- and the 1-inch-diameter windows was found to be roughly 2:1. This would seem to indicate that the displacements of 30° conical windows are proportional to their minor diameter.

Four-and-One-Half-Inch-Diameter, 60° Conical Windows

The 4.5-inch-diameter, 60° conical windows, except for the 0.25 t/D ratio specimens, were ejected completely from the mounting flange on failure. When the remains of the 4.5-inch-diameter, 0.25 t/D ratio windows (Figures B-43 and B-44), retained in the flange, were compared to the remains of 1-inch-diameter windows with the same t/D ratio, it became apparent that the mechanisms of failure must have been similar, for the appearance of the retained window fragment was the same in both cases. Since the center portion of the 4.5-inch-diameter, 0.25 t/D ratio window was not ejected from the vessel, due to premature pressure relief through a crack in that section, it was available for observation. The center portion showed deformation of both the high- and low-pressure faces. The deformation of the high-pressure face was a typical cold-flow crater, while the conical cavity on the low-pressure face was generated by fracturing of the material. The whole center portion of the window was separated from the rest of the window body by a shear cone surface. Thus, there were actually two fracture cones, the outer one which permitted the center portion of the window to separate from the ring-shaped fragment retained by the flange, and the inner one which allowed a conical cavity to be created on the low-pressure face of the window.

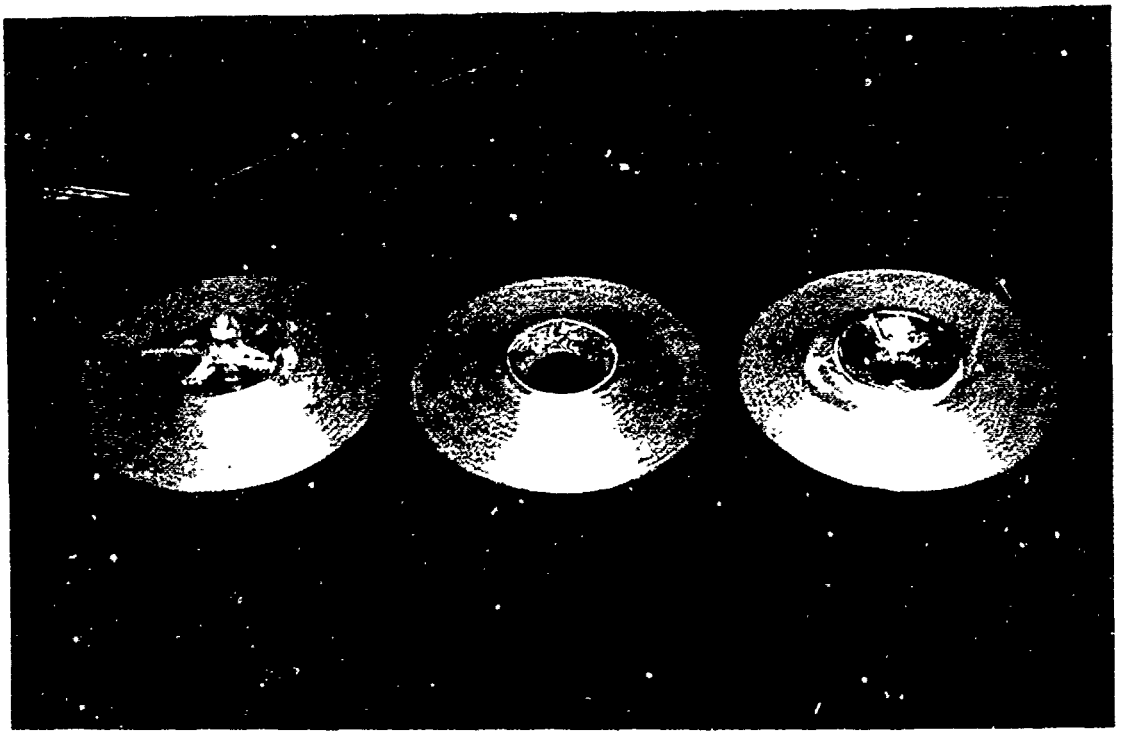

Figure B-34. Failed 1-inch-diameter, 150°, 0.25 t/D ratio windows, low-pressure faces.

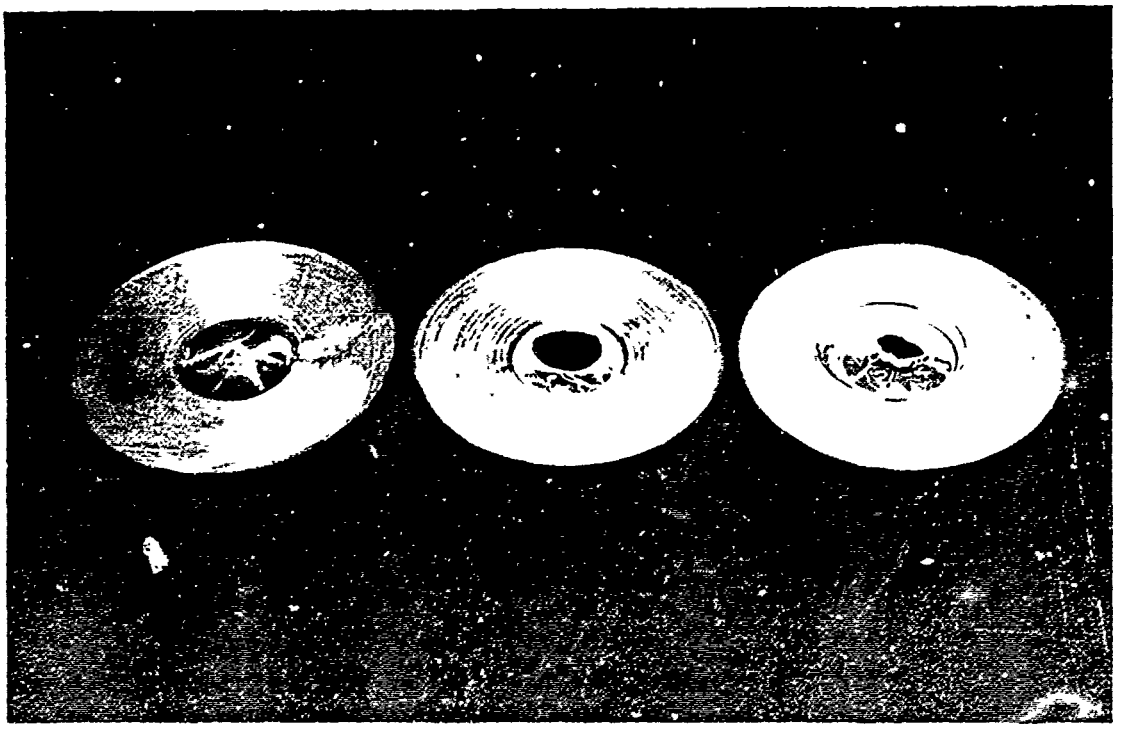

Figure B-35. Failed 1-inch-diameter, 150°, 0.25 t/D ratio windows, high-pressure faces.

Figure B-36. Failed 1-inch-diameter, 150°, 0.5 t/D ratio window, low-pressure face.

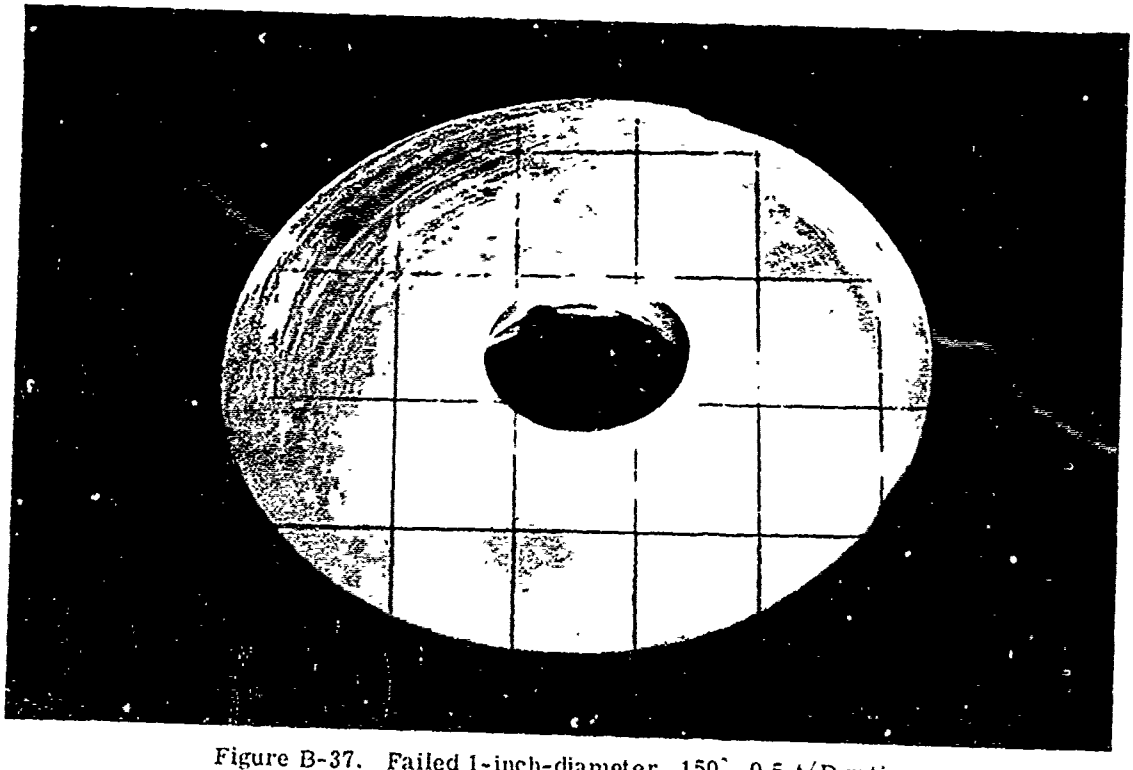

Figure B-37. Failed 1-inch-diameter, 150°, 0.5 t/D ratio window, high-pressure face.

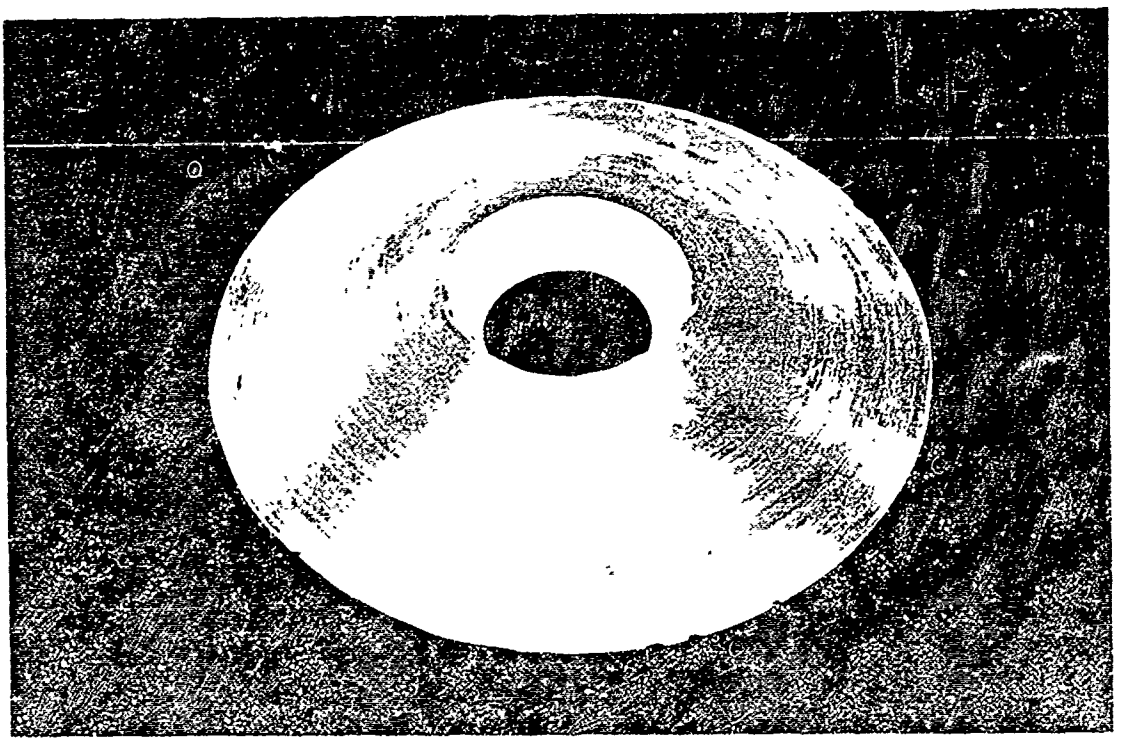

Figure B-38. Failed 1-inch-diameter, 150°, 0.625 t/D ratio window, low-pressure face.

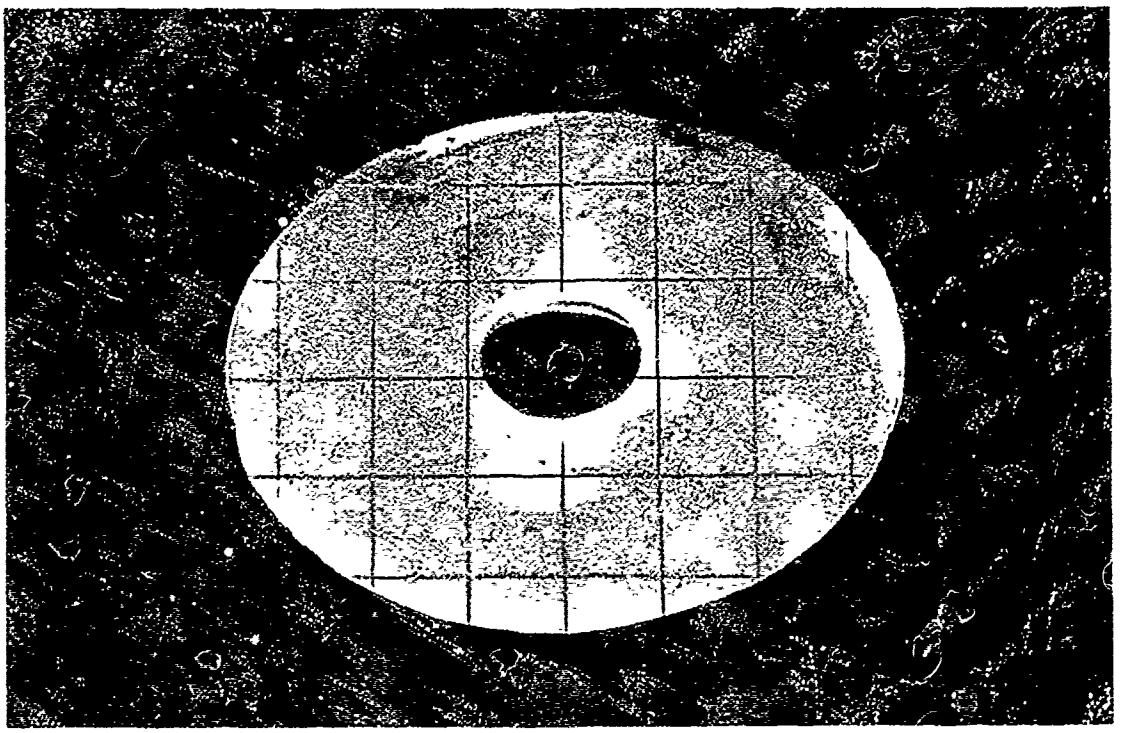

Figure B-39. Failed 1-inch-diameter, 150°, 0.625 t/D ratio window, high-pressure face.

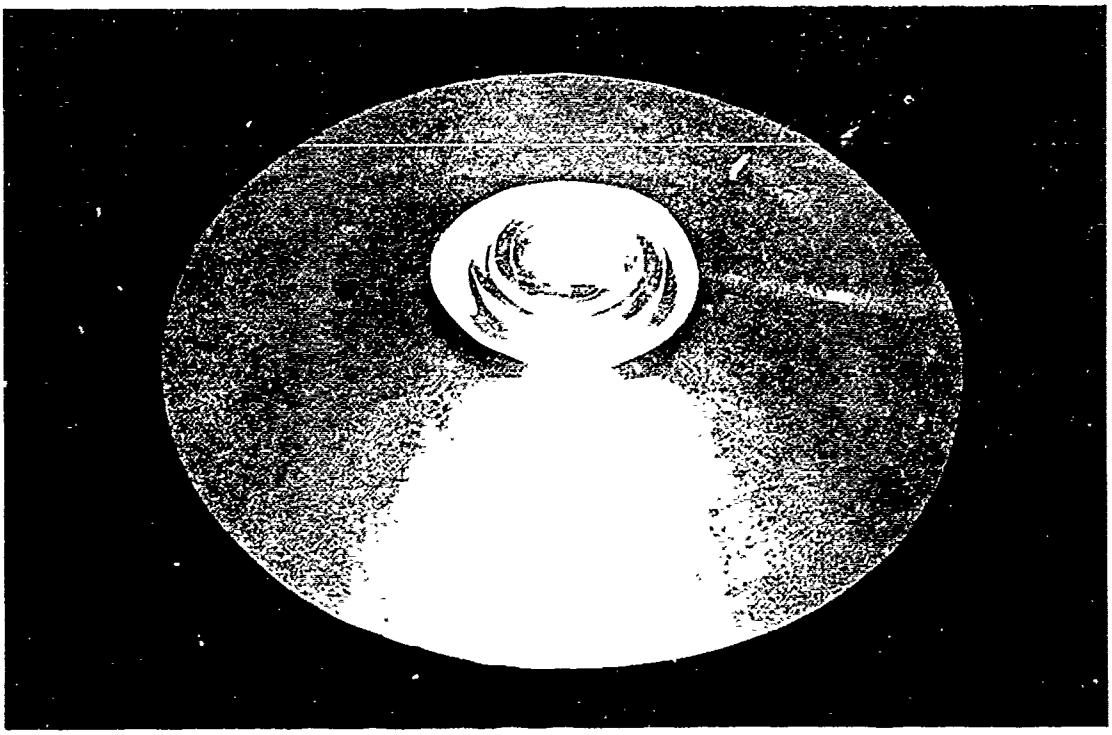

Figure B-40. Arrested failure of 1-inch-diameter, 150°, 0.625 t/D ratio window at 24, 000 psi, low-pressure face.

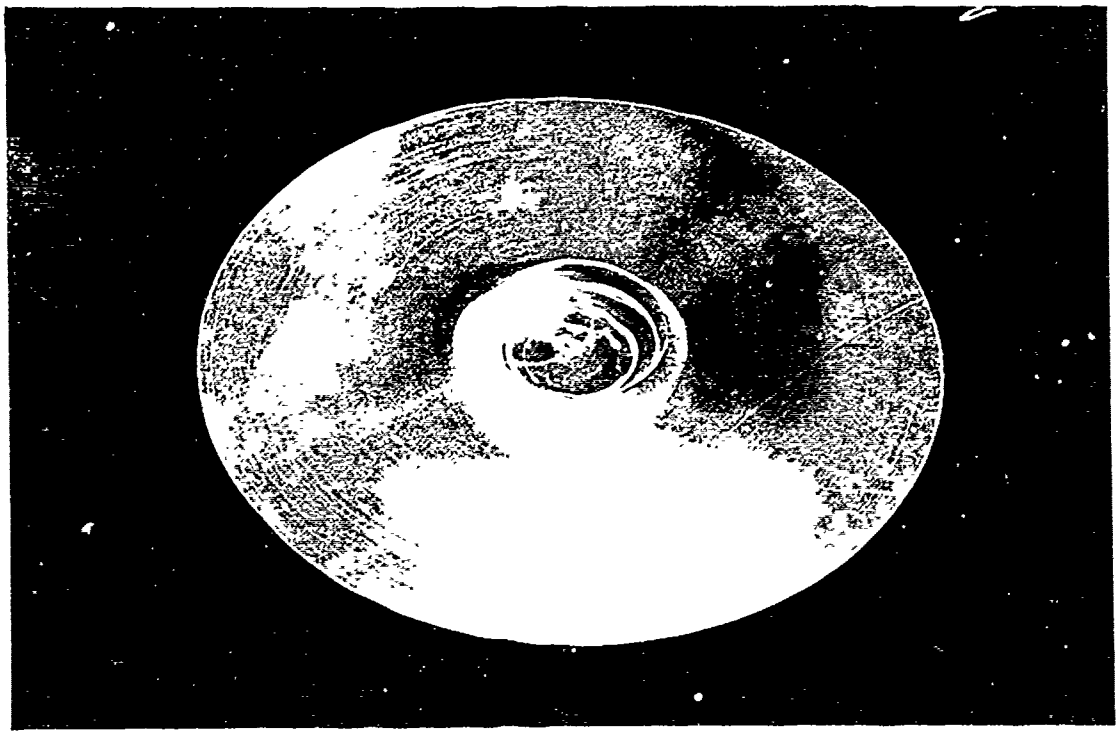

Figure B-41. Arrested failure of 1-inch-diameter, 150°, 0.625 t/D ratio window at 24, 000 psi, high-pressure face. (Cold-flow crater bounded by outer fracture cone.)

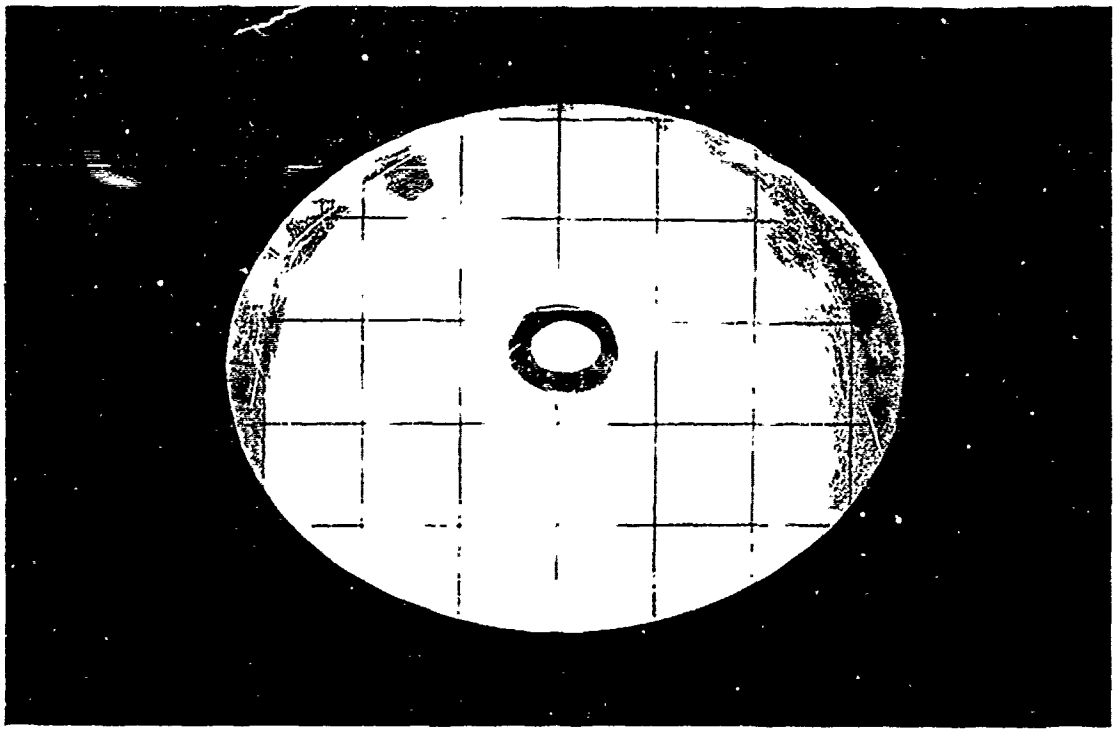

Figure B-42. Arrested failure of 1-inch-diameter, 150°, 0.625 t/D ratio window at 24,000 psi, high-pressure face. (No cold-flow crater beyond outer fracture cone.)

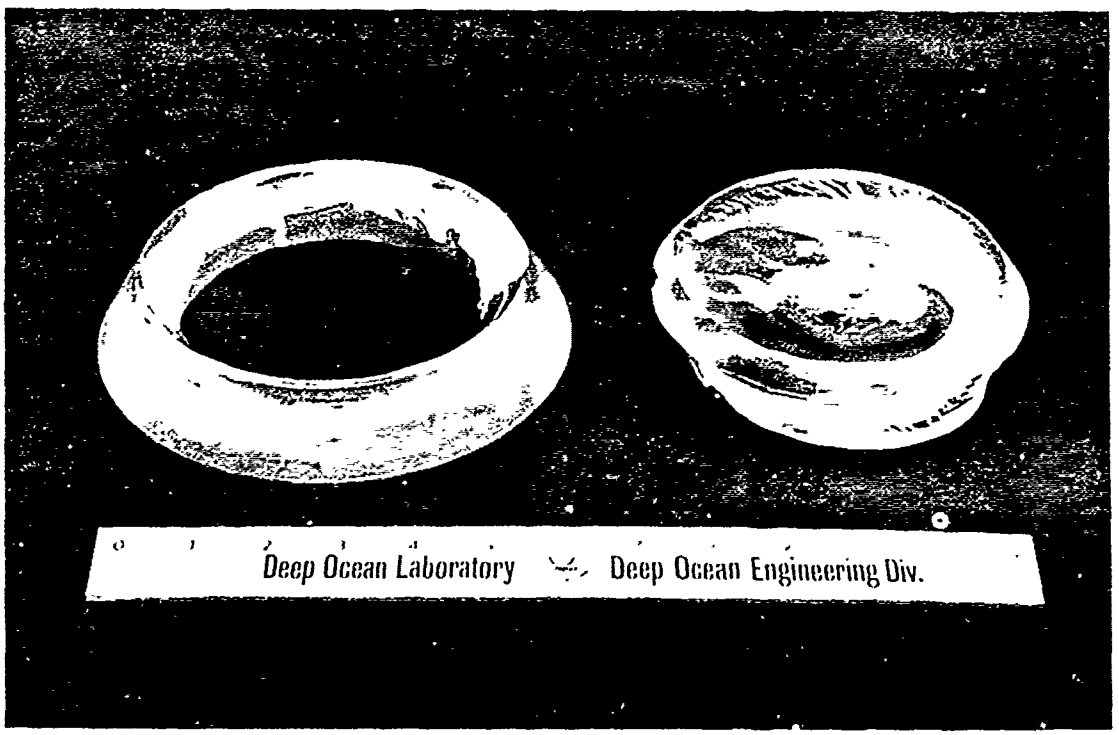

Figure B-43. Failed 4.5-inch-diameter, 60°, 0.25 t/D ratio window, low-pressure face, with center portion alongside.

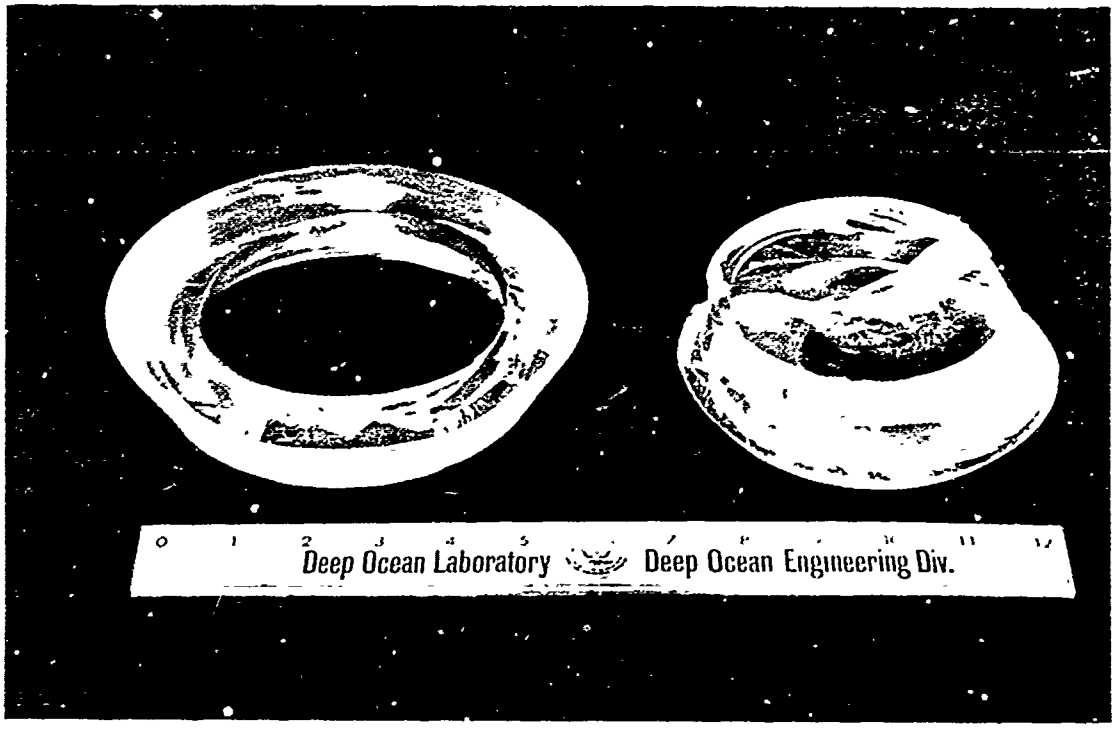

Figure B-44. Failed 4.5-inch-diameter, 60°, 0.25 t/D ratio window, high-pressure face, with center portion alongside.

Eight-Inch-Diameter, 90° Conical Windows

When the 8-inch-diameter, 4-inch-thick conical window with 90° included angle was subjected to increasing hydrostatic pressure, it failed by fracturing (Figure B-45) in a manner similar to 1-inch-diameter windows of the same t/D ratio (0.5) and included angle. The failure of the two types of windows at the same critical pressure lends considerable affirmation to the postulate that the critical pressure data obtained with 1-inch-diameter conical windows is applicable to larger conical windows provided they have the same included angle and t/D ratio.

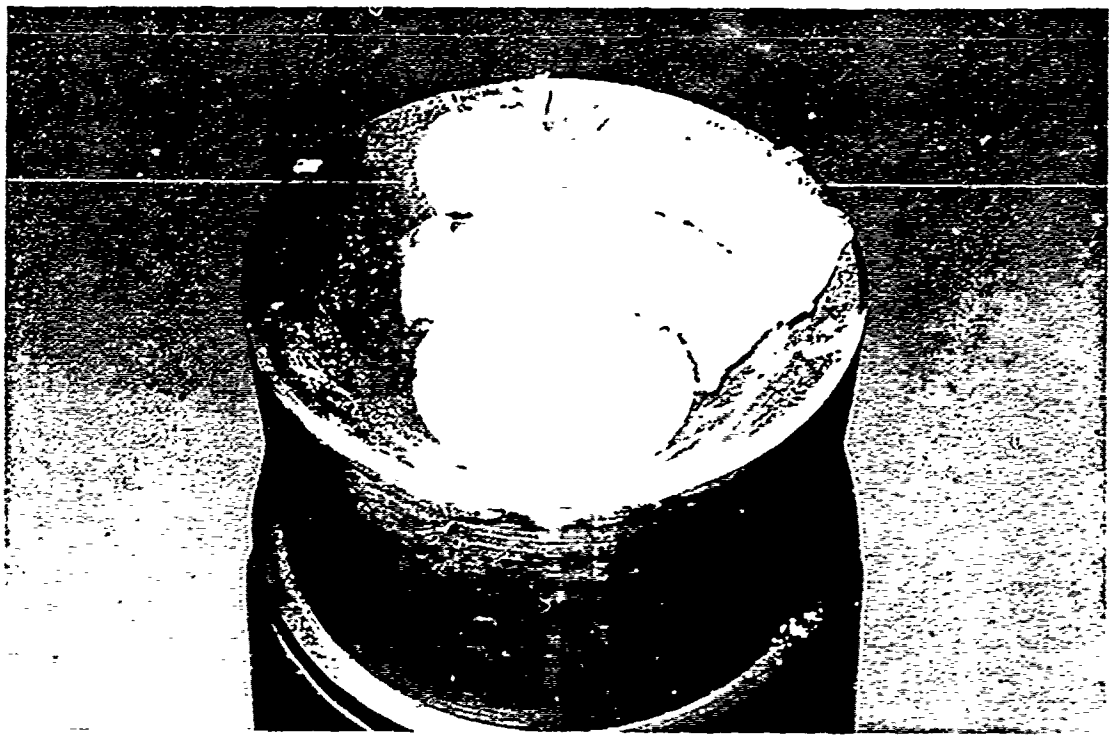

Figure B-45. Failed 8-inch-diameter, 90°, 0.5 t/D ratio window, high-pressure face, shown in mounting flange.

Appendix C

STATISTICAL EVALUATION OF THE SIZE OF THE SAMPLE GROUPS

To conduct a check as to whether the average of five experimental values is an adequate representation of the experimentally determined variable, ten specimens instead of five were tested for the 30° and 90° conical windows with a 0.5 t/D nominal ratio. The average critical pressure of the first five 30° windows tested was 8,600 psi (Table G-4, Appendix G) while that of the second five windows was 8,270 psi (Table G-5, Appendix G). When statistical methods were applied to determine the significance of the difference between the two means, it was found that the standard error of the difference was 366 psi. Since the difference between the means was 330 psi, and thus less than three standard errors of the difference for these two groups, it evidently resulted from chance and was of no significance.

The same type of analysis of experimental data derived from testing of two groups of 90° windows with five 0.5 t/D ratio windows in each (Tables G-20 and G-21, Appendix G) showed that the difference between the average critical pressures of 16,820 and 15,940 of the two groups was 880 psi, while the standard error of the difference amounted to 700 psi. This indicated that the difference between the average critical pressures of the two 90° window groups was also due solely to chance, since the difference betweeen the average critical pressures of the two groups was less than three standard errors of the difference for these two groups, and hence of no significance. Since the testing of an additional five windows of the same t/D ratio did not produce critical pressures that would be significantly different from the ones obtained by testing a single group of five windows, it can be postulated that the size of the window sample groups of same t/D ratio used in this study was sufficiently large and representative.

Appendix D

TEMPERATURE INFLUENCE EVALUATION TESTS

Besides the special tests performed on the 30° and 90° windows with a 0.5 t/D ratio to determine whether the experimental data produced by groups of five windows was repeatable, if additional groups of five were tested, tests were also performed to determine whether variation in the temperature of the mounting flange and the water adjacent to the window had significant influence on the critical pressure of the windows.

Low-temperature tests were conducted on a group of 30° windows with a 0.5 t/D ratio (Table G-6, Appendix G). The average critical pressure of the windows tested at temperatures of 35° to 40°F was higher than the average critical pressure of identical windows at 64° to 70°F in the standard temperature range (Table G-4, Appendix G) by 1,950 psi. When the standard error of the means was calculated for the critical pressures resulting from the low- and room-temperature tests, it was found to be 417 psi. Since the difference between the means of the low- and the room-temperature critical pressures was 1,950 psi, that difference was indicated as not due to chance but to some variable. Because no other additional variable was introduced into the tests other than temperature, it can be safely assumed that the difference in average critical pressures between the low- and room-temperature groups was caused by the influence of low temperature on the mechanical properties of acrylic plastic.

Appendix E

APPLICABILITY OF 1-INCH-DIAMETER WINDOW TEST DATA TO WINDOWS OF LARGER SIZES

The series of windows for the experimental validation of the t/D scaling ratio consisted of 2-inch-diameter, 30° windows with 0.125, 0.25 and 0.5 t/D ratios; 4.5-inch-diameter, 60° windows with 0.125, 0.25 and 0.5 t/D ratios; and 8-inch-diameter, 90° windows with 0.5 t/D ratios. It was reasoned that if the average critical pressures for these larger windows were approximately the same as for 1-inch-diameter windows of the same shape and t/D ratio, then the assumption that the t/D ratio is a valid scaling ratio would have been substantiated.

For the performance of critical pressure tests on the 2-inch-, 4.5-inch-, and 8-inch-diameter windows, the same experimental arrangement was followed as for the 1-inch-diameter windows except that larger mounting flanges of DOL Type I were used (Figures E-1, E-2, and E-3). Windows were fabricated again from Grade G Plexiglas to the same machining tolerances specified for the 1-inch-diameter windows. After being mounted in the appropriate flanges and subjected to the same experimental testing procedures as the 1-inch windows, the larger diameter windows were pressurized to failure.

A sufficient number of window specimens were so tested and compared in their critical pressures and displacements with 1-inch-diameter windows having the same t/D ratio and angle, that the relationship between the experimentally derived values for different window diameters could be established with reasonable confidence. The critical pressure curves (Figures 10, 12, 14, 16, 18) based on experimental data obtained with 1-inch-diameter windows were found to predict directly with reasonable accuracy the critical pressures of windows with diameters larger than 1 inch (Figures 20 and 22), provided they are composed of the same material, have the same t/D ratio and angle as the 1-inch-diameter windows, and are tested in DOL Type I mounting flanges.

The displacement curves based on experimental data derived from testing 1-inch-diameter windows (Figures 11, 13, 15, 17, and 19) do not predict directly the displacements of windows with a diameter larger than 1 inch (Figures 21 and 23). The displacements of windows with the same t/D ratio and angle but a diameter larger than 1 inch, however, are in the elastic range approximately proportional to the minor diameter of the window.

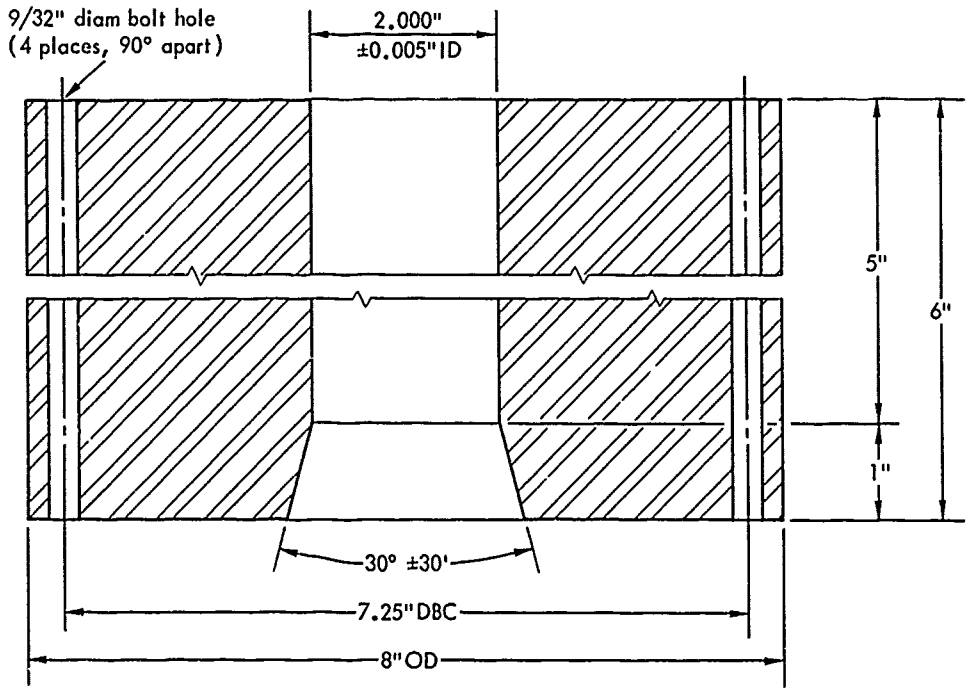

Figure E-1. DOL Type I configuration mounting flange for 2-inch-diameter, 30° conical window scaling factor validation tests.

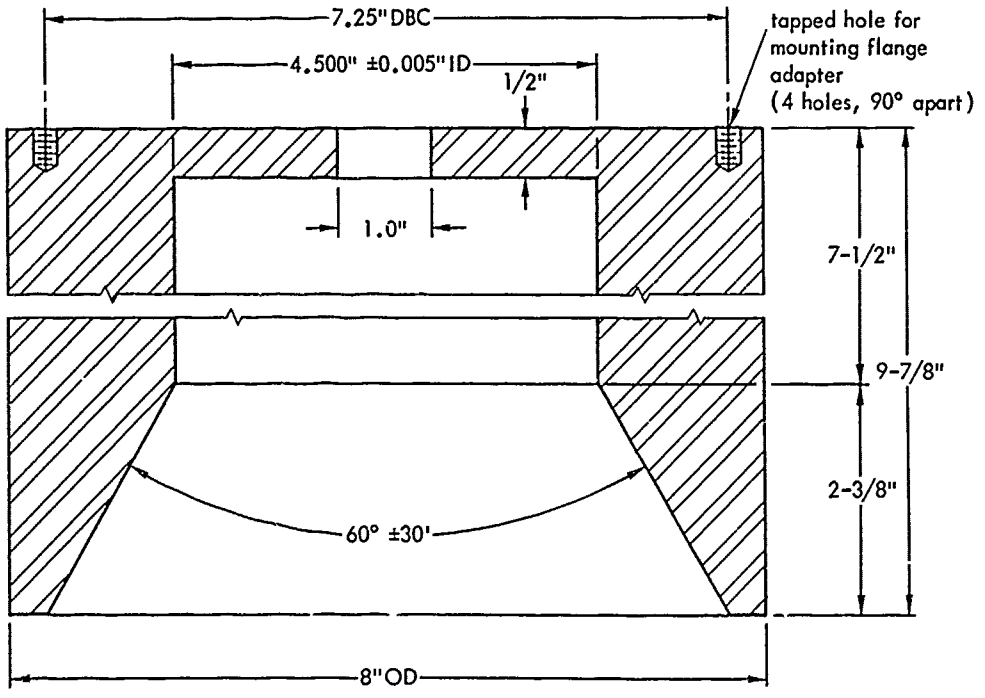

Figure E-2. DOL Type I configuration mounting flange for 4.5-[illegible] diameter, 60° conical window scaling factor validation tests.

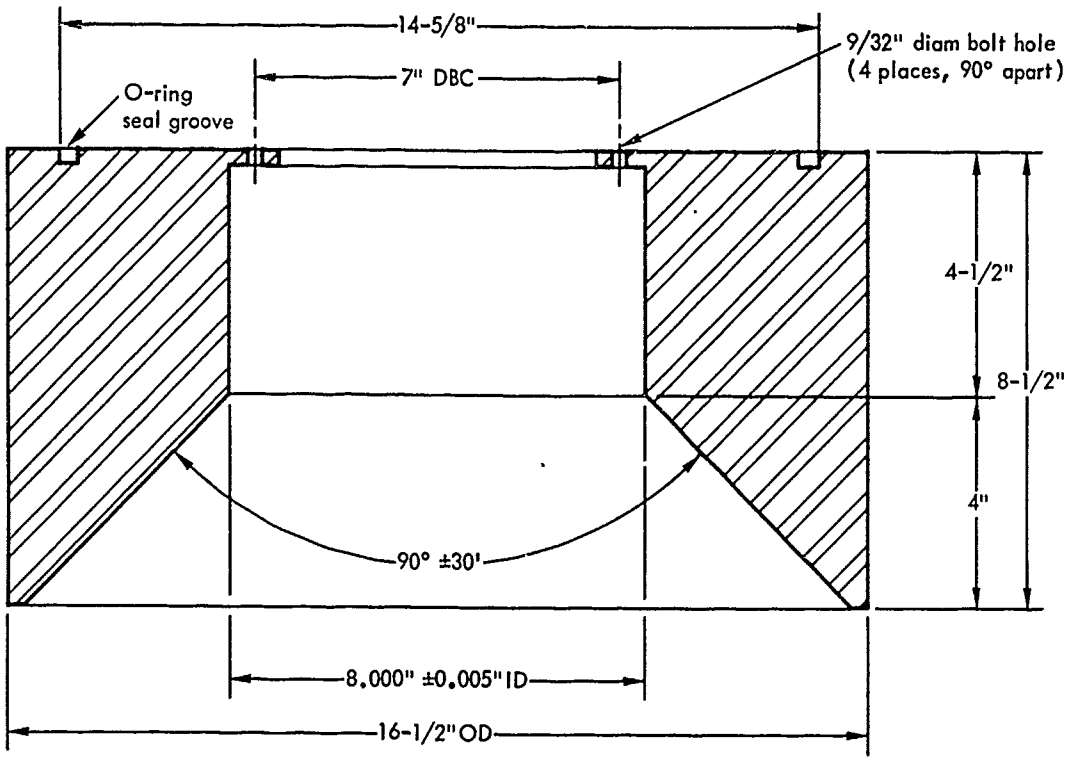

Figure E-3. DOL Type I configuration mounting flange for 8-inch-diameter, 90° conical window scaling factor validation tests.

Appendix F

EVALUATION OF OTHER WINDOW MOUNTING FLANGE CONFIGURATIONS

Since the configuration of the transition zone between the conical and the cylindrical cavities in the mounting flange may have considerable influence on the critical pressure of conical windows, several exploratory tests were conducted to determine whether a departure from the DOL Type I flange cavity configuration would influence greatly the critical pressure of conical windows under short-term hydrostatic loading. Although many flange cavity configurations are feasible for conical windows, only one in addition to the DOL Type I was utilized for exploratory investigation.

The second configuration, called DOL Type II, differed from Type I in only one vital respect. Type I was characterized by a long cylindrical cavity adjoining the conical cavity, with the same diameter as the minor diameter of the conical cavity, to provide the displaced portion of the window with radial support. In the DOL Type II configuration the cavity receiving the displaced portion was flared, with its diameter increasing beyond the juncture of the two cavities (Figure F-1). Thus, the window displaced portion was not provided with any radial support, and tended to separate from the window body retained in the flange conical cavity.

The exploratory tests conducted with 1-inch-diameter, 30° windows in a flange of the DOL Type II configuration showed that the window critical pressures were considerably lower than those obtained from testing the same windows in DOL Type I flanges. A comparison of the critical pressures of the 1-inch-diameter, 30° windows with a t/D of 1.0 in both types of flanges is as follows: DOL Type I - 27,600 psi; DOL Type II - 22,169 psi. Complete data on windows tested in DOL Type II configuration flanges are presented in Tables G-11 and G-37, Appendix G.

Since the flange configuration has such a pronounced effect on the critical pressure of the window, it is mandatory that whenever a designer wishes to apply critical pressure data from this report to a full-size window in deep submergence structure or pressure vessel, he must provide it with a DOL Type I flange. In order to achieve maximum critical pressure, the length of the cylindrical cavity in a full-size window flange must be equal to or greater than the maximum displacement that the particular window would experience prior to failure. The magnitude of the window displacements for 1-inch-diameter windows (Tables G-1 through G-10 and G-12 through G-33, Appendix G) would have to be scaled to the diameter of the window used in an actual application. The method for approximate scaling of displacements is presented in Appendix E.

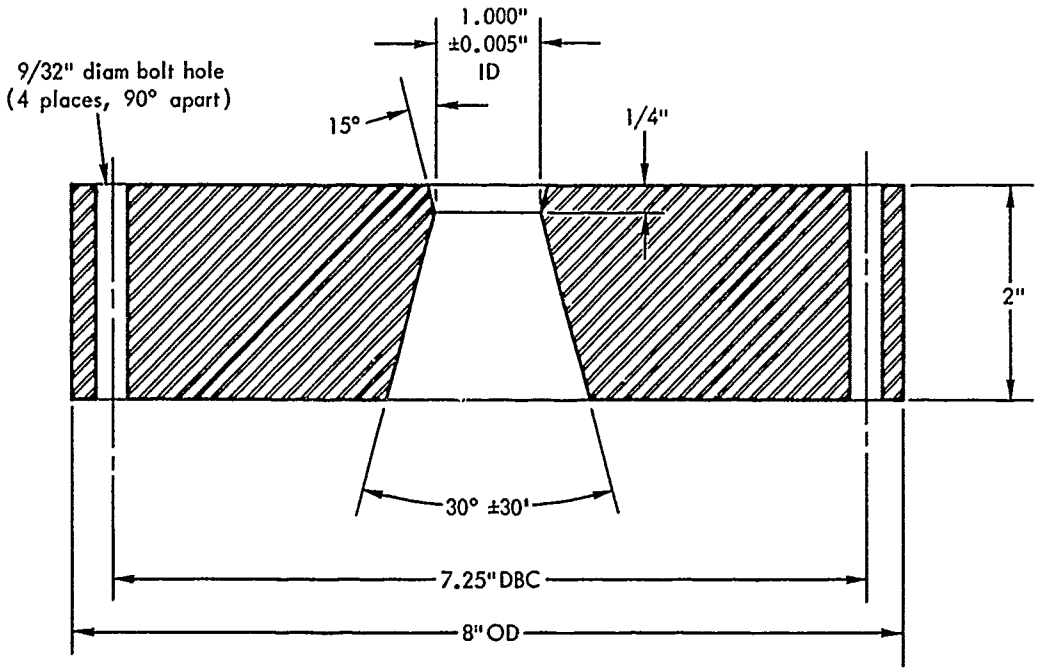

Figure F-1. DOL Type II configuration mounting flange for 1-inch-diameter, 30° conical window exploratory tests.

Appendix G

DATA FROM THE TESTING OF CONICAL ACRYLIC WINDOWS

(Tables G-1 Through G-40)

Table G-1. Test Data on 1-Inch-Diameter, 30° Windows With t/D Ratio of 0.125, in DOL Type I Flange

	Specimen Number					Maximum Value	Average Value	Minimum Value
	1	2	3	4	5			
Thickness, t (in.)	0.129	0.137	0.135	0.140	0.153	0.153	0.138	0.129
Temperature (°F)	65	69	68	68	66	69	67	66
Pressurization Rate (psi/min)	750	555	500	600	800	800	642	500
Pressure (psi)	Axial Displacement of Center Point on Window Low-Pressure Face (in.)							
—	←(All failed at pressures below 1,000 psi)→							
Pressure at Failure (psi)	800	850	850	750	880	850	826	750

Table G-2. Test Data on 1-Inch-Diameter, 30° Windows With t/D Ratio of 0.25 in DOL Type I Flange

	Specimen Number					Maximum Value	Average Value	Minimum Value
	6	7	8	9	10			
Thickness, t (in.)	0.250	0.253	0.250	0.250	0.251	0.253	0.251	0.250
Temperature (°F)	65	61	63	66	67	67	65	61
Pressurization Rate (psi/min)	800	680	700	740	680	800	720	680
Pressure (psi)	Axial Displacement of Center Point on Window Low-Pressure Face (in.)							
1,000	0.009	0.011	0.009	0.011	0.012	0.008	0.010	0.012
2,000	0.020	0.025	0.025	0.030	0.030	0.020	0.026	0.030
3,000	0.042	0.050	0.050	0.054	0.053	0.042	0.050	0.054
Pressure at Failure (psi)	4,200	3,900	3,850	3,900	3,750	4,200	3,900	3,750

Table G-3. Test Data on 1-Inch-Diameter, 30° Windows With t/D Ratio of 0.375, in DOL Type I Flange

	Specimen Number					Maximum Value	Average Value	Minimum Value
	11	12	13	14	15			
Thickness, t (in.)	0.344	0.348	0.340	0.338	0.340	0.348	0.342	0.338
Temperature (°F)	62	68.5	64	66	64.5	68.5	65	62
Pressurization Rate (psi/min)	560	570	630	690	650	690	615	560
Pressure (psi)	Axial Displacement of Center Point on Window Low-Pressure Face (in.)							
1,000	0.011	0.021	0.020	0.012	0.013	0.021	0.015	0.011
2,000	0.025	0.027	0.034	0.026	0.029	0.034	0.030	0.025
3,000	0.041	0.047	0.044	0.042	0.045	0.047	0.044	0.041
4,000	0.062	0.065	0.068	0.062	0.069	0.069	0.065	0.062
5,000	0.124	0.135	0.100	0.100	0.130	0.135	0.118	0.100
Pressure at Failure (psi)	5,200	5,250	5,600	5,100	5,300	5,600	5,300	5,100

Table G-4. Test Data on 1-Inch-Diameter, 30° Windows With t/D Ratio of 0.5, in DOL Type I Flange

	Specimen Number					Maximum Value	Average Value	Minimum Value
	16	17	18	19	20			
Thickness, t (in.)	0.510	0.490	0.480	0.488	0.488	0.510	0.490	0.480
Temperature (°F)	68.5	69.9	70.0	66.0	64.0	70	68	64
Pressurization Rate (psi/min)	610	620	675	780	905	975	720	610
Pressure (psi)	Axial Displacement of Center Point on Window Low-Pressure Face (in.)							
1,000	0.005	0.005	0.006	0.005	0.005	0.006	0.005	0.005
2,000	0.015	0.011	0.014	0.010	0.010	0.015	0.012	0.010
3,000	0.028	0.020	0.019	0.015	0.015	0.028	0.020	0.015
4,000	0.040	0.031	0.034	0.020	0.020	0.040	0.031	0.020
5,000	0.053	0.044	0.055	0.034	0.029	0.055	0.042	0.029
6,000	0.072	0.060	0.073	0.058	0.045	0.073	0.060	0.045
7,000	0.092	0.079	0.095	0.130	0.070	0.130	0.093	0.070
8,000	0.116	0.110	0.135		0.120	0.135	0.120	0.110
Pressure at Failure (psi)	9,200	8,800	8,700	7,700	8,600	9,200	8,600	8,300

Table G-5. Test Data on 1-Inch-Diameter, 30° Windows With t/D Ratio of 0.5, in DOL Type J Flange: Sample Group Size Validation Tests

	Specimen Number					Maximum Value	Average Value	Minimum Value
	21	22	23	24	25			
Thickness, t (in.)	0.500	0.490	0.512	0.497	0.515	0.515	0.503	0.490
Temperature (°F)	66	70	73	72	72	73	70	66
Pressurization Rate (psi/min)	980	740	1,000	940	332	1,000	800	332
Pressure (psi)	Axial Displacement of Center Point on Window Low-Pressure Face (in.)							
1,000	0.010	0.003	0.010	0.005	0.004	0.010	0.006	0.003
2,000	0.020	0.009	0.015	0.010	0.008	0.020	0.012	0.009
3,000	0.030	0.020	0.027	0.026	0.012	0.030	0.023	0.012
4,000	0.042	0.032	0.040	0.035	0.026	0.042	0.035	0.026
5,000	0.055	0.048	0.050	0.047	0.048	0.055	0.050	0.047
6,000	0.075	0.072	0.071	0.069	0.080	0.080	0.073	0.069
7,000	0.110	0.150	0.105	0.130	0.150	0.150	0.129	0.105
8,000					0.310			
Pressure at Failure (psi)	8,300	7,400	8,000	9,400	8,300	9,400	8,270	7,400

Table G-6. Test Data on 1-Inch Diameter, 30° Windows With t/D Ratio of 0.5, in DOL Type I Flange: Low-Temperature Tests

	Specimen Number					Maximum Value	Average Value	Minimum Value
	26	27	28	29	30			
Thickness, t (in.)	0.512	0.494	0.498	0.489	0.514	0.514	0.501	0.489
Temperature (°F)	38	36	35	40	40	40	38	35
Pressurization Rate (psi/min)	625	500	600	713	653	713	619	500
Pressure (psi)	Axial Displacement of Center Point on Window Low-Pressure Face (in.)							
1,000	0.006	0.005	0.006	0.010	0.005	0.010	0.006	0.005
2,000	0.009	0.015	0.016	0.015	0.008	0.016	0.013	0.008
3,000	0.014	0.019	0.025	0.020	0.014	0.025	0.018	0.014
4,000	0.022	0.031	0.039	0.030	0.030	0.039	0.030	0.022
5,000	0.041	0.039	0.050	0.040	0.035	0.050	0.041	0.035
6,000	0.045	0.048	0.057	0.050	0.054	0.057	0.051	0.045
7,000	0.060	0.060	0.075	0.070	0.075	0.075	0.068	0.060
8,000	0.081	0.083	0.090	0.090	0.080	0.090	0.085	0.080
9,000	0.117	0.108	0.112	0.125	0.095	0.125	0.112	0.095
10,000	0.250	0.110	0.148	0.250	0.130	0.250	0.178	0.110
11,000			0.200					
12,000			0.350					
Pressure at Failure (psi)	10,000	10,600	12,200	10,200	9,800	12,200	10,550	9,800

Table G-7. Test Data on 1-Inch-Diameter, 30° Windows With t/D Ratio of 0.625, in DOL Type I Flange

	Specimen Number					Maximum Value	Average Value	Minimum Value
	31	32	33	34	35			
Thickness, t (in.)	0.624	0.632	0.627	0.630	0.625	0.632	0.628	0.624
Temperature (°F)	67	67	67	66	62	67	65	62
Pressurization Rate (psi/min)	650	665	700	590	630	705	650	590
Pressure (psi)	Axial Displacement of Center Point on Window Low-Pressure Face (in.)							
1,000	0.015	0.008	0.012	0.011	0.018	0.018	0.013	0.008
2,000	0.024	0.012	0.021	0.022	0.026	0.026	0.021	0.012
3,000	0.032	0.020	0.030	0.031	0.036	0.036	0.030	0.020
4,000	0.043	0.028	0.039	0.040	0.047	0.047	0.039	0.028
5,000	0.052	0.040	0.049	0.049	0.054	0.054	0.049	0.040
6,000	0.063	0.046	0.058	0.060	0.065	0.065	0.058	0.046
7,000	0.077	0.058	0.069	0.072	0.076	0.077	0.070	0.058
8,000	0.092	0.070	0.082	0.087	0.090	0.09?	0.084	0.070
9,000	0.110	0.088	0.098	0.104	0.104	0.104	0.098	0.088
10,000	0.140	0.106	0.118	0.130	0.123	0.140	0.123	0.106
11,000	0.175	0.121	0.145	0.162	0.150	0.162	0.151	0.121
12,000	0.235	0.165	0.183	0.205	0.189	0.235	0.195	0.165
13,000	0.355	0.221	0.235	0.280	0.250	0.355	0.269	0.221
14,000		0.340	0.340	0.370	0.380	0.380	0.357	0.340
Pressure at Failure (psi)	13,800	14,800	14,900	15,300	14,900	15,300	14,700	13,800

Table G-8. Test Data on 1-Inch-Diameter, 30° Windows with t/D ratio of 0.75, in DOL Type I Flange

	Specimen Number					Maximum Value	Average Value	Minimum Value
	36	37	38	39	40			
Thickness, t (in.)	0.727	0.726	0.721	0.740	0.730	0.740	0.728	0.726
Temperature (°F)	70	68	74	65	68	74	69	65
Pressurization Rate (psi/min)	590	635	770	740	630	770	670	630
Pressure (psi)	Axial Displacement of Center Point on Window Low-Pressure Face (in.)							
1,000	0.003	0.005	0.007	0.015	0.011	0.003	0.008	0.015
2,000	0.008	0.011	0.015	0.025	0.021	0.008	0.016	0.025
3,000	0.014	0.016	0.018	0.033	0.030	0.014	0.022	0.033
4,000	0.022	0.025	0.022	0.041	0.040	0.022	0.030	0.041
5,000	0.032	0.033	0.028	0.050	0.049	0.028	0.039	0.050
6,000	0.041	0.043	0.037	0.057	0.060	0.037	0.048	0.060
7,000	0.053	0.055	0.046	0.066	0.071	0.053	0.058	0.071
8,000	0.067	0.068	0.059	0.078	0.085	0.067	0.072	0.078
9,000	0.084	0.082	0.075	0.095	0.100	0.075	0.087	0.100
10,000	0.104	0.099	0.095	0.115	0.121	0.099	0.107	0.121
11,000	0.130	0.121	0.118	0.132	0.150	0.118	0.130	0.150
12,000	0.160	0.147	0.160	0.153	0.190	0.147	0.162	0.190
13,000	0.197	0.179	0.230	0.179	0.245	0.179	0.206	0.245
14,000	0.251	0.210	0.330	0.209	0.328	0.210	0.265	0.330
15,000	0.335	0.257	0.440	0.250	0.415	0.250	0.339	0.440
Pressure at Failure (psi)	16,100	17,650	16,000	17,750	16,000	17,750	16,680	16,000

Table G-9. Test Data on 1-Inch-Diameter, 30° Windows With t/D Ratio of 0.875, in DOL Type I Flange

	Specimen Number					Maximum Value	Average Value	Minimum Value
	41	42	43	44	45			
Thickness, t (in.)	0.889	0.8[illegible]	0.879	0.880	0.877	0.889	0.860	0.877
Temperature (°F)	70	70	64	68	64	70	66	64
Pressurization Rate (psi/min)	935	725	642	712	696	935	742	642
Pressure (psi)	Axial Displacement of Center Point on Window Low-Pressure Face (in.)							
1,000	0.003	0.000	0.004	0.000	0.000	0.004	0.002	0.000
2,000	0.004	0.010	0.007	0.005	0.006	0.010	0.005	0.004
3,000	0.008	0.017	0.010	0.010	0.014	0.017	0.012	0.008
4,000	0.014	0.019	0.014	0.015	0.021	0.021	0.017	0.014
5,000	0.019	0.024	0.022	0.020	0.032	0.032	0.023	0.019
6,000	0.025	0.030	0.030	0.029	0.042	0.042	0.032	0.025
7,000	0.033	0.048	0.039	0.031	0.046	0.048	0.039	0.031
8,000	0.042	0.053	0.049	0.042	0.055	0.055	0.048	0.042
9,000	0.062	0.059	0.059	0.055	0.067	0.067	0.060	0.059
10,000	0.065	0.068	0.072	0.068	0.076	0.076	0.070	0.065
11,000	0.077	0.083	0.086	0.078	0.096	0.096	0.084	0.077
12,000	0.094	0.105	0.102	0.098	0.109	0.109	0.102	0.094
13,000	0.118	0.125	0.120	0.120	0.124	0.124	0.121	0.118
14,000	0.153	0.160	0.142	0.152	0.142	0.160	0.143	0.142
15,000	0.203	0.197	0.165	0.190	0.164	0.203	0.183	0.164
16,000	0.253	0.245	0.194	0.231	0.198	0.253	0.225	0.194
17,000	0.297	0.288	0.224	0.280	0.242	0.297	0.267	0.224
18,000	0.337	0.328	0.262	0.320	0.302	0.337	0.310	0.262
19,000	0.398	0.376	0.300	0.372	0.347	0.399	0.359	0.300
20,000	0.550	0.455	0.328	0.460	0.390	0.550	0.437	0.328
21,000		0.940	0.358	0.840	0.460	0.940	0.518	0.358
Pressure at Failure (psi)	20,300	21,800	23,300	21,000	22,500	23,300	21,800	20,300

Table G-10. Test Data on 1-Inch-Diameter, 30 Windows With t/D Ratio of 1.0, in DOL Type I Flange

	Specimen Number					Maximum Value	Average Value	Minimum Value
	46	47	48	49	50			
Thickness, t (in.)	0.950	0.978	0.977	0.980	0.969	0.980	0.970	0.950
Temperature (°F)	61	65	72	72	73	73	69	61
Pressurization Rate (psi/min)	500	610	715	600	640	715	613	500
Pressure (psi)	Axial Displacement of Center Point on Window Low-Pressure Face (in.)							
1,000	0.005	0.006	0.004	0.005	0.007	0.007	0.005	0.004
2,000	0.008	0.007	0.008	0.009	0.010	0.010	0.008	0.007
3,000	0.016	0.009	0.011	0.011	0.013	0.016	0.012	0.011
4,000	0.025	0.015	0.014	0.014	0.017	0.025	0.017	0.014
5,000	0.034	0.023	0.024	0.019	0.025	0.034	0.025	0.019
6,000	0.041	0.032	0.026	0.025	0.030	0.041	0.031	0.025
7,000	0.048	0.043	0.035	0.032	0.040	0.048	0.040	0.032
8,000	0.058	0.045	0.047	0.038	0.042	0.058	0.046	0.038
9,000	0.069	0.056	0.061	0.047	0.054	0.069	0.057	0.047
10,000	0.083	0.066	0.071	0.057	0.062	0.083	0.068	0.057
11,000	0.097	0.079	0.088	0.066	0.080	0.097	0.082	0.066
12,000	0.107	0.100	0.105	0.077	0.096	0.107	0.097	0.090
13,000	0.117	0.116	0.116	0.090	0.115	0.117	0.110	0.096
14,000	0.128	0.133	0.137	0.104	0.125	0.137	0.125	0.104
15,000	0.138	0.159	0.151	0.117	0.140	0.159	0.141	0.117
16,000	0.154	0.193	0.174	0.134	0.180	0.193	0.167	0.134
17,000	0.169	0.218	0.195	0.150	0.198	0.218	0.186	0.150
18,000	0.187	0.253	0.211	0.176	0.238	0.253	0.213	0.176
19,000	0.207	0.290	0.236	0.203	0.247	0.290	0.236	0.203
20,000	0.231	0.307	0.257	0.232	0.300	0.307	0.265	0.232
21,000	0.263	0.325	0.293	0.263	0.310	0.325	0.291	0.263
22,000	0.302	0.340	0.307	0.300	0.331	0.340	0.316	0.300
23,000	0.360	0.363	0.364	0.321	0.358	0.364	0.353	0.321
24,000	0.463	0.398	0.490	0.345	0.400	0.490	0.419	0.345
25,000	0.515	0.466	0.520	0.480	0.471	0.520	0.490	0.466
26,000	0.548		0.570	0.550	0.562	0.570	0.557	0.548
27,000	0.640		0.670	0.650	0.660	0.670	0.655	0.640
Pressure at Failure (psi)	29,100	26,100	27,600	28,200	27,000	29,100	27,600	26,100

Table G-11. Test Data on 1-Inch-Diameter, 30° Windows With t/D Ratio of 1.00, in DOL Type II Flange: Exploratory Tests

	Specimen Number					Maximum Value	Average Value	Minimum Value
	51	52	53	54	55			
Thickness, t (in.)	0.969	0.960	0.964	0.962	0.969	0.969	0.964	0.960
Temperature (°F)	64	65	65	65		65	65	64
Pressurization Rate (psi/min)	791	741	656	783		791	743	656
Pressure (psi)	Axial Displacement of Center Point on Window Low-Pressure Face (in.)							
1,000	0.001	0.002	0.001	0.002		0.002	0.002	0.001
2,000	0.009	0.011	0.009	0.010		0.001	0.008	0.009
3,000	0.016	0.016	0.017	0.016		0.017	0.016	0.016
4,000	0.019	0.022	0.024	0.023		0.024	0.022	0.019
5,000	0.027	0.030	0.030	0.030		0.030	0.029	0.027
6,000	0.040	0.036	0.037	0.036		0.040	0.037	0.036
7,000	0.049	0.044	0.044	0.042		0.049	0.045	0.042
8,000	0.057	0.050	0.053	0.051		0.057	0.053	0.050
9,000	0.068	0.062	0.062	0.060		0.068	0.063	0.060
10,000	0.079	0.069	0.070	0.069		0.079	0.072	0.069
11,000	0.093	0.078	0.082	0.080		0.093	0.083	0.078
12,000	0.108	0.089	0.095	0.091		0.108	0.096	0.089
13,000	0.125	0.099	0.107	0.103		0.125	0.109	0.099
14,000	0.144	0.110	0.125	0.112		0.144	0.123	0.110
15,000	0.165	0.122	0.141	0.130		0.165	0.140	0.122
16,000	0.194	0.136	0.158	0.146		0.194	0.159	0.136
17,000	0.223	0.152	0.181	0.162		0.223	0.180	0.162
18,000	0.280	0.172	0.204	0.180		0.280	0.209	0.172
19,000		0.195	0.231	0.199		0.195	0.208	0.195
20,000		0.217	0.273	0.219		0.217	0.236	0.217
21,000		0.250	0.325	0.245		0.325	0.273	0.245
22,000		0.285		0.277		0.285	0.281	0.277
23,000		0.415		0.351		0.415	0.383	0.351
Pressure at Failure (psi)	20,575	23,000	21,300	23,500		23,500	22,169	20,575

Table G-12. Test Data on 1-Inch-Diameter, 60° Windows With t/D Ratio of 0.125, in DOL Type I Flange

	Specimen Number					Maximum Value	Average Value	Minimum Value
	56	57	58	50	60			
Thickness, t (in.)	0.138	0.136	0.127	0.141	0.132	0.141	0.135	0.127
Temperature (°F)	68	69	69.5	67.5	70	70	69	68
Pressurization Rate (psi/min)	581	671	750	674	635	750	662	581
Pressure (psi)	Axial Displacement of Center Point on Window Low-Pressure Face (in.)							
1,000	(Failed)	0.047	0.038	0.037	0.0752	0.0752	0.049	0.037
Pressure at Failure (psi)	1,000	1,175	1,350	1,200	1,150	1,350	1,175	1,000

Table G-13. Test Data on 1-Inch-Diameter, 60° Windows With t/D Ratio of 0.25, in DOL Type I Flange

	Specimen Number					Maximum Value	Average Value	Minimum Value
	61	62	63	64	65			
Thickness, t (in.)	0.246	0.247	0.245	0.247	0.246	0.247	0.246	0.245
Temperature (°F)	71	68	70	65	68	71	68	65
Pressurization Rate (psi/min)	651	645	638	630	640	651	641	630
Pressure (psi)	Axial Displacement of Center Point on Window Low-Pressure Face (in.)							
1,000	0.004	0.0035	0.005	0.004	0.004	0.005	0.004	0.0035
2,000	0.015	0.008	0.008	0.007	0.010	0.015	0.0	0.007
3,000	0.028	0.017	0.012	0.015	0.015	0.028	0.017	0.012
4,000	0.044	0.030	0.027	0.028	0.020	0.044	0.030	0.020
5,000	0.105	0.068	0.053	0.057	0.040	0.105	0.064	0.040
Pressure at Failure (psi)	5,100	5,325	5,450	5,500	5,270	5,500	5,280	5,100

Table G-14. Test Data on 1-Inch-Diameter, 60° Windows With t/D Ratio of 0.375, in DOL Type I Flange

	Specimen Number					Maximum Value	Average Value	Minimum Value
	66	67	68	69	70			
Thickness, t (in.)	0.356	0.327	0.361	0.366	0.355	0.366	0.352	0.327
Temperature (°F)	67	68	70	72	64	72	68	64
Pressurization Rate (psi/min)	664	709	665	780	633	780	690	633
Pressure (psi)	Axial Displacement of Center Point on Window Low-Pressure Face (in.)							
1,000	0.004	0.003	0.004	0.003	0.004	0.004	0.0035	0 003
2,000	0.005	0.005	0.007	0.004	0.006	0.007	0.005	0.004
3,000	0.007	0.008	0.010	0.006	0.009	0.009	0.008	0.006
4,000	0.008	0.010	0.012	0.007	0.010	0.012	0.009	0.007
5,000	0.010	0.012	0.014	0.011	0.012	0.014	0.012	0.010
6,000	0.012	0.014	0.016	0.020	0.013	0.020	0.015	0.012
7,000	0.026	0.030	0.020	0.035	0.018	0.035	0.026	0.018
8,000	0.040	0.045	0.025	0.055	0.024	0.055	0. 3	0.024
Pressure at Failure (psi)	8,800	7,800	9,150	8,850	8,500	9,150	8,620	7,800

Table G-15. Test Data on 1-Inch-Diameter, 60° Windows With t/D Ratio of 0.5, in DOL Type I Flange

	Specimen Number					Maximum Value	Average Value	Minimum Value
	71	72	73	74	75			
Thickness, t (in.)	0.492	0.493	0.494	0.492	0.490	0.494	0.493	0,490
Temperature (°F)	66	69	69	69	67	69	68	66
Pressurization Rate (psi/min)	669	675	672	684	985	985	736	669
Pressure (psi)	Axial Displacement of Center Point on Window Low-Pressure Face (in.)							
1,000	0.004	0.007	0.005	0.004	0.001	0.007	0.005	0.001
2,000	0.005	0.010	0.007	0.005	0.0025	0.010	0.006	0.0025
3,000	0.007	0.012	0.008	0.008	0.005	0.012	0.008	0.005
4,000	0.008	0.013	0.010	0.010	0.006	0.013	0.009	0.006
5,000	0.009	0.015	0.011	0.015	0.007	0.015	0.011	0.007
6,000	0.010	0.016	0.013	0.020	0.0075	0.020	0.015	0.0075
7,000	0.012	0.019	0.015	0.026	0.022	0.026	0.019	0.012
8,000	0.014	0.022	0.017	0.032	0.028	0.032	0.023	0.014
9,000	0.016	0.034	0.023	0.041	0.036	0.041	0.030	0.016
10,000	0.022	0.046	0.033	0.055	0.046	0.055	0.040	0.022
11,000	0.038	0.064	0.044	0.079	0.048	0.079	0.055	0.038
12,000	0.073	0.107	0.068	0.210	0.059	0.210	0.103	0.059
13,000	0.260		0.113		0.079	0.260	0.150	0.079
14,000			0.610		0.137	0.610	0.373	0.137
Pressure at Failure (psi)	13,350	13,000	14,450	12,600	14,750	14,750	13,650	12,600

Table G-16. Test Data on 1-Inch-Diameter, 60° Windows With t/D Ratio of 0.625, in DOL Type I Flange

	Specimen Number					Maximum Value	Average Value	Minimum Value
	76	77	78	79	80			
Thickness, t (in.)	0.626	0.632	0.627	0.626	0.623	0.632	0.627	0.623
Temperature (°F)	68	70	70	65	73	73	69	65
Pressurization Rate (psi/min)	669	497	651	612	668	669	619	497
Pressure (psi)	Axial Displacement of Center Point on Window Low-Pressure Face (in.)							
1,000	0.012	0.010	0.010	0.006	0.004	0.012	0.008	0.004
2,000	0.014	0.012	0.014	0.008	0.005	0.014	0.012	0.005
3,000	0.016	0.014	0.018	0.010	0.007	0.018	0.013	0.007
4,000	0.018	0.016	0.022	0.012	0.008	0.022	0.015	0.008
5,000	0.018	0.025	0.026	0.014	0.010	0.026	0.019	0.010
6,000	0.021	0.030	0.029	0.015	0.011	0.030	0.021	0.011
7,000	0.023	0.032	0.033	0.017	0.013	0.033	0.024	0.013
8,000	0.027	0.037	0.037	0.019	0.015	0.037	0.027	0.015
9,000	0.031	0.043	0.041	0.024	0.017	0.043	0.031	0.017
10,000	0.035	0.047	0.046	0.038	0.018	0.047	0.037	0.018
11,000	0.040	0.055	0.051	0.040	0.021	0.055	0.041	0.021
12,000	0.045	0.060	0.057	0.042	0.024	0.060	0.046	0.024
13,000	0.052	0.067	0.062	0.050	0.028	0.067	0.052	0.028
14,000	0.060	0.073	0.068	0.053	0.033	0.073	0.057	0.033
15,000	0.068	0.083	0.077	0.058	0.044	0.083	0.066	0.044
16,000	0.078	0.094	0.086	0.066	0.054	0.094	0.076	0.054
17,000	0.088	0.104	0.097	0.077	0.067	0.104	0.087	0.067
18,000	0.103	0.120	0.110	0.088	0.083	0.120	0.101	0.083
19,000	0.119	0.147	0.134	0.109	0.108	0.147	0.122	0.108
20,000	0.146	0.177	0.174	0.133	0.153	0.177	0.157	0.146
21,000	0.205	0.220	0.246	0.173	0.250	0.250	0.219	0.173
22,000	0.330	0.280	0.305	0.247	0.358	0.358	0.304	0.247
23,000	0.440	0.355	0.347	0.347	0.405	0.440	0.379	0.347
24,000	0.518	0.410	0.390	0.391	0.452	0.518	0.432	0.390
25,000		0.435	0.415	0.415		0.435	0.422	0.415
26,000		0.478	0.438	0.459		0.478	0.485	0.458
27,000				0.494		0.484	0.484	0.484
28,000				0.498		0.498	0.497	0.489
Pressure at Failure (psi)	24,850	26,600	23,400	28,100	24,500	28,100	26,090	24,500

Table G-17. Test Data on 1-Inch-Diameter, 90 Windows With t/D Ratio of 0.125, in DOL Type I Flange

	Specimen Number					Maximum Value	Average Value	Minimum Value
	81	82	83	84	85			
Thickness, t (in.)	0.147	0.134	0.140	0.138	0.110	0.147	0.134	0.110
Temperature (°F)	74.3	73.4	72.5	72.5	72.5	74.3	73.2	72.5
Pressurization Rate (psi/min)	700	708	620	665	625	708	664	620
Pressure (psi)	Axial Displacement of Center Point on Window Low-Pressure Face (in.)							
1,000	←(Failed below 1,000 psi)→			0.018	←(Failed below 1,000 psi)→			
Pressure at Failure (psi)	1,000	800	800	1,150	600	1,150	870	600

Table G-18. Test Data on 1-Inch-Diameter, 90 Windows With t/D Ratio of 0.25, in DOL Type I Flange

	Specimen Number					Maximum Value	Average Value	Minimum Value
	86	87	88	89	90			
Thickness, t (in.)	0.260	0.258	0.248	0.255	0.254	0.260	0.255	0.248
Temperature (°F)	69.5	67.5	68.0	69.0	70.5	69.5	68.9	67.5
Pressurization Rate (psi/min)	679	658	638	675	650	679	660	638
Pressure (psi)	Axial Displacement of Center Point on Window Low-Pressure Face (in.)							
1,000	0.005	0.003	0.003	0.007	0.002	0.007	0.004	0.002
2,000	0.014	0.006	0.006	0.010	0.005	0.014	0.008	0.005
3,000	0.022	0.012	0.008	0.013	0.010	0.022	0.013	0.008
4,000	0.031	0.022	0.012	0.017	0.024	0.031	0.021	0.012
5,000	0.073	0.034	0.022	0.022	0.050	0.073	0.040	0.022
6,000		0.067	0.095	0.060		0.095	0.074	0.060
Pressure at Failure (psi)	5,300	6,300	6,100	6,200	5,300	6,300	5,840	5,300

Figure G-19. Test Data on 1-Inch-Diameter, 90° Windows With t/D Ratio of 0.375, in DOL Type I Flange

	Specimen Number					Maximum Value	Average Value	Minimum Value
	91	92	93	94	95			
Thickness, t (in.)	0.381	0.370	0.374	0.379	0.380	0.381	0.377	0.370
Temperature (°F)	75.2	71.6	76.1	75.2	73.4	76.1	74.3	71.6
Pressurization Rate (psi/min)	661	674	673	672	668	674	670	661
Pressure (psi)	Axial Displacement of Center Point on Window Low-Pressure Face (in.)							
1,000	0.009	0.008	0.010	0.006	0.005	0.010	0.008	0.005
2,000	0.011	0.012	0.012	0.007	0.010	0.012	0.010	0.007
3,000	0.013	0.014	0.014	0.009	0.013	0.014	0.012	0.009
4,000	0.014	0.016	0.016	0.010	0.017	0.017	0.015	0.010
5,000	0.015	0.019	0.018	0.013	0.022	0.022	0.017	0.013
6,000	0.017	0.022	0.020	0.016	0.027	0.027	0.022	0.016
7,000	0.037	0.028	0.022	0.020	0.033	0.037	0.028	0.020
8,000	0.039	0.036	0.025	0.026	0.039	0.039	0.033	0.025
9,000	0.042	0.043	0.030	0.033	0.047	0.047	0.039	0.030
10,000	0.046	0.055	0.043	0.045	0.060	0.060	0.050	0.043
11,000	0.075	0.078	0.118	0.067	0.090	0.118	0.086	0.067
Pressure at Failure (psi)	11,850	12,150	11,250	11,900	11,500	12,150	11,730	11,250

Table G-20. Test Data on 1-Inch-Diameter, 90° Windows With t/D Ratio of 0.5, in DOL Type I Flange

	Specimen Number					Maximum Value	Average Value	Minimum Value
	96	97	98	99	100			
Thickness, t (in.)	0.511	0.516	0.490	0.480	0.481	0.516	0.496	0.480
Temperature (° F)	71.6	68.4	65.3	63.5	69.8	71.6	67.7	63.5
Pressurization Rate (psi/min)	657	664	662	667	675	675	665	657
Pressure (psi)	Axial Displacement of Center Point on Window Low-Pressure Face (in.)							
1,000	0.004	0.003	0.002	0.002	0.002	0.004	0.003	0.002
2,000	0.008	0.007	0.004	0.003	0.004	0.008	0.005	0.003
3,000	0.012	0.011	0.007	0.003	0.005	0.012	0.008	0.003
4,000	0.015	0.015	0.008	0.005	0.007	0.015	0.010	0.005
5,000	0.018	0.018	0.010	0.007	0.009	0.018	0.012	0.007
6,000	0.021	0.021	0.011	0.009	0.012	0.021	0.015	0.009
7,000	0.024	0.025	0.013	0.013	0.017	0.025	0.018	0.013
8,000	0.027	0.028	0.015	0.016	0.020	0.028	0.021	0.015
9,000	0.031	0.032	0.017	0.020	0.026	0.032	0.025	0.017
10,000	0.035	0.036	0.019	0.024	0.031	0.036	0.029	0.019
11,000	0.039	0.041	0.023	0.029	0.037	0.041	0.034	0.023
12,000	0.045	0.046	0.028	0.035	0.044	0.046	0.040	0.028
13,000	0.051	0.053	0.035	0.042	0.058	0.058	0.048	0.035
14,000	0.058	0.062	0.046	0.051	0.077	0.077	0.059	0.046
15,000	0.069	0.073	0.065	0.073	0.122	0.122	0.080	0.065
16,000	0.086	0.091	0.127	0.114		0.127	0.105	0.086
Pressure at Failure (psi)	17,900	17,850	16,400	16,400	15,550	17,900	16,820	15,550

Table G-21. Test Data on 1-Inch-Diameter, 90° Windows With t/D Ratio of 0.5. in DOL Type I Flange: Sample Group Size Validation Tests

	Specimen Number					Maximum Value	Average Value	Minimum Value
	101	102	103	104	105			
Thickness, t (in.)	0.496	0.490	0.512	0.482	0.515	0.515	0.499	0.482
Temperature (F)	70	68	80	77	75	80	74	68
Pressurization Rate (psi/min)	672	634	670	672	570	570	837	634
Pressure (psi)	Axial Displacement of Center Point on Window Low-Pressure Face (in.)							
1,000	0.002	0.003	0.007	0.011	0.006	0.011	0.006	0.002
2,000	0.003	0.005	0.008	0.015	0.007	0.015	0.007	0.003
3,000	0.004	0.006	0.009	0.018	0.009	0.018	0.009	0.004
4,000	0.007	0.007	0.010	0.024	0.015	0.024	0.011	0.007
5,000	0.015	0.009	0.011	0.028	0.019	0.028	0.016	0.009
6,000	0.018	0.010	0.012	0.031	0.022	0.031	0.018	0.010
7,000	0.021	0.011	0.013	0.036	0.027	0.036	0.021	0.011
8,000	0.025	0.014	0.014	0.039	0.030	0.039	0.024	0.014
9,000	0.030	0.016	0.018	0.046	0.034	0.046	0.028	0.016
10,000	0.035	0.020	0.020	0.053	0.039	0.053	0.032	0.020
11,000	0.041	0.026	0.023	0.062	0.044	0.062	0.038	0.023
12,000	0.048	0.033	0.031	0.076	0.051	0.076	0.046	0.031
13,000	0.058	0.043	0.040	0.110	0.060	0.110	0.060	0.040
14,000	0.075	0.067	0.056		0.071	0.075	0.065	0.056
15,000	0.107	0.110	0.073		0.090	0.110	0.090	0.073
Pressure at Failure (psi)	15,850	15,700	16,550	13,850	17,750	17,750	15,940	13,850

Table G-22. Test Data on 1-Inch-Diameter, 90° Windows With t/D Ratio of 0.625, in DOL Type I Flange

	Specimen Number					Maximum Value	Average Value	Minimum Value
	106	107	108	109	110			
Thickness, t (in.)	0.626	0.632	0.633	0.631	0.631	0.633	0.631	0.626
Temperature (°F)	67.1	65.3	67.1	62.6	65.3	67.1	65.5	62.6
Pressurization Rate (psi/min)	669	702	851	934	613	934	754	613
Pressure (psi)	Axial Displacement of Center Point on Window Low-Pressure Face (in.)							
1,000	0.003	0.002		0.003	0.004	0.004	0.003	0.002
2,000	0.007	0.004	0.001	0.005	0.007	0.007	0.005	0.001
3,000	0.010	0.005	0.002	0.006	0.010	0.010	0.007	0.002
4,000	0.013	0.006	0.016	0.007	0.013	0.016	0.011	0.006
5,000	0.015	0.007	0.016	0.008	0.016	0.016	0.012	0.007
6,000	0.018	0.008	0.017	0.009	0.019	0.019	0.014	0.008
7,000	0.020	0.009	0.017	0.011	0.022	0.022	0.016	0.009
8,000	0.023	0.010	0.018	0.012	0.024	0.024	0.017	0.010
9,000	0.025	0.013	0.022	0.013	0.027	0.027	0.020	0.013
10,000	0.029	0.025	0.025	0.014	0.031	0.031	0.025	0.014
11,000	0.031	0.026	0.027	0.015	0.033	0.033	0.026	0.015
12,000	0.035	0.026	0.031	0.017	0.036	0.036	0.029	0.017
13,000	0.038	0.027	0.035	0.018	0.040	0.040	0.032	0.018
14,000	0.042	0.027	0.038	0.019	0.043	0.043	0.034	0.019
15,000	0.045	0.028	0.042	0.021	0.047	0.047	0.037	0.021
16,000	0.049	0.047	0.047	0.022	0.051	0.051	0.043	0.022
17,000	0.053	0.049	0.052	0.024	0.055	0.055	0.047	0.024
18,000	0.058	0.050	0.058	0.025	0.061	0.061	0.050	0.025
19,000	0.063	0.051	0.065	0.026	0.066	0.066	0.054	0.026
20,000	0.070	0.072	0.071	0.028	0.071	0.072	0.062	0.028
21,000	0.078	0.074	0.080	0.030	0.077	0.080	0.068	0.030
22,000	0.089	0.076	0.090	0.058	0.087	0.090	0.080	0.058
23,000	0.099	0.097	0.107	0.061		0.107	0.091	0.061
24,000	0.108	0.118	0.127	0.065	0.120	0.127	0.108	0.065
25,000	0.120	0.140	0.154	0.069	0.133	0.154	0.123	0.069
26,000	0.140	0.186	0.192	0.083		0.192	0.150	0.083
27,000	0.176	0.248	0.287	0.105		0.287	0.204	0.105
Pressure at Failure (psi)	28,850	27,400	27,700	29,900	27,100	29,900	28,190	27,100

Table G-23. Test Data on 1-Inch-Diameter, 120° Windows With t/D Ratio of 0.125, in DOL Type I Flange

	Specimen Number					Maximum Value	Average Value	Minimum Value
	111	112	113	114	115			
Thickness, t (in.)	0.120	0.120	0.121	0.120	0.120	0.121	0.120	0.120
Temperature (°F)	63.5	64	63.5	63	63	64	63.4	63
Pressurization Rate (psi/min)	329	524	429	449	372	524	421	329
Pressure (psi)	Axial Displacement of Center Point on Window Low-Pressure Face (in.)							
—	←(All failed at pressures below 1,000 psi)→							
Pressure Failure (psi)	850	750	750	750	850	850	780	750

Table G-24. Test Data on 1-Inch-Diameter, 120° Windows With t/D Ratio of 0.25, in DOL Type I Flange

	Specimen Number					Maximum Value	Average Value	Minimum Value
	116	117	118	119	120			
Thickness, t (in.)	0.241	0.240	0.244	0.243	0.239	0.244	0.243	0.239
Temperature (°F)	63	64	61	61	61	64	62	61
Pressurization Rate (psi/min)	705	657	642	623	651	703	655	623
Pressure (psi)	Axial Displacement of Center Point on Window Low-Pressure Face (in.)							
1,000	0.004	0.003	0.002	0.003	0.002	0.004	0.003	0.002
2,000	0.007	0.006	0.005	0.005	0.005	0.007	0.006	0.005
3,000	0.011	0.010	0.009	0.008	0.009	0.011	0.009	0.008
4,000		0.024	0.014	0.015	0.016	0.024	0.017	0.014
Pressure at Failure (psi)	3,500	4,400	4,950	4,400	4,350	4,950	4,320	3,500

Table G-25. Test Data on 1-Inch-Diameter, 120° Windows With t/D Ratio of 0.375, in DOL Type I Flange

	Specimen Number					Maximum Value	Average Value	Minimum Value
	121	122	123	124	125			
Thickness, t (in.)	0.349	0.331	0.330	0.328	0.337	0.349	0.335	0.328
Temperature (°F)	65.5	65.5	67	61.4	62.7	67	64.4	61.4
Pressurization Rate (psi/min)	716	717	833	680	674	833	724	674
Pressure (psi)	Axial Displacement of Center Point on Window Low-Pressure Face (in.)							
1,000	0.002	0.002	0.002	0.001	0.002	0.002	0.002	0.001
2,000	0.004	0.003	0.005	0.002	0.004	0.005	0.004	0.002
3,000	0.005	0.005	0.007	0.004	0.006	0.007	0.005	0.002
4,000	0.008	0.007	0.009	0.006	0.008	0.009	0.008	0.006
5,000	0.009	0.009	0.011	0.007	0.010	0.011	0.009	0.007
6,000	0.012	0.011	0.013	0.010	0.012	0.013	0.012	0.010
7,000	0.015	0.014	0.016	0.012	0.014	0.016	0.014	0.012
8,000	0.018	0.018	0.018	0.016	0.017	0.018	0.017	0.016
9,000	0.031	0.031	0.029	0.027	0.021	0.031	0.028	0.021
10,000	0.054	0.070	0.050	0.055	0.038	0.070	0.053	0.038
11,000					0.074			
Pressure at Failure (psi)	10,900	10,680	10,700	10,450	11,300	11,300	10,806	10,450

Table G-26. Test Data on 1-Inch-Diameter, 120° Windows With t/D Ratio of 0.5, in DOL Type I Flange

	Specimen Number					Maximum Value	Average Value	Minimum Value
	126	127	128	129	130			
Thickness, t (in.)	0.490	0.490	0.483	0.493	0.493	0.493	0.490	0.483
Temperature (°F)	67.5	68.0	69.0	67.5	66.5	69.0	67.7	66.5
Pressurization Rate (psi/min)	666	665	669	657	671	671	666	657
Pressure (psi)	Axial Displacement of Center Point on Window Low-Pressure Face (in.)							
1,000	0.002	0.001	0.001	0.000	0.001	0.002	0.001	0.000
2,000	0.005	0.002	0.003	0.001	0.002	0.005	0.003	0.001
3,000	0.005	0.003	0.004	0.003	0.004	0.005	0.004	0.003
4,000	0.006	0.005	0.005	0.004	0.005	0.006	0.005	0.004
5,000	0.008	0.006	0.007	0.005	0.006	0.008	0.006	0.005
6,000	0.009	0.008	0.008	0.007	0.008	0.009	0.008	0.007
7,000	0.010	0.009	0.010	0.008	0.009	0.010	0.009	0.008
8,000	0.011	0.011	0.012	0.009	0.010	0.012	0.011	0.009
9,000	0.013	0.012	0.013	0.010	0.011	0.013	0.012	0.010
10,000	0.014	0.014	0.014	0.012	0.013	0.014	0.013	0.012
11,000	0.016	0.015	0.015	0.018	0.016	0.018	0.016	0.015
12,000	0.017	0.017	0.017	0.020	0.017	0.020	0.018	0.017
13,000	0.019	0.018	0.019	0.022	0.020	0.022	0.020	0.018
14,000	0.022	0.045	0.021	0.032	0.025	0.045	0.029	0.021
15,000	0.025	0.048	0.025	0.035	0.031	0.048	0.033	0.025
16,000	0.030	0.052	0.034	0.048	0.039	0.052	0.041	0.030
17,000	0.065	0.070	0.045	0.052	0.050	0.070	0.056	0.045
18,000	0.142	0.100	0.060	0.080	0.066	0.142	0.090	0.060
19,000			0.148	0.200	0.130	0.200	0.159	0.130
Pressure at Failure (psi)	18,400	18,700	19,300	19,300	19,300	19,300	19,000	18,400

Table G-27. Test Data on 1-Inch-Diameter, 120 Windows With t/D Ratio of 0.625, in DOL Type I Flange

	Specimen Number					Maximum Value	Average Value	Minimum Value
	131	132	133	134	135			
Thickness, t (in.)	0.607	0.602	0.583	0.600	0.583	0.607	0.595	0.583
Temperature (°F)	63.5	65.5	67.0	67.5	67.5	67.5	66.2	63.5
Pressurization Rate (psi/min)	732	643	661	603	646	732	657	603
Pressure (psi)	Axial Displacement of Center Point on Window Low-Pressure Face (in.)							
1,000	0.002	0.000	0.003	0.001	0.001	0.003	0.001	0.000
2,000	0.004	0.001	0.005	0.002	0.003	0.005	0.003	0.001
3,000	0.005	0.002	0.007	0.003	0.004	0.007	0.004	0.002
4,000	0.007	0.003	0.009	0.004	0.005	0.009	0.006	0.003
5,000	0.008	0.004	0.010	0.005	0.006	0.010	0.007	0.004
6,000	0.009	0.005	0.011	0.006	0.007	0.011	0.008	0.005
7,000	0.010	0.005	0.012	0.007	0.009	0.012	0.009	0.005
8,000	0.011	0.007	0.013	0.007	0.010	0.013	0.010	0.007
9,000	0.012	0.008	0.015	0.008	0.011	0.015	0.011	0.008
10,000	0.014	0.009	0.015	0.009	0.019	0.019	0.013	0.009
11,000	0.015	0.010	0.017	0.010	0.020	0.020	0.014	0.010
12,000	0.016	0.011	0.018	0.011	0.021	0.021	0.015	0.011
13,000	0.018	0.012	0.020	0.012	0.023	0.023	0.017	0.012
14,000	0.040	0.013	0.021	0.014	0.024	0.040	0.022	0.013
15,000	0.041	0.041	0.022	0.015	0.025	0.041	0.029	0.015
16,000	0.042	0.041	0.024	0.017	0.027	0.042	0.030	0.017
17,000	0.044	0.043	0.025	0.018	0.043	0.044	0.035	0.018
18,000	0.045	0.044	0.027	0.037	0.045	0.045	0.040	0.027
19,000	0.047	0.046	0.029	0.037	0.047	0.047	0.041	0.029
20,000	0.049	0.048	0.031	0.039	0.049	0.049	0.043	0.031
21,000	0.075	0.050	0.051	0.040	0.067	0.075	0.057	0.040
22,000	0.079	0.076	0.054	0.054	0.070	0.079	0.067	0.054
23,000	0.080	0.078	0.057	0.055	0.094	0.094	0.073	0.055
24,000	0.084	0.081	0.073	0.077	0.098	0.098	0.083	0.073
25,000	0.109	0.085	0.093	0.080	0.116	0.116	0.097	0.080
26,000	0.119	0.110	0.204	0.195	0.199	0.204	0.165	0.110
27,000	0.170	0.190				0.190	0.180	0.170
Pressure at Failure (psi)	27,900	27,700	26,300	26,500	26,700	27,900	27,020	26,300

Table G-28. Test Data on 1-Inch-Diameter, 150° Windows With t/D Ratio of 0.125, in DOL Type I Flange

	Specimen Number					Maximum Value	Average Value	Minimum Value
	136	137	138	139	140			
Thickness, t (in.)	0.125	0.127	0.126	0.131	0.123	0.131	0.126	0.123
Temperature (°F)	65.5	61.9	66.5	67.1	69.1	69.1	66.0	61.9
Pressurization Rate (psi/min)	440	237	500	464	268	500	382	237
Pressure (psi)	Axial Displacement of Center Point on Window Low-Pressure Face (in.)							
—	←(All failed at pressures below 1,000 psi)→							
Pressure at Failure (psi)	550	575	600	650.	525	650	580	525

Table G-29. Test Data on 1-Inch-Diameter, 150° Windows With t/D Ratio of 0.25, in DOL Type I Flange

	Specimen Number					Maximum Value	Average Value	Minimum Value
	141	142	143	144	145			
Thickness, t (in.)	0.245	0.240	0.244	0.248	0.249	0.249	0.245	0.240
Temperature (°F)	68.1	68.4	69.1	69.0	68.1	69.1	68.5	68.1
Pressurization Rate (psi/min)	672	664	667	635	618	672	651	618
Pressure (psi)	Axial Displacement of Center Point on Window Low-Pressure Face (in.)							
1,000	0.003	0.004	0.002	0.002	0.003	0.004	0.003	0.002
2,000	0.005	0.007	0.005	0.004	0.005	0.007	0.005	0.004
3,000	0.007	0.013	0.012	0.011	0.009	0.013	0.010	0.007
4,000	0.011	0.047	0.023			0.047	0.027	0.011
5,000	0.024							
Pressure at Failure (psi)	5,450	4,550	4,750	3,950	3,800	5,450	4,500	3,800

Table G-30. Test Data on 1-Inch-Diameter, 150° Windows With t/D Ratio of 0.375, in DOL Type I Flange

	Specimen Number					Maximum Value	Average Value	Minimum Value
	146	147	148	149	150			
Thickness, t (in.)	0.360	0.375	0.343	0.357	0.335	0.375	0.354	0.335
Temperature (°F)	66.5	67.9	67.5	67.6	67.6	67.9	67.4	66.5
Pressurization Rate (psi/min)	663	652	678	669	. 667	678	666	652
Pressure (psi)	Axial Displacement of Center Point on Window Low-Pressure Face (in.)							
1,000	0.001	0.002	0.002	0.001	0.001	0.002	0.001	0.001
2,000	0.002	0.004	0.004	0.003	0.002	0.004	0.003	0.002
3,000	0.003	0.006	0.006	0.004	0.004	0.006	0.005	0.003
4,000	0.005	0.007	0.007	0.007	0.007	0.007	0.007	0.005
5,000	0.006	0.009	0.009	0.009	0.009	0.009	0.008	0.006
6,000	0.008	0.010	0.011	0.010	0.012	0.012	0.010	0.008
7,000	0.011	0.012	0.013	0.013	0.016	0.016	0.013	0.011
8,000	0.013	0.013	0.018	0.015	0.019	0.019	0.016	0.013
9,000	0.015	0.029	0.034	0.018	0.027	0.034	0.025	0.015
10,000	0.018	0.031	0.049	0.024	0.059	0.059	0.036	0.018
11,000	0.032	0.040		0.038		0.040	0.037	0.032
12,000		0.061				0.061	0.061	0.061
Pressure at Failure (psi)	11,500	12,525	10,550	11,300	10,100	12,525	11,195	10,100

Table G-31. Test Data on 1-Inch-Diameter, 150° Windows With t/D Ratio of 0.5, in DOL Type I Flange

	Specimen Number					Maximum Value	Average Value	Minimum Value
	151	152	153	154	155			
Thickness, t (in.)	0.465	0.461	0.468	0.467	0.467	0.468	0.466	0.461
Temperature (F)	67.9	67.2	68.2	68.1	67.4	68.2	67.8	67.2
Pressurization Rate (psi/min)	667	665	659	663	669	669	665	659
Pressure (psi)	Axial Displacement of Center Point on Window Low-Pressure Face (in.)							
1,000	0.001	0.001	0.001	0.001	0.002	0.002	0.001	0.001
2,000	0.002	0.003	0.002	0.003	0.003	0.003	0.003	0.002
3,000	0.003	0.004	0.003	0.004	0.004	0.004	0.004	0.003
4,000	0.004	0.005	0.005	0.005	0.006	0.006	0.005	0.004
5,000	0.005	0.006	0.006	0.007	0.007	0.007	0.006	0.005
6,000	0.007	0.007	0.006	0.008	0.008	0.008	0.007	0.006
7,000	0.008	0.008	0.008	0.010	0.009	0.010	0.009	0.008
8,000	0.009	0.009	0.011	0.011	0.010	0.011	0.010	0.009
9,000	0.010	0.010	0.013	0.013	0.011	0.013	0.011	0.010
10,000	0.011	0.011	0.018	0.015	0.013	0.018	0.014	0.011
11,000	0.012	0.013	0.021	0.016	0.014	0.021	0.015	0.012
12,000	0.015	0.015	0.027	0.019	0.016	0.027	0.018	0.015
13,000	0.017	0.017	0.031	0.040	0.018	0.031	0.025	0.017
14,000	0.027	0.020	0.042	0.043	0.021	0.043	0.031	0.020
15,000	0.030	0.022	0.046	0.045	0.023	0.048	0.034	0.022
16,000	0.046	0.026	0.064	0.065	0.026	0.065	0.045	0.026
17,000	0.070	0.034	0.095	0.091	0.030	0.095	0.064	0.030
18,000	0.150				0.056	0.150	0.103	0.056
Pressure at Failure (psi)	18,100	17,600	17,550	17,650	18,150	18,150	17,810	17,550

Table G-32. Test Data on 1-Inch-Diameter, 150° Windows With t/D Ratio of 0.5, in DOL Type I Flange: Sample Group Size Validation Tests

	Specimen Number					Maximum Value	Average Value	Minimum Value
	156	157	158	159	160			
Thickness, t (in.)	0.498	0.485	0.498	0.504	0.500	0.504	0.497	0.485
Temperature (°F)	65.8	69.1	67.9	66.1	68.5	69.1	67.5	65.8
Pressurization Rate (psi/min)	662	661	642	672	656	672	659	642
Pressure (psi)	Axial Displacement of Center Point on Window Low-Pressure Face (in.)							
1,000	0.003	0.001	0.003	0.002	0.002	0.003	0.002	0.001
2,000	0.004	0.002	0.004	0.003	0.0035	0.004	0.003	0.002
3,000	0.005	0.003	0.006	0.004	0.005	0.006	0.0045	0.003
4,000	0.006	0.0035	0.007	0.005	0.006	0.007	0.005	0.0035
5,000	0.007	0.004	0.008	0.006	0.007	0.008	0.006	0.004
6,000	0.008	0.011	0.009	0.007	0.008	0.011	0.009	0.007
7,000	0.009	0.012	0.010	0.008	0.009	0.012	0.010	0.008
8,000	0.0095	0.018	0.012	0.0085	0.012	0.018	0.012	0.0085
9,000	0.021	0.020	0.013	0.009	0.013	0.021	0.015	0.009
10,000	0.022	0.022	0.014	0.010	0.022	0.022	0.018	0.010
11,000	0.023	0.028	0.016	0.011	0.024	0.028	0.020	0.011
12,000	0.024	0.035	0.016	0.012	0.025	0.035	0.022	0.012
13,000	0.035	0.036	0.018	0.013	0.032	0.036	0.027	0.013
14,000	0.036	0.043	0.019	0.015	0.038	0.043	0.030	0.015
15,000	0.037	0.049	0.021	0.016	0.039	0.049	0.032	0.016
16,000	0.045	0.065	0.058	0.018	0.043	0.065	0.046	0.018
17,000	0.047	0.066	0.061	0.020	0.050	0.066	0.049	0.020
18,000	0.056	0.082	0.064	0.022	0.056	0.082	0.056	0.022
19,000	0.064	0.125	0.089	0.025	0.066	0.125	0.074	0.025
20,000	0.092		0.150	0.034	0.105	0.150	0.095	0.034
21,000	0.153			0.150		0.153	0.1515	0.150
Pressure at Failure (psi)	21,200	19,550	20,200	21,000	20,750	21,200	20,540	19,550

Table G-33. Test Data on 1-Inch-Diameter, 150° Windows With t/D Ratio of 0.625, in DOL Type I Flange

	Specimen Number					Maximum Value	Average Value	Minimum Value
	161	162	163	164	165			
Thickness, t (in.)	0.602	0.602	0.606	0.596	0.589	0.606	0.599	0.589
Temperature (°F)	67.7	69.0	66.0	70.4	68.4	70.4	68.3	66.0
Pressurization Rate (psi/min)	664	662	504	653	603	664	617	504
Pressure (psi)	Axial Displacement of Center Point on Window Low-Pressure Face (in.)							
1,000	0.002	0.005	0.004	0.002	0.003	0.005	0.0032	0.002
2,000	0.008	0.006	0.005	0.004	0.004	0.008	0.005	0.004
3,000	0.009	0.007	0.006	0.006	0.005	0.009	0.0066	0.005
4,000	0.010	0.008	0.007	0.007	0.006	0.010	0.0076	0.006
5,000	0.011	0.009	0.0085	0.008	0.007	0.011	0.0087	0.007
6,000	0.0115	0.010	0.0095	0.010	0.008	0.0115	0.0098	0.008
7,000	0.012	0.011	0.010	0.011	0.010	0.012	0.0108	0.010
8,000	0.013	0.012	0.012	0.012	0.011	0.013	0.012	0.011
9,000	0.014	0.013	0.013	0.013	0.011	0.014	0.013	0.011
10,000	0.014	0.014	0.0145	0.015	0.012	0.015	0.014	0.012
11,000	0.015	0.015	0.015	0.020	0.013	0.020	0.0156	0.013
12,000	0.016	0.016	0.0165	0.024	0.014	0.024	0.0173	0.014
13,000	0.017	0.017	0.018	0.026	0.015	0.026	0.0186	0.015
14,000	0.0175	0.018	0.0195	0.031	0.016	0.031	0.0204	0.016
15,000	0.018	0.020	0.0205	0.035	0.017	0.035	0.022	0.017
16,000	0.019	0.021	0.022	0.039	0.025	0.039	0.025	0.019
17,000	0.020	0.022	0.024	0.043	0.025	0.043	0.027	0.020
18,000	0.022	0.024	0.025	0.049	0.026	0.049	0.029	0.022
19,000	0.0245	0.025	0.027	0.055	0.032	0.055	0.035	0.0245
20,000	0.027	0.028	0.029	0.062	0.033	0.062	0.036	0.027
21,000	0.030	0.029	0.031	0.072	0.037	0.072	0.040	0.029
22,000	0.032	0.032	0.051	0.081	0.048	0.081	0.049	0.032
23,000	0.035	0.035	0.053	0.097	0.054	0.097	0.055	0.035
24,000	0.038	0.076	0.068	0.145	0.077	0.145	0.081	0.038
25,000	0.042	0.085	0.120			0.120	0.082	0.042
26,000	0.066	0.125	0.280			0.280	0.157	0.066
27,000	0.110					0.110	0.110	0.110
Pressure at Failure (psi)	27,500	26,850	26,150	24,800	24,700	27,500	26,000	24,700

Table G-34. Test Data on 2-Inch-Diameter, 30° Windows With t/D Ratio of 0.125, in DOL Type I Flange

	Specimen Number					Maximum Value	Average Value	Minimum Value
	166	167	168	169	170			
Thickness, t (in.)	0.244	0.254	0.257	0.265	0.264	0.265	0.257	0.244
Temperature (°F)	70.8	70.1	69.7	69.4	69.8	70.8	69.9	69.4
Pressurization Rate (psi/min)	697	570	687	517	662	697	627	517
Pressure (psi)	Axial Displacement of Center Point on Window Low-Pressure Face (in.)							
250	0.007	0.005	0.007	0.007	0.007	0.007	0.007	0.005
500	0.018	0.013	0.015	0.014	0.014	0.018	0.015	0.013
750	0.050	0.040	0.028	0.025	0.026	0.050	0.034	0.025
Pressure at Failure (psi)	850	850	900	900	900	900	880	850

Table G-35. Test Data on 2-Inch-Diameter, 30° Windows With t/D Ratio of 0.25, in DOL Type I Flange

	Specimen Number					Maximum Value	Average Value	Minimum Value
	171	172	173	174	175			
Thickness, t (in.)	0.490	0.485	0.490	0.485	0.485	0.490	0.487	0.485
Temperature (°F)	70.0	69.1	69.2	70.5	69.5	70.5	69.7	69.1
Pressurization Rate (psi/min)	658	604	659	679	655	679	651	604
Pressure (psi)	Axial Displacement of Center Point on Window Low-Pressure Face (in.)							
250	0.002	0.002	0.002	0.002	0.002	0.002	0.002	0.002
500	0.005		0.005	0.005	0.005	0.005	0.005	0.005
750	0.008		0.007	0.009	0.007	0.009	0.008	0.007
1,000	0.010	0.009	0.009	0.012	0.009	0.012	0.010	0.009
1,250	0.013	0.012	0.011	0.015	0.012	0.015	0.013	0.011
1,500	0.017	0.015	0.015	0.018	0.016	0.018	0.016	0.015
1,750	0.020	0.018	0.018	0.022	0.019	0.022	0.019	0.018
2,000	0.024	0.021	0.021	0.028	0.023	0.028	0.023	0.021
2,250	0.028	0.025	0.032	0.033	0.028	0.033	0.029	0.025
2,500	0.032	0.031	0.045	0.040	0.033	0.045	0.036	0.031
2,750	0.060	0.070	0.070	0.046	0.039	0.070	0.057	0.039
3,000	0.110	0.110	0.110	0.070	0.075	0.110	0.095	0.070
Pressure at Failure (psi)	3,225	3,175	3,250	3,250	3,275	3,275	3,235	3,175

Table G-36. Test Data on 2-Inch-Diameter, 30° Windows With t/D Ratio of 0.5, in DOL Type I Flange: t/D Ratio Validation Tests

	Specimen Number					Maximum Value	Average Value	Minimum Value
	176	177	178	179	180			
Thickness, t (in.)	0.957	0.954	0.954	0.971	0.965	0.971	0.960	0.954
Temperature (°F)	64.5	67	64.5	62.8	68	68	65.4	62.8
Pressurization Rate (psi/min)	435	657	663	613	657			
Pressure (psi)	Axial Displacement of Center Point on Window Low-Pressure Face (in.)							
1,000	0.005	0.011	0.008	0.007	0.011	0.011	0.008	0.005
2,000	0.013	0.028	0.019	0.012	0.029	0.029	0.020	0.012
3,000	0.021	0.048	0.037	0.025	0.050	0.050	0.036	0.021
4,000	0.050	0.076	0.061	0.048	0.075	0.076	0.062	0.048
5,000	0.078	0.104	0.091	0.074	0.105	0.105	0.090	0.074
6,000	0.113	0.151	0.128	0.110	0.154	0.154	0.132	0.110
7,000	0.200	0.249	0.207	0.189	0.250	0.250	0.219	0.189
8,000	0.450							
Pressure at Failure (psi)	8,100	7,400	7,450	7,900	7,300	8,100	7,630	7,300

Table G-37. Test Data on 2-Inch-Diameter, 30 Windows With t/D Ratio of 1.0, in DOL Type II Flange

	Specimen Number					Maximum Value	Average Value	Minimum Value
	181	182	183	184	185			
Thickness, t (in.)	2.008	0.981	1.981	1.993	2.001	2.008	1.993	1.981
Temperature (°F)	67	70	71	66	65	71	67.8	65
Pressurization Rate (psi/min)	658	655	666	655	661	666	659	655
Pressure (psi)	Axial Displacement of Center Point on Window Low-Pressure Face (in.)							
1,000	0.004	0.005	0.003	0.004	0.004	0.005	0.004	0.003
2,000	0.008	0.015	0.007	0.018	0.024	0.024	0.0144	0.007
3,000	0.013	0.027	0.042	0.046	0.034	0.046	0.0324	0.013
4,000	0.021	0.039	0.045	0.041	0.044	0.045	0.0380	0.021
5,000	0.034	0.051	0.073	0.057	0.061	0.073	0.0552	0.034
6,000	0.045	0.065	0.076	0.072	0.073	0.076	0.0662	0.045
7,000	0.059	0.082	0.099	0.088	0.092	0.099	0.0840	0.059
8,000	0.074	0.099	0.104	0.103	0.109	0.109	0.0978	0.074
9,000	0.093	0.117	0.110	0.118	0.124	0.118	0.1124	0.093
10,000	0.110	0.138	0.142	0.139	0.148	0.148	0.1354	0.110
11,000	0.133	0.165	0.156	0.168	0.171	0.171	0.1586	0.133
12,000	0.157	0.196	0.198	0.201	0.202	0.202	0.1908	0.157
13,000	0.190	0.240	0.234	0.228	0.240	0.240	0.2264	0.190
14,000	0.225	0.290	0.288	0.259	0.285	0.290	0.2694	0.225
15,000	0.267	0.335	0.334	0.299	0.325	0.335	0.3120	0.267
16,000	0.310	0.382	0.382	0.340	0.371	0.382	0.3570	0.310
17,000	0.349	0.429	0.442	0.379	0.425	0.442	0.4048	0.349
18,000	0.395	0.485	0.543	0.419	0.484	0.543	0.4652	0.395
19,000	0.440	0.570	0.675		0.581	0.675	0.5665	0.440
20,000	0.508				0.780	0.780	0.6440	0.508
Pressure at Failure (psi)	20,800	20,400	19,800	20,500	20,500	20,800	20,400	19,800

Table G-38. Test Data on 4.5-Inch-Diameter, 60° Windows With t/D Ratio of 0.125, in DOL Type I Flange

	Specimen Number					Maximum Value	Average Value	Minimum Value
	186	187	188	189	190			
Thickness, t (in.)	0.555	0.550	0.555	0.550	0.555	0.555	0.553	0.550
Temperature (°F)	67	67	67	67	67.5	67.5	67.1	67
Pressurization Rate (psi/min)	655	621	578	708	533	708	619	533
Pressure (psi)	Axial Displacement of Center Point on Window Low-Pressure Face (in.)							
250	0.010	0.011	0.018	0.015	0.032	0.032	0.017	0.010
500	0.044	0.042	0.055	0.050	0.078	0.078	0.054	0.042
750	0.088	0.090	0.095	0.090		0.095	0.090	0.088
Pressure at Failure (psi)	950	925	1,000	850	650	1,000	875	650

Table G-39. Test Data on 4.5-Inch-Diameter, 60° Windows With t/D Ratio of 0.25, in DOL Type I Flange

	Specimen Number					Maximum Value	Average Value	Minimum Value
	191	192	193	194	195			
Thickness, t (in.)	1.114	1.119	1.134	1.135	1.159	1.159	1.132	1.114
Temperature (°F)	67.1	67.0	65.5	68.8	70.7	70.7	67.8	65.5
Pressurization Rate (psi/min)	609	651	639	633	637	651	634	609
Pressure (psi)	Axial Displacement of Center Point on Window Low-Pressure Face (in.)							
1,000	0.022	0.013	0.015	0.014	0.014	0.022	0.016	0.013
2,000	0.052	0.044	0.042	0.040	0.044	0.052	0.044	0.040
3,000	0.089	0.079	0.078	0.072	0.080	0.089	0,080	0.072
4,000	0.136	0.130	0.128	0.121	0.132	0.136	0.129	0.121
5,000	0.208	0.212	0.201	0.195	0.197	0.212	0.203	0.195
Pressure at Failure (psi)	5,600	5,850	5,850	5,900	5,750	5,900	5,790	5,600

Table G-40. Test Data on 4.5-Inch-Diameter, 60° Windows With t/D Ratio of 0.5, in DOL Type I Flange: t/D Ratio Validation Tests

	Specimen Number					Maximum Value	Average Value	Minimum Value
	196	197	198	199	200			
Thickness, t (in.)	2.270	2.250	2.240	2.348	2.250	2.348	2.272	2.240
Temperature (°F)	62.5	67.5	64	69.5	63.5	69.5	65.4	62.5
Pressurization Rate (psi/min)	456	211	325	628	625	211	628	449
Pressure (psi)	Axial Displacement of Center Point on Window Low-Pressure Face (in.)							
1,000	0.006	0.008	0.008	0.011	0.004	0.011	0.007	0.004
2,000	0.014	0.019	0.023	0.017	0.029	0.029	0.020	0.014
3,000	0.020	0.036	0.038	0.026	0.034	0.038	0.031	0.020
4,000	0.032	0.053	0.055	0.045	0.055	0.055	0.048	0.032
5,000	0.048	0.070	0.071	0.062	0.065	0.071	0.063	0.048
6,000	0.066	0.089	0.089	0.081	0.091	0.091	0.083	0.066
7,000	0.086	0.112	0.108	0.103	0.122	0.122	0.106	0.086
8,000	0.108	0.136	0.129	0.127	0.128	0.133	0.126	0.108
9,000	0.137	0.168	0.155	0.155	0.160	0.168	0.155	0.137
10,000	0.175	0.224	0.198	0.181	0.188	0.224	0.191	0.175
11,000	0.211	0.303	0.230	0.213	0.234	0.303	0.238	0.211
12,000	0.241	0.412	0.294	0.274	0.282	0.412	0.301	0.241
13,000	0.282		0.436	0.337	0.363	0.436	0.354	0.282
14,000	0.341		0.700	0.438	0.490	0.700	0.492	0.341
15,000	0.441							
16,000	0.730							
Pressure at Failure (psi)	16,000	12,500	14,100	14,650	14,650	16,000	14,380	12,500

REFERENCES

1. Auguste Piccard. Earth, sky and the sea. New York, Oxford University Press, 1956.

2. Ocean Research Equipment, Inc. Staff Report 04651: Pressure tests of Plexiglas windows of ALVIN submarine. Falmouth, Mass., April 1965.

3. Allied Research Associates, Inc. Report ARA-F-271-5: Photoelastic investigation of stress in a penetrated atmosphere - final report, by H. Hamilton and H. Becker. Concord, Mass., Dec. 1964.

4. U. S. Naval Civil Engineering Laboratory. Technical Note TN-755: The conversion of 16-inch projectiles to pressure vessels. Port Hueneme, Calif., Aug. 1965.

U. S. Naval Civil Engineering Laboratory
WINDOW FOR EXTERNAL OR INTERNAL HYDROSTATIC PRESSURE VESSELS PART I – CONICAL ACRYLIC WINDOWS UNDER SHORT-TERM PRESSURE APPLICATION, by J. D. Stachiw and K. O. Gray
TR-512 100 p. illus Jan 1967 Unclassified

1. Undersea vessels 2. Conical acrylic windows I. Y-F015-01-07-001

Conical acrylic windows for fixed ocean-floor structures were placed under short-term loading (pressurization from zero to failure at a fixed rate). The windows, of different thicknesses and different included conical angles, were subjected to various applied pressures, and their subsequent behavior was studied.

Acrylic windows, in the form of truncated cones with included angles of 30°, 60°, 90°, 120°, and 150°, were tested to destruction at ambient room temperature by applying hydrostatic pressure to the base of the truncated cone at a continuous rate of 650 psi/min. The pressure at which the windows failed and the magnitude of displacement through the window mounting at different pressure levels were recorded. The ultimate strength of the conical windows (denoted by the critical pressure at which actual failure occurred) was found to be related both to thickness and included conical angle.

Graphs are presented defining the relationships of critical pressure versus thickness-to-diameter ratio, and pressure versus magnitude of displacement for the windows.

Nondimensional scaling factors for critical pressure and displacement applicable to large-diameter windows are discussed and presented in graphic form.

U. S. Naval Civil Engineering Laboratory
WINDOW FOR EXTERNAL OR INTERNAL HYDROSTATIC PRESSURE VESSELS PART I – CONICAL ACRYLIC WINDOWS UNDER SHORT-TERM PRESSURE APPLICATION, by J. D. Stachiw and K. O. Gray
TR-512 100 p. illus Jan 1967 Unclassified

1. Undersea vessels 2. Conical acrylic windows I. Y-F015-01-07-001

Conical acrylic windows for fixed ocean-floor structures were placed under short-term loading (pressurization from zero to failure at a fixed rate). The windows, of different thicknesses and different included conical angles, were subjected to various applied pressures, and their subsequent behavior was studied.

Acrylic windows, in the form of truncated cones with included angles of 30°, 60°, 90°, 120°, and 150°, were tested to destruction at ambient room temperature by applying hydrostatic pressure to the base of the truncated cone at a continuous rate of 650 psi/min. The pressure at which the windows failed and the magnitude of displacement through the window mounting at different pressure levels were recorded. The ultimate strength of the conical windows (denoted by the critical pressure at which actual failure occurred) was found to be related both to thickness and included conical angle.

Graphs are presented defining the relationships of critical pressure versus thickness-to-diameter ratio, and pressure versus magnitude of displacement for the windows.

Nondimensional scaling factors for critical pressure and displacement applicable to large-diameter windows are discussed and presented in graphic form.

U. S. Naval Civil Engineering Laboratory
WINDOW FOR EXTERNAL OR INTERNAL HYDROSTATIC PRESSURE VESSELS PART I – CONICAL ACRYLIC WINDOWS UNDER SHORT-TERM PRESSURE APPLICATION, by J. D. Stachiw and K. O. Gray
TR-512 100 p. illus Jan 1967 Unclassified

1. Undersea vessels 2. Conical acrylic windows I. Y-F015-01-07-001

Conical acrylic windows for fixed ocean-floor structures were placed under short-term loading (pressurization from zero to failure at a fixed rate). The windows, of different thicknesses and different included conical angles, were subjected to various applied pressures, and their subsequent behavior was studied.

Acrylic windows, in the form of truncated cones with included angles of 30°, 60°, 90°, 120°, and 150°, were tested to destruction at ambient room temperature by applying hydrostatic pressure to the base of the truncated cone at a continuous rate of 650 psi/min. The pressure at which the windows failed and the magnitude of displacement through the window mounting at different pressure levels were recorded. The ultimate strength of the conical windows (denoted by the critical pressure at which actual failure occurred) was found to be related both to thickness and included conical angle.

Graphs are presented defining the relationships of critical pressure versus thickness-to-diameter ratio, the pressure versus magnitude of displacement for the windows.

Nondimensional scaling factors for critical pressure and displacement applicable to large-diameter windows are discussed and presented in graphic form.

U. S. Naval Civil Engineering Laboratory
WINDOW FOR EXTERNAL OR INTERNAL HYDROSTATIC PRESSURE VESSELS PART I – CONICAL ACRYLIC WINDOWS UNDER SHORT-TERM PRESSURE APPLICATION, by J. D. Stachiw and K. O. Gray
TR-512 100 p. illus Jan 1967 Unclassified

1. Undersea vessels 2. Conical acrylic windows I. Y-F015-01-07-001

Conical acrylic windows for fixed ocean-floor structures were placed under short-term loading (pressurization from zero to failure at a fixed rate). The windows, of different thicknesses and different included conical angles, were subjected to various applied pressures, and their subsequent behavior was studied.

Acrylic windows, in the form of truncated cones with included angles of 30°, 60°, 90°, 120°, and 150°, were tested to destruction at ambient room temperature by applying hydrostatic pressure to the base of the truncated cone at a continuous rate of 650 psi/min. The pressure at which the windows failed and the magnitude of displacement through the window mounting at different pressure levels were recorded. The ultimate strength of the conical windows (denoted by the critical pressure at which actual failure occurred) was found to be related both to thickness and included conical angle.

Graphs are presented defining the relationships of critical pressure versus thickness-to-diameter ratio, the pressure versus magnitude of displacement for the windows.

Nondimensional scaling factors for critical pressure and displacement applicable to large-diameter windows are discussed and presented in graphic form.

Unclassified
Security Classification

DOCUMENT CONTROL DATA - R&D

(Security classification of title, body of abstract and indexing annotation must be entered when the overall report is classified)

1. ORIGINATING ACTIVITY *(Corporate author)*
U. S. Naval Civil Engineering Laboratory
Port Hueneme, California

2a. REPORT SECURITY CLASSIFICATION
Unclassified

2b. GROUP

3. REPORT TITLE
Window For External Or Internal Hydrostatic Pressure Vessels Part I — Conical Acrylic Windows Under Short-Term Pressure Application

4. DESCRIPTIVE NOTES *(Type of report and inclusive dates)*
Not Final; August 1965 - June 1966

5. AUTHOR(S) *(Last name, first name, initial)*
Stachiw, J. D.
Gray, K. O.

6. REPORT DATE	7a. TOTAL NO. OF PAGES	7b. NO. OF REFS
January 1967	100	4

8a. CONTRACT OR GRANT NO.	9a. ORIGINATOR'S REPORT NUMBER(S)
b. PROJECT NO. Y-F015-01-07-001	TR-512
c.	9b. OTHER REPORT NO(S) *(Any other numbers that may be assigned this report)*
d.	

10. AVAILABILITY/LIMITATION NOTICES
Distribution of this document is unlimited. Copies available at the Clearinghouse (CFSTI) $3.00.

11. SUPPLEMENTARY NOTES	12. SPONSORING MILITARY ACTIVITY
	Naval Facilities Engineering Command Washington, D. C.

13. ABSTRACT

Conical acrylic windows for fixed ocean-floor structures were placed under short-term loading (pressurization from zero to failure at a fixed rate). The windows, of different thicknesses and different included conical angles, were subjected to various applied pressures, and their subsequent behavior was studied.

Acrylic windows, in the form of truncated cones with included angles of 30°, 60°, 90°, 120°, and 150°, were tested to destruction at ambient room temperature by applying hydrostatic pressure to the base of the truncated cone at a continuous rate of 650 psi/min. The pressure at which the windows failed and the magnitude of displacement through the window mounting at different pressure levels were recorded. The ultimate strength of the conical windows (denoted by the critical pressure at which actual failure occurred) was found to be related both to thickness and included conical angle.

Graphs are presented defining the relationships of critical pressure versus thickness-to-diameter ratio, and pressure versus magnitude of displacement for the windows.

Nondimensional scaling factors for critical pressure and displacement applicable to large-diameter windows are discussed and presented in graphic form.

DD FORM 1 JAN 64 1473 *0101-807-6800*

Unclassified
Security Classification

14. KEY WORDS	LINK A		LINK B		LINK C	
	ROLE	WT	ROLE	WT	ROLE	WT
Undersea habitation Conical acrylic windows Hydrostatic pressure Short-term loading Failures						

INSTRUCTIONS

1. ORIGINATING ACTIVITY. Enter the name and address of the contractor, subcontractor, grantee, Department of Defense activity or other organization *(corporate author)* issuing the report.

2a. REPORT SECURITY CLASSIFICATION: Enter the overall security classification of the report. Indicate whether "Restricted Data" is included. Marking is to be in accordance with appropriate security regulations.

2b. GROUP: Automatic downgrading is specified in DoD Directive 5200.10 and Armed Forces Industrial Manual. Enter the group number. Also, when applicable, show that optional markings have been used for Group 3 and Group 4 as authorized.

3. REPORT TITLE: Enter the complete report title in all capital letters. Titles in all cases should be unclassified. If a meaningful title cannot be selected without classification, show title classification in all capitals in parenthesis immediately following the title.

4. DESCRIPTIVE NOTES: If appropriate, enter the type of report, e.g., interim, progress, summary, annual, or final. Give the inclusive dates when a specific reporting period is covered.

5. AUTHOR(S): Enter the name(s) of author(s) as shown on or in the report. Enter last name, first name, middle initial. If military, show rank and branch of service. The name of the principal author is an absolute minimum requirement.

6. REPORT DATE. Enter the date of the report as day, month, year; or month, year. If more than one date appears on the report, use date of publication.

7a. TOTAL NUMBER OF PAGES: The total page count should follow normal pagination procedures, i.e., enter the number of pages containing information.

7b. NUMBER OF REFERENCES: Enter the total number of references cited in the report.

8a. CONTRACT OR GRANT NUMBER. If appropriate, enter the applicable number of the contract or grant under which the report was written.

8b, 8c, & 8d. PROJECT NUMBER: Enter the appropriate military department identification, such as project number, subproject number, system numbers, task number, etc.

9a. ORIGINATOR'S REPORT NUMBER(S). Enter the official report number by which the document will be identified and controlled by the originating activity. This number must be unique to this report.

9b. OTHER REPORT NUMBER(S): If the report has been assigned any other report numbers *(either by the originator or by the sponsor)*, also enter this number(s).

10. AVAILABILITY/LIMITATION NOTICES: Enter any limitations on further dissemination of the report, other than those imposed by security classification, using standard statements such as:

(1) "Qualified requesters may obtain copies of this report from DDC."

(2) "Foreign announcement and dissemination of this report by DDC is not authorized."

(3) "U. S. Government agencies may obtain copies of this report directly from DDC. Other qualified DDC users shall request through _____."

(4) "U. S. military agencies may obtain copies of this report directly from DDC. Other qualified users shall request through _____."

(5) "All distribution of this report is controlled. Qualified DDC users shall request through _____."

If the report has been furnished to the Office of Technical Services, Department of Commerce, for sale to the public, indicate this fact and enter the price, if known.

11. SUPPLEMENTARY NOTES. Use for additional explanatory notes.

12. SPONSORING MILITARY ACTIVITY: Enter the name of the departmental project office or laboratory sponsoring *(paying for)* the research and development. Include address.

13. ABSTRACT: Enter an abstract giving a brief and factual summary of the document indicative of the report, even though it may also appear elsewhere in the body of the technical report. If additional space is required, a continuation sheet shall be attached.

It is highly desirable that the abstract of classified reports be unclassified. Each paragraph of the abstract shall end with an indication of the military security classification of the information in the paragraph, represented as *(TS), (S), (C), or (U)*

There is no limitation on the length of the abstract. However, the suggested length is from 150 to 225 words

14. KEY WORDS: Key words are technically meaningful terms or short phrases that characterize a report and may be used as index entries for cataloging the report. Key words must be selected so that no security classification is required. Identifiers, such as equipment model designation, trade name, military project code name, geographic location, may be used as key words but will be followed by an indication of technical context. The assignment of links, roles, and weights is optional.

Technical Report

R 773

NAVAL CIVIL ENGINEERING LABORATORY

Port Hueneme, California 93043

Sponsored by

NAVAL FACILITIES ENGINEERING COMMAND

August 1972

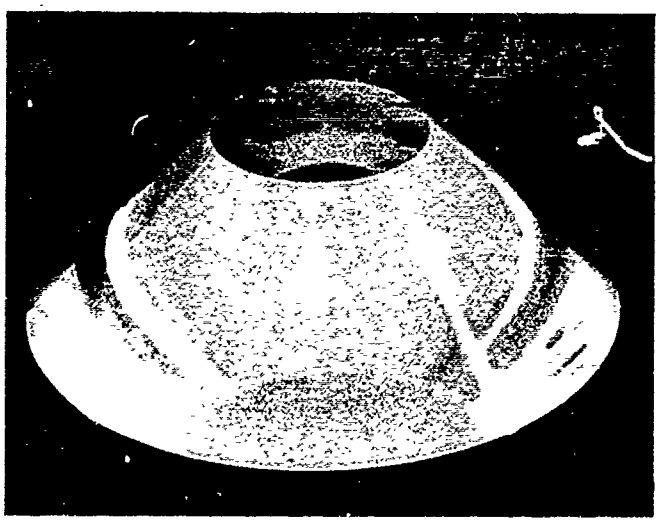

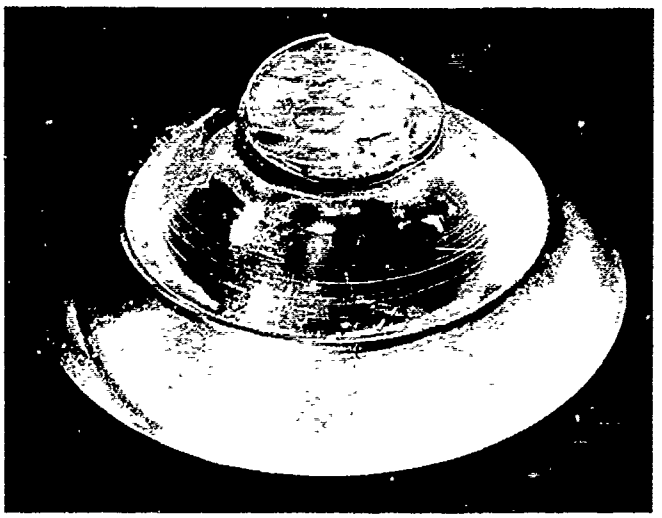

WINDOWS FOR EXTERNAL OR INTERNAL HYDROSTATIC PRESSURE VESSELS—PART VII. Effect of Temperature and Flange Configurations on Critical Pressure of 90-Degree Conical Acrylic Windows Under Short-Term Loading

WINDOWS FOR EXTERNAL OR INTERNAL HYDROSTATIC PRESSURE VESSELS—PART VII. Effect of Temperature and Flange Configurations on Critical Pressure of 90-Degree Conical Acrylic Windows Under Short-Term Loading

Technical Report R-773

YF 51.543.008.01.001

by

J. D. Stachiw and J. R. McKay

ABSTRACT

Conical acrylic windows of 90-degree included angle and 0.083 to 0.775 thickness-to-minor-diameter (t/D) ratios have been tested to ultimate failure under short-term hydrostatic loading. The ambient temperature was varied from 32°F to 90°F and the relationship between minor window diameter (D) and minor window cavity diameter in the flange (D_f) varied from 0.970 to 1.500. The test results show that the critical pressure of identical windows at 90°F is approximately *10% to 20%* less than at 70°F, and at 32°F it is approximately *15% to 25%* more than at 70°F. The increase in critical pressure of windows with identical t/D ratios due to changes in D/D_f ratio is as large as 100% from the critical pressures associated with the standard $D/D_f = 1.000$ ratio. As a rule, an increase in D/D_f ratio raised the critical pressure of windows with $t/D \geqslant 0.375$ significantly, while for windows with $t/D < 0.375$, it had no effect or very little. To improve the critical pressure of 90-degree conical acrylic windows, it is recommended that such windows be designed with a window/flange mismatch ratio of $D/D_f > 1.00$, the exact magnitude depending on the window's t/D ratio, service, and design considerations.

CONTENTS

INTRODUCTION

Background

Previous studies[1-3] of acrylic windows under short-term hydrostatic pressure were primarily directed towards the effect of hydrostatic pressure on windows of different structural shapes: conical frustums, flat discs, and spherical shell sectors. During the performance of the study of conical frustums,[1] it was discovered that both the ambient temperature and the location of the conical window's low-pressure face with respect to the edge of the beveled bearing surface in the flange cavity have a large effect on the ability of the window to withstand hydrostatic pressure without failure (Figure 1). The critical pressures (pressure at which ultimate failure of window occurs) of conical acrylic windows were found to vary during exploratory tests as much as 30% because of temperature changes in the 32°F-to-90°F range and as much as 60% because of changes in the window's elevation with respect to the bottom edge of the window seat in the flange. Therefore the effect of temperature and window seat elevation could not be considered as negligible. Recognizing the importance of these variables on the design of man-rated windows for undersea habitats, hyperbaric chambers, and internal pressure vessels for ocean simulation facilities, the Naval Facilities Engineering Command sponsored a study in this area as a part of the Ocean Engineering Program of the Naval Civil Engineering Laboratory (NCEL). This report is a summary of that study.

Objective

The objective of the study was to investigate the effect that (1) the ambient temperature and (2) window location with respect to the edge of the beveled bearing surface in the flange cavity have on the short-term critical pressure of conical acrylic windows. The data resulting from this study will permit the designers of window/flange assemblies for internal or external pressure vessels to (1) predict with greater certainty the ultimate short-term critical pressure of the selected window at any temperature and to (2) optimize the ultimate short-term strength of the window for the desired diameter by selecting the proper relationship between the minor diameter of the window (D) and the minor diameter of the conical flange cavity (D_f).

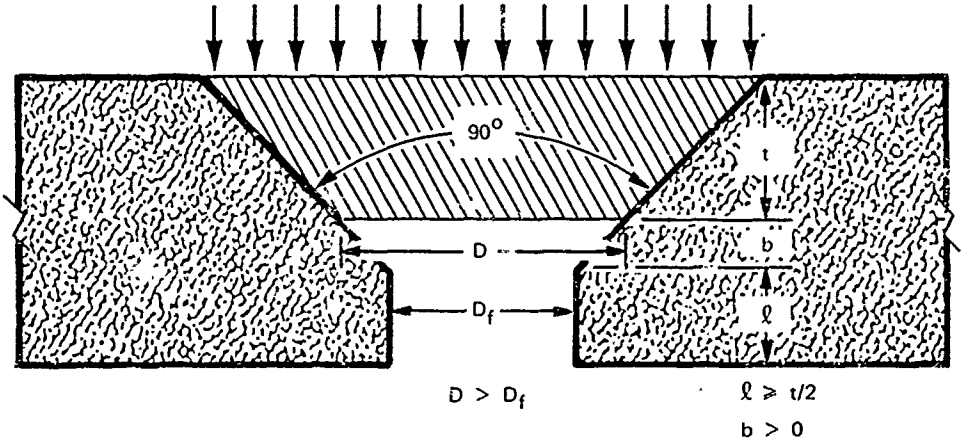

Note: D = minor diameter
D_f = minor flange opening diameter
t = window thickness

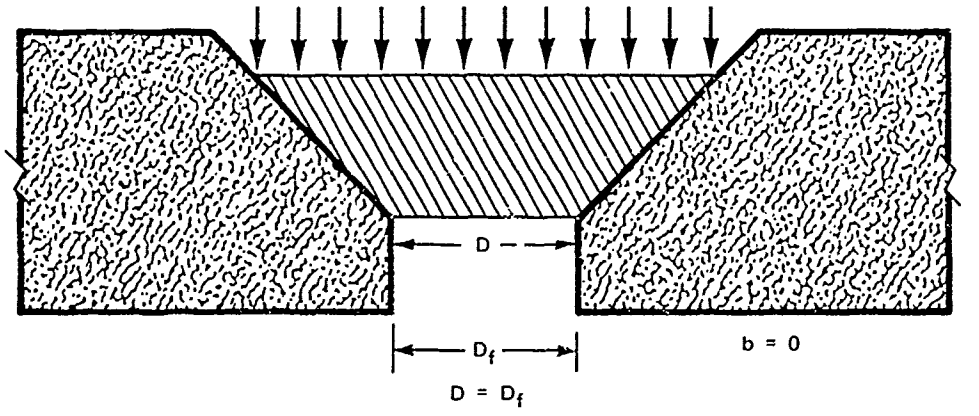

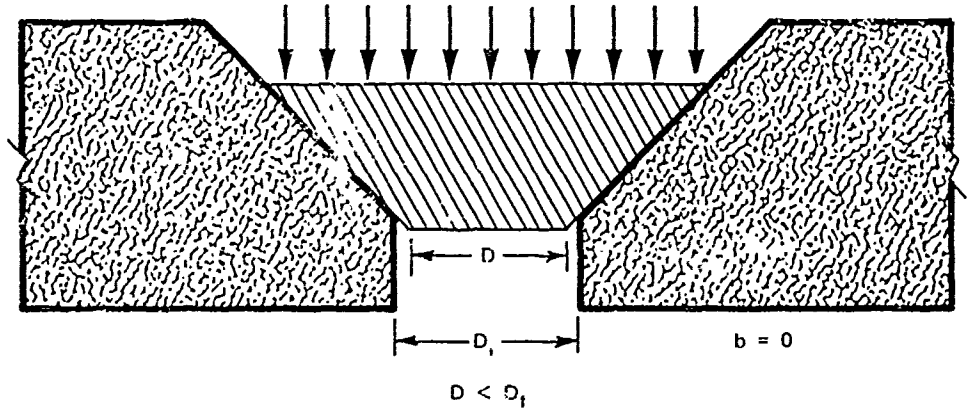

Figure 1. Typical window-seating arrangements for conical frustum acrylic windows. Critical pressure of window is maximized when b > 0; magnitude of b varies with t/D ratio.

Scope

The study was conducted experimentally and the relationships between variables derived empirically (Tables 1 and 2). Only short-term pressure loading was utilized to permit completion of the study within the existing framework of funding and pressure vessel availability. Since previous studies[1,4-6] have shown that windows of 90-degree included angle represent a good compromise between critical pressure, extrusion resistance, bulk, and cost for most typical pressure applications, only 90-degree windows were investigated at this time. The temperature variation was limited to 32°F-to-90°F range and it was varied in four discrete steps. The thickness-to-minor-diameter (t/D) ratio was varied from 0.083 to 0.775 in six steps; the relationship between minor diameter of the window (D) and minor diameter of the conical window cavity in the flange (D_f) was varied from 0.970 to 1.500 in seven steps. It was thought that by utilizing four different ambient temperatures, six t/D ratios, and seven D/D_f ratios in an experimental study limited to windows with only a single conical angle, an accurate picture would be generated of the interrelationship between these variables for 90-degree windows. Although the data generated by this study are true only for short-term loading conditions, with the proper selection of a safety factor they can serve also as conservative predictors for long-term loading conditions.

TEST SPECIMENS

The bulk of the test specimens were scale-model 90-degree conical acrylic windows (Figure 2). To validate the experimental data resulting from testing of the model windows, some full-scale windows were to be tested also (Figure 3). Both the model and full-scale windows were machined from commercially available Plexiglas G flat sheets and plates. The machining tolerances for model-scale windows were ±15 minutes for the included conical angle, ±0.002 inch for the minor diameter, and ±0.002 inch for the thickness. Dimensional tolerances for the full-scale windows were ±15 minutes for the angle, ±0.005 inch for the diameter, and ±0.010 inch for the thickness. The machining finish on the models' conical bearing surfaces was 63 rms, while the full-scale windows were polished all over after a finish of 63 rms was imparted by machining. After they were machined and polished, all windows were annealed at 175°F for 24 hours.

Table 1. Test Program for Investigation of Seating Arrangement Effect on Critical Pressure of 90-Degree Conical Acrylic Windows

(Material is unshrunk Plexiglas G (Federal Specification L-P-391 B); ambient temperature is 68°F to 72°F.)

Minor Diameter, D (in.)	No. of Specimens With Thickness, t of—						
	0.125 in.	0.250 in.	0.375 in.	0.500 in.	0.625 in.	0.750 in.	2.000 in.
0.970	5	5	5	5	5	5	–
1.000	5	5	5	5	5	5	–
1.030	5	5	5	5	5	5	–
1.060	5	5	5	5	5	5	–
1.125	5	5	5	5	5	5	–
1.250	5	5	5	5	5	5	–
1.500	5	5	5	5	5	5	–
3.880	–	–	–	–	–	–	4
4.000	–	–	–	–	–	–	1
4.120	–	–	–	–	–	–	1
4.240	–	–	–	–	–	–	4
4.500	–	–	–	–	–	–	1
5.000	–	–	–	–	–	–	1
6.000	–	–	–	–	–	–	4
6.400	–	–	–	–	–	–	2
8.500	–	–	–	–	–	–	2

Table 2. Test Program for Investigation of Temperature Effect on Critical Pressure of 90-Degree Conical Acrylic Windows

(Material is unshrunk Plexiglas G; ambient temperatures are shown below.)

Temperature (°F)	Minor Diameter, D (in.)	No. of Specimens With Thickness, t of—					
		0.125 in.	0.250 in.	0.375 in.	0.500 in.	0.625 in.	0.750 in.
32	1.000	5	5	5	5	5	5
	1.500	5	5	5	5	5	5
50	1.000	5	5	5	5	5	5
	1.500	5	5	5	5	5	5
90	1.000	5	5	5	5	5	5
	1.500	5	5	5	5	5	5

Material: Plexiglas G, Federal Specification L-P-391 B

Nomenclature

D = minor diameter (in.)
t = thickness (in.)
α = included conical angle (deg)

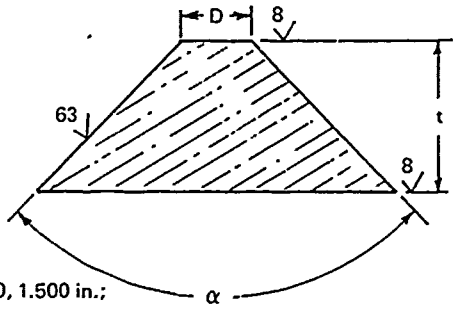

Dimensions

1. Model windows:

   D = 0.970, 1.000, 1.030, 1.060, 1.125, 1.250, 1.500 in.; tolerance = ±0.005
   t = 0.125, 0.250, 0.375, 0.500, 0.625, 0.750 in.; tolerance = ±0.002
   α = 90 deg; tolerance = ±15 min

2. Full-scale windows:

   D = 4.0 in.; tolerance = ±0.010
   t = 3.880, 4.000, 4.120, 4.240, 4.500, 5.000, 6.000, 6.400, 8.500 in.; tolerance = ±0.010
   α = 90 deg; tolerance = ±15 min

Figure 2. Typical model and full-scale acrylic plastic windows.

Since, from the previous studies[1-12] with acrylic windows and complete acrylic pressure hulls, it is known that the mechanical and physical properties of Plexiglas G do not vary significantly (1) from one sheet of material to another, and (2) between sheets of different thickness, no material test program was undertaken during this study. Because of this reproducibility in material properties inherent in Plexiglas G, it is assumed that all the data generated in this study are interrelated without any conversion factor with the data generated in the previous NCEL window and pressure hull studies that also utilized Plexiglas G material.

TEST FLANGES

For the testing of windows, two kinds of flanges of 90-degree included angle were employed The flange for testing models had a window cavity with 1-inch minor diameter (Figure 4a), while the one for the full-scale windows had a 4-inch minor diameter (Figure 4b). In both cases, the dimensional tolerances for the minor diameter were ±0.001 inch, while for the included conical angle they were ±5 minutes. The machining finish on the conical bearing surface in each case was 63 rms. Since dimensional changes of the flanges can influence the critical pressure of windows significantly, precautions were taken to make the flanges as rigid as possible. Because of the massive construction selected for the flanges, they were assumed to be perfectly rigid with respect to the windows tested.

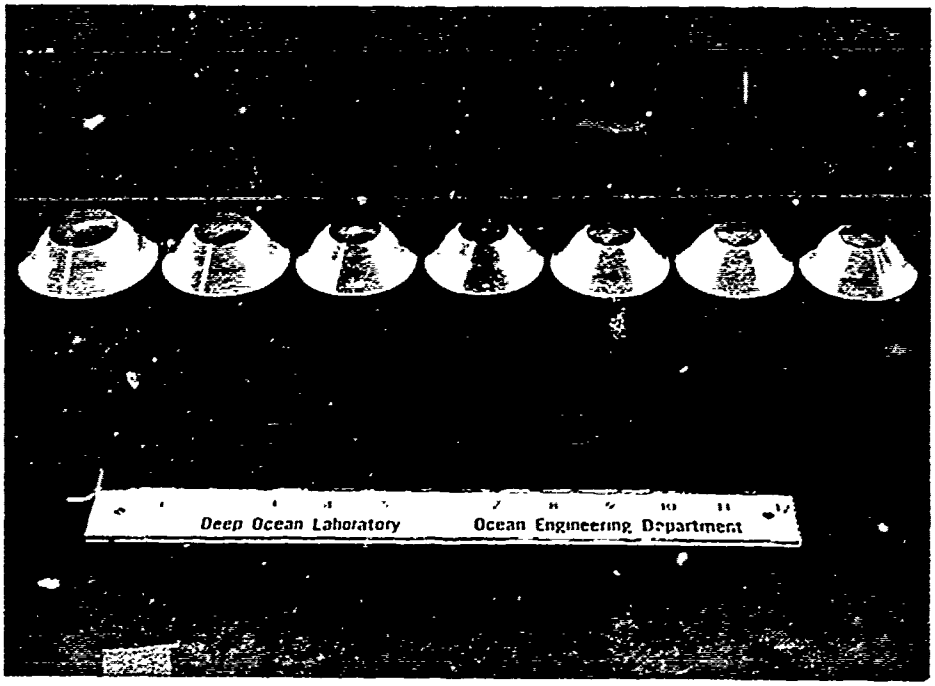

Figure 3a. Typical model acrylic plastic windows.

Figure 3b. Typical full-scale acrylic plastic windows.

Nomenclature

M = external flange diameter (in.)
α = included conical angle (deg)

Dimensions

α = 90 deg; tolerance = ±15 min
M = 4 in.

Material: 4130 steel

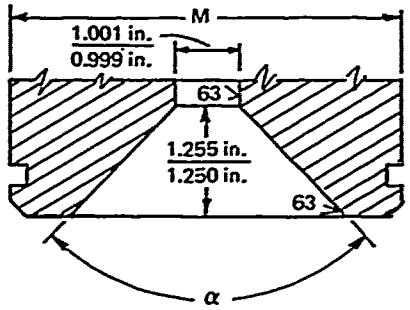

Figure 4a. Dimensions of flange for testing model windows.

Nomenclature

M = external flange diameter (in.)
L = overall flange thickness (in.)
k = cylindrical passage length (in.)
α = included conical angle (deg)

Dimensions

α = 90 deg; tolerance = ±5 min
M = 17-3/4 ± 1/64 in.
k = 1 ± 1/64 in. for 90-deg windows
L = 5 ± 1/64 in. for 90-deg windows

Material: 4130 steel

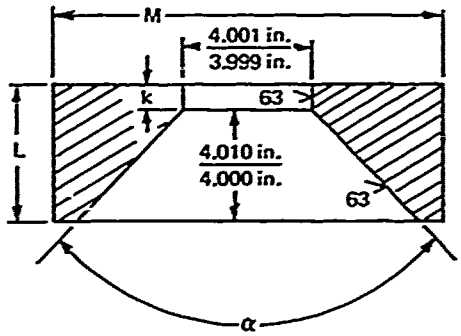

Figure 4b. Dimensions of flange for testing full-scale windows.

TEST ARRANGEMENT

Pressure Vessels

The hydrostatic testing of the windows was performed in two different vessels because of the large variation in sizes of windows tested and pressures required for their ultimate failure.

The *model windows* were tested in a 50,000-psi maximum operational pressure vessel. This 50,000-psi operational pressure vessel was a 5-inch-diameter vessel custom-built for testing windows at high pressure (Figure 5). The special features of the vessel are (1) the window flange being integral with the end closure and (2) temperature control in 32°F-to-120°F range.

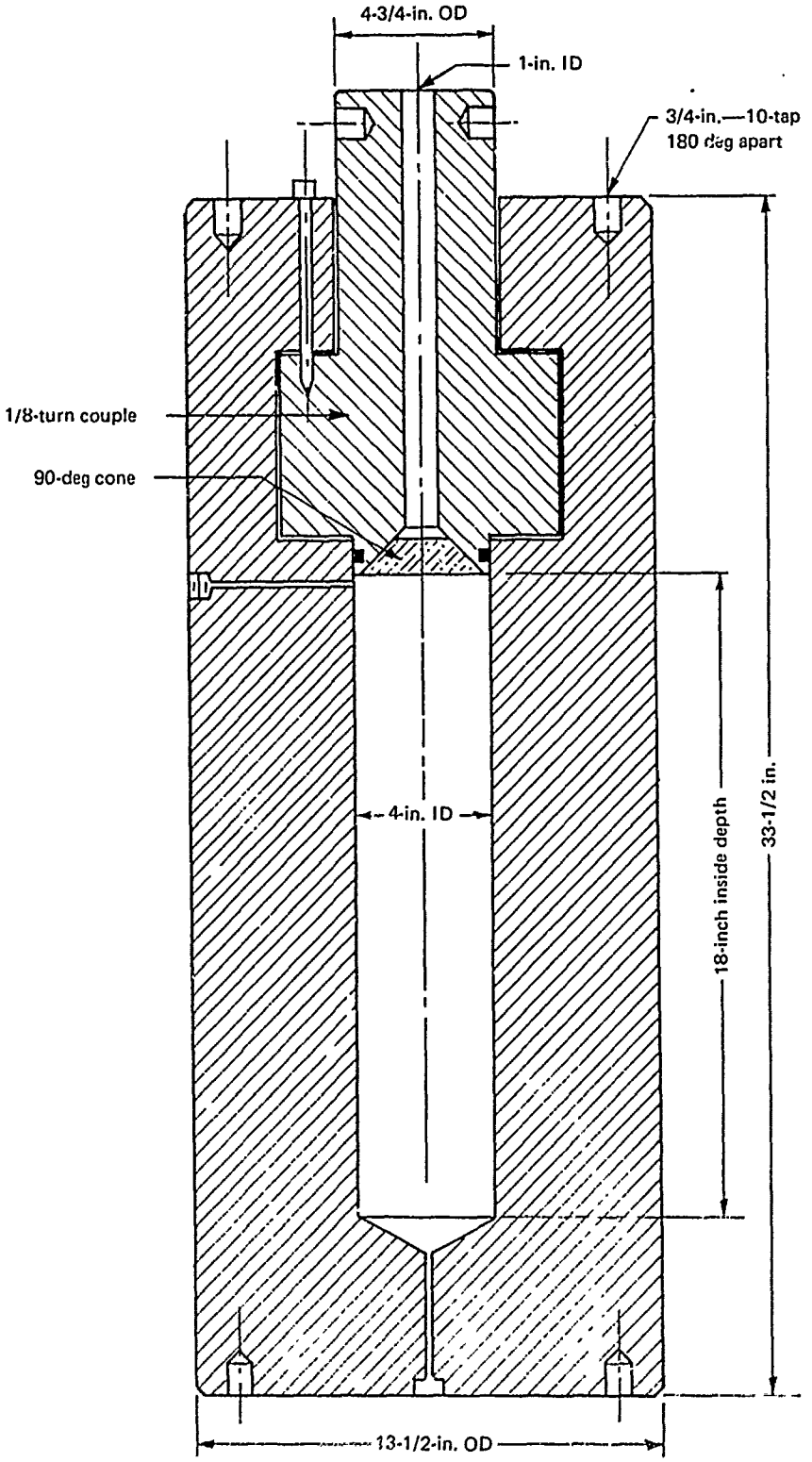

Figure 5. Ocean-pressure simulator with 50,000-psi capability used for testing model windows.

The *full-scale windows* were tested in an 18-inch-diameter vessel with 20,000-psi internal pressure capability (Figure 6). The special features of the vessel were (1) temperature control in 32°F-to-120°F range and (2) trunnion mounting, permitting the orientation of the vessel either in vertical or horizontal attitude.

Pumps

Pressurization of all the vessels was accomplished by means of air-operated, positive-displacement pumps. The pressurizing medium used in the 18-inch-diameter pressure vessel was tap water, while in the 5-inch-diameter vessel it was hydraulic oil. In all cases, the pressurization rate was controlled by manual throttling of pressurized air operating the pumps. Because of the precision with which the supply of pressurized air could be regulated, the pressurization rate of the vessels could be controlled within ±50 psi/min around the specified 650-psi/min rate.

Instrumentation

The instrumentation for the measurement of *test conditions* consisted of a remotely reading Bourdon-tube-type thermometer with 1°F resolution and remotely reading Bourdon-tube-type pressure gages with 1-psi resolution in the 0-to-1,000-psi, 10-psi in the 1,000-to-10,000-psi, 20-psi in the 10,000-to-30,000-psi, and 50-psi in the 30,000-to-50,000-psi pressure range. The *displacement* of the window through the flange opening was measured with a mechanical measuring device consisting of a dial indicator, and wire/pulley system connecting the dial indicator with the center of the window's low-pressure face (Figure 7). The wire was anchored to the center of the window's low-pressure face by means of an acrylic post bonded with acrylic cement to the window face. Since the anchor was bonded and not mechanically fastened to the window surface, it did not affect in any manner the window's strength under hydrostatic loading.

The ultimate failure of the window at critical pressure was accompanied by a loud explosion and ejection of a high-pressure jet of water from the vessel's interior through the flange opening. To protect the test personnel from any hazards associated with the forceful emission of water and window fragments, the dial indicator readings were transmitted by television camera and video console system from the vessel to the test control center located behind massive concrete blast deflectors. In this manner, the source of error in the displacement readout system was minimized by keeping the wire between the dial indicator and the window as short as possible while at the same time maximizing the safety of the test operator by removing him from the immediate vicinity of the vessel.

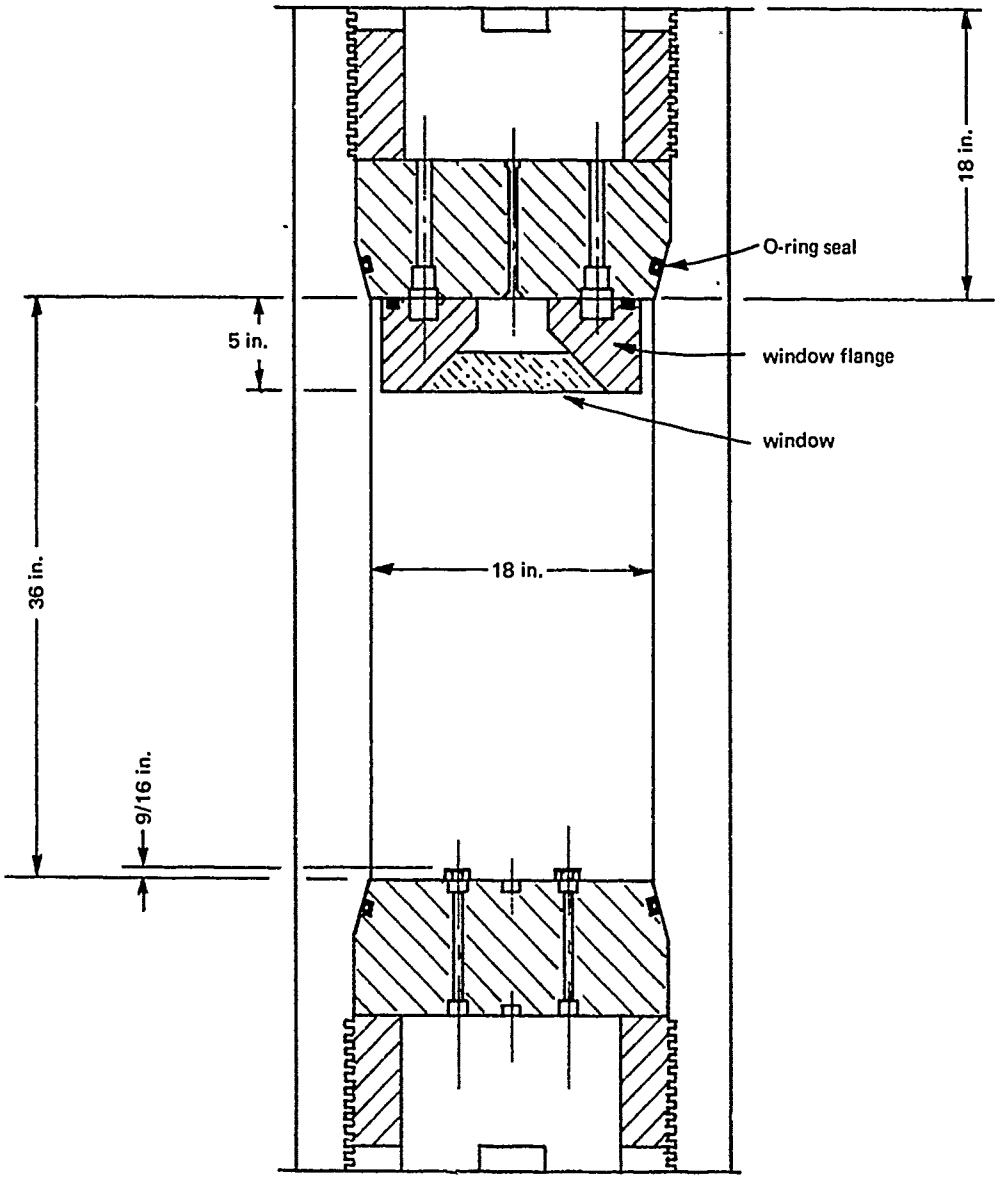

Figure 6. Ocean-pressure simulator with 20,000-psi capability used for testing full-scale windows.

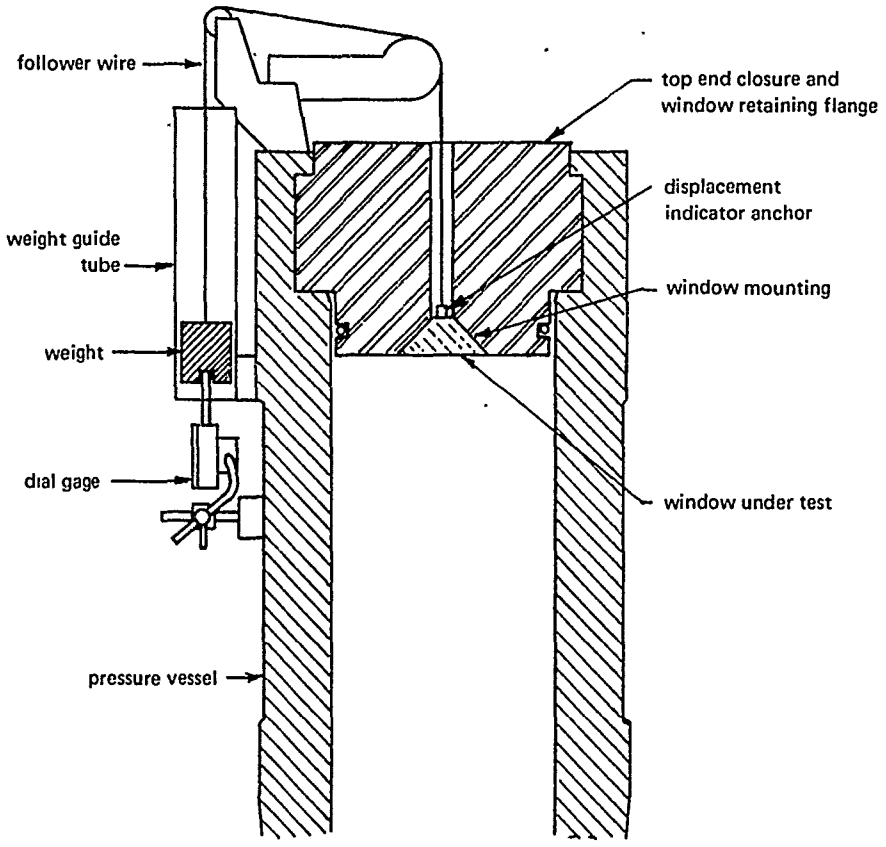

Figure 7. Arrangement for measuring window displacements through retaining flange.

TEST PROCEDURE

To standardize the test conditions for the window test program, a procedure was developed that was followed during all the tests in this study. This procedure had as its objective to ensure that (1) the thickness of the grease, (2) the length of exposure to ambient water temperature, and (3) the rate of pressurization to failure did not introduce additional variables into the test program.

The *effect of grease thickness* on the flange seating surface was minimized by preloading each window in the flange with hydrostatic pressure for 5 minutes. The preloading pressure (t x 500 psi for model windows and t x 125 psi for full-scale windows) was considered sufficient to squeeze out all the grease surplus from between the window and the flange, while at the same time the pressure was not high enough to induce any permanent deformation of the window. At the conclusion of the preloading period, the pressure on the window was reduced to zero and the displacement measurement system rezeroed by adjusting the dial indicator.

The *effect of temperature exposure duration* was minimized by temperature conditioning all of the windows that were to be tested at temperatures above or below 70°F room temperature. The temperature conditioning was performed by placing the window overnight in a water bath at the same temperature as the pressure vessel before mounting the window into the flange for testing. After removal from the temperature conditioning bath, the window was mounted into the flange (Figures 8 and 9) and immediately lowered (Figures 10 and 11) into the pressure vessel already filled with the pressurizing medium preconditioned to the desired temperature. After locking of the end closure (Figure 12), the windows were immediately hydrostatically preloaded, bringing pressurizing fluid in contact with the window and the end closure. Because the windows were temperature preconditioned and subsequently during the test kept at the desired ambient temperature by leaving the high-pressure face of the window wetted by the pressurizing fluid at preset temperature, it can be safely assumed that the temperature of the acrylic during the application of hydrostatic pressure was essentially the same as the ambient temperature of the pressurizing medium.

The *effect of pressurizing rate* was minimized by controlling the pressurization rate accurately. The pressurization rate was maintained at 650 psi/min with ±50-psi/min variation limits. The selection of 650 psi/min as the standard pressurization rate was based on the fact that all other previous short-term pressurization tests on windows at NCEL utilized this particular rate. In view of this, a comparison of critical pressures for different t/D and D/D_f ratios or temperatures is feasible, as the pressurization rate in all of these studies was a constant rather than a variable.

TEST OBSERVATIONS

The test observations were limited to three factors: (1) displacement, (2) mode of failure at critical pressure, and (3) critical pressure. Some aspects of observations (like magnitude of displacement and critical pressure) lent themselves to quantifying and recording in digital form. Other aspects of observations could only be recorded qualitatively. Such aspects were character of displacement (jerky, smooth, sudden, etc.), rate of energy release at failure (loud bang or quiet hiss), and mechanism of failure (flexure, plug extrusion, etc.).

Appendixes A and B discuss the presentation of experimental data from the observations and the application of such data to design of pressure-resistant windows.

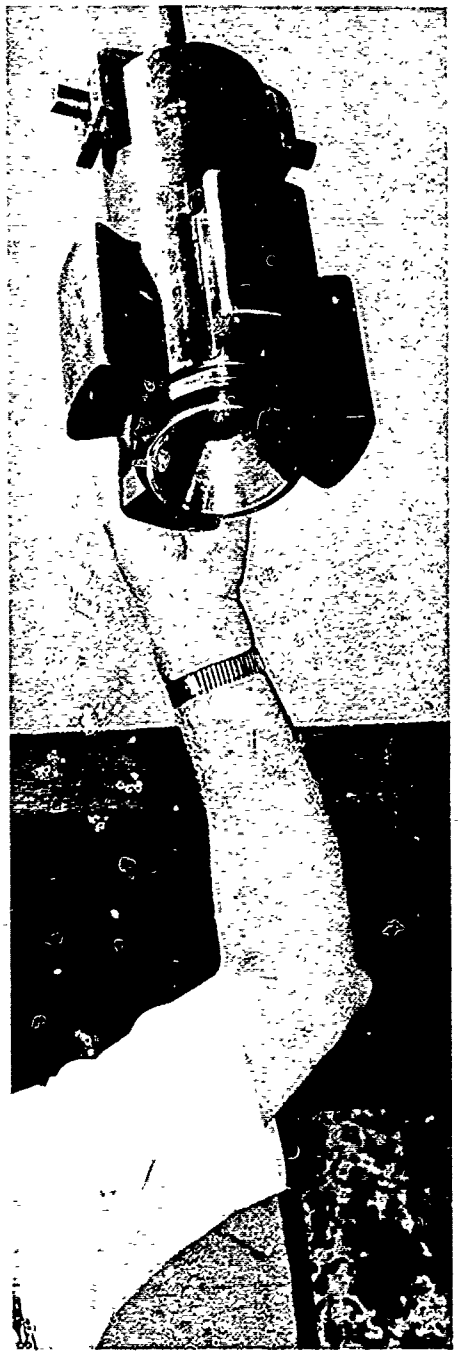

Figure 8. Vessel end closure with integral window flange before installation of model window for testing to 50,000 psi.

Figure 9. Installation of window.

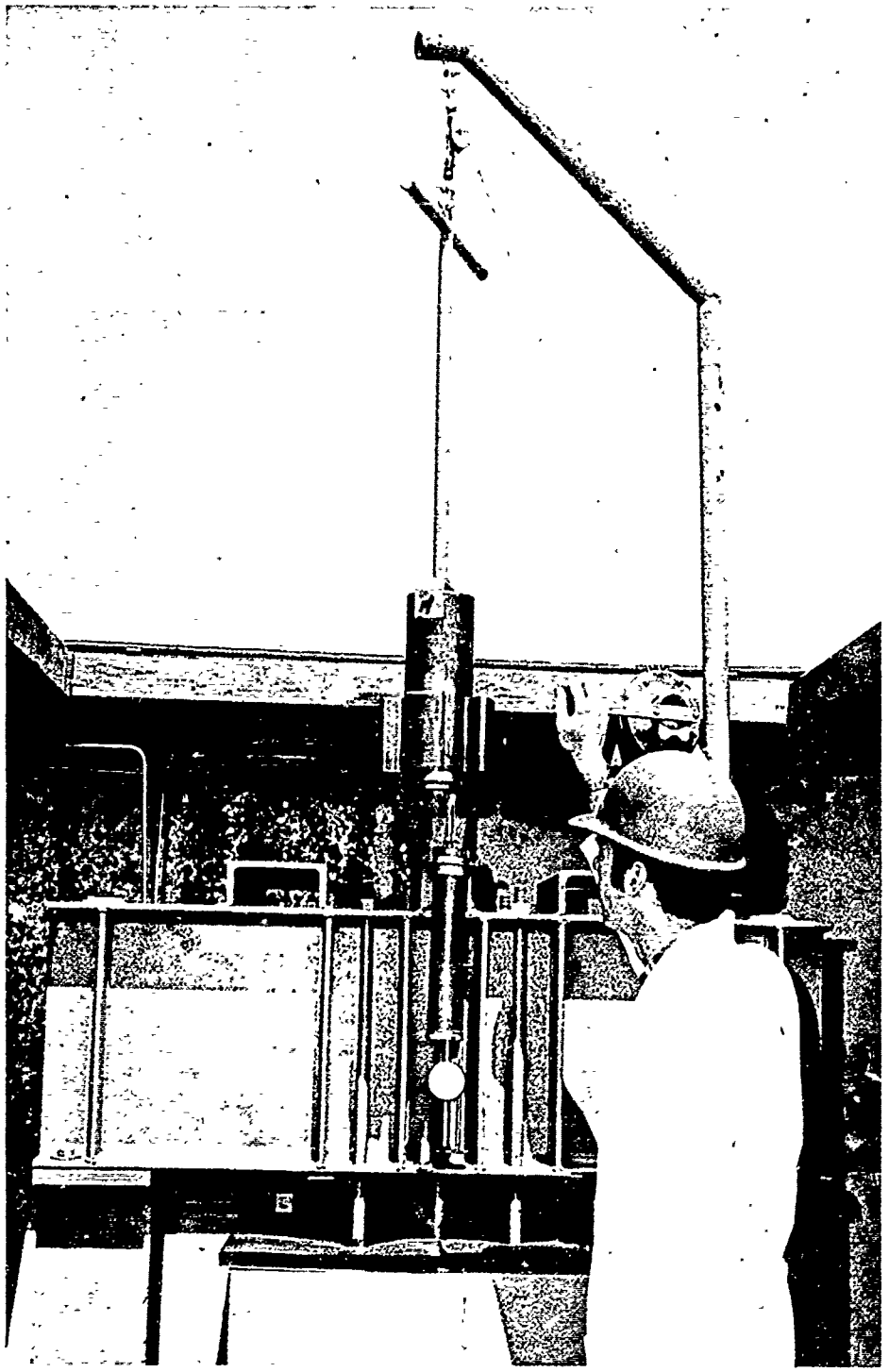

Figure 10. Lowering end closure into pressure vessel.

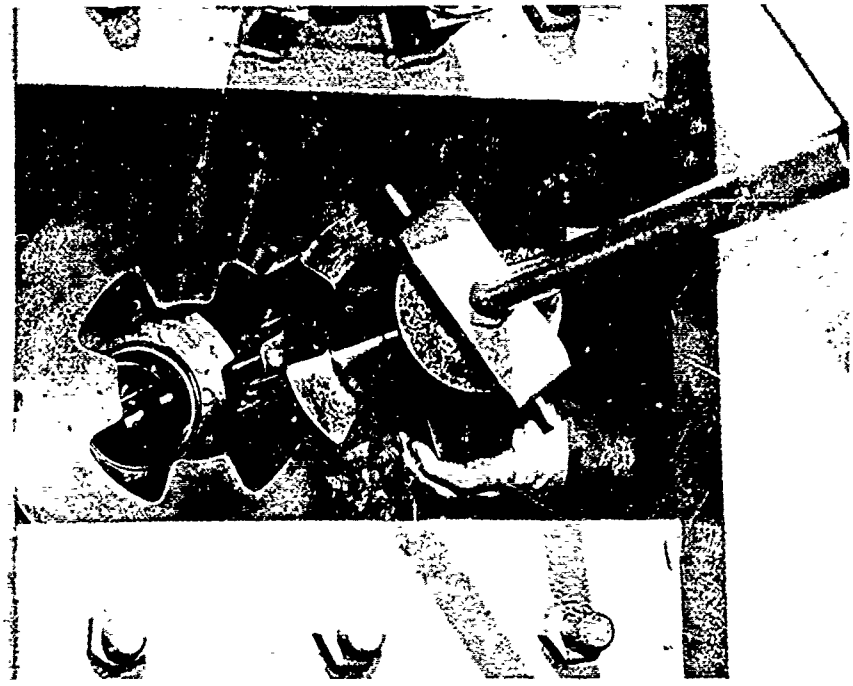

Figure 11. Aligning end closure lugs with slots in pressure vessel.

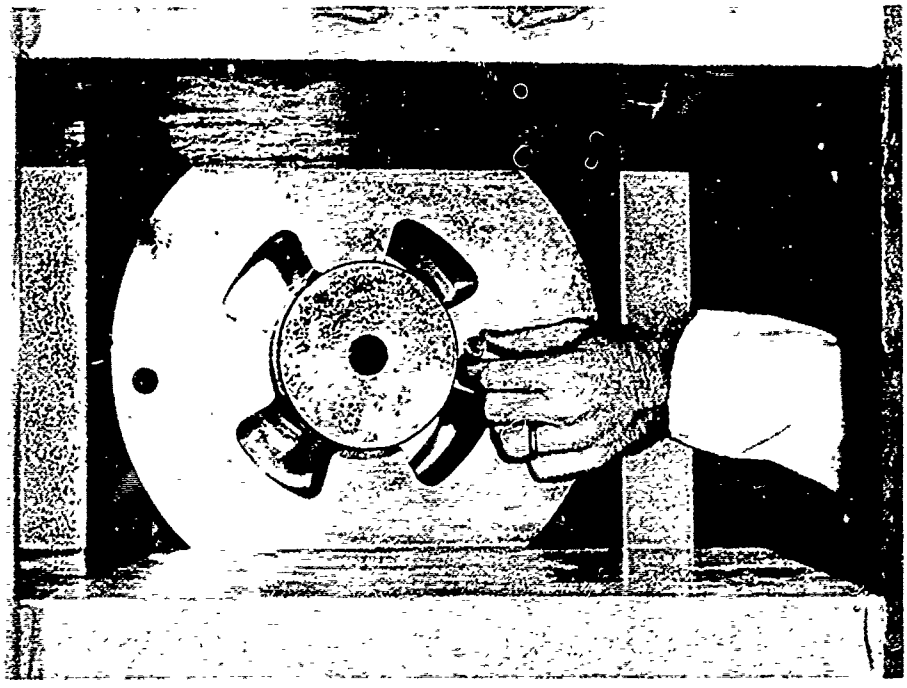

Figure 12. Securing locked assembly with pins.

Displacement

All windows displaced with an increase in hydrostatic pressure. However, whereas the displacement of windows with $t/D \leqslant 0.125$ was stepped, that of thicker windows was smooth. This stepped displacement coincided with the pulsation in pressure resulting from the action of the positive-large displacement pump on a small volume of contained liquid.

Windows with $t/D \geqslant 0.500$ displaced at a reasonably constant rate until moments before failure where an order-of-magnitude increase in displacement rate would take place. Windows with $t/D \geqslant 0.625$ did not exhibit a sudden increase in displacement rate at any time before failure. For these windows, the displacement rate was relatively steady and constant until failure actually took place.

The magnitude of displacement was not only a function of the window's t/D ratio but also of the temperature and the window/flange D/D_f ratio. For windows of a given t/D ratio, the magnitude of displacement at any particular pressure was directly related to temperature and inversely to D/D_f ratio. For example, at $32^{\circ}F$ the displacement of windows with $t/D = 0.500$ under 10,000-psi loading was 0.22D for $D/D_f = 1.000$, while for $D/D_f = 1.500$, it was 0.015D. At $90^{\circ}F$, the displacement of windows with $t/D = 0.500$ under 10,000-psi loading was, on the other hand, 0.051D for $D/D_f = 1.000$ and 0.032D for $D/D_f = 1.500$ (Appendix A—Figures A-1 through A-13).

Modes of Failure

Not all of the windows failed, as the pressurizing capability of the pump was limited to 48,000 psi, which in many cases did not prove to be sufficient for blowing out some of the thick windows with $t/D = 0.750$. There were basically four modes of failures among those windows that failed, depending on the window's t/D and window/flange D/D_f ratios.

The windows with $t/D = 0.125$, regardless of their D/D_f ratio, failed in a pattern typical of thin membranes under flexure: radial cracks radiate from the center of the windows towards the periphery (Figure 13). The destruction of the windows was total, with most of the fragments resembling circular sectors. A sudden loud blast accompanied the failure.

Windows with $0.250 \leqslant t/D \leqslant 0.375$, regardless of their D/D_f ratio, failed in a pattern typical of thick membranes under flexure: the radial cracks radiate from the center of the windows, but before failure of the window the cracks coalesce into a rough conical fracture surface. The apex of the conical fracture surface intersected the center of the window's high-pressure face, while the base of the fracture surface intersected the

window's low-pressure face at its very edge (in some cases, it intersected the bearing surface near the edge of the low-pressure face). The failure was characterized by (1) very little cold flow on the high and low-pressure window faces, and by (2) the ejection of the acrylic fragments contained within the fracture cone (Figure 14), and (3) slow release of pressure from the interior of the vessel through the relatively small hole in the window's high-pressure face. The release of pressure was accompanied by a loud hiss rather than a bang.

The windows with $t/D \geq 0.500$ failed in a manner that was dependent on the window/flange D/D_f ratio. Windows with $0.970 \leq D/D_f \leq 1.060$ failed in a manner similar to windows with $0.250 \leq t/D \leq 0.375$ but with a loud bang. No fragments of the window remained in the flange, since the high-velocity stream of pressurizing fluid ($P_c > 18{,}000$ psi) tore from the flange even the annular fragment of the window that was restricting its flow by the relatively small fracture hole in its center.

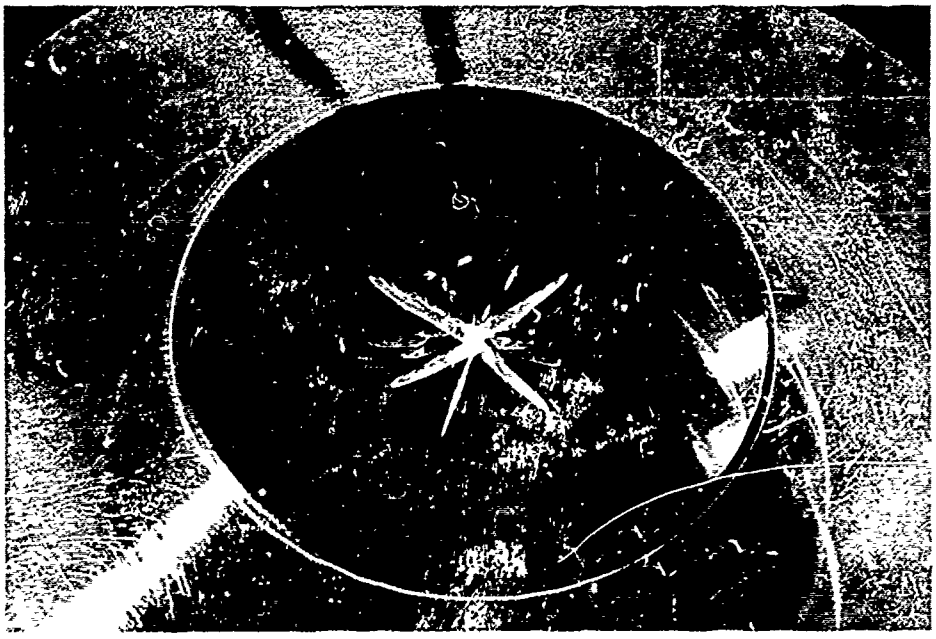

Figure 13. Typical thin-membrane flexure failure of windows with $t/D \leq 0.125$; low-pressure face.

Windows with $t/D \geq 0.500$, but window/flange arrangement $D/D_f \geq 1.125$, failed in two phases (Figure 15). The *first phase* of the failure was a shear-type failure characterized by (a) large cold-flow cratering on the high-pressure face (Figure 16), (b) considerable cold-flow extrusion on the low-pressure face, and (c) gradual separation of a cone-shaped fragment of acrylic from the rest of the window body. The shear cone intersected

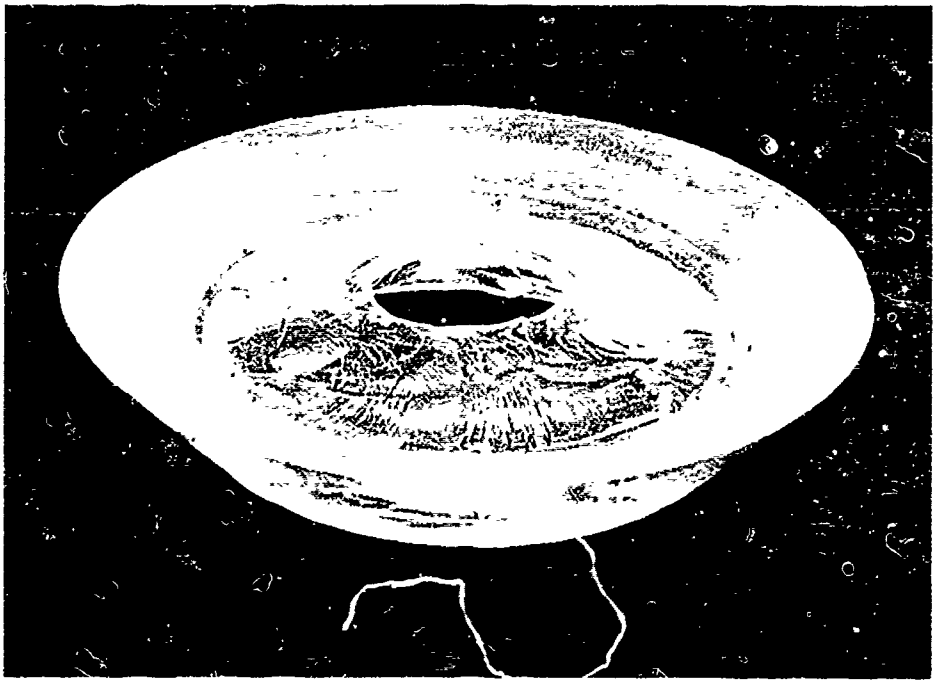

(a) High-pressure face.

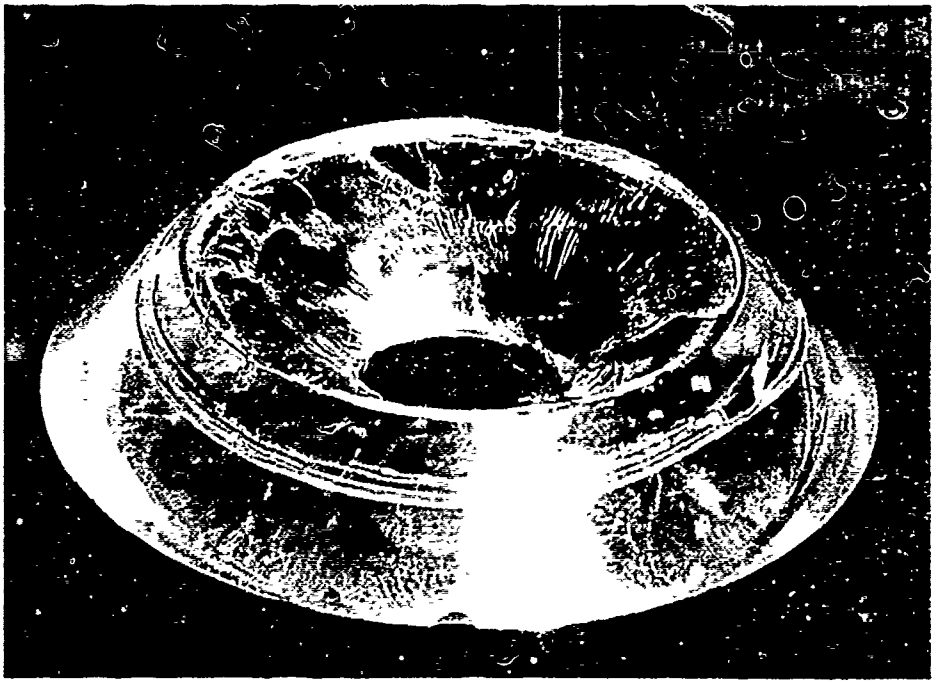

(b) Low-pressure face.

Figure 14. Typical thick-membrane flexure failure of windows with $0.250 \leqslant t/D \leqslant 0.375$.

both the high-pressure face and the bearing area of the window. Interestingly enough, the bearing surface was intersected approximately midway between the low- and high-pressure faces. The intersection of the shear cone and of the high-pressure face resulted in a penetration significantly larger than the penetrations observed during failure of windows with t/D ratio in the 0.250-to-0.375 range. Measurement of the penetration diameter revealed that it was invariably equal to or slightly larger than the D_f of the flange, while the penetrations for the $0.250 \leqslant t/D \leqslant 0.375$ windows were generally less than $0.5D_f$ of the flange.

Another interesting feature of the shear-cone failure was the smoothness of the conical fracture (Figure 16) surface, so strikingly different from the roughness of the flexure-type fracture surface found in 0.250 and 0.375 t/D windows. No flow of water took place during the first phase of the failure, as the central fragment of the window was still substantial enough to act as a plug in the flange.

The *second phase* of the failure was a massive flow extrusion failure of the central window fragment. During this phase while the central window fragment was extruded through the minor flange diameter, the annular window fragment resulting from the shear failure of the first phase did not see any further action, as it was subjected now only to purely isostatic loading. The second phase of failure concluded after further operation of the pressurizing pump with the forceful ejection of the central window fragment through the small bottom opening in the flange cavity. Since the diameter of the penetration in the annular window fragment was larger than the diameter of the small bottom opening in the flange, no restriction was imposed on the jet of rapidly escaping pressurizing medium and thus the annular window fragment was not torn from the flange during the rapid depressurization.

Critical Pressures

The magnitude of critical pressures was found to be a function of temperature, and D/D_f and t/D ratios. The fact that the critical pressure of a window is a function of these variables was established in previous studies, but only the effect of t/D ratio was quantitatively described. This study permitted quantitative establishment of the effect of D/D_f and temperature also. Comparison was made of the magnitudes of critical pressures for windows with different t/D and D/D_f ratios but at the same ambient temperature. It was noted that the D/D_f ratio has a very significant effect on the critical pressure of some windows but a negligible effect on others, depending on their t/D ratio (Figure 17). In general, as the t/D ratio increased so did the effect of the D/D_f ratio. For t/D ratios $\leqslant 0.300$, the

effect of changing the D/D_f ratio for a given t/D ratio was negligible, while for t/D ratios $\geq$0.300, the effect was significant. For example, windows with t/D = 0.500 experienced a gain in critical pressure of approximately 20,000 psi (about 100%) when the D/D_f parameter was varied from 0.970 to 1.500. For windows with larger t/D ratios, the effect should be even more pronounced, but the lack of experimental data on windows with t/D > 0.500 precludes any quantitative description (Appendix A—Figures A-14 through A-19).

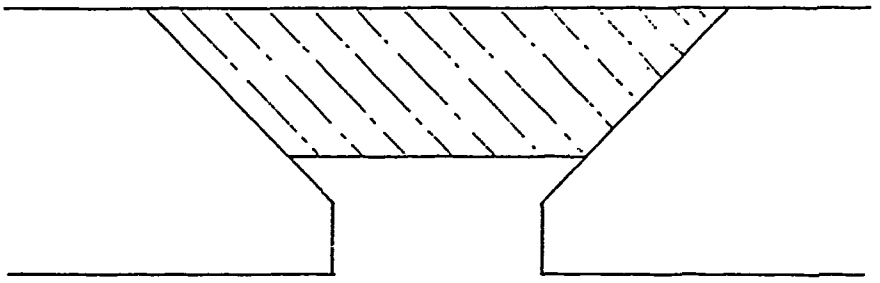

(a) Window before pressurization.

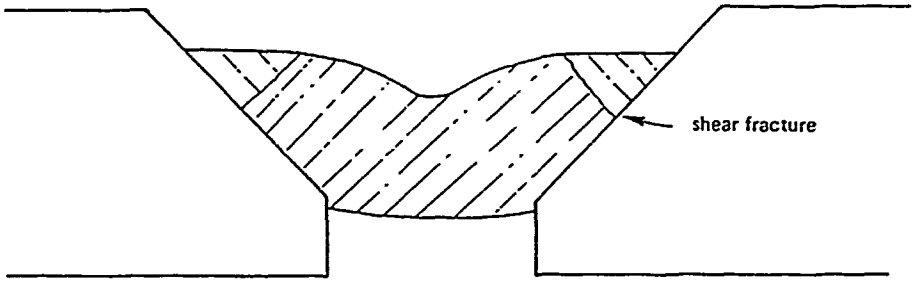

(b) Window under pressure. First phase—annular fracture completed, separation begins between center plug and annular fragment.

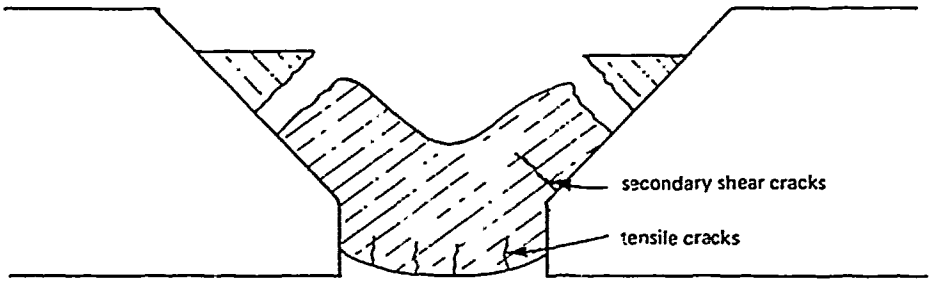

(c) Window under pressure. Second phase—center plug separates, secondary fractures appear in plug, and plug is ejected through opening.

Figure 15. Shear failure mechanism in windows with t/D $\geq$ 0.500.

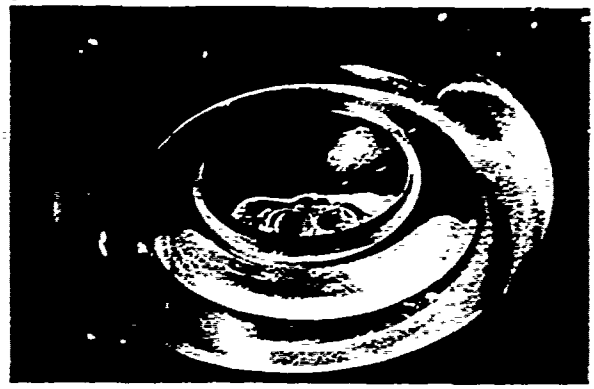

(a) High-pressure face of fractured window.

(b) High-pressure faces of fragments after disassembly of fractured window.

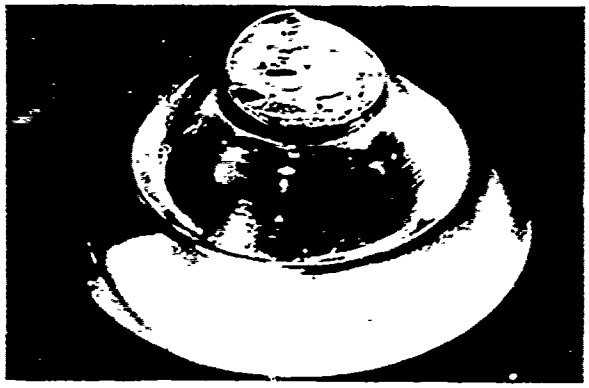

(c) Low-pressure face of fractured window.

(d) Low-pressure faces of fragments after disassembly of fractured window.

Figure 16. Typical shear failure in windows with $t/D \geq 0.500$ and $D/D_f = 1.500$.

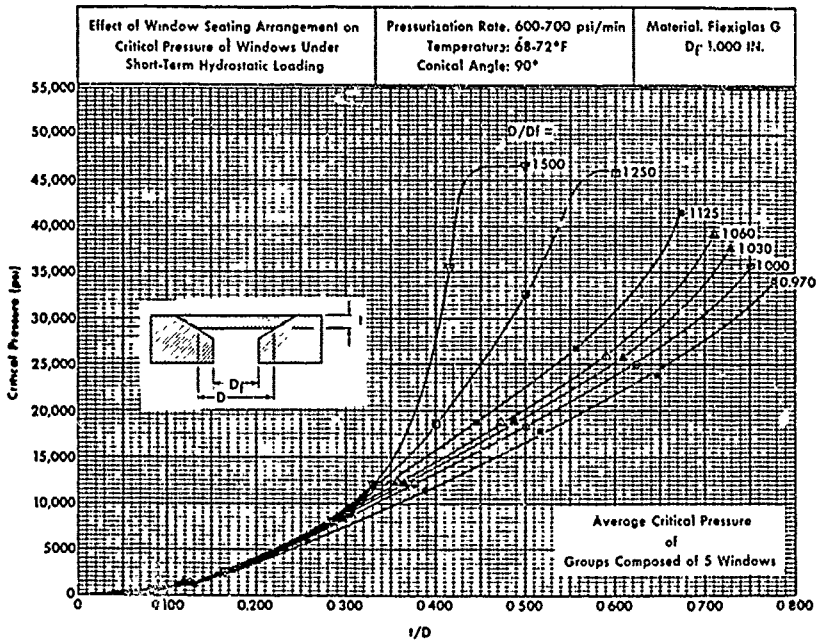

Figure 17. Effect of seating arrangement and t/D ratio on critical pressure of conical acrylic windows under short-term hydrostatic loading in 68°F-to-72°F temperature range.

Ambient temperature was noted to have a significant effect (Figure 18) on the critical pressure also, but its effect in the 32°F-to-90°F range was as a rule considerably less than that of the D/D_f ratio (Figure 19). It appears that the temperature changed the critical pressures by the same percentage regardless of their t/D or D/D_f ratio. To use again the 0.500 t/D windows as an example, the gain in critical pressure when the temperature was decreased from 90°F to 32°F was approximately 7,300 psi (about 45%).

The scatter in critical pressures for each group (expressed in percent of group's mean) of windows composed of five identical test specimens varied with the t/D ratio (Figures A-14 through A-19). For groups with $t/D \leqslant 0.250$ the total scatter was in the 40-to-30% (of calculated group's mean) range, while for windows with $t/D \geqslant 0.375$ it was in the 3-to-10% range. It would thus appear that the predominant reasons for magnitude-of-scatter range are variations in surface finish and bevel-angle mismatch which vary at random and which cause a discrete difference in critical pressure between individual window specimens regardless of the window's thickness. Since the critical pressures of thin windows are low, the small, discrete differences in critical pressure are interpreted as a larger percentage in scatter than for thick windows, which have high critical pressures. No change in scatter magnitude was observed to be associated with changes in ambient temperature, which substantiated the observations of other studies that the notch sensitivity of acrylic plastic does not increase with a decrease in temperature.[13]

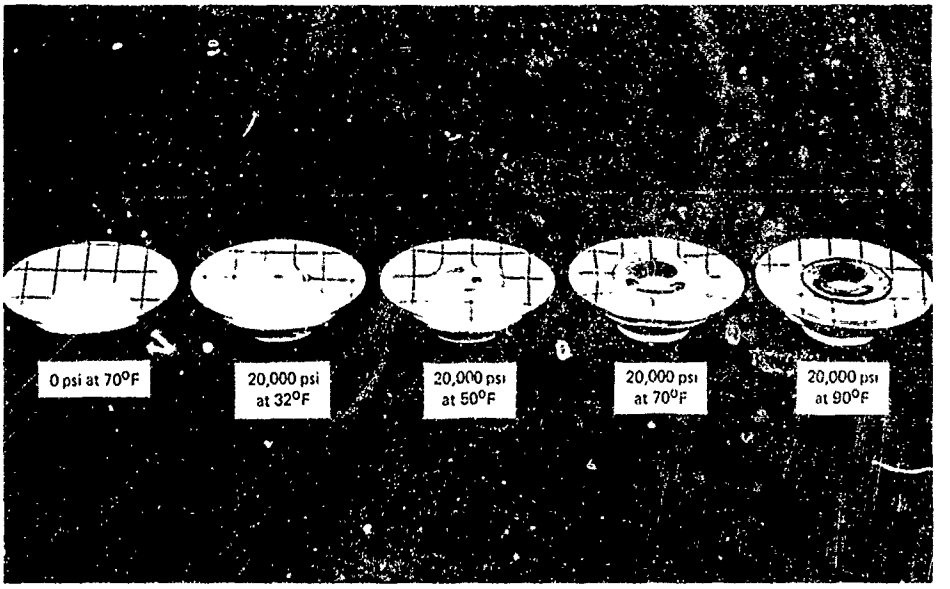

(a) High-pressure faces.

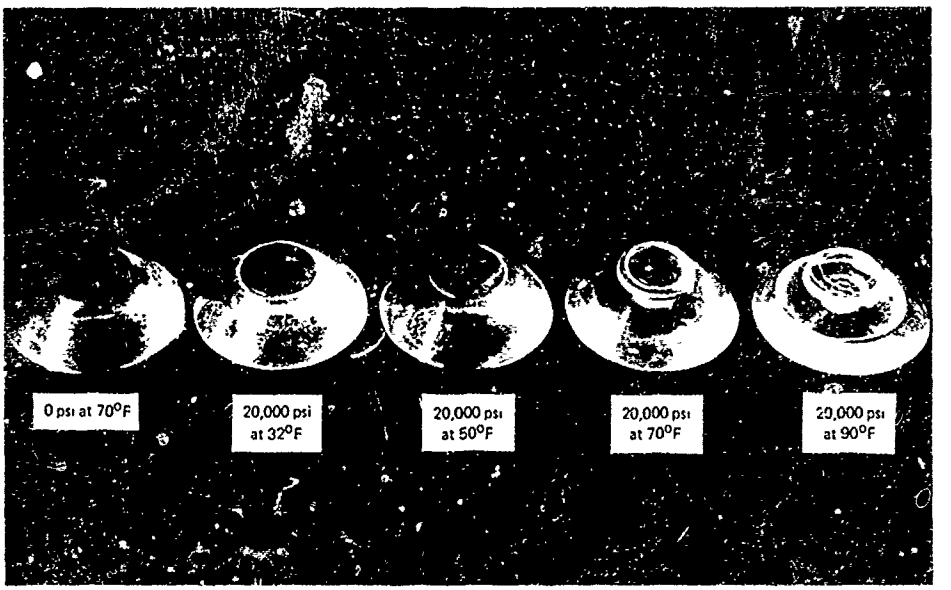

(b) Low-pressure faces.

Figure 18. Effect of ambient temperature on permanent deformation of 90-degree conical acrylic windows subjected to sustained 20,000-psi hydrostatic loading for 1 hour; $t/D = 0.625$, $D/D_f = 1.000$.

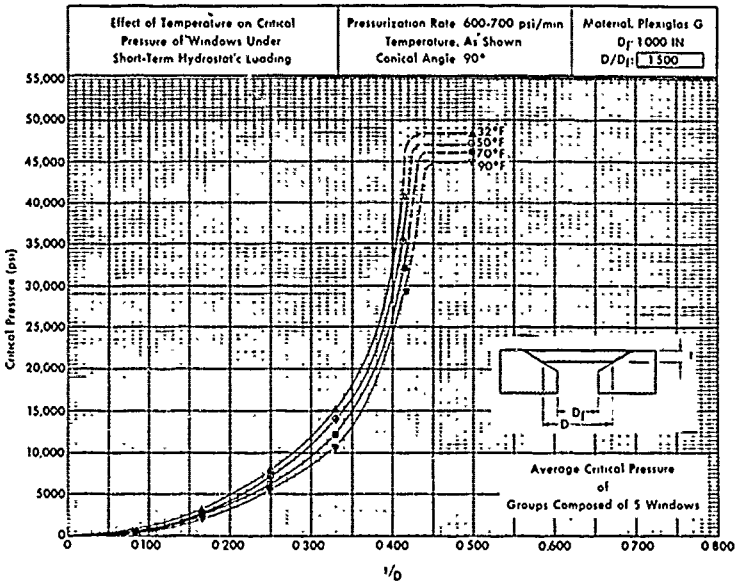

(a) $D/D_f = 1.500$.

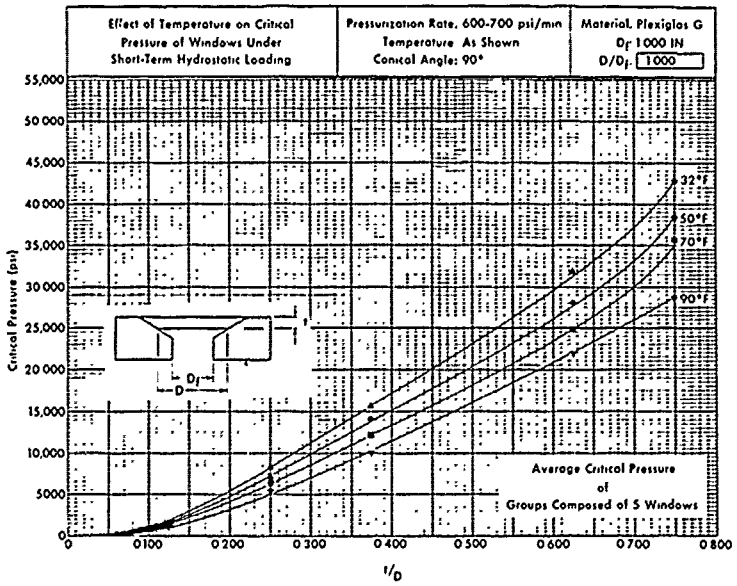

(b) $D/D_f = 1.000$.

Figure 19. Effect of ambient temperature and t/D ratio on critical pressure of 90-degree conical acrylic windows under short-term hydrostatic loading.

No difference was observed between the magnitudes of critical pressures for model (Figure A-17), and full-scale windows (Figure A-20), with the same t/D and t/D_f ratios under identical ambient temperatures. This (1) further substantiates findings of previous studies denoting that t/D is a valid nondimensional factor, and (2) establishes the fact the D/D_f is also a valid nondimensional factor useful in design of window/flange systems.

FINDINGS

All findings are based on conical acrylic plastic windows of 90-degree included angle and thus apply *quantitatively* to such windows only. These findings also apply to conical windows with other included angles, but only in a qualitative manner.

1. The mismatch (D/D_f ratio) between minor diameter of the window (D) and minor diameter of the conical window cavity in the flange (D_f) affected significantly the critical pressure (P_c) of acrylic conical windows. The magnitude of increase in P_c was directly related to the window's t/D and D/D_f ratios, but it became significant only for windows with $t/D \geqslant 0.300$ and $D/D_f > 1.030$. The magnitude of the increase in P_c (above P_c associated with $D/D_f = 1.0$) due to D/D_f ratios $\geqslant 1.500$ exceeded 100% for windows with $t/D \geqslant 0.500$.

2. The change in ambient temperature also affected significantly the critical pressure of conical acrylic windows. The relative (in terms of percent) increase in P_c was independent of t/D and D/D_f ratios, but it was inversely related to the ambient temperature of the pressurizing medium. The increase in P_c was of 30%-to-50% magnitude in the 32^{o}F-to-90^{o}F ambient temperature range.

3. The scatter of P_c values for identical windows tested under the same test conditions was independent of ambient temperature and was in the 30%-to-40% range for windows with $t/D \leqslant 0.250$ ratios and 3%-to-10% range for $t/D \geqslant 0.375$ ratios.

4. The D/D_f ratio, a quantitative indicator of window location in the conical cavity of the flange, was found to be a truly nondimensional parameter like the t/D ratio.

CONCLUSIONS

Designers of conical acrylic plastic windows should pay as much attention to the selection of the proper window-seating ratio (D/D_f) as to the choice of thickness-to-diameter ratio (t/D), because with judicious selection of D/D_f ratio they can double the critical pressure of such windows.

Appendix A

PRESENTATION OF EXPERIMENTAL DATA

DISPLACEMENTS

The displacements of windows have been presented as the averages of each window group with the same t/D, t/D_f, and D/D_f ratios tested under the same ambient temperature. Since there were generally about five windows in each group, the plotted averages represent fairly reliable typical displacement values for windows with a given set of dimensional parameters. The displacements of model windows tested in flanges with $D_f = 1.000$ inch have been plotted separately (Figures A-1 through A-13) from the displacements of full-scale windows (Figures A-21 through A-28) so that a comparison could be made between the displacements of model and full-scale windows with identical dimensional parameters. The comparison indicates that the displacements of full-scale windows are larger than those of model windows by a scaling factor that can be represented as the ratio of full-scale to model window diameters. In some cases the displacements were smaller for the full-scale windows than predicted by the scaling factor, but in no cases were they any larger.

CRITICAL PRESSURES

The critical pressures of window groups have been plotted in such a manner that not only the average but also the maximum and minimum values are shown (Figures A-14 through A-20). This method of plotting was selected to give the window designers an appreciation for typical ranges of critical pressures associated with given t/D_f and D/D_f ratios. Comparison of critical pressures for model (Figure A-17) and full-scale windows (Figure A-20) indicated that they are the same if the dimensional and test parameters of windows are the same. The typical range of critical pressures for the full-scale windows (Figure A-20) was found to be also of the same magnitude as for the model windows (Figure A-17), indicating that the critical pressure data generated by testing of model windows are applicable without any scaling or conversion factors to full-scale windows.

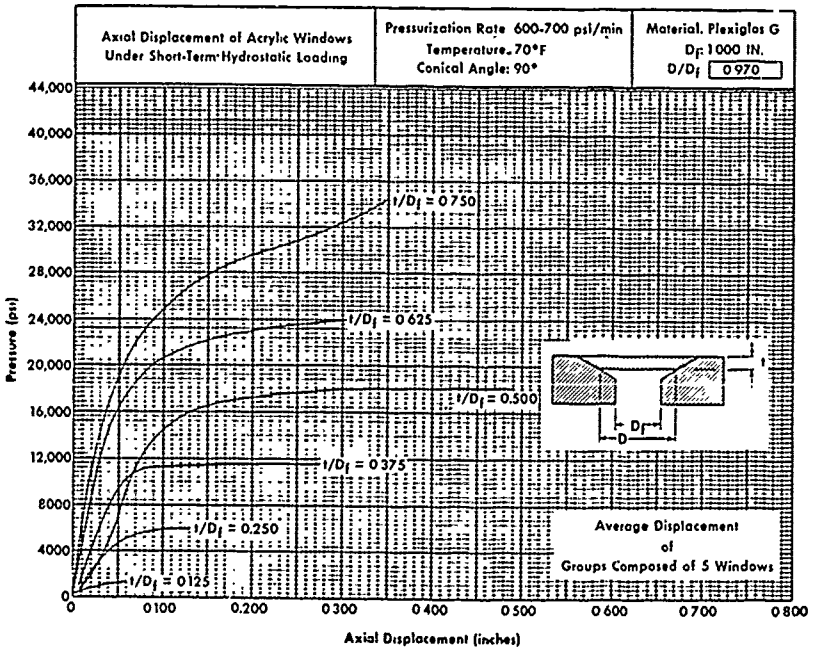

Figure A-1. Effect of short-term hydrostatic loading on axial displacement of 90-degree conical acrylic windows at 70°F ambient temperature; D_f = 1.000 inch, D/D_f = 0.970.

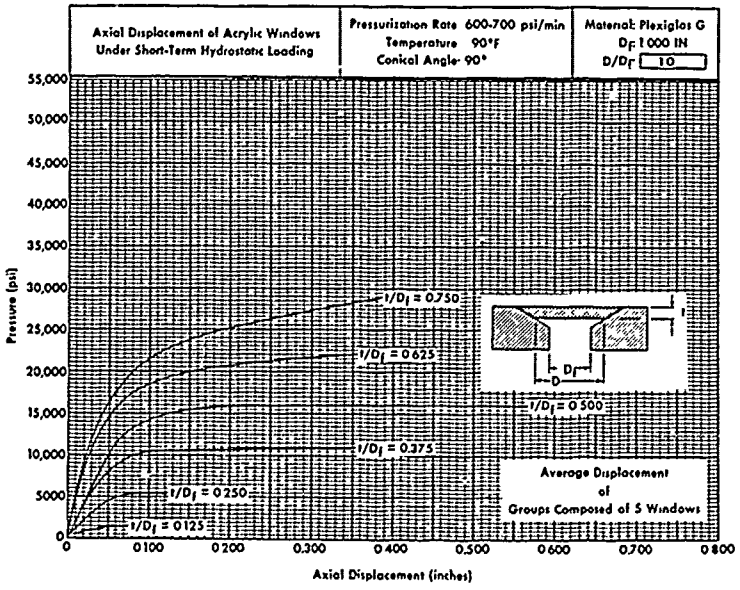

Figure A-2. Effect of short-term hydrostatic loading on axial displacement of 90-degree conical acrylic windows at 90°F ambient temperature; D_f = 1.000 inch, D/D_f = 1.000.

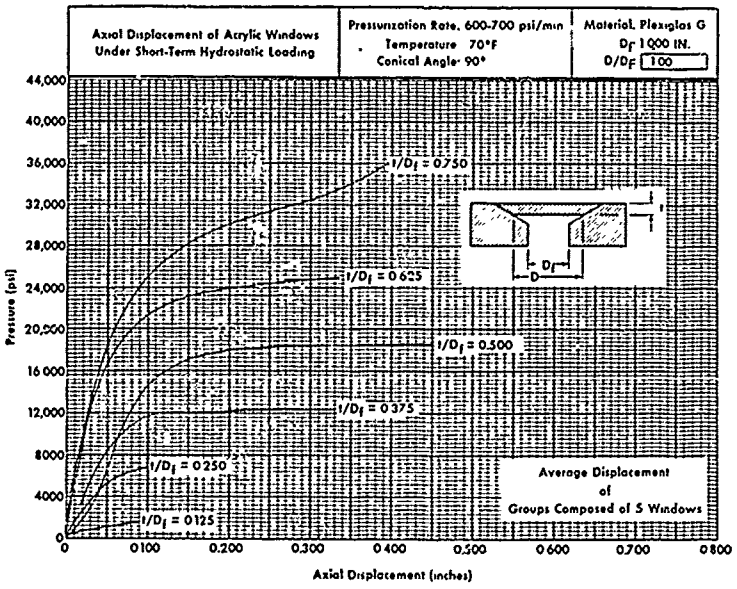

Figure A-3. Effect of short-term hydrostatic loading on axial displacement of 90-degree conical acrylic windows at 70°F ambient temperature; D_f = 1.000 inch, D/D_f = 1.000.

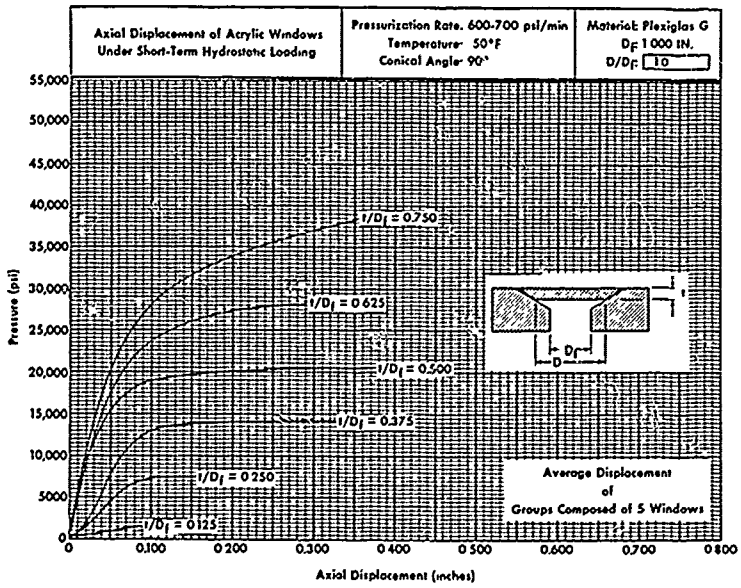

Figure A-4. Effect of short-term hydrostatic loading on axial displacement of 90-degree conical acrylic windows at 50°F ambient temperature; D_f = 1.000 inch, D/D_f = 1.000.

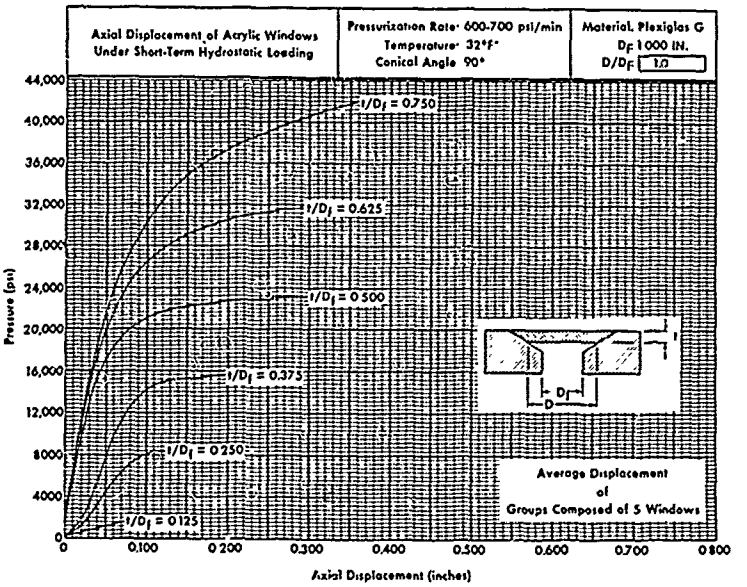

Figure A-5. Effect of short-term hydrostatic loading on axial displacement of 90-degree conical acrylic windows at 32°F ambient temperature; D_f = 1.000 inch, D/D_f = 1.000.

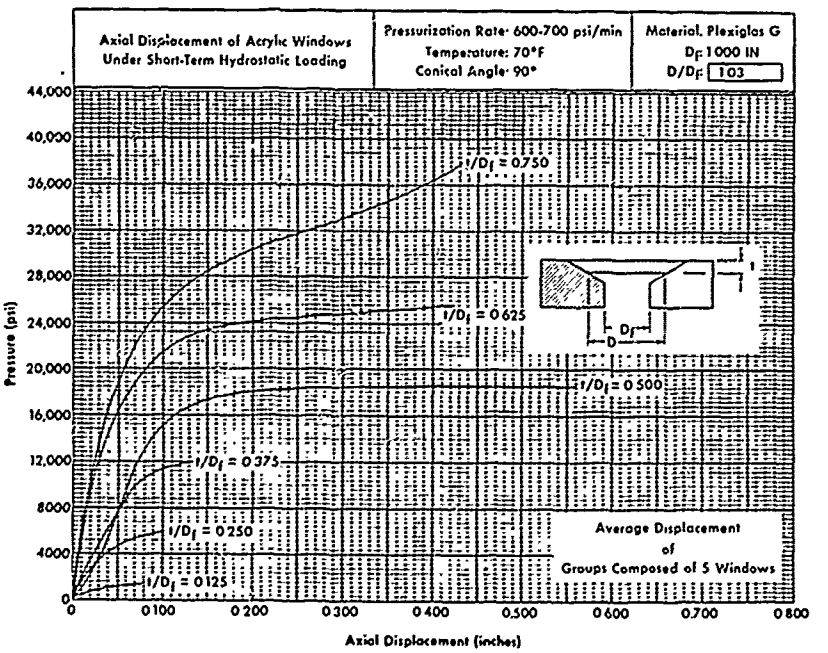

Figure A-6. Effect of short-term hydrostatic loading on axial displacement of 90-degree conical acrylic windows at 70°F ambient temperature; D_f = 1.000 inch, D/D_f = 1.030.

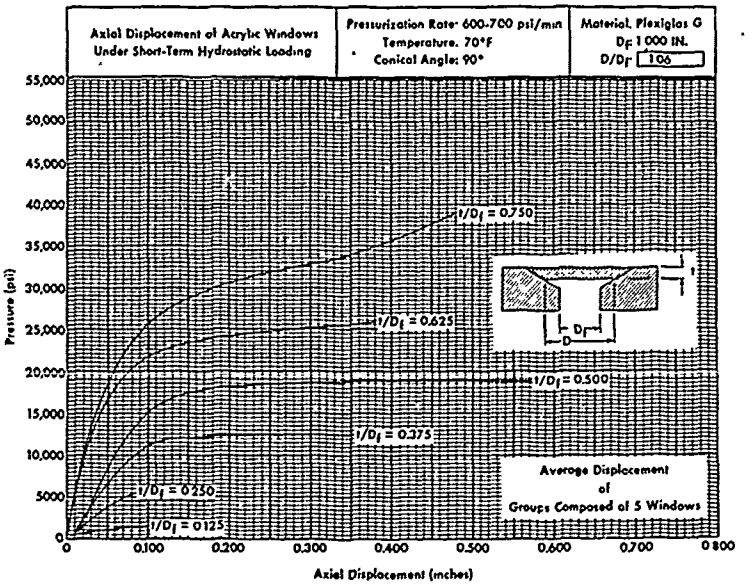

Figure A-7. Effect of short-term hydrostatic loading on axial displacement of 90-degree conical acrylic windows at 70°F ambient temperature; D_f = 1.000 inch, D/D_f = 1.060.

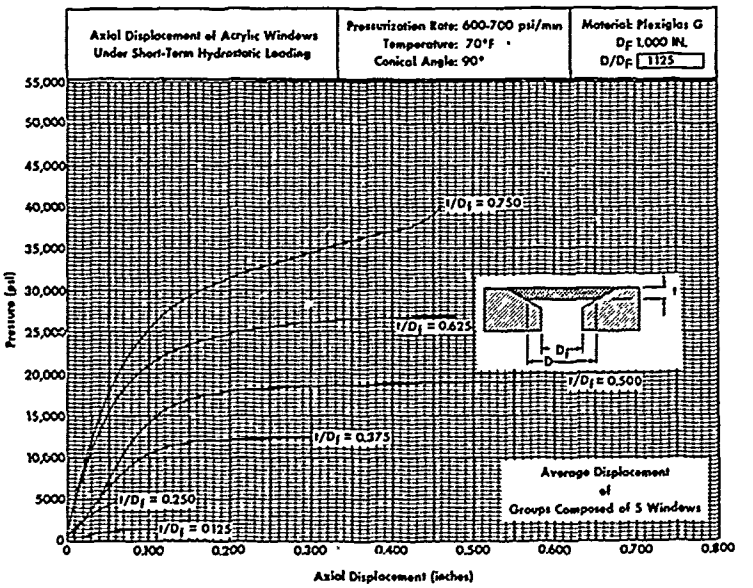

Figure A-8. Effect of short-term hydrostatic loading on axial displacement of 90-degree conical acrylic windows at 70°F ambient temperature; D_f = 1.000 inch, D/D_f = 1.125.

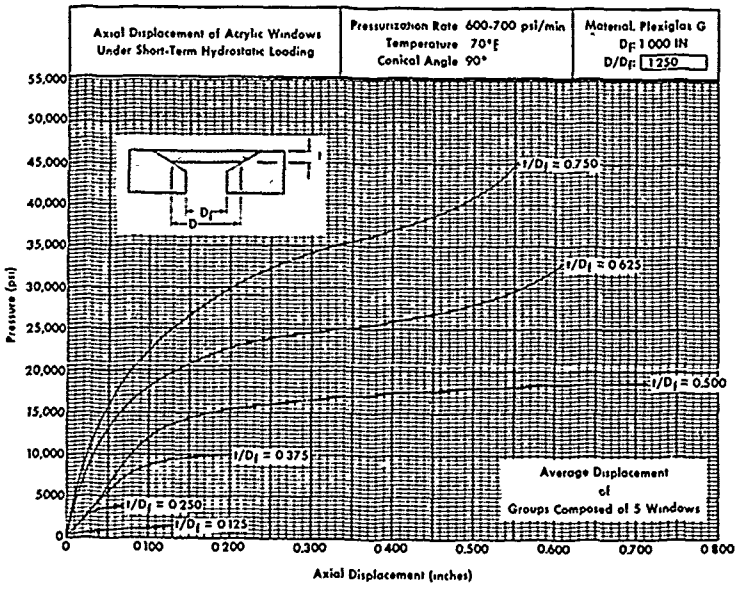

Figure A-9. Effect of short-term hydrostatic loading on axial displacement of 90-degree conical acrylic windows at 70°F ambient temperature; D_f = 1.000 inch, D/D_f = 1.250.

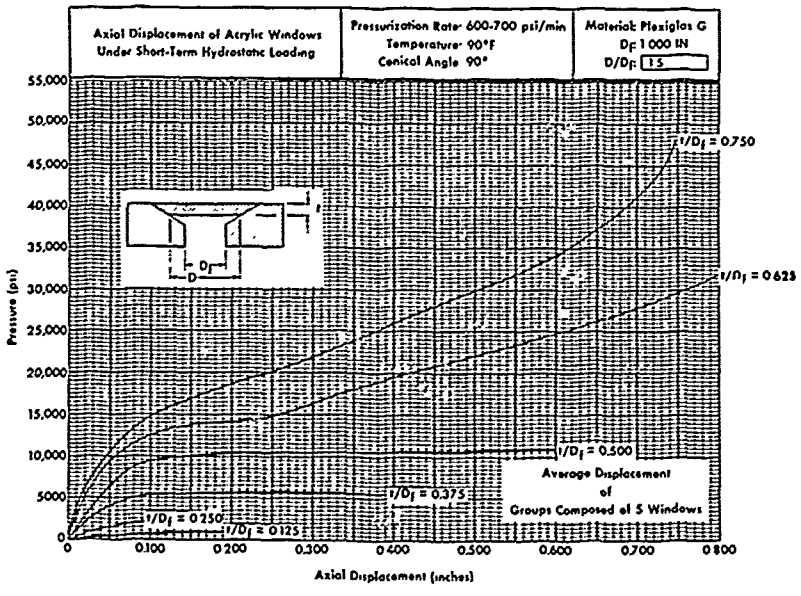

Figure A-10. Effect of short-term hydrostatic loading on axial displacement of 90-degree conical acrylic windows at 90°F ambient temperature; D_f = 1.000 inch, D/D_f = 1.500.

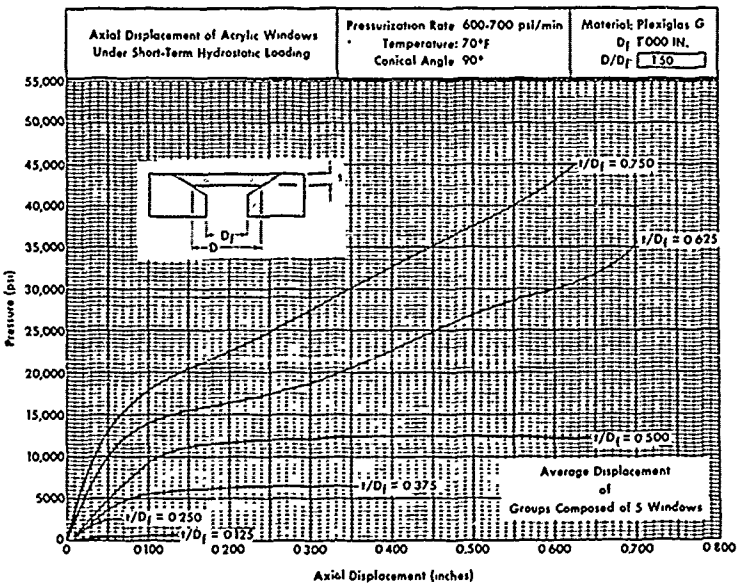

Figure A-11. Effect of short-term hydrostatic loading on axial displacement of 90-degree conical acrylic windows at 70°F ambient temperature; D_f = 1.000 inch, D/D_f = 1.500.

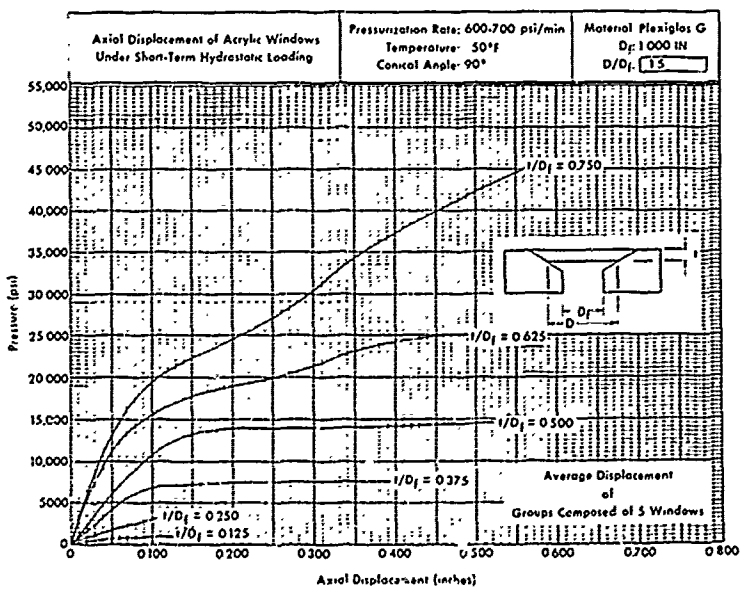

Figure A-12. Effect of short-term hydrostatic loading on axial displacement of 90-degree conical acrylic windows at 50°F ambient temperature; D_f = 1.000 inch, D/D_f = 1.500.

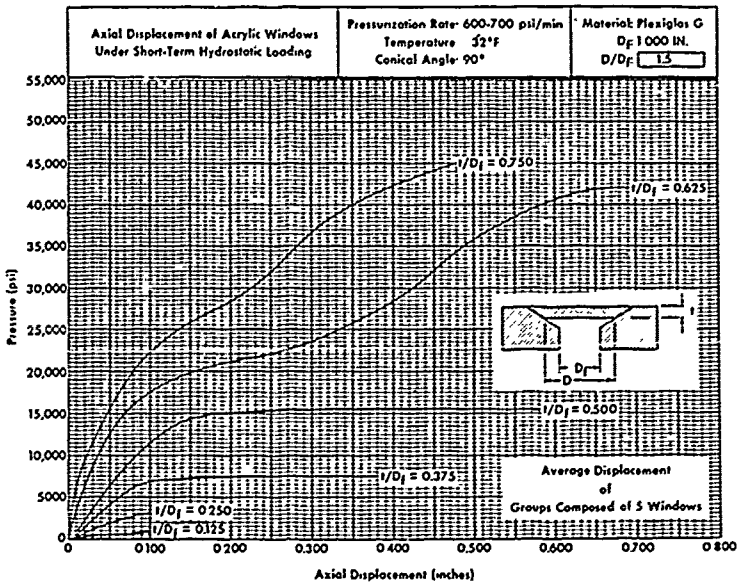

Figure A-13. Effect of short-term hydrostatic loading on axial displacement of 90-degree conical acrylic windows at 32°F ambient temperature; D_f = 1.000 inch, D/D_f = 1.500.

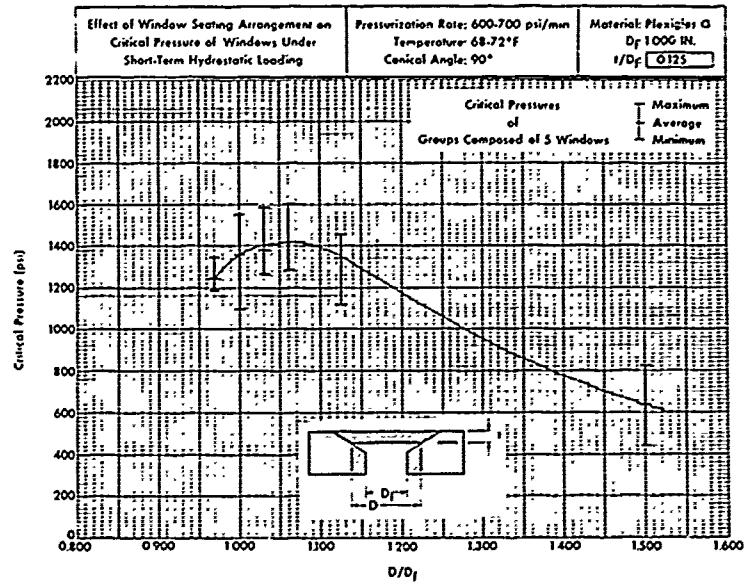

Figure A-14. Effect of seating arrangement on critical pressure of 90-degree conical acrylic windows under short-term hydrostatic loading at 70°F ambient temperature; D_f = 1.000 inch, t/D_f = 0.125.

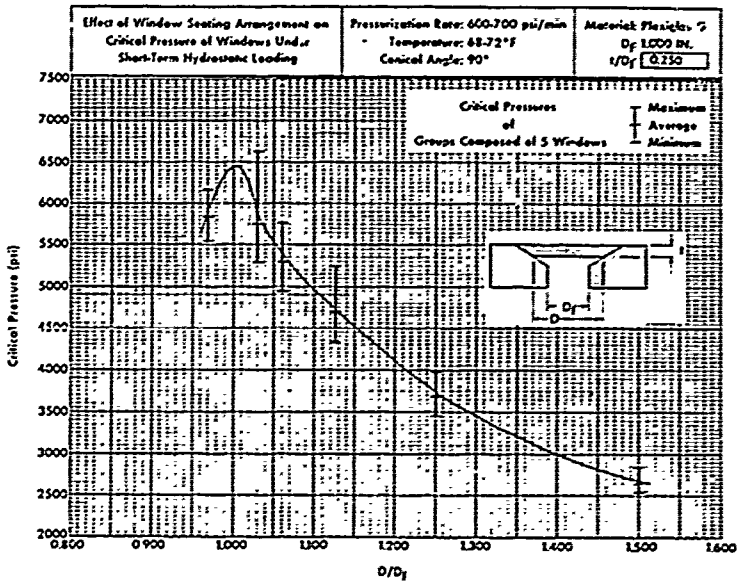

Figure A-15. Effect of seating arrangement on critical pressure of 90-degree conical acrylic windows under short-term hydrostatic loading at 70°F ambient temperature; D_f = 1.000 inch, t/D_f 0.250.

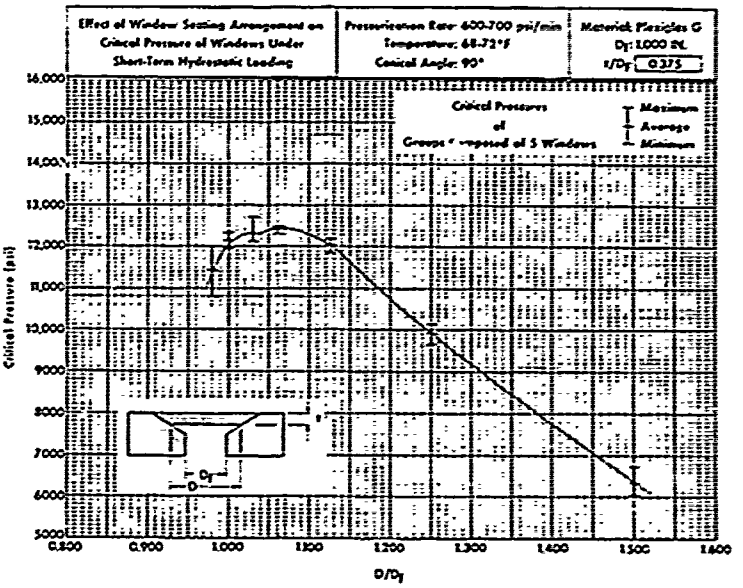

Figure A-16. Effect of seating arrangement on critical pressure of 90-degree conical windows under short-term hydrostatic loading at 70°F ambient temperature; D_f = 1.000 inch, t/D_f = 0.375.

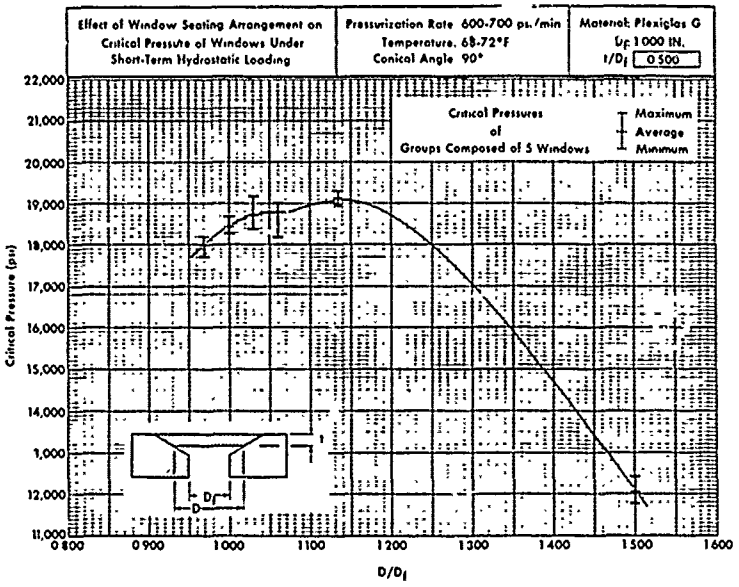

Figure A-17. Effect of seating arrangement on critical pressure of 90-degree conical acrylic windows under short-term hydrostatic loading at 70°F ambient temperature; D_f = 1.000 inch, t/D_f = 0.500.

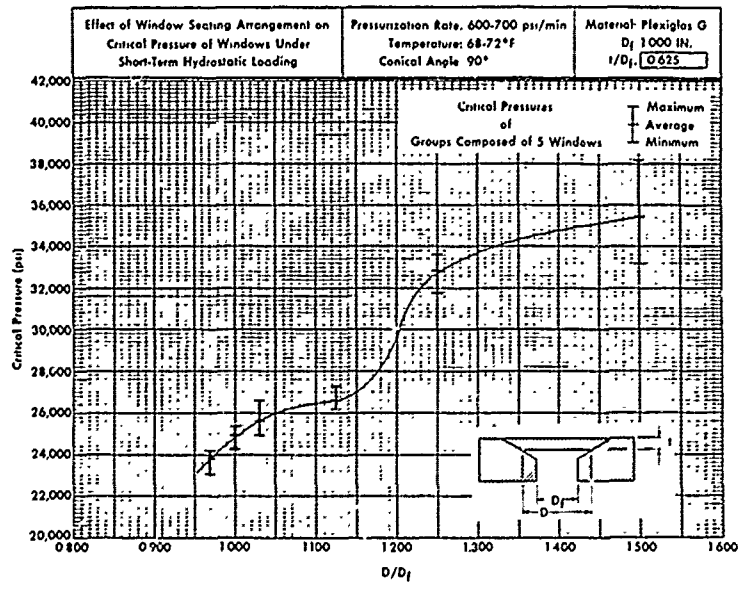

Figure A-18. Effect of seating arrangement on critical pressure of 90-degree conical acrylic windows under short-term hydrostatic loading at 70°F ambient temperature; D_f = 1.000 inch, t/D_f = 0.625.

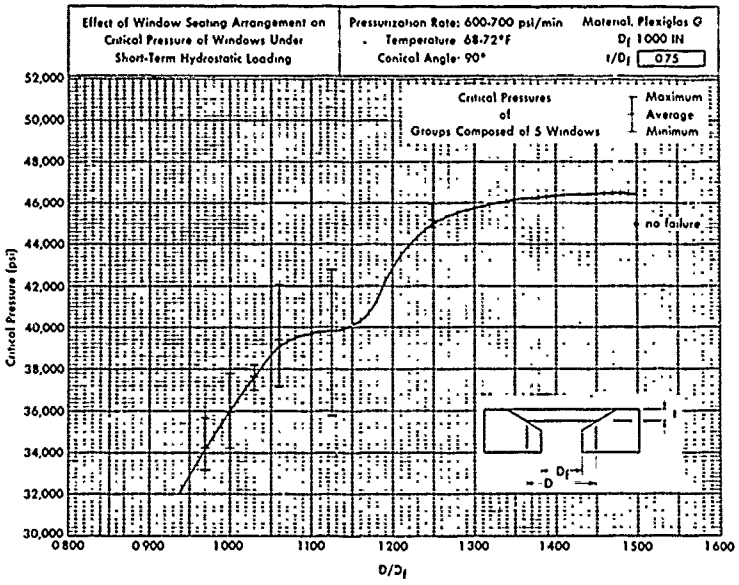

Figure A-19. Effect of seating arrangement on critical pressure of 90-degree conical acrylic windows under short-term hydrostatic loading at 70°F ambient temperature; D_f = 1.000 inch, t/D_f = 0.750.

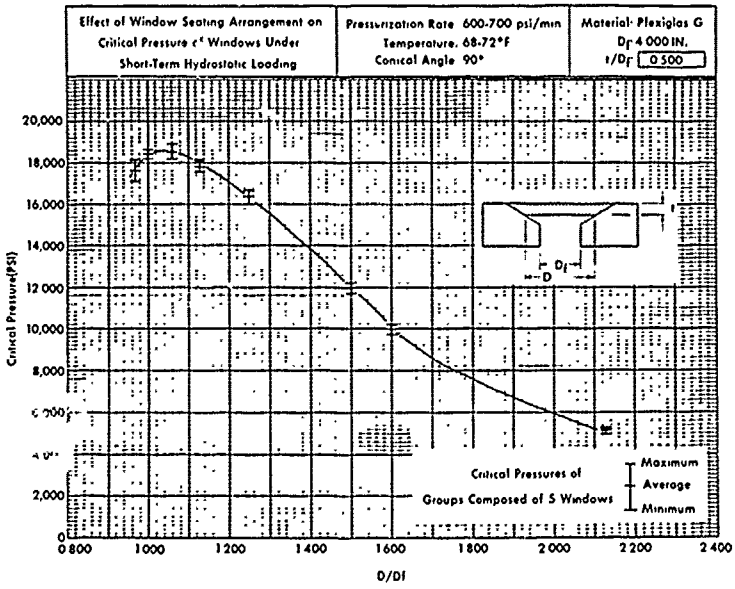

Figure A-20. Effect of seating arrangement on critical pressure of 90-degree conical acrylic windows under short-term hydrostatic loading at 70°F ambient temperature; D_f = 4.000 inches, t/D_f = 0.500.

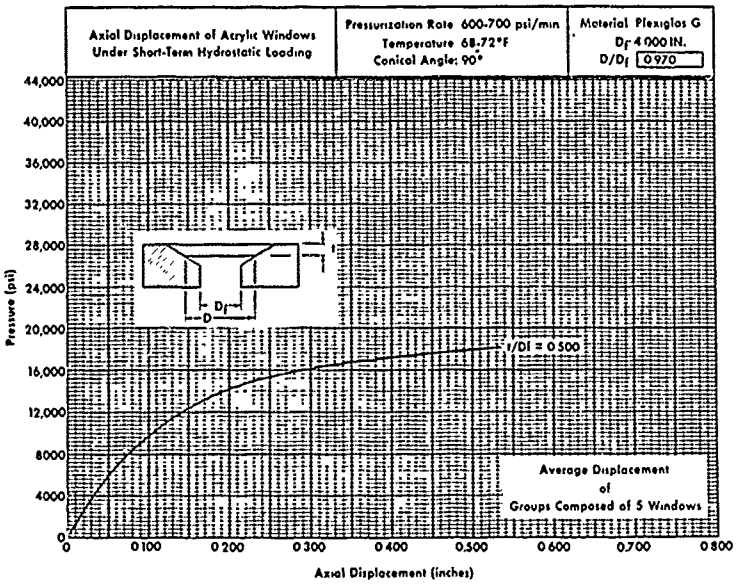

Figure A-21. Effect of short-term hydrostatic loading on axial displacement of 90-degree conical acrylic windows at 70°F ambient temperature; D_f = 4.000 inches, t/D_f = 0.500, D/D_f = 0.970.

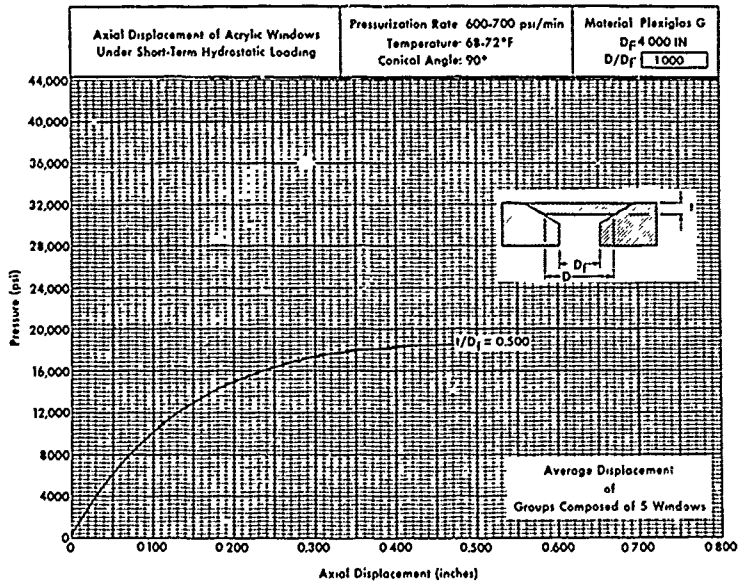

Figure A-22. Effect of short-term hydrostatic loading on axial displacement of 90-degree conical acrylic windows at 70°F ambient temperature; D_f = 4.000 inches, t/D_f = 0.500, D/D_f = 1.000.

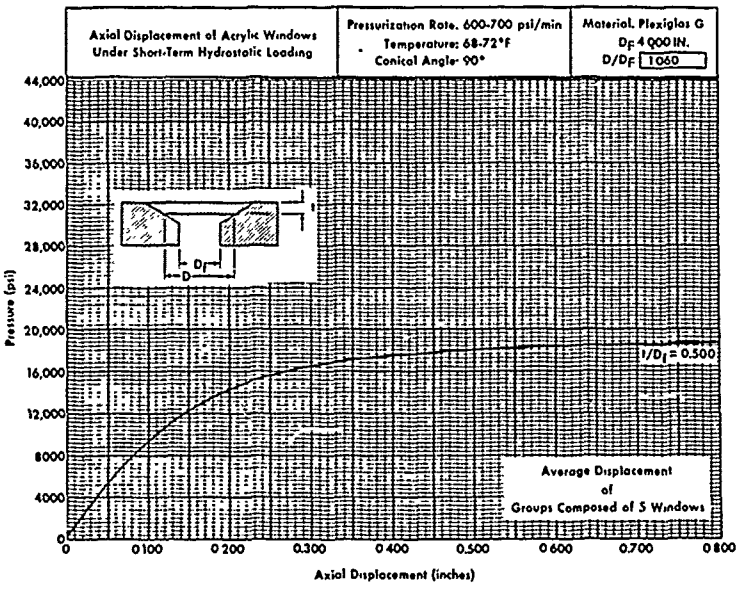

Figure A-23. Effect of short-term hydrostatic loading on axial displacement of 90-degree conical acrylic windows at 70°F ambient temperature; D_f = 4.000 inches, t/D_f = 0.500, D/D_f = 1.060.

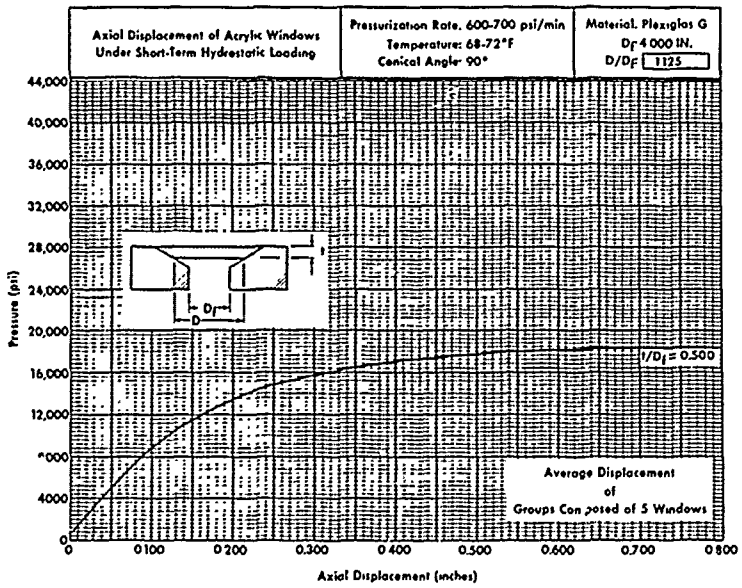

Figure A-24. Effect of short-term hydrostatic loading on axial displacement of 90-degree conical acrylic windows at 70°F ambient temperature; D_f = 4.000 inches, t/D_f = 0.500, D/D_f = 1.125.

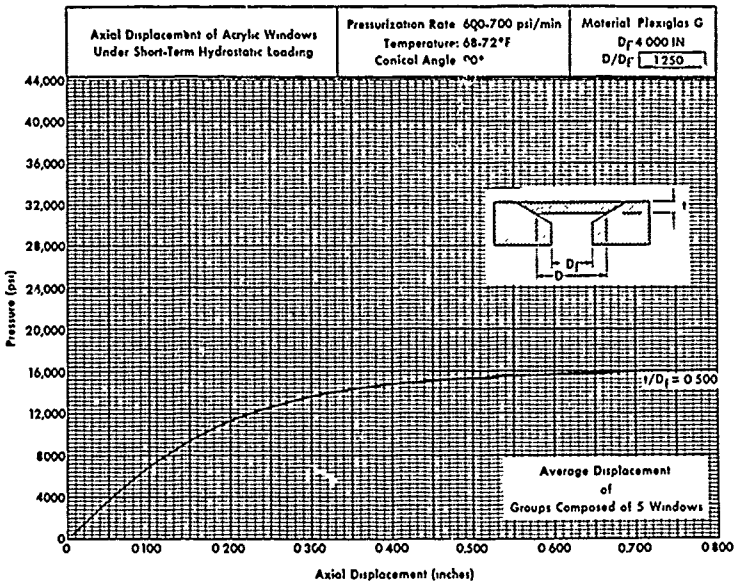

Figure A-25. Effect of short-term hydrostatic loading on axial displacement of 90-degree conical acrylic windows at 70°F ambient temperature; D_f = 4.000 inches, t/D_f = 0.500, D/D_f = 1.250.

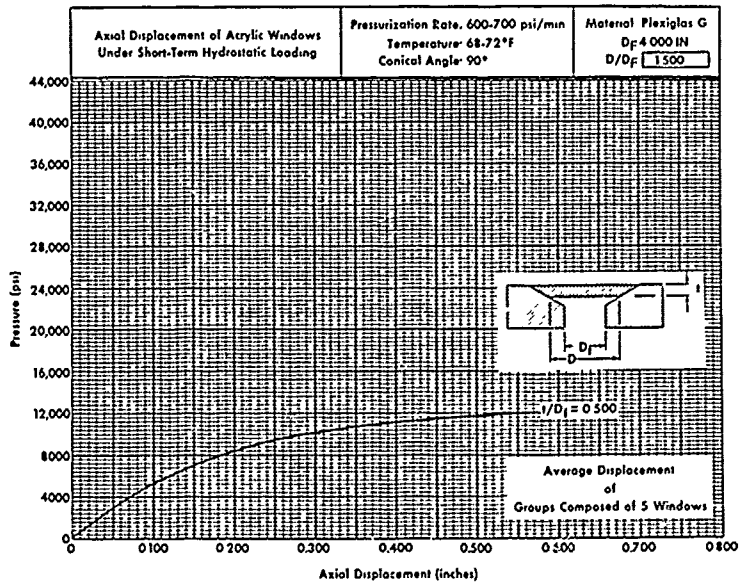

Figure A-26. Effect of short-term hydrostatic loading on axial displacement of 90-degree conical acrylic windows at 70°F ambient temperature; D_f = 4.000 inches, t/D_f = 0.500, D/D_f = 1.500.

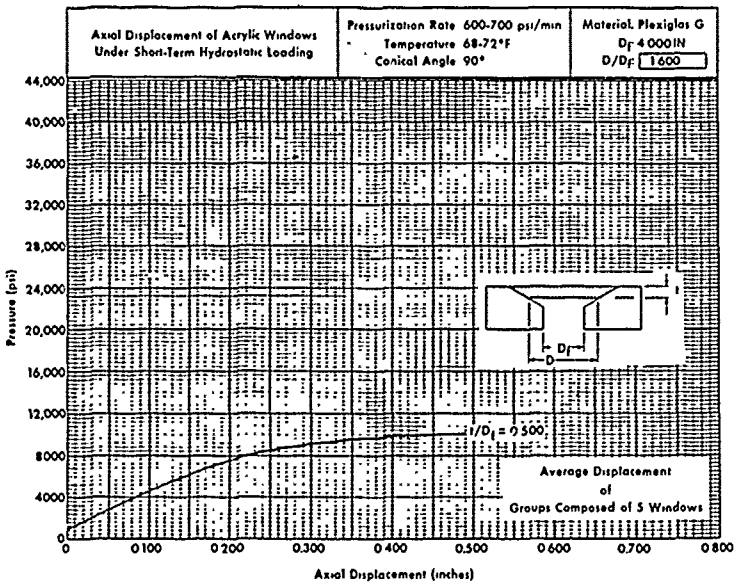

Figure A-27. Effect of short-term hydrostatic loading on axial displacement of 90-degree conical acrylic windows at 70°F ambient temperature; D_f = 4.000 inches, t/D_f = 0.500, D/D_f = 1.600.

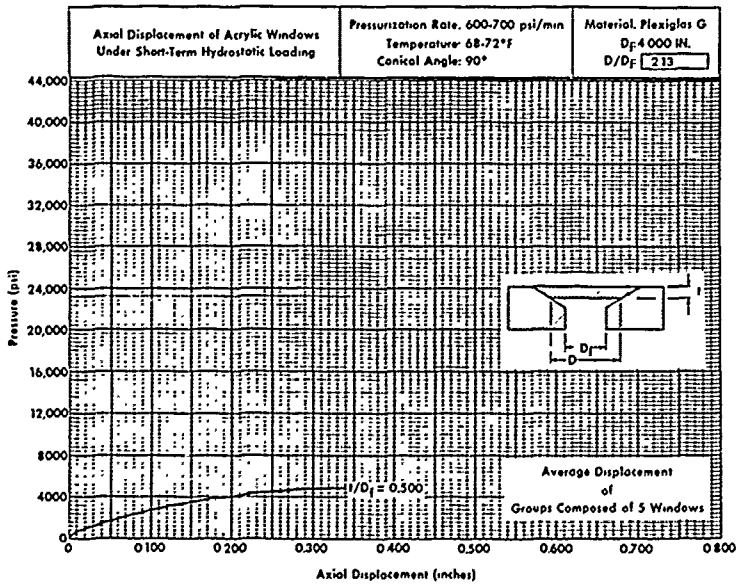

Figure A-28. Effect of short-term hydrostatic loading on axial displacement of 90-degree conical acrylic windows at 70°F ambient temperature; D_f = 4.000 inches, t/D_f = 0.500, D/D_f = 2.130.

Appendix B

APPLICATION OF EXPERIMENTAL DATA TO DESIGN OF PRESSURE-RESISTANT WINDOWS

BACKGROUND

Conical frustum acrylic plastic windows have been utilized in submersibles, personnel transfer capsules, deck decompression chambers, and deep ocean simulators since they were introduced to such applications by Professor Auguste Piccard through his pioneering FNRS-2 submersible in 1939. Considerable experimental and analytical data have been amassed over the years describing the effects of conical angle and thickness-to-diameter ratio (t/D) on the critical pressure, deformation, and axial displacement of such windows under hydrostatic loadings of different durations. Although this information is sufficient for design of safe conical acrylic windows in the 0-to-20,000-psi operational pressure range, it is insufficient to permit maximization of the windows' short-term critical pressure potential through variation in the window seating inside the window containment flange.

That the relationship between the minor diameter of the window (D) and that of the flange (D_f) affects the critical pressure of the conical acrylic window has been known for a long time[14] but data were not available to permit quantifying this effect. This is not to imply that specific D/D_f ratios were not recommended for design of windows. Recommendations have been made in the past on choice of proper D/D_f ratios for different operational pressures, but those recommendations were aimed only at increasing the static and cyclic fatigue life rather than short-term strength of windows. Now that the experimental data on the relationship between short-term critical pressure and D/D_f ratio are available, it is possible also to specify D/D_f ratios that will substantially increase the short-term critical pressure that is so important during occurrence of transient depth increases for submersibles or pressure surges inside of deep ocean simulators.

DISCUSSION

Since this experimental study has shown (Figure 17) that raising D/D_f ratios over 1.000 (which in all the NCEL window studies is considered the benchmark ratio) is *never harmful*, and for $t/D > 0.300$ increasing the ratio is beneficial in raising of short-term critical pressure potential, the designer may be tempted to make the D/D_f ratio as high as possible so

that a very high short-term critical pressure may be obtained for the window he is designing. This temptation should be resisted, as there are some drawbacks associated also with unlimited D/D_f increase.

The drawbacks associated with D/D_f increase are (1) greater costs for window and flange fabrication and (2) increased weight of the window/flange assembly. The increased cost and weight are results of the increased window and flange sizes for a given D_f. For example, a 90-degree window with t/D = 0.5 located in a flange with D_f = 4.000 inches increased 50% in thickness when the D/D_f ratio and accompanying critical pressure potential are increased from 1.000 (P_c = 19,000 psi) to 1.500 (P_c = 47,000 psi). The accompanying change in flange thickness will be anywhere from 50% to 100% depending on its structural design. This increase in weight and cost is not followed by any increase in viewing field, as this is always controlled by D_f, which remains constant.

For this reason, a detailed trade-off study must be conducted between increase in short-term critical pressure potential on one hand and increase in weight and cost of the structure on the other hand before an intelligent decision can be made on what D/D_f to select for a given window. However, because such trade-off studies may be too long or too complicated for a window designer hard pressed for an answer, a simple set of design guides has been prepared for his use. These simple design guides will permit the designer to rapidly choose a window-seating arrangement (D/D_f) that improves not only the short-term critical pressure potential of the window but also its static and cyclic fatigue life.

DESIGN GUIDES

The simple design guides developed for the benefit of the window designer rest on two basic observations. $D/D_f > 1.000$ is desirable to give an axially displacing window radial and axial support to its conical bearing surface so that (1) the window's short-term critical pressure potential is increased for unforeseen temporary overload and (2) static and fatigue life of the window is prolonged by eliminating contact between the sharp corner of the flange and the window's bearing surface during pressurizations of the window to its rated operational depth.

From these two basic observations, two general guidelines can be deduced that become helpful in choosing of D/D_f ratios:

1. Since every window in service will experience static and cyclic fatigue regardless of the relationship between short-term critical pressure and operational pressure chosen, it behooves the designer to prolong the

fatigue life by choosing such a D/D_f ratio that the conical bearing of the window *never* extends past the supporting conical flange seat during pressurizations to operational depth (Figure B-1). These D/D_f ratios are considered to be *minimums* and should be met in all operational window designs. Experimental studies have been already conducted for some selected operational depths (20,000 psi, 10,000 psi, and 5,000 psi) and the minimum D/D_f ratios have been recommended for providing necessary bearing support to the axially displacing windows. Thus for 90-degree conical windows a $t/D = 2.0$ and $D/D_f = 1.25$ are recommended for 20,000 psi, $t/D = 1.0$ and $D/D_f = 1.15$ for 10,000 psi, and $t/D = 0.625$ and $D/D_f = 1.06$ for 5,000 psi. For pressures less than 5,000 psi, experimentally obtained D/D_f ratio for static or cyclic fatigue do not exist, but a conservative assumption dictates the use of the same minimum D/D_f ratio as for 5,000-psi operational pressure.

2. Once the minimum D/D_f ratios required for containment of window axial displacements under operational pressure have been met, further increase of D/D_f ratios can be justified only by the desire to improve further the short-term critical pressure potential of the window (Figure B-1). What the limit to the improvement should be is, of course, a matter to be decided by the designer, but an increase of more than 50% is very hard to justify, particularly since the proof pressures to which windows may be subjected never exceed the operational pressure by more than 50%.

EXAMPLE A

Problem

Choose the proper D/D_f ratio for a 90-degree conical acrylic window to be utilized in a deep ocean simulator rated for 5,000-psi operational pressure. The service that the window will see will involve long-term, short-term, and dynamic pressure loadings. Before it is placed into service, the window will be proof-tested to 1.5 times its operational pressure.

Solution

The *minimum* t/D ratio required to satisfy the static and cyclic fatigue requirements of 5,000-psi service is 0.625 (see Reference 6). The *minimum* D/D_f ratio that will provide adequate bearing support for the axial window displacement under 5,000-psi operational pressure is 1.06

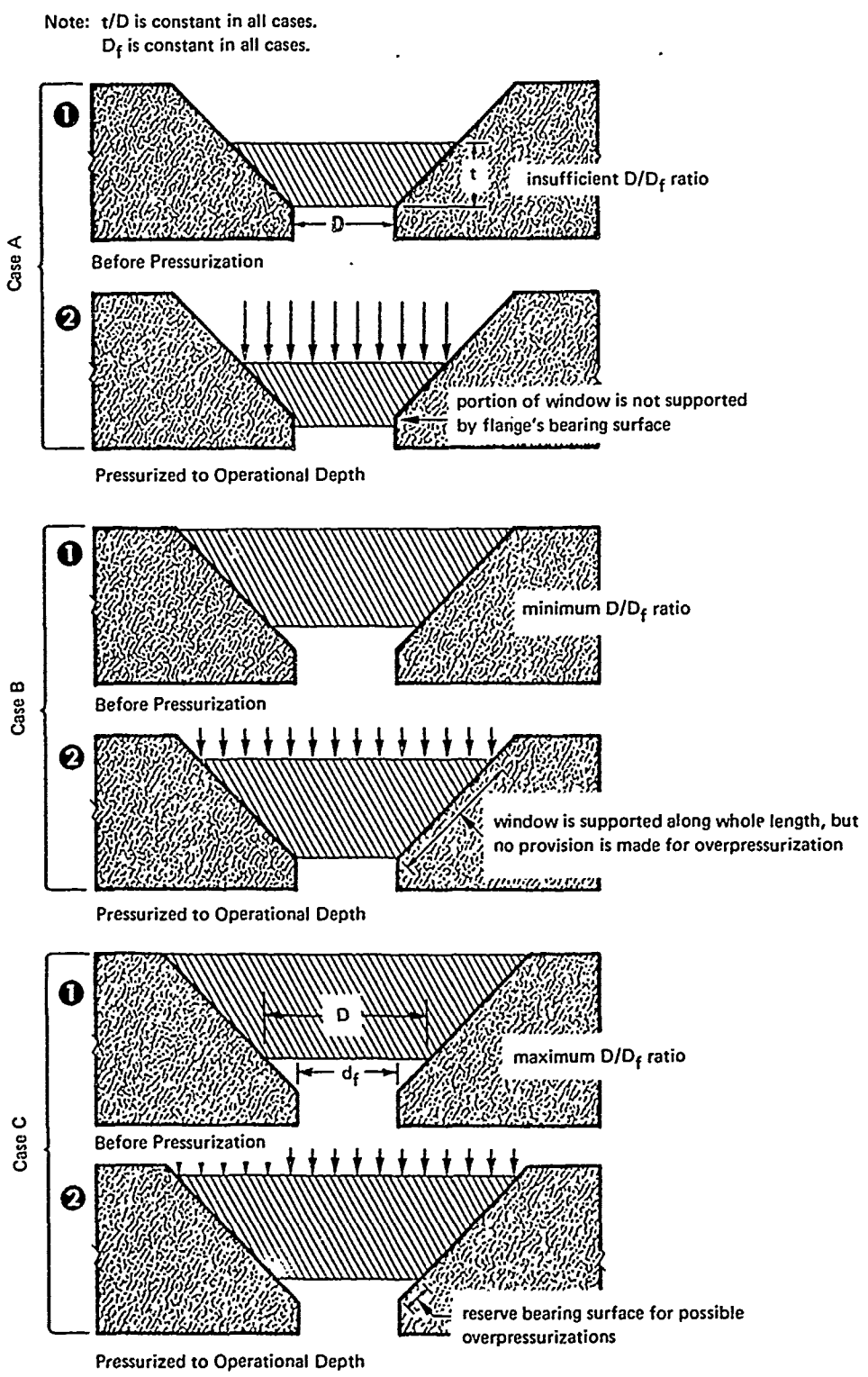

Figure B-1. Effect of D/D_f ratio on support of window's bearing surface during hydrostatic loading.

(see Reference 6). The *maximum* recommended D/D_f ratio for the t/D = 0.625 is 1.175 based on planned 50% increase in critical pressure of the window. A D/D_f of 1.175 was chosen for the window.

EXAMPLE B

Problem

Choose the proper D/D_f ratio for a 90-degree conical window utilized in a research submersible with abyssal depth capability of 36,000 feet. The window will be subjected mostly to cyclic pressure loadings with maximum possible sustained loading of 36-hour durations. Before it is put in service, the window will be proof-tested to 1.25 times its operational pressure.

Solution

The minimum t/D ratio required to satisfy the cyclic fatigue requirements of 36,000-foot depth is 2.00 (see Reference 4). The *minimum* D/D_f ratio that will provide adequate bearing support for the axial window displacement at 36,000-foot depth is 1.25 (see Reference 4). The maximum D/D_f cannot be determined in this case from curves in Figure 17, since windows of t/D = 2.00 were not tested in the present window-seating study. It would appear however that D/D_f = 1.25 can also serve in this case as the maximum ratio, since observation of curves in Figure 17 leads to the conclusion that D/D_f = 1.25 probably increases the critical pressure more than 24% over D/D_f = 1.000 unless the plastic extrusion pressure is reached sooner. A D/D_f of 1.250 was chosen for the window.

EXAMPLE C

Problem

Choose the proper D/D_f ratio for a 90-degree conical acrylic window utilized in a submersible for 1,000-foot operational service. The loading on the window will be primarily of cyclic nature with maximum sustained loading of 36-hour duration. Before it is placed into service, the window will be proof-tested to 1.50 times its operational pressure.

Solution.

Since extensive window studies were not conducted previously at 1,000-foot operational depth, specific recommendations do not exist for the selection of t/D and D/D_f ratio. Because of this, recourse must be taken to a more arbitrary approach of choosing t/D ratios. This approach, whatever it lacks in accuracy, makes up through conservatism in application of high safety factors. This approach is based on the observation (Reference 14) that if the short-term critical pressure (Figure 17 at $D/D_f = 1.00$) is divided by a conversion factor of four then the long-term critical pressure is approximately fixed. To insure that the approximately arrived at long-term critical pressure (static fatigue) is valid for (1) repeated pressurization and (2) proof test (overload), it is further divided by a safety factor of two. To summarize, when the short-term critical pressure is divided by a factor of eight, a safe operational pressure has been fixed.

In the case of the 1,000-foot operational depth, it means that a t/D must be chosen that at $D/D_f = 1.00$ has a short-term critical pressure of 3,600 psi (that is, 450 psi x 8). The t/D corresponding to 3,600-psi short-term critical pressure is found to be 0.200. Since the operational pressure is less than 5,000 psi, the recommended minimum $D/D_f = 1.06$. Maximum $D/D_f = 1.06$ also, since increasing the D/D_f ratio further does not affect the critical pressure. Thus the final ratios for 1,000-foot operational depth 90-degree conical window are $t/D = 0.200$ and $D/D_f = 1.06$.

Examples A through C refer to applications where the ambient temperature will be in the $65^{\circ}F$-to-$75^{\circ}F$ range. If the ambient temperature is lower, no corrections need to be made to the chosen t/D ratios, as the error is on the conservative side and thus acceptable. The situation is slightly different if the ambient temperatures are above the $65^{\circ}F$-to-$75^{\circ}F$ range. If no corrections were made, the error would be on the unsafe side, resulting in windows with lower safety factors. For this reason, when choosing windows on the basis of their short-term critical pressure (see Example C), effects of higher temperature should be taken into account. Thus Figure 19a, instead of Figure 17, should be used as the basis for determining short-term critical pressure, because Figure 19a takes the effects of temperature into account. Since Figure 19 has only curves for $D/D_f = 1.00$ and $D/D_f = 1.50$, critical pressure values for other D/D_f ratios must be found by interpolation.

REFERENCES

1. Naval Civil Engineering Laboratory. Technical Report R-512: Windows for external or internal hydrostatic pressure vessels, pt. 1. Conical acrylic windows under short-term pressure application, by J. D. Stachiw and K. O. Gray. Port Hueneme, Calif., Jan. 1967. (AD 646882)

2.————. Technical Report R-527: Windows for external or internal hydrostatic pressure vessels, pt. 2. Flat acrylic windows under short-term pressure application, by J. D. Stachiw, G. M. Dunn, and K. O. Gray. Port Hueneme, Calif., May 1967. (AD 652343)

3.————. Technical Report R-631: Windows for external or internal hydrostatic pressure vessels, pt. 3. Critical pressure of acrylic spherical shell windows under short-term pressure application, by J. D. Stachiw and F. W. Brier. Port Hueneme, Calif., June 1969. (AD 689789)

4.————. Technical Report R-645: Windows for external or internal hydrostatic pressure vessels, pt. 4. Conical acrylic windows under long-term pressure applications at 20,000 psi, by J. D. Stachiw. Port Hueneme, Calif., Oct. 1969. (AD 697272)

5.————. Technical Report R-708: Windows for external or internal hydrostatic pressure vessels, pt. 5. Conical acrylic windows under long-term pressure application of 10,000 psi, by J. D. Stachiw and W. A. Moody. Port Hueneme, Calif., Jan. 1970. (AD 718812)

6.————. Technical Report R-747: Windows for external or internal hydrostatic pressure vessels, pt. 6. Conical acrylic windows under long-term pressure application at 5,000 psi, by J. D. Stachiw and K. O. Gray. Port Hueneme, Calif., June 1971. (AD 736594)

7.————. Technical Note N-1127: Flat disc acrylic plastic windows for man-rated hyperbaric chambers at the USN Experimental Diving Unit, by J. D. Stachiw. Port Hueneme, Calif., Nov. 1970. (AD 716751)

8.————. Technical Report R-676: Development of a spherical acrylic plastic pressure hull for hydrospace application, by J. D. Stachiw. Port Hueneme, Calif., Apr. 1970. (AD 707363)

9.————. Technical Note N-1113: The spherical acrylic pressure hull for hydrospace application, pt. 2. Experimental stress evaluation of prototype NEMO capsule, by J. D. Stachiw and K. L. Mack. Port Hueneme, Calif., Oct. 1970. (AD 715772)

10. Naval Civil Engineering Laboratory. Technical Note N-1094: The spherical acrylic pressure hull for hydrospace application, pt. 3. Comparison of experimental and analytical stress evaluations for prototype NEMO capsule, by H. Ottsen. Port Hueneme, Calif., Mar. 1970. (AD 709914)

11.————: Technical Note N-1134: The spherical acrylic pressure hull for hydrospace application, pt. 4. Cyclic fatigue of NEMO capsule #3, by J. D. Stachiw. Port Hueneme, Calif., Oct. 1970. (AD 715345)

12.————. Technical Report R-675: Stress analysis of a conical acrylic viewport, by M. R. Snoey and J. E. Crawford. Port Hueneme, Calif., Apr. 1970. (AD 708009)

13. Armed Forces Supply Support Center. Military Handbook 17: Plastics for flight vehicles, pt. 2. Transparent glazing materials. Washington, D. C., Aug. 1961.

14. M. R. Snoey and J. D. Stachiw. "Windows and transparent hulls for man in hydrospace," in a critical look at marine technology; transactions of the 4th annual MTS conference and exhibit, Washington, D. C., July 8-10, 1968. Washington, D. C., Marine Technology Society, 1968, pp. 419-463.

DISTRIBUTION LIST

SNDL Code	No. of Activities	Total Copies	
—	1	12	Defense Documentation Center
FKAIC	1	10	Naval Facilities Engineering Command
FKNI	6	6	NAVFAC Engineering Field Divisions
FKN5	9	9	Public Works Centers
FA25	1	1	Public Works Center
..	9	9	RDT&E Liaison Officers at NAVFAC Engineering Field Divisions and Construction Battalion Centers
—	316	316	NCEL Special Distribution List No. 9 for persons and activities interested in reports on Deep Ocean Studies

Naval Civil Engineering Laboratory
WINDOWS FOR EXTERNAL OR INTERNAL HYDROSTATIC PRESSURE VESSELS—PART VII. Effect of Temperature and Flange Configurations on Critical Pressure of 90-Degree Conical Acrylic Windows Under Short-Term Loading (Final), by J. D. Stachiw and J. R. McKay
TR-773 51 p. illus August 1972 Unclassified

1. Pressure vessel windows—Conical acrylic plastic I. YF 51.543.008.01.001

Conical acrylic windows of 90-degree included angle and 0.083 to 0.775 thickness-to-minor-diameter (t/D) ratios have been tested to ultimate failure under short-term hydrostatic loading. The ambient temperature was varied from 32°F to 90°F and the relationship between minor window diameter (D) and minor window cavity diameter in the flange (D_f) varied from 0.970 to 1.500. The test results show that the critical pressure of identical windows at 90°F is approximately *10% to 20%* less than at 70°F, and at 32°F it is approximately *15% to 25%* more than at 70°F. The increase in critical pressure of windows with identical t/D ratios due to changes in D/D_f ratio is as large as 100% from the critical pressures associated with the standard D/D_f = 1.000 ratio. As a rule, an increase in D/D_f ratio raised the critical pressure of windows with t/D ⩾ 0.375 significantly, while for windows with t/D < 0.375, it had no effect or very little. To improve the critical pressure of 90-degree conical acrylic windows, it is recommended that such windows be designed with a window/flange mismatch ratio of D/D_f > 1.00, the exact magnitude depending on the window's t/D ratio, service, and design considerations.

Naval Civil Engineering Laboratory
WINDOWS FOR EXTERNAL OR INTERNAL HYDROSTATIC PRESSURE VESSELS—PART VII. Effect of Temperature and Flange Configurations on Critical Pressure of 90-Degree Conical Acrylic Windows Under Short-Term Loading (Final), by J. D. Stachiw and J. R. McKay
TR-773 51 p. illus August 1972 Unclassified

1. Pressure vessel windows—Conical acrylic plastic I. YF 51.543.008.01.001

Conical acrylic windows of 90-degree included angle and 0.083 to 0.775 thickness-to-minor-diameter (t/D) ratios have been tested to ultimate failure under short-term hydrostatic loading. The ambient temperature was varied from 32°F to 90°F and the relationship between minor window diameter (D) and minor window cavity diameter in the flange (D_f) varied from 0.970 to 1.500. The test results show that the critical pressure of identical windows at 90°F is approximately *10% to 20%* less than at 70°F, and at 32°F it is approximately *15% to 25%* more than at 70°F. The increase in critical pressure of windows with identical t/D ratios due to changes in D/D_f ratio is as large as 100% from the critical pressures associated with the standard D/D_f = 1.000 ratio. As a rule, an increase in D/D_f ratio raised the critical pressure of windows with t/D ⩾ 0.375 significantly, while for windows with t/D < 0.375, it had no effect or very little. To improve the critical pressure of 90-degree conical acrylic windows, it is recommended that such windows be designed with a window/flange mismatch ratio of D/D_f > 1.00, the exact magnitude depending on the window's t/D ratio, service, and design considerations.

Naval Civil Engineering Laboratory
WINDOWS FOR EXTERNAL OR INTERNAL HYDROSTATIC PRESSURE VESSELS—PART VII. Effect of Temperature and Flange Configurations on Critical Pressure of 90-Degree Conical Acrylic Windows Under Short-Term Loading (Final), by J. D. Stachiw and J. R. McKay
TR-773 51 p. illus August 1972 Unclassified

1. Pressure vessel windows—Conical acrylic plastic I. YF 51.543.008.01.001

Conical acrylic windows of 90-degree included angle and 0.083 to 0.775 thickness-to-minor-diameter (t/D) ratios have been tested to ultimate failure under short-term hydrostatic loading. The ambient temperature was varied from 32°F to 90°F and the relationship between minor window diameter (D) and minor window cavity diameter in the flange (D_f) varied from 0.970 to 1.500. The test results show that the critical pressure of identical windows at 90°F is approximately *10% to 20%* less than at 70°F, and at 32°F it is approximately *15% to 25%* more than at 70°F. The increase in critical pressure of windows with identical t/D ratios due to changes in D/D_f ratio is as large as 100% from the critical pressures associated with the standard D/D_f = 1.000 ratio. As a rule, an increase in D/D_f ratio raised the critical pressure of windows with t/D ⩾ 0.375 significantly, while for windows with t/D < 0.375, it had no effect or very little. To improve the critical pressure of 90-degree conical acrylic windows, it is recommended that such windows be designed with a window/flange mismatch ratio of D/D_f > 1.00, the exact magnitude depending on the window's t/D ratio, service, and design considerations.

Naval Civil Engineering Laboratory
WINDOWS FOR EXTERNAL OR INTERNAL HYDROSTATIC PRESSURE VESSELS—PART VII. Effect of Temperature and Flange Configurations on Critical Pressure of 90-Degree Conical Acrylic Windows Under Short-Term Loading (Final), by J. D. Stachiw and J. R. McKay
TR-773 51 p. illus August 1972 Unclassified

1. Pressure vessel windows—Conical acrylic plastic I. YF 51.543.008.01.001

Conical acrylic windows of 90-degree included angle and 0.083 to 0.775 thickness-to-minor-diameter (t/D) ratios have been tested to ultimate failure under short-term hydrostatic loading. The ambient temperature was varied from 32°F to 90°F and the relationship between minor window diameter (D) and minor window cavity diameter in the flange (D_f) varied from 0.970 to 1.500. The test results show that the critical pressure of identical windows at 90°F is approximately *10% to 20%* less than at 70°F, and at 32°F it is approximately *15% to 25%* more than at 70°F. The increase in critical pressure of windows with identical t/D ratios due to changes in D/D_f ratio is as large as 100% from the critical pressures associated with the standard D/D_f = 1.000 ratio. As a rule, an increase in D/D_f ratio raised the critical pressure of windows with t/D ⩾ 0.375 significantly, while for windows with t/D < 0.375, it had no effect or very little. To improve the critical pressure of 90-degree conical acrylic windows, it is recommended that such windows be designed with a window/flange mismatch ratio of D/D_f > 1.00, the exact magnitude depending on the window's t/D ratio, service, and design considerations.

Unclassified

Security Classification

DOCUMENT CONTROL DATA - R & D

(Security classification of title, body of abstract and indexing annotation must be entered when the overall report is class fied)

1. ORIGINATING ACTIVITY *(Corporate author)*

Naval Civil Engineering Laboratory
Port Hueneme, California 93043

2a. REPORT SECURITY CLASSIFICATION

Unclassified

2b. GROUP

3. REPORT TITLE

WINDOWS FOR EXTERNAL OR INTERNAL HYDROSTATIC PRESSURE VESSELS—PART VII. Effect of Temperature and Flange Configurations on Critical Pressure of 90-Degree Conical Acrylic Windows Under Short-Term Loading

4. DESCRIPTIVE NOTES *(Type of report and inclusive dates)*

Final; June 1969–June 1970

5. AUTHOR(S) *(First name, middle initial, last name)*

J. D. Stachiw and J. R. McKay

6. REPORT DATE	7a. TOTAL NO. OF PAGES	7b. NO. OF REFS
August 1972	51	14

8a. CONTRACT OR GRANT NO.	9a. ORIGINATOR'S REPORT NUMBER(S)
b. PROJECT NO. YF 51.543.008.01.001	TR-773
c.	9b. OTHER REPORT NO(S) *(Any other numbers that may be assigned this report)*
d.	

10. DISTRIBUTION STATEMENT

Approved for public release; distribution unlimited.

11. SUPPLEMENTARY NOTES	12. SPONSORING MILITARY ACTIVITY
	Naval Facilities Engineering Command Washington, D. C. 20390

13. ABSTRACT

Conical acrylic windows of 90-degree included angle and 0.083 to 0.775 thickness-to-minor-diameter (t/D) ratios have been tested to ultimate failure under short-term hydrostatic loading. The ambient temperature was varied from 32°F to 90°F and the relationship between minor window diameter (D) and minor window cavity diameter in the flange (D_f) varied from 0.970 to 1.500. The test results show that the critical pressure of identical windows at 90°F is approximately *10% to 20%* less than at 70°F, and at 32°F it is approximately *15% to 25%* more than at 70°F. The increase in critical pressure of windows with identical t/D ratios due to changes in D/D_f ratio is as large as 100% from the critical pressures associated with the standard D/D_f = 1.000 ratio. As a rule, an increase in D/D_f ratio raised the critical pressure of windows with $t/D \geq 0.375$ significantly, while for windows with $t/D < 0.375$, it had no effect or very little. To improve the critical pressure of 90-degree conical acrylic windows, it is recommended that such windows be designed with a window/flange mismatch ratio of $D/D_f > 1.00$, the exact magnitude depending on the window's t/D ratio, service, and design considerations.

DD FORM 1 NOV 65 1473 (PAGE 1)

S/N 0101-807-6801

Unclassified

Security Classification

14. KEY WORDS	LINK A		LINK B		LINK C	
	ROLE	WT	ROLE	WT	ROLE	WT
Pressure vessel windows						
Acrylic plastic						
Conical windows						
Short-term pressurization						
Long-term pressurization						
Failure modes						
Displacement						
Deformation						
Fracture patterns						
Window flange designs						
Submersible windows						
Undersea habitat windows						
Deep-submergence windows						
Viewports						
Hyperbaric chamber windows						

R 527

Technical Report

WINDOWS FOR EXTERNAL OR INTERNAL HYDROSTATIC PRESSURE VESSELS

PART II. Flat Acrylic Windows Under Short-Term Pressure Application

May 1967

NAVAL FACILITIES ENGINEERING COMMAND

NAVAL CIVIL ENGINEERING LABORATORY

Port Hueneme, California

WINDOWS FOR EXTERNAL OR INTERNAL HYDROSTATIC PRESSURE VESSELS
PART II. Flat Acrylic Windows Under Short-Term Pressure Application

Technical Report R-527

Y-F015-01-07-001

by

J. D. Stachiw, G. M. Dunn, and K. O. Gray

ABSTRACT

Flat, disk-shaped acrylic windows of different thickness-to-diameter ratios have been tested to destruction under short-term hydrostatic loading at room temperatures, where short-term loading is defined as pressurizing the window hydrostatically on its high-pressure face at a 650-psi/minute rate till failure of the window takes place. Critical pressures and displacements of windows with thickness to effective diameter ratios less than 1.0 have been recorded and plotted. The critical pressures derived from testing flat windows in flanges with 1.5-inch, 3.3-inch, and 4.0-inch openings have been found applicable also to flanges with larger openings, so long as the larger windows are of the same t/D_i and D_o/D_i ratios, where t is thickness of the window, D_i is the clear opening in the flange and therefore the effective diameter of the window exposed to ambient atmospheric pressure and D_o is overall diameter of the window face exposed to hydrostatic pressure. The performance of flat windows under short-term hydrostatic pressure has been found to be comparable to that of conical windows with included angle equal to, or larger than 90 degrees.

CONTENTS

TERMINOLOGY

D_i The diameter of the clear opening in the flange and therefore the effective diameter of the window.

D_o The overall diameter of the window, or diameter of opening on high-pressure side of flange (minus clearance).

P_c Critical pressure or the pressure at which complete failure of the window occurs, resulting in explosive release of pressure from the vessel and fragmentation of the window.

t The nominal or exact measured thickness of the acrylic window.

INTRODUCTION

The Naval Facilities Engineering Command is responsible for the construction and maintenance of underwater structures attached to the ocean floor. Such structures may include instrumented or manned underwater surveillance or observation posts that will rely (at least in part) on visual observation and the transmission and reception of electromagnetic radiation through nonopaque areas of the hull for the performance of their mission. The Deep Ocean Laboratory of the Naval Civil Engineering Laboratory (NCEL) is carrying out studies to provide information on the design of underwater windows. The first report[1] on these studies discussed the behavior of conical acrylic windows under short-term pressurization. The report in hand presents information on the behavior of flat, disk-shaped acrylic windows under short-term pressurization.

Flat, disk-shaped acrylic windows for high-hydrostatic-pressure applications have received very limited attention, and only a few facets of their behavior under hydrostatic loading have been investigated.[2] Since flat windows possess characteristics not inherent in conical acrylic windows currently in use in underwater structures, it was considered desirable to investigate this type of window.

The major advantage of flat windows is the commercial availability of glass, acrylic, epoxy, and polycarbonate material in polished transparent sheets or plates. Conical windows require considerable precision machining to adapt flat sheets or plates to the window flange. On the other hand, flat windows require only simple cutting and turning to transform flat material into usable windows. Furthermore, the fabrication of the flat-window mounting flange is also much simpler. Since the mating surfaces of both the window and flange are plane, the problem of replacement of windows is simplified when they become defective due to mechanical damage or the cracking which precedes failure under pressure. There may, of course, be some disadvantages associated with flat windows, such as smaller angle of vision for the same flange opening, but there are sufficient advantages inherent in flat windows to make them worthy of investigation for underwater structural applications.

The underwater structures in which flat windows could be incorporated may be subjected to a variety of hydrostatic loadings. Thus a series of studies must be conducted to determine their behavior under short-term, long-term, cyclic, and dynamic loading. The first of the studies conducted deals with the short-term hydrostatic loading of flat acrylic windows, where short-term hydrostatic loading is defined as pressurizing the window on its high-pressure face at a 650-psi/min rate from zero (atmospheric) pressure to its failure pressure. The purpose of this report is to document the first experimental study.

EXPERIMENTAL PROCEDURE

The objective of the experimental study was to generate a set of performance curves that would serve as the basis for designing flat acrylic windows for use under short-term hydrostatic pressure. Also the critical pressures for windows had to be determined before further optical studies could be undertaken. Therefore, experimental data not only had to cover the whole range of depths encountered in the ocean, but also had to be applicable to flat windows of different thicknesses and diameters.

To meet these objectives, window test specimens had to be designed that upon testing would provide the necessary data on which generalized window design curves could be based. This was accomplished by selecting two nondimensional parameters for dimensioning the windows. Use of the t/D_i ratio and the D_o/D_i ratio (see "Terminology" and Figure 1) permitted not only the adequate description of any window, but also scaling window dimensions up or down. In order to cover the whole depth range in the ocean, the thickness component (t) of the t/D_i ratio was varied from 0.125 inch to 2 inches, while to prove the applicability of experimental data to all possible window sizes the flange opening diameter (D_i) component of the ratio was varied from 1.5 inches to 4.0 inches (Table 1). Flanges and some of the windows are shown in Figures 2, 3, and 4. The flange seat diameter ratio (D_o/D_i) was not varied during the generation of the experimental data serving as basis for generalized design curves because there were indications (see Appendix A) that varying this parameter would unduly complicate the study. For the same reason the various methods for retaining the window in the flange were not investigated, although earlier exploratory experimental data shows[3] that for some t/D_i and t/D_o ratios, the type of edge restraint used on the window has a considerable influence on the critical pressure of the window. To avoid confounding the data, the windows in this study were not clamped or lapped in place, but simply sealed with grease into the flange cavity with approximately 0.005 to 0.010 inch radial clearance between them and the flange. This type of flat acrylic window mounting (shown in Figure 1) will be referred to in this report as the DOL type III flange.

Although in designing a flat acrylic window to be safe for underwater application it is necessary to know the behavior of such windows under various types of hydrostatic loading, only the short-term strength of windows was considered in this study. The experimental evaluation of long-term and cyclic hydrostatic loading was relegated to future studies on this subject. In the present study it is considered sufficient for design purposes to have reliable data on only the magnitude of the displacement of the center on the window's low-pressure face and the critical pressure at which a window of any t/D_i ratio fails under short-term loading.

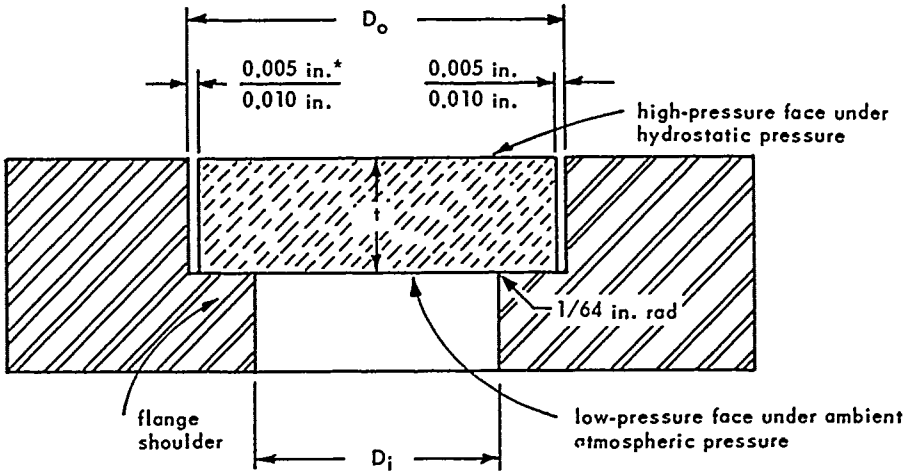

$$D_o = 1.5 \times D_i$$

* Indicates maximum and minimum dimensions allowable.

Figure 1. DOL type III flange configuration for short-term testing of flat acrylic windows.

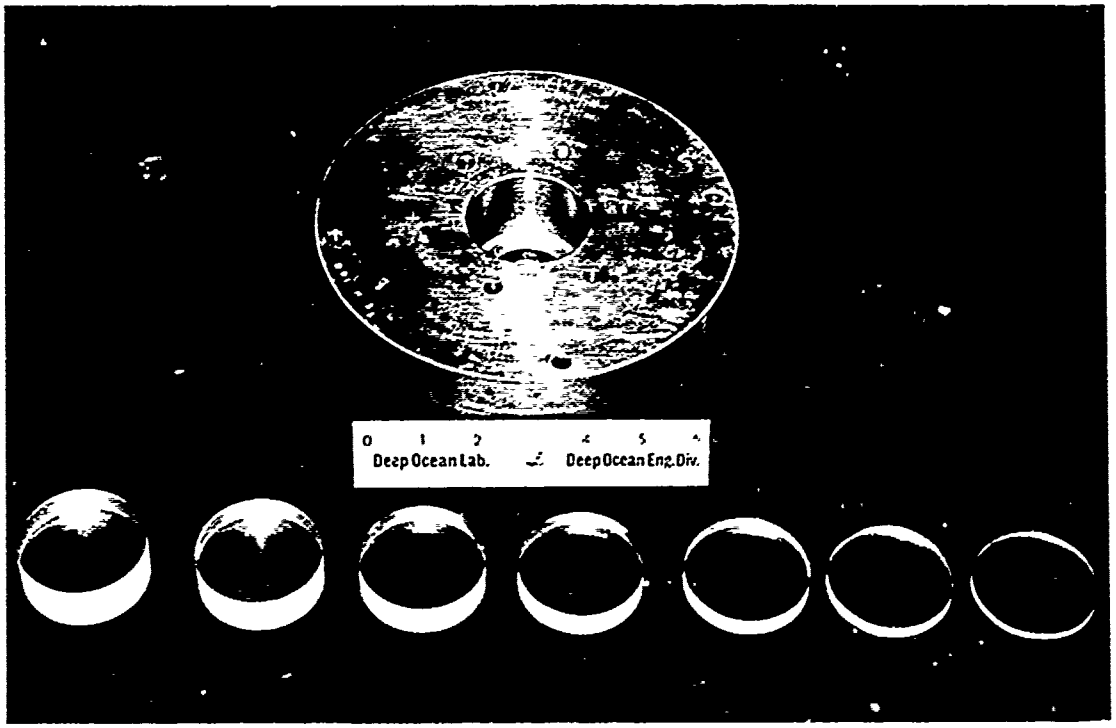

Figure 2. Flat acrylic windows and 1.50-inch (D_i) flange used to determine the relationship between the window's critical pressure and t/D_i ratio.

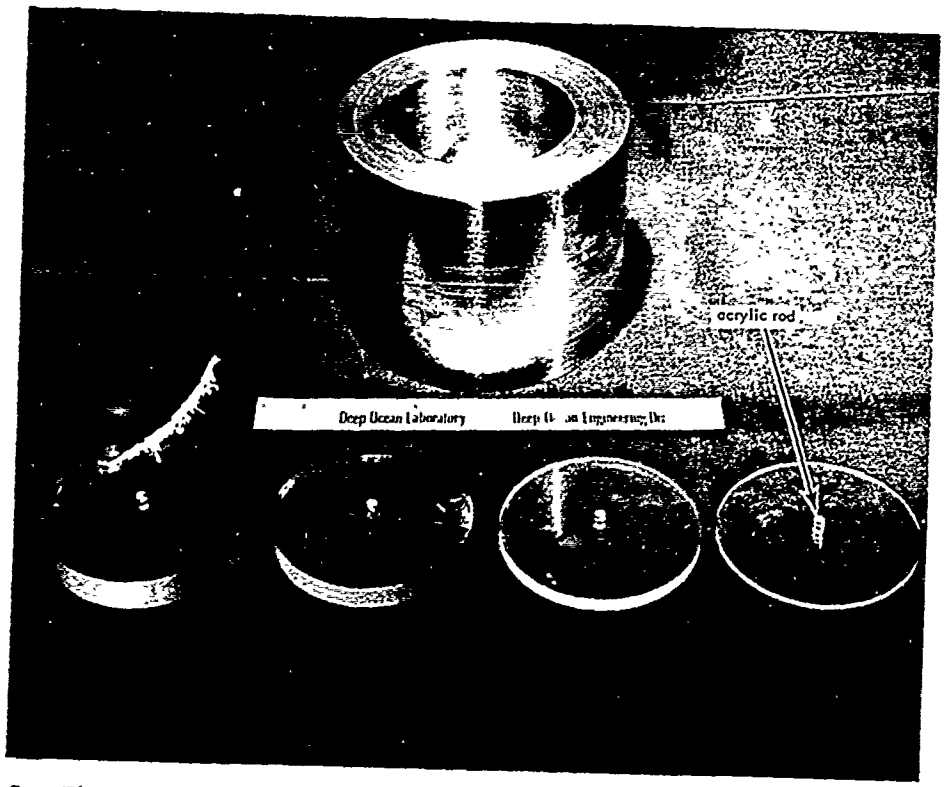

Figure 3. Flat acrylic windows and 3.33-inch (D_i) flange used to determine the relationship between the window's critical pressure and t/D_i ratio.

Figure 4. Flat acrylic windows and 4.00-inch (D_i) flange used to determine the relationship between the window's critical pressure and t/D_i ratio.

Table 1. Flat Disk Window Test Specimens

(* represents a test group of five window specimens)

Nominal Thickness (in.)	D_i = 1.50 in. D_o = 2.25 in.	D_i = 3.33 in. D_o = 5.00 in.	D_i = 4.00 in. D_o = 6.00 in.
1/8	*	*	
1/4	*		*
3/8	*	*	
1/2	*		*
5/8	*	*	
3/4	*		
7/8	*	*	
1	*		*
1-1/8		*	
1-1/2		*	
2		*	*

In order to simulate the loads encountered by flat acrylic windows in underwater structures, window specimens were subjected to hydrostatic pressure loading in a hydrospace simulation chamber. The pressurization of the windows was conducted in a 16-inch naval gun shell converted into a pressure vessel[4] with water at room temperature serving as the pressurization medium. The water was pressurized by two air-driven, positive-displacement pumps whose pumping rate was controlled within ±50 psi/minute. Since previous studies[1] have shown that critical pressure of windows depends on water temperature as well as on pressurization rate, an effort was made to hold these variables constant for all the window tests. The standard pressurization rate was 650 psi/minute, and water temperature was held between 65°F and 75°F.

The window test specimens for this study (Table 1) were fabricated by lathe turning Plexiglas grade G sheet stock. The circular disks (Figure 1) thus formed had an overall diameter (D_o) of 0.010 inch to 0.020 inch less than the flange's high-pressure opening diameter (D_o), permitting the window to seat in its flange cavity with 0.005 to 0.010 inch radial clearance. The manufacturer's tolerances for variation in the nominal thickness of commercial sheets were accepted for the thickness tolerance of the finished circular flat windows. The finish of the disk edges was held to 32 rms. Dimensions recorded were the average of micrometer measurements taken at three different locations for the window's diameter and for its thickness.

The hydrostatic testing consisted of pressurizing a flange-mounted window (Figure 5) until failure occurred. Since the window flange is open on one side to the atmosphere, window fragments were ejected upon its failure (Figure 6). The displacement of the window's low-pressure face during pressurization was measured to ±0.001 inch by means of a wire that transmitted the displacement of the window to a mechanical dial indicator over a pulley system without any mechanical amplification (Figures 5 and 7). To permit the attachment of a displacement indicator wire to the center of the window's low-pressure face, a short acrylic rod with a small transverse hole in one end was bonded to the window's surface with solvent-type cement. The displacement of the window under hydrostatic pressure was read directly from the dial indicator with a closed-circuit television system that permitted the operators to be in a safe location during the ejection of the window from its retaining flange when critical pressure was reached (Figures 8 and 9).

As discussed in Appendix A, silicone grease was used as a pressure seal between the window and flange. The grease was spread by hand on the contact area of the low-pressure face and edge of the window. Sealing was completed when the window was placed in the flange cavity, rotated in place and pushed inward against the flange. This was done to distribute the grease uniformly over the area of contact and also to eliminate any small air bubbles trapped between the window and flange. This procedure proved to be adequate as it allowed no leakage of water to occur between the window and the flange. Care was exercised to insure that both the flange cavity and window were clean, since the flange was used for successive testing and tended to retain small fragments of previously tested specimens.

Since the ejection of windows in many cases fragmented them into very small pieces, a reconstruction of the mechanism of material failure was usually impossible. To provide data that would give an insight into the mechanism of failure, some of the windows were pressurized only to a fraction of the window's critical pressure and then removed for inspection of their deformation and cracks (Appendix B).

The explosive release of energy which accompanied window failure at higher critical pressures was quite harmful to O-rings, bolts, and flanges. To decrease the shock effects of this energy release, the cylindrical passage in the flange and the adaptor flange was filled with water after the window was in place. At the moment the window failed the water was forced through a 1/2-inch-diameter restrictive opening in the adaptor flange. This shock-damping method was sufficient to prevent the breaking of the eight 1/4-inch-diameter high-strength bolts connecting the window flange and adaptor flange.

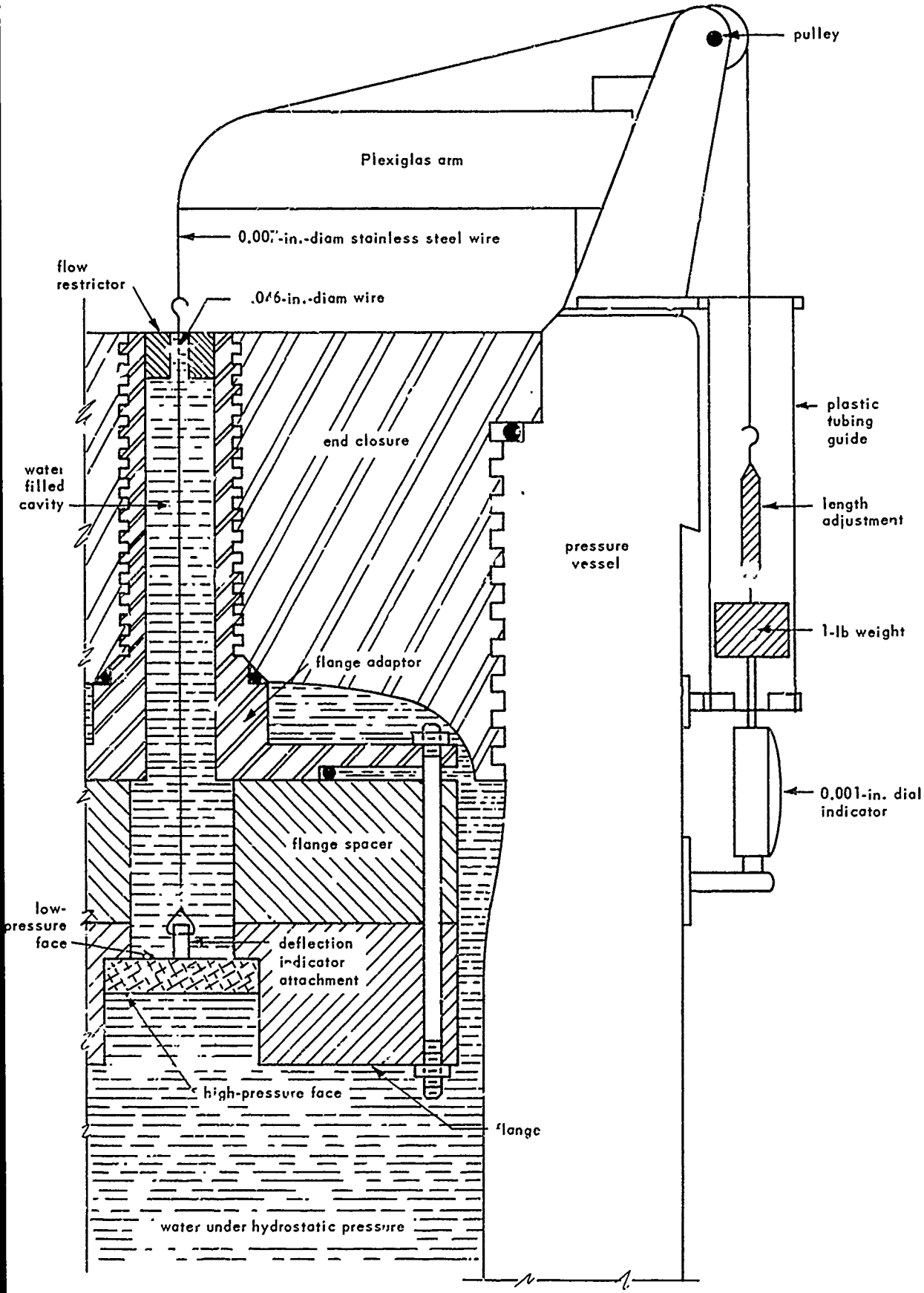

Figure 5. Schematic drawing of deflection measuring apparatus and flange mounting used in the testing of windows.

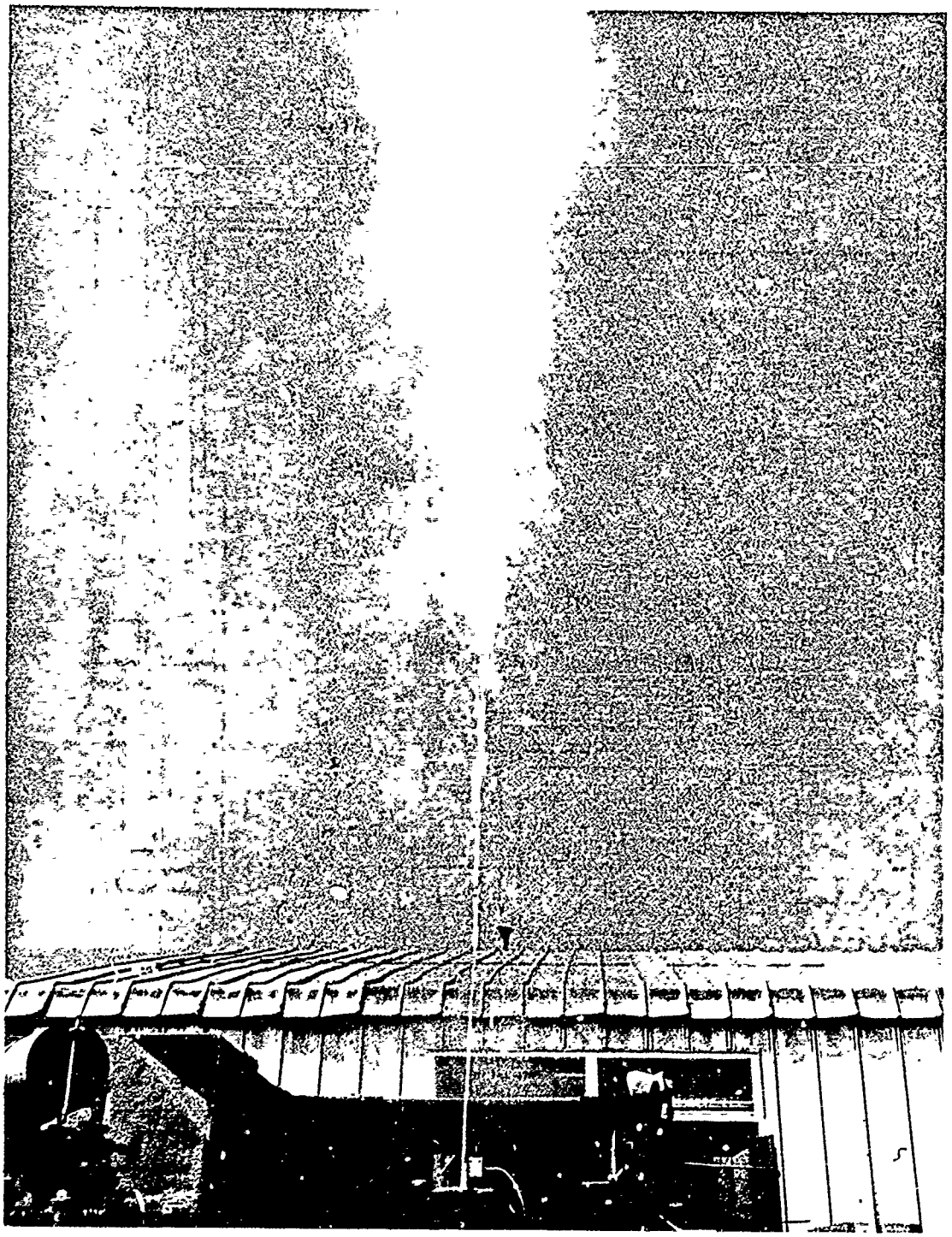

Figure 6. Ejection of window fragments by a high-pressure jet of water upon failure of the window.

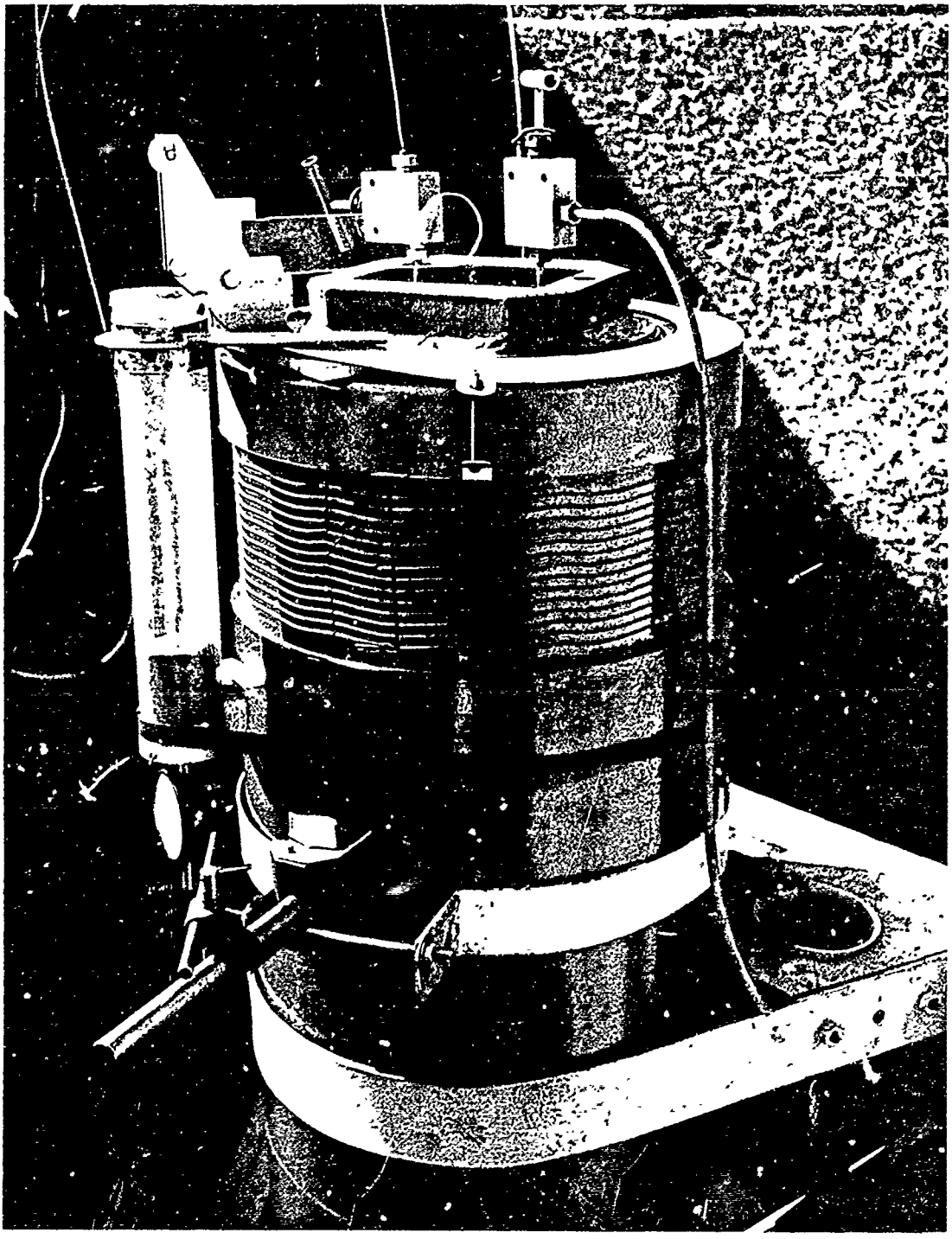

Figure 7. Deflection-measuring apparatus in place on pressure vessel.

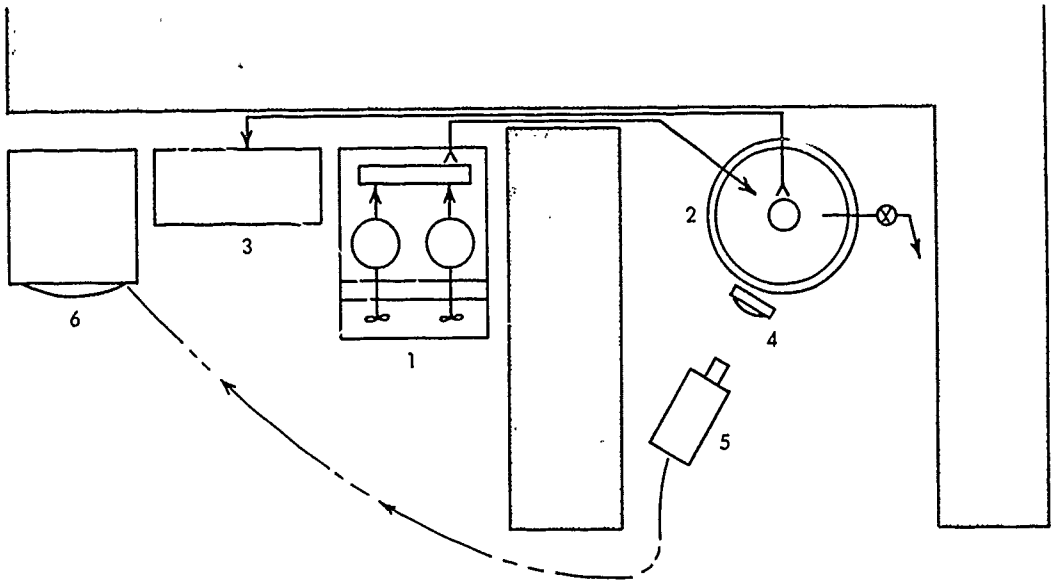

Air-driven positive displacement pumps (1) supply water under pressure to the Mk I 9-in. pressure vessel (2). Pressure is monitored by gage (3) and recorded. Dial indicator (4) is watched via closed-circuit television camera (5) and monitor (6). Operator is thus enabled to record data behind safety barricade.

Figure 8. Schematic plan of experimental setup.

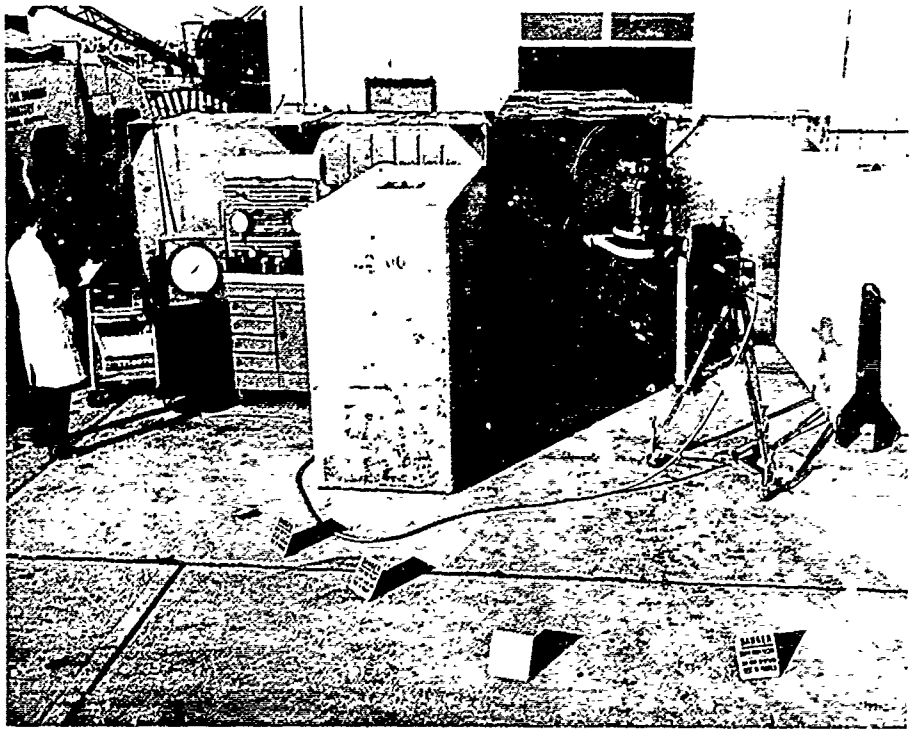

Figure 9. Pressure gages, pumps, and closed-circuit television monitor used behind barricade during testing.

DISCUSSION

General

The flat acrylic windows failed either in flexure or in shear, depending on their t/D_i ratio. The failure modes and mechanisms are discussed in detail in Appendix B, and deflection data are presented in Appendix C. In most cases, the center of the window was ejected in the form of small fragments, while in few cases in the low t/D_i ratio range the center was not ejected, as the formation of large cracks in the window at low pressure vented the pressurized water, and thus removed the energy required for ejection of the window. The critical pressures of windows were found to vary exponentially with their t/D_i ratio. When the critical pressures of windows with the same D_o/D_i and t/D_i ratios, and effective diameters of 1.50, 3.33, and 4.00 inches were plotted on the same graph (Figure 10) they were found to fall in the same failure region. This indicates that the critical pressure of a flat acrylic window is dependent only on the t/D_i ratio (and the mounting of the window in the flange).

The displacement of the windows also varied with their t/D_i ratio. Comparison of displacements of windows having effective diameters (D_i) of 1.50 inches (Figure 11), 3.33 inches (Figure 12), and 4.00 inches (Figure 13) shows that the displacements, besides being a function of t/D_i ratio are also a function of D_i. Although there are insufficient experimental data to establish a reliable relationship between the magnitude of displacement and the D_i of the window in DOL type III flange, it appears that the displacement is directly proportional to the D_i of the window.

The critical pressures of flat acrylic windows when compared to the critical pressures of conical acrylic windows investigated in previous studies[1] were found to be approximately of the same magnitude as the critical pressures of conical windows of same t/D_i ratio and having an included angle equal to, or larger than 90 degrees. Thus, it would appear that the flat acrylic windows mounted in the DOL type III flange are as resistant to short-term hydrostatic loading as the conical windows with included angle equal to, or larger than 90 degrees.

A technical discussion of the relationship between the critical pressure, D_o/D_i ratio, radial clearance between the window and the flange, and the method of sealing is presented in detail in Appendix A.

A technical discussion of the mode of failure of flat acrylic windows is presented in detail in Appendix B.

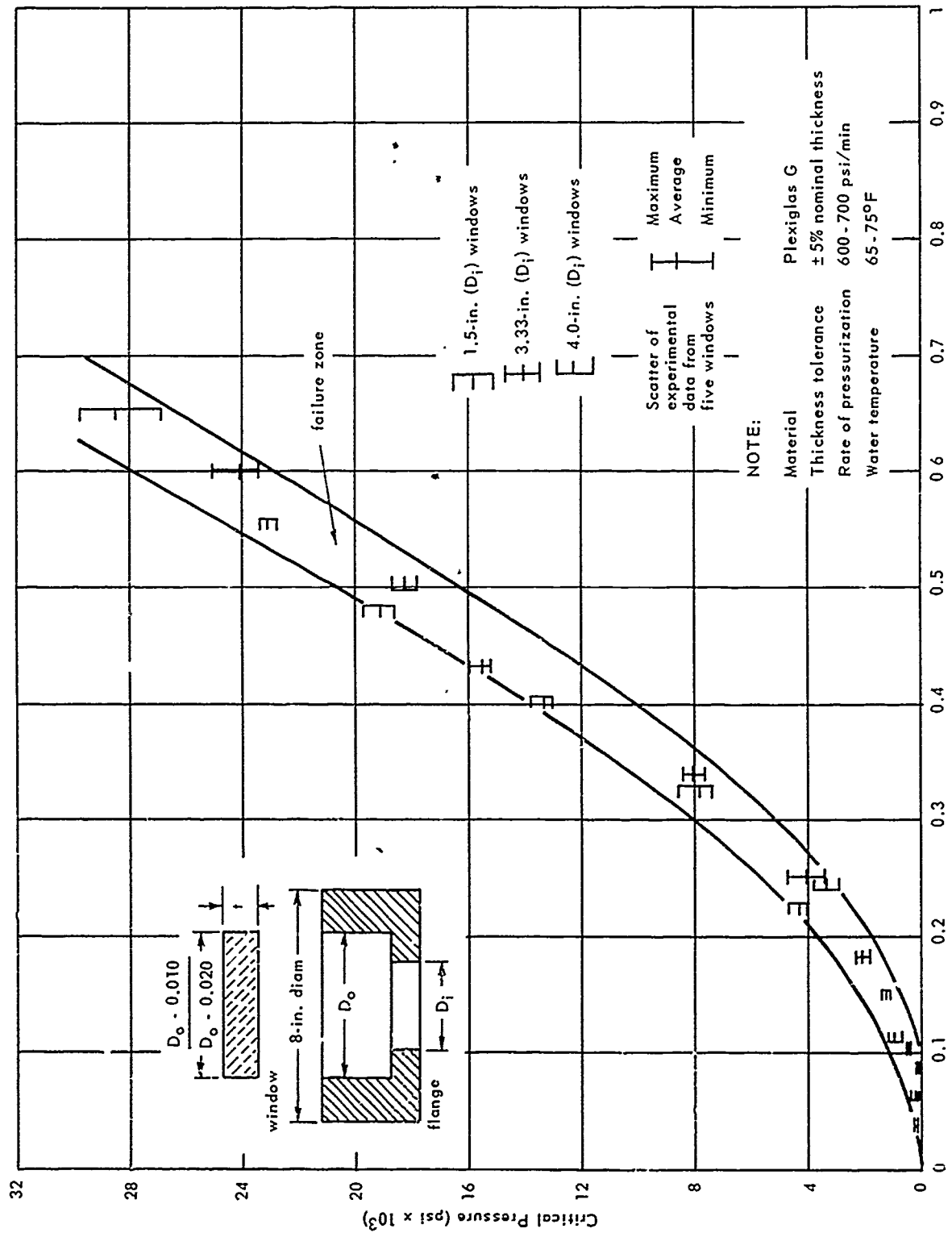

Figure 10. The experimental relationship between critical pressure and t/D_i ratio for flat acrylic windows with D_o/D_i ratio equal to 1.5.

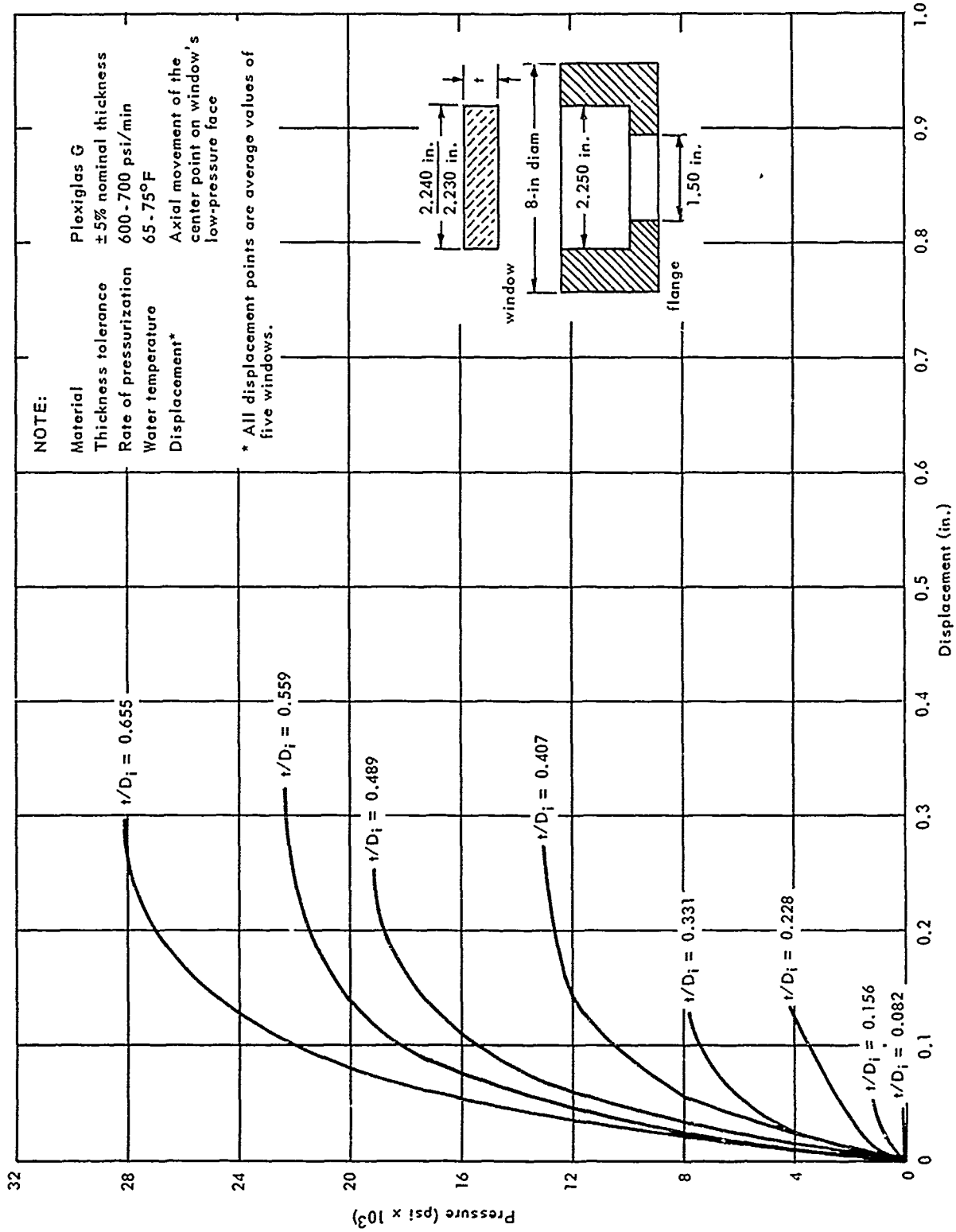

Figure 11. The experimental relationship between displacement and t/D_i ratio of flat acrylic windows with 1.5-inch D_i and with D_o/D_i ratio equal to 1.5.

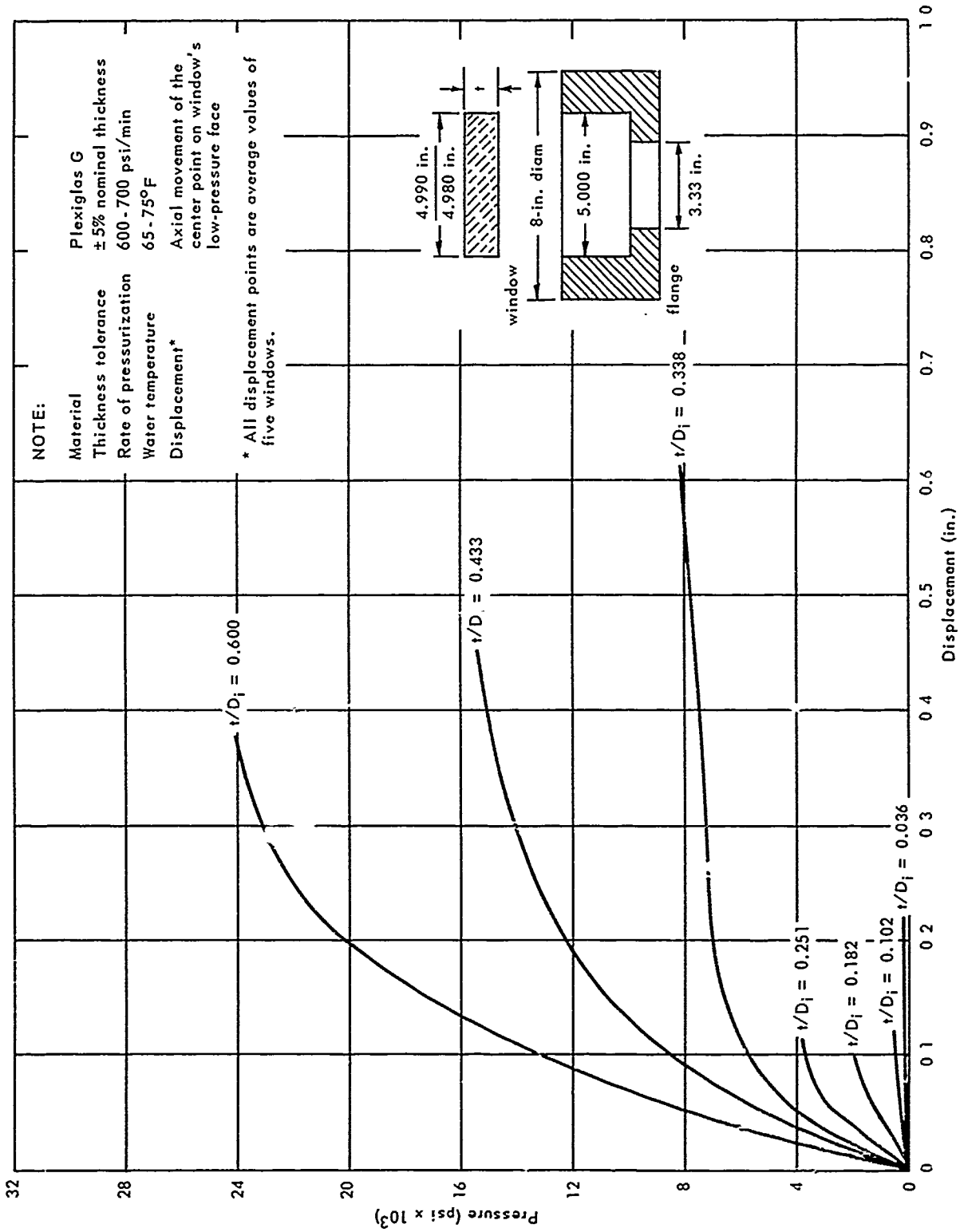

Figure 12. The experimental relationship between displacement and t/D_i ratio of flat acrylic windows with 3.33-inch D_i and with D_o/D_i ratio equal to 1.5.

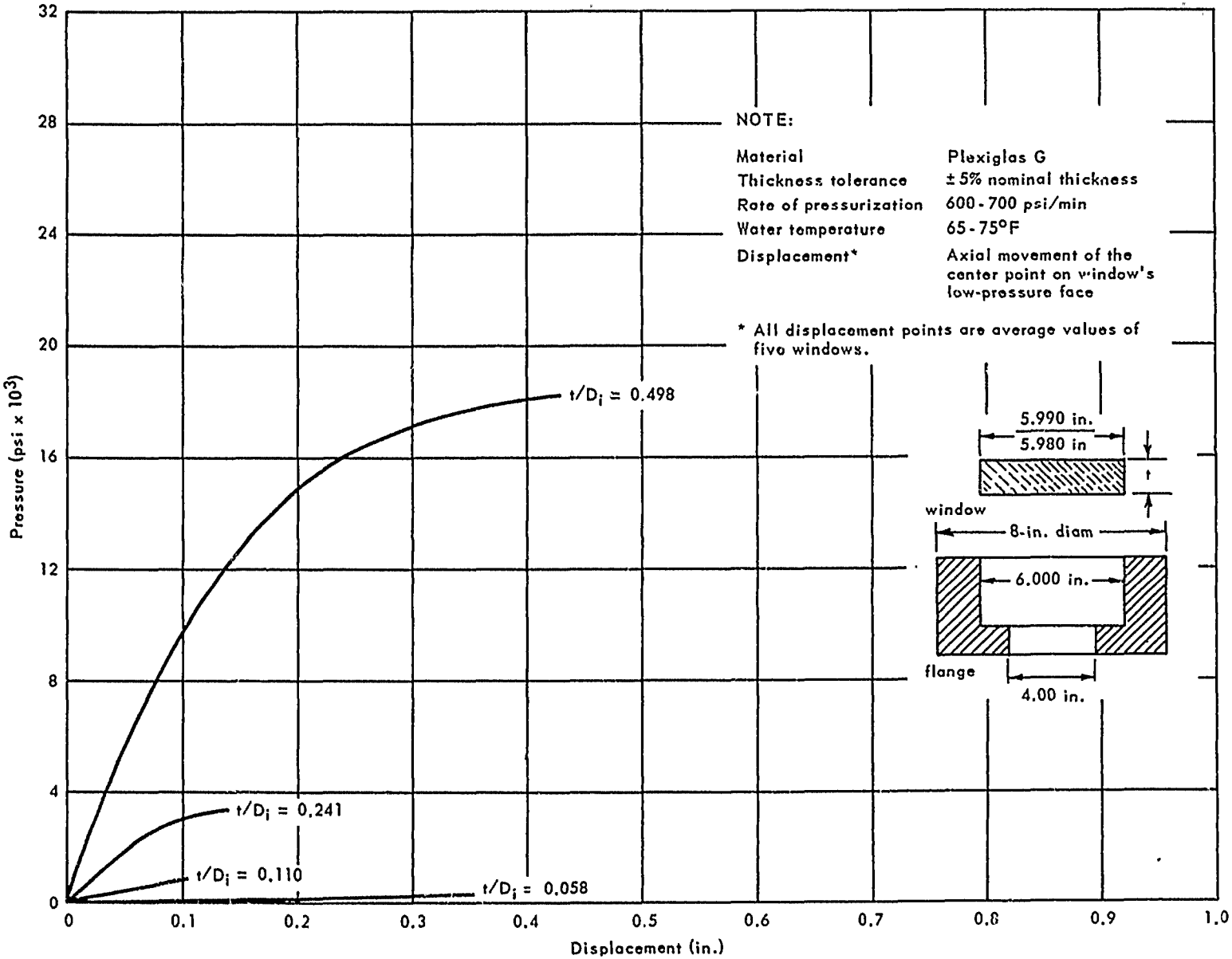

Figure 13. The experimental relationship between displacement and t/D_i ratio of flat acrylic windows with 4.00-inch D_i and with D_o/D_i ratio equal to 1.5.

Effect of Loading Conditions

Preliminary results .rom other studies in progress indicate that the critical pressures and deflections of acrylic windows are adversely affected by higher temperatures, and sustained or cyclical pressure loading. The designer is therefore cautioned that the data presented in this report pertains only to short-term pressure loading as defined for this study. If the short-term critical pressure data is used as a design basis for windows subjected to long term or cyclical loading, a safety factor of at least four, based on the short-term critical pressure, is recommended for the preliminary selection of window thickness. Subsequently a full-scale window with dimensions selected on the basis previously described should be tested under the full loading expectancy of the design. When experimental data for long-term and cyclical pressure loading become available the presently recommended approximate safety factor will be replaced by precise critical-pressure design curves plotted as a function of loading duration or number of pressure cycles.

Effect of Variations in Flange Design

Effects of flange designs different from DOL type III have not yet been investigated. Variations of direct influence on deflection and critical pressure would be (1) the use of a retaining ring against the high-pressure face, (2) the use of gaskets with or without a retaining ring, (3) using a radial clearance less than 0.005 inch between the window and flange, and (4) using a different flange shoulder thickness at D_i.

It is postulated that use of a retaining ring incorporated in a flange design would increase the critical pressure capabilities and decrease deflections of windows whose t/D_i ratio is less than about 0.4 to 0.5. This size window, failing predominantly by flexure would be more drastically influenced than would be the windows of t/D_i ratios greater than about 0.5, which fail predominantly by shear.

Flat bearing gaskets employed in a flange design are postulated to have varying effects, depending on the gasket's thickness and hardness and whether a retaining ring is also employed. Again the smaller t/D_i ratio windows would probably be more affected than would be the larger t/D_i ratio windows.

The magnitude of the flange thickness should not affect the window's short-term critical pressure so long as it is sufficiently thick to restrain radially the extruding portion of the window's low-pressure face prior to its failure. Also, the flange shoulder must be sufficiently thick to be rigid in comparison to the flexural rigidity of the flat acrylic window supported by the shoulder.

FINDINGS

1. The critical pressure of flat acrylic windows under short-term hydrostatic loading has been found to be solely a function of their t/D_i ratios, so long as their material composition and D_o/D_i ratios, the rate of pressurization, temperature of pressurizing medium, and the method of retaining the window in the flange are the same.

2. The axial displacement of the window's low-pressure face center has been found to vary both with the window's t/D_i ratio and its D_i.

3. The critical pressures of flat acrylic windows under short-term hydrostatic loading in a DOL type III flange have been found to be approximately the same as the critical pressures of conical acrylic windows with included angle equal to, or larger than 90 degrees, tested in DOL type I flanges under the same temperature and pressurization conditions.[1]

CONCLUSIONS

1. Flat acrylic windows have been found to perform successfully under short-term pressure application in pressure vessels and hydrospace structures.

2. Flat acrylic windows may be substituted for conical windows of 90 degrees or greater included angle, of similar thickness and effective diameter for short-term pressurization applications.

Appendix A

DISCUSSION OF WINDOW MOUNTINGS

INTRODUCTION

Variables Investigated

In conjunction with the experimental program investigating the relationship between the t/D_i ratio of flat acrylic windows and their critical pressure, an exploratory study was initiated to investigate several window-mounting variables which probably influence this relationship. The variables investigated were: (1) the relationship between the overall diameter (D_o) of the window disk and the effective diameter (D_i) of the window's unsupported viewing area as defined by the supporting shoulder of the window flange; (2) the method of making a pressure-tight seal between the window and the flange; and (3) the effect of radial clearance between the window and the flange. For these preliminary investigations, several test arrangements were devised and a number of windows were tested using each arrangement (Table A-1).

Experimental Methods

For the evaluation of the effect of the D_o/D_i ratio of windows on their critical pressure, two different flanges were fabricated that had the same D_i but different D_o openings (Figures A-1a, A-1c, and A-2). Windows (Figures A-3a and A-3c) of the same thickness, but with a D_o that matched the D_o of the flanges were tested in these flanges.

To evaluate the influence of the sealing method on the critical pressure of flat windows, two different types of seals were used in both the large and the small D_o/D_i ratio windows. The two types of seals used were an O-ring seal (Figures A-3b, A-3d, and A-4) under radial compression located around the circumference of the window, and a grease, surface-to-surface seal (Figures A-3a, A-3c, and A-5) between the window's low-pressure face and the flange's facing (Figures A-1a and A-1c). If the collapse pressure of windows tested in them remained the same regardless of the seal used, it could be postulated that the two methods of sealing were equivalent, and exerted no influence on the collapse pressure of windows. Collapse pressures of different magnitude resulting from the use of different sealing systems would, on the other hand, be indicative of seal's influence on the collapse pressure, and thus the collapse pressure of windows would have to be evaluated for each different kind of sealing method.

Table A-1. Flanges and Windows Used in the Evaluation of Seals, D_o/D_i Ratios, and Radial Clearances for Flat Acrylic Windows

Flanges			Windows Sealed With Grease					Windows Sealed With O-Rings				
D_i (in.)	D_o (in.)	Figure	D_o (in.)	Thickness[1] (in.)	Critical Pressure[2] (psi)	Displacement[2] at 16,000 psi (in.)	Figure	D_o (in.)	Thickness[1] (in.)	Critical Pressure[2] (psi)	Displacement[2] at 16,000 psi (in.)	Figure
1.501[3] / 1.499	2.001 / 2.000	A-1a	1.960 / 1.940	0.750	18,490	0.100	A-3a	1.999 / 1.998	0.750	19,060	0.086	A-3b
1.501 / 1.499	2.250 / 2.248	A-1b	1.960 / 1.940	0.750	16,960	0.079	A-3a	—	—	—	—	—
1.501 / 1.499	4.001 / 4.000	A-1c	3.960 / 3.940	0.750	19,190	0.117	A-3c	3.999 / 3.998	0.750	19,270	0.112	A-3d

1/ Nominal stock thickness of the five window specimens.

2/ Represents an average value of five window specimens.

3/ Indicates maximum and minimum dimensions allowable.

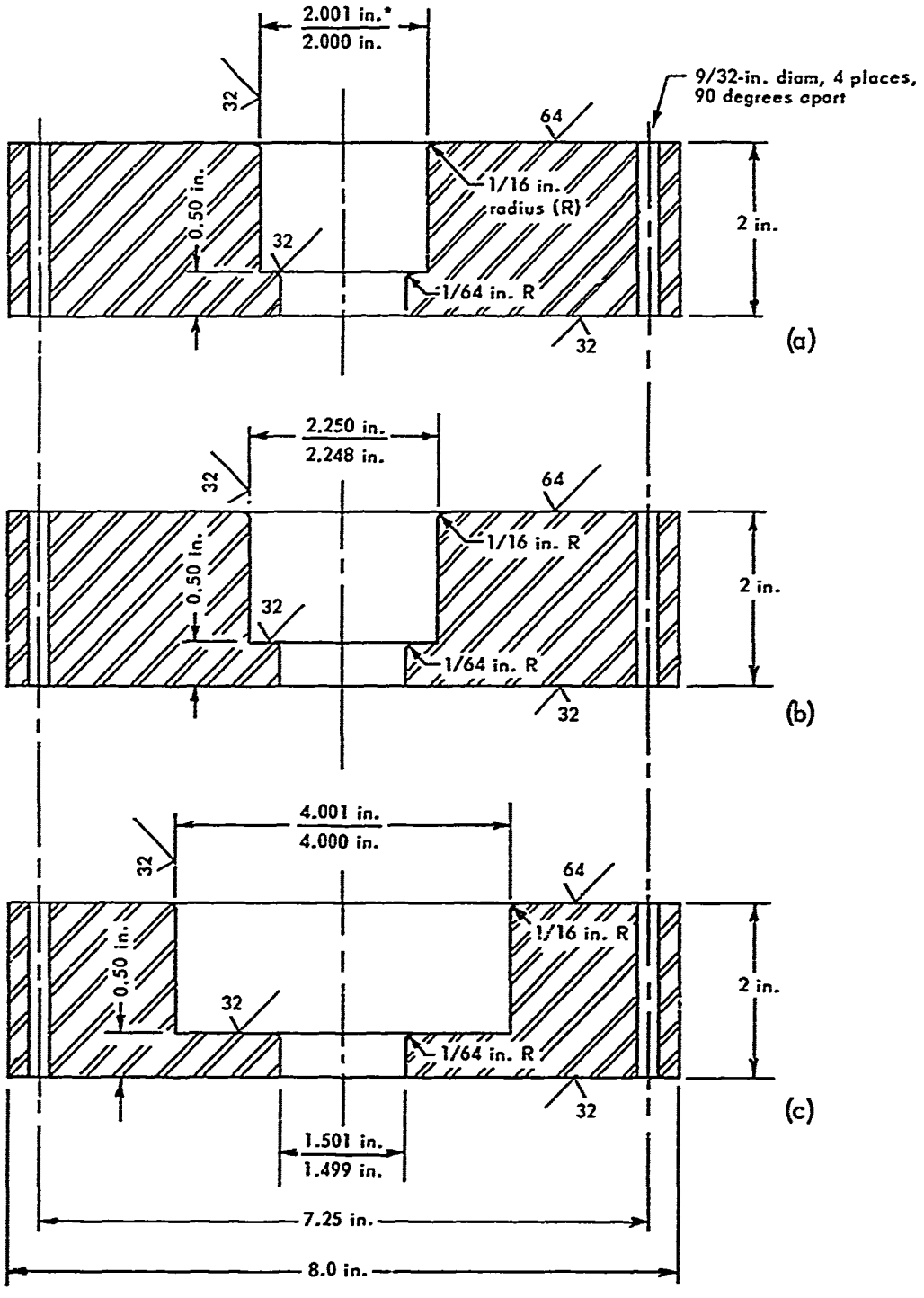

* Indicates maximum and minimum dimensions allowable.

Figure A-1. Flanges employed in investigation of window mountings.

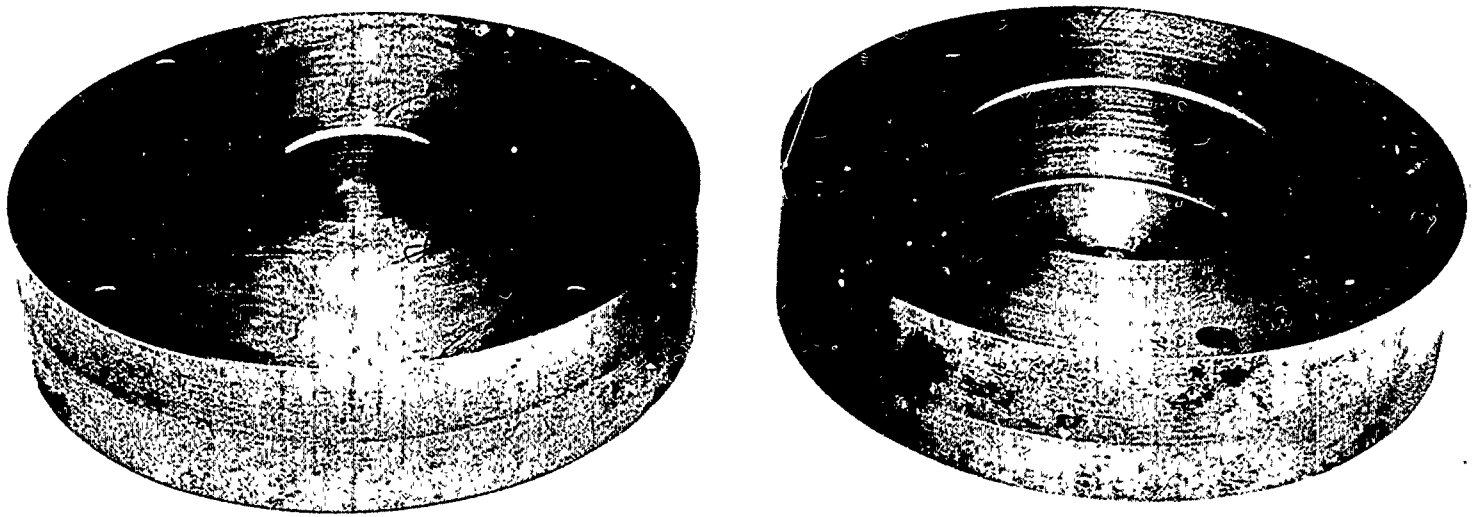

Figure A-2. Flanges (1.5-inch D_i) used in the window mounting investigation; 2.0-inch (D_o) (left) and 4.0-inch (D_o) (right).

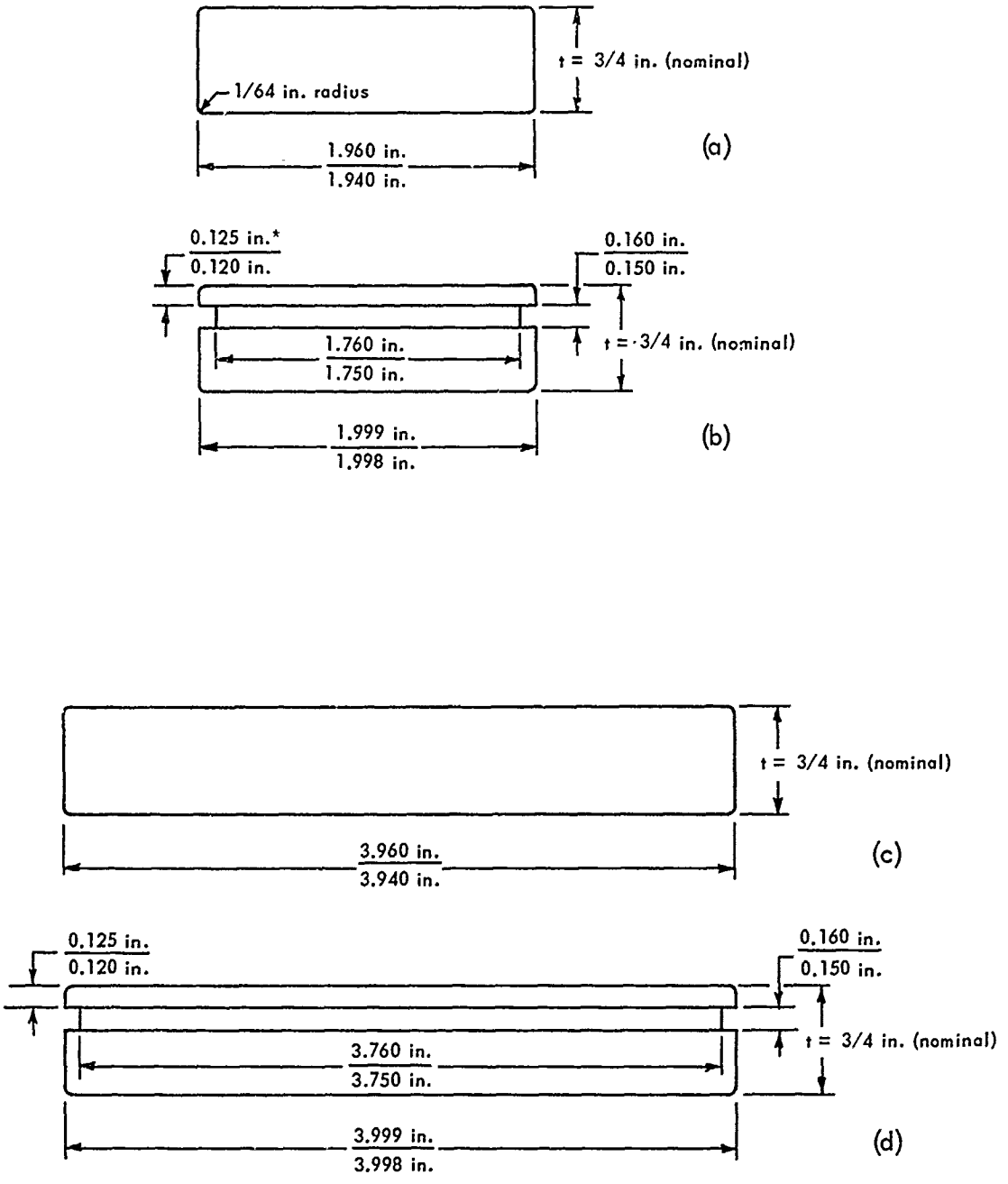

* Indicates maximum and minimun dimensions allowable.

Figure A-3. Details of flat acrylic windows used in investigation of window mountings.

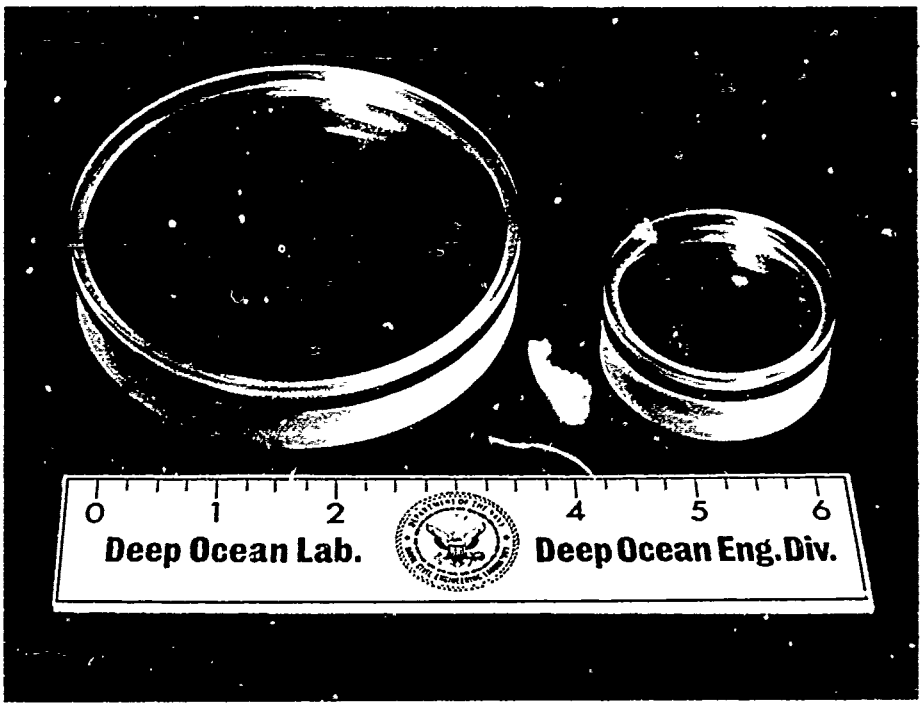

Figure A-4. Flat acrylic windows used with O-ring sealing technique in the investigation of window mountings.

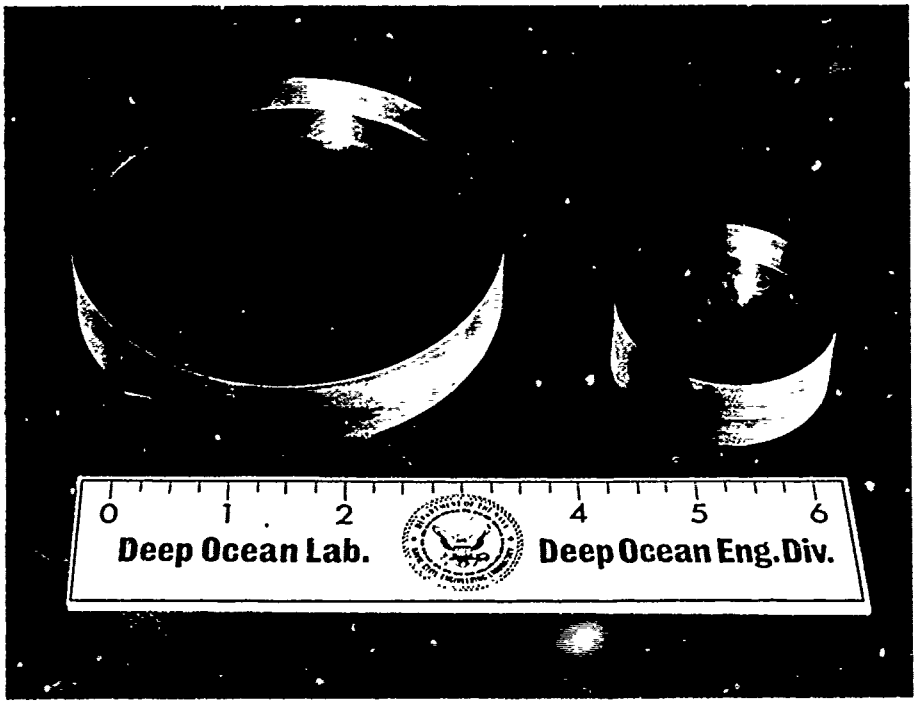

Figure A-5. Flat acrylic windows used with plane surface (grease) sealing technique in the investigation of window mountings.

The influence of window fit on the critical pressure was investigated with windows having the same D_o/D_i ratio and thickness (Figures A-3a and A-3b) fitted into flanges with different major diameters (Figures A-1a and A-1b). In one of the flanges (Figure A-1a) the pretest radial clearance between the windows and the flange was either 0.001 inch (Figure A-3b) or 0.025 inch (Figure A-3a), while in the other flange (Figure A-1b) the clearance was 0.125 inch. A radial clearance of 0.001 or 0.025 inch when the window is subjected to hydrostatic pressures above 10,000 psi is calculated to result in an interference fit between the window and the flange, thus resulting in a lateral constraint of the window. The flange (Figure A-1b) and window (Figure A-3a) assembly with the initially larger radial clearance of 0.150 inch, even when subjected to hydrostatic pressures that destroyed the window, did not cause it to be wedged inside the flange opening. With such an arrangement it was possible to determine whether the wedging in of the window in the flange under hydrostatic pressure had any measurable influence on the critical pressure of flat windows.

DISCUSSION

Relationship Between Critical Pressure and D_o/D_i Ratio

Tests to determine the relationship between critical pressure and D_o/D_i ratio were conducted with five 2-inch (D_o) windows in a 1.5-inch (D_i) flange and five 4-inch (D_o) windows in a 1.5-inch (D_i) flange. The windows were sealed in the flange with the aid of silicone grease, which was liberally applied to the bearing as well as the radial surfaces of the flat circular window. For both the 2-inch and the 4-inch (D_o) windows, the radial clearance between the window and the flange was 0.025 inch.

When tested to destruction, the average critical pressure of 2-inch (D_o) windows was 18,490 psi (Table C-1), while the critical pressure of 4-inch (D_o) windows was 19,190 psi (Table C-16). The small difference between the average critical pressures of the 2-inch and the 4-inch (D_o) windows with a 0.5 t/D_i ratio seemed to indicate that varying the D_o/D_i ratio from 1.33 to 2.67 did not significantly influence the critical pressure of flat acrylic windows, since the maximum collapse pressure found in 2-inch (D_o) windows (18,900 psi, Table C-1) overlapped the minimum collapse pressure found in 4-inch (D_o) windows (18,800 psi, Table C-16).

Since the critical pressures of windows with 1.33 and 2.67 D_o/D_i ratios are approximately the same so long as their t/D_i ratios are identical, a flange with an intermediate D_o/D_i ratio of 1.5 was selected for the conduct of the main flat-window study program.

Relationship Between Critical Pressure and Sealing Technique

The evaluation of window sealing methods was conducted with a total of 20 windows (10 untested windows in addition to the 10 already tested in the evaluation of D_o/D_i ratio study). Five of the additional windows had a 1.33 D_o/D_i ratio and a 0.5 t/D_i ratio and a D_o of 2 inches (Figure A-3b), while the five others had a 2.67 D_o/D_i ratio and a 0.5 t/D_i ratio with a D_o of 4 inches (Figure A-3d). All 10 windows had a nominal 1/8-inch-diameter radial O-ring seal located in a groove machined in the window 0.125 inch below its high-pressure face.

When the windows were tested to destruction in appropriate flanges (Figures A-1a and A-1c), the critical pressures of the O-ring-equipped acrylic flat windows were 19,060 (Table C-2) and 19,270 psi (Table C-17) — reasonably close to the pressures (18,490 and 19,190 psi, Tables C-1 and C-16) of the corresponding windows sealed in the flange with silicone grease. The displacements of the O-ring-equipped windows were approximately the same as the displacements of grease-sealed windows with the identical D_o/D_i and t/D_i ratios (Table A-1).

Thus, both seal designs are of equal desirability, so long as the sole criterion for their selection is their influence on the critical pressure of the flat acrylic window. For the main body of the flat window study program, where the relationship between the t/D_i ratio and critical pressure is investigated, the grease-seal design was selected. This design permitted the investigation of very thin, flat windows into whose body an O-ring seal could not be incorporated.

Relationship Between Critical Pressure and Window Fit

Evaluation of the effect on critical pressure of radial clearance between the flat acrylic window and the steel flange was conducted with a total of 25 windows (5 untested windows in addition to the 20 tested in previous tests). The radial clearance between the acrylic window and its flange varied from one group of window specimens to another. One group of 10 windows tested previously had a radial clearance of 0.001 inch (Figures A-3b and A-3d); another previously tested group of 10 had a clearance of 0.025 inch (Figures A-3a and A-3c). The group of 5 windows tested in addition to the 20 windows tested previously had a radial clearance of 0.150 inch (Figure A-3a). Appropriate flanges (Figures A-1a, A-1b, and A-1c) were used with the windows to result in 0.001-inch, 0.025-inch, and 0.150-inch clearances.

When the critical pressures of all the window groups were compared to each other, no significant difference in critical pressures could be found between the groups of windows possessing radial clearances of 0.001 inch and 0.025 inch, respectively. There was, however, a significant difference between the 16,960-psi (Table C-3) critical pressures of the window group with a radial clearance of 0.150 inch and the

pressures of two window groups with the 0.001-inch (19,060 psi and 19,270 psi) and 0.025-inch (18,490 psi and 19,190 psi) radial clearances. The difference in the average critical pressure was approximately 10%, the windows with the 0.150-inch radial clearance failing at the lower critical pressures.

It would thus appear that it is to the designer's advantage to specify small clearances between the flat acrylic window and its flange, since by doing this he accomplishes two desirable objectives. His design not only results in a window that has superior critical pressure, but also is easier to seal in the flange. The small radial clearances are ideal for sealing the window in the flange with a radial O-ring seal, or silicone rubber potting-type seal. Because of these findings, the main body of window test program was conducted with windows that fit into the steel flanges with a 0.005- to 0.010-inch radial clearance.

FINDINGS

The exploratory tests in the window mounting investigation seemed to indicate that (1) varying the D_o/D_i ratio from 1.33 to 2.67, (2) changing the radial clearance between the window and the flange from 0.001 inch to 0.025 inch, and (3) substituting a radial O-ring seal for a grease seal have no significant influence on the critical pressures of flat acrylic windows with a 0.5 t/D_i ratio. When the radial clearance is increased to 0.150 inch, the critical pressure of the 0.5 t/D_i ratio window is reduced.

Whether these conclusions are applicable to flat acrylic windows with t/D_i ratios other than 0.5 is unknown. Some of the data generated in the main body of the flat window program have raised serious doubts that the conclusions hold for the whole t/D_i range. For example, the critical pressure of windows with a nominal 0.167 t/D_i ratio and a 1.5 D_o/D_i ratio was discovered to be 723 psi for a radial clearance of 0.005 inch and 2,100 psi for a radial clearance of 0.001 inch.

Thus, it would appear that for t/D_i ratios less than 0.5, any change in radial clearance below 0.005 inch influences its critical pressure considerably. Future studies will attempt to clarify this problem.

Appendix B

FAILURE MODES OF FLAT ACRYLIC WINDOWS

DISCUSSION

In nearly all cases for all sizes of windows tested, failure began with radial cracking on the window's low-pressure face. Radiating outward from near the center, the cracks commonly formed a nonsymmetrical, three- or four-pointed figure. This form of cracking preceded failure in nearly all cases and is assumed to be the beginning of failure (Figures B-1 and B-2). Depth of cracking was found to be a function of the thickness, t/D_i ratio of the window, and the pressure of the fluid. Since audible cracking was noted during testing, it is postulated that these radial cracks were rapidly formed, terminating at the window's D_i. Depth of cracking in the low-pressure face in most cases was found to be a small fraction of the window's thickness.

With additional pressurization, a second stage of failure began to develop. A conchoidal or "cupped cone" fracture was established, emanating from the base of the radial cracks and proceeding radially inward and circumferentially (Figures B-3 and B-4). The formation of a conchoidal fracture surface preceded failure in all cases observed.

Simultaneously, as the conchoidal fracture surface was formed, the radial cracks increased slightly in depth (Figures B-5 and B-6). Cracks did not deepen uniformly and new cracks developed with further pressurization. The additional cracking gave rise to formation of new and deeper conchoidal fracture surfaces. Additional pressurization caused the circumferential expansion and coalescence of the conchoidal fracture surfaces into one conical fracture surface as well as an increase in fracture depth (Figures B-7 and B-8). Cracking and formation of conchoidal fracture surfaces continued (Figures B-9 and B-10) deeper into the window's thickness until the critical pressure was finally reached resulting in the fragmentation and expulsion of the window's low-pressure face (Figures B-11 and B-12). The size of the central hole was a function of t/D_i ratio and D_i. The conical cavity resulting from the expulsion of the center portion of the window consistently assumed an approximate angle of 30 degrees with the high-pressure face.

Cracking between the window's D_i and D_o occurred concentrically with the window's circumference, nearly perpendicular to and emanating from the low-pressure face. This cracking was sometimes accompanied by small radial intersecting cracks (Figure B-9). This form occurred with larger t/D_i ratios, failure still assuming the conical surface form. The circumferential cracks sometimes penetrated the window's thickness but still did not constitute a plane of failure.

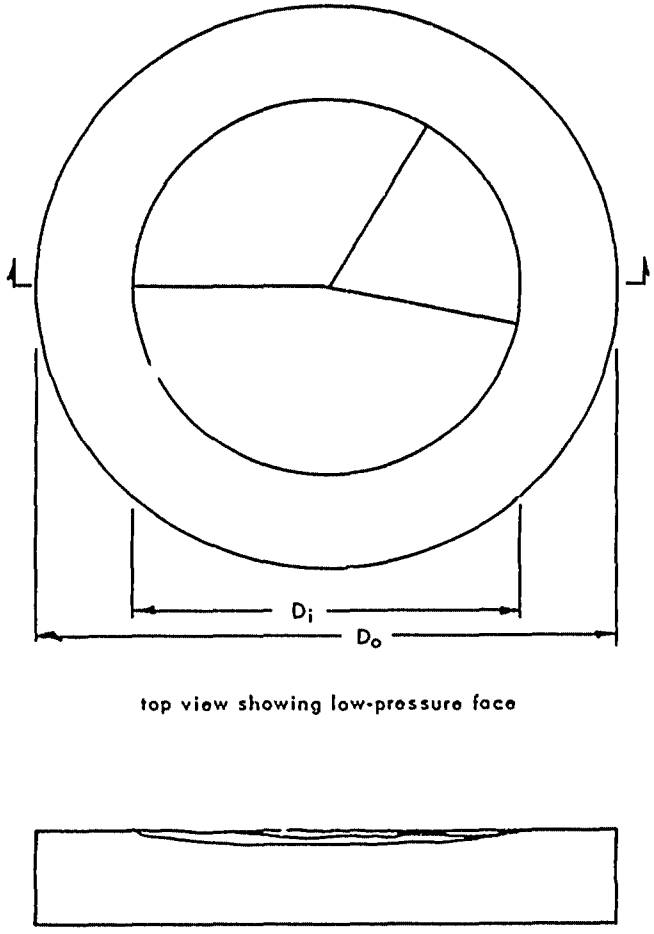

Figure B-1. Initial radial crack pattern in low-pressure face of windows.

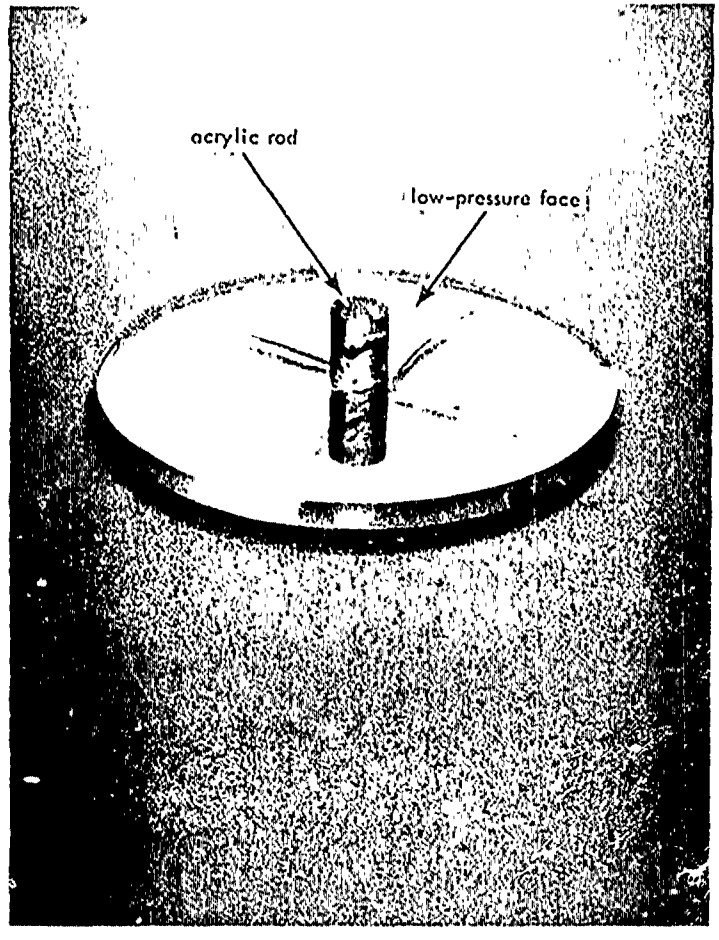

Figure B-2. Crack pattern in failed 0.122-inch-thick window with a t/D_i ratio of 0.081. Maximum pressurization 62 psi.

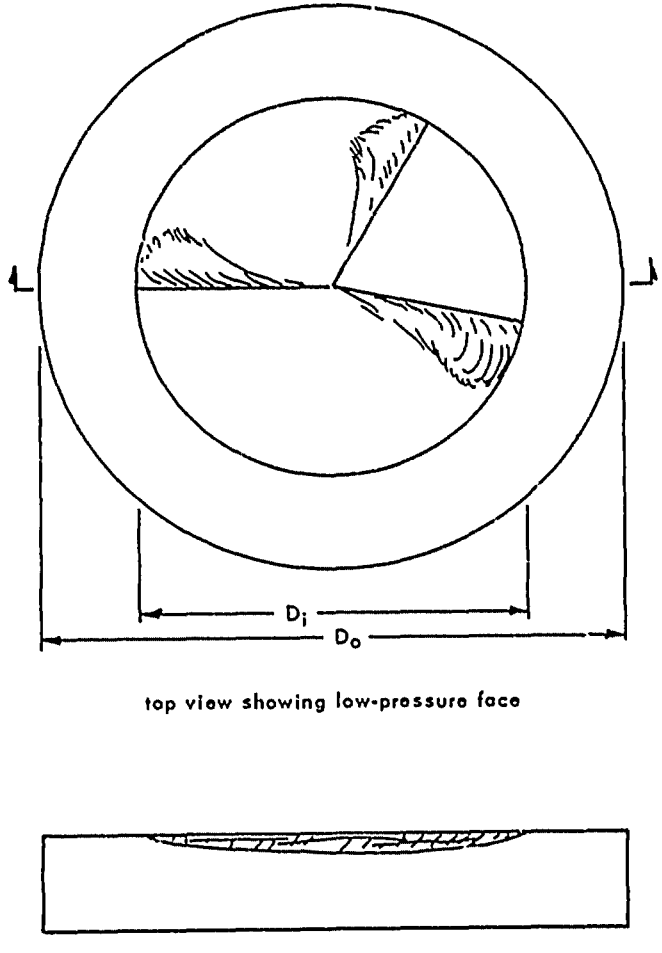

Figure B-3. Second stage conchoidal fracture pattern, early development.

Figure B-4. Conchoidal fracture pattern in partially failed 0.355-inch-thick window with a t/D_i ratio of 0.237. Maximum pressurization 2,990 psi.

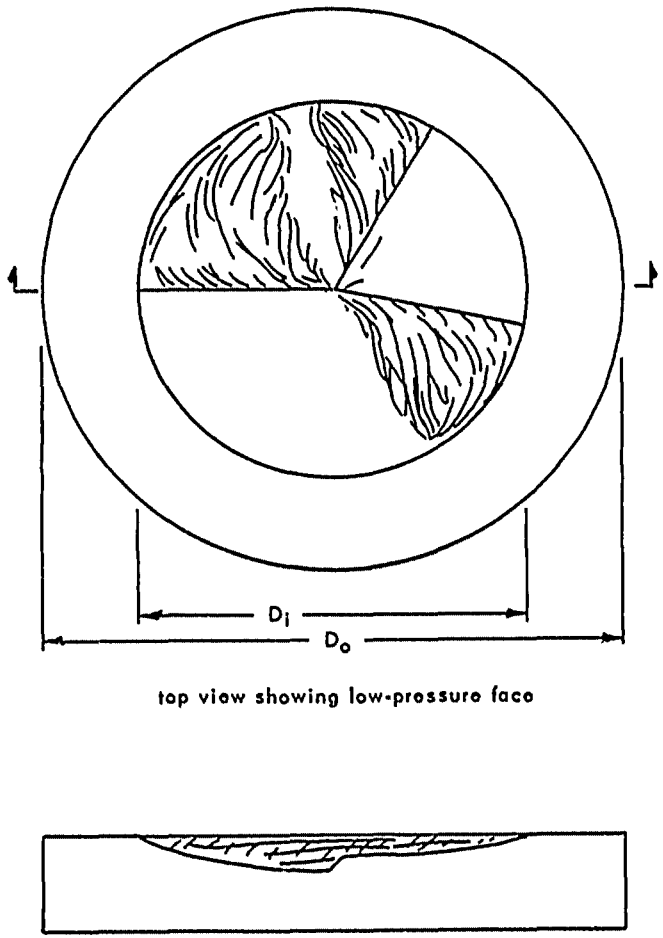

Figure B-5. Conchoidal fracture pattern, advanced stage of development.

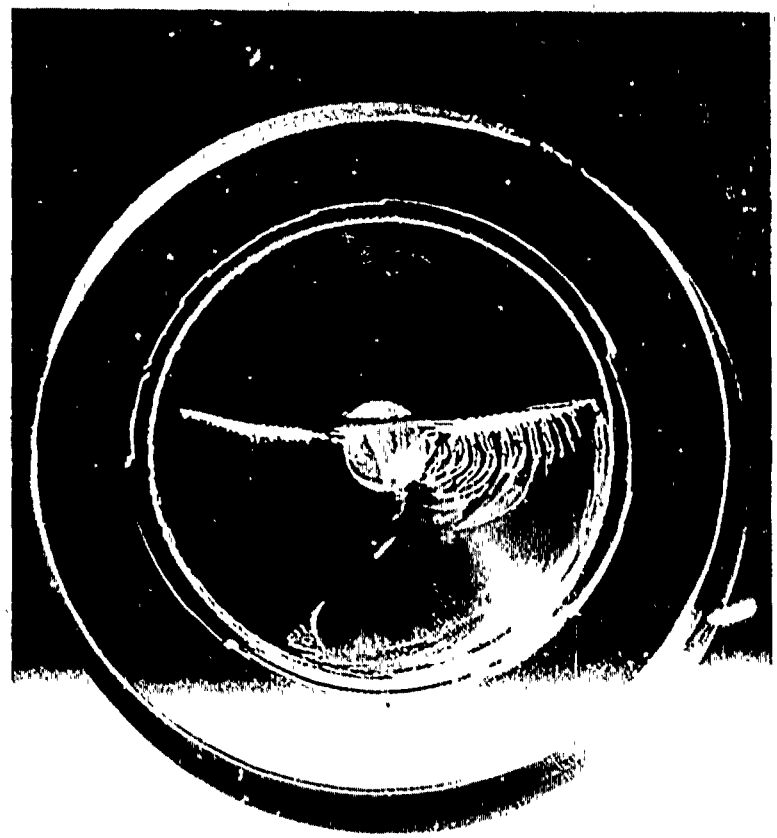

Figure B-6. Advanced stage of conchoidal fracture pattern in 0.857-inch-thick window with a t/D_i ratio of 0.572. Maximum pressurization 20,100 psi.

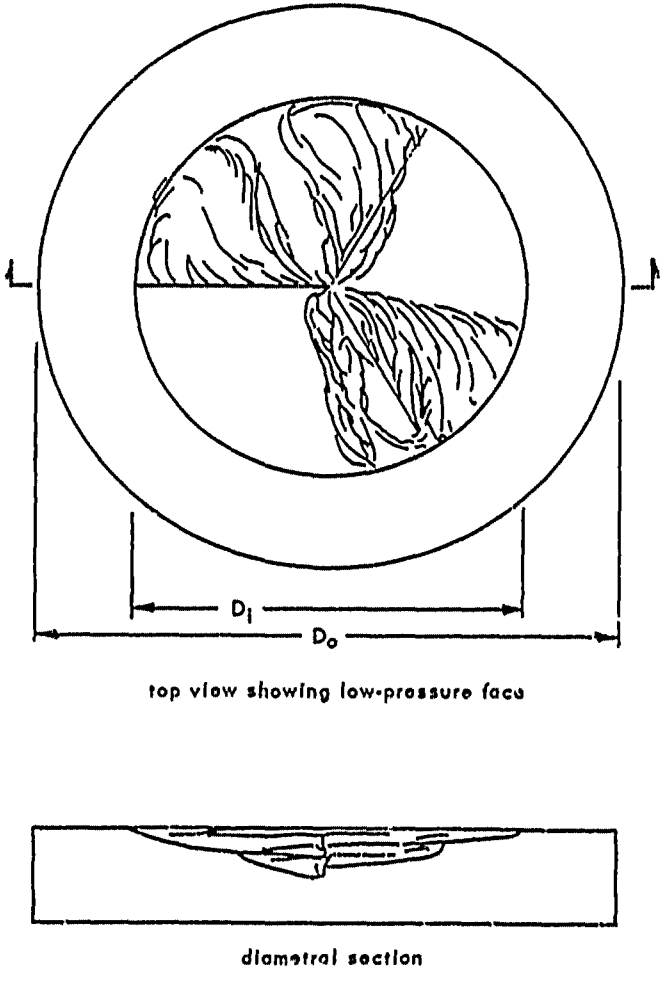

Figure B-7. Imminent coalescence of conchoidal fractures as critical pressure is approached.

Figure B-8. Coalescing conchoidal fractures just prior to failure in a 0.735-inch-thick window with a t/D_i ratio of 0.490; maximum pressurization 18,600 psi.

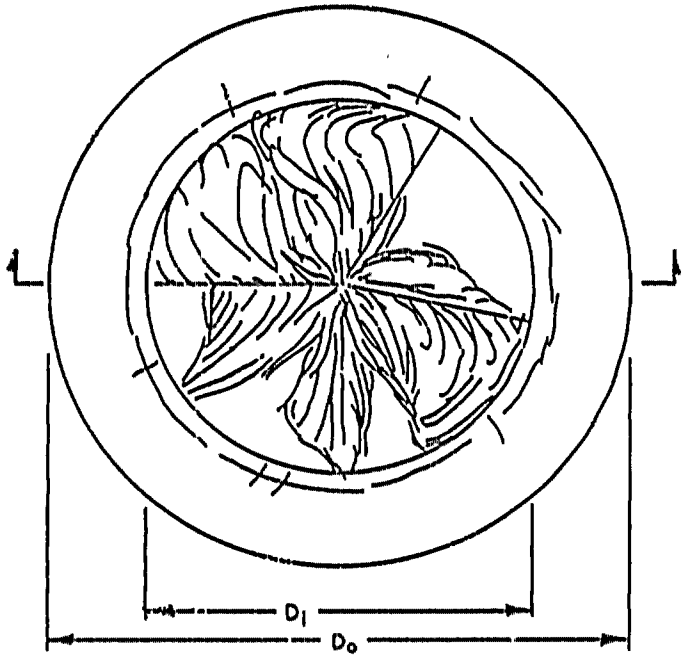

Figure B-9. An advanced stage of coalescence of conchoidal fractures as critical pressure is approached.

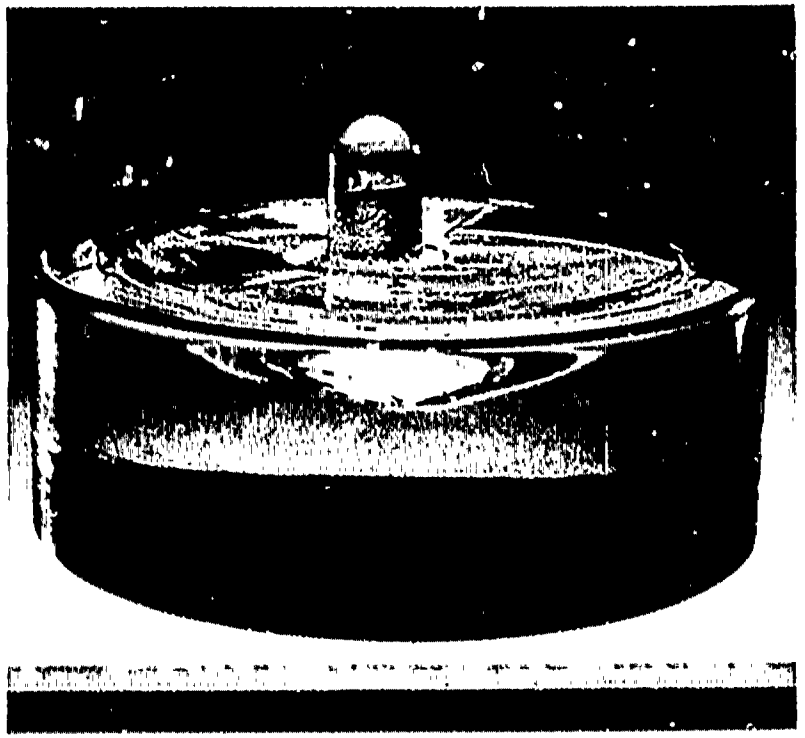

Figure B-10. A 0.735-inch-thick window with t/D_i ratio of 0.490 pressurized to 19,000 psi. Note extrusion at the window's D_i and penetration depth of the conchoidal fracture into the window.

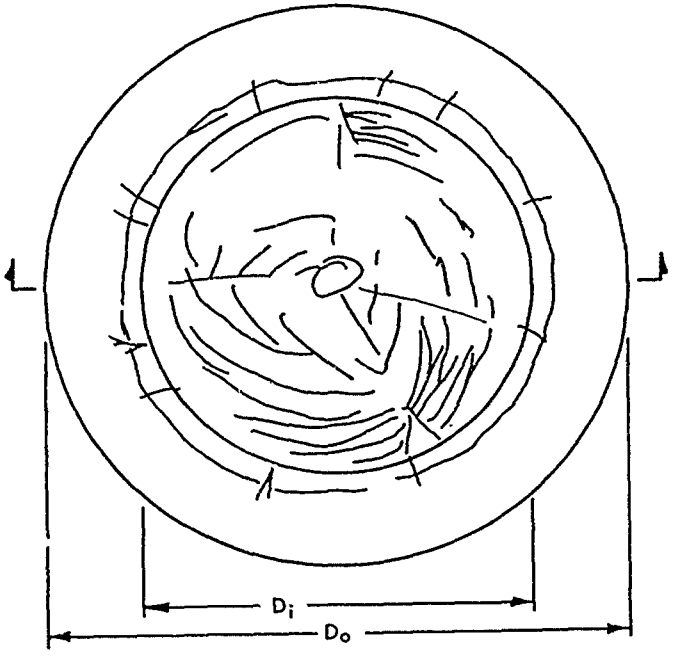

Figure B-11. The type of failure which follows complete coalescence of conical fracture surfaces.

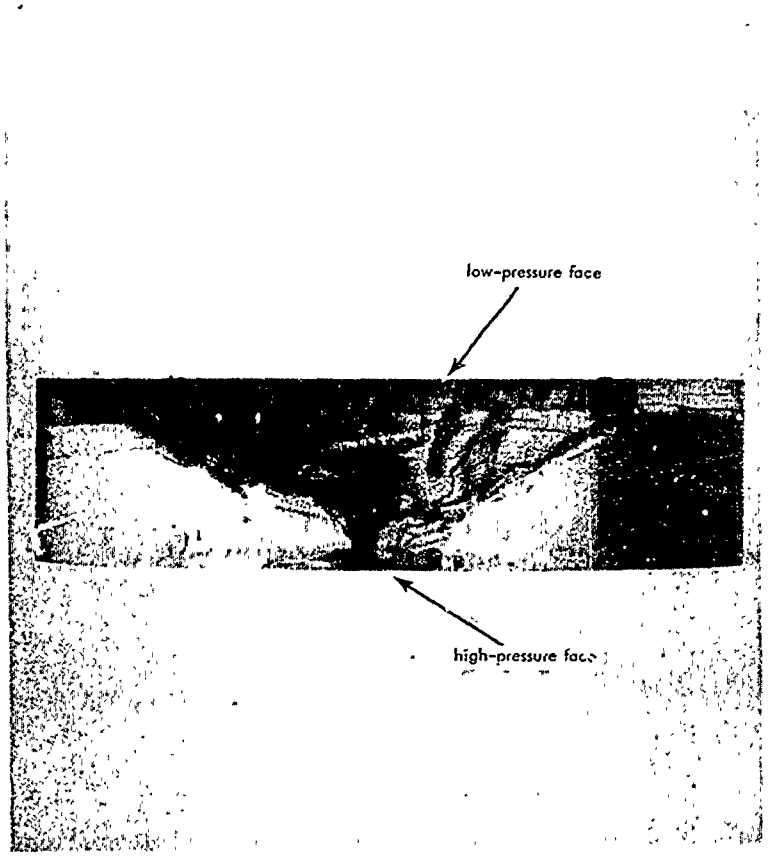

Figure B-12. A 0.600-inch-thick window with a t/D_i ratio of 0.400 which failed at 13,000 psi.

Considerable cold-flow cratering occurred on the high-pressure face before the critical pressure was reached (Figure B-13). Both elastic and plastic extrusion on the low-pressure face were also experienced by the window at this time (Figure B-14).

Windows whose t/D_i ratios exceeded about 0.50 failed predominately by shear; the conical fracture surface was unable to penetrate the thickness of the material (Figures B-15 and B-16). At the critical pressure, the entire window was penetrated by discontinuous cracks and the central portion (bounded by D_i) was completely ejected.

RESULTS OF TESTS

1.5-Inch (D_i) Windows

The 1.5-inch (D_i) windows were tested in groups of five; the nominal t/D_i ratios included the range from 0.083 to 0.667. For each group, critical pressure was plotted against the t/D_i ratio (Figure B-17) and pressure was plotted against the window's central displacement.

The windows having t/D_i ratios less than 0.2 exhibited both flexural and conical failures. Parametric considerations were the window's radial clearance, pressurization rate, and grease-seal thickness. No attempt was made to isolate these effects in this study.

For a t/D_i ratio between 0.2 and 0.4 the principal failure was conical, the cone's apex reaching the high-pressure face toward the upper limit of critical pressure (Figure B-12). Audible cracking during pressurization occurred mostly at levels above 75% of critical pressure and occurred fairly consistently between 90% of critical pressure and failure.

Windows of t/D_i ratios greater than 0.4 failed predominantly by shear, fragmentation being so complete that sometimes none of the window material was retained in the flange. Extrusion of these windows caused audible cracking to occur many times before critical pressure was reached. For t/D_i ratios of less than about 0.25 pressurization to approximately 70% of critical pressure resulted in no visible evidence (to the naked eye) that the windows had been pressurized. For t/D_i ratios between 0.25 and 0.55, the extrusion of the window at 70% of critical pressure caused a shallow impression of the flange seat to appear (Table B-1); however, on examination after release of pressure no visible impairment of optical quality inside this impression was apparent to the naked eye. For windows of t/D_i ratios greater than 0.55, the development of cracks accompanied extrusion and depression.

Details of flanges used in testing the 1.5-inch (D_i) windows are shown in Figure B-18 and an in-place schematic is shown in Figure B-19.

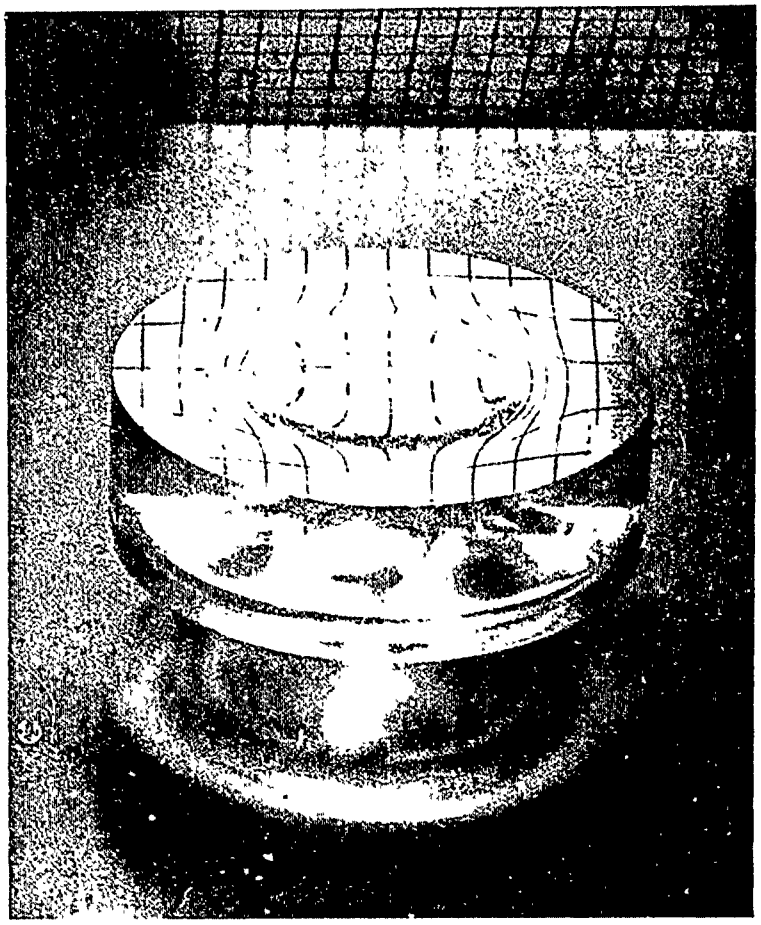

Figure B-13. Plastic flow cratering on the high-pressure side of a 0.735-inch-thick, 0.490 t/D_i ratio window subjected to 18,600 psi pressure.

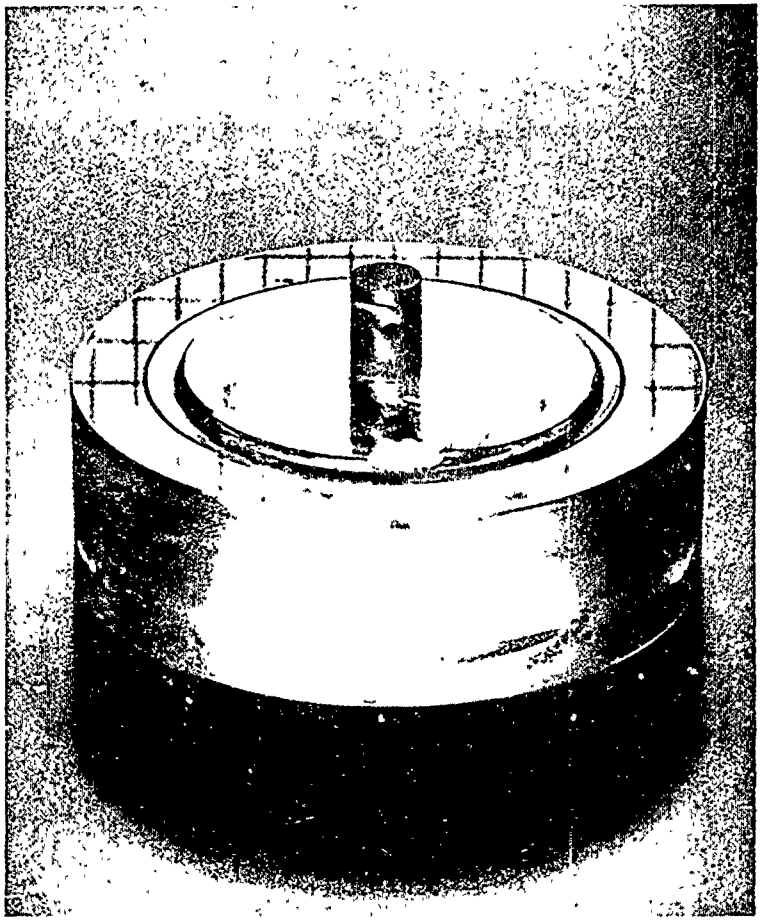

Figure B-14. Extrusion of the unsupported low-pressure face of a 0.735-inch-thick, 0.490 t/D_i ratio window subjected to 18,600 psi pressure.

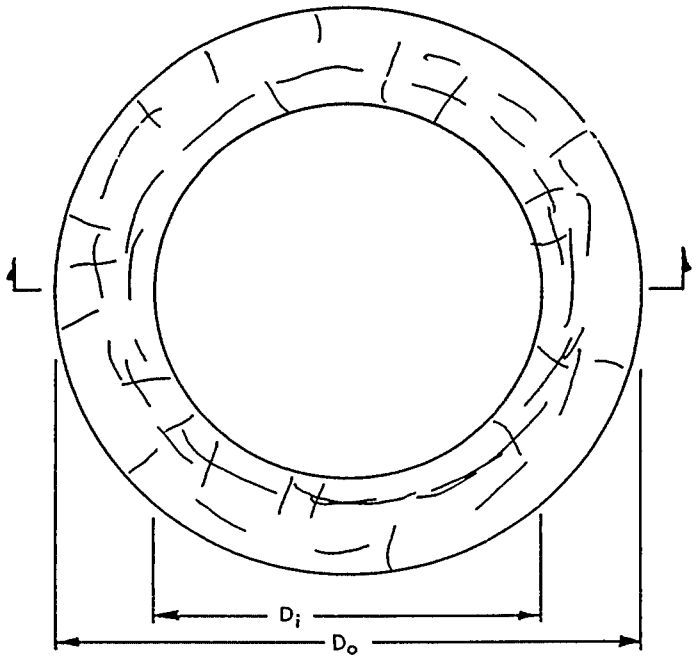

Figure B-15. Shear-type failure common to windows with large t/D_i ratios.

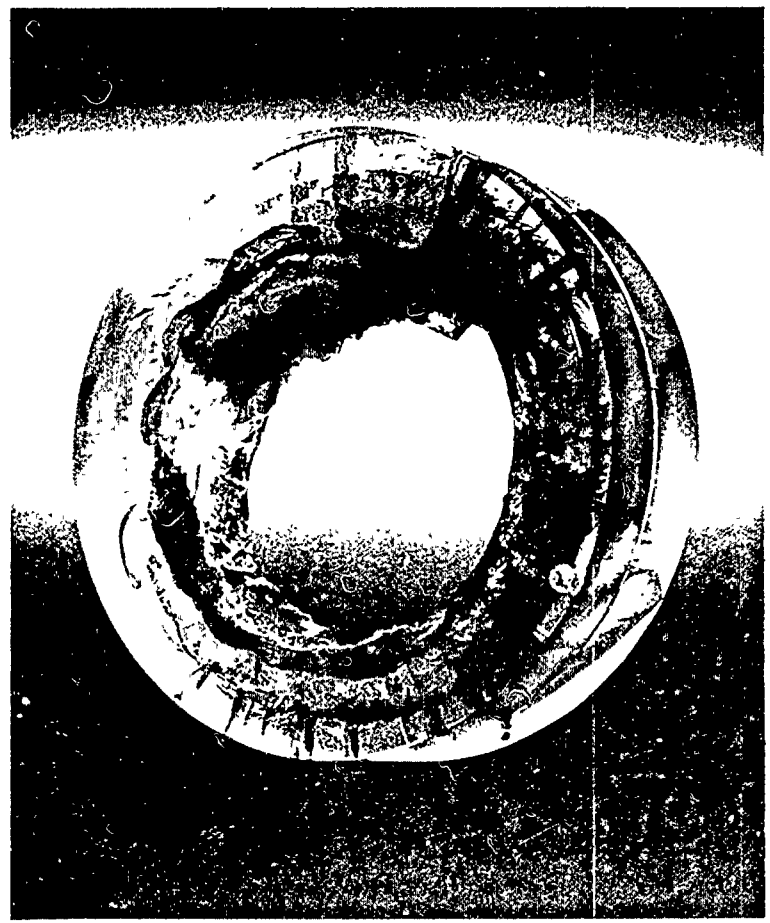

Figure B-16. Shear-type failure in a 1.432-inch-thick, 0.500 t/D_i ratio window which failed at 15,300 psi.

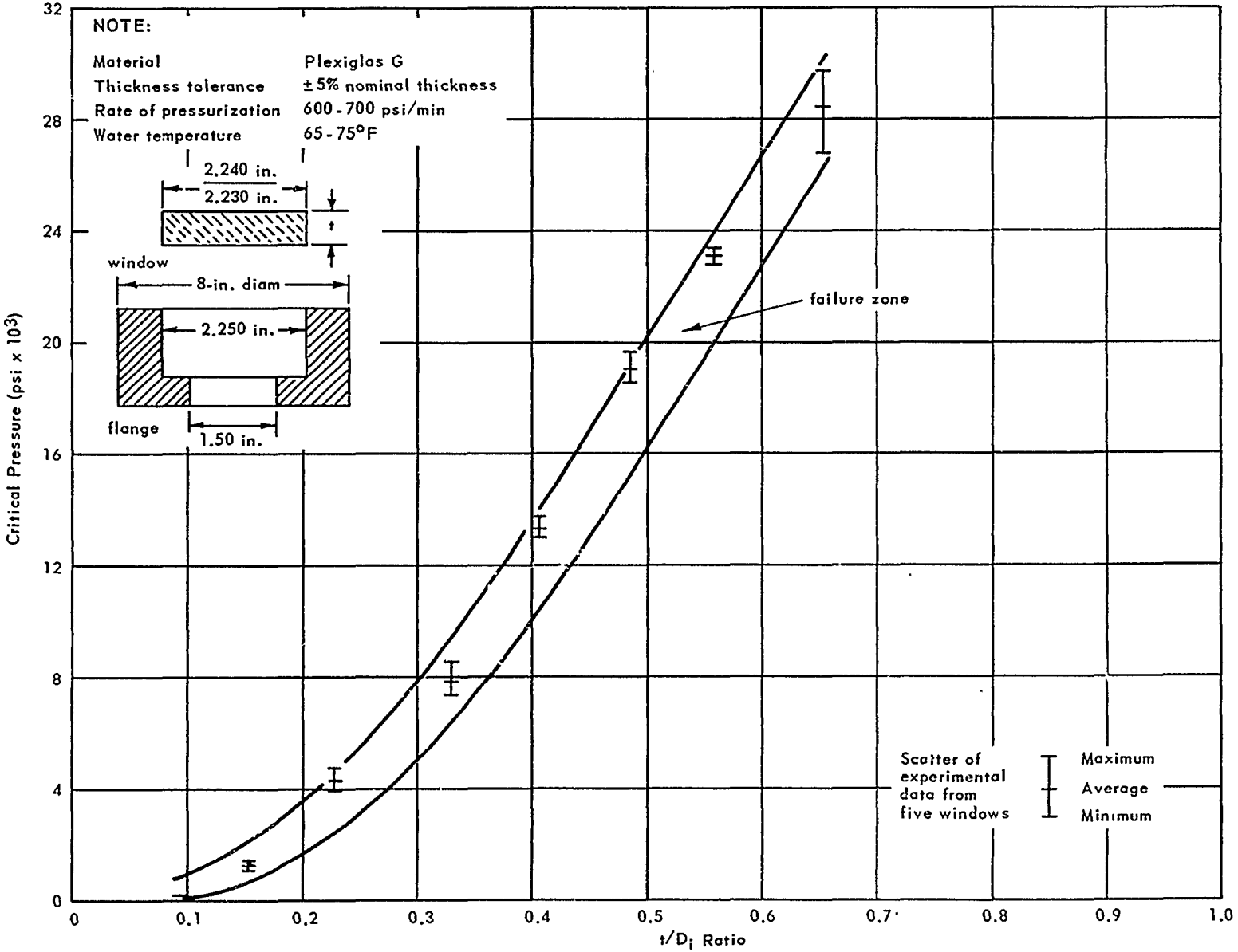

Figure 3-17. Relationship between critical pressure and t/D_i ratio of 1.50-inch (D_i) flat acrylic windows.

Table B-1. Extrusions of Some Flat Disk Windows Measured After Pressurization

Specimen No.	t[1]	t/D_i Ratio	Measured[2] Set (in.)	% of Group Average Critical Pressure
141	0.125	0.083	0.000	70
142	0.248	0.165	0.000	70
143	0.355	0.237	0.000	68
144	0.497	0.331	0.001	70
145	0.613	0.409	0.002	70
146	0.735	0.490	0.026	98
147	0.735	0.490	0.002	67[3]
148	0.857	0.572	0.011	87
149	0.982	0.655	0.024	92
150	0.983	0.655	0.029	85
151	0.121	0.036	0.000	70
152	0.349	0.102	0.000	70
153	0.607	0.182	0.000	65
154	0.848	0.254	0.000	70
155	1.130	0.339	0.004	70
156	1.452	0.436	0.003	70
157	2.000	0.600	0.004	68
158	1.991	0.598	0.034	99
159	2.008	0.602	0.037	98
160	0.233	0.058	0.000	64
161	0.455	0.107	0.000	63
162	0.968	0.242	0.000	59
163	1.987	0.496	0.002	55

1/ Thickness measured prior to pressurization.
2/ Measured 7 days after pressurization.
3/ See Figure B-26.

Note: The maximum pressure was immediately relieved by either (a) bleeding pressurized fluid from the vessel or (b) the development of leaks around the window caused by deformation of the window under pressure.

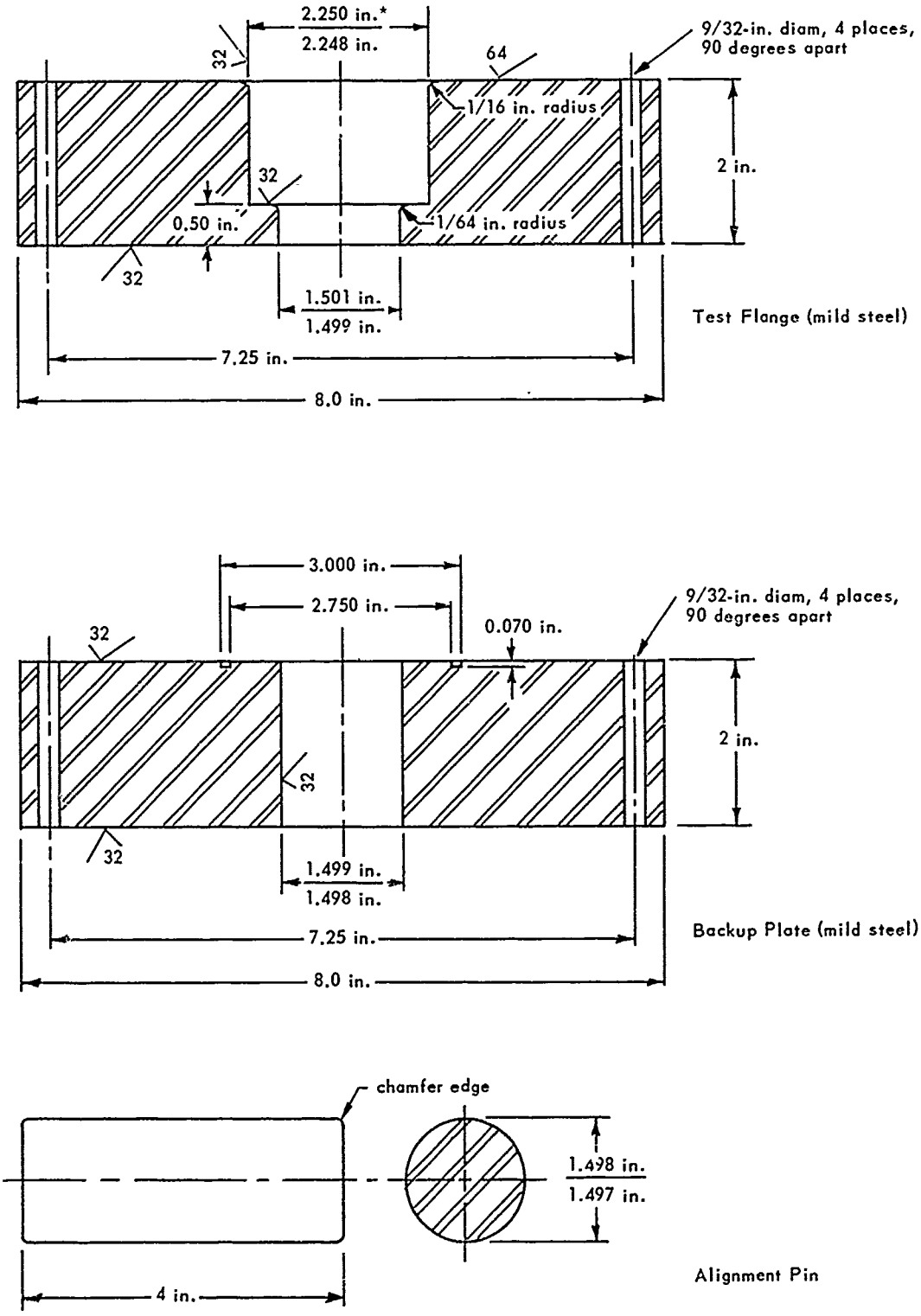

* Indicates maximum and minimum dimensions allowable.

Figure B-18. Details of flange assembly used to determine the relationship between the window's critical pressure and t/D_i ratio for 1.50-inch (D_i) windows.

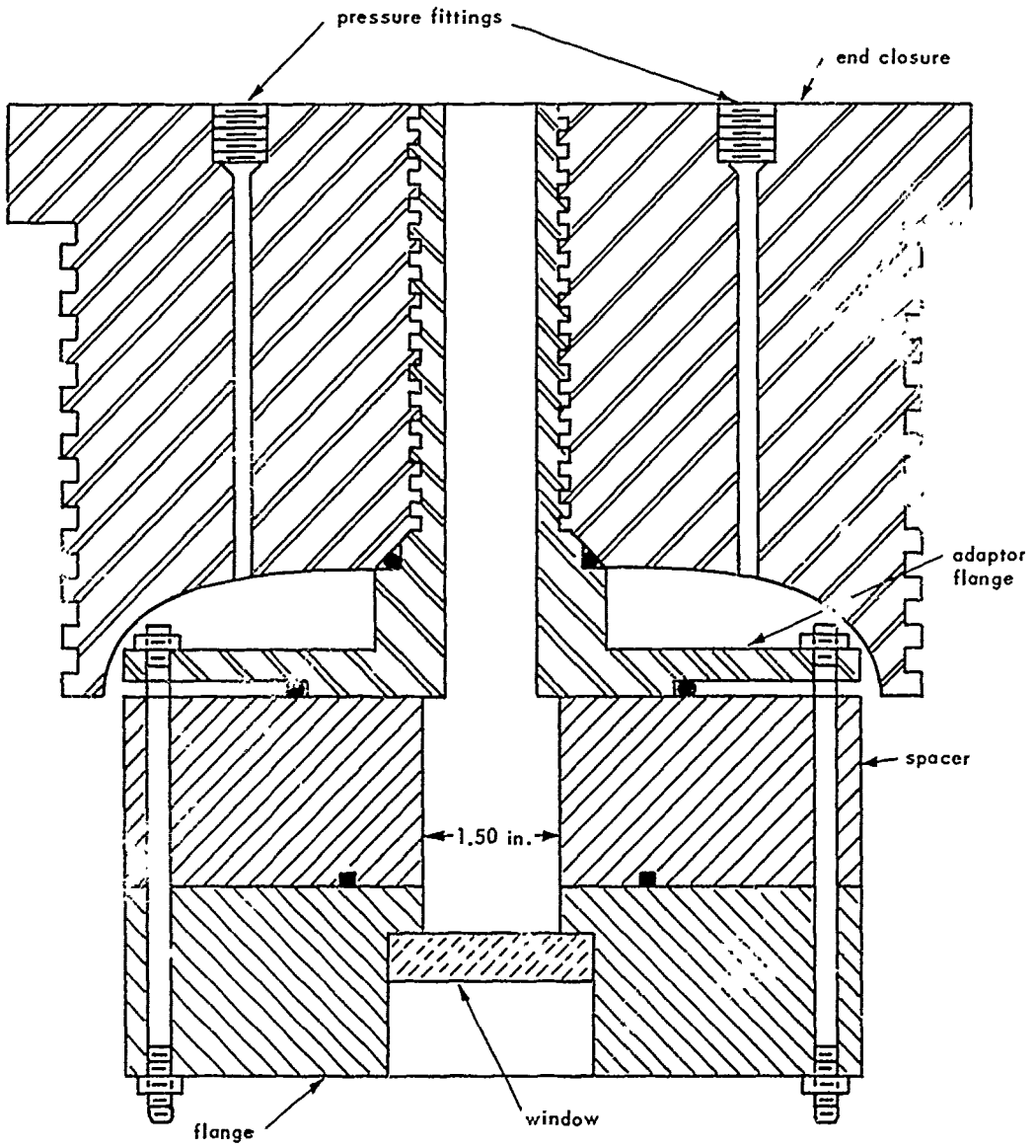

Figure B-19. Schematic of a typical window and flange test assembly secured to the end closure of a Mk I 9-inch pressure vessel.

3.33-Inch (D_i) Windows

The 3.33-inch (D_i) windows were tested in groups of five and had t/D_i ratios ranging from 0.036 to 0.600. For each group the critical pressure was plotted against the t/D_i ratio (Figure B-20) and the pressure was plotted against deflection.

Windows with t/D_i ratios of less than 0.1 exhibited both the conical and flexural failure modes whereas windows with t/D_i ratios between 0.1 and 0.4 failed only in the conical fracture mode previously described. Concentric cracking was observed toward the upper t/D_i limit. These cracks propagated from the low-pressure face.

Shear failures were characteristic of windows whose t/D_i ratios were greater than about 0.4 (Figure B-16). Combined with the shear failure pattern were the various combinations of radial and circumferential cracks discontinuous throughout the window. Details of flanges used in testing the 3.33-inch (D_i) windows are shown in Figure B-21 and an in-place schematic is shown in Figure B-22.

4.00-Inch (D_i) Windows

The t/D_i ratios of the 4.00-inch (D_i) specimens ranged from 0.058 to 0.498. Four groups consisting of five windows each were used in the comparative study. Critical pressure was plotted against the t/D_i ratio (Figure B-23) and pressure was plotted against deflection.

Results of limited testing of 4.00-inch (D_i) windows were consistently comparable with those for the 1.50-inch, and 3.33-inch (D_i) specimens. Flexural and conical surface failures were witnessed for t/D_i ratios less than 0.1 and conical failures were observed for t/D_i ratios between 0.1 and about 0.4. Shear failure was dominant for t/D_i ratios greater than about 0.4.

Details of flanges used in testing the 4.00-inch (D_i) specimens are shown in Figure B-24 and an in-place schematic is shown in Figure B-25. Extrusion, retained as permanent set in the specimens (Figure B-26), is summarized in Table B-1 for specimens which were not pressurized to critical pressure.

SUMMARY

Failure mechanisms characteristic of the 1.50-inch (D_i) windows were found also to be characteristic of the 3.33-inch and 4.00-inch (D_i) windows so long as t/D_i ratios were similar. Critical pressures derived from testing of windows having a different D_i in the DOL type III flange design were found to be comparable so long as the D_o/D_i ratio was maintained at 1.5, temperatures were within the 65°F to 75°F range, and the radial clearance was kept to less than 0.010 inch.

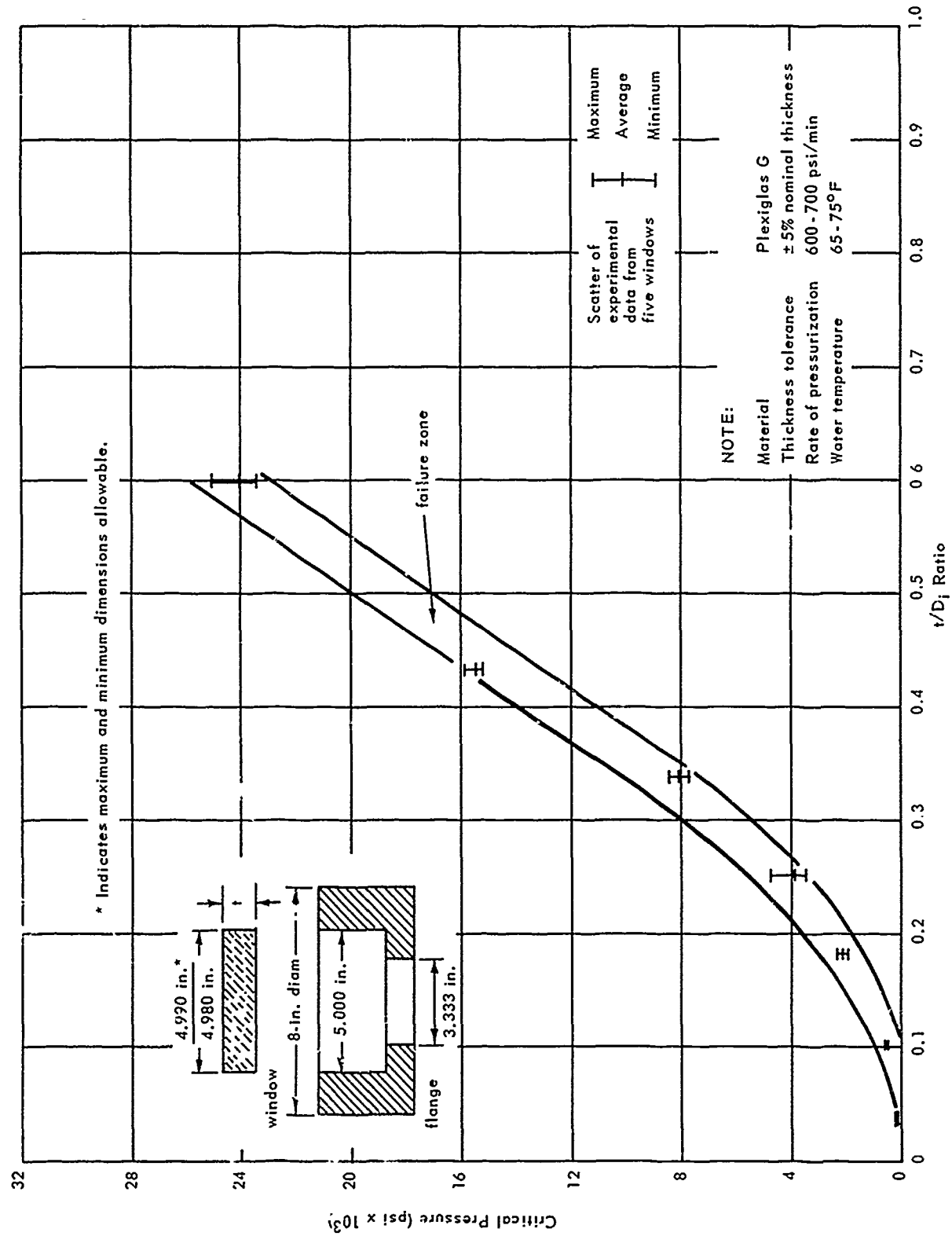

Figure B-20. Relationship between critical pressure and t/D_j ratio of 3.33-inch (D_j) flat acrylic windows.

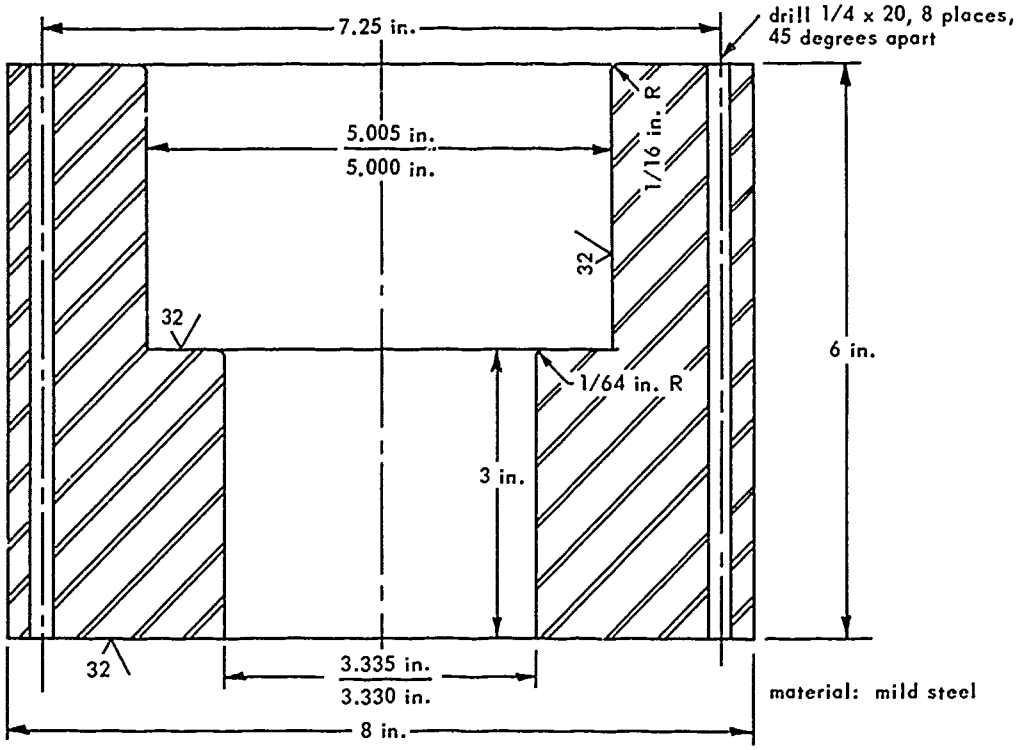

Figure B-21. Details of assembly used to determine the relationship between the window's critical pressure and t/D_i ratio for 3.33-inch (D_i) windows.

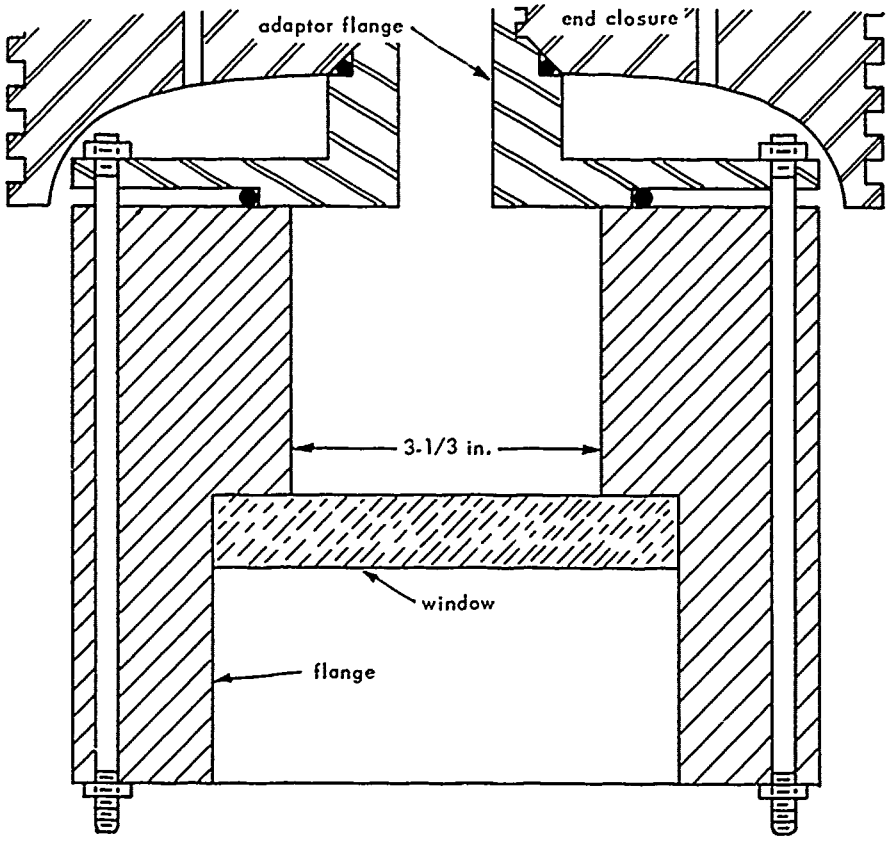

Figure B-22. Schematic of 3.33-inch (D_i) window and flange in end closure of Mk I 9-inch pressure vessel.

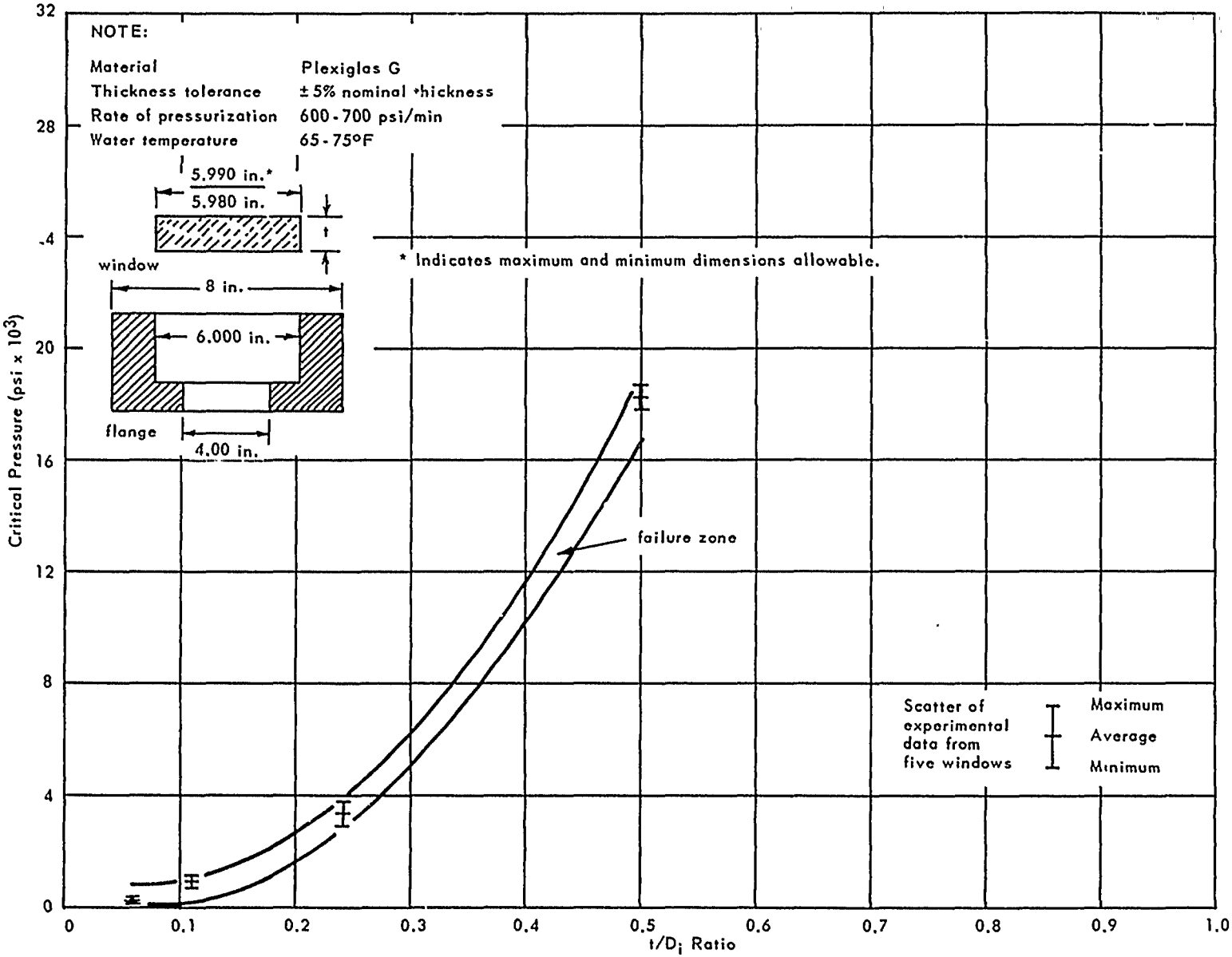

Figure B-23. Relationship between the critical pressure and t/D_i ratio of 4.00-inch (D_i) flat acrylic windows.

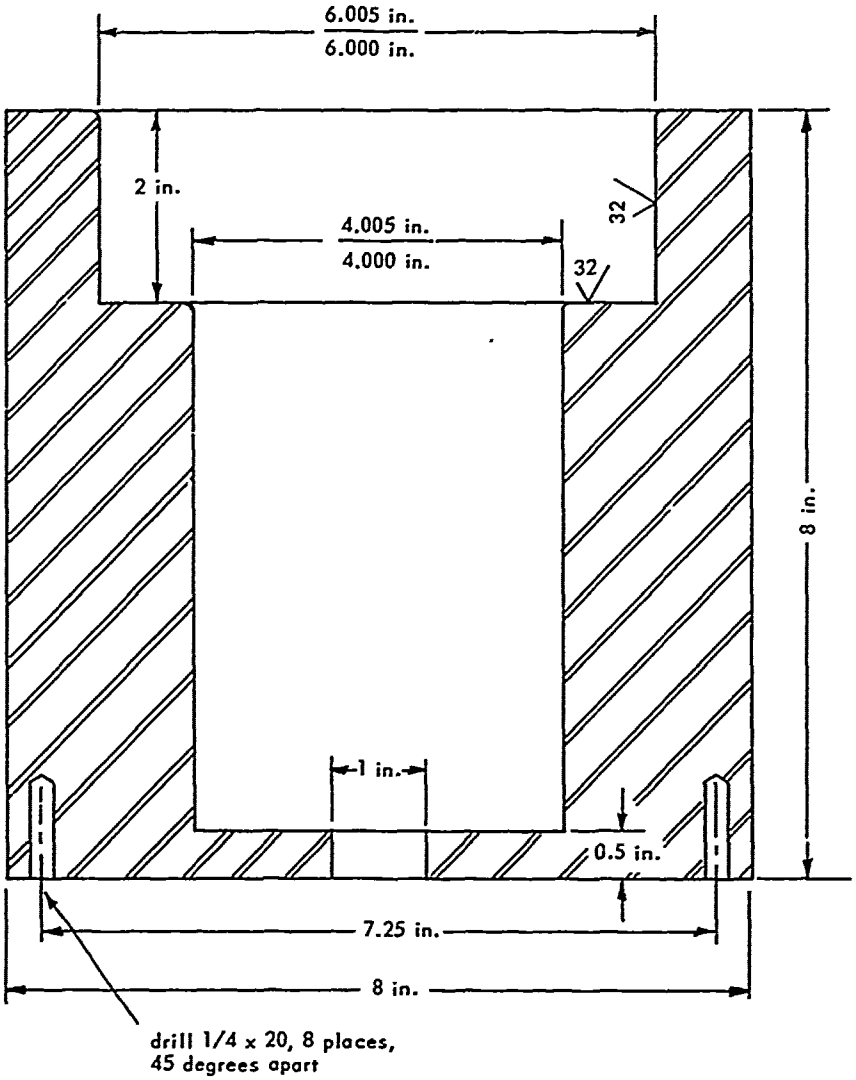

Figure B-24. Details of flange used to determine the relationships between the window's critical pressure and t/D_i ratio for 4.00-inch (D_i) windows.

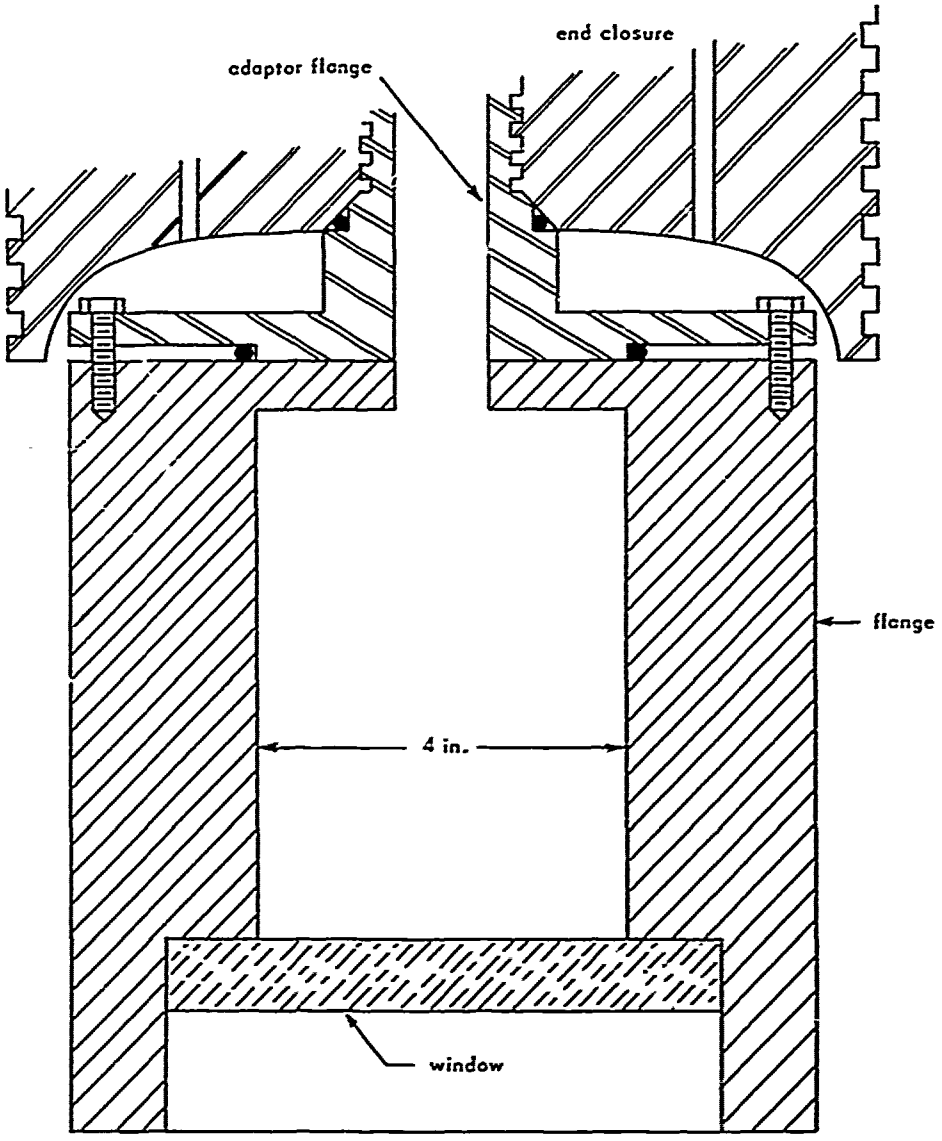

Figure B-25. Schematic of 4.00-inch (D_i) window and test flange assembled to the end closure of the Mk I 9-inch pressure vessel.

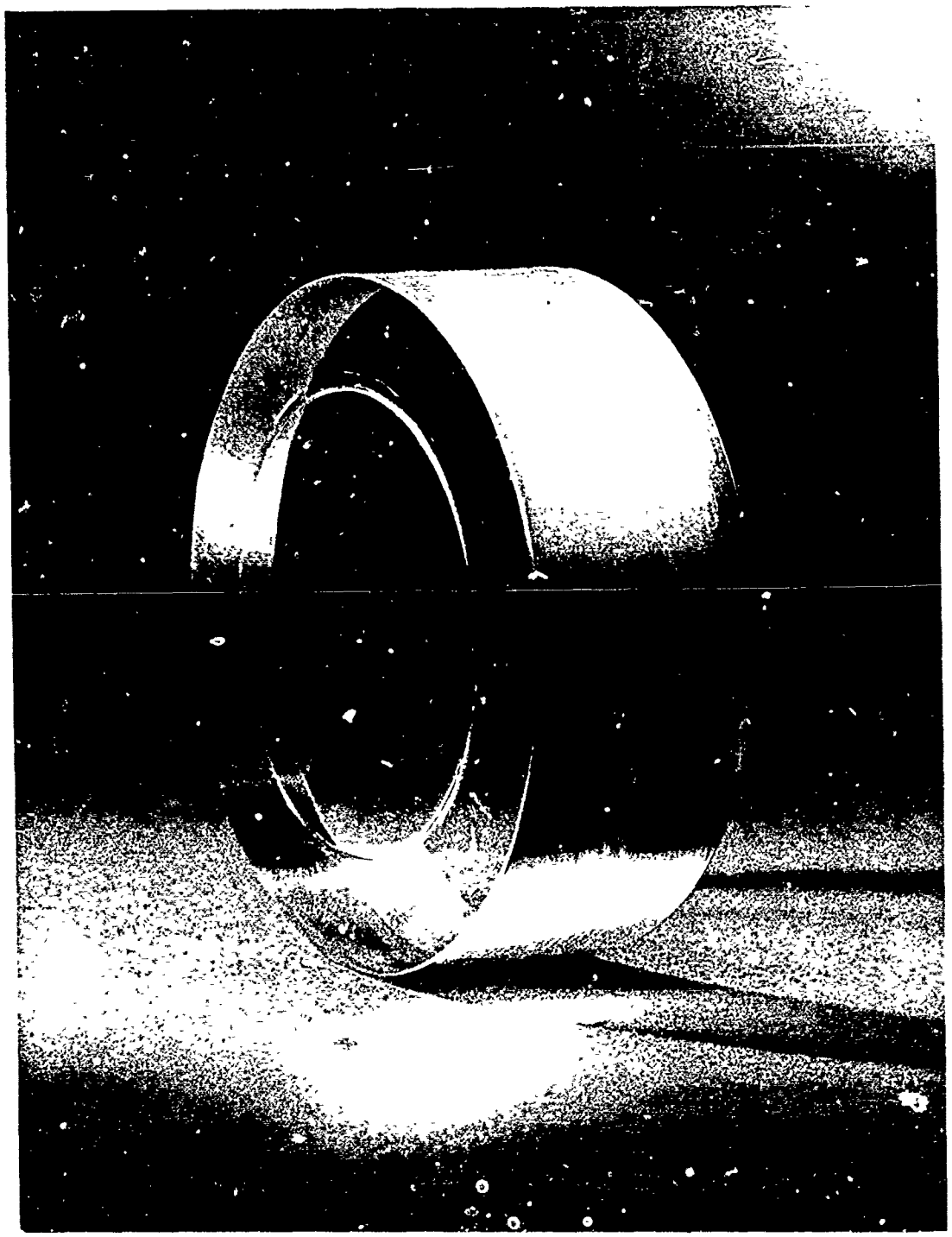

Figure B-26. Permanent extrusion of low-pressure face of a flat acrylic window having a 0.490 t/D_i ratio; window pressurized to 67% of ultimate critical pressure.

Appendix C

AXIAL DISPLACEMENT AND CRITICAL PRESSURES OF FLAT ACRYLIC WINDOWS SUBJECTED TO HYDROSTATIC PRESSURE IN DOL TYPE III FLANGES

Table C-1. Hydrostatic Test Data for Nominal 1.50-Inch (D_i) - 2.00-Inch (D_o) Flat Acrylic Windows, Test Specimens 1 - 5

(Sealed with grease; radial clearance 0.020 to 0.030 inch; nominal D_o/D_i ratio 1.33)

Parameter	Specimen Number					Value		
	1	2	3	4	5	Max	Avg	Min
Thickness (in.)	0.735	0.744	0.741	0.730	0.744	0.744	0.739	0.730
D_o (actual, in.)	1.960	1.950	1.955	1.951	1.945	1.960	1.952	1.945
Temperature (°F)	66.0	66.5	64.5	63.5	65.5	66.5	65.3	63.5
t/D_i Ratio (actual)	0.490	0.496	0.493	0.487	0.496	0.496	0.492	0.487
Pressurization Rate (psi/min)	686	662	783	665	1,201 1/	783	699	662
Pressure (psi)	Axial Displacement of Center Point on Window's Low-Pressure Face (in.)							
1,000		0.001	0.001	0.001	0.002	0.002	0.001	0.001
2,000	0.001	0.003	0.003	0.003	0.005	0.005	0.003	0.001
3,000		0.005	0.005	0.009	0.008	0.009	0.007	0.005
4,000	0.005	0.008	0.007	0.015	0.012	0.015	0.009	0.005
5,000	0.007	0.009	0.008	0.020	0.015	0.020	0.012	0.00
6,000	0.008	0.011	0.010	0.025	0.021	0.025	0.015	0.008
7,000	0.010	0.013	0.011	0.032	0.027	0.032	0.019	0.010
8,000	0.011	0.015	0.013	0.036	0.032	0.036	0.022	0.013
9,000	0.014	0.018	0.031	0.042	0.038	0.042	0.030	0.018
10,000	0.019	0.022	0.032	0.048	0.044	0.048	0.034	0.022
11,000	0.026	0.030	0.034	0.055	0.050	0.055	0.041	0.030
12,000	0.035	0.037	0.036	0.064	0.058	0.064	0.048	0.036
13,000	0.045	0.043	0.054	0.076	0.065	0.076	0.059	0.043
14,000	0.055	0.050		0.086	0.075	0.086	0.071	0.050
15,000	0.074	0.060		0.099	0.086	0.099	0.084	0.060
16,000	0.091	0.087		0.112	0.109	0.112	0.100	0.087
17,000	0.127	0.107		0.127	0.127	0.127	0.120	0.107
18,000		0.137		0.160	0.165	0.165	0.154	0.137
Pressure at Failure (psi)	17,500	18,600	18,600	18,900	18,850	18,900	18,490	17,500

1/ Not included in average pressure value.

Table C-2. Hydrostatic Test Data for Nominal 1.50-Inch (D_i) - 2.00-Inch (D_o) Flat Acrylic Windows, Test Specimens 6 - 10

(Sealed with O-ring; radial clearance 0.0005 to 0.0010 inch; nominal D_o/D_i ratio 1.33)

Parameter	Specimen Number					Value		
	6	7	8	9	10	Max	Avg	Min
Thickness (in.)	0.749	0.745	0.729	0.747	0.733	0.749	0.741	0.729
D_o (actual, in.)	1.999	1.998	1.999	1.988	1.988	1.999	1.998	1.998
Temperature (°F)	65.0	67.5	62.5	64.5	65.5	67.5	65.0	62.5
t/D_i Ratio (actual)	0.499	0.496	0.486	0.498	0.488	0.499	0.493	0.486
Pressurization Rate (psi/min)	668	664	655	651	657	668	661	651
Pressure (psi)	Axial Displacement of Center Point on Window's Low-Pressure Face (in.)							
1,000	0.002	0.001	0.003	0.003	0.002	0.003	0.002	0.001
2,000	0.003	0.006	0.004	0.006	0.008	0.008	0.005	0.003
3,000	0.005	0.010	0.005	0.008	0.014	0.014	0.008	0.005
4,000	0.012	0.011	0.007	0.010	0.020	0.020	0.012	0.007
5,000	0.013	0.021	0.009	0.013	0.024	0.024	0.016	0.009
6,000	0.023	0.026	0.011	0.015	0.030	0.030	0.021	0.011
7,000	0.024	0.032	0.012	0.017	0.033	0.033	0.024	0.012
8,000	0.033	0.038	0.014	0.019	0.039	0.039	0.029	0.014
9,000	0.034	0.043	0.016	0.021	0.044	0.044	0.032	0.016
10,000	0.045	0.049	0.018	0.023	0.050	0.050	0.037	0.018
11,000	0.047	0.054	0.021	0.026	0.058	0.058	0.041	0.021
12,000	0.056	0.063	0.023	0.029	0.065	0.065	0.047	0.023
13,000	0.064	0.070	0.026	0.031	0.074	0.074	0.053	0.026
14,000	0.075	0.081	0.035	0.042	0.083	0.083	0.063	0.035
15,000	0.085	0.091	0.039	0.046	0.096	0.096	0.071	0.039
16,000	0.096	0.103	0.058	0.062	0.110	0.110	0.086	0.058
17,000	0.110	0.122	0.083	0.080	0.137	0.137	0.106	0.083
18,000	0.146	0.155	0.114	0.110	0.185	0.185	0.142	0.110
19,000	0.206	0.206					0.206	
Pressure at Failure (psi)	19,450	19,150	19,000	18,850	18,850	19,450	19,060	18,850

Table C-3. Hydrostatic Test Data for Nominal 1.50-Inch (D_i) - 2.00-Inch (D_o) Flat Acrylic Windows, Test Specimens 11 - 15

(Sealed with grease; radial clearance 0.145 to 0.155 inch; nominal D_o/D_i ratio 1.33)

Parameter	Specimen Number					Value		
	11	12	13	14	15	Max	Avg	Min
Thickness (in.)	0.753	0.743	0.735	0.743	0.734	0.753	0.742	0.734
D_o (actual, in.)	1.960	1.955	1.950	1.945	1.951	1.960	1.952	1.945
Temperature (°F)	69.0	69.0	68.5	69.1	67.2	69.1	68.6	67.2
t/D_i Ratio (actual)	0.502	0.495	0.490	0.495	0.489	0.502	0.494	0.489
Pressurization Rate (psi/min)	665	791	659	665	670	791	690	659
Pressure (psi)	Axial Displacement of Center Point on Window's Low-Pressure Face (in.)							
1,000	0.001	0.001	0.001	0.002	0.001	0.002	0.001	0.001
2,000	0.002	0.002	0.003	0.003	0.003	0.003	0.003	0.002
3,000	0.004	0.003	0.005	0.004	0.005	0.005	0.004	0.003
4,000	0.005	0.005	0.006	0.006	0.006	0.006	0.006	0.005
5,000	0.006	0.006	0.007	0.008	0.007	0.008	0.007	0.006
6,000	0.007	0.008	0.009	0.009	0.009	0.009	0.008	0.007
7,000	0.009	0.009	0.010	0.011	0.010	0.011	0.010	0.009
8,000	0.012	0.011	0.012	0.013	0.012	0.013	0.012	0.011
9,000	0.013	0.013	0.014	0.014	0.014	0.014	0.014	0.013
10,000	0.014	0.015	0.016	0.017	0.016	0.017	0.016	0.014
11,000	0.015	0.017	0.018	0.019	0.018	0.019	0.017	0.015
12,000	0.019	0.020	0.020	0.021	0.020	0.021	0.020	0.019
13,000	0.022	0.024	0.023	0.027	0.037	0.037	0.022	0.022
14,000	0.025	0.040	0.038	0.033	0.040	0.040	0.035	0.025
15,000		0.059	0.068	0.050	0.044	0.068	0.055	0.044
16,000		0.090		0.06[illegible]	0.079	0.090	0.079	0.069
17,000				0.100				
18,000								
Pressure at Failure (psi)	17,700	16,700	15,650	17,900	16,850	17,900	16,960	15,650

Table C-4. Hydrostatic Test Data for Nominal 1.50-Inch (D_i) - 2.25-Inch (D_o) Flat Acrylic Windows, Test Specimens 16 - 20

(Sealed with grease; radial clearance 0.005 to 0.010 inch; nominal D_o/D_i ratio 1.5)

Parameter	Specimen Number					Value		
	16	17	18	19	20	Max	Avg	Min
Thickness (in.)	0.123	0.112	0.117	0.115	0.120	0.123	0.117	0.117
D_o (actual, in.)	2.245	2.243	2.240	2.238	2.241	2.245	2.241	2.238
Temperature (°F)		68	68	68	69	69	68	68
t/D_i Ratio (actual)	0.082	0.075	0.078	0.077	0.080	0.082	0.079	0.075
Pressurization Rate (psi/min)	153	200	292	144	480	480	254	144
Pressure (psi)	Axial Displacement of Center Point on Window's Low-Pressure Face (in.)							
50	0.010	0.026	0.014	0.027	0.017	0.027	0.019	0.010
100	0.017	0.042	0.030	0.047	0.038	0.047	0.035	0.017
150			0.036		0.046	0.046	0.041	0.036
200			0.041		0.050	0.050	0.046	0.041
250			0.051		0.052	0.052	0.051	0.051
300			0.057		0.057	0.057	0.057	0.057
350					0.063			
400					0.073			
450					0.083			
Displacement at Failure (in.)	0.067	0.060	0.050		0.083	0.083	0.065	0.050
Pressure at Failure (psi)	147	160	338	124	450	450	244	124

Notes:

1. Pressurized slowly to facilitate taking displacement data.
2. Grease sealing and pressurization procedure may have caused erratic results.

Table C-5. Hydrostatic Test Data for Nominal 1.50-Inch (D_i) - 2.25-Inch (D_o) Flat Acrylic Windows, Test Specimens 21 - 25

(Sealed with grease; radial clearance 0.002 to 0.005 inch; nominal D_o/D_i ratio 1.5)

Parameter	Specimen Number					Value		
	21	22	23	24	25	Max	Avg	Min
Thickness (in.)	0.121	0.119	0.119	0.119	0.119	0.121	0.119	0.119
D_o (actual, in.)	2.245	2.244	2.246	2.247	2.246	2.247	2.246	2.244
Temperature (°F)	70	70	70	70	70	70	70	70
t/D_i Ratio (actual)	0.081	0.079	0.079	0.079	0.079	0.081	0.079	0.079
Pressurization Rate (psi/min)	310	293	429	272	326	429	326	272
Pressure (psi)	Axial Displacement of Center Point on Window's Low-Pressure Face (in.)							
50	0.012	0.021	0.008	0.033	0.030	0.033	0.021	0.008
100					0.047		0.047	
150								
200								
Displacement at Failure (in.)	0.028	0.038		0.044	0.049	0.049	0.040	0.028
Pressure at Failure (psi)	90	85	60	79	111	111	85	60

Note: Grease seal was thin.

Table C-6. Hydrostatic Test Data for Nominal 1.50-Inch (D_i) - 2.25-Inch (D_o) Flat Acrylic Windows, Test Specimens 26 - 30

(Sealed with grease; radial clearance 0.002 to 0.005 inch; nominal D_o/D_i ratio 1.5)

Parameter	Specimen Number					Value		
	26	27	28	29	30	Max	Avg	Min
Thickness (in.)	0.122	0.121	0.123	0.124	0.126	0.126	0.123	0.121
D_o (actual, in.)	2.246	2.246	2.245	2.247	2.246	2.247	2.246	2.245
Temperature (°F)	66	67	67	67	68	68	67	66
t/D_i ratio (actual)	0.081	0.081	0.082	0.083	0.084	0.084	0.082	0.081
Pressurization Rate (psi/min)	162	188	210	173		210	183	162
Pressure (psi)	Axial Displacement of Center Point on Window's Low-Pressure Face (in.)							
50	0.003	0.035	0.035	0.012	0.023	0.035	0.021	0.003
100					0.045		0.045	
Displacement at Failure (in.)	0.045	0.043	0.039	0.037	0.050	0.050	0.043	0.037
Pressure at Failure (psi)	74	62	61	83	129	129	94	61

Note: Grease liberally applied.

Table C-7. Hydrostatic Test Data for Nominal 1.50-Inch (D_i) - 2.25-Inch (D_o) Flat Acrylic Windows, Test Specimens 31 - 35

(Sealed with grease; radial clearance 0.005 to 0.010 inch; nominal D_o/D_i ratio 1.5)

Parameter	Specimen Number					Value		
	31	32	33	34	35	Max	Avg	Min
Thickness (in.)	0.236	0.234	0.238	0.231	0.229	0.238	0.234	0.229
D_o (actual, in.)	2.238	2.238	2.236	2.237	2.236	2.238	2.237	2.236
Temperature (°F)	68	69	70	65	66	70	68	65
t/D_i Ratio (actual)	0.157	0.156	0.158	0.154	0.153	0.158	0.156	0.153
Pressurization Rate (psi/min)	682	712	675	685	648	712	680	648
Pressure (psi)	Axial Displacement of Center Point on Window's Low-Pressure Face (in.)							
200	0.003	0.001	0.001	0.002	0.001	0.003	0.002	0.001
400	0.010	0.012	0.001	0.007	0.001	0.012	0.006	0.001
600	0.015	0.017	0.015	0.015	0.002	0.017	0.013	0.002
800	0.023	0.024	0.015	0.022	0.010	0.024	0.019	0.010
1,000	0.031	0.029	0.026	0.030	0.060	0.060	0.035	0.026
1,200	0.075	0.037		0.040		0.075	0.051	0.037
1,400	0.098							
1,600								
Pressure at Failure (psi)	1,430	1,210	1,140	1,320	1,100	1,430	1,240	1,100

Note: Erratic deflection.

Table C-8. Hydrostatic Test Data for Nominal 1.50-Inch (D_i) - 2.25-Inch (D_o) Flat Acrylic Windows, Test Specimens 36 - 40

(Sealed with grease; radial clearance 0.005 to 0.010 inch; nominal D_o/D_i ratio 1.5)

Parameter	Specimen Number					Value		
	118	119	120	121	122	Max	Avg	Min
Thickness (in.)	0.235	0.237	0.240	0.237	0.234	0.240	0.237	0.234
D_o (actual, in.)	2.239	2.237	2.240	2.237	2.240	2.240	2.239	2.237
Temperature (°F)	70	68	69	68	69	70	69	68
t/D_i Ratio (actual)	0.157	0.158	0.160	0.158	0.156	0.160	0.158	0.156
Pressurization Rate (psi/min)	590	497	524	627	560	627	560	497
Pressure (psi)	Axial Displacement of Center Point on Window's Low-Pressure Face (in.)							
100	0.002	0.005	0.001	0.002	0.004	0.005	0.003	0.001
200	0.006	0.007	0.002	0.002	0.006	0.007	0.005	0.002
300	0.007	0.010	0.002	0.002	0.008	0.010	0.006	0.002
400	0.009	0.014	0.003	0.003	0.011	0.014	0.011	0.003
500	0.013	0.017	0.003	0.004	0.015	0.017	0.010	0.003
600	0.016		0.009	0.009	0.018	0.018	0.014	0.009
700	0.019		0.012	0.012		0.019	0.014	0.012
800	0.024							
900								
1,000								
Displacement at Failure (in.)	0.046	0.045	0.048	0.053	0.064	0.064	0.051	0.045
Pressure at Failure (psi)	840	642	733	702	695	840	723	642

Notes:

1. Thin grease seal coating.
2. Amount of cement used on deflection pin may have significant effect on thin windows.

Table C-9. Hydrostatic Test Data for Nominal 1.50-Inch (D_i) - 2.25-Inch (D_o) Flat Acrylic Windows, Test Specimens 41 - 45

(Sealed with grease; radial clearance 0.000 to 0.005 inch; nominal D_o/D_i ratio 1.5)

Parameter	Specimen Number					Value		
	41	42	43	44	45	Max	Avg	Min
Thickness (in.)	0.243	0.246	0.249	0.248	0.249	0.249	0.247	0.243
D_o (actual, in.)	2.249	2.246	2.247	2.249	2.248	2.249	2.248	2.246
Temperature (°F)	66	68	68	67	66	68	67	66
t/D_i Ratio (actual)	0.162	0.164	0.166	0.165	0.166	0.166	0.165	0.162
Pressurization Rate (psi/min)	560	482	673	648	633	673	599	482
Pressure (psi)	Axial Displacement of Center Point on Window's Low-Pressure Face (in.)							
100	0.001	0.000	0.001	0.001	0.001	0.001	0.001	0.000
200	0.001	0.001	0.001	0.001	0.001	0.001	0.001	0.001
300	0.001	0.012	0.009	0.001	0.001	0.012	0.005	0.001
400	0.002	0.017	0.010	0.002	0.002	0.017	0.007	0.002
500	0.002	0.021	0.016	0.002	0.002	0.021	0.009	0.002
600	0.002	0.024	0.018	0.011	0.003	0.024	0.012	0.002
700	0.003	0.028	0.023	0.012	0.003	0.028	0.013	0.003
800	0.020	0.051	0.024	0.019	0.011	0.051	0.025	0.011
900	0.021	0.055	0.034	0.029	0.014	0.055	0.031	0.014
1,000	0.026	0.059	0.051	0.030	0.040	0.059	0.041	0.026
1,100		0.064	0.057	0.046	0.040	0.064	0.052	0.040
1,200		0.067	0.064	0.046	0.047	0.067	0.056	0.046
1,300	abort	0.075	0.064	0.054	0.047	0.075	0.060	0.047
1,400		0.083	0.072	0.055	0.052	0.083	0.066	0.052
1,500		0.088	0.072	0.063	0.058	0.088	0.070	0.058
1,600		0.092	0.079	0.063	0.062	0.092	0.074	0.062
1,700		0.096	0.086	0.071	0.070	0.096	0.081	0.070
1,800		0.102	0.086	0.071	0.073	0.102	0.083	0.071
1,900		0.124	0.093	0.078	0.078	0.124	0.093	0.078
2,000		0.139	0.099	0.085	0.081	0.139	0.101	0.081
2,100			0.100	0.085	0.088		0.091	
2,200					0.093			
Displacement at Failure (in.)		0.142	0.100	0.085	0.093	0.142	0.105	0.085
Pressure at Failure (psi)		2,000	2,100	2,100	2,200	2,200	2,100	2,000

Notes:

1. Abort caused by use of 1,000-psi gage.
2. Grease liberally applied.
3. Audible cracking at about 900 psi and 1,600 psi.

Table C-10. Hydrostatic Test Data for Nominal 1.50-Inch (D_i) - 2.25-Inch (D_o) Flat Acrylic Windows, Test Specimens 46 - 50

(Sealed with grease; radial clearance 0.005 to 0.010 inch; nominal D_o/D_i ratio 1.5)

Parameter	Specimen Number					Value		
	46	47	48	49	50	Max	Avg	Min
Thickness (in.)	0.338	0.342	0.344	0.341	0.344	0.344	0.342	0.338
D_o (actual, in.)	2.240	2.242	2.238	2.241	2.241	2.242	2.240	2.238
Temperature (°F)	67	67	69	65	65	69	67	65
t/D_i Ratio (actual)	0.225	0.228	0.229	0.227	0.229	0.229	0.228	0.225
Pressurization Rate (psi/min)	660	668	660	665	685	685	668	660
Pressure (psi)	Axial Displacement of Center Point on Window's Low-Pressure Face (in.)							
500	0.003	0.002	0.001	0.001	0.008	0.008	0.003	0.001
1,000	0.011	0.003	0.011	0.002	0.015	0.015	0.009	0.003
1,500	0.037	0.007	0.016	0.022	0.023	0.037	0.021	0.007
2,000	0.052	0.036	0.036	0.030	0.031	0.052	0.037	0.030
2,500	0.067	0.052	0.067	0.059	0.056	0.067	0.060	0.052
3,000	0.085	0.063	0.085	0.072	0.087	0.087	0.078	0.063
3,500	0.106	0.077	0.103	0.089	0.105	0.106	0.096	0.077
4,000	0.134	0.095	0.123		0.121	0.134	0.103	0.095
4,500					0.148			
5,000								
Displacement at Failure (in.)		0.119	0.148	0.106	0.161	0.161	0.134	0.106
Pressure at Failure (psi)	4,100	4,400	4,225	3,950	4,700	4,700	4,275	3,950

Note: Grease liberally applied.

Table C-11. Hydrostatic Test Data for Nominal 1.50-Inch (D_i) - 2.25-Inch (D_o) Flat Acrylic Windows, Test Specimens 51 - 55

(Sealed with grease; radial clearance 0.005 to 0.010 inch; nominal D_o/D_i ratio 1.5)

Parameter	Specimen Number					Value		
	51	52	53	54	55	Max	Avg	Min
Thickness (in.)	0.496	0.497	0.496	0.499	0.497	0.499	0.497	0.496
D_o (actual, in.)	2.237	2.240	2.237	2.237	2.238	2.240	2.238	2.237
Temperature (°F)	69	66	68	68	68	69	68	66
t/D_i Ratio (actual)	0.330	0.331	0.330	0.333	0.331	0.333	0.331	0.330
Pressurization Rate (psi/min)	680	695	689	662	670	695	679	662
Pressure (psi)	Axial Displacement of Center Point on Window's Low-Pressure Face (in.)							
1,000	0.003	0.001	0.001	0.001	0.003	0.003	0.002	0.001
2,000	0.014	0.007	0.012	0.002	0.010	0.014	0.009	0.002
3,000	0.022	0.016	0.018	0.012	0.018	0.022	0.017	0.012
4,000	0.029	0.023	0.028	0.021	0.027	0.029	0.026	0.021
5,000	0.040	0.036	0.036	0.031	0.036	0.040	0.036	0.031
6,000	0.077	0.053	0.065	0.040	0.062	0.077	0.059	0.040
7,000	1/	0.088	0.085	0.052	0.088	0.088	0.079	0.052
8,000		0.120	0.119		1/	0.120	0.120	0.119
9,000								
10,000								
Displacement at Failure (in.)		0.152	0.146	0.122		0.152	0.130	0.122
Pressure at Failure (psi)	7,300	8,550	8,450	7,450	7,300	8,550	7,810	7,300

1/ Deflection wire became disengaged.

Notes:

1. Grease liberally applied.
2. 500-psi preload.
3. Audible cracking at about 7,000 psi.

Table C-12. Hydrostatic Test Data for Nominal 1.50-Inch (D_i) - 2.25-Inch (D_o) Flat Acrylic Windows, Test Specimens 56 - 60

(Sealed with grease; radial clearance 0.005 to 0.010 inch; nominal D_o/D_i ratio 1.5)

Parameter	Specimen Number					Value		
	56	57	58	59	60	Max	Avg	Min
Thickness (in.)	0.607	0.604	0.622	0.620	0.600	0.622	0.611	0.600
D_o (actual, in.)	2.240	2.239	2.240	2.239	2.237	2.240	2.239	2.237
Temperature (°F)	68	67	68	68	64	68	67	64
t/D_i Ratio (actual)	0.405	0.402	0.414	0.413	0.400	0.414	0.407	0.400
Pressurization Rate (psi/min)	670	665	665	668	663	670	666	663
Pressure (psi)	Axial Displacement of Center Point on Window's Low-Pressure Face (in.)							
1,000	0.002	0.009	0.011	0.004	0.001	0.011	0.005	0.001
2,000	0.003	0.015	0.019	0.012	0.009	0.019	0.012	0.003
3,000	0.008	0.021	0.024	0.019	0.012	0.024	0.019	0.008
4,000	0.015	0.028	0.030	0.025	0.023	0.030	0.024	0.015
5,000	0.021	0.037	0.039	0.031	0.030	0.039	0.031	0.021
6,000	0.027	0.043	0.043	0.038	0.036	0.043	0.039	0.027
7,000	0.034	0.050	0.053	0.045	0.043	0.053	0.045	0.033
8,000	0.046	0.057	0.059	0.053	0.055	0.058	0.054	0.046
9,000	0.059	0.055	0.068	0.061	0.070	0.070	0.065	0.059
10,000	0.092	0.073	0.103	0.104	0.083	0.104	0.091	0.083
11,000	0.117	0.084	0.146	0.145	0.114	0.146	0.121	0.114
12,000	0.163	1/	0.199	0.186	0.174	0.199	0.144	0.163
13,000	0.228		1/	0.318	1/	0.318	0.273	0.228
14,000								
15,000								
Displacement at Failure (in.)	0.392							
Pressure at Failure (psi)	13,300	13,800	13,075	13,150	13,000	13,800	13,265	13,000

1/ Deflection wire became disengaged.

Notes:

1. Grease liberally applied.
2. 500-psi preload.
3. Cracking at about 9,000 psi and 13,000 psi.

Table C-13. Hydrostatic Test Data for Nominal 1.50-Inch (D_i) - 2.25-Inch (D_o) Flat Acrylic Windows, Test Specimens 61 - 65

(Sealed with grease; radial clearance 0.005 to 0.010 inch; nominal D_o/D_i ratio 1.5)

Parameter	Specimen Number					Value		
	61	62	63	64	65	Max	Avg	Min
Thickness (in.)	0.733	0.733	0.734	0.735	0.735	0.735	0.734	0.733
D_o (actual, in.)	2.239	2.239	2.241	2.241	2.240	2.241	2.240	2.239
Temperature (°F)	67	69	71	66	68	71	68	66
t/D_i Ratio (actual)	0.488	0.488	0.489	0.490	0.490	0.490	0.489	0.488
Pressurization Rate (psi/min)	670	670	682	669	637	682	656	637
Pressure (psi)	Axial Displacement of Center Point on Window's Low-Pressure Face (in.)							
1,000	0.001	0.000	0.002	0.001	0.002	0.002	0.001	0.000
2,000	0.001	0.000	0.011	0.002	0.003	0.011	0.005	0.000
3,000	0.013	0.012	0.018	0.016	0.003	0.018	0.012	0.003
4,000	0.021	0.012	0.023	0.017	0.004	0.023	0.015	0.004
5,000	0.022	0.018	0.029	0.026	0.017	0.029	0.022	0.017
6,000	0.029	0.025	0.034	0.026	0.017	0.034	0.026	0.017
7,000	0.029	0.033	0.035	0.027	0.018	0.035	0.028	0.018
8,000	0.036	0.033	0.040	0.039	0.035	0.040	0.036	0.033
9,000	0.043	0.038	0.048	0.039	0.035	0.048	0.041	0.035
10,000	0.046	0.045	0.053	0.052	0.036	0.053	0.046	0.036
11,000	0.052	0.052	0.061	0.053	0.047	0.061	0.053	0.047
12,000	0.059	0.059	0.068	0.065	0.048	0.068	0.060	0.048
13,000	0.071	0.064	0.075	0.065	0.063	0.075	0.068	0.063
14,000	0.078	0.090	0.095	0.072	0.076	0.095	0.082	0.076
15,000	0.097	0.099	0.106	0.084	0.095	0.106	0.096	0.084
16,000	0.112	0.121	0.129	0.107	0.109	0.129	0.116	0.107
17,000		0.143	0.145	0.125	0.131	0.145	0.135	0.125
18,000		0.174	0.185	0.143	0.164	0.185	0.161	0.143
19,000		0.236		0.177		0.236	0.202	0.177
Displacement at Failure (in.)		0.252	0.255	0.256		0.256	0.253	0.252
Pressure at Failure (psi)		19,200	18,600	19,650		19,650	19,100 1/	18,600

1/ Averaged with preliminary tests.

Notes:

1. Abort due to pump failure at 16,600 psi.
2. Audible cracking at about 14,000 psi.

Table C-14. Hydrostatic Test Data for Nominal 1.50-Inch (D_i) - 2.25-Inch (D_o) Flat Acrylic Windows, Test Specimens 66 - 70

(Sealed with grease; radial clearance 0.005 to 0.010 inch; nominal D_i/D_o ratio 1.5)

Parameter	Specimen Number					Value		
	66	67	68	69	70	Max	Avg	Min
Thickness (in.)	0.833	0.838	0.840	0.845	0.857[1]	0.845	0.839	0.833
D_o (actual, in.)	2.238	2.238	2.239	2.239	2.238	2.239	2.238	2.238
Temperature (°F)	68	67	68	70	66	70	68	67
t/D_i Ratio (actual)	0.555	0.558	0.560	0.563	0.572	0.572	0.559	0.555
Pressurization Rate (psi/min)	695	662	660	663	650	695	670	660
Pressure (psi)	Axial Displacement of Center Point on Window's Low-Pressure Face (in.)							
1,000	0.001	0.001	0.001	0.001	0.001	0.001	0.001	0.001
2,000	0.002	0.002	0.002	0.002	0.001	0.002	0.002	0.001
3,000	0.002	0.002	0.003	0.002	0.002	0.003	0.002	0.002
4,000	0.006	0.005	0.004	0.003	0.003	0.006	0.004	0.003
5,000	0.012	0.011	0.005	0.003	0.005	0.012	0.008	0.003
6,000	0.016	0.015	0.010	0.004	0.006	0.016	0.011	0.004
7,000	0.021	0.016	0.015	0.011	0.009	0.021	0.016	0.011
8,000	0.025	0.021	0.021	0.015	0.010	0.025	0.020	0.015
9,000	0.030	0.025	0.027	0.020	0.019	0.030	0.026	0.020
10,000	0.034	0.031	0.031	0.026	0.020	0.034	0.031	0.026
11,000	0.039	0.035	0.036	0.031	0.020	0.039	0.035	0.031
12,000	0.044	0.041	0.041	0.035	0.035	0.044	0.040	0.035
13,000	0.050	0.045	0.047	0.040	0.036	0.050	0.045	0.040
14,000	0.056	0.054	0.052	0.047	0.037	0.056	0.052	0.047
15,000	0.063	0.059	0.059	0.053	0.039	0.063	0.059	0.053
16,000	0.070	0.069	0.066	0.064	0.040	0.070	0.067	0.064
17,000	0.078	0.076	0.077	0.072	0.041	0.078	0.076	0.072
18,000	0.091	0.087	0.087	0.083	0.042	0.091	0.087	0.083
19,000	0.103	0.097	0.099	0.096	0.064	0.103	0.099	0.096
20,000	0.119	0.110	0.118	0.111	0.080	0.119	0.115	0.110
21,000	0.144	0.132	0.139	0.137	1/	0.144	0.138	0.132
22,000	0.180	0.163	0.170	0.183		0.183	0.174	0.163
23,000	0.282	0.232	0.230			0.282	0.248	0.230
Displacement at Failure (in.)		0.325	0.330			0.330	0.328	0.325
Pressure at Failure (psi)	23,100	23,400	23,350	22,800		23,400	23,160	22,800

1/ Abort due to leak at 20,100 psi, not averaged.

Table C-15. Hydrostatic Test Data for Nominal 1.50-Inch (D_i) - 2.25-Inch (D_o) Flat Acrylic Windows, Test Specimens 71 - 75

(Sealed with grease; radial clearance 0.002 to 0.005 inch; nominal D_o/D_i ratio 1.5)

Parameter	Specimen Number					Value		
	71	72	73	74	75	Max	Avg	Min
Thickness (in.)	0.982	0.982	0.982	0.985	0.984	0.985	0.983	0.982
D_o (actual, in.)	2.243	2.242	2.243	2.243	2.243	2.243	2.243	2.242
Temperature (°F)	68	69	69	70	67	70	69	67
t/D_i Ratio (actual)	0.655	0.655	0.655	0.656	0.656	0.656	0.655	0.655
Pressurization Rate (psi/min)	660	670	663	677	665	677	670	660
Pressure (psi)	Axial Displacement of Center Point on Window's Low-Pressure Face (in.)							
1,000	0.000	0.000	0.001	0.000	0.001	0.001	0.000	0.000
2,000	0.006	0.001	0.002	0.001	0.002	0.006	0.002	0.001
3,000	0.010	0.002	0.004	0.001	0.002	0.010	0.004	0.001
4,000	0.015	0.002	0.015	0.001	0.004	0.015	0.007	0.001
5,000	0.019	0.003	0.015	0.002	0.009	0.019	0.010	0.002
6,000	0.023	0.008	0.025	0.003	0.015	0.025	0.015	0.003
7,000	0.027	0.015	0.025	0.010	0.015	0.027	0.018	0.010
8,000	0.031	0.015	0.025	0.012	0.016	0.031	0.020	0.012
9,000	0.035	0.016	0.034	0.016	0.026	0.035	0.025	0.016
10,000	0.038	0.021	0.034	0.021	0.027	0.038	0.028	0.021
11,000	0.042	0.026	0.034	0.026	0.027	0.042	0.031	0.026
12,000	0.046	0.033	0.045	0.030	0.040	0.046	0.039	0.030
13,000	0.050	0.034	0.045	0.035	0.041	0.050	0.041	0.034
14,000	0.055	0.041	0.046	0.039	0.041	0.055	0.044	0.039
15,000	0.060	0.045	0.058	0.044	0.041	0.060	0.050	0.041
16,000	0.066	0.051	0.058	0.049	0.054	0.066	0.056	0.049
17,000	0.071	0.060	0.069	0.054	0.055	0.071	0.062	0.054
18,000	0.075	0.066	0.070	0.060	0.070	0.075	0.068	0.060
19,000	0.083	0.073	0.082	0.067	0.071	0.083	0.075	0.067
20,000	0.088	0.080	0.082	0.076	0.071	0.088	0.079	0.071
21,000	0.095	0.089	0.094	0.084	0.087	0.095	0.090	0.084
22,000	0.103	0.113	0.102	0.093	0.088	0.113	0.100	0.088
23,000	0.112	0.118	0.112	0.104	0.103	0.118	0.110	0.103
24,000	0.132	0.125	0.116	0.114	0.104	0.132	0.118	0.104
25,000	0.138	0.173	0.128	0.129	0.118	0.138	0.129	0.118
26,000	0.150	0.237	0.148	0.148	0.132	0.150	0.145	0.132
27,000	2/	1/	0.180	0.173	0.148	0.180	0.160	0.148
28,000			0.210	0.230	0.160	0.230	0.200	0.160
29,000					0.194			
Pressure at Failure (psi)		26,800	28,800	28,600	29,800	29,800	28,500	26,800

1/ Time stopped to fix leak at 22,000 psi.
2/ Abort due to pump failure at 26,350 psi.

Table C-16. Hydrostatic Test Data for Nominal 1.50-Inch (D_i) - 4.00-Inch (D_o) Flat Acrylic Windows, Test Specimens 76 - 80

(Sealed with grease; radial clearance 0.020 to 0.030 inch; nominal D_o/D_i ratio 2.67)

Parameter	Specimen Number					Value		
	76	77	78	79	80	Max	Avg	Min
Thickness (in.)	0.729	0.731	0.729	0.738	0.730	0.738	0.731	0.729
D_o (actual, in.)	3.951	3.950	3.950	3.960	3.945	3.960	3.952	3.945
Temperature (°F)	64.5	64.0	65.5	65.0	64.0	65.5	64.6	64.0
t/D_i Ratio (actual)	0.486	0.487	0.486	0.492	0.487	0.492	0.487	0.486
Pressurization Rate (psi/min)	674	602	667	606	652	674	640	602
Pressure (psi)	Axial Displacement of Center Point on Window's Low-Pressure Face (in.)							
1,000	0.009	0.003	0.008	0.008	0.008	0.009	0.007	0.003
2,000	0.023	0.008	0.015	0.024	0.015	0.024	0.017	0.008
3,000	0.030	0.013	0.018	0.029	0.023	0.030	0.023	0.013
4,000	0.036	0.018	0.025	0.036	0.031	0.036	0.029	0.018
5,000	0.042	0.023	0.031	0.042	0.035	0.042	0.035	0.023
6,000	0.047	0.032	0.037	0.047	0.042	0.047	0.041	0.032
7,000	0.052	0.037	0.042	0.053	0.047	0.053	0.046	0.037
8,000	0.058	0.040	0.048	0.057	0.060	0.060	0.053	0.040
9,000	0.063	0.046	0.051	0.075	0.065	0.075	0.060	0.046
10,000	0.068	0.052	0.058	0.078	0.071	0.078	0.065	0.052
11,000	0.073	0.057	0.062	0.083	0.078	0.083	0.071	0.057
12,000	0.080	0.062	0.070	0.088	0.084	0.088	0.077	0.062
13,000	0.101	0.068		0.096	0.090	0.101	0.089	0.068
14,000	0.107	0.074		0.113	0.098	0.113	0.098	0.074
15,000	0.115	0.094		0.118	0.106	0.118	0.108	0.094
16,000	0.125	0.102		0.128	0.114	0.128	0.117	0.102
17,000	0.136	0.112		0.142		0.142	0.130	0.112
18,000	0.154	0.133				0.154	0.143	0.133
19,000	0.175							
20,000								
Pressure at Failure (psi)	19,500	18,950	19,100	18,800	19,600	19,600	19,190	18,800

Table C-17. Hydrostatic Test Data for Nominal 1.50-Inch (D_i) - 4.00-Inch (D_o) Flat Acrylic Windows, Test Specimens 81 - 85

(Sealed with O-ring; radial clearance 0.0005 to 0.001 inch; nominal D_o/D_i ratio 2.67)

Parameter	Specimen Number					Value		
	81	82	83	84	85	Max	Avg	Min
Thickness (in.)	0.740	0.733	0.739	0.747	0.738	0.747	0.739	0.733
D_o (actual, in.)	3.999	3.999	3.999	3.998	3.998	3.999	3.998	3.998
Temperature (°F)	65.0	64.0	64.0	63.5	63.0	65.0	63.9	63.0
t/D_i Ratio (actual)	0.493	0.488	0.492	0.498	0.492	0.498	0.492	0.488
Pressurization Rate (psi/min)	651	620	673	666	658	673	654	620
Pressure (psi)	Axial Displacement of Center Point on Window's Low-Pressure Face (in.)							
1,000	0.020	0.009	0.014	0.026	0.001	0.026	0.014	0.001
2,000	0.040	0.019	0.020	0.041	0.005	0.041	0.025	0.005
3,000	0.055	0.027	0.024	0.050	0.011	0.055	0.033	0.011
4,000	0.064	0.036	0.026	0.056	0.019	0.064	0.040	0.019
5,000	0.069	0.039	0.028	0.061	0.026	0.069	0.045	0.026
6,000	0.075	0.046	0.030	0.066	0.032	0.075	0.050	0.030
7,000	0.080	0.050	0.032	0.072	0.037	0.080	0.054	0.032
8,000	0.085	0.055	0.035	0.078	0.043	0.085	0.059	0.035
9,000	0.091	0.067	0.038	0.082	0.049	0.091	0.065	0.038
10,000	0.097	0.075	0.040	0.089	0.055	0.047	0.071	0.040
11,000	0.102	0.080	0.043	0.117	0.060	0.117	0.080	0.043
12,000		0.085	0.065	0.118	0.067	0.118	0.084	0.065
13,000		0.091	0.069	0.120	0.073	0.120	0.088	0.069
14,000		0.099	0.076	0.128	0.079	0.128	0.095	0.076
15,000		0.102	0.082	0.136	0.086	0.136	0.101	0.082
16,000		0.118	0.092	0.145	0.095	0.145	0.112	0.092
17,000		0.130	0.108	0.154	0.106	0.154	0.124	0.106
18,000		0.157	0.121	0.167	0.119	0.167	0.141	0.119
19,000		0.180			0.135	0.180	0.157	0.135
20,000					0.173			
21,000					0.247			
Pressure at Failure (psi)	19,150	19,300	18,300	18,400	21,200	21,200	19,270	18,300

Table C-18. Hydrostatic Test Data for Nominal 3.33-Inch (D_i) - 5.00-Inch (D_o) Flat Acrylic Windows, Test Specimens 86 - 90

(Sealed with grease; radial clearance 0.005 to 0.010 inch; nominal D_o/D_i ratio 1.5)

Parameter	Specimen Number					Value		
	86	87	88	89	90	Max	Avg	Min
Thickness (in.)	0.123	0.123	0.119	0.121	0.119	0.123	0.121	0.119
D_o (actual, in.)	4.988	4.988	4.989	4.989	4.990	4.990	4.989	4.988
Temperature (°F)	66	66	66	67	67	67	66	66
t/D_i Ratio (actual)	0.037	0.037	0.036	0.036	0.036	0.037	0.036	0.036
Pressurization Rate (psi/min)	150	111	151	175	192	192	156	111
Pressure (psi)	Axial Displacement of Center Point on Window's Low-Pressure Face (in.)							
50	0.132	0.140	0.150	0.157	0.171	0.171	0.150	0.132
100	0.176	0.194	0.203	0.209	0.224	0.224	0.201	0.176
Displacement at Failure (in.)	0.197	0.194	0.240	0.216	0.244	0.194	0.218	0.244
Pressure at Failure (psi)	112	100	145	105	125	145	117	100

Table C-19. Hydrostatic Test Data for Nominal 3.33-Inch (D_i) - 5.00-Inch (D_o) Flat Acrylic Windows, Test Specimens 91 - 95

(Sealed with grease; radial clearance 0.002 to 0.005 inch; nominal D_o/D_i ratio 1.50)

Parameter	Specimen Number					Value		
	91	92	93	94	95	Max	Avg	Min
Thickness (in.)	0.360	0.347	0.347	0.348	0.349	0.360	0.350	0.347
D_o (actual, in.)	4.995	4.996	4.995	4.995	4.994	4.996	4.995	4.994
Temperature (°F)	70	71	65	66	66	71	68	65
t/D_i Ratio (actual)	0.104	0.102	0.102	0.102	0.102	0.104	0.102	0.102
Pressurization Rate (psi/min)	760	690	840[1]	687	688	760	671	687
Pressure (psi)	Axial Displacement of Center Point on Window's Low-Pressure Face (in.)							
100	0.003	0.016	0.024	0.039	0.032	0.039	0.023	0.003
200	0.026	0.032	0.044	0.050	0.046	0.050	0.040	0.026
300	0.039	0.045		0.065	0.060	0.065	0.050	0.039
400	0.053	0.096	0.073	0.079	0.077	0.096	0.076	0.053
500		0.124	0.086	0.092	0.091	0.124	0.095	0.086
600			0.101					
700			0.115					
800			0.132[1]					
Displacement at Failure (in.)		0.131	0.132	0.107	0.103	0.132	0.118	0.103
Pressure at Failure (psi)	570	545	800[1]	590	570	590	569	545

[1] Not included in averaged values.

Table C-20. Hydrostatic Test Data for Nominal 3.33-Inch (D_i) - 5.00-Inch (D_o) Flat Acrylic Windows, Test Specimens 96 - 100

(Sealed with grease; radial clearance 0.002 ro 0.005 inch; nominal D_o/D_i ratio 1.50)

Parameter	Specimen Number					Value		
	96	97	98	99	100	Max	Avg	Min
Thickness (in.)	0.603	0.604	0.606	0.607	0.607	0.607	0.605	0.603
D_o (actual, in.)	4.994	4.995	4.995	4.994	4.994	4.995	4.994	4.994
Temperature (°F)	66	68	68	68	69	69	68	66
t/D_i Ratio (actual)	0.181	0.182	0.182	0.182	0.182	0.182	0.182	0.181
Pressurization Rate (psi/min)	617	634	668	588	682	682	638	588
Pressure (psi)	Axial Displacement of Center Point on Window's Low-Pressure Face (in.)							
200	0.008	0.025	0.024	0.011	0.004	0.025	0.014	0.004
400	0.015	0.034	0.030	0.019	0.015	0.034	0.023	0.015
600	0.024	0.040	0.040	0.028	0.024	0.040	0.031	0.024
800	0.032	0.049	0.047	0.036	0.037	0.049	0.040	0.032
1,000	0.038	0.055	0.055	0.043	0.039	0.055	0.046	0.038
1,200	0.044	0.066	0.063	0.054	0.052	0.066	0.056	0.044
1,400	0.053	0.071	0.070	0.058	0.055	0.071	0.061	0.053
1,600	0.101	0.079	0.078	0.067	0.064	0.101	0.078	0.064
1,800	0.112	0.087	0.087	0.076	0.074	0.112	0.088	0.074
2,000		0.098	0.095	0.080		0.098	0.091	0.080
2,200		0.106					0.106	
Displacement at Failure (in.)	0.138	0.109	0.100	0.081	0.076	0.138	0.100	0.076
Pressure at Failure (psi)	1,910	2,300	2,100	2,025	1,960	2,300	2,060	1,910

Table C-21. Hydrostatic Test Data for Nominal 3.33-Inch (D_i) - 5.00-Inch (D_o) Flat Acrylic Windows, Test Specimens 101 - 105

(Sealed with grease; radial clearance 0.002 to 0.005 inch; nominal D_o/D_i ratio 1.5)

Parameter	Specimen Number					Value		
	101	102	103	104	105	Max	Avg	Min
Thickness (in.)	0.841	0.836	0.847	0.831	0.830	0.847	0.837	0.830
D_o (actual, in.)	4.995	4.995	4.994	4.995	4.994	4.995	4.995	4.994
Temperature (°F)	70	69	65	65	64	70	67	64
t/D_i Ratio (actual)	0.252	0.251	0.254	0.249	0.249	0.254	0.251	0.249
Pressurization Rate (psi/min)	660	664 1/	669	652	620	669	653	620
Pressure (psi)	Axial Displacement of Center Point on Window's Low-Pressure Face (in.)							
500	0.019	0.010	0.004	0.002	0.011	0.019	0.009	0.002
1,000	0.030	0.018	0.019	0.012	0.022	0.030	0.020	0.012
1,500	0.040	0.025	0.029	0.019	0.031	0.040	0.029	0.019
2,000	0.050	0.039	0.037	0.034	0.042	0.050	0.040	0.034
2,500		0.046	0.045	0.042	0.053	0.053	0.047	0.042
3,000	0.072	0.058	0.052	0.050	0.061	0.072	0.059	0.050
3,500	0.084	0.129 1/		0.130		0.130	0.114	0.084
4,000	0.102				0.084			
4,500	0.117							
Displacement at Failure (in.)	0.124			0.138	0.084	0.138	0.115	0.084
Pressure at Failure (psi)	4,750	3,550	3,400	3,600	4,000	4,750	3,860	3,400

1/ Preloaded pressure unknown, plugged gage line.

Table C-22. Hydrostatic Test Data for Nominal 3.33-Inch (D_i) - 5.00-Inch (D_o) Flat Acrylic Windows, Test Specimens 106 - 110

(Sealed with grease; radial clearance 0.005 to 0.010 inch; nominal D_o/D_i ratio 1.5)

Parameter	Specimen Number					Value		
	106	107	108	109	110	Max	Avg	Min
Thickness (in.)	1.109	1.131	1.132	1.131	1.127	1.132	1.126	1.109
D_o (actual, in.)	4.986	4.983	4.984	4.983	4.986	4.986	4.984	4.983
Temperature (°F)	65	69	68	68	69	69	68	65
t/D_i Ratio (actual)	0.333	0.339	0.340	0.339	0.338	0.340	0.338	0.333
Pressurization Rate (psi/min)	710	633	664	655	672	710	669	633
Pressure (psi)	Axial Displacement of Center Point on Window's Low-Pressure Face (in.)							
500	0.001	0.002	0.002	0.001	0.001	0.002	0.001	0.001
1,000	0.011	0.002	0.010	0.001	0.020	0.020	0.009	0.001
1,500	0.012	0.008	0.018	0.010	0.020	0.020	0.016	0.008
2,000	0.021	0.013	0.027	0.019	0.020	0.027	0.020	0.013
2,500	0.030	0.018	0.034	0.026	0.033	0.034	0.028	0.018
3,000	0.039	0.027	0.042	0.032	0.045	0.045	0.037	0.027
3,500	0.048	0.033	0.047	0.036	0.045	0.048	0.042	0.033
4,000	0.056	0.043	0.054	0.048	0.056	0.056	0.051	0.043
4,500	0.064	0.050	0.059	0.059	0.095	0.095	0.065	0.050
5,000	0.074	0.060	0.067	0.068	0.097	0.097	0.075	0.060
5,500	0.083	0.067	0.114	0.070	0.113	0.114	0.089	0.067
6,000	0.091	0.109	0.128	0.115	0.128	0.128	0.114	0.091
6,500	0.099	0.142	0.136	0.131	0.142	0.142	0.130	0.099
7,000	0.130	0.176	0.255	0.292	0.155	0.292	0.201	0.130
7,500	0.489	0.386	0.336	0.447	1/	0.489	0.415	0.336
8,000	0.572		0.456					
Displacement at Failure (in.)	0.782	0.610	0.456	0.536		0.782	0.596	0.456
Pressure at Failure (psi)	8,300	7,825	8,025	7,650	8,450	8,450	8,050	7,650

1/ Deflection wire disengaged suddenly.

Note: Cracking at about 5,000 psi and 7,000 psi.

Table C-23. Hydrostatic Test Data for Nominal 3.33-Inch (D_i) -5.00-Inch (D_o) Flat Acrylic Windows, Test Specimens 111 - 115

(Sealed with grease; radial clearance 0.005 to 0.010 inch; nominal D_o/D_i ratio 1.5)

Parameter	Specimen Number					Value		
	111	112	113	114	115	Max	Avg	Min
Thickness (in.)	1.446	1.432	1.439	1.437	1.449	1.449	1.441	1.432
D_o (actual, in.)	4.986	4.988	4.986	4.985	4.987	4.988	4.987	4.985
Temperature (°F)	65	66	65	68	65	68	66	65
t/D_i Ratio (actual)	0.435	0.429	0.432	0.431	0.436	0.436	0.433	0.429
Pressurization Rate (psi/min)	673	658	669 1/	645	662	673	661	645
Pressure (psi)	Axial Displacement of Center Point on Window's Low-Pressure Face (in.)							
1,000	0.002	0.001		0.010	0.009	0.010	0.005	0.001
2,000	0.016	0.019	0.027	0.018	0.016	0.027	0.019	0.016
3,000	0.029	0.030	0.037	0.033	0.026	0.037	0.031	0.026
4,000	0.031	0.036	0.049	0.040	0.040	0.049	0.039	0.031
5,000	0.045	0.044	0.060	0.042	0.050	0.060	0.048	0.042
6,000	0.059	0.061	0.070	0.055	0.059	0.070	0.059	0.055
7,000	0.072	0.069	0.081	0.070	0.080	0.081	0.074	0.069
8,000	0.085	0.089	0.094	0.090	0.095	0.095	0.091	0.085
9,000	0.099	0.109	0.107	0.120	0.104	0.120	0.108	0.099
10,000	0.122	0.124	0.123	0.138	0.143	0.143	0.130	0.122
11,000	0.168	0.156	0.175	0.170	0.184	0.184	0.171	0.156
12,000	0.205	0.196	0.211	0.216	0.216	0.216	0.209	0.196
13,000	0.230	0.230	0.253	0.244	0.257	0.257	0.243	0.230
14,000	0.285	0.284	0.310	0.302	0.306	0.310	0.298	0.284
15,000	0.365	0.371	0.427	0.389	0.384	0.427	0.387	0.365
Displacement at Failure (in.)	0.428	0.424	0.464 1/	0.454	0.486	0.486	0.451	0.424
Pressure at Failure (psi)	15,750	15,300	15,200	15,475	15,400	15,750	15,425	15,200

1/ Held 2 minutes at 500 psi to fix leak.

Notes:

1. 500-psi preload.
2. Audible cracks at about 9,000 psi and 11,000 psi.

Table C-24. Hydrostatic Test Data for Nominal 3.33-Inch (D_i) - 5.00-Inch (D_o) Flat Acrylic Windows, Test Specimens 116 - 120

(Sealed with grease; radial clearance 0.005 to 0.010 inch; nominal D_o/D_i ratio 1.5)

Parameter	Specimen Number					Value		
	116	117	118	119	120	Max	Avg	Min
Thickness (in.)	2.000	1.991	1.995	1.996	2.008	2.008	1.998	1.991
D_o (actual, in.)	4.993	4.987	4.988	4.987	4.990	4.993	4.989	4.987
Temperature (°F)	65	66	66	66	66	66	66	65
t/D_i Ratio (actual)	0.600	0.598	0.599	0.599	0.602	0.602	0.600	0.598
Pressurization Rate (psi/min)	662	660	665	663	664	665	663	660
Pressure (psi)	Axial Displacement of Center Point on Window's Low-Pressure Face (in.)							
1,000	0.001	0.001	0.004	0.001	0.001	0.004	0.002	0.001
2,000	0.010	0.002	0.013	0.001	0.011	0.013	0.007	0.001
3,000	0.021	0.010	0.022	0.012	0.018	0.022	0.017	0.010
4,000	0.025	0.018	0.030	0.019	0.026	0.030	0.024	0.018
5,000	0.033	0.026	0.037	0.026	0.033	0.037	0.031	0.026
6,000	0.040	0.033	0.044	0.033	0.041	0.044	0.038	0.033
7,000	0.046	0.040	0.052	0.041	0.048	0.052	0.045	0.040
8,000	0.052	0.050	0.059	0.048	0.056	0.059	0.053	0.048
9,000	0.067	0.057	0.066	0.056	0.064	0.067	0.062	0.056
10,000	0.073	0.066	0.074	0.064	0.072	0.074	0.070	0.064
11,000	0.083	0.075	0.083	0.073	0.080	0.083	0.079	0.073
12,000	0.091	0.083	0.092	0.083	0.090	0.092	0.088	0.083
13,000	0.101	0.092	0.101	0.091	0.098	0.101	0.097	0.091
14,000	0.114	0.103	0.111	0.101	0.109	0.114	0.108	0.103
15,000	0.127	0.114	0.122	0.115	0.119	0.127	0.119	0.114
16,000	0.137	0.125	0.132	0.128	0.135	0.137	0.131	0.125
17,000	1/	0.137	0.146	0.140	0.148	0.148	0.143	0.137
18,000		0.152	0.160	0.156	0.161	0.161	0.157	0.152
19,000		0.170	0.177	0.171	0.181	0.181	0.175	0.170
20,000		0.197	0.192	0.191	0.198	0.198	0.195	0.191
21,000		0.221	0.223	0.208	0.220	0.223	0.218	0.208
22,000		0.248	0.252	0.251	0.253	0.253	0.251	0.248
23,000		0.288	0.292	0.294	0.301	0.301	0.294	0.288
24,000			0.380					
Displacement at Failure (in.)		0.359	0.395	0.360	0.326	0.395	0.380	0.326
Extrusion Set (in.)	0.010	0.068 2/			0.076 2/			
Pressure at Failure (psi)		23,900	24,150	23,650	23,450	24,150	24,050	23,450

1/ Abort at 16,250 psi due to pump failure.
2/ Extrusion and bending caused seal to fail, release of pressure.

Note: 1,000-psi preload; smooth deflections.

Table C-25. Hydrostatic Test Data for Nominal 4.00-Inch (D_i) - 6.00-Inch (D_o) Flat Acrylic Windows, Test Specimens 121 - 125

(Sealed with grease; radial clearance 0.005 to 0.010 inch; nominal D_o/D_i ratio 1.5)

Parameter	Specimen Number					Value		
	121	122	123	124	125	Max	Avg	Min
Thickness (in.)	0.236	0.235	0.228	0.231	0.235	0.236	0.233	0.228
D_o (actual, in.)	5.987	5.989	5.988	5.985	5.987	5.989	5.987	5.985
Temperature (°F)	68	69	69	69	69	69	69	68
t/D_i Ratio (actual)	0.059	0.059	0.057	0.058	0.059	0.059	0.058	0.057
Pressurization Rate (psi/min)	157	400	673	425	391	673	409	157
Pressure (psi)	Axial Displacement of Center Point on Window's Low-Pressure Face (in.)							
50	0.084	0.129	0.108	0.111	0.128	0.129	0.112	0.084
100		0.186		0.155	0.160	0.186	0.167	0.155
150	0.174			0.192	0.208	0.208	0.192	0.174
200			0.283		0.240	0.283	0.261	0.240
250					0.270			
300			0.332		0.300	0.332	0.316	0.300
350			0.390		0.320	0.390	0.355	0.320
Displacement at Failure (in.)	0.200	0.186	0.422			0.422	0.269	0.186
Pressure at Failure (psi)	190	100	350	170	360	360	234	100

Notes:

1. Pressurization rate hard to hold due to pumping gage lag and air in line.
2. Reading difficult to make at close intervals.

Table C-26. Hydrostatic Test Data for Nominal 4.00-Inch (D_i) - 6.00-Inch (D_o) Flat Acrylic Windows, Test Specimens 126 - 130

(Sealed with grease; radial clearance 0.005 to 0.010 inch; nominal D_o/D_i ratio 1.5)

Parameter	Specimen Number					Value		
	126	127	128	129	130	Max	Avg	Min
Thickness (in.)	0.451	0.484	0.460	0.463	0.460	0.484	0.464	0.451
D_o (actual, in.)	5.988	5.984	5.989	5.990	5.987	5.990	5.988	5.984
Temperature (°F)	68	68	68	68	65	68	67	65
t/D_i Ratio (actual)	0.106	0.121	0.108	0.108	0.107	0.121	0.110	0.106
Pressurization Rate (psi/min)	689	657	638	669	737	737	678	637
Pressure (psi)	Axial Displacement of Center Point on Window's Low-Pressure Face (in.)							
100				0.022	0.017			
200	0.015	0.010	0.028	0.028	0.027	0.028	0.022	0.010
300	0.029			0.038	0.034			
400	0.038	0.032	0.050	0.048	0.044	0.050	0.042	0.032
500	0.049			0.058	0.060			
600	0.060	0.053	0.075	0.070	0.073	0.075	0.068	0.053
700				0.082	0.090			
800	0.090	0.078	0.096	0.096		0.096	0.090	0.078
900				0.108				
1,000		0.109		0.131				
1,100				0.151				
Displacement at Failure (in.)				0.157	0.090			
Pressure at Failure (psi)	910	1,030	940	1,170	700	1,170	950	700

Note: 50-psi preload.

Table C-27. Hydrostatic Test Data for Nominal 4.00-Inch (D_i) - 6.00-Inch (D_o) Flat Acrylic Windows, Test Specimens 131 - 135

(Sealed with grease; radial clearance 0.005 to 0.010 inch; nominal D_o/D_i ratio 1.5)

Parameter	Specimen Number					Value		
	131	132	133	134	135	Max	Avg	Min
Thickness (in.)	0.957	0.972	0.957	0.976	0.963	0.976	0.965	0.957
D_o (actual, in.)	5.986	5.981	5.984	5.980	5.985	5.986	5.984	5.980
Temperature (°F)	64	65	65	65	66	66	65	64
t/D_i Ratio (actual)	0.239	0.243	0.239	0.244	0.241	0.244	0.241	0.239
Pressurization Rate (psi/min)	651	725	652	685	698	725	682	651
Pressure (psi)	Axial Displacement of Center Point on Window's Low-Pressure Face (in.)							
500	0.009	0.002	0.006	0.014	0.030	0.030	0.012	0.002
1,000	0.023	0.016	0.019	0.026	0.044	0.044	0.026	0.016
1,500	0.036	0.034	0.037	0.051	0.057	0.057	0.042	0.031
2,000	0.048	0.047	0.042	0.062	0.063	0.063	0.052	0.042
2,500	0.060	0.058	0.057	0.076	0.078	0.078	0.066	0.057
3,000	0.105		0.070	0.091	0.092	0.105	0.090	0.070
3,500	0.137				0.106			
Displacement at Failure (in.)		0.068	0.150	0.101	0.106	0.150	0.106	0.068
Pressure at Failure (psi)	3,550	2,900	3,100	3,800	3,500	3,800	3,370	2,900

Notes:

1. 50-psi preload.
2. Audible cracking at about 2,500 psi.

Table C-28. Hydrostatic Test Data for Nominal 4.00-Inch (D_i) - 6.00-Inch (D_o) Flat Acrylic Windows, Test Specimens 136 - 140

(Sealed with grease; radial clearance 0.005 to 0.010 inch; nominal D_o/D_i ratio 1.5)

Parameter	Specimen Number					Value		
	136 1/	137	138	139	140	Max	Avg	Min
Thickness (in.)	2.144 1/	1.989	1.997	1.984	1.986	1.997	1.989	1.984
D_o (actual, in.)	5.985 1/	5.984	5.981	5.982	5.982	5.984	5.982	5.981
Temperature (°F)	66 1/	68	67	68	67	68	67	67
t/D_i Ratio (actual)	0.536 1/	0.498	0.500	0.496	0.496	0.500	0.498	0.496
Pressurization Rate (psi/min)	668 1/	663	674	668	678	678	668	663
Pressure (psi)	Axial Displacement of Center Point on Window's Low-Pressure Face (in.)							
1,000	0.009	0.009	0.002	0.001	0.002	0.009	0.005	0.001
2,000	0.018	0.018	0.015	0.012	0.017	0.018	0.016	0.012
3,000	0.027	0.024	0.021	0.028	0.030	0.030	0.026	0.021
4,000	0.041	0.038	0.035	0.037	0.040	0.041	0.038	0.035
5,000	0.046	0.046	0.044	0.045	0.051	0.051	0.046	0.044
6,000	0.055	0.055	0.052	0.055	0.057	0.057	0.055	0.052
7,000	0.067	0.070	0.060	0.070	0.071	0.071	0.068	0.060
8,000	0.083	0.080	0.073	0.081	0.081	0.083	0.080	0.073
9,000	0.095	0.094	0.084	0.090	0.092	0.095	0.091	0.084
10,000	0.107	0.110	0.095	0.103	0.106	0.110	0.104	0.095
11,000	0.122	0.120	0.130	0,121	0.118	0.130	0.122	0.118
12,000	0.135	0.136	0.142	0.136	0.131	0.142	0.136	0.131
13,000	0.155	2/	0.164	2/	0.152	0.164	0.157	0.152
14,000	0.170		0.183		0.173	0.183	0.175	0.170
15,000	0.205		0.213		0.191	0.213	0.203	0.191
16,000	2/		0.238		0.216	0.238	0.227	0.216
17,000			0.280		2/			
18,000			0.350					
Displacement at Failure (in.)			0.427					
Pressure at Failure (psi)	19,550	18,350	18,700	18,100	17,800	18,700	18,240	17,800

1/ Not averaged because of thickness variation.
2/ Deflection post popped off suddenly.

Note: Audible cracking at about 13,000 and 15,000 psi.

REFERENCES

1. U. S. Naval Civil Engineering Laboratory. Technical Report R-512: Windows for external or internal hydrostatic pressure vessels: Part I. Conical acrylic windows under short-term pressure application, by J. D. Stachiw and K. O. Gray. Port Hueneme, Calif., Jan. 1967.

2. C. E. Bodey. Private communication concerning pressure effects on Plexiglas circular discs. Autonetics Division, North American Aviation, Anaheim, Calif., Apr. 22, 1965.

3. Rohm and Haas Company. Plexiglas handbook for aircraft engineers, 2nd ed. Philadelphia, Pa., 1952.

4. U. S. Naval Civil Engineering Laboratory. Technical Note N-755: The conversion of 16-inch projectiles to pressure vessels, by K. O. Gray and J. D. Stachiw. Port Hueneme, Calif., June 1965.

U. S. Naval Civil Engineering Laboratory
WINDOWS FOR EXTERNAL OR INTERNAL HYDROSTATIC PRESSURE VESSELS — PART II. Flat Acrylic Windows Under Short-Term Pressure Application, by J. D. Stachiw, G. M. Dunn, and K. O. Gray
TR-527 77 p. illus May 1967 Unclassified

1. Flat acrylic windows — Hydrostatic pressure tests I. Y-F015-01-07-001

Flat, disk-shaped acrylic windows of different thickness-to-diameter ratios have been tested to destruction under short-term hydrostatic loading at room temperatures, where short-term loading is defined as pressurizing the window hydrostatically on its high-pressure face at a 650-psi/minute rate till failure of the window takes place. Critical pressures and displacements of windows with thickness to effective diameter ratios less than 1.0 have been recorded and plotted. The critical pressures derived from testing flat windows in flanges with 1.5-inch, 3.3-inch, and 4.0-inch openings have been found applicable also to flanges with larger openings, so long as the larger windows are of the same t/D_i and D_o/D_i ratios, where t is thickness of the window, D_i is the clear opening in the flange and therefore the effective diameter of the window exposed to ambient atmospheric pressure and D_o is overall diameter of the window face exposed to hydrostatic pressure. The performance of flat windows under short-term hydrostatic pressure has been found to be comparable to that of conical windows with included angle equal to, or larger than 90 degrees.

U. S. Naval Civil Engineering Laboratory
WINDOWS FOR EXTERNAL OR INTERNAL HYDROSTATIC PRESSURE VESSELS — PART II. Flat Acrylic Windows Under Short-Term Pressure Application, by J. D. Stachiw, G. M. Dunn, and K. O. Gray
TR-527 77 p. illus May 1967 Unclassified

1. Flat acrylic windows — Hydrostatic pressure tests I. Y-F015-01-07-001

Flat, disk-shaped acrylic windows of different thickness-to-diameter ratios have been tested to destruction under short-term hydrostatic loading at room temperatures, where short-term loading is defined as pressurizing the window hydrostatically on its high-pressure face at a 650-psi/minute rate till failure of the window takes place. Critical pressures and displacements of windows with thickness to effective diameter ratios less than 1.0 have been recorded and plotted. The critical pressures derived from testing flat windows in flanges with 1.5-inch, 3.3-inch, and 4.0-inch openings have been found applicable also to flanges with larger openings, so long as the larger windows are of the same t/D_i and D_o/D_i ratios, where t is thickness of the window, D_i is the clear opening in the flange and therefore the effective diameter of the window exposed to ambient atmospheric pressure and D_o is overall diameter of the window face exposed to hydrostatic pressure. The performance of flat windows under short-term hydrostatic pressure has been found to be comparable to that of conical windows with included angle equal to, or larger than 90 degrees.

U. S. Naval Civil Engineering Laboratory
WINDOWS FOR EXTERNAL OR INTERNAL HYDROSTATIC PRESSURE VESSELS — PART II. Flat Acrylic Windows Under Short-Term Pressure Application, by J. D. Stachiw, G. M. Dunn, and K. O. Gray
TR-527 77 p. illus May 1967 Unclassified

1. Flat acrylic windows — Hydrostatic pressure tests I. Y-F015-01-07-001

Flat, disk-shaped acrylic windows of different thickness-to-diameter ratios have been tested to destruction under short-term hydrostatic loading at room temperatures, where short-term loading is defined as pressurizing the window hydrostatically on its high-pressure face at a 650-psi/minute rate till failure of the window takes place. Critical pressures and displacements of windows with thickness to effective diameter ratios less than 1.0 have been recorded and plotted. The critical pressures derived from testing flat windows in flanges with 1.5-inch, 3.3-inch, and 4.0-inch openings have been found applicable also to flanges with larger openings, so long as the larger windows are of the same t/D_i and D_o/D_i ratios, where t is thickness of the window, D_i is the clear opening in the flange and therefore the effective diameter of the window exposed to ambient atmospheric pressure and D_o is overall diameter of the window face exposed to hydrostatic pressure. The performance of flat windows under short-term hydrostatic pressure has been found to be comparable to that of conical windows with included angle equal to, or larger than 90 degrees.

U. S. Naval Civil Engineering Laboratory
WINDOWS FOR EXTERNAL OR INTERNAL HYDROSTATIC PRESSURE VESSELS — PART II. Flat Acrylic Windows Under Short-Term Pressure Application, by J. D. Stachiw, G. M. Dunn, and K. O. Gray
TR-527 77 p. illus May 1967 Unclassified

1. Flat acrylic windows — Hydrostatic pressure tests I. Y-F015-01-07-001

Flat, disk-shaped acrylic windows of different thickness-to-diameter ratios have been tested to destruction under short-term hydrostatic loading at room temperatures, where short-term loading is defined as pressurizing the window hydrostatically on its high-pressure face at a 650-psi/minute rate till failure of the window takes place. Critical pressures and displacements of windows with thickness to effective diameter ratios less than 1.0 have been recorded and plotted. The critical pressures derived from testing flat windows in flanges with 1.5-inch, 3.3-inch, and 4.0-inch openings have been found applicable also to flanges with larger openings, so long as the larger windows are of the same t/D_i and D_o/D_i ratios, where t is thickness of the window, D_i is the clear opening in the flange and therefore the effective diameter of the window exposed to ambient atmospheric pressure and D_o is overall diameter of the window face exposed to hydrostatic pressure. The performance of flat windows under short-term hydrostatic pressure has been found to be comparable to that of conical windows with included angle equal to, or larger than 90 degrees.

Unclassified

Security Classification

DOCUMENT CONTROL DATA - R & D

(Security classification of title, body of abstract and indexing annotation must be entered when the overall report is classified)

1 ORIGINATING ACTIVITY *(Corporate author)*

Naval Civil Engineering Laboratory
Port Hueneme, California 93041

2a. REPORT SECURITY CLASSIFICATION

Unclassified

2b GROUP

3. REPORT TITLE

WINDOWS FOR EXTERNAL OR INTERNAL HYDROSTATIC PRESSURE VESSELS – PART II.
Flat Acrylic Windows Under Short-Term Pressure Application

4. DESCRIPTIVE NOTES *(Type of report and inclusive dates)*

Not final, January 1, 1966 to June 30, 1966

5. AUTHOR(S) *(First name, middle initial, last name)*

Stachiw, J. D.
Dunn, G. M.
Gray, K. O.

6. REPORT DATE	7a. TOTAL NO OF PAGES	7b. NO OF REFS
May 1967	77	4

8a. CONTRACT OR GRANT NO	9a. ORIGINATOR'S REPORT NUMBER(S)
b. PROJECT NO. Y-F015-01-07-001	TR-527
c.	9b. OTHER REPORT NO(S) *(Any other numbers that may be assigned this report)*
d.	

10. DISTRIBUTION STATEMENT

Distribution of this report is unlimited. Copies available at the Clearinghouse for Federal Scientific & Technical Information (CFSTI), Sills Building, 5285 Port Royal Road, Springfield, Va. 22151 – Price $3.00

11. SUPPLEMENTARY NOTES	12. SPONSORING MILITARY ACTIVITY
	Naval Facilities Engineering Command

13. ABSTRACT

Flat, disk-shaped acrylic windows of different thickness-to-diameter ratios have been tested to destruction under short-term hydrostatic loading at room temperatures, where short-term loading is defined as pressurizing the window hydrostatically on its high-pressure face at a 650-psi/minute rate till failure of the window takes place. Critical pressures and displacements of windows with thickness to effective diameter ratios less than 1.0 have been recorded and plotted. The critical pressures derived from testing flat windows in flanges with 1.5-inch, 3.3-inch, and 4.0-inch openings have been found applicable also to flanges with larger openings, so long as the larger windows are of the same t/D_i and D_o/D_i ratios, where t is thickness of the window, D_i is the clear opening in the flange and therefore the effective diameter of the window exposed to ambient atmospheric pressure and D_o is overall diameter of the window face exposed to hydrostatic pressure. The performance of flat windows under short-term hydrostatic pressure has been found to be comparable to that of conical windows with included angle equal to, or larger than 90 degrees.

DD FORM 1 NOV 65 1473 (PAGE 1)

S/N 0101-807-6801

Unclassified

Security Classification

14 KEY WORDS	LINK A		LINK B		LINK C	
	ROLE	WT	ROLE	WT	ROLE	WT
Undersea structures						
Flat acrylic windows						
Hydrostatic pressure						
Short-term loading						

R631

Technical Report

WINDOWS FOR EXTERNAL OR INTERNAL HYDROSTATIC PRESSURE VESSELS—PART III.

Critical Pressure of Acrylic Spherical Shell Windows Under Short-Term Pressure Applications

June 1969

Sponsored by

NAVAL FACILITIES ENGINEERING COMMAND

NAVAL CIVIL ENGINEERING LABORATORY

Port Hueneme, California

WINDOWS FOR EXTERNAL OR INTERNAL HYDROSTATIC PRESSURE VESSELS—PART III. Critical Pressure of Acrylic Spherical Shell Windows Under Short-Term Pressure Applications

Technical Report R-631

YF 38.535.005.01.005

by

J. D. Stachiw and F. W. Brier

ABSTRACT

Model and full-scale acrylic windows in the form of spherical shell lenses with parallel convex and concave surfaces have been imploded by loading their convex surface hydrostatically at a 650-psi/min rate while their concave surface was exposed to atmospheric pressure. The thickness of the model windows varied from 0.250 to 1.200 inches and of the full-scale windows from 0.564 to 4.000 inches, while the included spherical sector angle of the lens and the bevel angle of its edge varied from 30 to 180 degrees in 30-degree increments. The low-pressure face diameters of the model windows varied from 1.423 to 5.500 inches, while those of the full-scale windows varied from 6.200 to 35.868 inches. In addition to critical pressures, displacements of the lens under hydrostatic pressure were recorded and plotted as functions of pressure.

CONTENTS

STATEMENT OF THE PROBLEM

Underwater vehicles, ocean bottom habitats, and instrumentation capsules frequently require optically transparent windows for the observation of hydrospace in which their mission is performed. Since the windows must withstand a large pressure differential between the atmospheric interior of the pressure hull and the hydrospace outside, high stresses are generated in them. To keep these stresses low, the diameters of the deep-submergence hydrospace windows are generally small in comparison to their thickness, thus severely restricting the windows' field of view. To increase the field of view of deep-submergence windows without further increasing their thickness, exploratory studies are being conducted on various shapes of acrylic windows. To date, exploratory investigations on the effects of short-term hydrostatic loading* have been completed with truncated cone windows[1] with spherical sector angles of 30, 60, 90, 120, and 150 degrees, and with flat disc windows.[2] Previous to this study, no acrylic window shape has been found to possess higher resistance to hydrostatic pressure than the conical windows of same thickness and diameter.

It was thought that a regular spherical shell sector (hereafter referred to as spherical window) might be the configuration that would significantly increase the resistance of acrylic hydrospace windows to external hydrostatic pressure. This report describes the experimental study of spherical windows under short-term hydrostatic loading conducted by the Naval Civil Engineering Laboratory as part of the Ocean Engineering Program sponsored by the Naval Facilities Engineering Command.

OBJECTIVES

1. To establish experimentally the relationship between a window's critical pressure and the ratio of its thickness to the diameter of its low-pressure face.

2. To establish experimentally the relationship between a window's critical pressure and the ratio of its thickness to the spherical radius of its concave surface.

---

* Pressurization of the window's convex surface with water at 650-psi/minute rate.

3. To establish experimentally the relationship between a window's critical pressure and the spherical sector angle for each ratio of thickness to concave surface spherical radius.

4. To establish experimentally the relationship between hydrostatic loading on the windows and their displacement in the flange as a function of spherical sector angles (α), t/D_i, and t/R_i ratios.*

PURPOSE

This experimental study will serve the following purposes: .

1. The critical pressures established for spherical windows will serve as basis of comparison for the selection of deep-submergence window shapes, as the data will complement studies already completed on conical and flat acrylic windows under short-term hydrostatic loading.

2. The empirical data will serve as a guide for designing spherical windows subjected to short-term hydrostatic loading.

3. The experimentally determined resistance to implosion of spherical windows under short-term loading can be used as base reference in future studies on long-term or cyclic pressure loadings of spherical windows.

SCOPE OF INVESTIGATION

The investigation of spherical acrylic windows under short-term loading utilized model test specimens with $0.090 \leqslant t/R_i \leqslant 0.436$ and spherical sector angles 30 degrees $\leqslant \alpha \leqslant$ 180 degrees. The concave surface spherical radius for all model scale windows was 2.750 inches except in the few cases in which full-scale windows with 6.200-, 29.000-, 30.500-inch concave radii were used to check the proposed nondimensional scaling factors for acrylic windows.

The main experimental investigation of spherical acrylic windows under short-term loading was limited to determining the critical pressure of such windows and the axial displacement of the windows through the conical flange under hydrostatic pressure applied to the windows' convex surface. In a few tests diametral contraction of the windows was also measured.

---

* See foldout for definition of terms.

BACKGROUND DISCUSSION

The investigation of spherical acrylic windows is an extension of studies performed in previous years at the Naval Civil Engineering Laboratory. The earlier studies concerned conical or flat windows, and with spherical acrylic hulls for underwater vehicles.[3] When the critical pressures of flat or conical acrylic windows under short-term hydrostatic loading were compared to the critical pressures of spherical acrylic hulls (Figure 1), also under short-term loading, it was found that the critical pressure of the spherical shape is several magnitudes higher. To some extent this was not an accurate comparison as the flat or conical windows rest on rigidly fixed steel flanges, while the spherical hull is not subjected to this boundary condition. Still, there were indications that if a portion of the spherical hull was equipped with a steel end closure the gain in the pressure resistance over a flat or conical window of the same low-pressure face diameter could be on the order of 100%, or higher. The probability of such a gain in pressure resistance justified the initiation of an experimental study into the behavior of spherical windows under hydrostatic loading. The first phase of this study, as with the studies of conical and flat acrylic windows, deals with the strength of spherical windows under short-term hydrostatic loading.

EXPERIMENT DESIGN

To meet the objectives of the study, three dimensional parameters of the model test specimens (Figure 2) were varied while the response of the window in the form of its displacement and critical pressure were noted. The three dimensional parameters varied were the thickness of the window, the spherical sector angle, and the diameter of the window's low-pressure face. The only dimensional parameter held constant for the model windows was the spherical radius of the window's concave surface. It was postulated that by providing seven variations in the thickness parameter of the windows, six variations in the spherical sector angle parameter, and six variations in their low-pressure face diameter parameter, sufficient variations would be introduced into the critical pressure response of the windows to determine what combination of dimensional parameter values results in a spherical window with optimized critical pressure response. Since the configuration of the steel window flange seat also has considerable influence on the critical pressure of hydrospace windows, all of the flanges were conceived to give equal amount of support to the seating surfaces of all the spherical windows tested (Figure 3).

Figure 1. Pressure-resistant spherical acrylic hull, 15-inch OD and 13-inch ID, whose critical pressure (5,000 psi) was used as standard for comparing the performance of spherical acrylic windows with different geometries.

In addition to the main experimental study dealing with the short-term critical pressure of model spherical windows, several subordinate investigations were also performed. The objective of these investigations was to clarify, or at least explore, some of the questions which impinge on the evaluation of main study test results. Thus, for example, one of the questions that had to be answered before the data generated in the main study could be applied to the design of full-scale hydrospace windows was: what is the influence of stress-loading rates on strain rates of acrylic plastic? (See Appendix A.) Other subjects to which the subordinate investigations addressed themselves were isotropy of mechanical properties in commercial acrylic plate (Appendix B), influence of temperature on short-term critical pressure of spherical windows (Appendix C), the optical properties of spherical windows (Appendix D), applicability of the test results obtained with model windows to operational full-scale windows (Appendix E), effect of stress raisers on critical pressure of spherical windows (Appendix F), behavior of spherical windows under constant pressure (Appendix G), and design of spherical window and flange systems for operational use (Appendix H). The tabulated data for the short-term pressurization tests are presented in Appendix I.

Parameters varied

α = 30, 60, 90, 120, 150, 180 degrees
t = 0.250, 0.375, 0.500, 0.625, 0.750, 1.000, 1.200 inches
D_i = 1.423, 2.750, 3.889, 4.763, 5.312, 5.500 inches

Parameters held constant

R_i = 2.750 inches
Bearing surface perpendicular to high- and low-pressure faces.

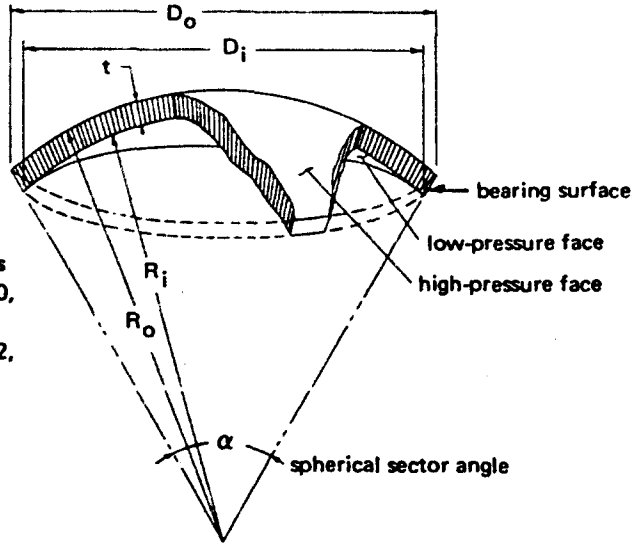

Figure 2. Dimensional parameters of model spherical window specimen test series.

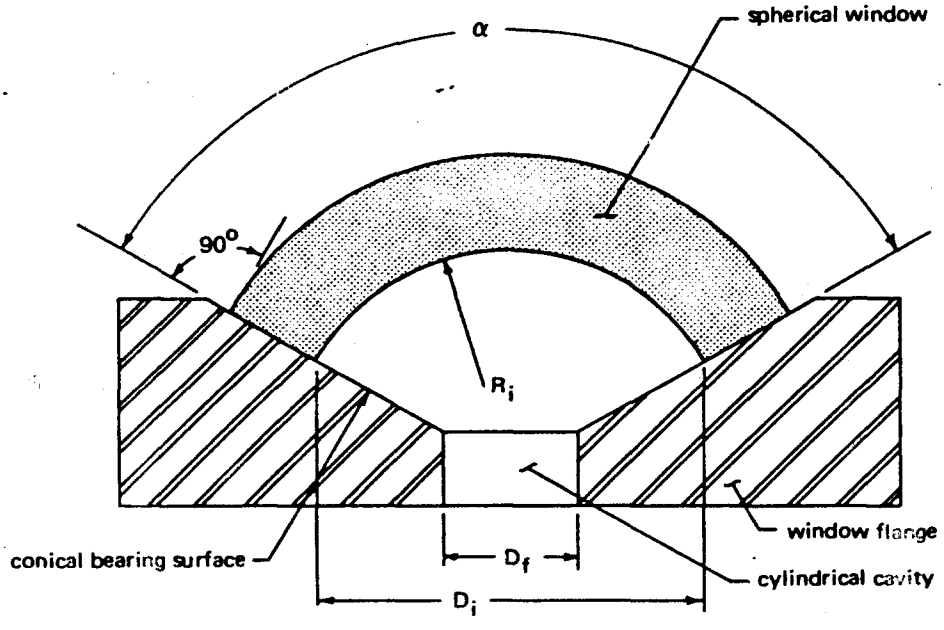

$D_i - D_f$ = constant for all spherical bevel angles (α)

$D_i - D_f = 0.2\ R_i$

Figure 3. DOL Type IV flange design for spherical windows.

Window Test Specimens

The model specimens (Figures 2 through 5) were fabricated from 4-inch-thick acrylic plates by sawing the plates into small blocks, which subsequently were turned in a lathe. The material used was commercial quality grade "G" Plexiglas, the physical properties of which are described in Appendixes A, B, and H. This off-the-shelf standard acrylic material was chosen with the designer in mind, permitting him to specify and easily procure fairly inexpensive stock for his own experimentation, or fabrication of operational full-scale windows.

All of the window specimens were machined first to within 0.125 inch of finished dimensions and then annealed according to time schedule recommended by the supplier (Table 1). During annealing, the windows were supported in such a manner that no stresses were induced in them by sagging of material. After annealing, the specimens were machined to required dimensional tolerances (Figure 6) and all surfaces were finished to a 32-rms finish; for some selected specimens the high- and low-pressure faces were subsequently polished to an optical finish.

Table 1. Annealing Specifications for Acrylic Windows

(Annealing temperature, 175°F.)

Window Thickness (in.)	Heating Time (hr)	Cooling-Off Periods	
		Maximum Cooling Rate (°F/hr)	Time (hr)
1/4	10-1/2	49	1/2
1/2	11	25	3/4
3/4	11	25	3/4
1	11-1/2	18	1
4	22	5	5

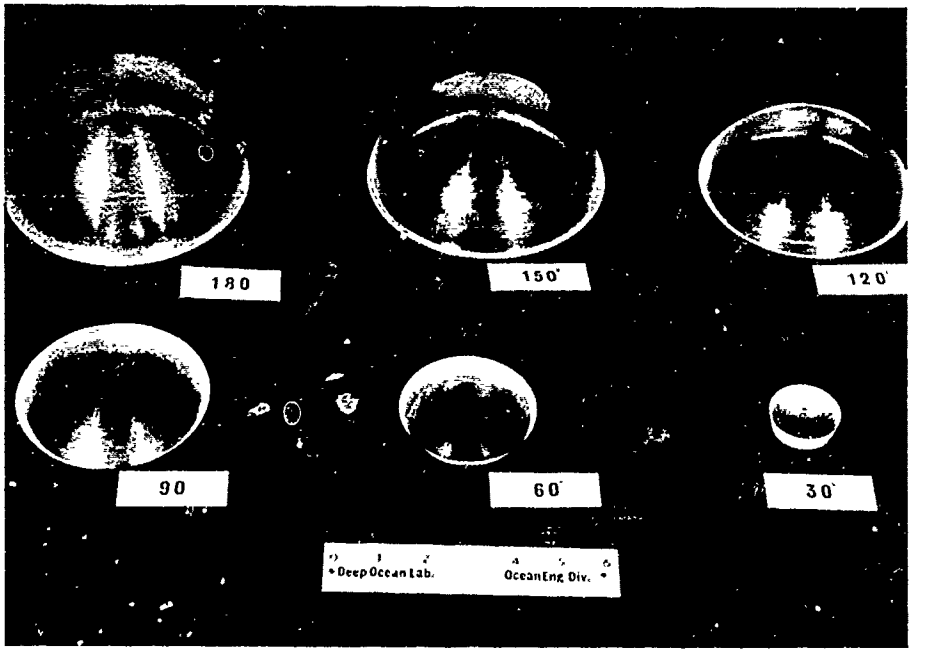

Figure 4. Convex high-pressure faces of typical model spherical acrylic windows with internal spherical radii of 2.750 inches.

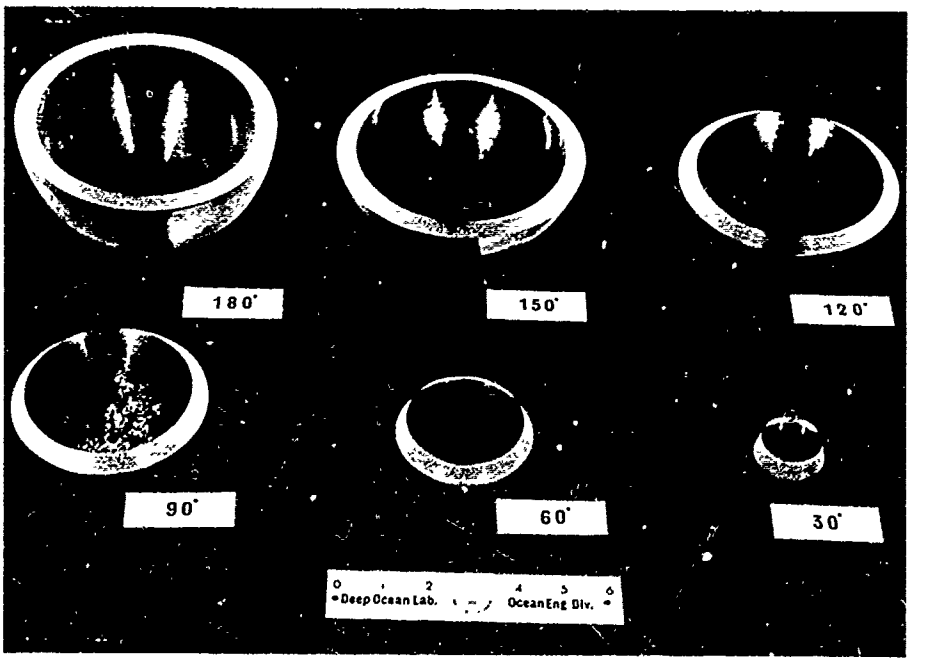

Figure 5. Concave low-pressure faces of typical model spherical acrylic windows with internal spherical radii of 2.750 inches.

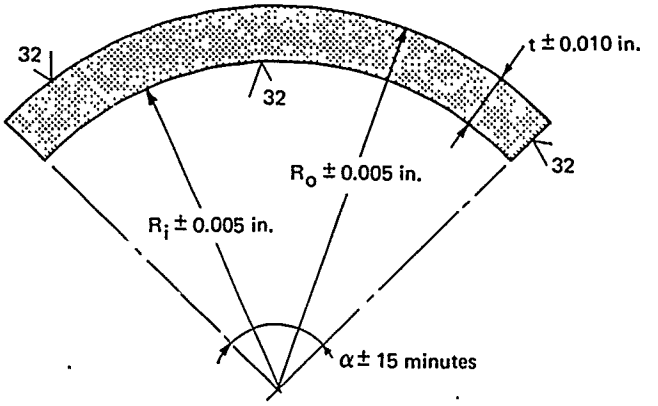

Spherical Sector Angle, α (deg)	Low-Pressure-Face Diameter, D_i (in.)	Nominal t/D_i Ratio at a Nominal Thickness (in.) of—						
		0.25	0.375	0.50	0.625	0.75	1.00	1.200
30	1.423	0.176	0.264	0.351	0.439	0.527	0.703	–
60	2.750	0.091	–	0.182	–	0.273	0.364	0.436
90	3.889	0.064	–	0.129	–	0.193	0.257	0.309
120	4.763	0.052	–	0.105	–	0.158	0.210	–
150	5.312	0.047	–	0.094	–	0.141	0.188	–
180	5.500	0.045	–	0.091	–	0.136	0.182	–
		Nominal t/R_i Ratio at a Nominal Thickness (in.) of—						
		0.25	0.375	0.50	0.625	0.75	1.00	1.200
For all angles	For all D_i	0.091	0.136	0.182	0.227	0.273	0.364	0.436

Figure 6. Geometry of model spherical acrylic window test specimens with R_i = 2.750 inches and $0.250 \leqslant t \leqslant 1.200$ inches.

Since the windows were machined from more than one plate of commercially available acrylic material, small variations were anticipated in the performance of windows under hydrostatic pressure. These small variations would be caused by minute differences in the manufacturing process of each individual plate, as well as due to differences in polymerization process from one point in the plate to another (Appendix B). These small variations in mechanical properties when combined with the variations in window dimensions defined by the allowable machining tolerances (Figure 6) were expected to result in a noticeable scatter of experimentally determined displacements and critical pressures of windows.

A designer utilizing this data can determine from the range of scatter what deviations of window strength may be expected when ordinary machine shop tolerances are used on grade "G" Plexiglas material received from various manufacturers. Knowing what deviations to expect from the average window strengths, he will be able to introduce an appropriate safety factor to account for such deviations.

Window Flanges

The model test specimens were mounted in metallic flanges (Figure 7) designed to fit into the standard end closure of the pressure vessel made available for this study. The pressure vessel employed for most of the tests was NCEL's Mk-I modification of the U. S. 16-inch naval gun shell[4] with an inside diameter of 9.45 inches. This diameter determined the choice of the 2.750-inch internal spherical radius for the model-scale series of window test specimens, since even the largest spherical acrylic window specimens in the model window series with R_o = 3.950 inches could be tested in the same vessel.

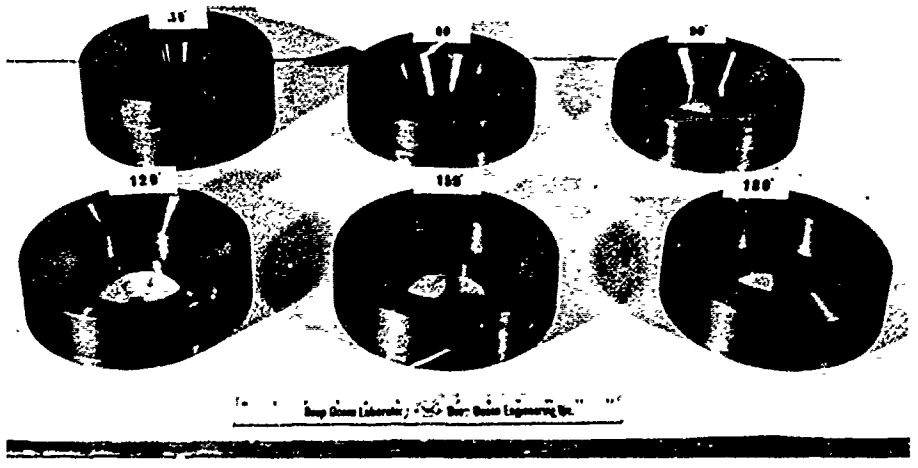

Figure 7. DOL Type IV steel flanges for testing model spherical acrylic windows.

The flanges, which were machined from mild steel, were of sufficient thickness to withstand all but minor deformation during application of hydrostatic pressure to the window specimens. In addition to the dimensional stability offered by the rigidity of the comparatively massive flange construction, the hydrostatic loading caused by surrounding fluid under pressure also acted on the flange to minimize its expansion from the wedging

action of the windows with small spherical sector angles. It can, therefore, be postulated that for all practical purposes the window flanges were rigid, and only the acrylic windows were deformed during testing.

For each of the six spherical sector angles a flange was provided with a matching conical bearing surface (Figure 8). To standardize all aspects of testing, each flange was provided with a cylindrical cavity of different diameter. The cylindrical cavity in each flange was so designed that the edge of the window's low-pressure surface would be positioned 0.275 inch from the edge of the cavity, measured radially and horizontally towards the vertical axis of the flange. The 0.275-inch distance was selected on the basis of calculations which indicated that this is the distance between the edge of the cylindrical cavity in the flange and edge of window required to give continuous bearing support to the thickest 180-degree sector angle window while its diameter decreased under hydrostatic pressure prior to failure. As the thickness of the windows tested varied, the high-pressure faces extended to different elevations in the flange cavity, while the low-pressure faces prior to testing always rested at the same distance from edge of cylindrical cavity in flange.

The same principle was followed in the design of flanges for large-scale spherical windows used for the verification of data gen rated with model windows (Appendix E).

INSTRUMENTATION

The instrumentation consisted of a thermometer, a series of pressure gages, and two displacement-measuring devices. The thermometer was used to measure with $1^{o}C$ accuracy the temperature of the water in contact with the convex face of the window in the vessel; the pressure gages measured with 10-psi accuracy the pressure of the water in the vessel, and the displacement measuring devices measured with an accuracy of 0.001 inch the displacement of the center and edge of the window low-pressure face as it extruded or deflected into the conical cavity of the flange.

The axial displacement measuring device consisted of 0.010-inch-diameter piano wire which had one end cemented to the window's low-pressure face by means of an acrylic anchor and the other end fastened to a weight which rested on a mechanical dial indicator (Figure 9). The edge displacement measuring device consisted of a strain-gaged wire ring connected to a strain-balancing and readout unit (Figure 10). The strain-gaged wire ring in conjunction with the strain-balancing and readout unit measured the decrease in the low-pressure face's diameter as the hydrostatic pressure forced the window to extrude through the conical cavity of

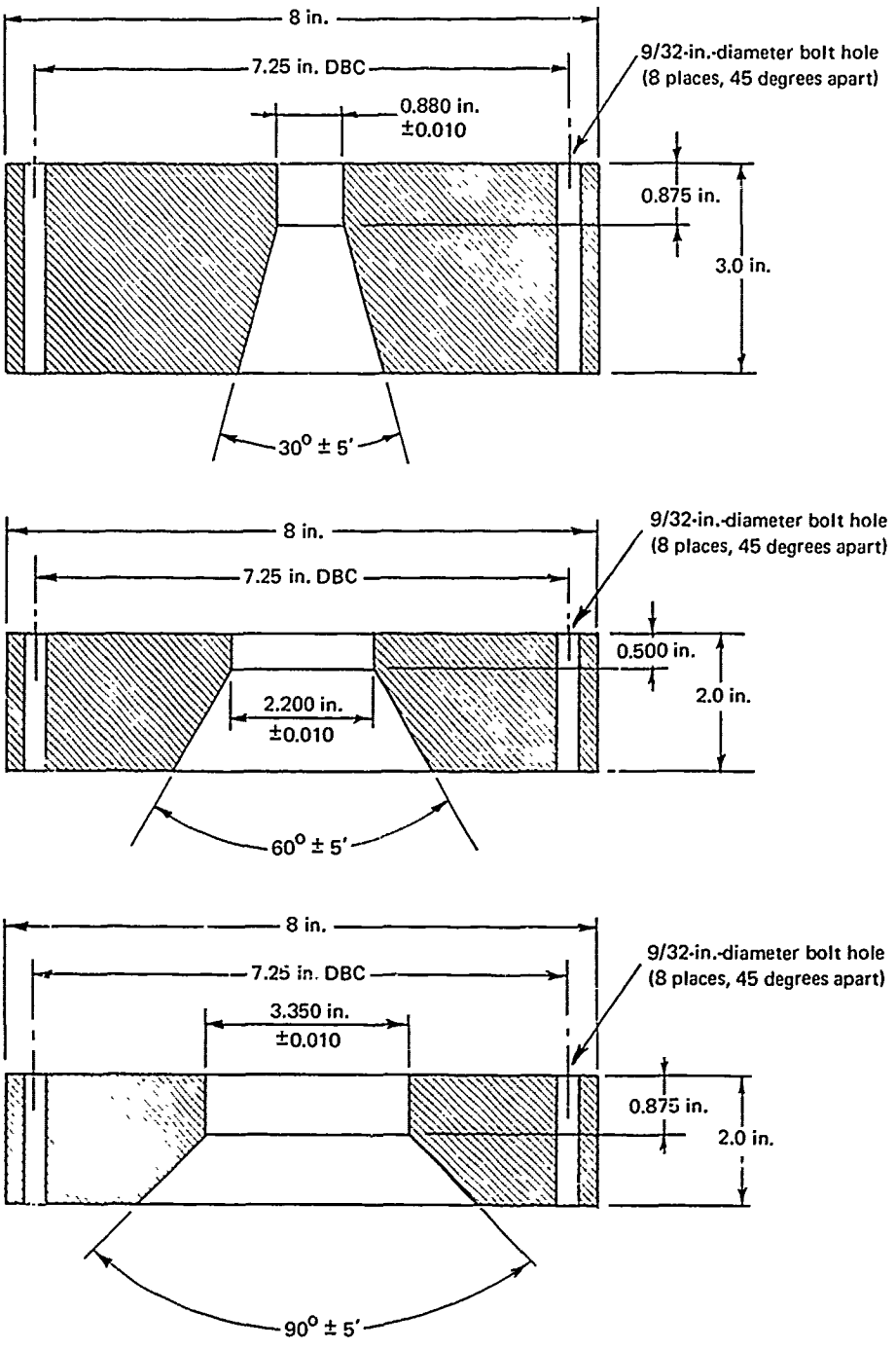

Figure 8. Geometry of DOL Type IV steel flanges for model windows with various spherical sector angles.

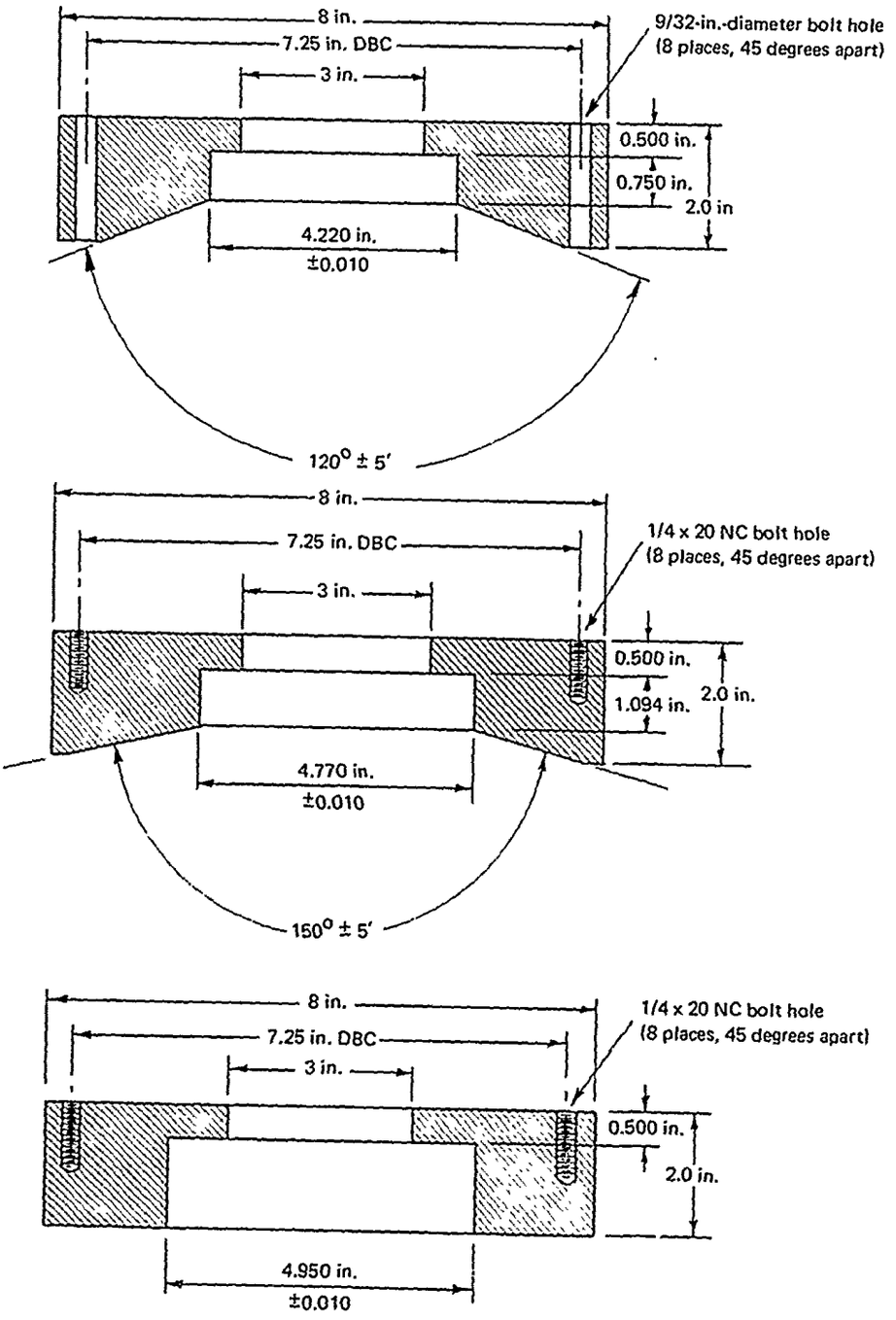

Figure 8. Continued.

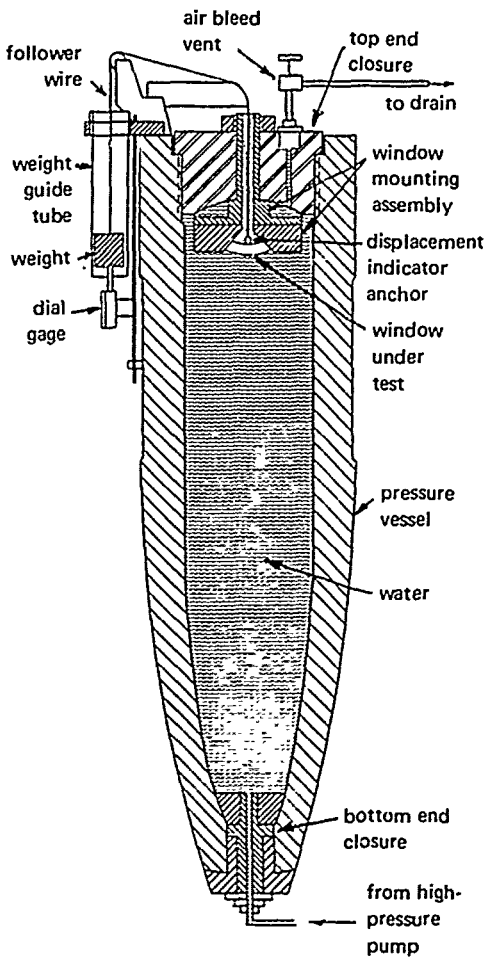

Figure 9. Device for measurement of axial displacement at the center of window's low-pressure face during hydrostatic pressurization.

the flange. The change in the low-pressure face's diameter was converted mathematically to sliding displacement of the windows circumferential edge. The strain gage was placed on the inside surface of the 0.045-inch-diameter spring wire ring to protect it from injury as the window extruded through the flange. The gage was then coated with a waterproofing agent to protect it from water which had been placed in the cavity to keep the strain gage at a constant temperature.

TEST PROCEDURE

The window flange with the appropriate spherical angle was placed on the flange adapter in the vessel end closure and was bolted in position. The window, to which the displacement indicator wire was already fastened by means of a small acrylic anchor piece cemented onto its low-pressure face, was coated with a thin film of silicone lubricant on its bearing surface and inserted into the mounting flange (Figure 11).

Rubber bands were used as retainers to keep the window from sliding or falling out of the flange. The steel wire connected to the acrylic anchor was then fastened to a dead weight of 1 pound. The wire was of such length that when it was positioned over pulleys and one end was centered over the window and the other over a dial indicator rod, the weight attached to that end came to rest on the dial indicator rod depressing it slightly. During the experiment the weight was kept from shifting on the dial indicator rod by a plastic guide tube and a recess on the bottom of the weight into which the indicator rod fitted (Figures 9 and 12).

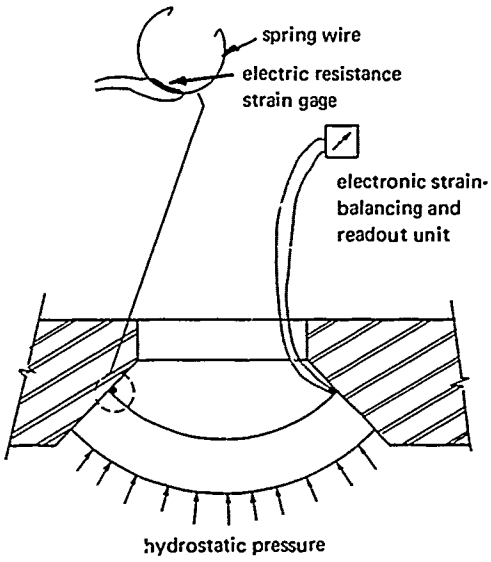

Figure 10. Device for measurement of window's sliding displacement on the bearing surface of steel flange.

To permit pressurization of the vessel, two entries were provided. The entry in the bottom end closure was used to admit the pressurizing fluid to the vessel, while the one in the top end closure served to remove entrapped air and to relieve the pressure in the vessel in case of test termination prior to window ejection. The pressure inside the vessel was monitored at all times with pressure gages connected by a 1/16-inch-OD tubing to a fitting in the main pressurizing manifold between the high-pressure pumping unit and the vessel. The use of such an extremely fine tubing ameliorated to a large degree the dynamic pressure surges in the hydraulic system at the instant of explosive window failure. Before pressurization began, the cylindrical cavity in the vessel end closure on the low-pressure side of the window was filled with water. This was done to keep the window temperature constant during the test and to lessen the shock wave created when the window failed. The pressurization of the vessel was accomplished by means of an air-driven pump.

Although different rates of pressurization were feasible, a pumping rate of 650 ± 50 psi/min was selected because previous window studies at NCEL have used that pressurization rate, and thus it has become accepted as a standard for short-term pressure tests at NCEL. The temperature of the pressurizing medium (freshwater) and of the vessel was maintained in the general range of 68°F to 72°F, although for some selected tests it was reduced to a range of 50°F to 52°F. The temperature readings were recorded before and after window failure to obtain an average reading.

The pressurization procedure varied, depending on the type of test. For the tests in which groups of five windows for each α and t/R_i were tested to failure, displacement readings were recorded at 1,000-psi intervals without interruption of the pressurization. The pressurization was continued until window failure occurred with an explosive release of compressed water and window fragments. Water and fragments were ejected high into the air through the cylindrical cavity in the end closure. To protect the operator of the pressurizing system from possible failure of the vessel, he as well as the monitoring equipment were separated from the test area by a massive

concrete block. For this reason the mechanical dial indicator readings were observed by means of a closed-circuit television system consisting of a television monitor (Figure 13) with the camera focused on the dial of the mechanical displacement indicator (Figure 12).

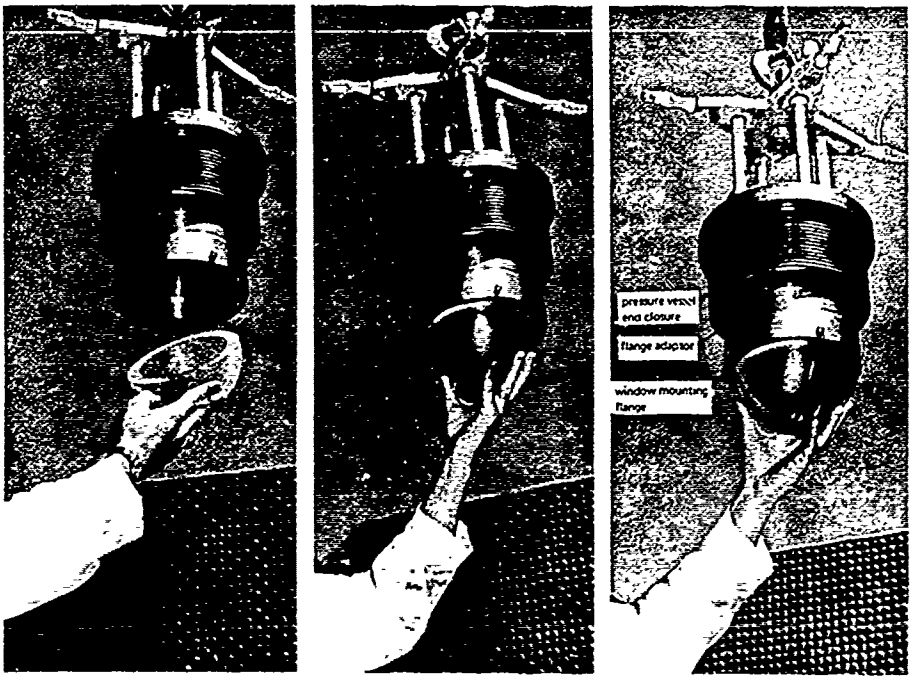

Figure 11. Steel flange for 180-degree spherical sector model windows attached to the end closure of pressure vessel.

For tests in which the diametral contraction of the low-pressure face was measured by means of the strain-gaged wire ring, the pressurization was terminated at 70% to 80% of critical pressure so that explosive failure of the window did not take place. The pressure was held for approximately 15 minutes before it was relieved through the air-bleed vent in the top end closure of the pressure vessel. By holding the pressure constant for 15 minutes, exploratory data was generated on the time-dependent displacement rates of spherical acrylic windows under sustained loading.

For this series of windows, a strain-gaged wire ring (Figure 10) was placed in the circumferential corner formed by the intersection of the low-pressure window face and the steel mounting flange, the leads were brought out of the vessel through the cylindrical cavity in the flange, and a strain-balancing and readout unit was hooked up to the leads.

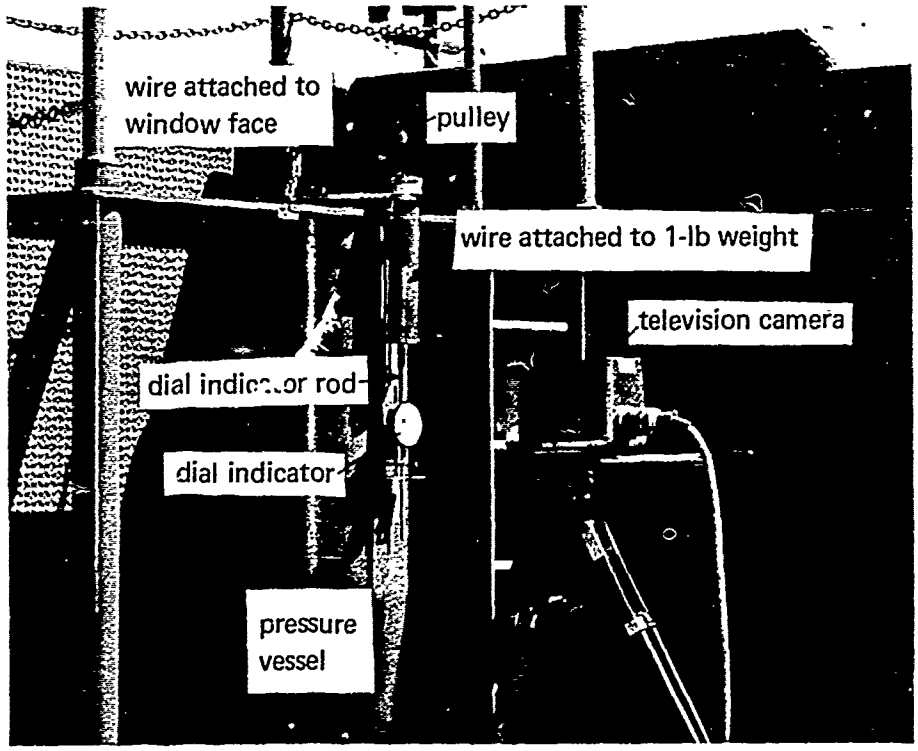

Figure 12. Window displacement monitoring setup.

As the window extruded through the flange, the diameter of the low-pressure face decreased, causing a decrease in the diameter of the wire ring and a change in the resistance of the strain gage. Each strain-gaged wire ring was precalibrated, allowing the resistance readings to be converted directly to magnitude of sliding displacement upon the conical flange seat surface.

TEST OBSERVATIONS

Modes of Failure

Not all model spherical windows tested under short-term pressure loading failed, as some of the windows were of such proportions that they could withstand 30,000 psi—the highest available pressure at the NCEL pressure test facility. The windows that did not fail at pressures less than 30,000 psi under short-term loading in this study were those with $t/D_i > 0.525$ and a spherical sector angle of 30 degrees. The only marks left on

these windows by the short-term pressurization to 30,000 psi were cracks on the bearing surface, a small extrusion plug on the low-pressure face (Figure 14), and cold-flow cratering on the high-pressure face (Figure 15).

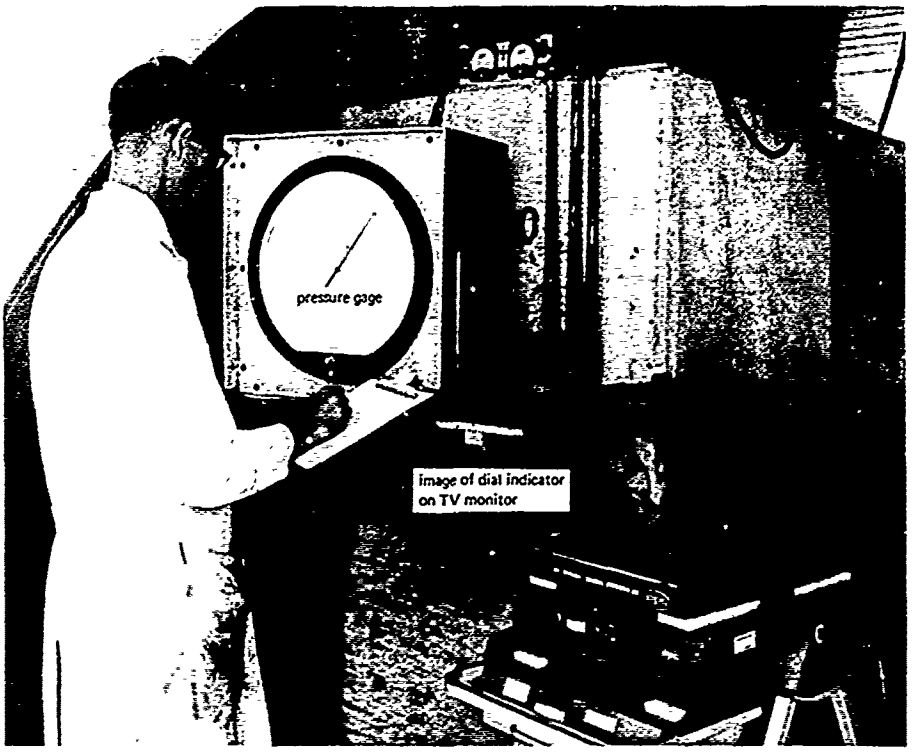

Figure 13. Control center for conducting window tests.

The windows that failed did so in one of two ways, the type of failure depending on the spherical sector angle and the t/D_i ratio of the window. One kind of failure was characterized by elastoplastic instability of the spherical window center as evidenced by formation of a local flat spot at the center of the window prior to failure. The failure occurred when either (1) the biaxial tensile flexural stress at the center of the low-pressure face generated by formation of a local flat spot or (2) the shear stress around the circumference of the flat spot exceeded by a sufficiently large margin the superimposed triaxial compressive stress field present in the window due to overall hydrostatic loading of the spherical window shape. Since the flat spot generally formed at the center of the window, and since its extent was rather limited, the fracture of the window took place in the form of a fragmented disc being torn out from the center of the window (Figure 16). The diameter of the hole torn was a fair indicator of the diameter of the flat spot formed at that location prior to initiation of fracture. This type of failure occurred

in all of the spherical windows with spherical sector angles of 90, 120, 150 and 180 degrees, regardless of their t/D_i ratio. In windows with spherical sector angles of 30 degrees or 60 degrees, this type of failure took place only when the t/D_i ratio was less than 0.275.

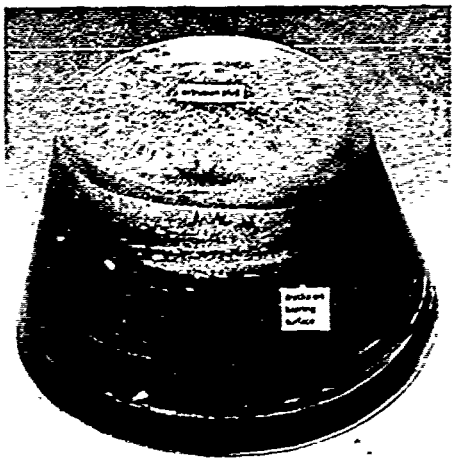

Figure 14. Cold-flow plug on the low-pressure face of a spherical acrylic window after short-term hydrostatic loading to 30,000 psi; 30-degree sector angle, $t/D_i = 0.527$.

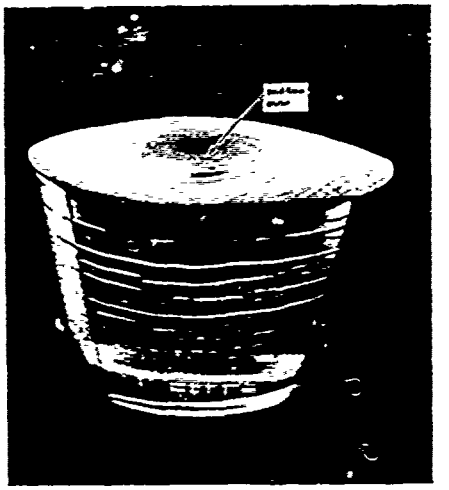

Figure 15. Initiation of cold-flow cratering on the high-pressure face of a spherical acrylic window after short-term hydrostatic loading to 30,000 psi; 30-degree sector angle, $t/D_i = 0.527$.

The other kind of observed window failure was the plug extrusion type. In this case the proportions of windows were such that although a flat spot did appear at the center of the window, the tensile flexural stresses on the low-pressure-face center of the window did not exceed the compressive stress generated there by the wedging of the window in the conical seat of the flange. Because of the wedging, a flexural fracture of the window did not take place. In this type of window failure, the diameter of the window decreased under compression until the window could slip through the cylindrical passage in the center of the window flange. Upon ejection complete fragmentation of the window took place. Moments before ejection such windows showed a very deep cold-flow crater on the high-pressure face (Figure 17) and a well-developed extrusion plug with a convex surface on the low-pressure face (Figure 18). The extrusion plug type of failure was observed only in 30-degree and 60-degree spherical sector windows with t/D_i ratios larger than 0.360.

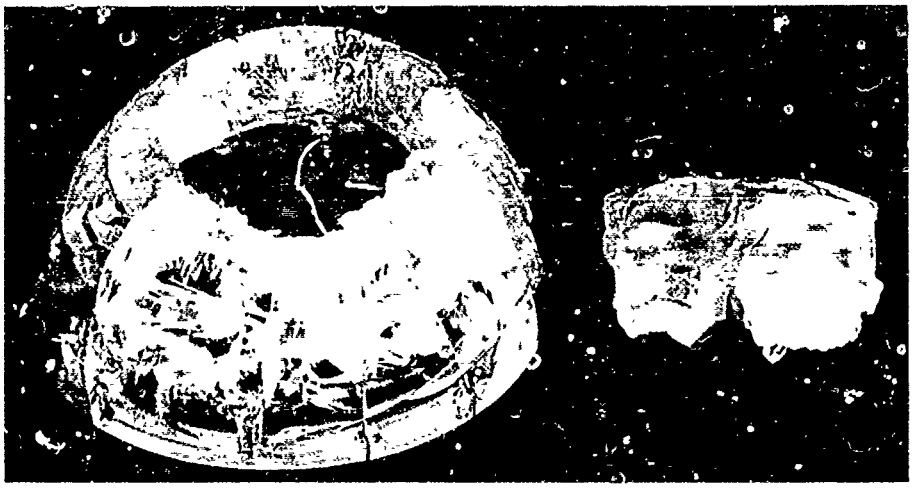

Figure 16. Spherical acrylic window that failed at 15,500 psi after formation of a flat spot in the center of the window; 180-degree sector angle, $t/D_i = 0.182$.

Figure 17. Well-developed cold-flow crater on the high-pressure face of a spherical acrylic window just prior to ejection of the window through the central opening in the flange at 30,000 psi; 60-degree sector angle, $t/D_i = 0.436$.

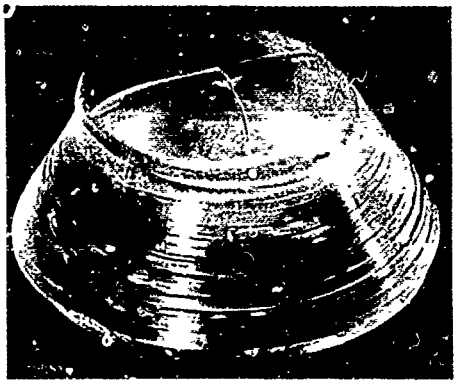

Figure 18. Well-formed extrusion plug on the low-pressure face of a spherical acrylic window just prior to ejection of the window through the central opening in the flange at 30,000 psi; 60-degree sector angle, $t/D_i = 0.436$.

Besides the cold-flow deformation of the window in the form of flat spots or cratering in the center of the high-pressure face of the window and the corresponding formation of plug extrusion on the low-pressure face, some cold flow also occurred on the bearing surface. The plastic deformation of the bearing surface took place by rounding of the bevel on the previously flat conical bearing surface (Figure 19). This deformation of the bearing surface was particularly pronounced only in windows with t/D_i ratios larger than 0.090 and spherical sector angles larger than 60 degrees (Figures 20, 21, and 22). In addition, the bearing surface of the window was penetrated by many fine cracks originating at the bearing surface proceeding into the interior of the window at right angles to the same bearing surface (Figure 23). At any given hydrostatic pressure the number of cracks in windows of the same thickness but different sector angles was different for each sector angle (Figure 24). The cracks were most numerous in windows with a spherical sector angle of 90 degrees (Figure 25) and were almost completely absent in windows with 150-degree angle (Figure 26). Furthermore, when windows of different thickness but of same sector angle were pressurized to a high percentage of a given window's critical pressure (Figure 27), it was noticed that the number of cracks in the bearing surfaces varied with thickness of the window. The thicker the window, the more numerous were the cracks. A few of those cracks were observed to appear some time interval after depressurization and removal of the window from the flange.

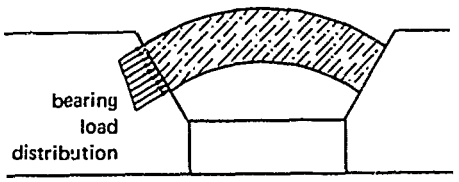

Typical surface bearing load distribution at hydrostatic loading less than 25% of critical pressure

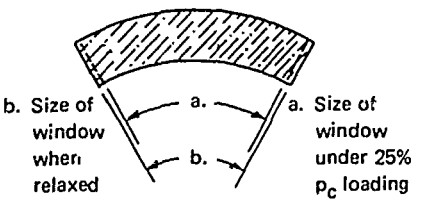

Typical relaxation of a window when hydrostatic pressure of 0.25 p_c magnitude is removed

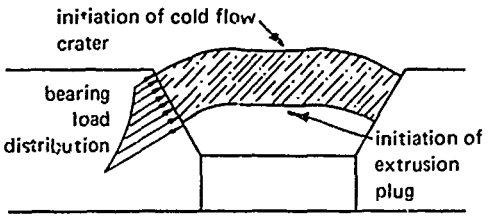

Typical surface bearing load distribution at hydrostatic loading higher than 75% of critical pressure

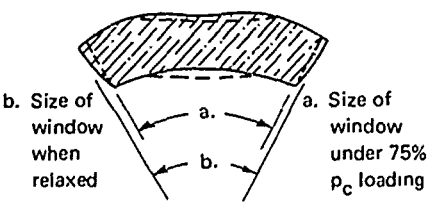

Typical relaxation of a window when hydrostatic pressure of 0.75 p_c magnitude is removed

Figure 19. Deformation processes responsible for rounding of bearing surfaces of spherical acrylic windows.

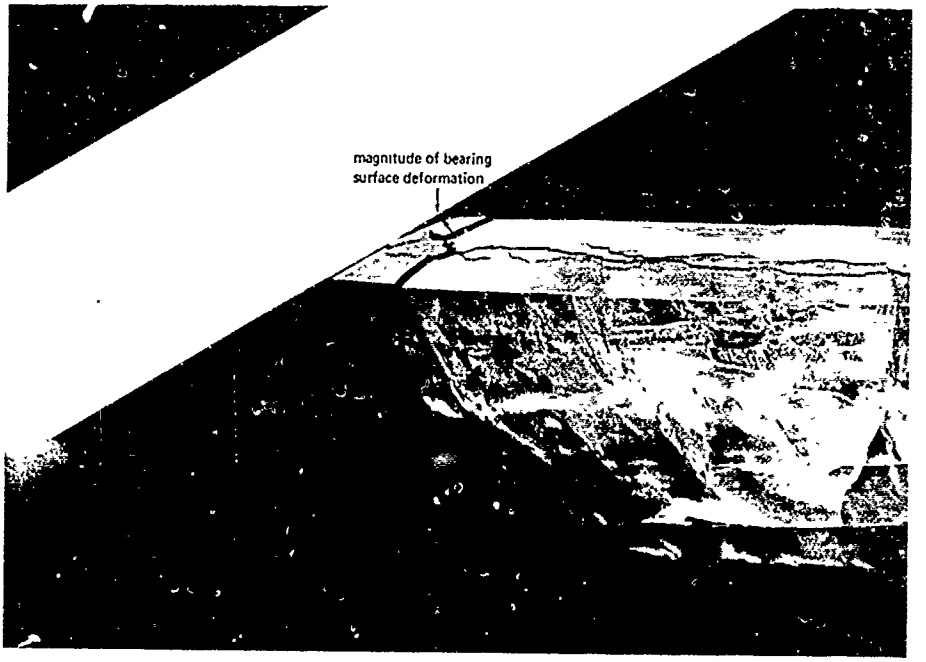

Figure 20. Pronounced permanent deformation of bearing surface on a spherical window that failed at 15,000-psi hydrostatic pressure; 120-degree sector angle, $t/D_i = 0.158$.

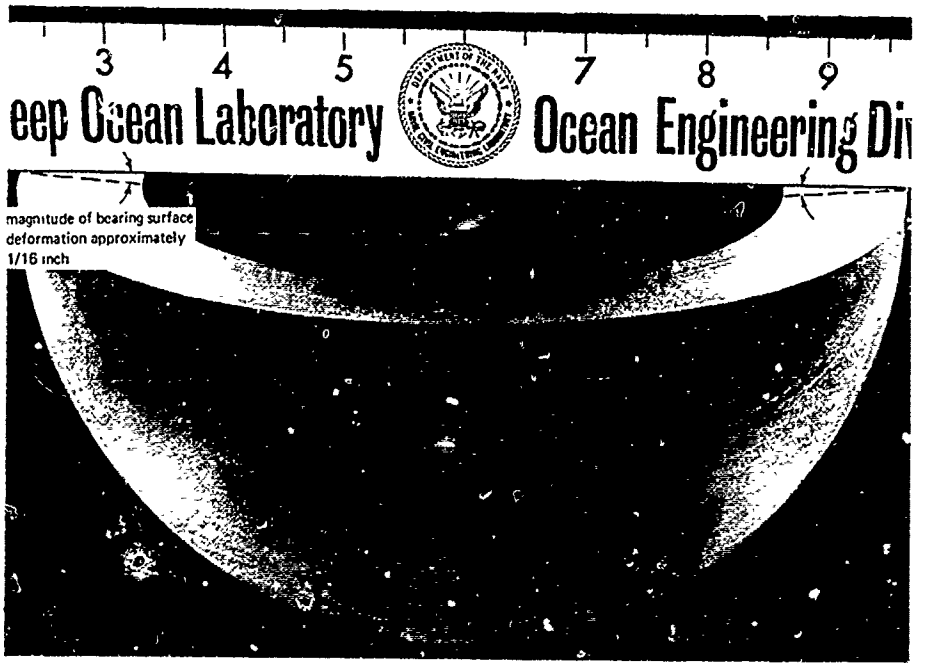

Figure 21. Pronounced permanent deformation of bearing surface on a thick spherical window pressurized to 72% of short-term critical pressure; 180-degree sector angle, $t/D_i = 0.182$.

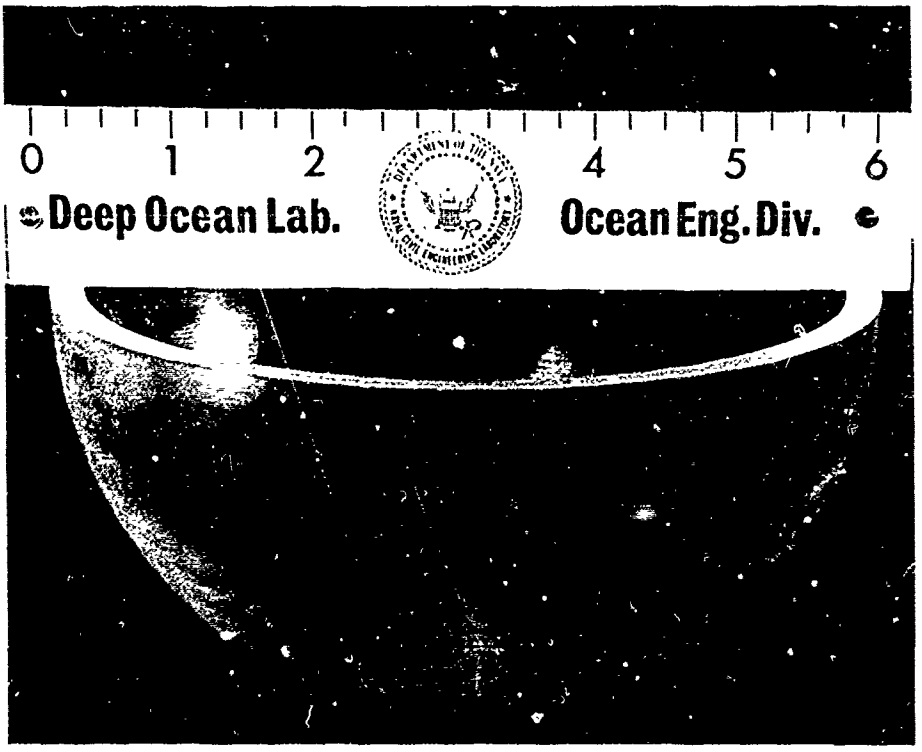

Figure 22. Absence of permanent deformation of bearing surface on a thin spherical window pressurized to 70% of short-term critical pressure; 180-degree sector angle, $t/D_i = 0.045$.

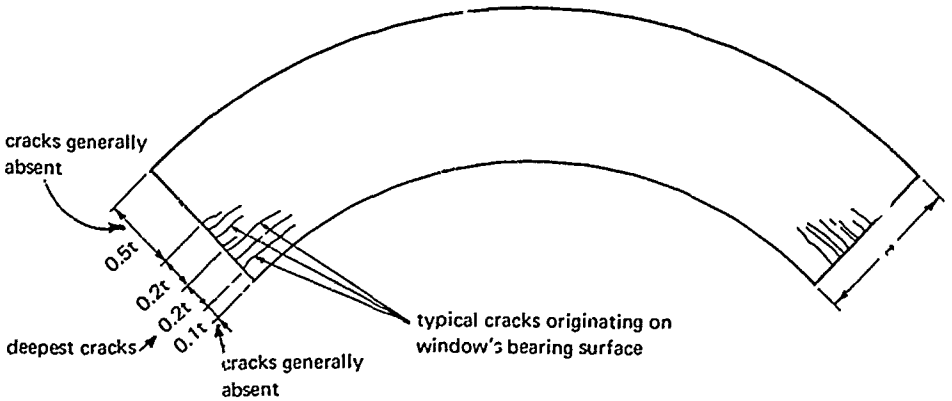

Figure 23. Direction and distribution of cracks originating on the window's bearing surface.

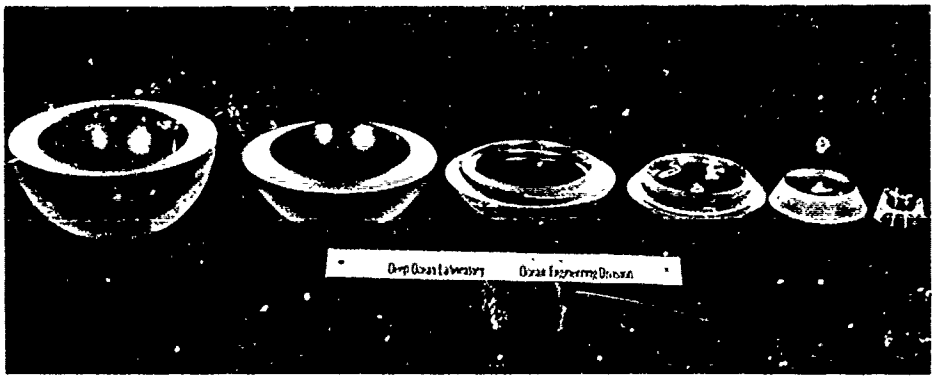

Figure 24. Overview of cracks in the bearing surfaces of 1-inch-thick windows after being subjected to 11,500 psi of sustained hydrostatic pressure for 15 minutes. Note the severe cracks in 90-degree and 120-degree windows.

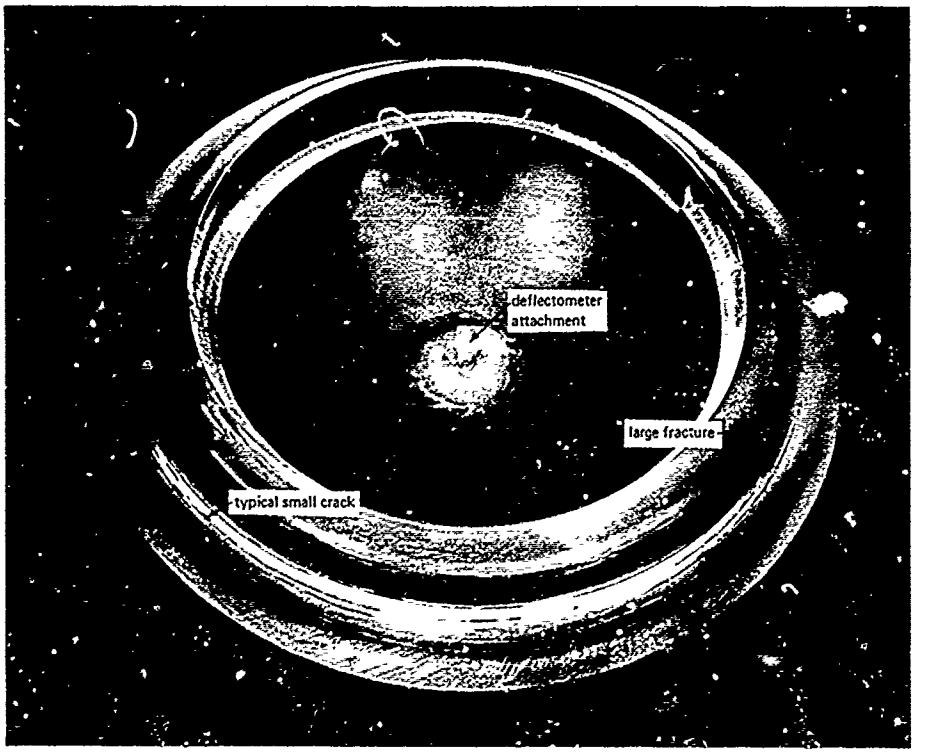

Figure 25. Severe cracks developed in 90-degree sector angle, 1-inch-thick window after 15 minutes of sustained pressure at 11,500 psi, equal to 75% of window's short-term critical pressure.

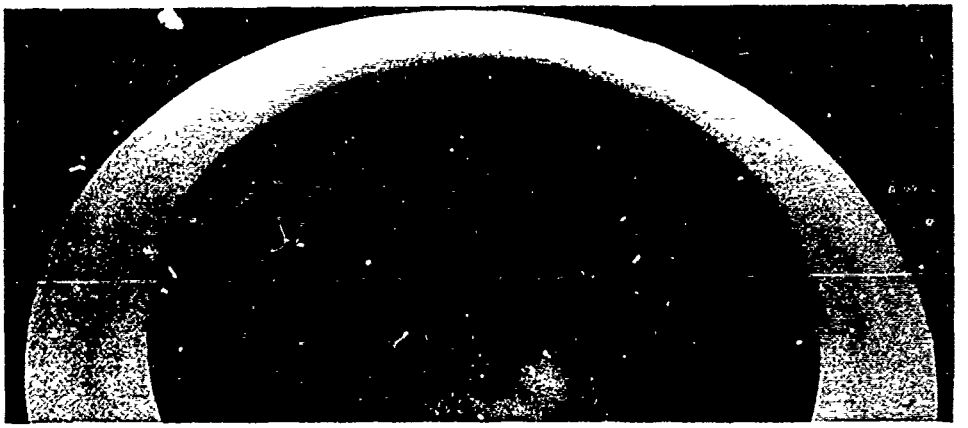

Figure 26. Only small cracks are visible in 150-degree sector angle, 1-inch-thick windows after 15 minutes of sustained pressure at 11,500 psi, equal to to 75% of window's short-term critical pressure.

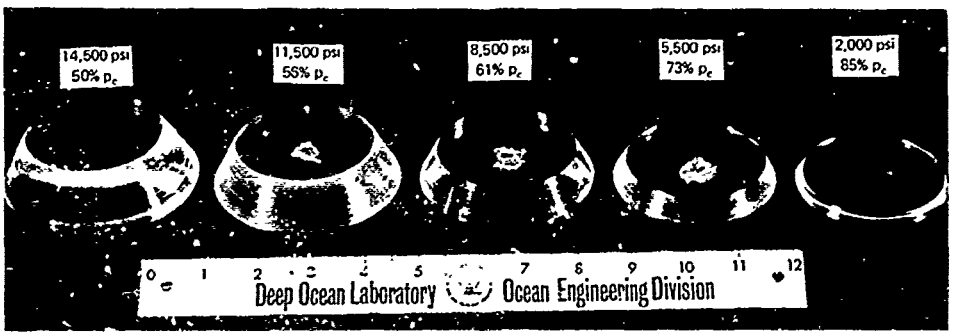

Figure 27. Overview of cracks in the bearing surfaces of 60-degree sector angle windows of different thickness; all sustained hydrostatic pressures for 15 minutes. Note that there are more cracks in 1-inch-thick window than in 0.25-inch-thick window although the thick window was loaded to a lower fraction of its short-term critical pressure.

Short-Term Critical Pressures

The critical pressure of windows with different t/D_i ratios and spherical sector angles varied with the t/D_i ratio, spherical sector angle, temperature of pressurizing medium, and length of loading. Generally speaking, an increase in t/D_i ratio was always followed by an increase in critical pressure, however the relationship between t/D_i and critical pressure was different for each spherical sector angle (Figures 28 through 33). For any given t/D_i ratio, an increase in spherical sector angle was always followed by an increase in critical pressure (Figure 34).

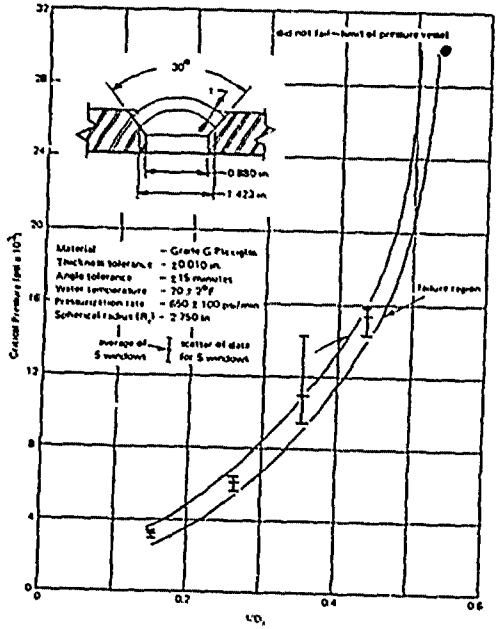

Figure 28 Critical pressures of 30-degree sector angle model spherical acrylic windows with different t/D_i ratios under short term pressure loading

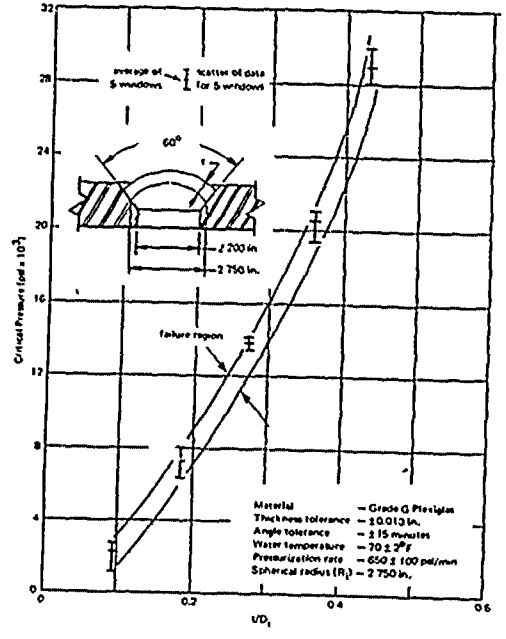

Figure 29 Critical pressures of 60-degree sector angle model spherical acrylic windows with different t/D_i ratios under short-term pressure loading.

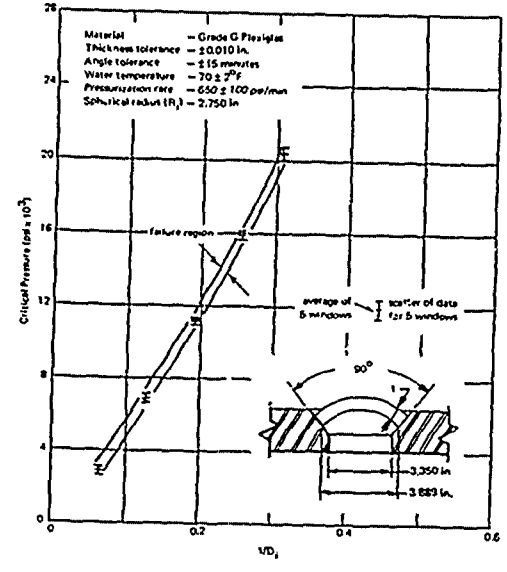

Figure 30. Critical pressures of 90-degree sector angle model spherical acrylic windows with different t/D_i ratios under short-term pressure loading.

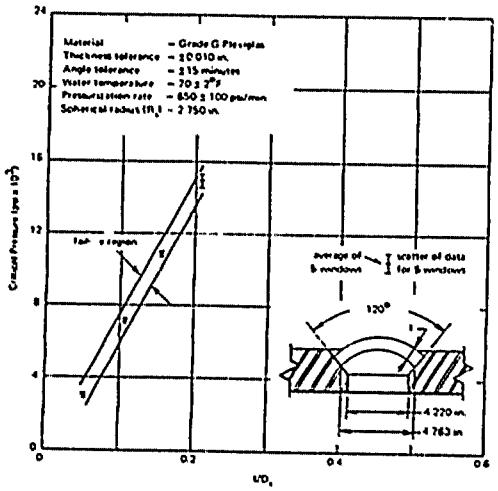

Figure 31 Critical pressures of 120-degree sector angle model spherical acrylic windows with different t/D_i ratios under short term pressure loading

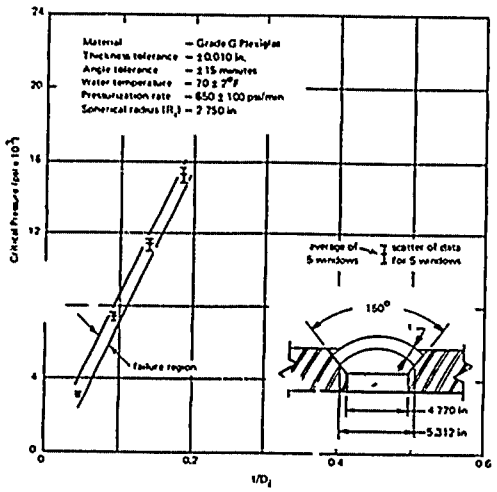

Figure 32. Critical pressures of 150-degree sector angle model spherical acrylic windows with different t/D_i ratios under short term pressure loading.

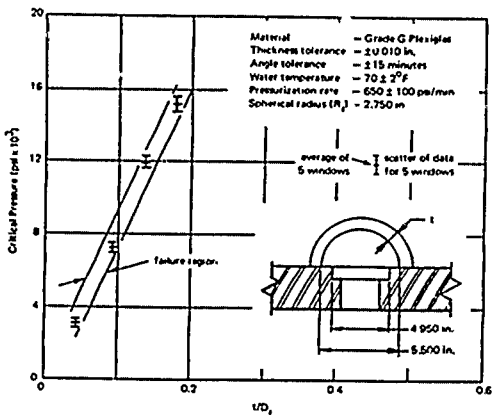

Figure 33 Critical pressures of 180-degree sector angle model spherical acrylic windows with different t/D_i ratios under short-term pressure loading

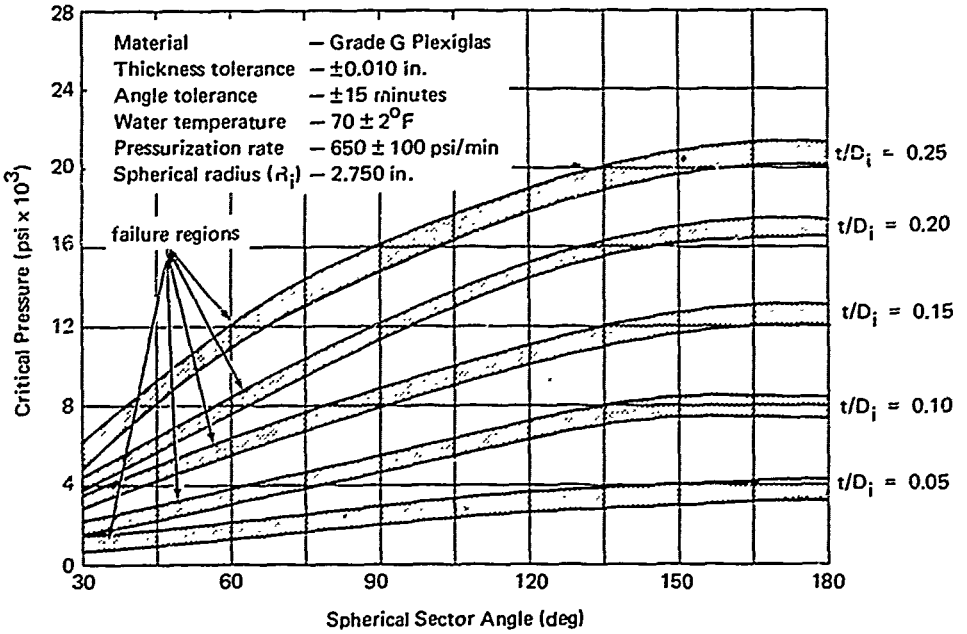

Figure 34. Critical pressure of model acrylic windows with different t/D_i ratios as a function of the spherical sector angle.

Critical pressures of windows with the same spherical sector angle but different t/R_i ratios increased with the magnitude of the t/R_i ratio. However, the exact relationship between t/R_i ratio and p_c was distinctly different for each spherical sector angle (Figures 35 through 40). When one observed the critical pressures of windows with the same t/R_i ratio but different spherical sector angles, it appeared that changing the spherical sector angle has no influence on windows with $t/R_i < 0.182$ (Figure 41). The situation was quite different for windows with $t/R_i \geq 0.182$, for which a definite change in critical pressure occurred in windows of the same t/R_i but different sector angles. As may be noted in Figure 41, the largest increase in critical pressure occurred when the spherical sector angle was decreased from a 90-degree to a 30-degree angle; very little, if any, variation took place in the 180-degree-to-90-degree region. This indicates that the edge effect in windows of same t/R_i exists only for relatively thick windows with a spherical angle less than 90 degrees. Windows with larger spherical sector angles fail at critical pressures that are in the same range as the collapse pressures of complete monolithic hollow acrylic spheres of same t/R_i ratio. For example, the 5,200-to-6,200-psi critical pressure range of 180-degree windows with $t/R_i = 0.143$ compared favorably with 5,000-psi critical pressure of an acrylic sphere of same t/R_i ratio (Figure 1).

When the temperature of the pressurizing medium was lowered from the 68°F-to-72°F room temperature range (in which most of the implosion tests were conducted) to the 50°F-to-52°F temperature range more common in the ocean depths, the critical pressures of spherical windows increased by approximately 20% (Appendix C). Thus the data generated by implosion testing of windows at room temperature is conservative when applied to the design of windows that will operate in hydrospace at lower ambient temperatures.

Since a total of only 20 large-scale windows (Appendix E), as compared to 170 model windows, was tested, tests results obtained with model windows cannot be completely validated. The 60-degree spherical sector angle is the only one for which a fairly accurate comparison between the large- and small-scale windows exists (Appendix E). This comparison indicates that the critical pressure data generated with model windows appears to be applicable to large-scale windows of the same t/R_i, t/D_i, and spherical sector angle, even though the critical pressures of full-scale spherical windows were somewhat lower than those of the model windows (Appendix E). No explanation for this has been found experimentally. However, the difference in critical pressures between the model and full-scale windows is less than 20%, while the spherical radii of model and full-scale windows differ by a factor of more than two. Thus it would appear that the critical pressures of model windows can be used with a reasonable degree of confidence in designing full-scale spherical windows, particularly if the safety factors recommended in Appendix H are applied.

The critical pressures of spherical windows with built-in stress raisers on the convex surface did not differ significantly from critical pressures of identical spherical windows without stress raisers (Appendix F). Since only windows with one t/D_i ratio and spherical sector angle were evaluated with stress raisers, a general observation cannot be made about all spherical windows. However, on the basis of data generated with windows having a 150-degree spherical angle and 0.094 t/D_i ratio and incorporating numerous stress raisers, it would appear that very serious stress raisers can be incorporated into the high-pressure face of 150-degree spherical windows without significantly lowering the critical pressure of the window.

Displacements Under Short-Term Pressure

When pressurized, all windows underwent displacement in their respective flanges. Since the axial displacement was measured only at the center for the majority of model windows and only a few had their displacement measured along the circumference of the window, the generated data describes with statistical confidence only axial displacements. However, by comparing the measurements taken at the center and at the circumference of the windows, a good idea can be formed on how the window of a given t/R_i and α is deforming under hydrostatic loading.

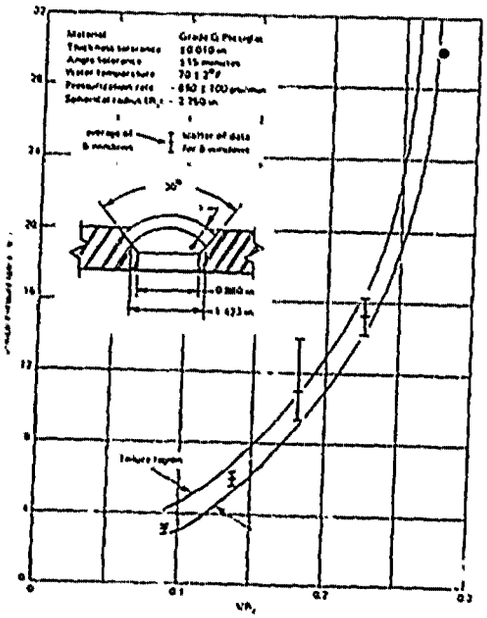

Figure 35. Critical pressures of 30 degree sector angle model spherical acrylic windows with different t/R_i ratios under short-term pressure loading.

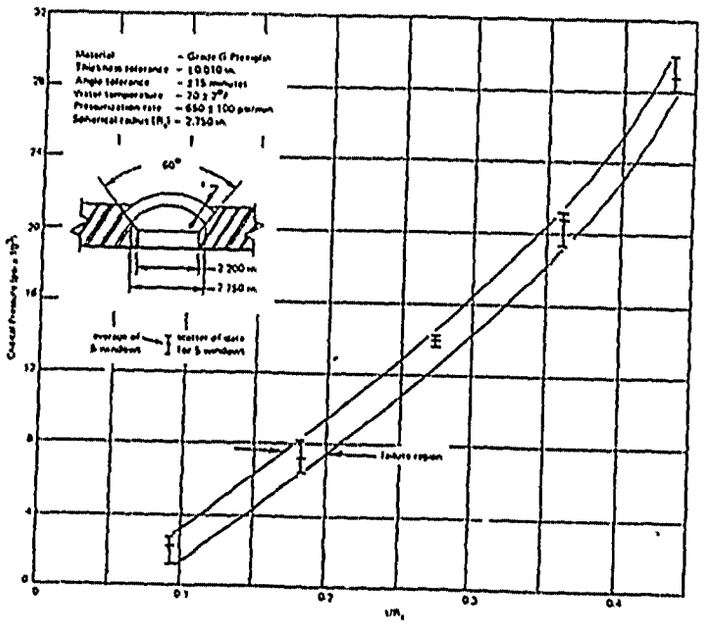

Figure 36. Critical pressures of 60 degree sector angle model spherical acrylic windows with different t/R_i ratios under short-term pressure loading.

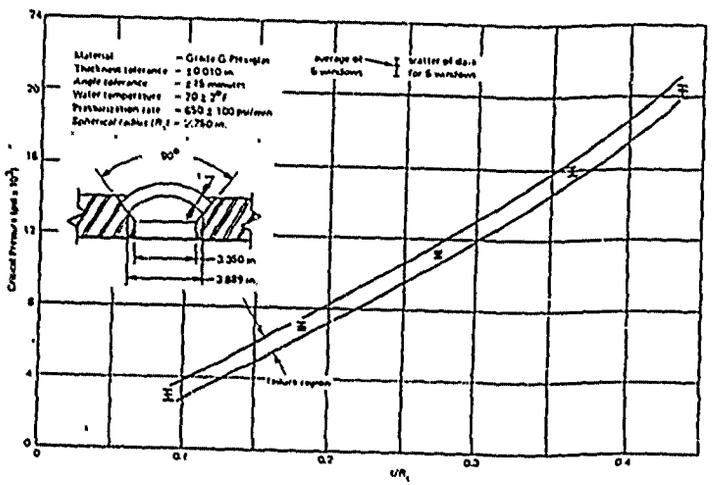

Figure 37. Critical pressures of 90 degree sector angle model spherical acrylic windows with different t/R_i ratios under short-term pressure loading.

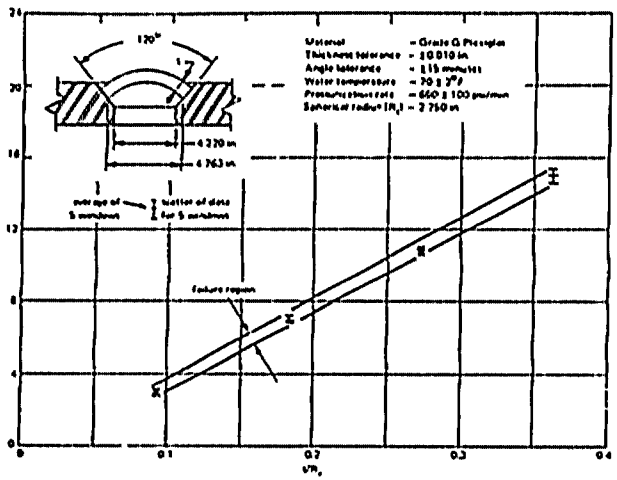

Figure 38. Critical pressures of 120-degree sector angle model spherical acrylic windows with different t/R_i ratios under short term pressure loading.

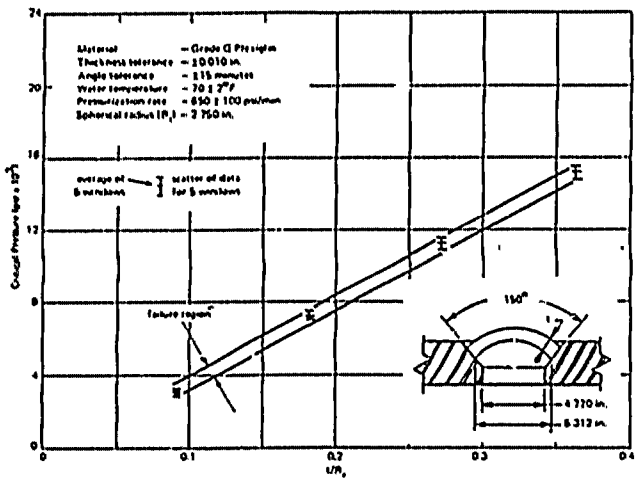

Figure 39. Critical pressures of 150-degree sector angle model spherical acrylic windows with different t/R_i ratios under short term pressure loading.

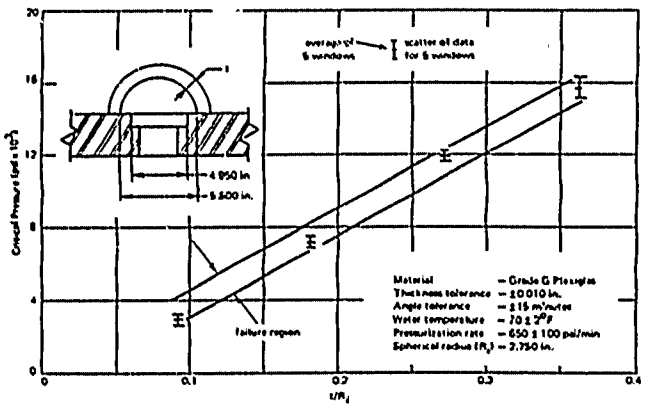

Figure 40. Critical pressures of 180-degree sector angle model spherical acrylic windows with different t/R_i ratios under short-term pressure loading.

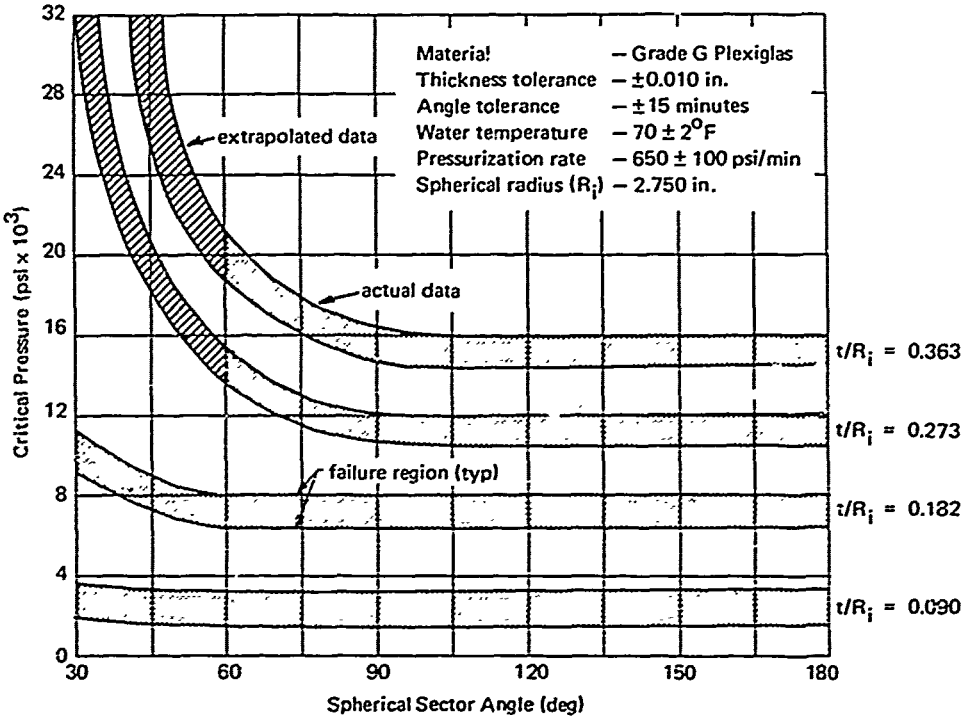

Figure 41. Critical pressures of model acrylic windows with different t/R_i ratios as a function of the spherical sector angle.

The axial displacements of spherical windows for any selected t/R_i ratio and magnitude of short-term pressure loading were observed to be approximately the same for all spherical sector angles (Figures 42 through 47) so long as the pressure selected was a small fraction of the window's critical pressure. The displacements were not the same however for a given short-term pressure and spherical sector angle when the t/R_i differed. Thus, it appears that for any chosen radius of curvature R_i and shell thickness t, the axial displacements vary only with short-term pressure, and not with the spherical sector angle if the pressure is only a small fraction of the window's critical pressure. When all parameters except short-term pressure are held constant in the comparison, the magnitude of axial displacement has been observed to vary with the pressure in a nonlinear manner.

The axial displacements of spherical windows, for any chosen short-term pressure and t/D_i vary inversely with the spherical sector angle, the 180-degree windows having the least displacement (Figures 42 through 47).

Since all the data on sliding displacement of windows in the flanges under short-term loading represents not the average of five window groups but only the test results from one model window specimen for each t/R_i and angle, less confidence can be placed on this data. Nevertheless, the plotted graphs do indicate the general trend and magnitude of the window's sliding under hydrostatic loading.

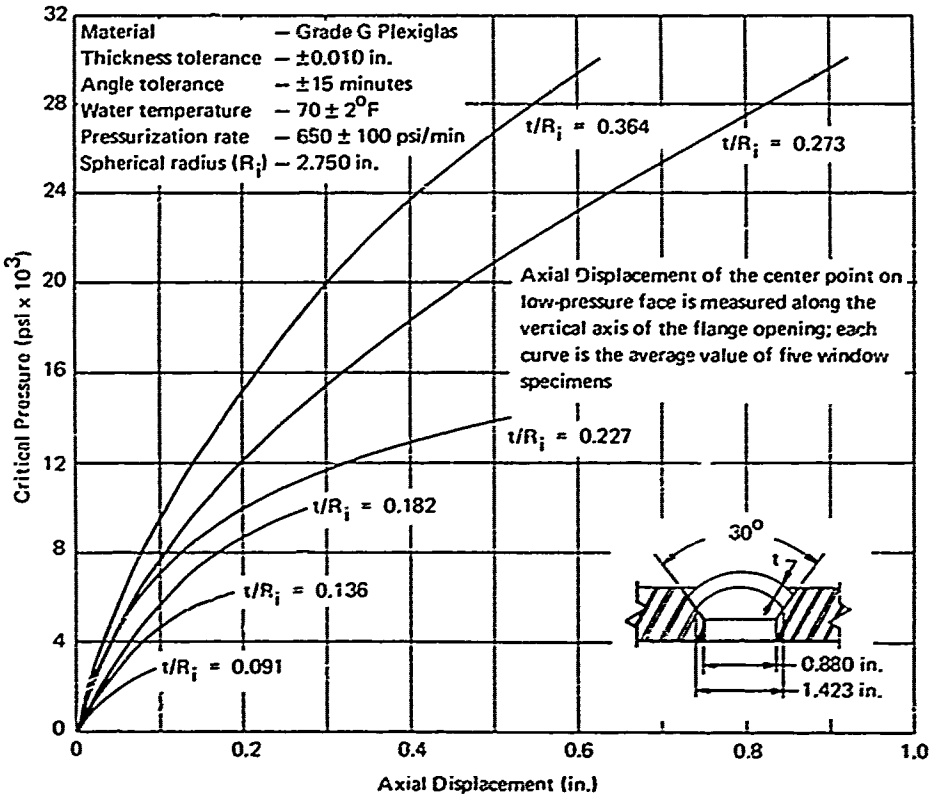

Figure 42. Axial displacements of 30-degree sector angle model spherical acrylic windows under short-term pressure loading.

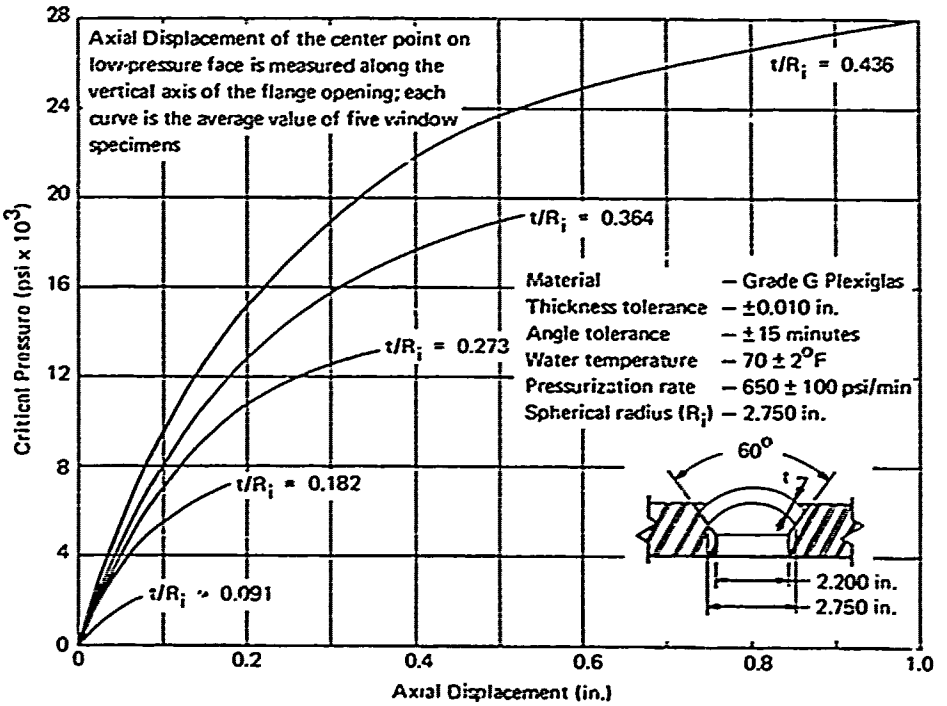

Figure 43. Axial displacements of 60-degree sector angle model spherical acrylic windows under short-term pressure loading.

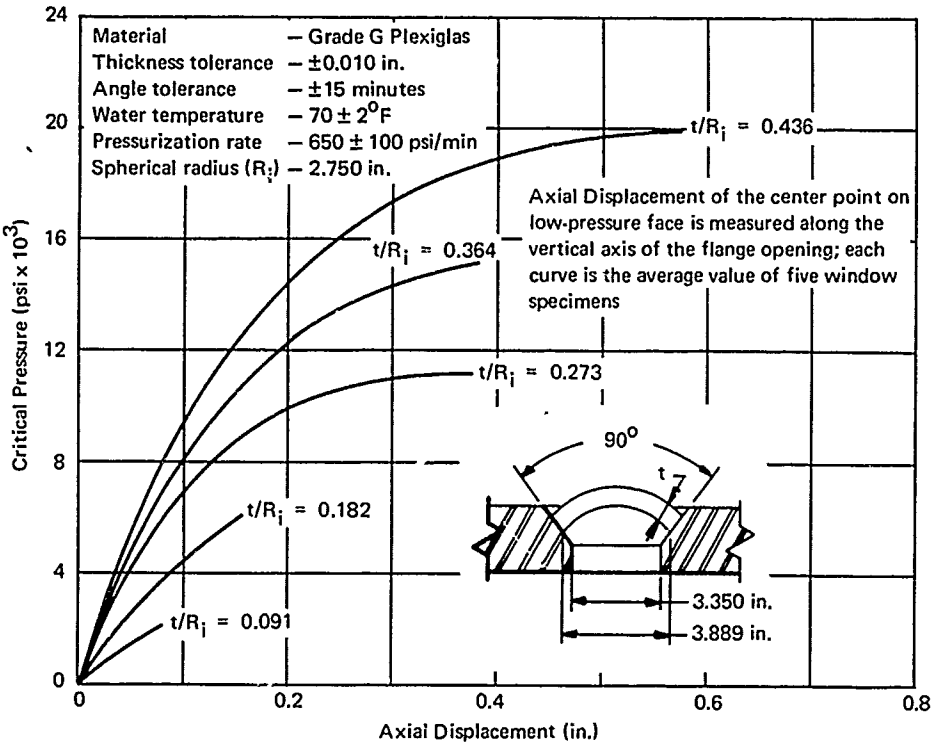

Figure 44. Axial displacements of 90-degree sector angle model spherical acrylic windows under short-term pressure loading.

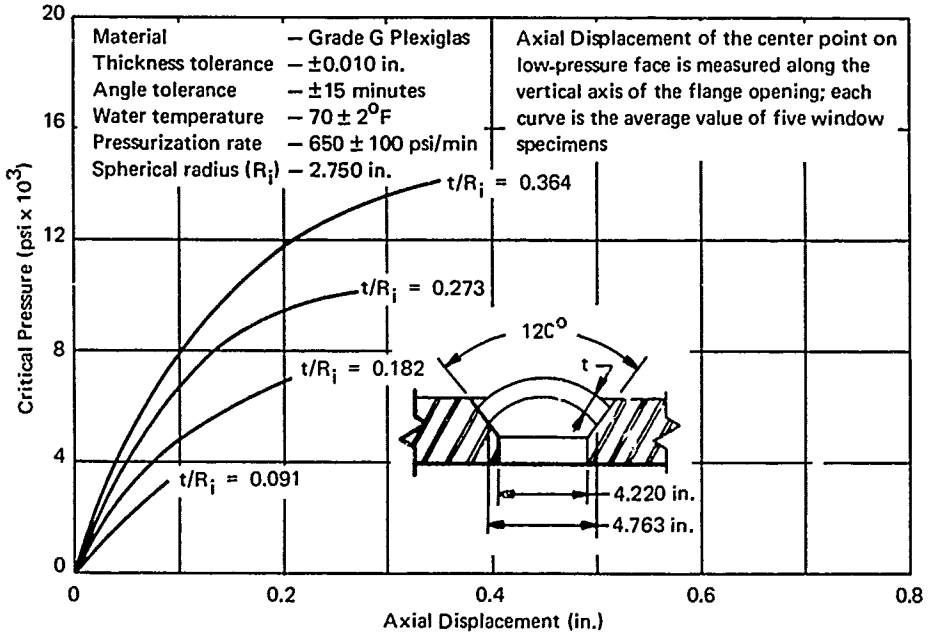

Figure 45. Axial displacements of 120-degree sector angle model spherical acrylic windows under short-term pressure loading.

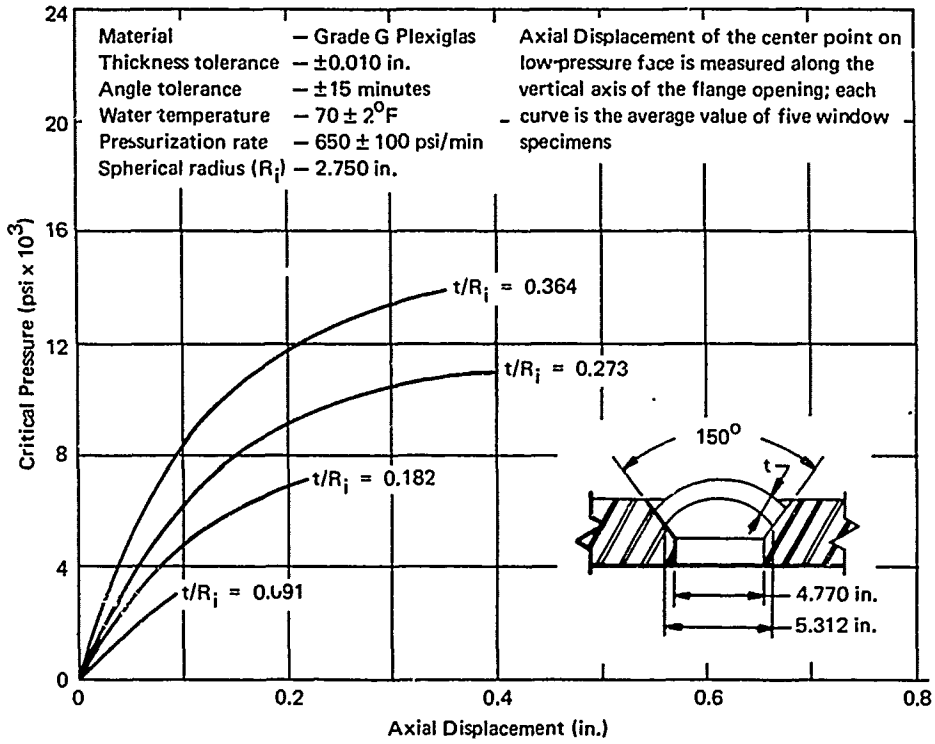

Figure 46. Axial displacements of 150-degree sector angle model spherical acrylic windows under short-term pressure loading.

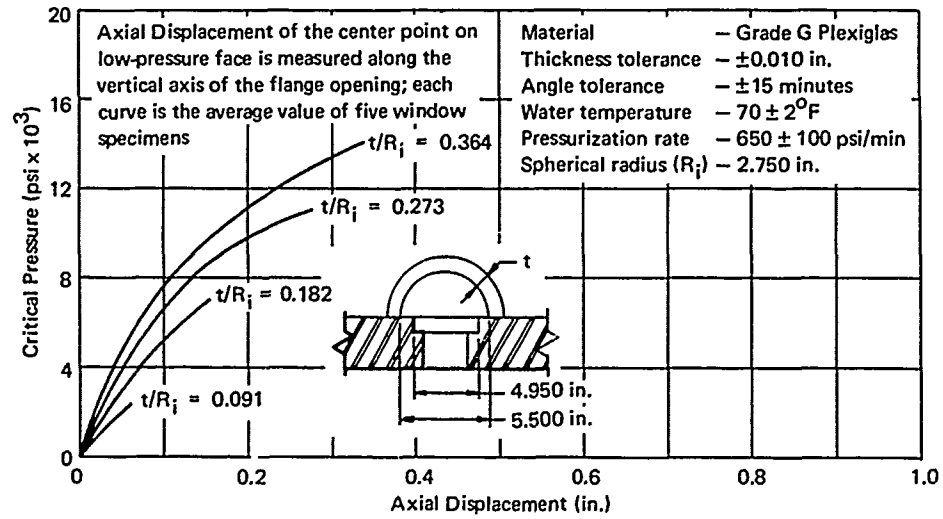

Figure 47. Axial displacements of 180-degree sector angle model spherical acrylic windows under short-term pressure loading.

The sliding of window's beveled edge on the window seat in the flange was somewhat less in magnitude than the axial displacement of the window under the same short-term pressurization, indicating the effect of friction between the window's edge and the flange. When a comparison was made of the magnitudes of the sliding displacements for windows with different spherical sector angles but the same t/R_i ratio and pressure, it appeared that the displacements do not vary significantly from one spherical sector angle to another (Figures 48 through 53). When all parameters are held constant, the magnitude of sliding is observed to vary with the pressure in a nonlinear manner.

FINDINGS

All findings, except 10 and 11, are based on data from model regular spherical sector acrylic windows with R_i = 2.750 inches tested in the 68°F-to-72°F temperature range. Finding 10 is also based on model tests but in the low temperature range, while finding 11 is based on full-scale window tests (Appendix E), where R_i differs from 2.750 inches.

1. Critical pressure of windows having $t/R_i > 0.090$ with identical thickness but different low-pressure-face diameters and associated spherical sector angles was found to be an inverse function (Figure 41 and 54) of the spherical sector angle in the 30-degree $\leqslant \alpha \leqslant$ 90-degree range. For windows with $t/R_i \leqslant 0.090$ the critical pressure was approximately the same for all the spherical angles.

2. Critical pressure of windows with the same thickness-to-low-pressure-face-diameter ratio but different spherical sector angle, diameter, and thickness was found to be a function of the spherical sector angle. An increase in the spherical sector angle was always accompanied by an increase in critical pressure in the 30-degree $\leqslant \alpha \leqslant$ 180-degree range (Figures 34 and 55).

3. For any given thickness-to-low-pressure-face-diameter ratio, the critical pressure of spherical windows was found (Figure 56) to be always higher than the critical pressure of conical windows of same sector angle mated to DOL Type I flanges.[1]

4. Axial displacement of the spherical windows with same thickness but with different low-pressure-face diameter and associated spherical sector angles was found to be fairly constant for all angles at any given pressure loading.

5. Axial displacement of spherical windows with the same thickness-to-low-pressure-face-diameter ratio but different spherical sector angle, diameter, and thickness was found to be an inverse function of the angle.

6. For any given thickness-to-low-pressure-face-diameter ratio and sector angle the axial displacement of spherical windows was less than that of conical acrylic windows with flat parallel viewing surfaces (Figure 57).

7. The sliding displacement of the window's bearing edge was found to be significantly less than axial displacement of any given window.

8. The spherical windows act as optical lenses with magnification of less than one. No optical distortion has been observed when the observer's eye is located at the center of a window's low-pressure-face curvature (Appendix D).

9. Stress raisers on the convex surface of the spherical windows do not appear to decrease the critical pressure of the window (Appendix F).

10. Critical pressure of spherical windows was found to increase with a decrease in ambient temperature. The increase in critical pressure of windows due to lowering the temperature of the pressurizing medium from the 68°F-to-72°F room-temperature range to the 50°F-to-52°F range was approximately 20% (Appendix C).

11. The critical pressures and axial displacements of full-scale spherical acrylic windows can be predicted with fair accuracy on the basis of critical pressures generated by testing to destruction of model windows with identical t/R_i, t/D_i, and α (Appendix E).

CONCLUSION

Spherical acrylic windows provide not only a larger field of view for the observer, but also fail at higher hydrostatic pressures than conical or flat disc acrylic windows of same thickness-to-diameter ratio.

RECOMMENDATION

In view of the superior performance shown by spherical acrylic windows under short-term pressure loading further studies should be conducted to evaluate their performance under long-term and cyclical pressure loading.

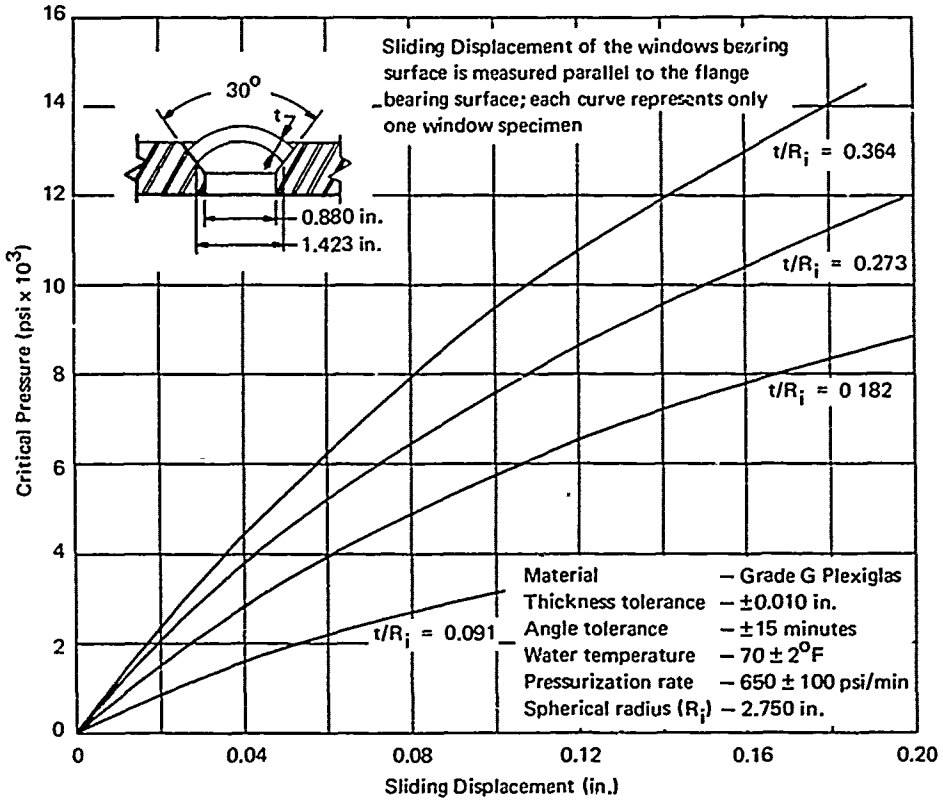

Figure 48. Sliding displacements of 30-degree sector angle model acrylic windows along flange seat under short-term hydrostatic pressure loading.

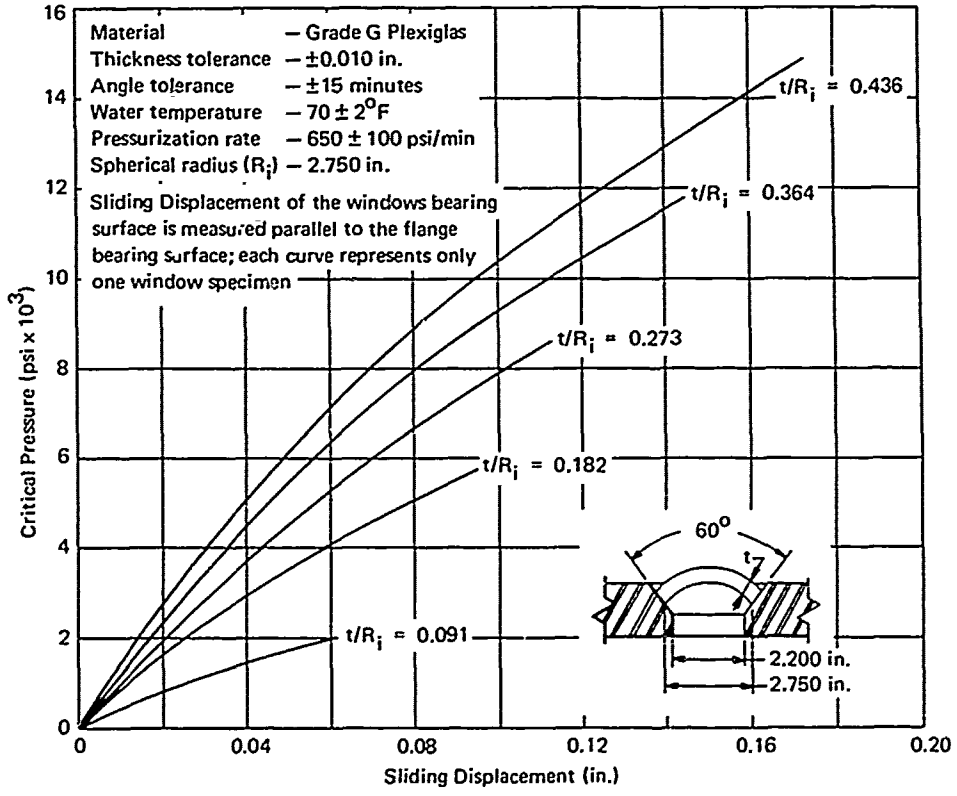

Figure 49. Sliding displacements of 60-degree sector angle model acrylic windows along flange seat under short-term hydrostatic pressure loading.

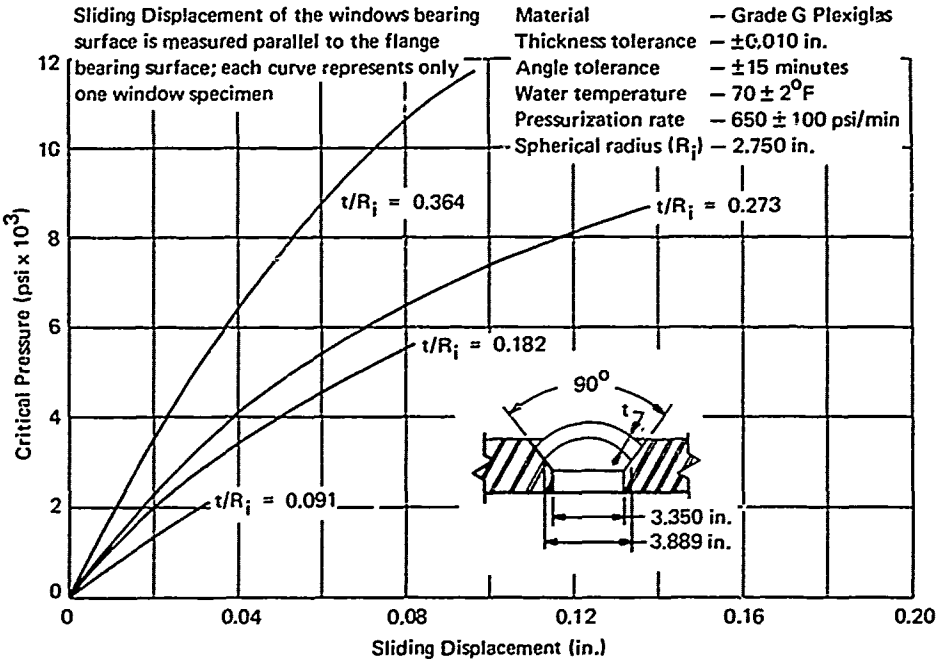

Figure 50. Sliding displacements of 90-degree sector angle model acrylic windows along flange seat under short-term hydrostatic pressure loading.

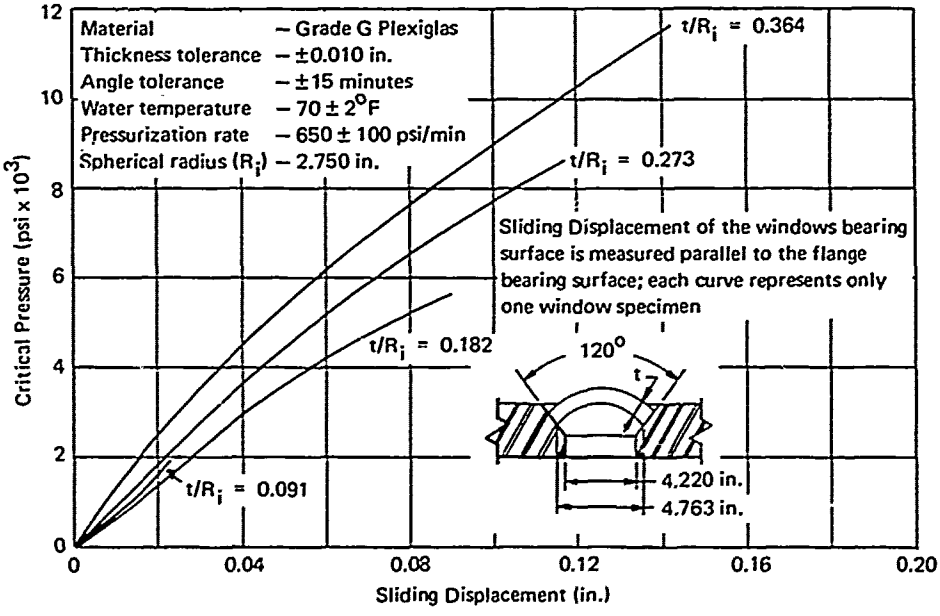

Figure 51. Sliding displacements of 120-degree sector angle model acrylic windows along flange seat under short-term hydrostatic pressure loading.

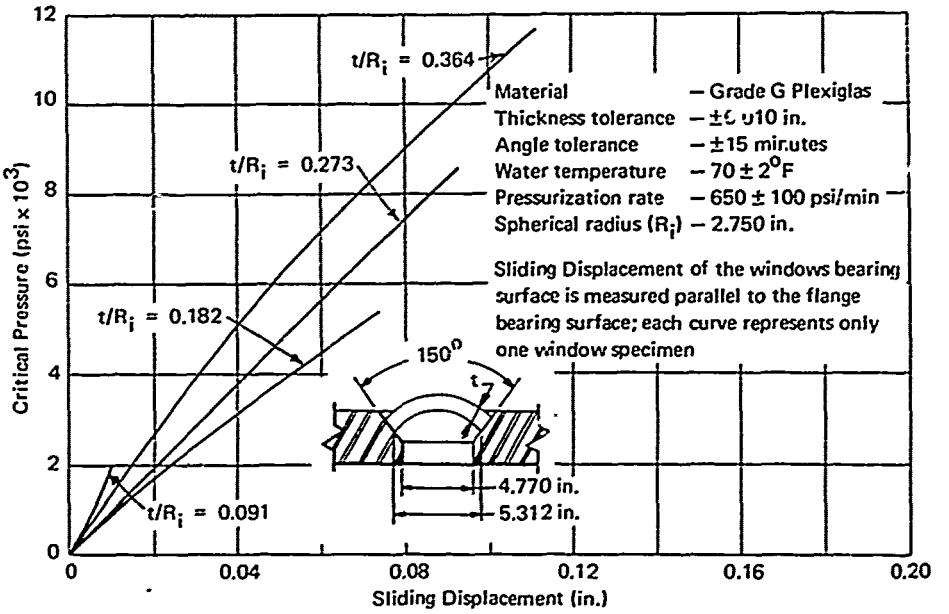

Figure 52. Sliding displacements of 150-degree sector angle model acrylic windows along flange seat under short-term hydrostatic pressure loading.

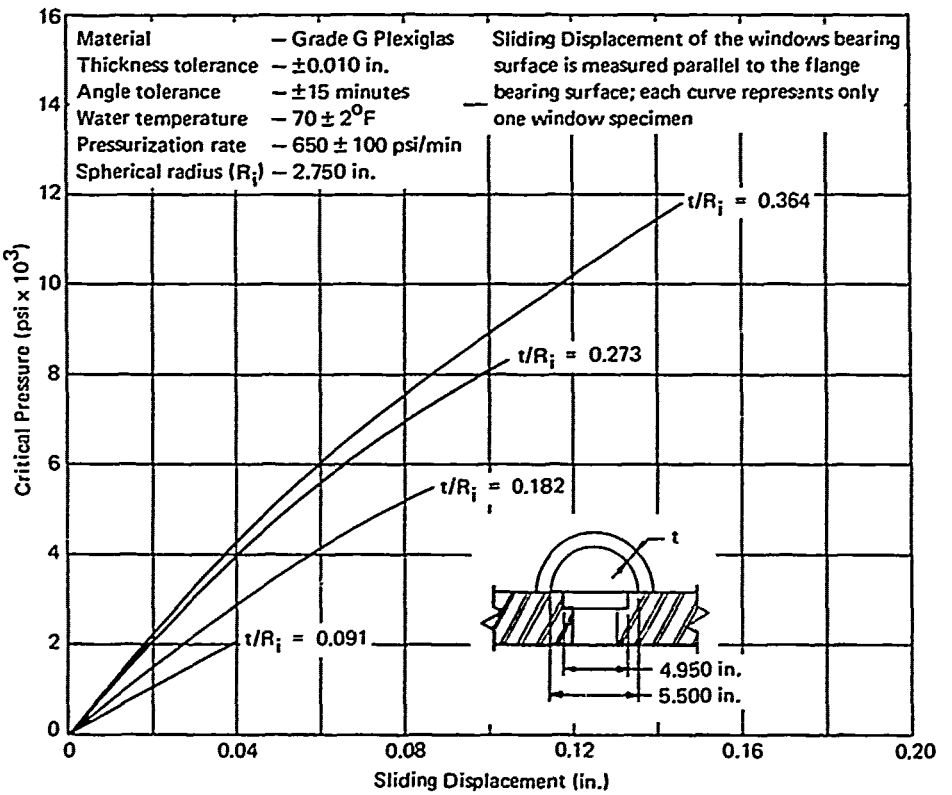

Figure 53. Sliding displacements of 180-degree sector angle model acrylic windows along flange seat under short-term hydrostatic pressure loading.

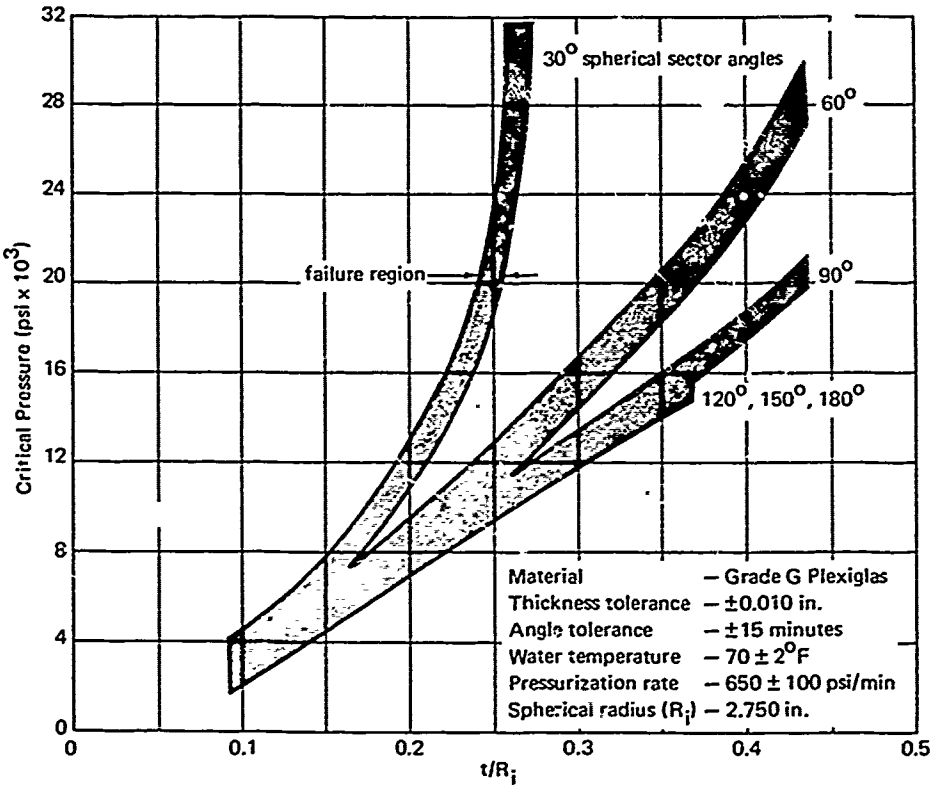

Figure 54. Summary of critical pressures as a function of t/R_i for all model spherical acrylic windows under short-term pressure loading.

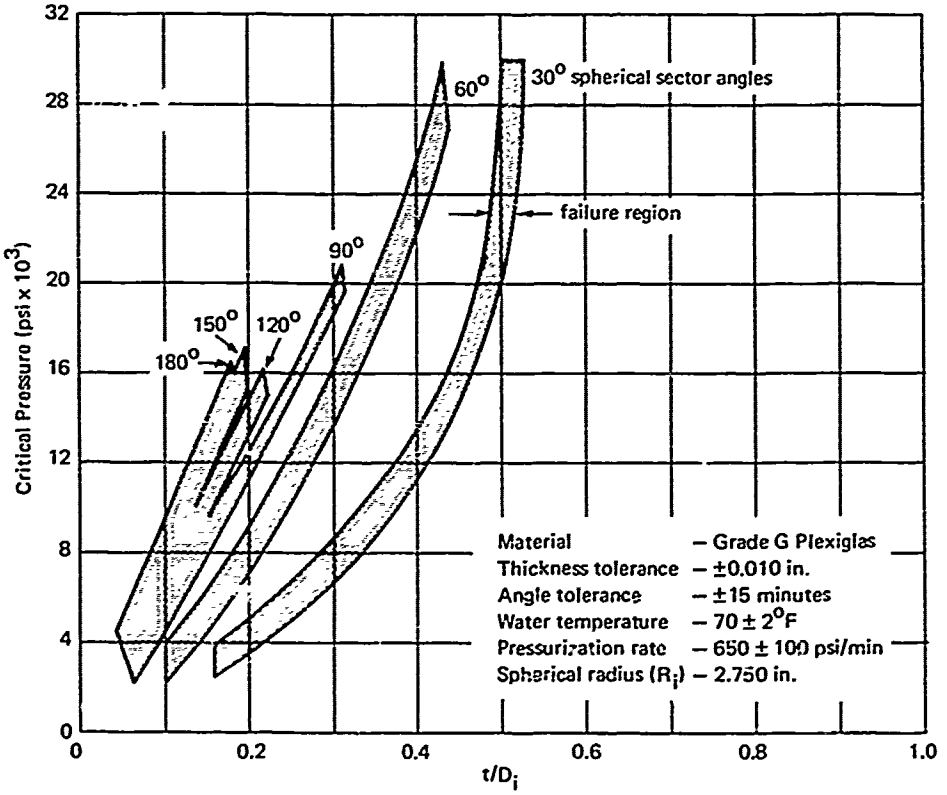

Figure 55. Summary of critical pressures as a function of t/D_i for all model spherical acrylic windows under short-term pressure loading.

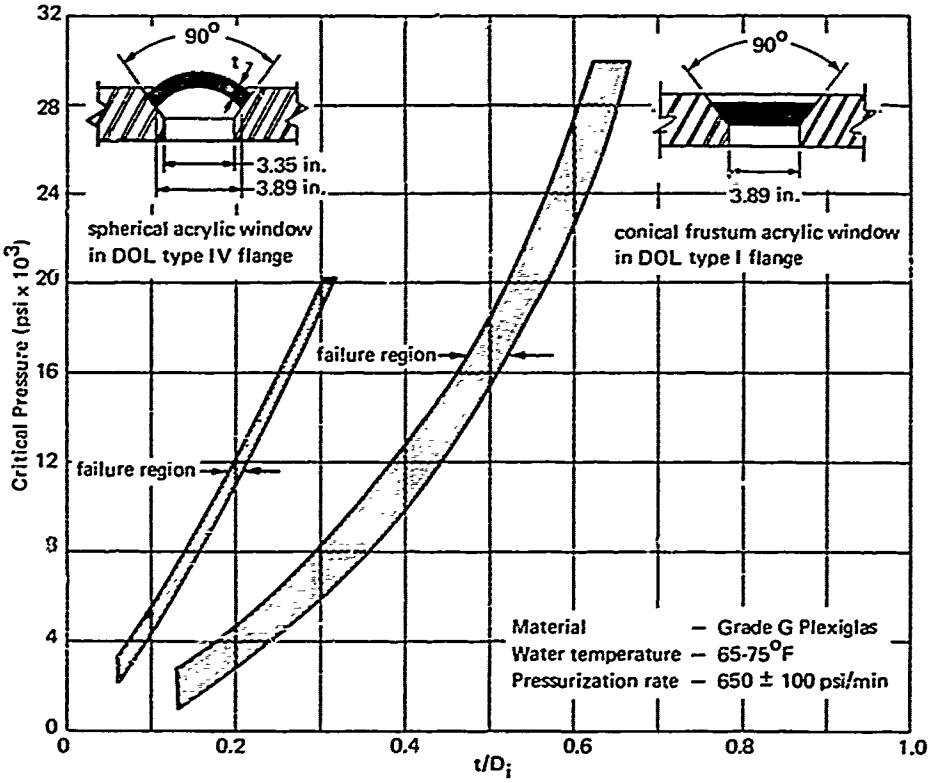

Figure 56. Comparison of critical pressures for 90-degree spherical and conical frustum acrylic windows under short-term loading.

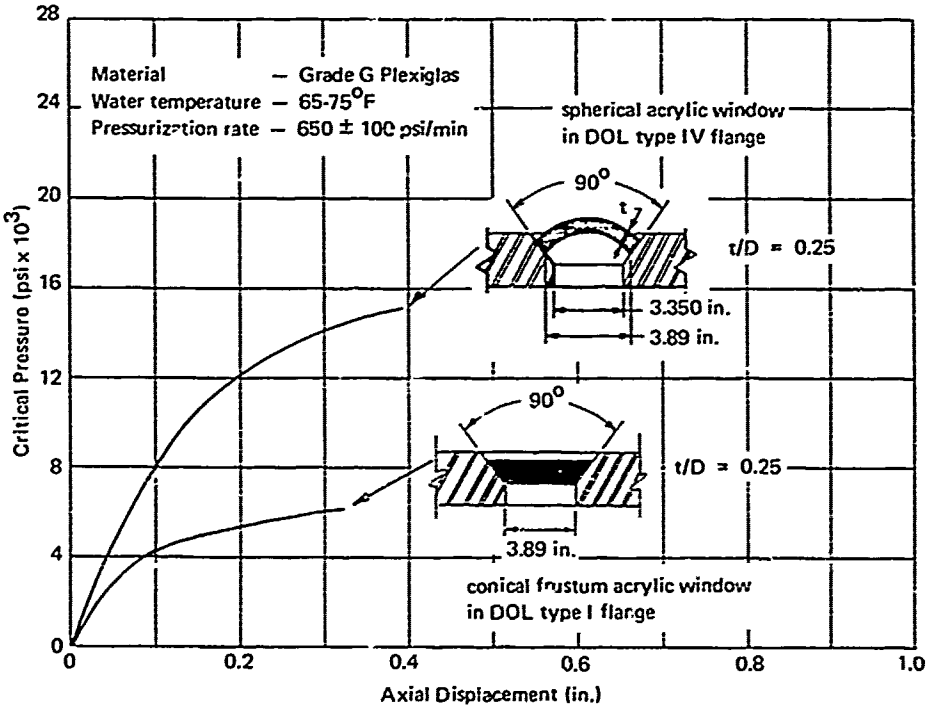

Figure 57. Comparison of axial displacements for 90-degree spherical and conical frustum acrylic windows with D_i = 3.890 inches under short-term loading.

Appendix A

EFFECT OF STRAIN RATE ON THE MECHANICAL PROPERTIES OF ACRYLIC PLASTIC

The spherical acrylic windows tested in this study were pressurized at the rate of 650 psi/min; however, the resultant stress rates varied with the thickness of the window tested. The minimum stress rate for the specimens was on the order of 1,200 psi/min for the 1.000-inch-thick windows, while the maximum stress rate was 3,900 psi/min for the 0.250-inch-thick windows. Since the maximum stressing rate is approximately three times larger than the minimum stress rate, it was conceivable that the response of the window material differed between these stress rates.

To find whether stress rate has any effect on the strength, strain, modulus of elasticity, or Poisson's ratio of grade "G" Plexiglas, cylindrical specimens were tested in axial compression at different loading rates. Assuming that the critical pressures of the windows are directly proportional to the mechanical properties of the cylindrical specimens, the information obtained from the cylindrical specimens would show to what extent the windows are affected by the varying of stress rate.

There are many factors which influence the critical pressure of the windows, such as thickness, spherical angle, flange shape, and temperature of environment. Still, the effect of each variable can be separated from the others by changing the dimensional proportions of the specimens, or testing environment. The effect of varying the stress rate could also be determined by testing windows at various loading rates, but testing cylindrical specimens would give approximately the same results, and the limited number of expensive spherical window specimens could thus be used for determination of more important structural parameters of the window.

To find how cylindrical specimens are affected by varying the stress rate 10 specimens were tested, two at each of five different loading rates: 80 psi/min, 1,220 psi/min, 2,225 psi/min, 3,900 psi/min, and 12,750 psi/min.

The range of the loading rates selected was such that there was in addition to stressing rates comparable to those in the windows also one rate considerably higher and one considerably lower than the maximum and minimum stress rates of the spherical window specimens. The highest loading rate for the cylindrical specimens was approximately three times the maximum stress rate of the window specimens, and the lowest loading rate was approximately 1/15 of the minimum stress rate found in the windows. It was hoped that if the simulated window stress rates differing by a factor of 3 did not produce any marked difference in material response, then the exaggerated maximum and minimum stress rates differing by approximately a factor of 150 would.

The physical proportions of the cylindrical specimens were chosen to conform essentially to ASTM Specification D695-63T; the specimens could be cut from a 4-inch-thick plate, the same material from which the spherical window specimens were made. The specimens, 4.00 inches in length and 2.00 inches in diameter (Figure A-1). were cut with their major axis parallel to the 4-inch-thick side of the plate.

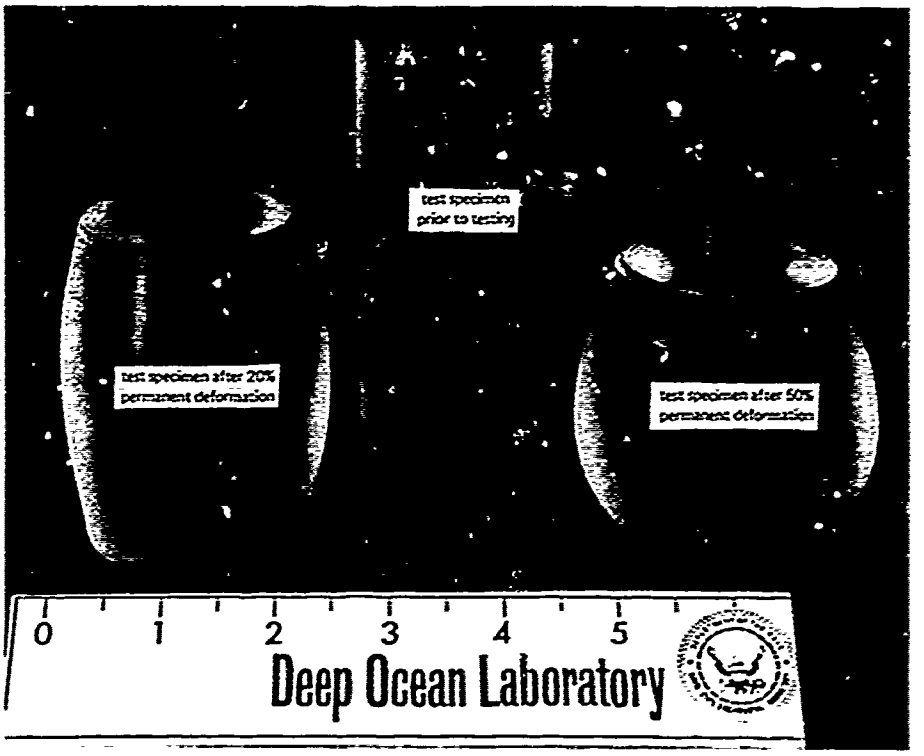

Figure A-1. Acrylic cylindrical test specimens before and after compression testing.

The cylindrical specimens were tested at a room temperature range of 75°F-to-80°F in a 400,000-pound-capacity Baldwin-Tate-Emery Universal Testing Machine. The load was applied axially on the lower face of the cylinder by a pump-driven hydraulic ram which compressed the specimen against a stationary platen.

The deformation during testing of each specimen was measured in both the axial and transverse directions by mechanical dial indicators, readings were taken at 5,000-pound intervals. The dial indicator used for measuring the transverse deformation was equipped with a T-shaped rod, thus allowing the maximum displacement to be measured whether it appeared above or below the center of the specimen (Figure A-2). Although this type of arrangement is not the one recommended by ASTM for accurate determination of material properties, it is useful for comparison of strains under different loading rates. The specimens were loaded until they reached a

point where the strain rate was increasing faster than the Universal Testing Machine could apply the load. One specimen was tested to failure so that the approximate ultimate stress would be known, and the mode of failure could be observed.

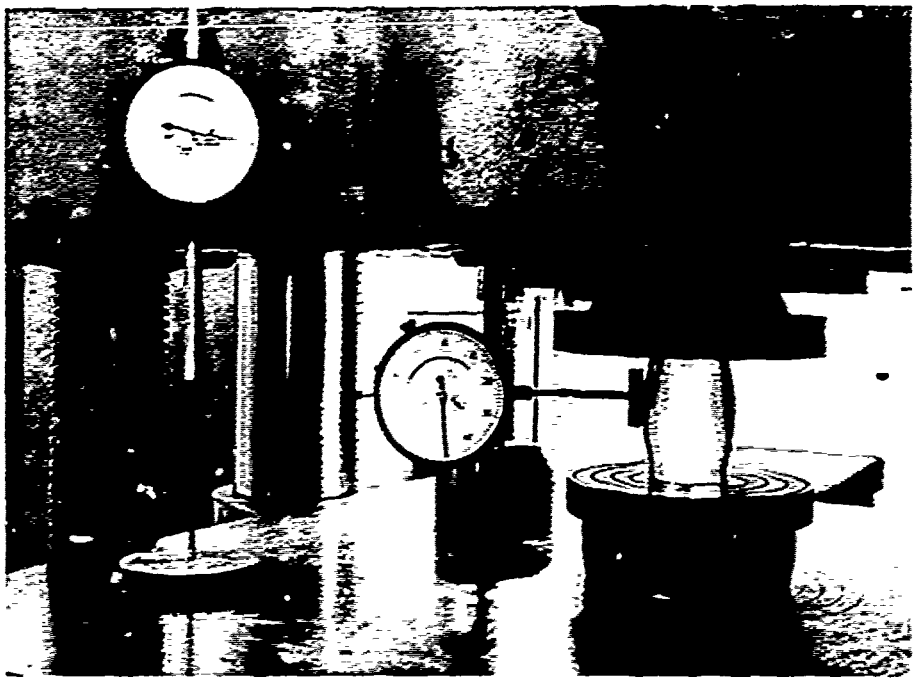

Figure A-2. Experimental setup for the measurement of axial and transverse strains in acrylic test specimens under uniaxial compression; at 14,500-psi stress level.

From the stress–strain curves (Figures A-3 and A-4), which are based on the original cross-sectional area, it can be seen that at all stress levels an increase in loading rate results in a decrease of strain rate. It can be seen from Figure A-4 that the tangent modulus of elasticity, and the secant modulus of elasticity also change with loading rates. In the case of the moduli of elasticity, their magnitude decreases as the loading rate decreases (Figures A-5 and A-6). An increase in loading rate is invariably followed by a decrease of Poisson's ratio (Figure A-7).

The specimen that was tested to destruction (Figure A-8) had a conical surface failure at both the upper and lower bearing surfaces. Fragments from the cylindrical specimen were ejected in all directions when failure occurred at a load of 103,000 pounds. At this load the specimen had been compressed to approximately 2 inches, or 50% of its original length.

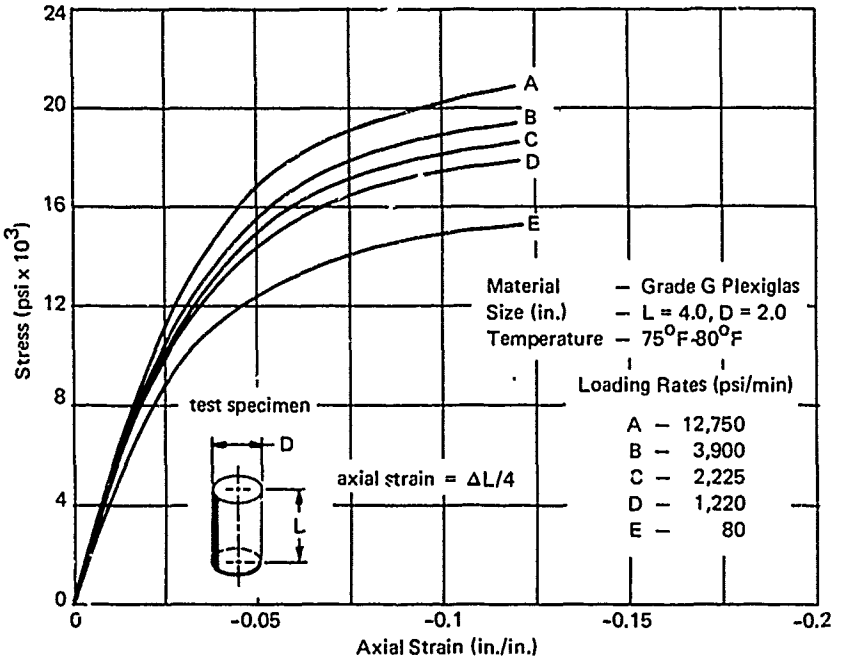

Figure A-3. Axial strain in acrylic test specimens under uniaxial compression.

Testing of the cylindrical specimens proved that the loading rate has an effect on the mechanical properties of grade "G" Plexiglas. However, it should be noted that the difference in strain rates, tangent and secant moduli of elasticity, and Poisson's ratio for the simulated maximum and minimum stressing rates of the spherical windows in this study (curves B and D on Figures A-3 through A-7) was less than 15% in the 0-to-10,000-psi stress range and thus could be ignored.

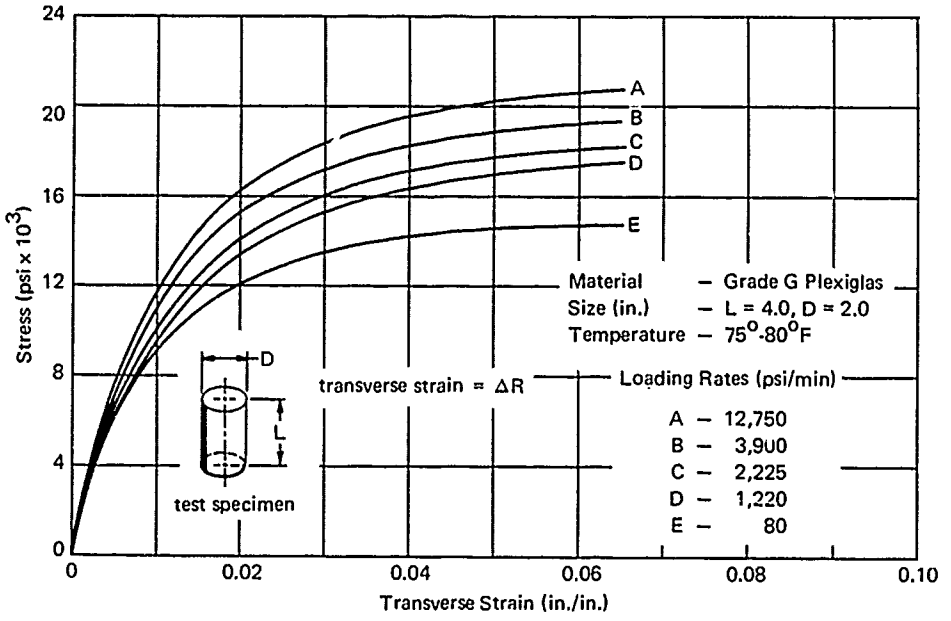

Figure A-4. Transverse strain in acrylic test specimens under uniaxial compression.

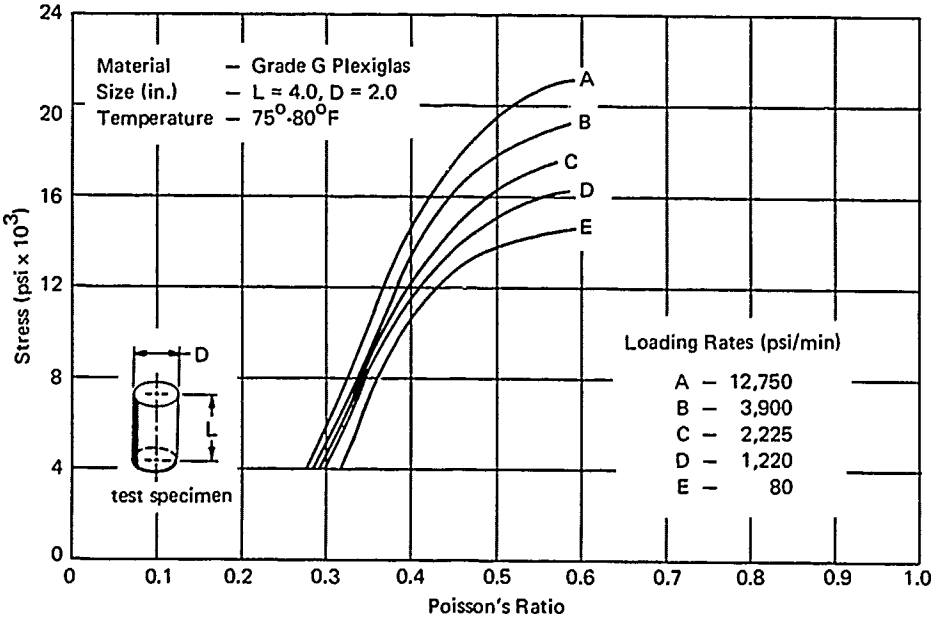

Figure A-5. Poisson's ratio in acrylic test specimens under uniaxial compression.

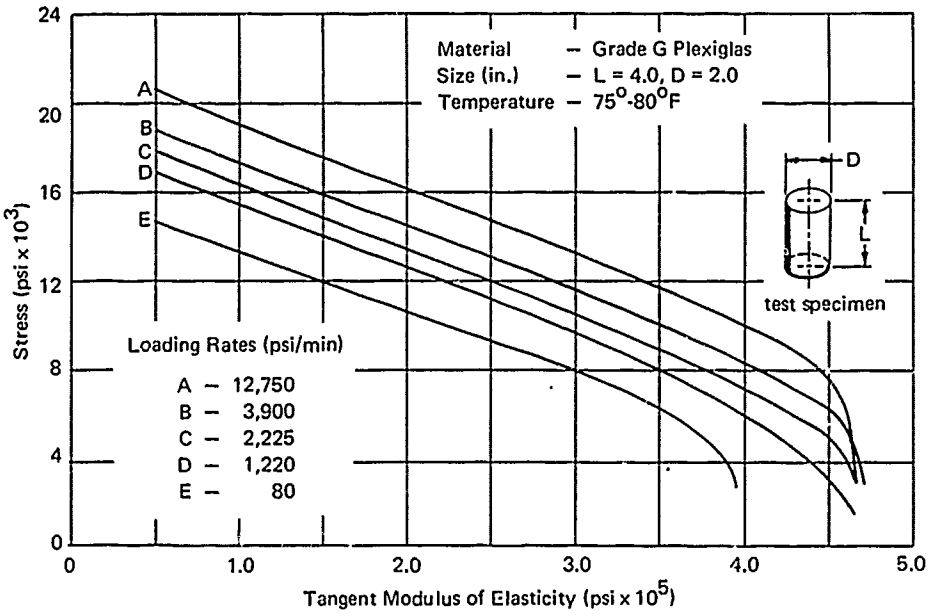

Figure A-6. Tangent modulus of elasticity in acrylic test specimens under uniaxial compression.

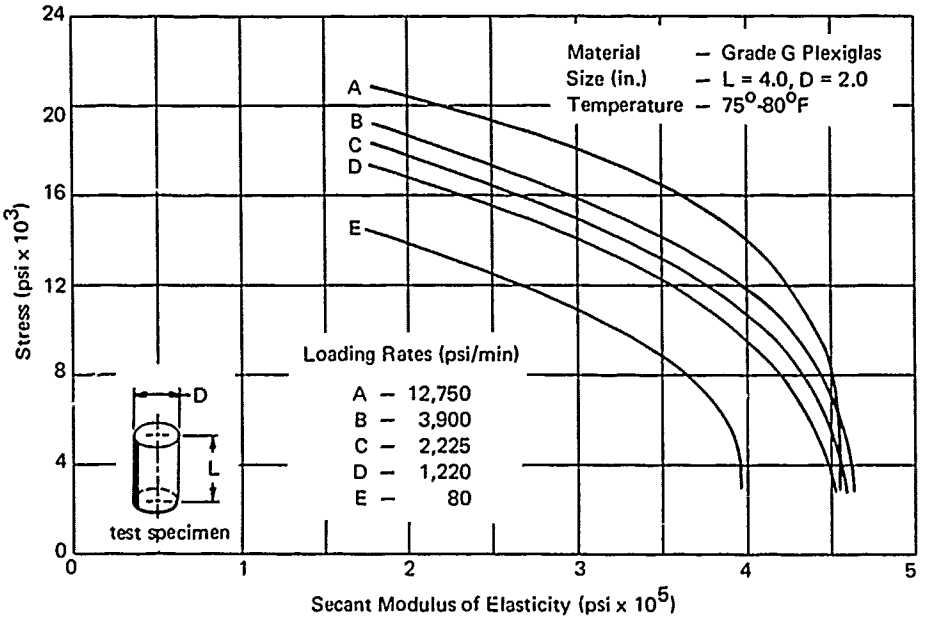

Figure A-7. Secant modulus of elasticity in acrylic test specimens under uniaxial compression.

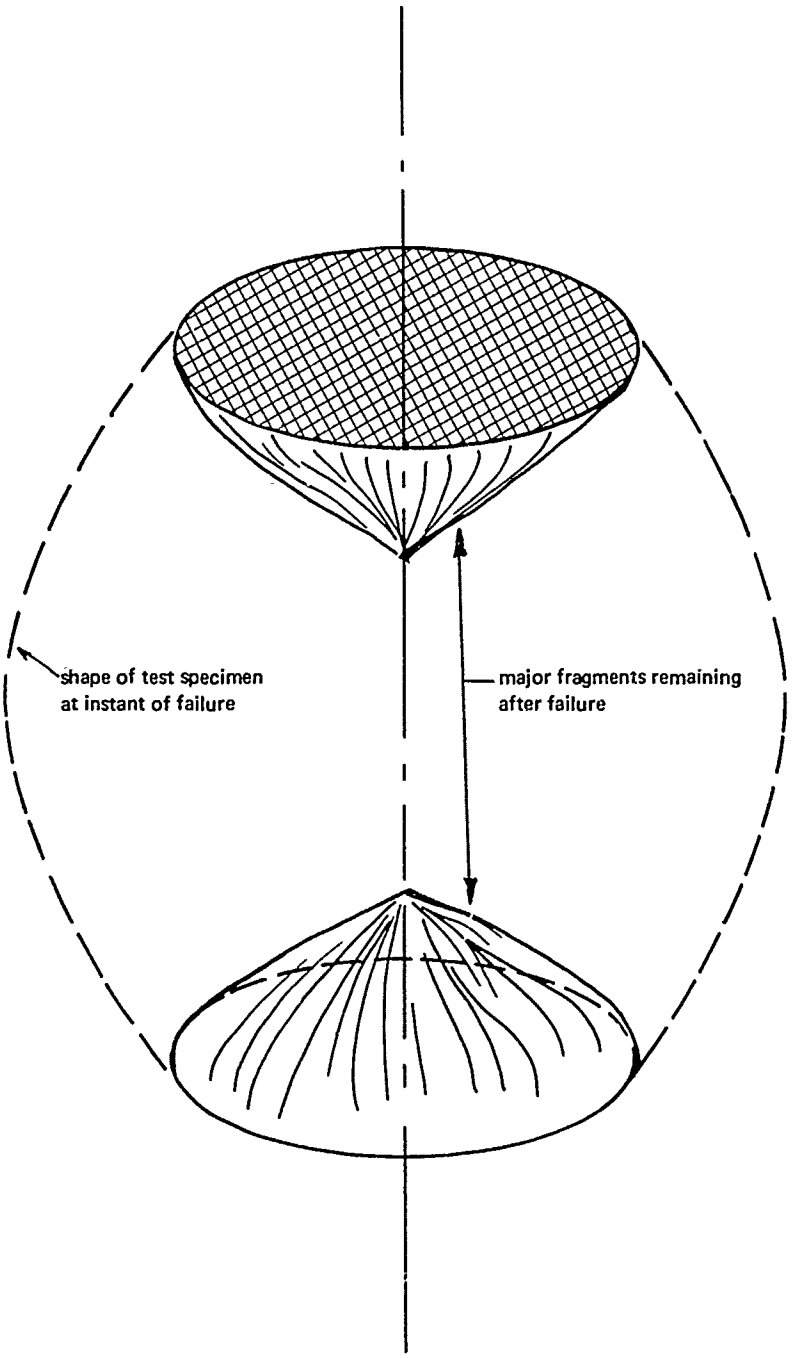

Figure A-8. Shape of fragments remaining after failure of cylindrical test specimen under uniaxial compression.

Appendix B

MECHANICAL PROPERTIES OF 4-INCH-THICK CAST ACRYLIC PLATE

The spherical windows tested in this study were machined from 4.0-inch-thick plates of acrylic plastic. The large hemispherical window specimens were cut with their central axis perpendicular to the polished surface of the plates as this was the only way that hemispherical windows of 2.750-inch internal radius could be machined from plate only 4 inches thick. However, the 30-degree spherical angle windows were machined with their central axis parallel to the polished surface of the plate, as in this manner more specimens could be cut from a given piece of acrylic plate.

Since at one stage of the manufacturing of acrylic plates, acrylic in a liquid state is poured into molds between sheets of glass and allowed to harden, it was conceivable that as a result of sedimentation of denser liquids or variation in hardening time at different planes in the plate that the physical properties of acrylic would vary between the axial and transverse axis of the plate. To find whether specimens which have been cut with their axis along different directions in the plate have the same physical properties, cylindrical specimens were selected to be tested in axial compression. Six cylindrical specimens, half of which were cut with major axis parallel and half with major axis perpendicular to the polished surface of the acrylic plate (Figure B-1), were tested at room temperature (75^{o} to 80^{o}F) in a 400,000-pound-capacity Baldwin-Tate-Emery Universal Testing Machine, at the rate of 1,450 psi/min. The dimensions of the cylinders, 4.00 inches in length and 2.00 inches in diameter, were chosen to permit cutting the specimens from a 4-inch-thick plate of grade "G" Plexiglas. This was the same material from which all spherical windows were made; dimensions of the test cylinders conformed to ASTM Specification DG95-63T.

The testing procedure was identical to that set forth in Appendix A, except that the loading rate was constant for all specimens. After conclusion of tests, the magnitudes of strains were compared to determine whether any significant differences existed between strain values measured on the different test cylinders. A comparison of results disclosed no significant differences in compressive strengths of test cylinders (Figure B-2), regardless of their orientation in the plate prior to machining. Because of the insignificant variation in strain of the cylindrical specimens cut along different axes in plate it can be safely assumed that for the current spherical window study no variables have been introduced into the experimental program by having the windows machined from the acrylic plate along different planes.

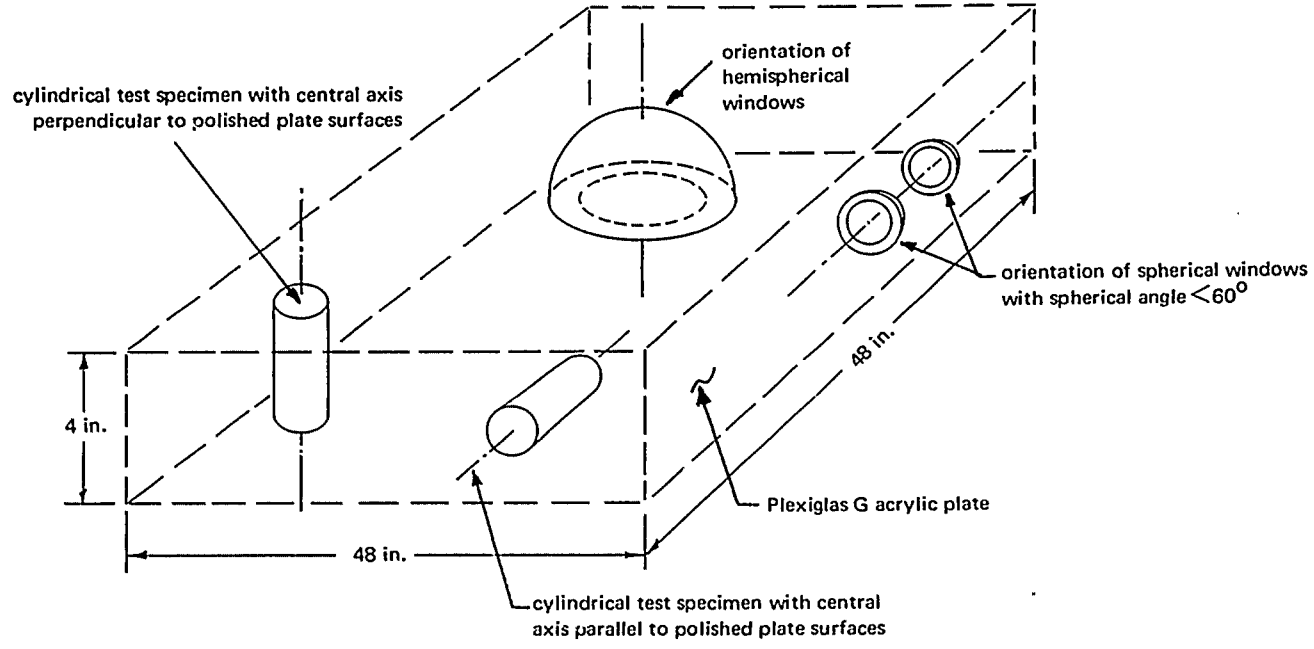

Figure B-1. Orientation of window and cylindrical test specimen axis with respect to material stock surfaces prior to machining operations.

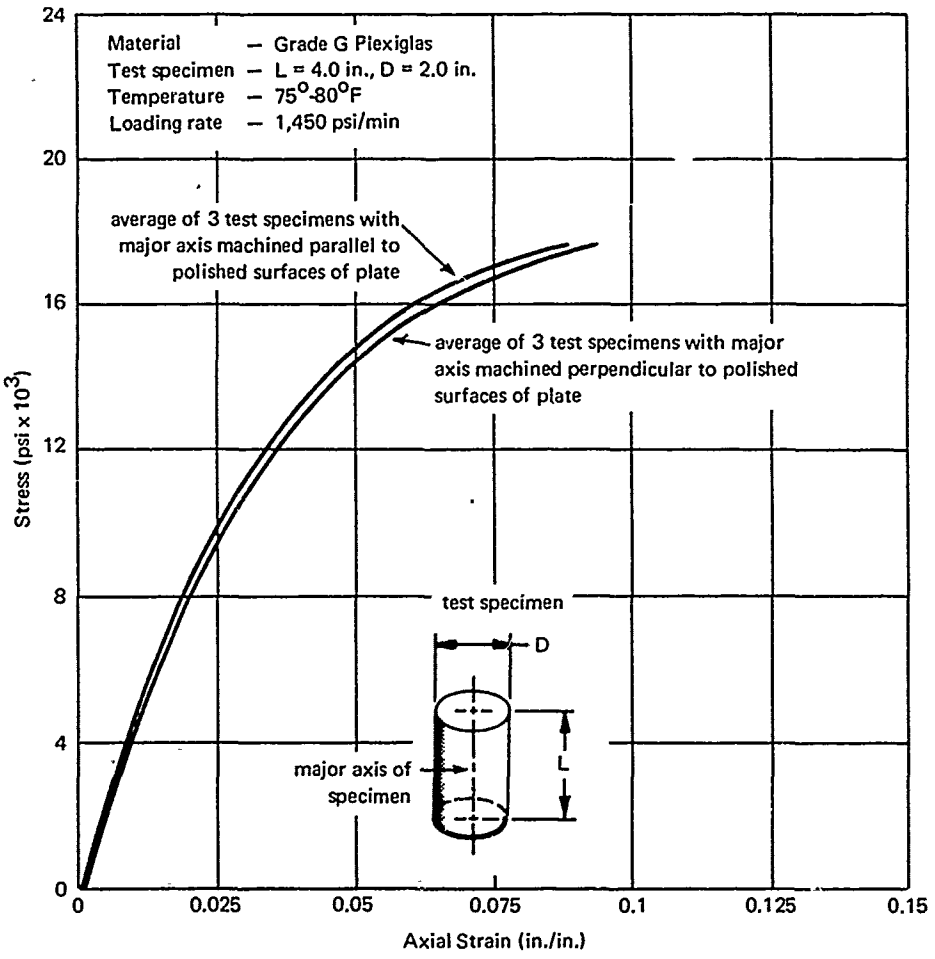

Figure B-2. Axial strains in acrylic test specimens under uniaxial compression.

Appendix C

EFFECT OF TEMPERATURE ON THE CRITICAL PRESSURE OF SPHERICAL SHELL ACRYLIC WINDOWS

It is a known fact[5] that the compressive strength of acrylic plastic increases with a decrease of temperature under which it is tested. Previous studies[1] performed at NCEL confirmed this by showing that the critical pressures of conical acrylic windows under short-term hydrostatic pressure loading were influenced by changes in temperature. For this reason, it was deemed necessary also to explore the influence of temperature on the critical pressure and displacement of spherical acrylic windows.

To find this effect, a group of four windows with 180-degree spherical angles, internal radii of 2.750 inches, and nominal thicknesses of 0.750 inch were tested in the temperature range of 50°F to 52°F. The testing procedure for the low-temperature specimens was identical to that used in the standard test series, except for the water temperature.

The change in pressurizing-medium temperature influenced both the magnitude of strains as well as critical pressure of windows tested. The strains in windows exposed to the low-temperature pressurization medium were found to be less by approximately 20% to 40% than in identical windows tested in the 69°F-to-70°F temperature range (Figure C-1). The average critical pressures of the window specimens tested in the low-temperature range (Table C-1) were found to be higher than the average critical pressure of identical windows in 69°F-to-70°F temperature range (Table C-2) by 17%, or 2,042 psi. The standard error of the difference between means for the critical pressure resulting from the low and standard temperature tests was calculated to be 102 psi. Since the difference between the average critical pressures of windows in the low and standard temperature ranges was 2,042 psi, it can be concluded that the difference is significant and not due to scatter of test data. Because no additional variable was introduced into the tests other than water temperature, it can be assumed that the difference in average critical pressure between the 51°F and 70°F temperature test groups was caused by the influence of low temperature on the mechanical properties of acrylic plastic.

Table C-1. Axial Displacement and Critical Pressure of Windows Tested at Average Temperature of 52°F

Specimen No.	Temperature (°F)	Pressurization Rate (psi/min)	Axial Displacement of Center Point on Low-Pressure Face (in.) at a Pressure (psi) of—													Pressure at Failure (psi)
			1,000	2,000	3,000	4,000	5,000	6,000	7,000	8,000	9,000	10,000	11,000	12,000	13,000	14,000	
153	50	675	0.000	0.000	0.002	0.022	0.034	0.051	0.070	0.089	0.104	0.132	0.169	0.209	0.296	–	13,900
154	52	660	0.010	0.026	0.040	0.052	0.066	0.081	0.098	0.115	0.140	0.162	0.198	0.245	0.308	–	13,850
155	52	663	0.002	0.012	0.025	0.039	0.052	0.066	0.082	0.098	0.120	0.146	0.178	0.220	0.285	0.410	14,100
156	51	634	0.008	0.024	0.035	0.048	0.061	0.075	0.091	0.108	0.128	0.152	0.181	0.254	0.283	0.350	14,200
Max Value	52	675	0.010	0.026	0.040	0.052	0.066	0.081	0.098	0.115	0.140	0.162	0.198	0.254	0.308	–	14,200
Avg Value	51	665	0.005	0.016	0.025	0.040	0.053	0.068	0.085	0.103	0.123	0.148	0.187	0.232	0.293	–	14,012
Min Value	50	660	0.000	0.000	0.002	0.022	0.034	0.051	0.070	0.089	0.104	0.132	0.169	0.209	0.283	–	13,850

Table C-2. Axial Displacement and Critical Pressure of Windows Tested at Average Temperature of 69°F

Specimen No.	Temperature (°F)	Pressurization Rate (psi/min)	Axial Displacement of Center Point on Low-Pressure Face (in.) at a Pressure (psi) of—											Pressure at Failure (psi)
			1,000	2,000	3,000	4,000	5,000	6,000	7,000	8,000	9,000	10,000	11,000	12,000	
117	69	667	0.023	0.035	0.047	0.063	0.079	0.096	0.110	0.141	0.172	0.223	0.283	–	11,750
118	69	645	0.003	0.014	0.028	0.040	0.055	0.071	0.089	0.111	0.138	0.175	0.241	0.325	12,300
119	70	660	0.017	0.031	0.046	0.061	0.077	0.094	0.110	0.140	0.172	0.215	0.277	–	11,850
120	69	660	0.023	0.038	0.051	0.064	0.080	0.096	0.116	0.140	0.168	0.210	0.272	0.380	12,850
121	70	658	0.018	0.033	0.047	0.061	0.078	0.095	0.115	0.140	0.171	0.213	0.292	–	11,900
Max Value	70	667	0.023	0.038	0.051	0.064	0.080	0.096	0.116	0.141	0.172	0.223	0.292	–	12,300
Avg Value	69	658	0.017	0.030	0.044	0.058	0.074	0.090	0.109	0.134	0.164	0.207	0.273	–	11,970
Min Value	69	645	0.003	0.014	0.028	0.040	0.055	0.071	0.089	0.111	0.138	0.175	0.241	–	11,750

Since only one group of windows with a t/R_i ratio of 0.272 and a 180-degree spherical angle was tested at 51 ± 1°F temperature, it is not known how much the critical pressures of spherical windows with different t/R_i ratios and angles are increased in 51°F temperature environment. Furthermore, it is not known how much further the critical pressure will increase if the temperature of the pressurizing medium decreases to the 32°F-to-34°F temperature range typical of deep ocean environment. It can be postulated, however, that since it is known that the strength of acrylic plastic increases with a decrease in temperature environment (regardless of whether the material is tested in tension, flexure, shear or compression[5]), the critical pressure of any acrylic spherical window will increase also in such an environment since all the windows fail by one, or a combination of these failure mechanisms.

Thus it can be concluded that the critical pressures plotted in the main body of the report represent conservative values, as the critical pressures of spherical acrylic windows in the 32°F-to-34°F temperature environment found in ocean depths will be higher. The magnitude of the critical pressure increase is unknown, but predictions based solely on the increase of material strength place it in the 15%-to-25% range

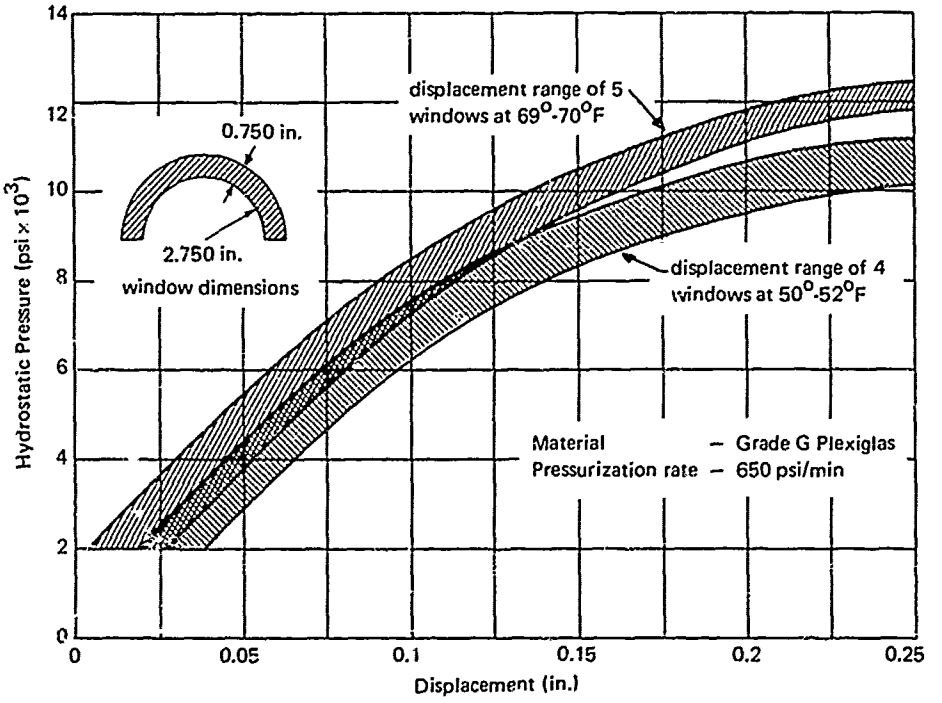

Figure C-1. Axial displacements of spherical acrylic windows tested under short-term hydrostatic pressure at different temperatures; $t/R_i = 0.273$, $\alpha = 180$ degrees.

Appendix D

OPTICAL PROPERTIES OF SPHERICAL SHELL ACRYLIC WINDOWS

DISCUSSION

The fundamental reason for existence of windows in hydrospace structures is to permit the observation of the surrounding hydrospace. An ideal hydrospace window would be strong enough to withstand the pressure found in the deepest part of the ocean, and at the same time would absorb very little light, cause no distortion of the image, require only a small penetration in the hull, and afford the observer a large field of view. Currently the most widely used shape of hydrospace windows is a 90-degree angle cone frustum, and the material utilized is acrylic plastic. Although the conical windows possess many good features, like good resistance to implosion for a given t/D_i ratio, ease of fabrication, and fairly large field of vision for a given hull penetration diameter, their optical properties leave a lot to be desired. The major optical shortcomings of conical windows are a severe image distortion when the observer's eye is close to the window's low-pressure face and a relatively small field of vision when the observer's eye is one or two window diameters away from the low-pressure face. Thus, for example, to utilize the 90-degree field of vision afforded by the 90-degree conical window, the observer has to have his face against the window surface with the resulting distortion of image. This distortion is caused by the difference in length of paths that the rays must traverse through a thick conical window when the eye is against the low-pressure face of the window. When the observer steps back from the window in order to minimize the distortion, he finds that his field of vision decreases from a 90-degree cone to 30 degrees or less, depending on his distance from the window. Thus the observer is forced to continually trade off field of vision for lack of distortion.

A different problem presents itself when spherical shell* windows are substituted for conical windows. In the spherical window, having the high- and low-pressure surfaces concentric to each other permits undistorted viewing of hydrospace when the observer's eye is located at the window's center of curvature. Since binocular vision is desirable, spherical windows with large radii are desirable. Use of large radius windows decreases the image distortion introduced by the impossibility of placing both eyes simultaneously in the center of curvature.

* For brevity these windows are usually referred to simply as "spherical windows" in this report.

While achievement of a 90-degree field of vision through the use of 90-degree conical windows is rather difficult because of the uncomfortable proximity to the window's surface that the observer must maintain, such a wide field is quite easy to attain with spherical windows. In fact, achievement of a 120-degree or even 150-degree field of vision through use of spherical windows is relatively easy and comfortable because the observer's eye is not required to be any closer to the window's surface than the distance between center of curvature and window's low-pressure surface. Although spherical windows of any radius of curvature can be employed in hydrospace structures, it is desirable for comfortable monocular viewing to use a radius of internal curvature longer than 7 cm, while for binocular vision the radius should be longer than 30 cm.

Severe image distortion results when spherical windows in the shape of a hemisphere are used for hydrospace observation with the observer removed from the center of curvature. When the observer is placed five to ten radii of curvature away from the window's low-pressure face, no image distortion is noticeable when the field of vision is limited to less than 5 degrees (Figure D-1). Very noticeable distortion appears at the periphery of the field of vision when the field of vision is enlarged to 10 degrees. The distortion becomes unbearable when the field is further increased beyond the 10-degree angle (Figure D-2). Thus it would appear that windows with spherical sector angles larger than 30 degrees are desirable only when the observer will perform most of his observations from a place only one to two radii of curvature removed from the window's low-pressure surface. If frequent observations are also to be conducted from a position five to ten radii away from the window's surface, a spherical window with spherical sector angle of 30 degrees or less is recommended, as any part of the image beyond the 10-degree field of vision will be severely distorted.

An interesting feature of spherical acrylic windows is that they act as true optical lenses producing erect images whose magnification can be calculated. For the purposes of this report, several simplifying assumptions have been made in order to make the following derivation of the lens magnification more mathematically manageable. Because of the simplifications made in the derivation, the resulting plotted data is to be used only as a first approximation of the actual lens magnification. For precise calculation of optical properties for a spherical window of given dimensions a special computation, quite beyond the scope of this report, is to be made that includes not only the determination of magnification but also of distortion.

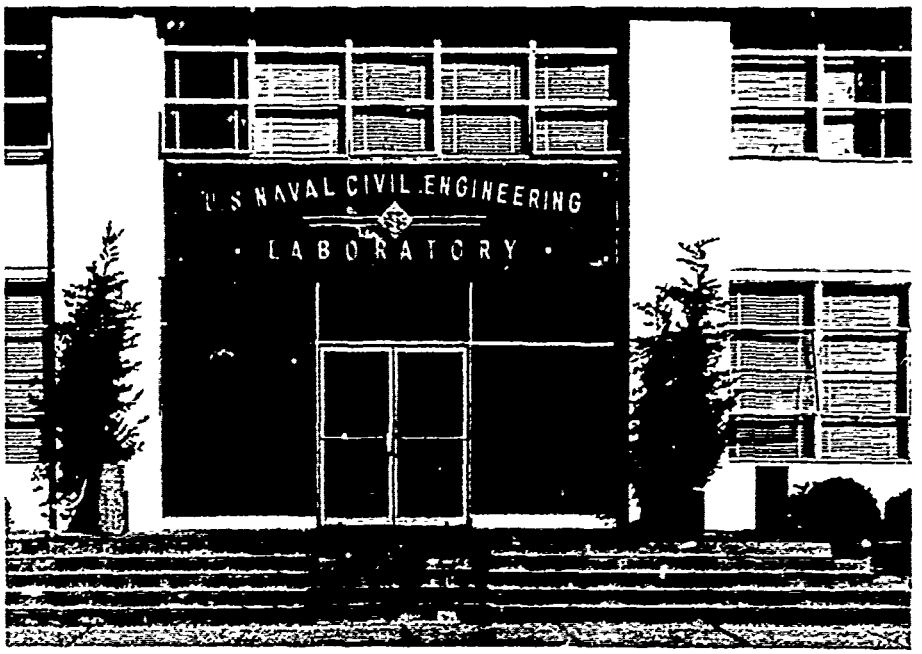

Figure D-1. View through a spherical acrylic window with internal curvature of 7 cm and external curvature of 9.5 cm. The observer's eye is located at the center of the curvature of the window.

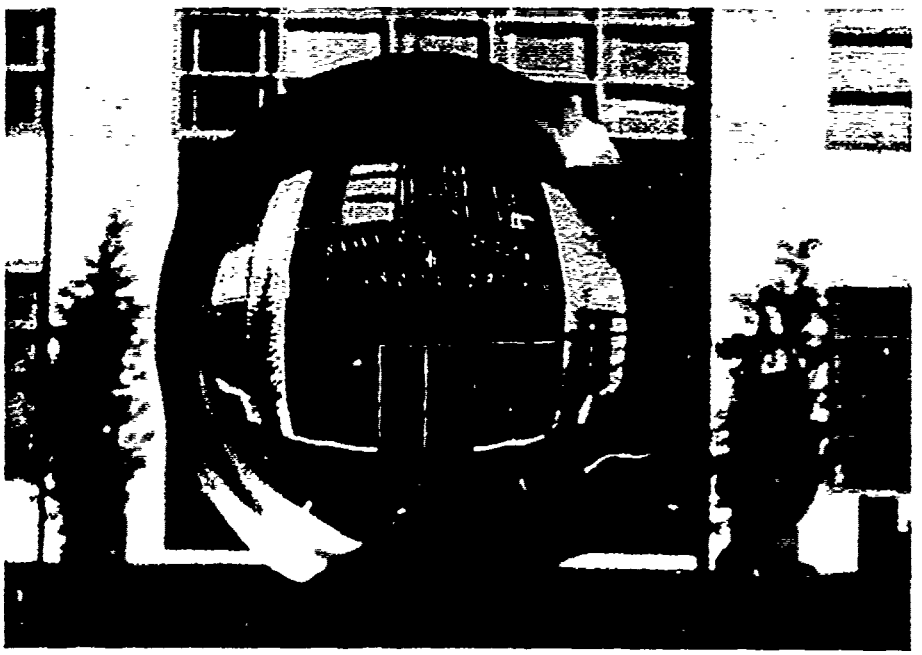

Figure D-2. View through a spherical acrylic window with internal curvature of 7 cm and external curvature of 9.5 cm. The observer is located 100 cm away from the window.

Calculation of Spherical Window Magnification*

The focal length of a thin** lens is given by***

$$\frac{1}{f} = \left(\frac{n_1}{n_2} - 1\right)\left(\frac{1}{R_o}\right) - \left(\frac{n_1 - n_0}{n_2}\right)\left(\frac{1}{R_i}\right) \qquad (1)$$

where n_1, is the index of refraction of the lens; n_0 and n_2 are the indices of refraction of the media to the right and left, respectively; R_0 and R_i are the radii of curvature of the left and right surfaces, respectively. Figure D-3 is a schematic of the spherical-shell lens in which the left-hand medium is water (n_2 = 1.333), and the right-hand medium is air (n_0 = 1). The radii, R_0 and R_i, are both positive since the center of curvature is to the right of the lens.

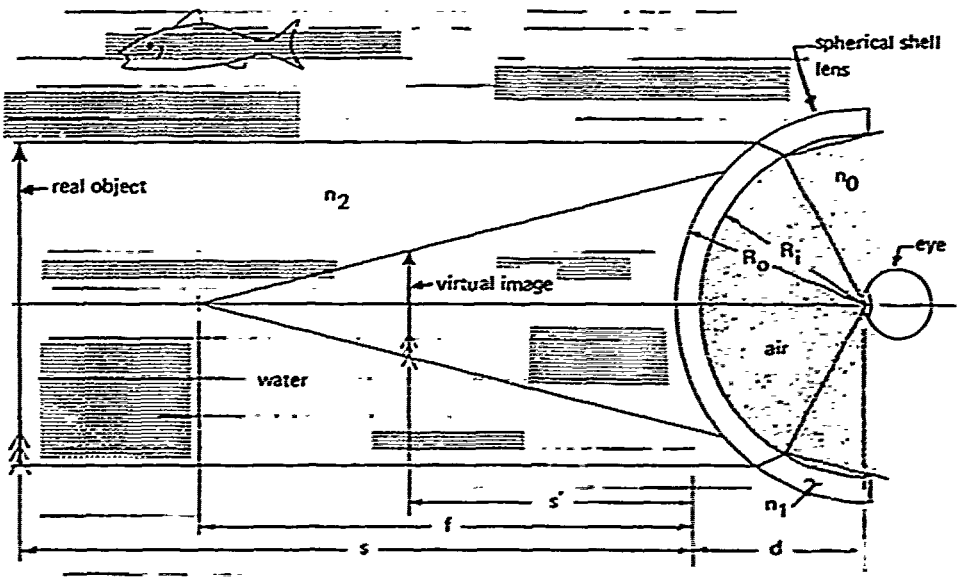

Figure D-3. Schematic of spherical window's lens optics.

---

* The section on calculation of spherical window magnification was written by Mr. R. D. Hitchcock, NCEL.

** A lens is considered "thin" if its thickness is small compared to its focal length.

*** This formula applies strictly to paraxial rays (i.e., rays at an angle, γ_o, with the optic axis where $\sin \gamma_o \cong \gamma_o$); for $\gamma > \gamma_o$, the results are sufficiently accurate for purposes of this analysis.

Because $R_0 > R_i$ and $n_1 > n_0$, the focal length, f, is negative for $n_2 \geq 1$; i.e., the spherical shell is a diverging lens. Thus, for any positive* object distance (s), the erect image distance (s′) must be negative* as shown by the relation

$$\frac{1}{f} = \frac{1}{s} + \frac{1}{s'} \tag{2}$$

With the object in the medium to the left of the lens (i.e., in the water), the lateral magnification of the system of Figure D-3 is computed as follows:

m_1 = lateral magnification of spherical shell

$$= \left(\frac{-s'}{s}\right)\left(\frac{n_2}{n_0}\right) \tag{3}$$

m_2 = lateral magnification of eye, with virtual image acting as real object

$$= \frac{-s'_e}{d - s'} \tag{4}$$

where s'_e is the image distance of the eye and is constant.** Hence, the lateral magnification M of the system is

$$M = m_1 m_2 = \left(\frac{-s'}{s}\right)\left(\frac{-s'_e}{d - s'}\right)\left(\frac{n_2}{n_0}\right)$$

Substituting the expressions for s′ as obtained from Equation 2, we get

$$M = \frac{s'_e\left(\frac{n_2}{n_0}\right)}{\left(\frac{ds}{f}\right) - (s + d)} \tag{5}$$

---

* By convention, s is positive if the object is to the left of the lens; s′ is positive if the image is to the right of the lens, a negative s′ means a virtual image.

** The focal length of the eye is changed involuntarily; and it is the image distance which must be considered in computing lateral magnification.

For the case of a plane window, $f = \infty$, and

$$M_\infty = \left(\frac{-s'_e}{s + d}\right)\left(\frac{n_2}{n_1}\right) \tag{6}$$

Dividing Equation 5 by Equation 6 and noting that $f < 0$ for this problem gives the relative magnification

$$M_r = \frac{s + d}{\left(\frac{sd}{|f|}\right) + (s + d)} \tag{7}$$

Equation 7 is plotted in Figures D-4 through D-6 as a function of object distance, s.

Equation 7 shows that as d varies from zero to ∞, M_r varies from unity to $f/(s + |f|)$ monotonically. The relative magnification,* M_r, is the ratio of the lateral dimension of an object as seen through the lens to that of the object when the lens is replaced by a plane window of same thickness and material.

When one studies briefly Figures D-4 through D-6, several phenomena become apparent. It becomes obvious that the relative magnification of the spherical window is always less than 1 when the observer is either at the center of curvature or further back of it. The decrease of the object image varies with the shell thickness, the distance of the observer from the window's low-pressure surface, the distance of the object from lens, and the radius of sphericity of the window. Scaling the window dimensions, i.e., changing R_0 and R_i such that R_0/R_i = constant, will change the relative magnification for a given s and d. Increasing the radii causes the spherical shell to approach a plane window and hence, M_r to approach unity, decreasing the radii causes M_r to approach zero.

In general it appears that the size of image of an object in water viewed through a spherical window is minimized when the object is far from the high-pressure face, the viewer is far back from the low-pressure face, the radius of window curvature is short, and the thickness of the window is considerable. The size of image is maximized when the object in water is close to the high-pressure face of window, the observer in the submersible is close to the low-pressure face of the window, the radius

* The true magnification is $(n_2/n_0)\, M_r$; this is the well-known feature of underwater optics, namely, a submerged object is enlarged in proportion to the refractive-index ratio for paraxial observation through a plane surface.

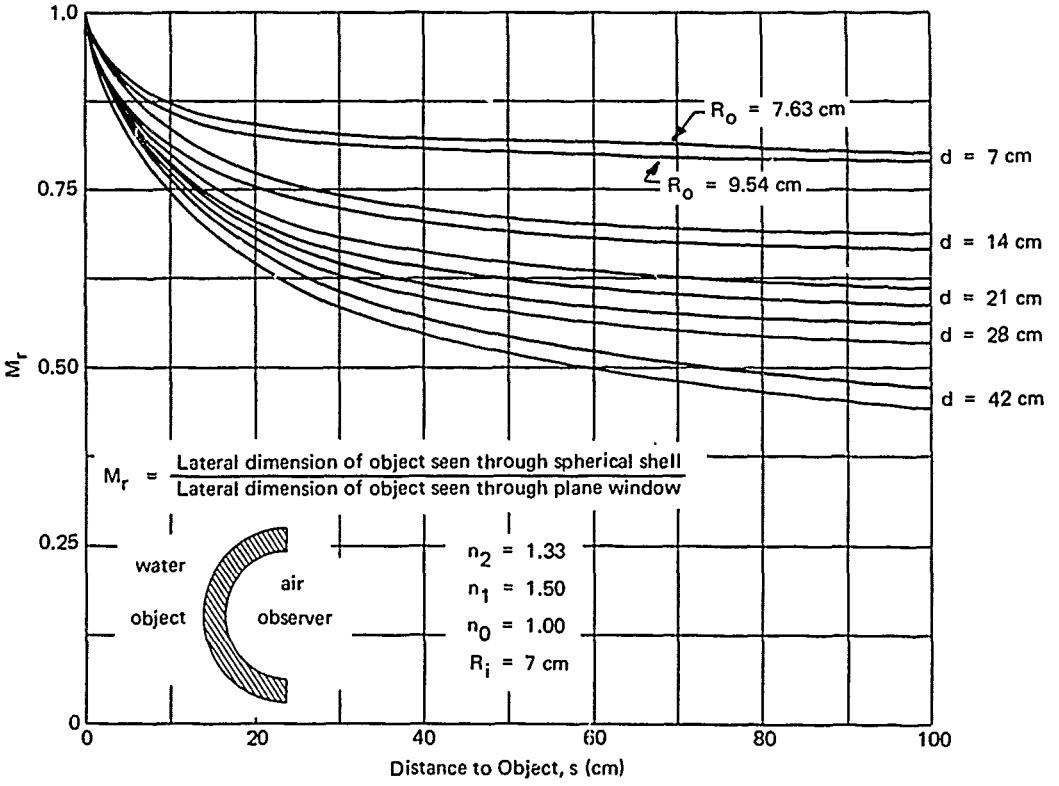

Figure D-4. Apparent magnification of objects in water viewed through acrylic spherical windows with internal curvature of 7 cm.

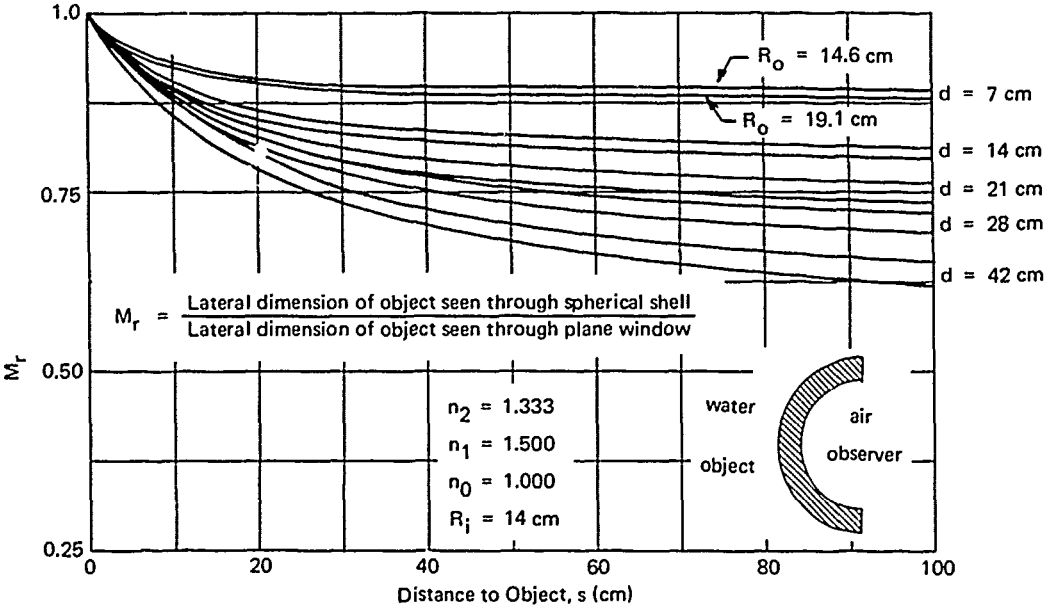

Figure D-5. Apparent magnification of objects in water viewed through acrylic spherical windows with internal curvature of 14 cm.

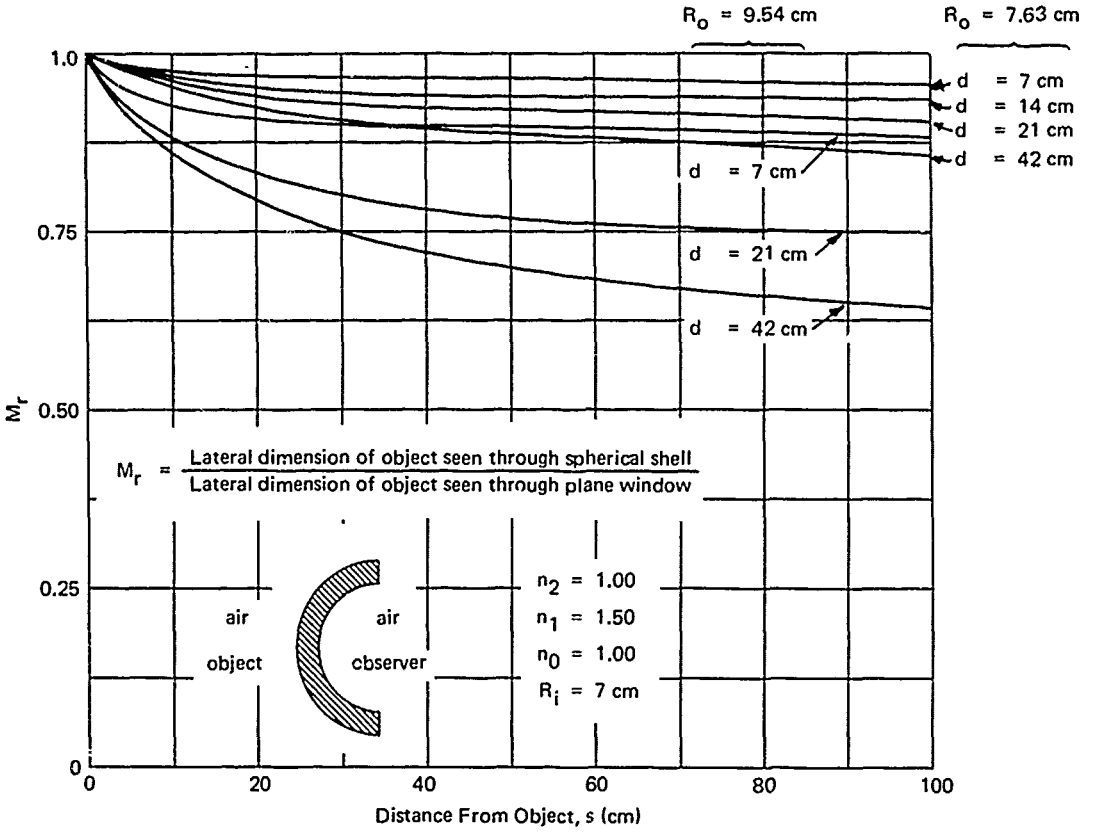

Figure D-6. Apparent magnification of objects in air viewed through acrylic spherical windows.

of window curvature is large, and the window is thin. In general though, so long as the object viewed in water is more than two R_i radii away from the window, the observer is within one R_i radius of the window, and the thickness of the window is less than one-half of R_i, the objects will appear erect and approximately 20% smaller than they actually are; this decrease in magnitude will remain relatively constant even if the object moves further away from the window during observation.

The Figures D-4 and D-5, besides graphically depicting the magnification of spherical windows with R_i equal to 7 or 14 cm, can be also used to predict the magnification of spherical windows with different R_i—so long as proper scaling procedures are observed. The basis of the scaling procedure in this case is the division of all dimensional variables appearing on the graphs by the R_i for which the curves are plotted, so that they become R_0/R_i, d/R_i and s/R_i. Once this is done the magnification of the spherical windows can be predicted. Thus, for example, the magnification of a spherical window with R_i = 28 cm and R_0 = 38.2 cm at s = 56 cm and d = 28 cm is the same as for the spherical window (Figures D-4 and D-5) with R_i = 7 cm, R_0 = 9.54 cm, s = 14 cm and d = 7 cm because the R_0/R_i,

s/R_i and d/R_i ratios are in both cases the same.* Because the data calculated for R_i = 7 cm and R_i = 14 cm can be scaled, the plotted magnification values on Figures D-4 and D-5 will be found to be very helpful in any design feasibility studies involving spherical windows for submersibles.

For those applications where spherical windows may be utilized for separating a pressurized air environment from a nonpressurized one, as in the case of decompression chambers, the magnification of spherical windows has been calculated with air being in contact with the low- and high-pressure faces of the windows (Figure D-6). Comparison of object magnification when air is on both sides of window, versus magnification when the high-pressure face is wetted by water shows that the presence of water makes the erect image of the object appear to be smaller than when water is absent.

* This can be seen by dividing numerator and denominator of the right side of Equation 7 by R_i. The result is: M_r = constant, provided R_0/R_i, s/R_i, and d/R_i are constant.

Appendix E

SCALING OF SPHERICAL SHELL ACRYLIC WINDOWS

OBJECTIVE

Model windows with R_i of 2.750 inches were used in the primary investigation for economy and because small pressure vessels capable of hydrostatically testing such specimens to destruction were available. Theoretical considerations based on known laws of structural mechanics indicated that the test results generated with model windows are applicable either directly or indirectly with the help of a scaling factor to full-scale spherical windows. It remained to prove experimentally that the theoretical considerations on which this premise rested were valid for spherical windows of viscoelastic material.

TEST SPECIMENS

The validation of the experimental data generated with model windows for applicability to large-scale windows was conducted with two separate series of full-scale windows (Table E-1). For the first series of windows an internal radius of 6.200 inches and spherical sector angle (α) of 60 degrees were chosen. These dimensions permitted the fabrication of the whole window series by machining 4-inch-thick commercially available grade "G" Plexiglas plate. Since the model windows were machined also from 4-inch-thick Plexiglas plate, the additional variable of a different window fabrication method would not be introduced. For the second series of full-scale windows (Figure E-1) an external radius of 33 inches and spherical sector angle of 72 degrees was chosen. The choice of that particular spherical radius and spherical sector angle was based on two factors: availability of a vacuum mold with 33-inch radius of curvature and the 48 x 48-inch size of the largest commercially available acrylic plates of 2.5- and 4-inch thickness from which the molding blanks could be cut. Because of these two limitations the largest spherical sector angle that could be specified was 72 degrees. Since the thickest available acrylic plate is only 4 inches thick, the t/R_i ratios and thus critical pressures of these windows are relatively low. Their importance, however, does not lie in the magnitude of their critical pressure but in the fact that they were molded, rather than machined from a casting, and that they represent the maximum size spherical window that can be built today from

Table E-1. Specifications for Full-Scale Spherical Acrylic Window Test Specimens

Internal Spherical Radius, R_i (in.)	Spherical Sector Angle, α (deg)	Low-Pressure-Face Diameter, D_i (in.)	Nominal Thickness, t (in.)	t/R_i Ratio	t/D_i Ratio
6.200	60	6.200	0.564	0.091	0.091
			1.127	0.182	0.182
			1.690	0.273	0.273
			2.254	0.364	0.364
			2.710	0.436	0.436
30.500*	72	35.868	2.500	0.082	0.069
29.000*	72	34.075	4.000	0.138	0.117

* R_o = 33 in.

Figure E-1. Largest acrylic spherical window tested at NCEL; R_o = 33 inches, spherical sector angle = 72 degrees, t = 2.5 inches

off-the-shelf commercial acrylic plate stock. Because these windows were formed in a mold with 33-inch curvature, the external radius is the same regardless whether the thickness is 4 or 2.5 inches. For this reason these windows are referred to by their R_o rather than R_i as is the case for machined windows whose R_i was held constant, while R_o varied depending on their thickness.

TEST ARRANGEMENT AND TESTING

The full-scale spherical acrylic windows were tested in steel flanges (Figures E-2, E-3, and E-4) similar in design to the flanges used in testing the model windows. This meant that the window seat in the flanges (Figures E-2 and E-4) was made sufficiently wide to provide the same measure of support to the sliding edge of the full-scale window as was provided in the model flanges for the model windows. The pressurization of windows with R_i = 6.200 inches took place in the same pressure vessel as the implosion testing of model windows, while the very large windows with R_o = 33 inches were tested in the 72-inch-ID pressure vessel. The test arrangement for the 33-inch-R_o windows differed considerably from the one used for the 2.750-inch-R_i and 6.200-inch-R_i windows. Where in the tests of the smaller windows only one opening in the flange was closed with a spherical acrylic shell, in the test arrangement for the 33-inch-R_o windows both openings in the flange were closed with spherical acrylic shells (Figure E-5). The drawback of this arrangement was that although two windows were simultaneously exposed to the hydrostatic pressure, the implosion pressure of a single window only would be available for the study, as both windows would not implode simultaneously. The advantage of this test arrangement that considerably overshadowed this drawback was that only a very light and inexpensive flange was required for the test. If a standard flange were used in which one opening is closed by the window while the other is closed by a steel bulkhead, the weight of the flange would be several thousand pounds heavier, and the flange would be at least twice as expensive.

One 33-inch-R_o window was instrumented with electric resistance strain gages (Figures E-6 and E-7) prior to implosion testing. The instrumentation leads were fed from the interior of the vessel to the readout and recording system by a rigid pipe that at the same time supported the whole window test assembly (Figure E-8). Since the catastrophic implosion of a large window inside the pressure chamber generates undesirable dynamic pressure loading on the vessel, steps were taken to minimize the magnitude of the dynamic pressure peak. This was accomplished by filling the space between the two windows with water vented to the exterior of the pressure vessel (Figure E-9). Thus, although the interior of the window

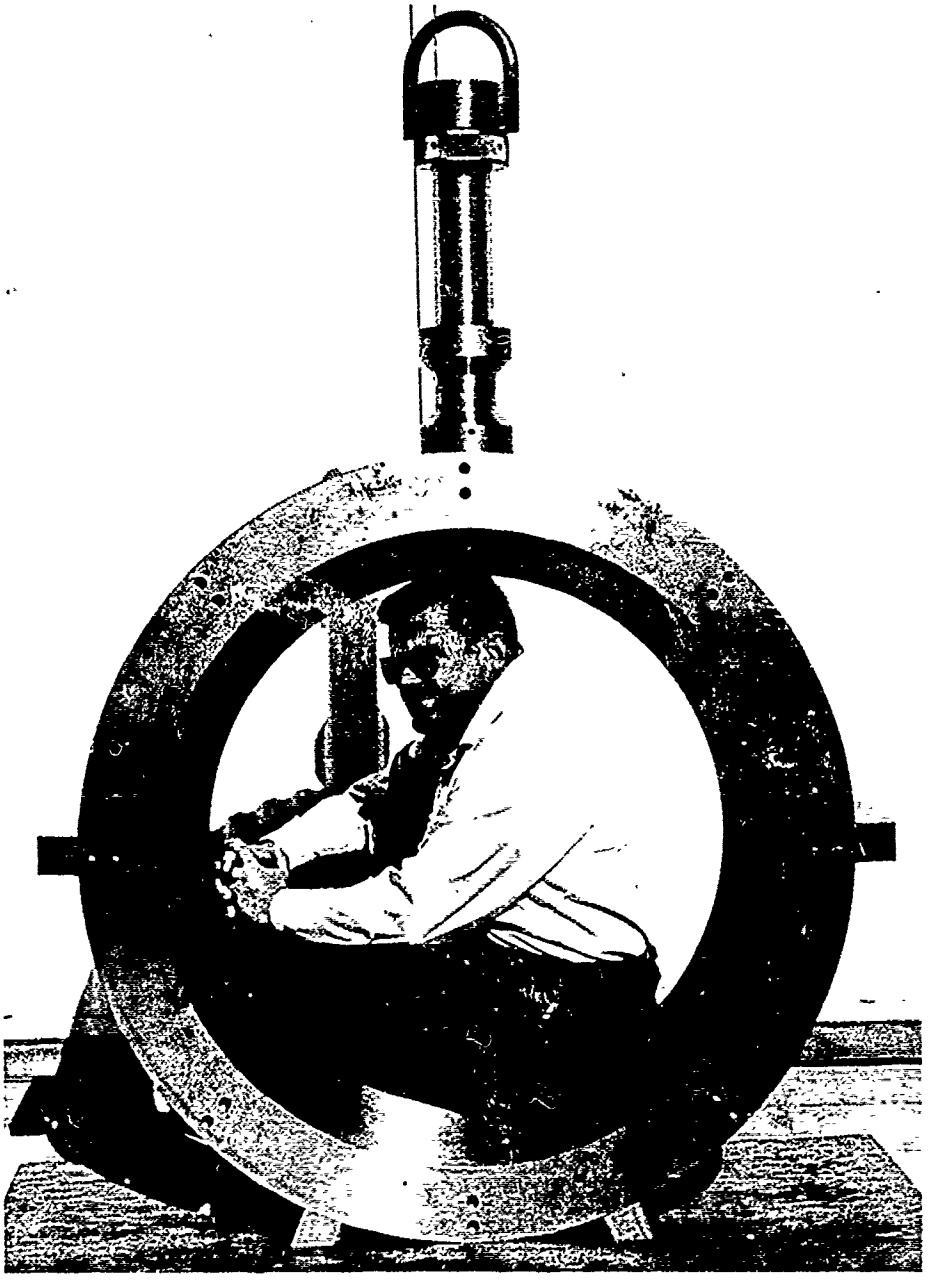

Figure E-2. Flange for testing spherical acrylic windows with R_o of 33 inches and 72-degree spherical sector angle.

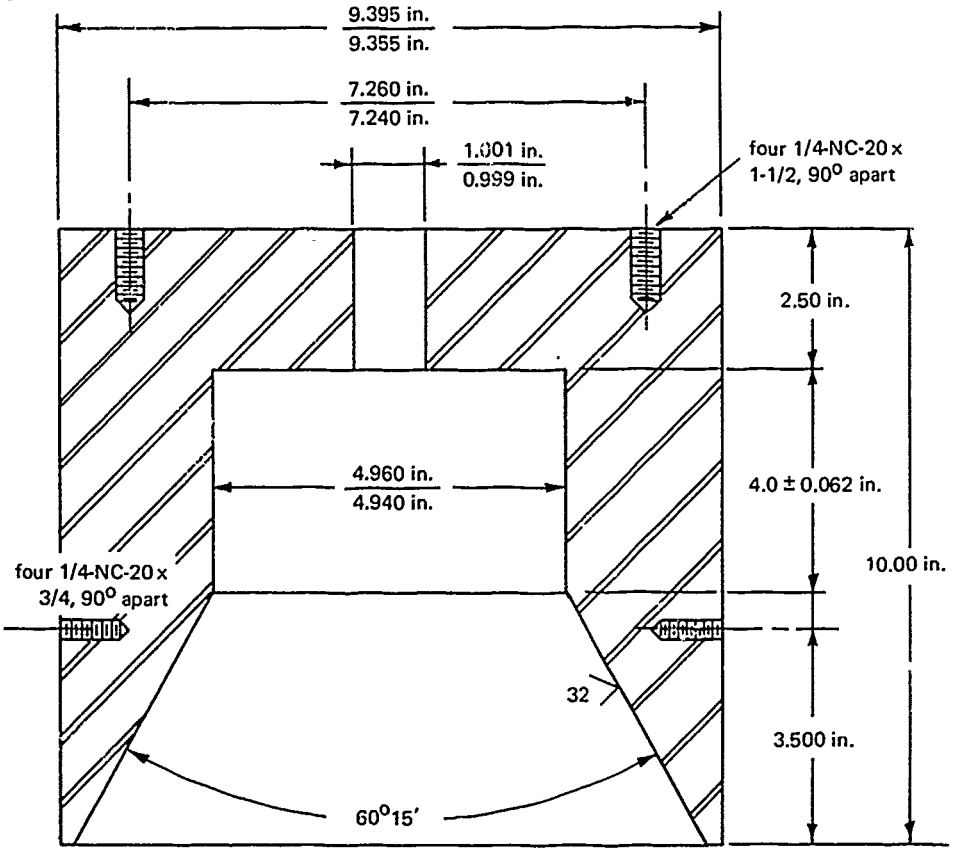

Figure E-3. Dimensions of flange for testing windows with R_i of 6.200 inches and 60-degree spherical sector angle.

test assembly was exposed to atmospheric pressure, an air-filled cavity was not present into which the water could surge upon implosion and generate a high dynamic pressure peak. In addition to mitigating the magnitude of shock wave, filling the test assembly interior with fluid permitted measurement of window displacement under hydrostatic loading. As the windows were deformed by hydrostatic pressure they displaced the fluid from the flange cavity through the vent pipe, which traversed the flange pipe hanger, to the exterior of the pressure vessel, where the volume of the fluid was measured. Upon implosion of one of the windows in the flange assembly, the water in its interior was ejected through the vent pipe and guided harmlessly to the exterior of the building by means of a duct that extended from the end closure on the pressure vessel to a vent in the roof (Figures E-8, E-9, and E-10). The windows were pressurized at a 650-psi/minute rate with tap water in the 68°F-to-70°F range. The pressure was raised at that rate until failure of the window occurred by implosion.

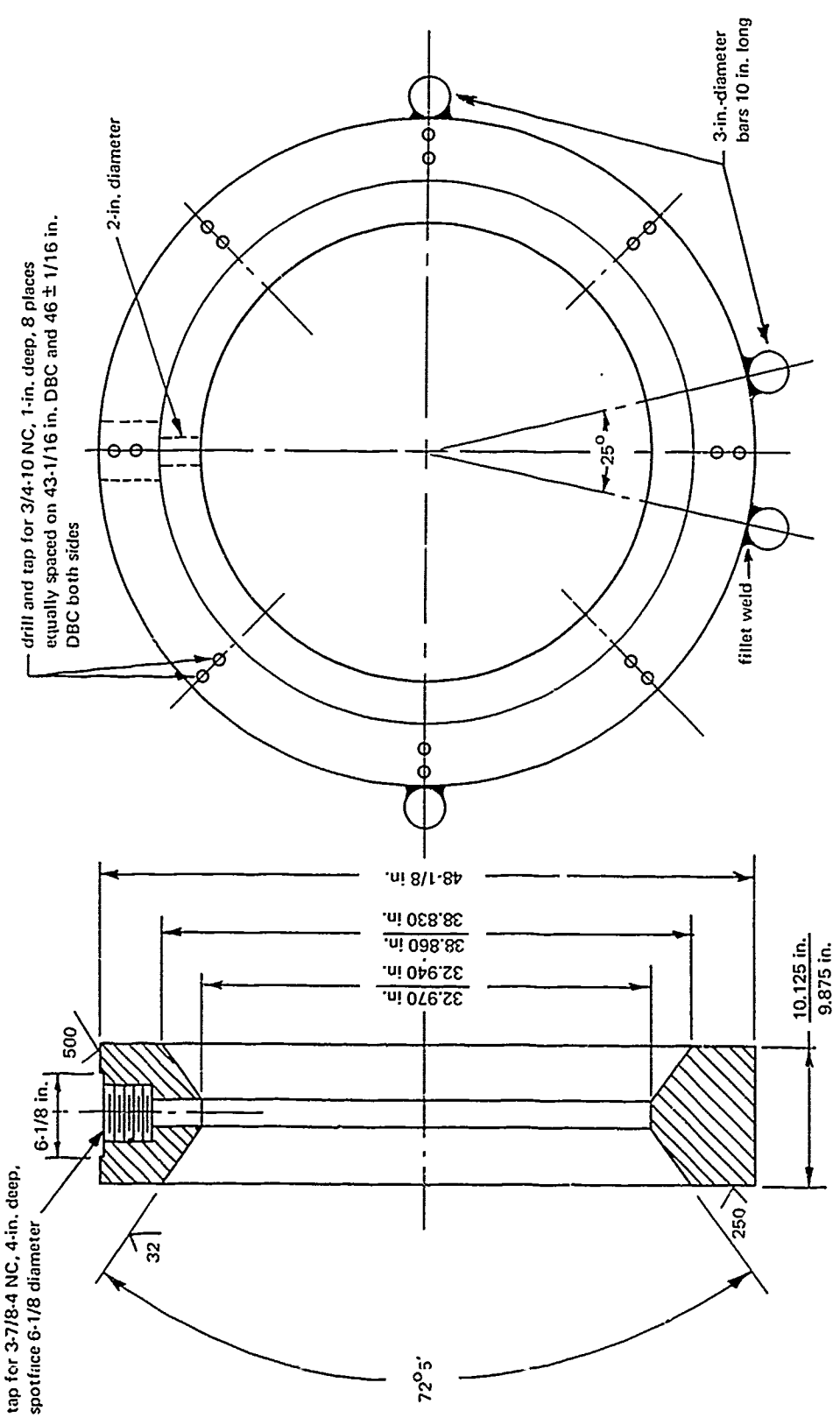

Figure E-4. Dimensions of flange for testing of windows with R_o of 33 inches and 72-degree spherical sector angle.

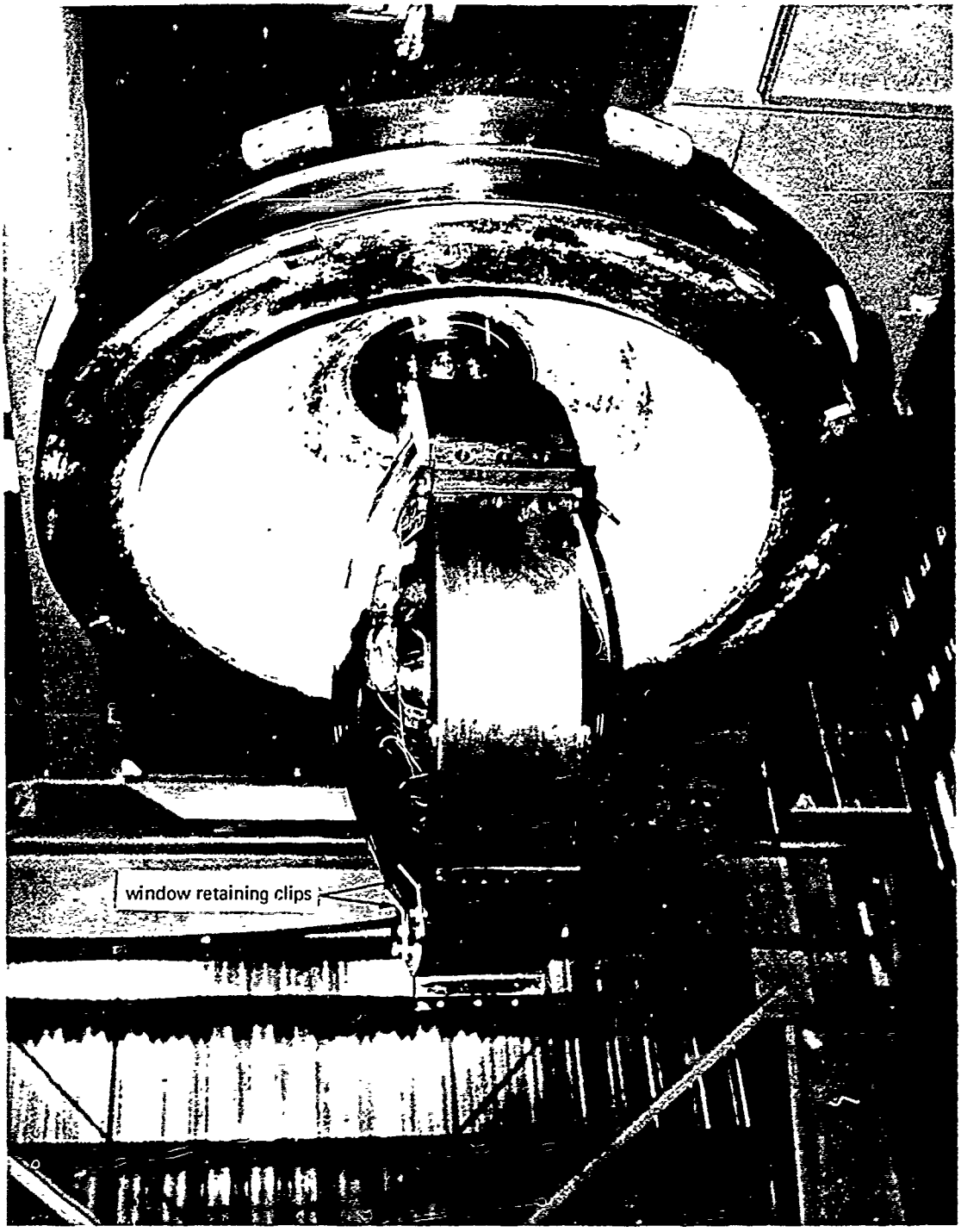

Figure E-5. Spherical window test assembly for very large windows with R_o of 33 inches attached to end closure of 72-inch-diameter pressure vessel at NCEL.

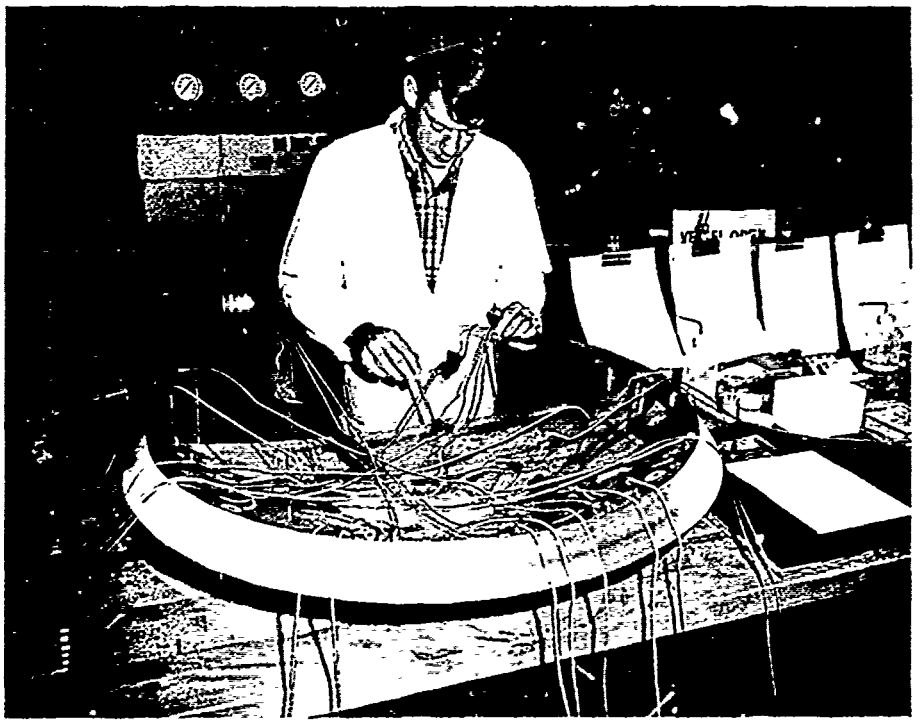

Figure E-6. Placement of electrical resistance strain gages on the spherical window with R_o = 33 inches.

TEST RESULTS

Window's With R_i = 6.200 Inches

Critical pressures of the full-scale windows with R_i = 6.200 inches were not identical but were close to pressures of model windows with R_i = 2.750 inches. The difference in critical pressure was in the 0%-to-20% range, the large windows generally failing at slightly lower pressures than the model windows (Figures E-11 and E-12). The difference in critical pressures is large enough to be significant, but not large enough to make the data generated with model windows inapplicable for prediction of safe operational pressures for large windows. No single proven explanation is available for the small difference in critical pressures between the model and full-scale windows. The safest explanation at the present time appears to be that the difference in critical pressures is caused by a combination of ordinary factors like minute differences in material properties, machining tolerances, flange seat finish, rigidity of window flanges, larger number of flaws in a large window than in a small window, a higher temperature rise in the window during pressurization because of disproportionate increase in mass of material versus heat transfer surface and others.

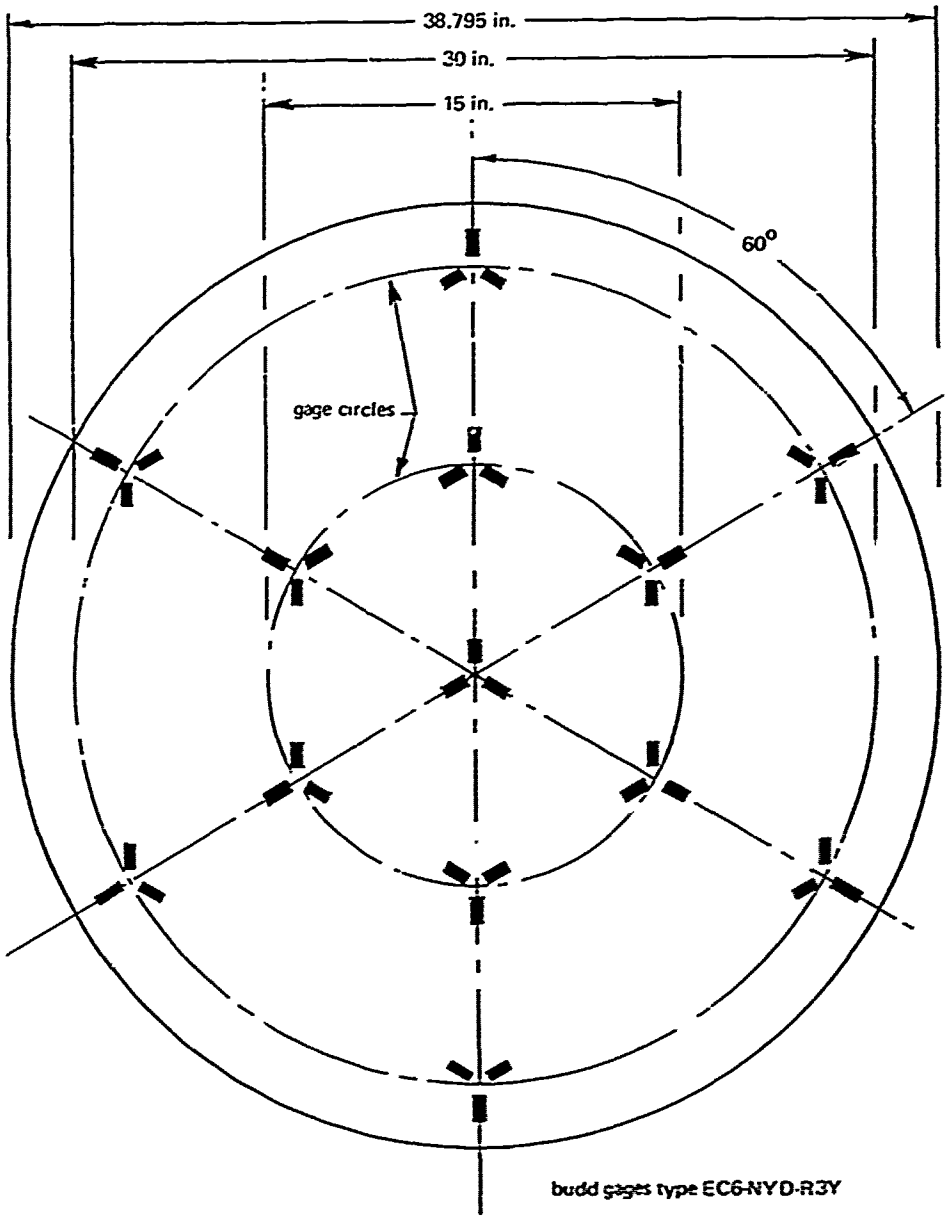

Figure E-7. Location of gages on the low-pressure face of the window with R_o = 33 inches.

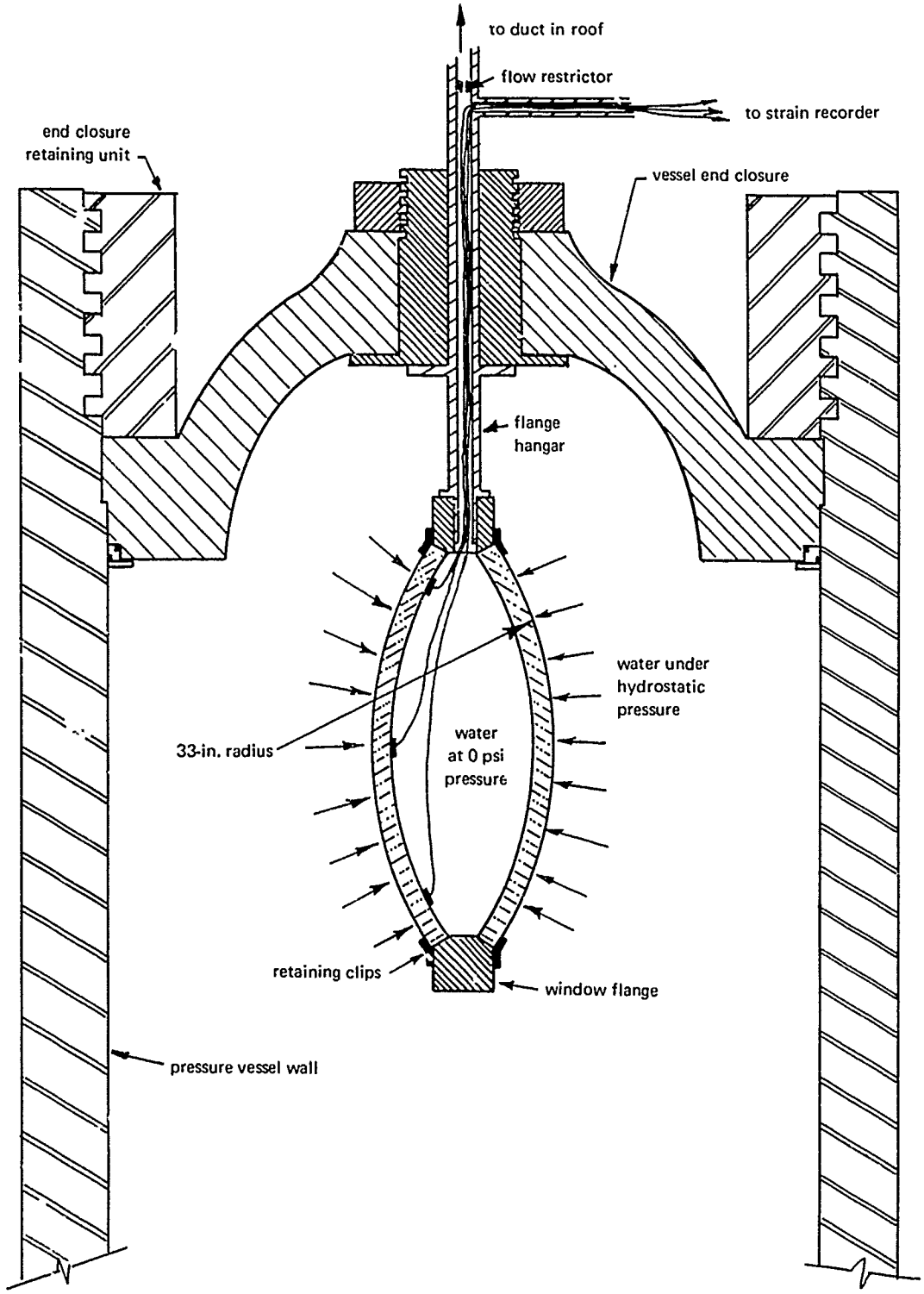

Figure E-8. Schematic of test assembly for very large spherical windows in the 72-inch-diameter pressure vessel.

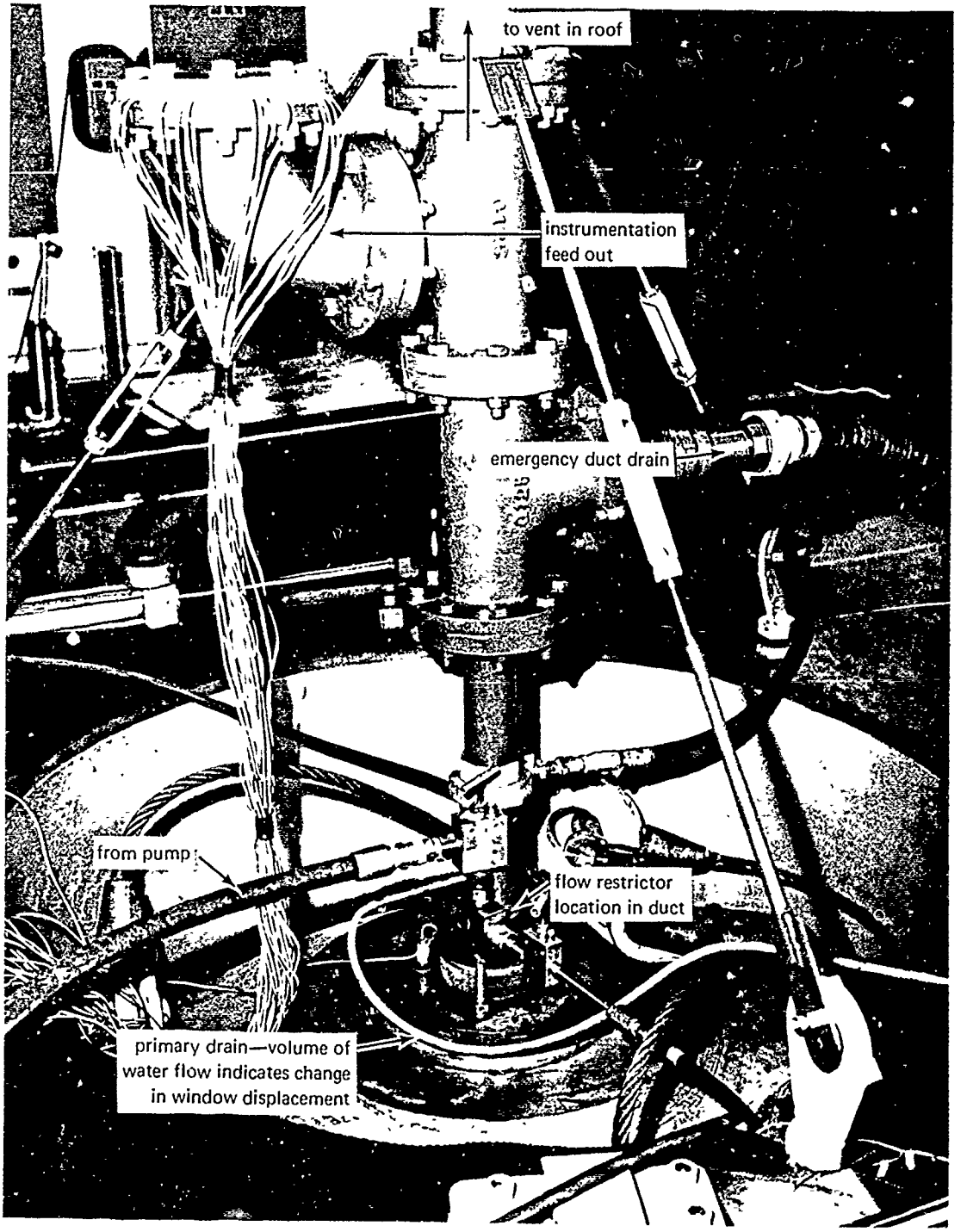

Figure E-9. Christmas tree for the ejection of fluid from the interior of the very large window test assembly inside the 72-inch-diameter pressure vessel.

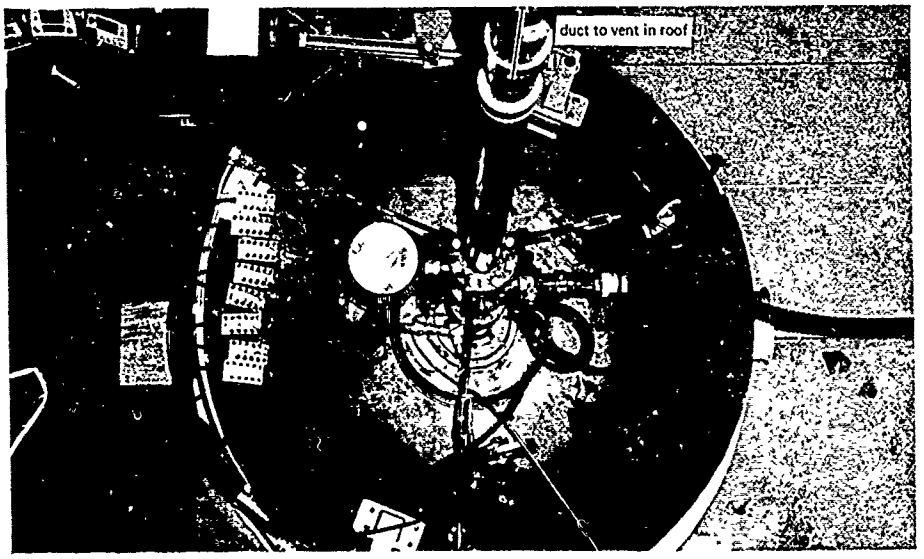

Figure E-10. Duct for the guidance of ejected water from the Christmas tree on the vessel to the vent in the roof.

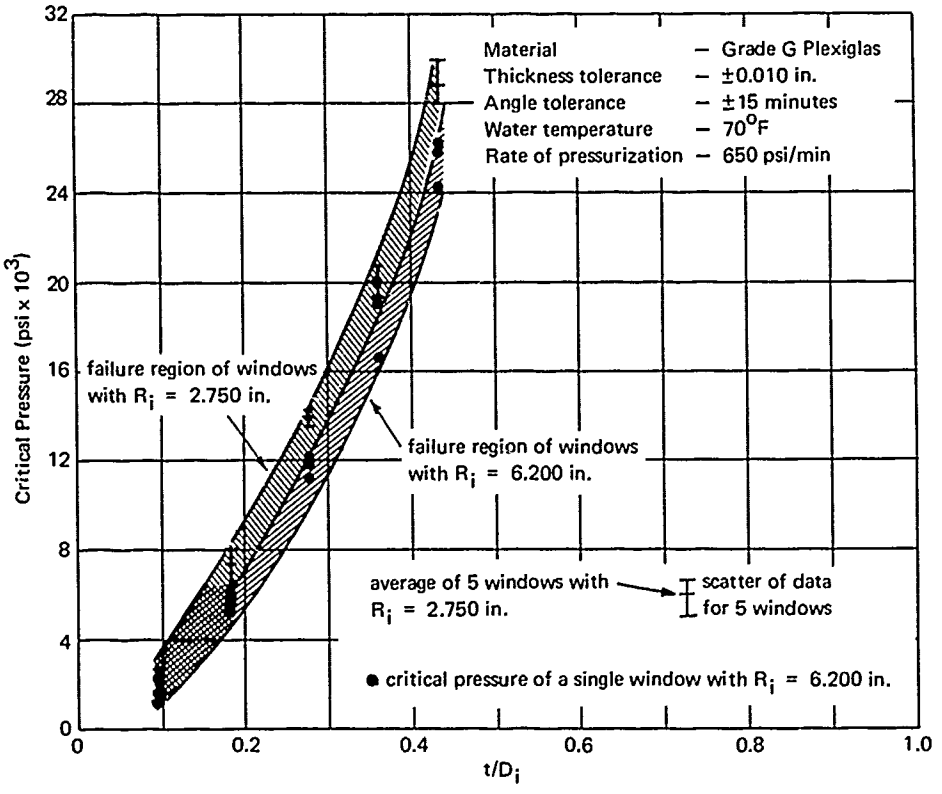

Figure E-11. Critical pressures of model windows with R_i = 2.750 inches and large windows with R_i = 6.200 inches under short-term hydrostatic loading as a function of t/D_i ratio.

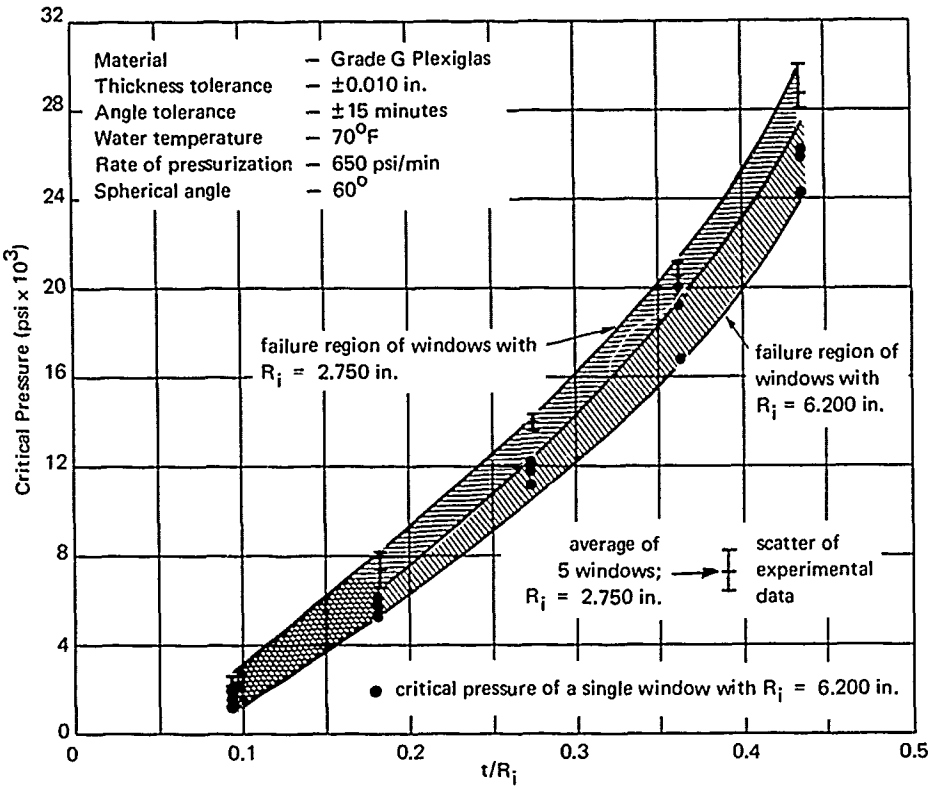

Figure E-12. Critical pressures of model windows with R_i = 2.750 inches and large windows with R_i = 6.200 inches under short-term hydrostatic loading as a function of t/R_i ratio.

Considerable trouble was experienced in getting reliable values for the critical pressure of 6.200-inch-R_i windows with t/R_i = 0.091. Several windows with these dimensions failed at pressures 50% or lower than the critical pressure of model windows with α = 60 degrees and t/R_i = 0.091. Subsequent observation of windows that failed at unexpectedly low pressures disclosed that these failures were caused by uneven sliding of the window in the flange; this resulted in severe damage to the beveled edge of the window at one location on its circumference. Very little fracturing took place in those cases, and then it was limited to a single location on the window's circumference. The data resulting from these failures was not plotted, as it represented a special set of circumstances not representative of window strength for that t/R_i. However, it was concluded from these failures that for 60-degree windows with small t/R_i ratios, mechanical restraints are needed against the edge of high-pressure face to keep the window from tilting during the initial stages of hydrostatic pressurization.

The axial displacement of the center point on the window's low-pressure face was measured on all large spherical windows with R_i = 6.200 inches. The displacements were much larger than for model

windows (Figure E-13), but as in model windows the magnitude of displacement of large windows varied with t/R_i ratio and hydrostatic pressure level. In order to compare the displacements of the large windows with the displacements of the model windows, they were scaled down by multiplying the displacements with a scaling ratio consisting of the large and model window diameters (2.750 inches/6.200 inches). When the scaled-down displacements of the large windows were plotted together with the displacements of the model windows on the same coordinates it was found that they were basically the same (Figure E-14). This serves as an effective support to the postulate that the strain data generated by testing model windows is applicable to full-scale windows so long as the applicable linear scaling factor is applied.

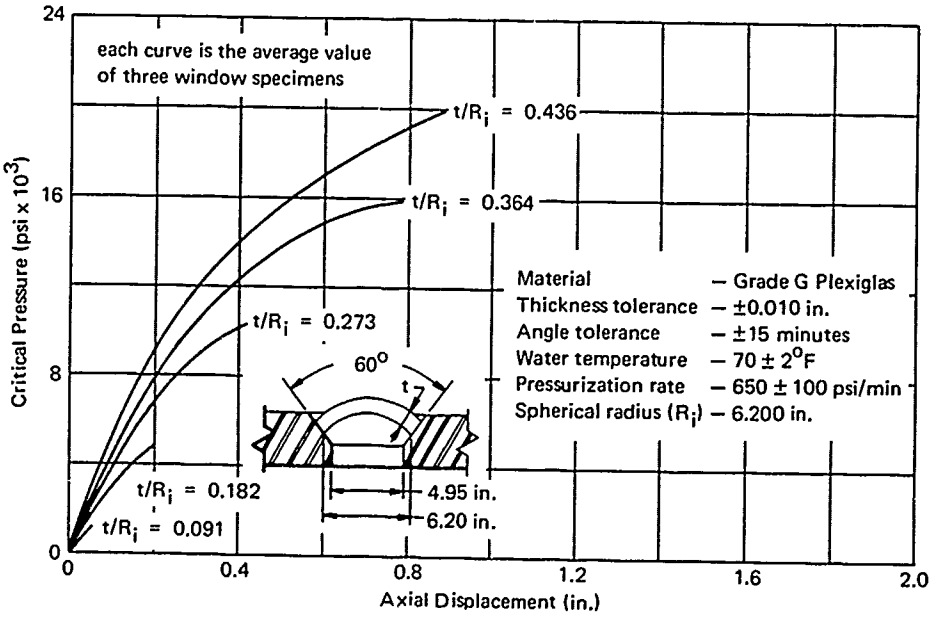

Figure E-13. Axial displacement of 60-degree spherical acrylic windows with R_i = 6.200 inches under short-term hydrostatic loading.

Windows With R_o = 33 Inches

Pressures at which the very large windows failed varied from one specimen to another for the same t/R_i ratio, depending on the magnitude of restraining force exerted by the retaining clips on the edge of the high-pressure face. Thus, the first window with a t/R_i of 0.082 tested to

implosion under short-term pressurization failed at 765 psi. The window was fractured only locally around a section of its circumference, and the retaining clips in that area were bent outwards by the edge of the window moving out of the flange (Figure E-15). The retaining clips were of 6061-T6 aluminum and had only a 0.25-in.^{2} cross section that could be bent rather readily. When the aluminum clips were replaced with substantially stronger steel clips of 1-inch cross section the following window of $t/R_i = 0.082$ failed at 1,550 psi. This implosion pressure corresponded rather well with implosion pressures of model windows having the same t/R_i ratio and temperature range.

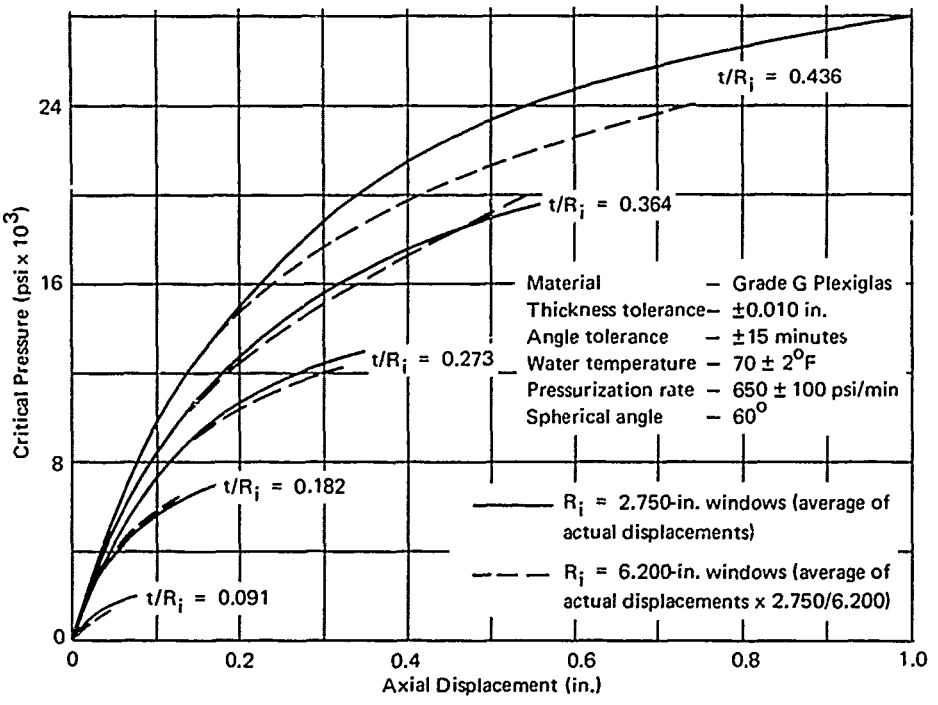

Figure E-14. Comparison of axial displacements measured on model and full-scale spherical acrylic windows under short-term hydrostatic loading.

The same problem presented itself during the testing of the very large windows with $t/R_i = 0.138$. Although this window was held in place by the improved steel retaining clips, it also became unstable during the test in the flange and bent the clips locally outwards. This occurred at 1,780 psi. Since there were no more windows available for testing, no further work was done to increase the strength of retaining clips or to replace them by a substantial

retaining ring. There is no doubt that the implosion strength of the very large windows with $t/R_i = 0.138$ is probably 40% to 50% higher than 1,780 psi. This conclusion is based on the following observations:

1. The failed window with $t/R_i = 0.138$ exhibited the same highly localized fracture as the very large window with $t/R_i = 0.082$ that failed prematurely by becoming statically unstable in the flange.

2. The retaining steel clips on the flange were in one location bent outwards, and this location corresponds to the location of the fracture on the circumference of the window.

3. The other window with $t/R_i = 0.138$ that was subjected to 1,780 psi when tested in pair with the failed window in the same flange exhibited none of the cracks or crazing which generally appear when a window has been pressurized in excess of 60% of its implosion pressure.

The strains (Figure E-16) measured on the window with $t/R_i = 0.082$ are linear and fairly uniform to at least the 765-psi pressure level under short-term hydrostatic loading. It is not known at what pressure loading the strains become nonlinear prior to failure at 1,550 psi. The test was terminated prematurely by the failure of retaining clips on the other window in the flange; this severely damaged the instrumentation on this window and thus no strain data were generated during the subsequent tests.

The stresses (Figure E-17) calculated on the basis of these strains were found to be linear and of moderate magnitude in the 0-to-765-psi pressure range. On the basis of these stresses it appears that the window with $R_o =$ 33 inches and $t/R_i = 0.082$ is probably safe for long-term submersion to 600 feet depth. By the same token the $t/R_i = 0.138$ window is probably safe to a depth of 1,000 feet if proper retaining rings are used to hold the window in the flange. Before, however, these very large windows are employed in actual manned installations they should be subjected to long-term tests so that their life at these depths can be accurately determined.

The displacement of the water (Figure E-18) from the interior of the flange enclosed by the two spherical windows with $t/R_i = 0.082$ was linear with pressure until a very short time before the failure of one of the windows occurred prematurely at 765 psi. The initial linearity of the displacement followed by the distinct nonlinearity prior to failure of one of the windows in the flange can serve in this type of window test as a warning system, which if heeded will permit termination of the hydrostatic test short of actual window failure. Although similar nonlinearity could have been observed if the failed window was instrumented with strain gages, the hydrostatic displacement indicator requires no prior instrumentation, or rapid strain-balancing and printout system.

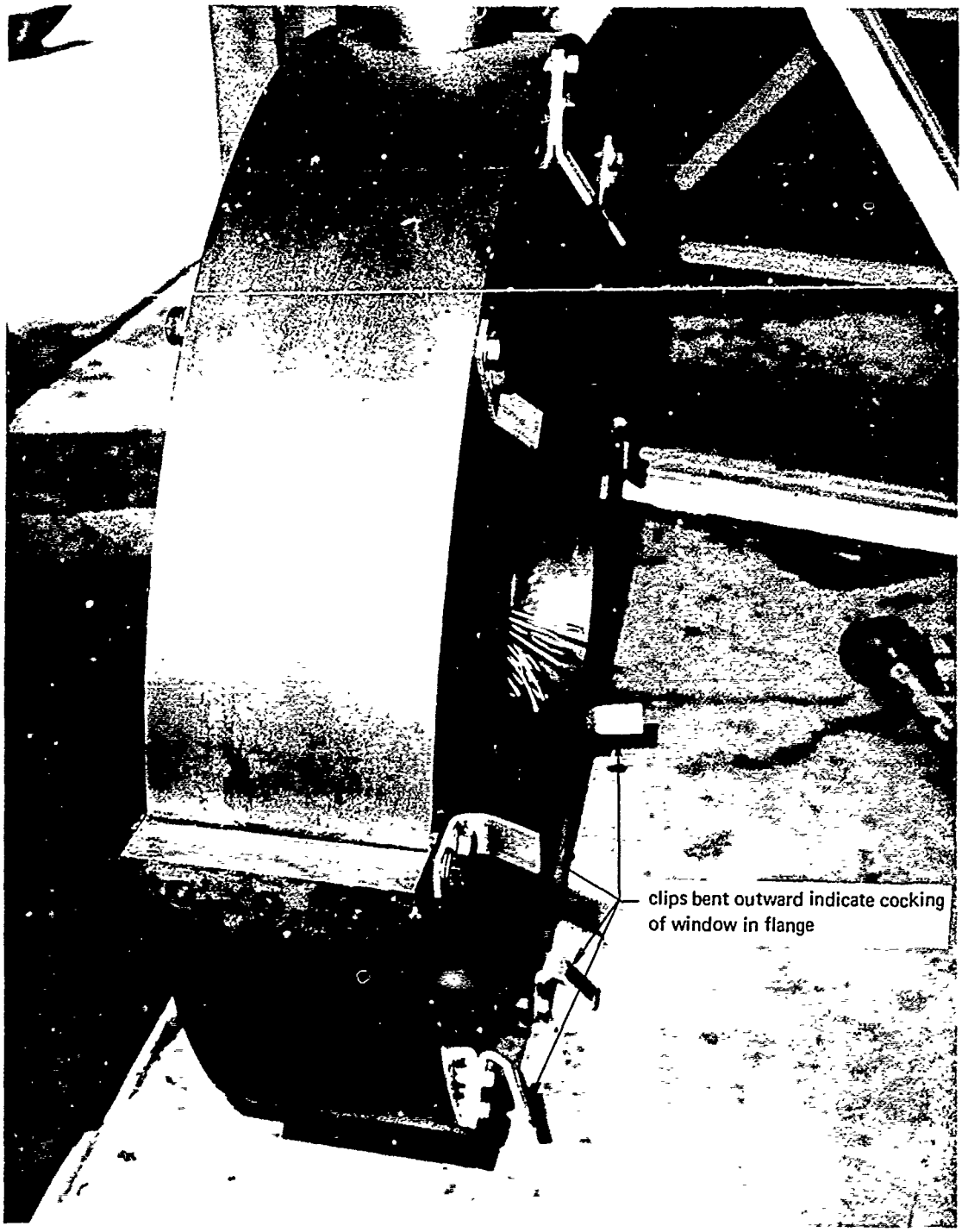

Figure E-15. Irregular failure of the spherical window with R_o = 33 inches and t = 2.5 inches resulted in some of the retaining clips being bent outwards, indicating that window cocked in flange before implosion.

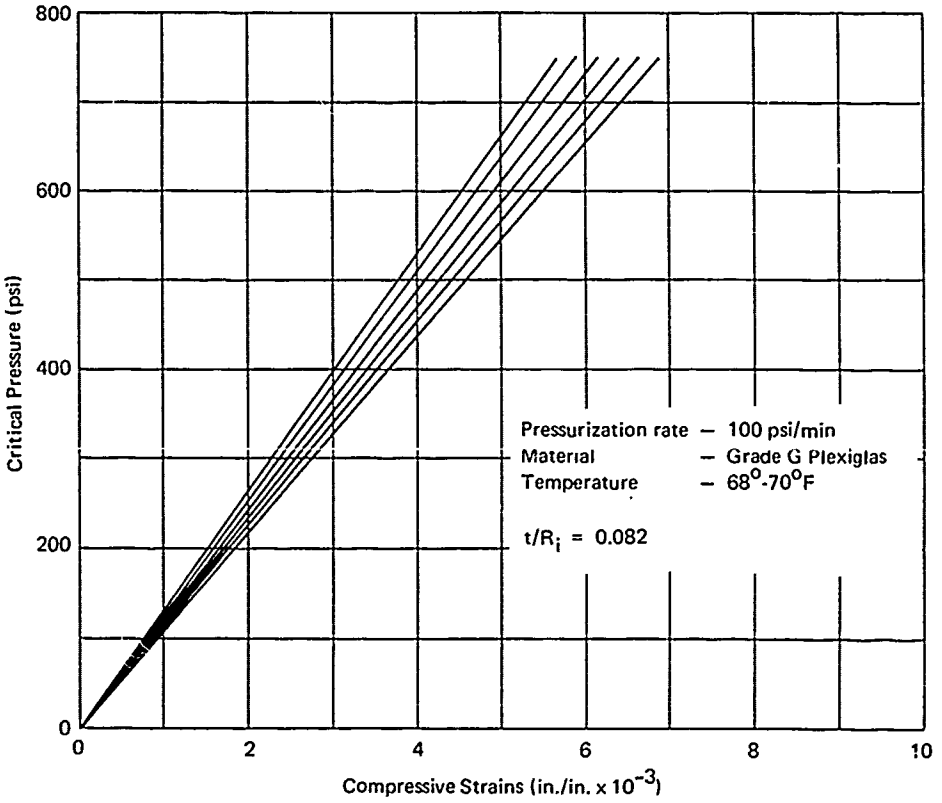

Figure E-16. Maximum principal compressive strains on the low-pressure face of the spherical acrylic window with R_o = 33 inches, t = 2.5 inches, and α = 72 degrees.

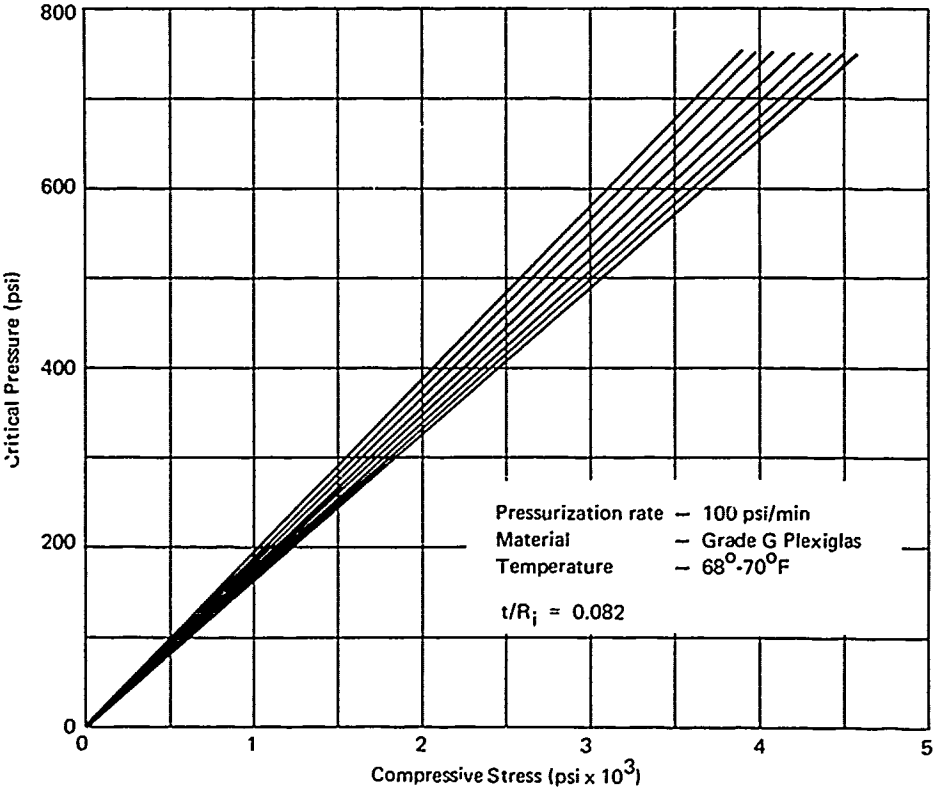

Figure E-17. Maximum principal compressive stresses on the low-pressure face of the spherical acrylic window with R_o = 33 inches, t = 2.5 inches, and α = 72 degrees.

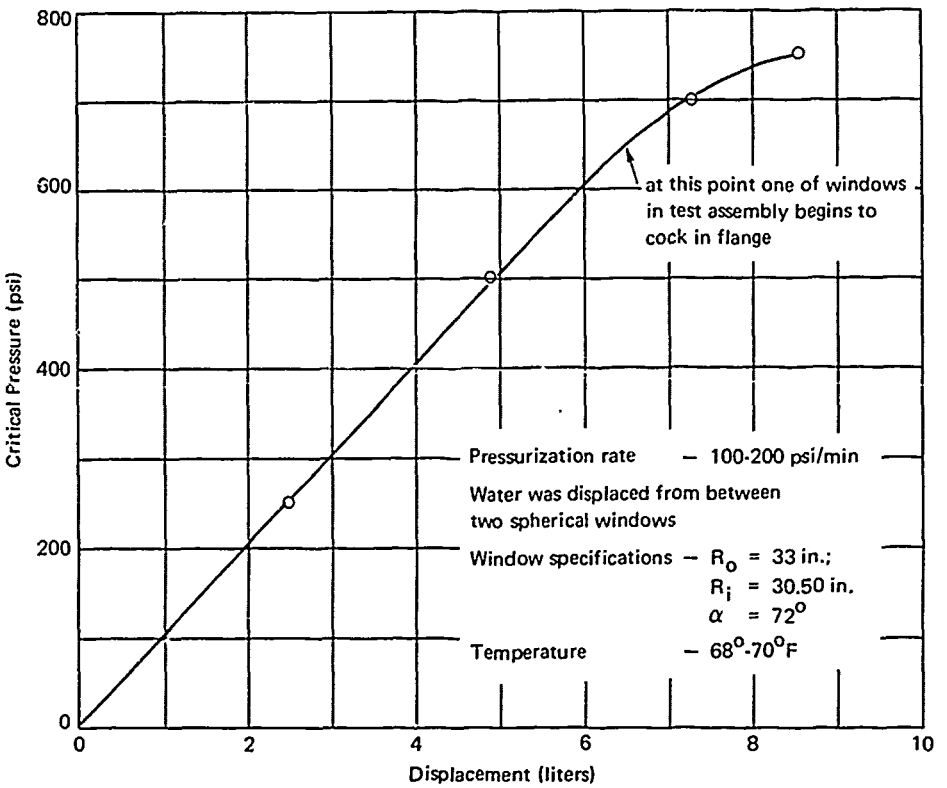

Figure E-18. Change in displacement of the volume enclosed by two spherical acrylic windows of R_o = 33 inches and t = 2.5 inches as shown in Figure E-8.

When the displacement of water is converted analytically into axial displacement of the window it appears that the axial displacement of the very large window is approximately what the scaled-up axial displacements of model windows would predict it to be (Figure E-19).

SUMMARY

Testing of two sizes of full-scale windows with R_i = 6.200 and R_o = 33 inches, respectively, has shown that the strains and implosion pressure of model windows with R_i = 2.750 inches can serve as a fair basis for predicting the strains and failure pressures of full-scale windows—providing that both the full-scale and the model windows fail in a regular, rather than irregular manner. It was unfortunate that some of the very large windows with R_o = 33 inches tested to implosion failed irregularly by becoming unstable in the flange at a very low pressure level and thus made it impossible to compare the implosion pressure of some of the very large windows with that of model windows.

The tendency of the low-t/R_i-ratio windows in the 60-to-72-degree spherical angle range to become statically unstable in the flange at pressures considerably lower than those at which regular implosion occurs presents a problem to the designer who must design the retaining ring for the window of such dimensions that it restrains the window from nonuniform displacement in the flange. As has been shown conclusively with the window of 33-inch R_o and $t/R_i = 0.082$, the uneven displacement of the window in the flange can be prevented with retaining clips or a ring of adequate strength, thus improving the performance of the window.

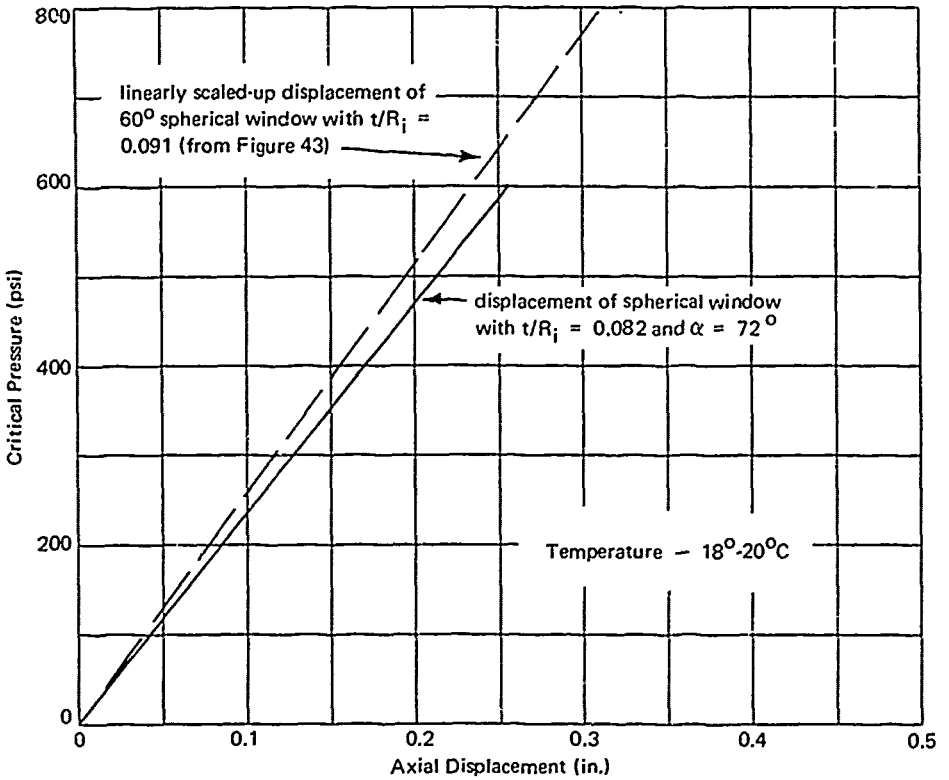

Figure E-19. Axial displacement of window with R_o = 33 inches, t = 2.5 inches, and α = 72 degrees. (Calculated on the basis of displaced water shown in Figure E-18.)

Appendix F

EFFECT OF STRESS RAISERS ON THE CRITICAL PRESSURE OF SPHERICAL SHELL ACRYLIC WINDOWS

All of the windows tested in the primary study had a $\sqrt{32}$ or better surface finish that eliminated most surface stress raisers. Because of this smooth finish, the experimentally established relationships between critical pressure and t/D_i or t/R_i ratios were not influenced by the effect of surface stress raisers. So long as the testing of spherical acrylic windows takes place in laboratory environment, very little danger exists that careless handling of the test specimens will result in the creation of surface stress raisers due to impact of the window against some fixed object. A different picture presents itself when spherical acrylic windows are incorporated into the hull of a submersible, or fixed ocean bottom habitat. There they are exposed to impacts by other objects during launching or docking operations that may deeply scratch the window's high-pressure face. If such scratches or gouges are extremely detrimental to the strength of the window, transparent shields will have to be installed to protect the windows against such damage to prevent the window from imploding during the subsequent dive. On the other hand, if moderately deep scratches or gouges do not markedly lower the critical pressure of the window during the first subsequent dive, such shields may be omitted for the sake of improved light transmissibility and decreased structural bulk.

To determine the effect of surface stress raisers on the critical pressure of a spherical acrylic window conclusively and exhaustively would require a long test program in which all the variables would be singly and jointly evaluated. Neither funding nor manpower was available for such an evaluation at the time the primary study was conducted. However, to obtain at least some insight into the problem presented by surface stress raisers, several exploratory tests were conducted.

The exploratory study was conducted with six windows of only a single t/R_i ratio and spherical sector angle. The t/R_i ratio chosen was 0.182 with 150-degree spherical sector angle. In order to generate as much data as possible from the limited number of specimens, each window was fabricated to have a stress raiser in a different location on the window surface. In this manner at least a qualitative conclusion could be reached that would show which location on the spherical window is most sensitive to the presence of stress raisers. Since the exterior of the window is more exposed to impacts during launching or docking operations, and thus has the greater probability of being scratched, it was selected as the surface in which to generate stress raisers for five test specimens. Only one specimen had the stress raiser placed on its interior surface.

The stress raisers consisted either of grooves, or of partially drilled holes. The drilled holes were used on two specimens only. In one specimen, the 0.062-inch-diameter x 0.062-inch-deep hole was in the center of the high-pressure face, while in the other specimen, it was in the center of the low-pressure face. Each of the other four specimens had a stress raiser consisting of one 0.062-inch-wide x 0.062-inch-deep circular groove with square cross section (Figure F-1). The grooves were machined in the window surface as circumferential bands located at different elevations. (Figures F-2 and F-3). Since the grooves were circular, continuous, and had a square cross section with sharp 90-degree corners, a maximized stress-raiser effect was generated.

Testing the spherical windows with stress raisers was performed in window flanges. The test methods were identical to those used in testing the windows without stress raisers described in the main body of the report. No measurement of axial displacement or sliding displacement on the flange seat was taken. Only the critical pressure was measured and subsequently compared to the critical pressures of windows without stress concentrations. When the critical pressures of windows with stress raisers (Table F-1) and their mode of failure were compared to the critical pressures and modes of failure for windows without stress raisers, several tentative conclusions appear to be supported by experimental data.

It appears that the presence of very severe stress raisers on the high-pressure face does not decrease the short-term critical pressure of the spherical acrylic window, regardless of where the stress raiser may be located. This is borne out by the fact that the critical pressures of window specimen with stress raisers at different locations on the high-pressure face are not only all approximately the same, but also equal to critical pressures of similar spherical windows without stress raisers tested previously in the program. This would seem to indicate that if a scratch or gouge is put accidentally into the high-pressure face of the spherical window during launching and is not noticed prior to the dive no danger to the crew exists, as the window will not fail during that dive to the submarine's operational depth. When the submarine returns from the dive and the gouge is detected during dockside inspection of the submarine then the window can be replaced with a new one if the severity of the crack warrants it. How severe a scratch or gouge it must be before it had deleterious effect on the cyclic pressure life of the window is unknown, as no experiments, even of exploratory nature, have been conducted.

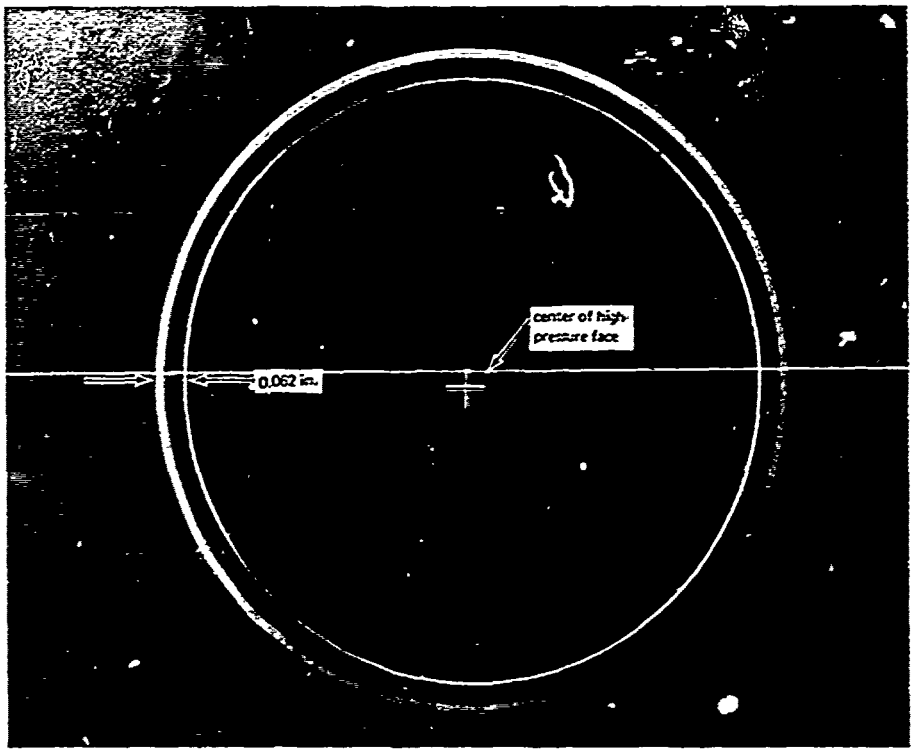

Figure F-1. Typical circular groove machined in high-pressure face of spherical window.

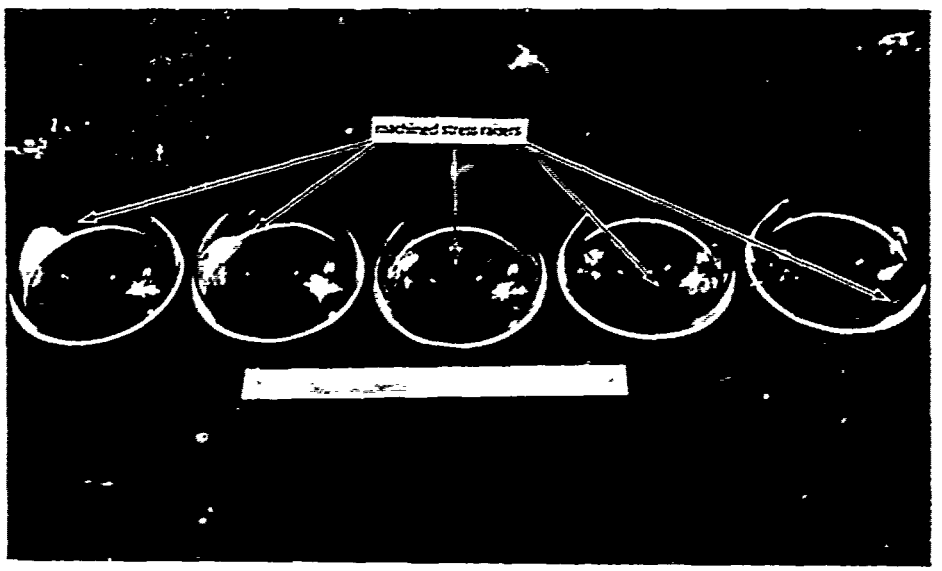

Figure F-2. Spherical windows with machined stress raisers before implosion testing.

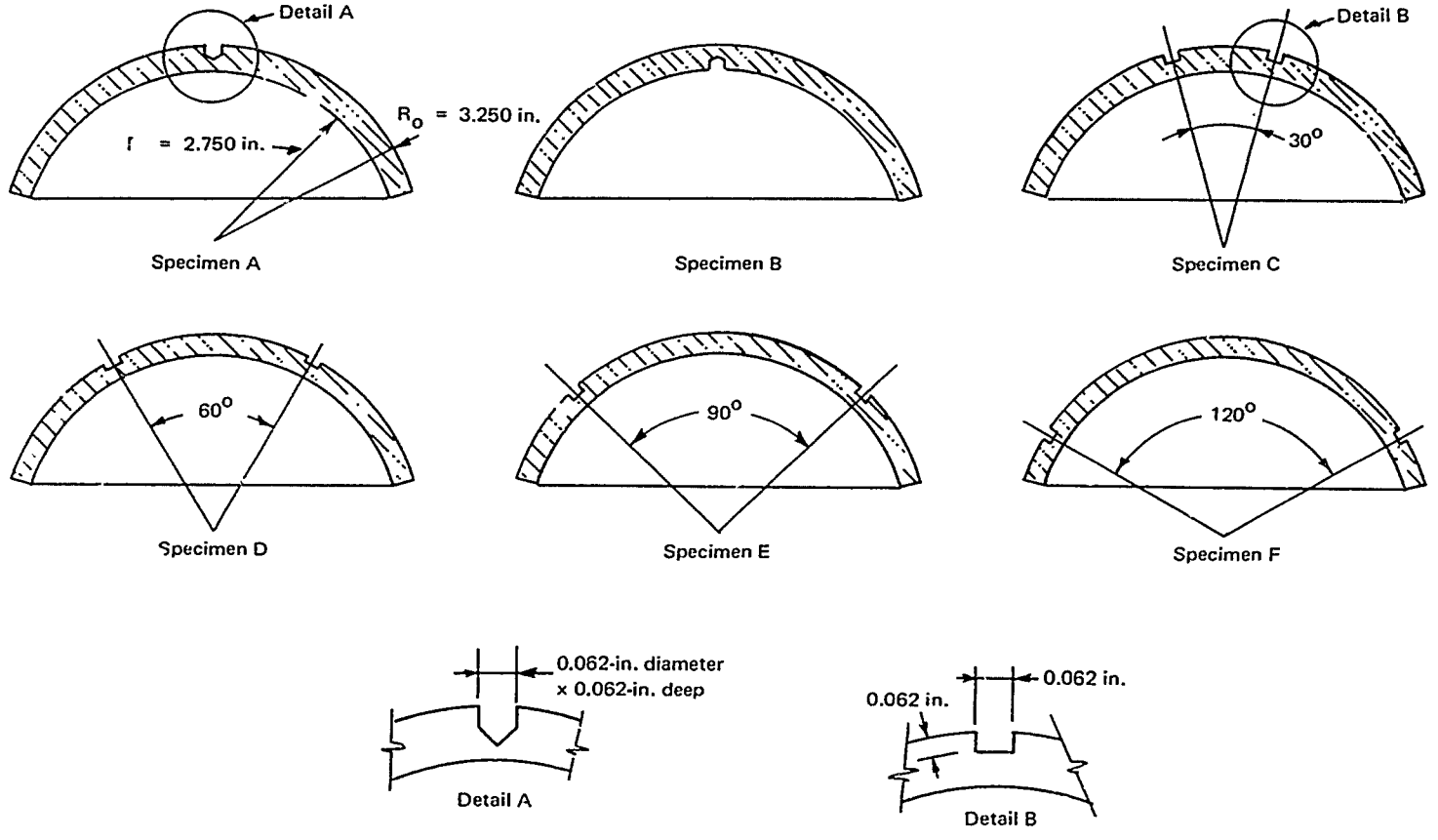

Figure F-3. Location of machined stress raisers on spherical window faces.

Table F-1. Comparison of Critical Pressures of Spherical Acrylic Windows With and Without Stress Raisers

(t/R_i = 0.182 and spherical sector angle = 150 degrees.)

Specimen	Nominal Thickness, t (in.)	Internal Spherical Radius, R_i (in.)	Temperature, T (^oF)	Pressurization Rate (psi/min)	Critical Pressure, p_c (psi)
Windows Without Stress Raisers					
106	0.505	2.751	70	632	7,400
107	0.495	2.751	70	669	7,250
108	0.500	2.750	71	670	7,300
109	0.496	2.748	71	670	7,250
110	0.510	2.750	71	681	7,600
Windows With Stress Raisers					
A	0.500	2.751	69.5	671	7,520
B	0.448	2.750	69.5	665	7,250
C	0.445	2.750	71.1	668	7,200
D	0.448	2.749	71.1	667	7,325
E	0.448	2.751	71.5	662	7,100
F	0.502	2.750	71	670	7,460

Since only a single window specimen was tested with a stress raiser on the low-pressure face, the conclusions reached are much more tentative than was the case for windows with stress raisers on the high-pressure face. The conclusion, based on the fact that the single window specimen with a stress raiser in the center of the low-pressure face failed in the same pressure range as windows without stress raisers, is that a stress raiser on the interior of a spherical window is not detrimental to its strength.

In view of the fact that all the above-mentioned exploratory tests with stress raisers have been conducted with spherical windows of one t/R_i ratio and spherical sector angle the conclusions reached apply directly only to that ratio and spherical sector angle. Still, it can be postulated with a fair degree of confidence that spherical windows with other t/R_i ratios and spherical sector angles will also be found quite insensitive to stress raisers in single-cycle service to operational depth because the compressive stresses in the window do not permit cracks to originate at the raisers.

All of the windows with stress raisers disintegrated into very small fragments upon implosion, and therefore no statements can be made on the mode of failure. It can be postulated, however, that since the windows with stress raisers failed at the same pressure as those without stress raisers their mode of failure was the same. The discussion of failure mode observed on windows without stress raisers can be found in the main body of the report.

Appendix G

DISPLACEMENTS OF SPHERICAL SHELL WINDOWS UNDER LONG-TERM LOADING

Observations were made of time-dependent axial and sliding displacements of 26 model spherical shell windows under sustained hydrostatic pressure of 15-minute duration (Table G-1). This technically constitutes a long-term loading, even though of very short duration, as distinct from the short-term loading used throughout the investigation that is the main subject of this report. On the basis of these exploratory tests, some insights were gained into the behavior of spherical windows under long-term loading. The data in Appendix G on long-term loading of spherical windows represents results from individual test specimens for each distinct combination of variables only rather than the average of five specimens as was the case in the main investigation. Therefore, considerable scatter exists between the plotted curves, as local flattening of the window may occur off center radically changing the magnitude of measured displacements. Only general trends and magnitudes of displacement can be tentatively established from the observed behavior of the individual test specimens.

All of the windows, regardless of their t/R_i ratio or spherical sector angle, experienced time-dependent axial and sliding displacements (Figures G-1 through G-11). When the axial displacements of windows with the same t/R_i ratio and under identical pressure loading were compared to each other (Figures G-1 through G-6), it was found that the magnitude of time-dependent axial displacement varied with the spherical sector angle. The largest time-dependent axial displacements were found in windows with 180-degree spherical sector angles, while the smallest ones were noted in 30-degree spherical sector windows.

The major change in time-dependent axial displacement was observed in the 30-to-90-degree spherical sector range, while the least change took place in the 90-to-180-degree range. Since the pressure levels at which the long-term tests were conducted were rather high, generating compressive stresses in 12,000-to-20,000-psi range, they resulted in high magnitudes of time-dependent axial displacement. Because the same magnitude of pressure was applied to all windows of the same thickness and spherical radius R_i but different spherical sector angles, it meant that each of the windows with $t/R_i \geqslant 0.182$ was loaded to a different percentage of its short-term critical pressure. Thus, while the 90-, 120-, 150-, and 180-degree spherical sector windows with $t/D_i \geqslant 0.182$ were loaded to approximately 75% of

short-term critical pressure, the 60-degree windows were loaded to only 55% and the 30-degree to 25%. For the windows with $t/R_i \leq 0.182$, the long-term pressure was approximately 75% of their short-term pressure, regardless of what their individual spherical sector angles may have been.

Table G-1. Pressures to Which Windows Were Subjected Under Long-Term Loading

(R_i = 2.750, water temperature = 68°F to 70°F, pressurization rate = 650 psi/min, duration = 15 minutes.)

Shell Thickness (in.)	Percent of Critical Pressure (p_c)* Applied at Sector Angle of—						Maximum Pressurization (psi)
	30°	60°	90°	120°	150°	180°	
	------ % p_c ------						
0.250	60	85†	70	65	63	67	2,000
0.500	50	73	80	76	75	75	5,500
0.750	25	61	76	78	74	71	8,500
1.000	‡	56	72	77	75	73	11,500
1.200	–	50	71	–	–	–	14,500

* p_c = average short-term critical pressure of windows.

† Specimen failed while under sustained pressure loading.

‡ Unknown, but definitely less than 30.

Some additional observations have been made, keeping in mind that although the long-term pressure applied to a group of windows with same t/R_i ratio but different spherical sector angles is the same, it does not necessarily constitute the same percentage of their short-term critical pressure. It appears that when the windows are subjected to long-term constant hydrostatic pressure equal to 75% of short-term pressure, the rate of time-dependent axial displacement during the first 15 minutes of constant pressure application is so high that in all probability the window would fail in less than 100 hours. When the long-term pressure tests of the windows are run at approximately 50% of short-term critical pressure, the rate of time-dependent axial displacement would seem to indicate that probably

the windows will implode only after more than 1,000 hours of loading. It is only when the windows are subjected to long-term loadings of less than 25% of short-term critical pressure that the rate of time-dependent axial displacement decreases to a level at which in all probability the windows would not implode in less than 10,000 hours. It appears that when the windows are loaded to 25% of their short-term critical pressure they will safely withstand long-term pressure loadings. However, it is not prudent at the present time to use a full-scale spherical window in an application where it will be subjected to long-term pressure loading equal to 25% of its short-term critical pressure without evaluating the prototype of such a window under long-term loading conditions similar to those to be encountered in actual service. The exploratory long-term data of Appendix G and the short-term data in the main body of the report can serve at the present time only as the basis for selection of the prototype window dimensions on the basis of a conversion factor of 12. When in the future long-term pressurization studies of 1,000-hour duration are conducted with spherical windows, the need for testing each prototype window designed with a conversion factor less than 12 will be eliminated. Until such studies are completed, prototype service windows must be tested when a conversion factor of less than 12 based on short-term critical pressure is used.

The sliding displacement of the spherical windows (Figures G-7 through G-12) under long-term loading was somewhat different from the axial displacement described before. In the first place, the magnitude of the sliding displacement was considerably less than the axial displacement measured on the same window at any particular time during the long-term pressure loading. Only for the 30-degree spherical sector windows were the magnitudes approximately the same. Second, the magnitude of sliding displacement for any given t/R_i ratio and pressure was fairly constant for all spherical sector angles except 150 degrees, for which it was smaller. The second observation correlates fairly well with the observed phenomenon that the 150-degree windows have fewer cracks (Figure 26) on their bearing surface than windows with any other sector angle. (See discussion on failure modes of windows in the main body of this report.) It would appear then that when the sliding displacement is minimized, so is the formation of cracks on the bearing surface of the windows. The reduction of sliding must result, however, from the geometry of window, and not from bonding of the window's bearing surfaces to the flange or a mechanical detent, as otherwise the window would prematurely fail from elastic instability or local bending stresses.

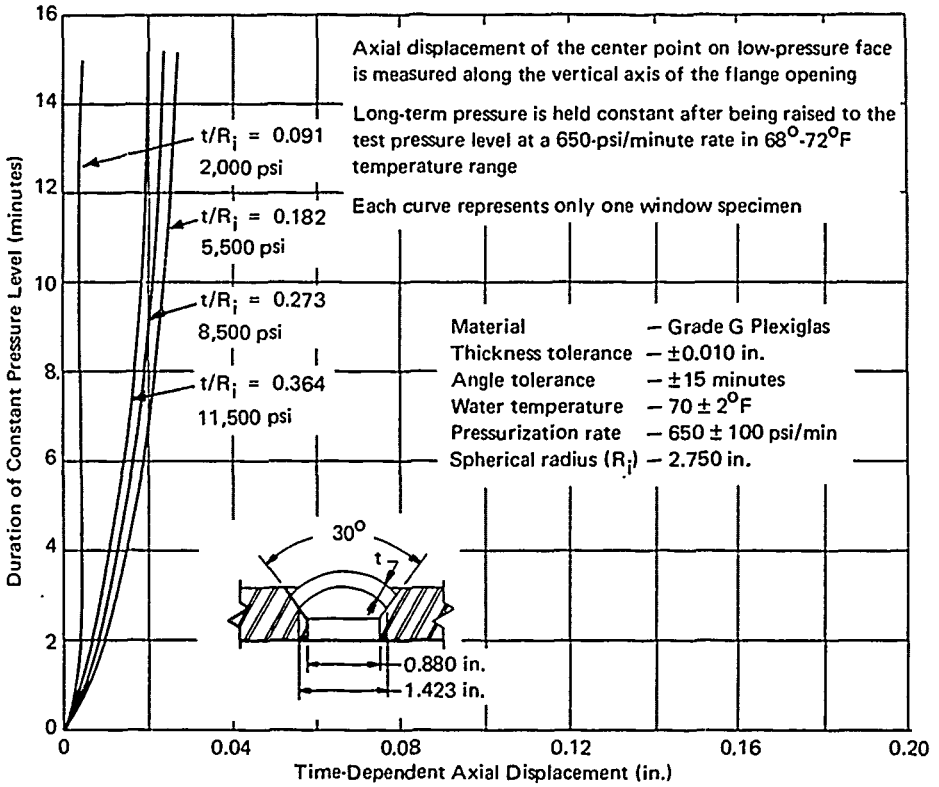

Figure G-1. Axial displacement of 30-degree spherical acrylic windows under long-term hydrostatic pressure.

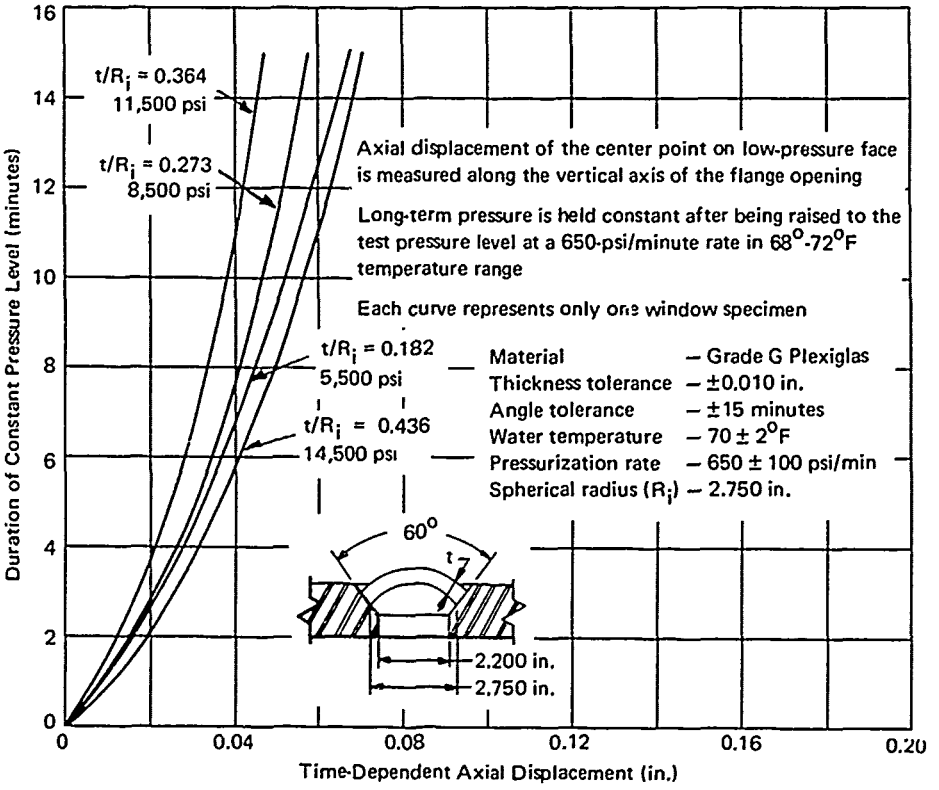

Figure G-2. Axial displacement of 60-degree spherical acrylic windows under long-term hydrostatic pressure.

Material	— Grade G Plexiglas
Thickness tolerance	— ±0.010 in.
Angle tolerance	— ±15 minutes
Water temperature	— 70 ± 2°F
Pressurization rate	— 650 ± 100 psi/min
Spherical radius (R_i)	— 2.750 in.

Axial displacement of the center point on low-pressure face is measured along the vertical axis of the flange opening

Long-term pressure is held constant after being raised to the test pressure level at a 650-psi/minute rate in 68°-72°F temperature range

Each curve represents only one window specimen

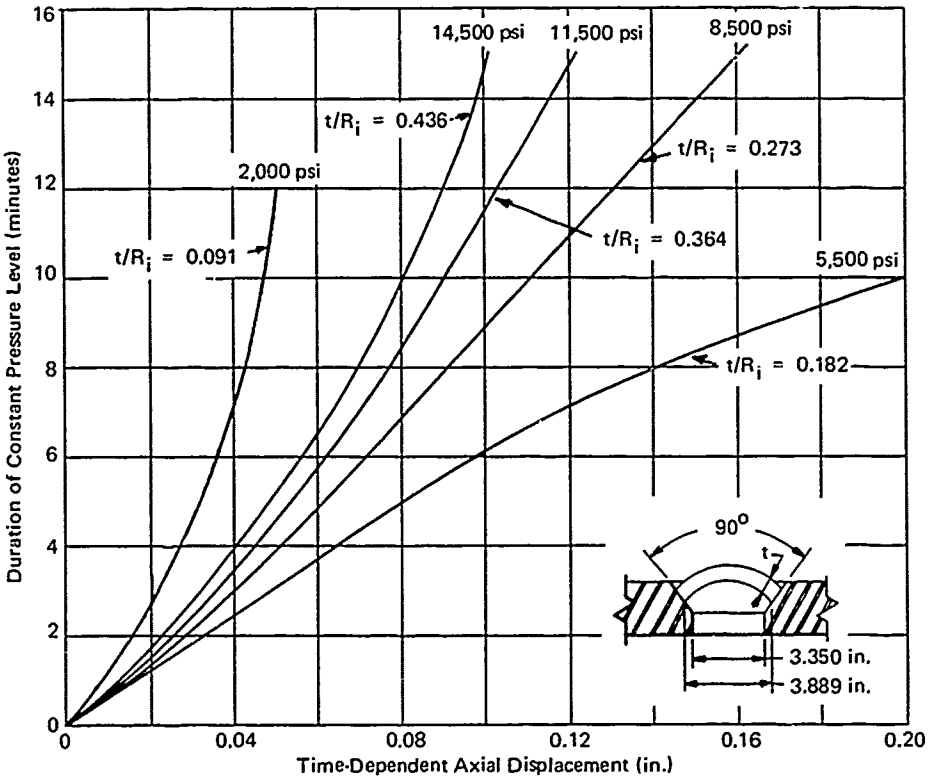

Figure G-3. Axial displacement of 90-degree spherical acrylic window under long-term hydrostatic pressure.

Material — Grade G Plexiglas
Thickness tolerance — ±0.010 in.
Angle tolerance — ±15 minutes
Water temperature — 70 ± 2°F
Pressurization rate — 650 ± 100 psi/min
Spherical radius (R_i) — 2.750 in.

Axial displacement of the center point on low-pressure face is measured along the vertical axis of the flange opening

Long-term pressure is held constant after being raised to the test pressure level at a 650-psi/minute rate in 68°-72°F temperature range

Each curve represents only one window specimen

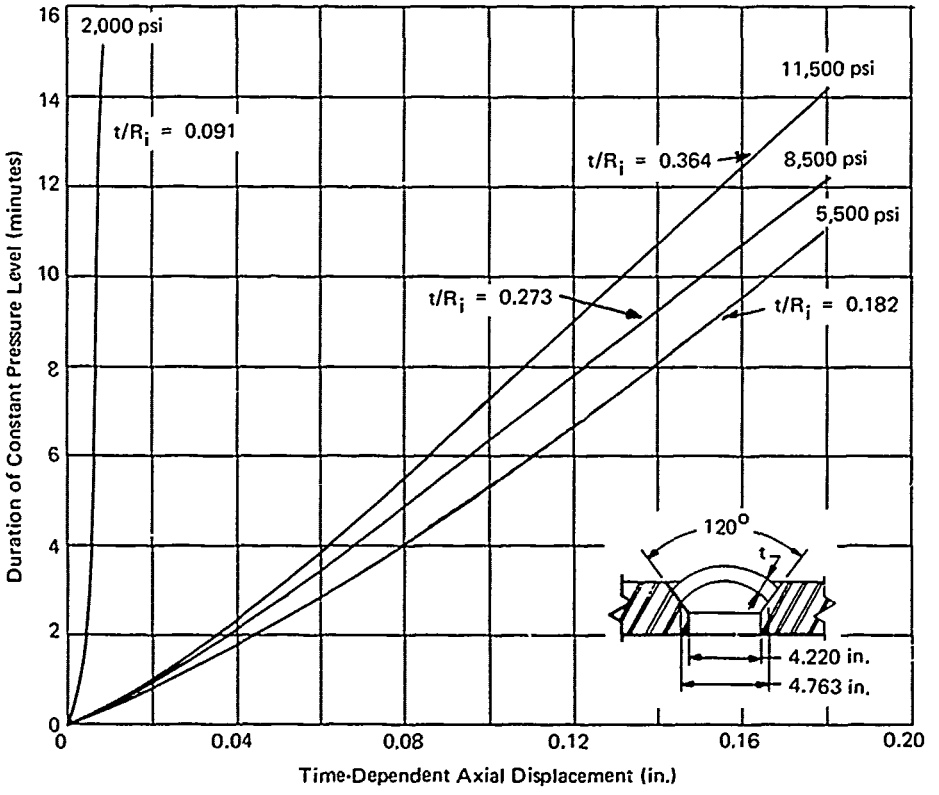

Figure G-4. Axial displacement of 120-degree spherical acrylic windows under long-term hydrostatic pressure.

Material	– Grade G Plexiglas
Thickness tolerance	– ±0.010 in.
Angle tolerance	– ±15 minutes
Water temperature	– 70 ± 2°F
Pressurization rate	– 650 ± 100 psi/min
Spherical radius (R_i)	– 2.750 in.

Axial displacement of the center point on low-pressure face is measured along the vertical axis of the flange opening

Long-term pressure is held constant after being raised to the test pressure level at a 650-psi/minute rate in 68°-72°F temperature range

Each curve represents only one window specimen

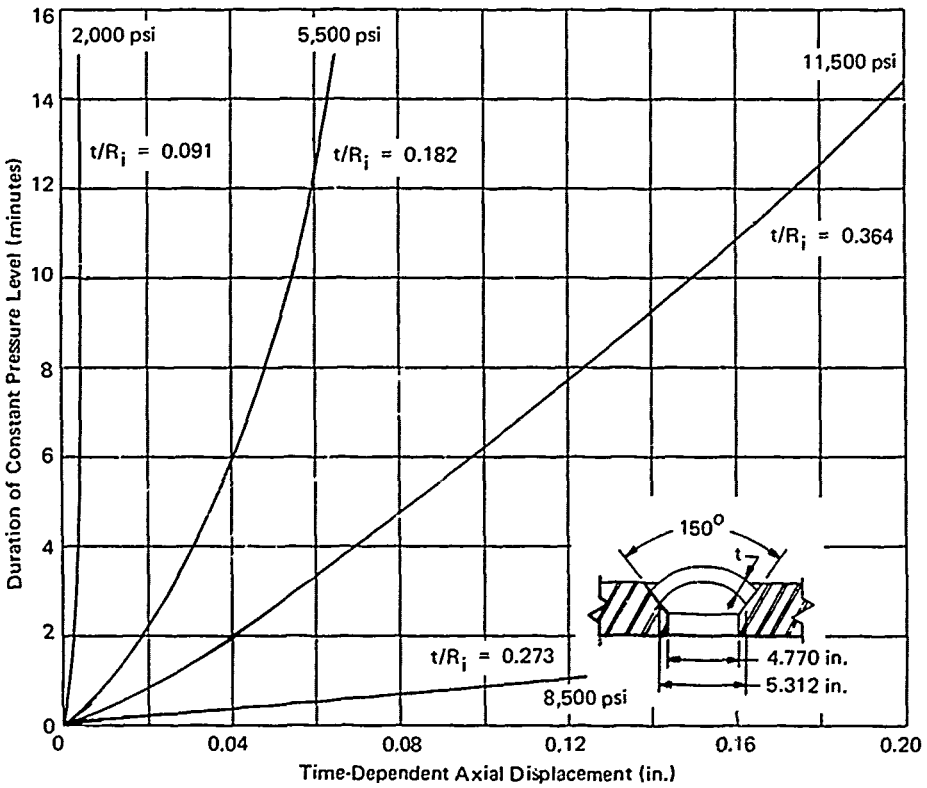

Figure G-5. Axial displacement of 150-degree spherical acrylic windows under long-term hydrostatic pressure.

Material — Grade G Plexiglas
Thickness tolerance — ±0.010 in.
Angle tolerance — ±15 minutes
Water temperature — 70 ± 2°F
Pressurization rate — 650 ± 100 psi/min
Spherical radius (R_i) — 2.750 in.

Axial displacement of the center point on low-pressure face is measured along the vertical axis of the flange opening

Long-term pressure is held constant after being raised to the test pressure level at a 650-psi/minute rate in 68°-72°F temperature range

Each curve represents only one window specimen

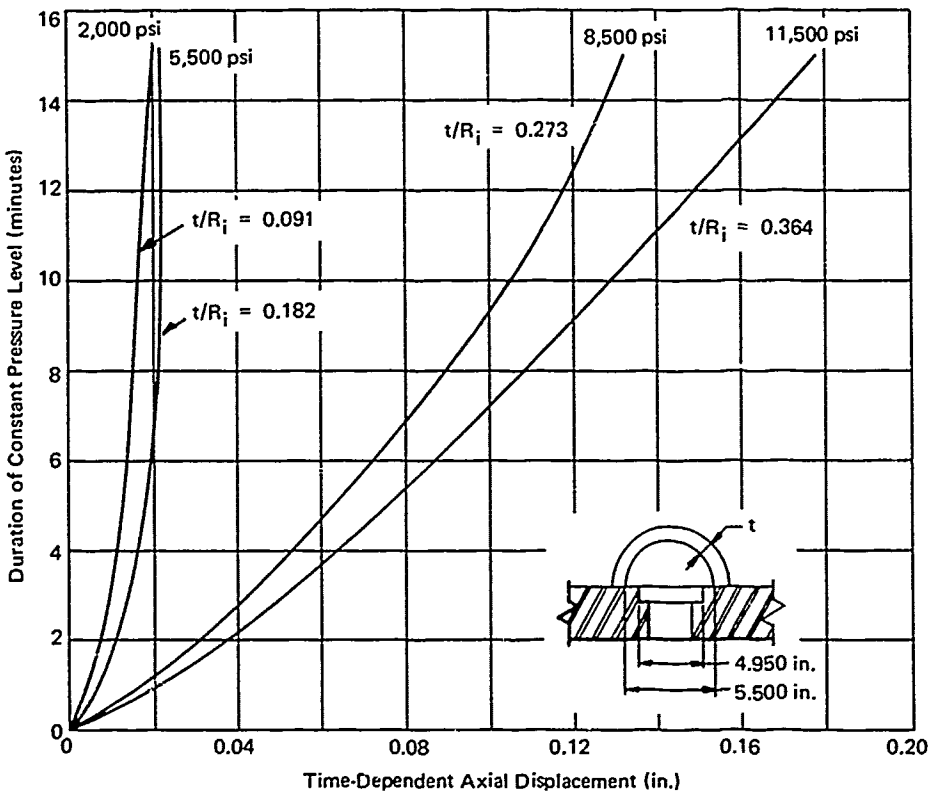

Figure G-6. Axial displacement of 180-degree spherical acrylic window under long-term hydrostatic pressure.

Material	– Grade G Plexiglas
Thickness tolerance	– ±0.010 in.
Angle tolerance	– ±15 minutes
Water temperature	– 70 ± 2°F
Pressurization rate	– 650 ± 100 psi/min
Spherical radius (R_i)	– 2.750 in.

Sliding Displacement of the windows bearing surface is measured parallel to the flange bearing surface.

Long-term pressure is held constant after being raised to the test pressure level at a 650-psi/minute rate in 68°-72°F temperature range

Each curve represents only one window specimen

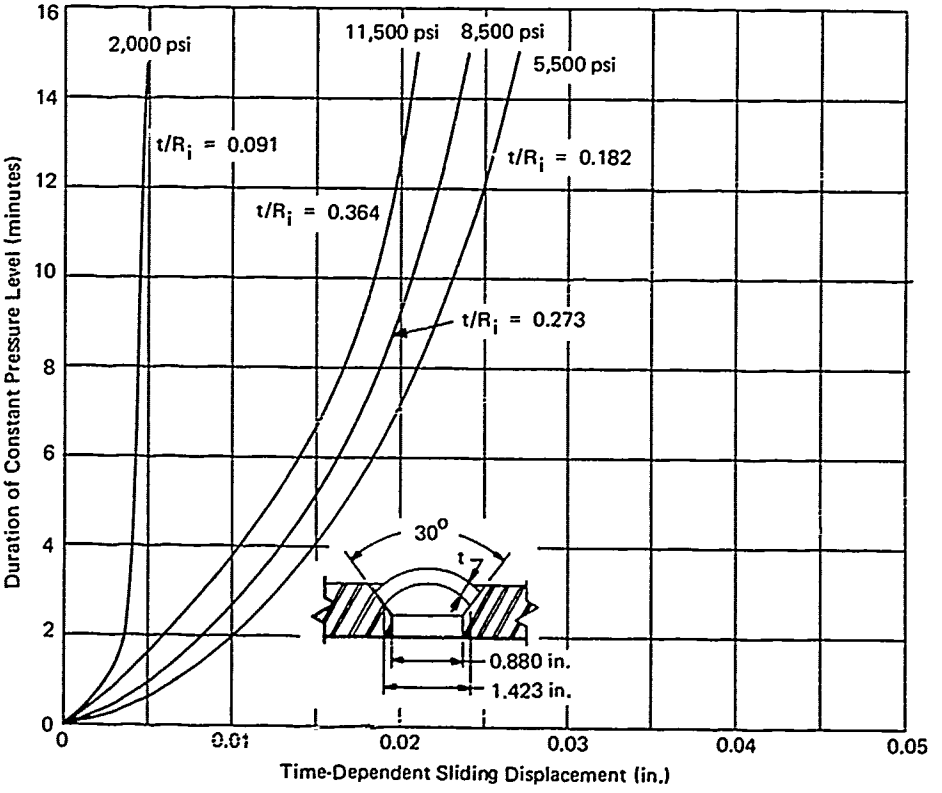

Figure G-7. Sliding displacement of 30-degree spherical acrylic windows under long-term hydrostatic pressure.

Material — Grade G Plexiglas
Thickness tolerance — ±0.010 in.
Angle tolerance — ±15 minutes
Water temperature — 70 ± 2°F
Pressurization rate — 650 ± 100 psi/min
Spherical radius (R_i) — 2.750 in.

Sliding Displacement of the windows bearing surface is measured parallel to the flange bearing surface.

Long-term pressure is held constant after being raised to the test pressure level at a 650-psi/minute rate in 68°-72°F temperature range

Each curve represents only one window specimen

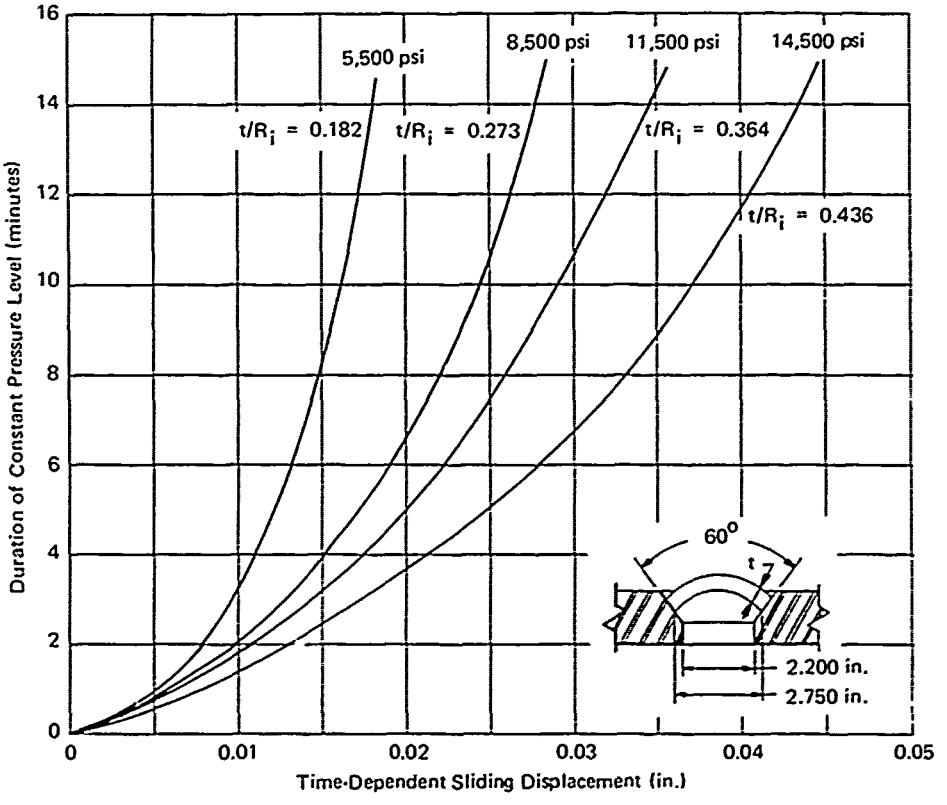

Figure G-8. Sliding displacement of 60-degree spherical acrylic windows under long-term hydrostatic pressure.

Material — Grade G Plexiglas
Thickness tolerance — ±0.010 in.
Angle tolerance — ±15 minutes
Water temperature — 70 ± 2°F
Pressurization rate — 650 ± 100 psi/min
Spherical radius (R_i) — 2.750 in.

Sliding Displacement of the windows bearing surface is measured parallel to the flange bearing surface.

Long-term pressure is held constant after being raised to the test pressure level at a 650-psi/minute rate in 68°-72°F temperature range

Each curve represents only one window specimen

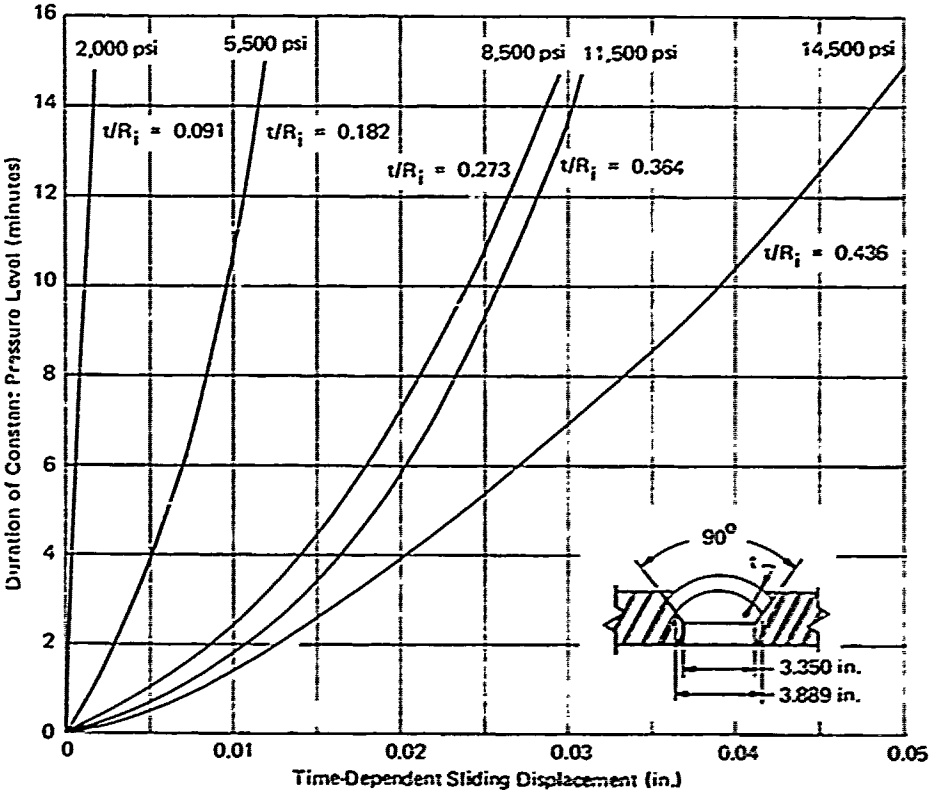

Figure G-9. Sliding displacement of 90-degree spherical acrylic windows under long-term hydrostatic pressure.

Material – Grade G Plexiglas
Thickness tolerance – ±0.010 in.
Angle tolerance – ±15 minutes
Water temperature – 70 ± 2°F
Pressurization rate – 650 + 100 psi/...
Spherical radius (R_i) – 2.750 in.

Sliding Displacement of the windows bearing surface is measured parallel to the flange bearing surface.

Long-term pressure is held constant after being raised to the test pressure level at a 650-psi/minute rate in 68°-72°F temperature range

Each curve represents only one window specimen

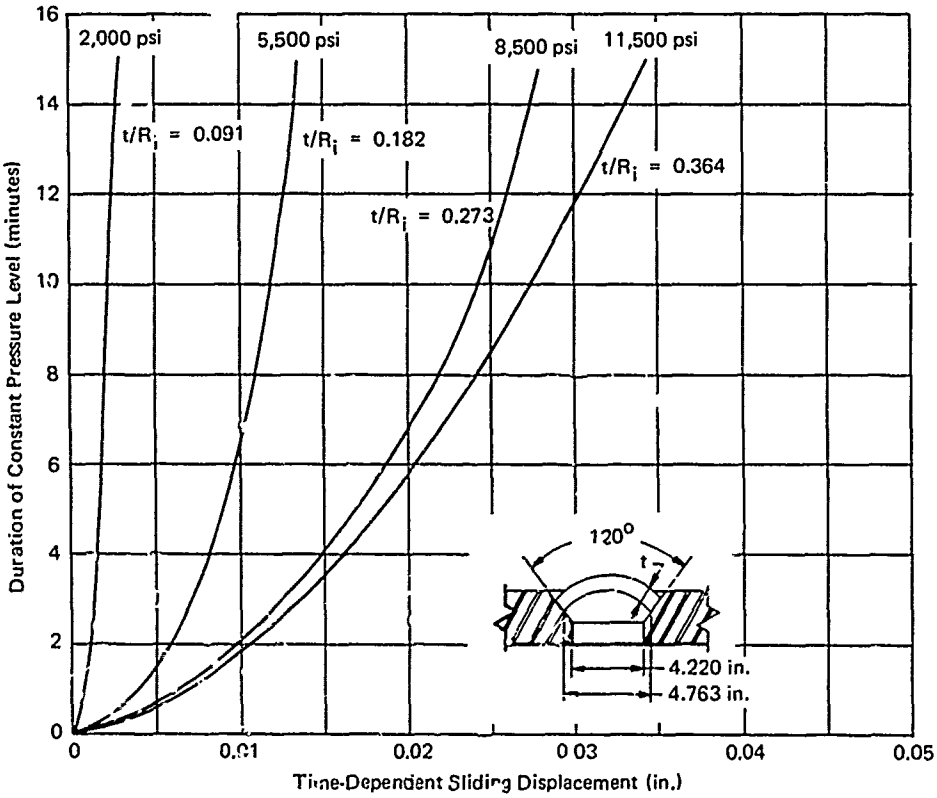

Figure G-10. Sliding displacement of 120-degree spherical acrylic windows under long-term hydrostatic pressure.

Material — Grade G Plexiglas
Thickness tolerance — ±0.010 in.
Angle tolerance — ±15 minutes
Water temperature — 70 ± 2°F
Pressurization rate — 650 ± 100 psi/min
Spherical radius (R_i) — 2.750 in.

Sliding Displacement of the windows bearing surface is measured parallel to the flange bearing surface.

Long-term pressure is held constant after being raised to the test pressure level at a 650-psi/minute rate in 68°-72°F temperature range

Each curve represents only one window specimen

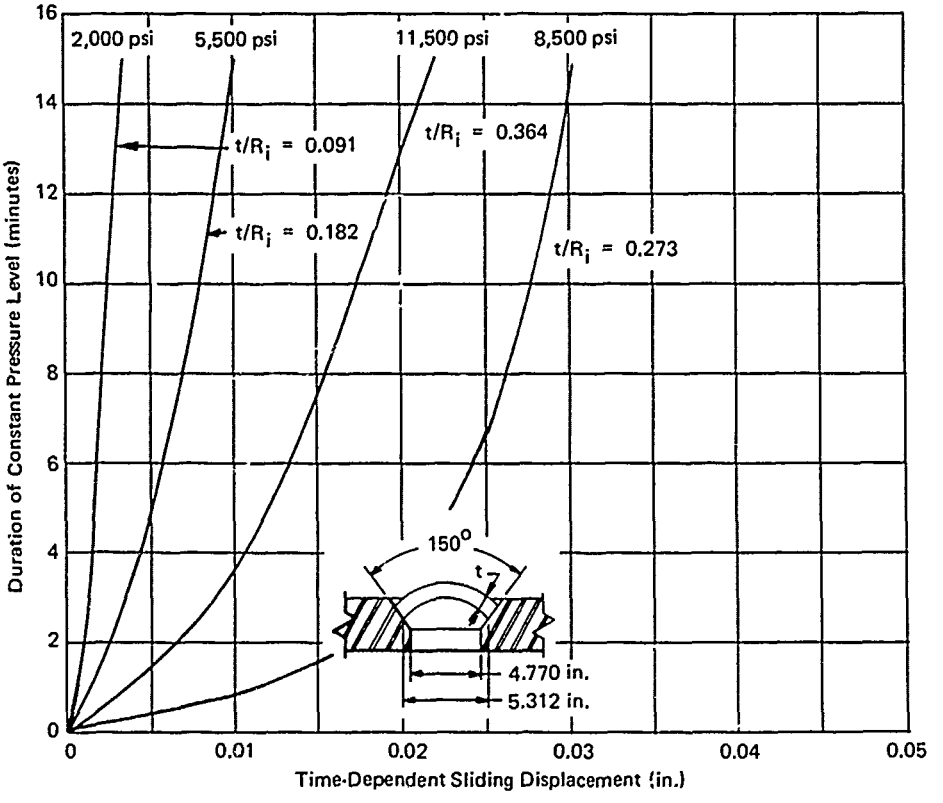

Figure G-11. Sliding displacement of 150-degree spherical acrylic windows under long-term hydrostatic pressure.

Material — Grade G Plexiglas
Thickness tolerance — ±0.010 in.
Angle tolerance — ±15 minutes
Water temperature — 70 ± 2°F
Pressurization rate — 650 ± 100 psi/min
Spherical radius (R_i) — 2.750 in.

Sliding Displacement of the windows bearing surface is measured parallel to the flange bearing surface.

Long-term pressure is held constant after being raised to the test pressure level at a 650-psi/minute rate in 68°-72°F temperature range

Each curve represents only one window specimen

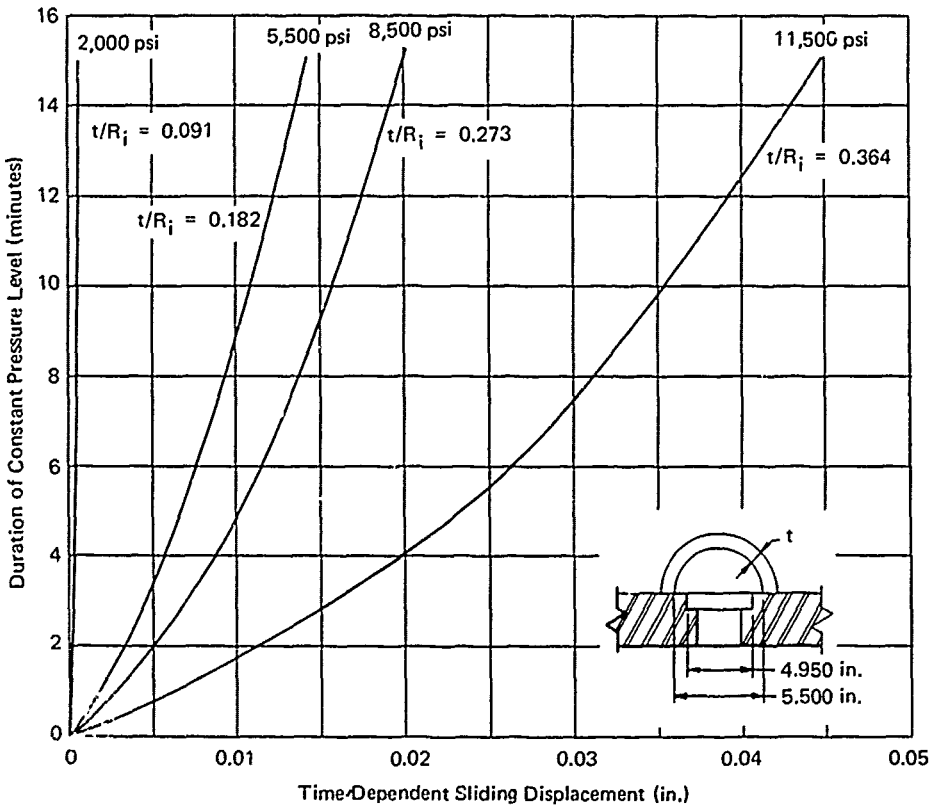

Figure G-12. Sliding displacement of 180-degree spherical acrylic windows under long-term hydrostatic pressure.

Appendix H

DESIGN CONSIDERATIONS FOR SPHERICAL SHELL WINDOW SYSTEMS

WINDOWS

Selection of Dimensions

The bulk of the data and observations generated in the primary investigation of this study pertains directly only to short-term loading under hydrostatic pressure. Only a few scattered observations were made to explore the many variables that must be considered when a spherical acrylic window is placed into actual service. However, until detailed studies are made of each variable influencing the performance of a spherical acrylic window in field service, these few indications must serve together with the short-term data as a design guide for windows under long-term or cyclic pressure loadings.

Because long-term sustained pressure and cyclic pressure loadings induce creep and static or cyclic fatigue cracks in the windows, data generated primarily with specimens under short-term loading cannot be applied to these quite different operational conditions without the use of some conversion factor. The proper magnitude of this conversion factor is not known at the present time. There are, however, indications that a conversion factor of 4 must be considered as the *absolute minimum* when the short-term critical pressures are utilized as indicators of what the critical pressure may be for windows under long-term or cyclic pressure loading. In practice this means, for example, that the window for long-term or cyclic pressure service at 2,000 psi must have the thickness required to fail at a *minimum* of 8,000 psi under short-term loading. The conversion factor chosen by the designer may be higher than 4 but never less. Exploratory long-term data discussed in Appendix G and data for a single window cycled at 25% of its short-term pressure seem to bear out the postulate that the minimum value of the conversion factor is approximately 4. The conversion factor of 4 is not to be considered a safety factor (SF) of 4, but of 1. If a safety factor is utilized it is then used to multiply the basic conversion factor of four. Thus, if a safety factor of 3 is desired, the conversion factor becomes 12, arrived at by multiplying 4 times 3.

In practice, the designer should choose at least three different window thicknesses for evaluation as full-scale prototype windows if he wishes to optimize his window design. The thinnest window would be chosen to have a conversion factor of 4 (SF of 1), the middle one a factor of 8 (SF of 2), and the thickest one a factor of 12 (SF of 3) in relation to the short-term critical pressure. (Thus, for service at 2,000-psi pressure, short-term critical pressures of 8,000 psi, 16,000 psi, and 24,000 psi would be required.) All three prototype windows should be subjected to hydrostatic tests simulating the actual service life of the window. Periodically the tests should be stopped and the specimen inspected for cracks. After a test period equivalent to 1 year's operational life of the window, the test should be stopped. At that time the final selection of the window should be made. If replacement of windows after every year of service is not considered unduly expensive, a window that exhibits some minor cracking on its bearing surface after 1 year of simulated service can be chosen. For applications where a yearly replacement of windows in service is not considered feasible or economically desirable, only a window that exhibits no cracks on the bearing surface after 1 year of simulated service should be considered. Although there exists a widely held design philosophy that windows should have a service life equal to the pressure hull of the submersible, there are very few practical arguments to support it. The arguments supporting the design philosophy stating that the operational life of the window should be 1 year are numerous. The most important ones are:

1. Testing of full-scale prototype windows for a period equal to the life of the submersible hull prior to selecting the proper window configuration is not feasible, as hull life is generally in the 10-to-20-year range.

2. A submersible must be overhauled at least once a year, when most components of mechanical and hydraulic subsystems which are wetted by seawater must be replaced. Thus, replacement of windows, if inspection of their bearing surfaces detects cracks, would involve no additional expense except the cost of new windows. The cost of new windows (anywhere from $100 to $1,000 per window depending on diameter and thickness) would be only a minor part of the total cost of overhaul, which depending on the size of the submarine is in the $50,00-to-$100,000 range.

3. Selection of windows with adequate thickness to insure an operational life equal to the life of the hull penalizes the occupants of the submersible with inadequate visibility, for in such a case the windows must be small in diameter.

Experience has shown that in most cases the testing of only three prototype windows with thicknesses that were chosen on the basis of conversion factors of 4, 8, and 12 with respect to short-term pressures is sufficient for the proper choice of window for operational conditions distinctly different from short-term pressure loading. In those cases where the window designer cannot subject several windows with different thicknesses to at least 1 year of simulated operational pressure loading prior to selecting the thinnest window that meets his approval, a simplified window selection procedure is proposed.

The simplified window selection procedure requires that the thickness of the window be selected on the basis of short-term data derated by a conversion factor of 12 (SF of 3). No pretesting of the window prior to installation in the submersible is then required so long as the window is monolithic and fabricated either by molding or machining of commercially available flat acrylic plates with mechanical properties equal to grade "G" Plexiglas. Since in the simplified window selection process all hydrostatic tests of the window prior to installation in the submersible have been dispensed with, lamination of several acrylic plates to generate a thicker window is not recommended. The strength of laminated windows is known to vary from one fabricator to another, depending on his experience and quality control, thus laminated windows must be evaluated prior to each application for use in submersibles. Since the thickest acrylic plate currently available as an off-the-shelf item is 4 inches thick, the designer following the simplified window design procedure is limited to windows with a thickness of 4 inches or less. If thicker windows are required, several thin plates can be laminated or the whole window can be machined from a massive custom casting. In either case, a prototype window should be then subjected to simulated hydrostatic loading for at least a year prior to installation in the pressure hull of other windows fabricated in an identical manner and from identical material. When more is learned about behavior of laminated windows or custom-cast windows so that meaningful specifications for their fabrication can be written, the requirement for testing of a prototype window based on a conversion factor of 12 (SF of 3) will be eliminated.

In addition to selection of the window's t/D_i and t/R_i ratios, some thought must be given to the choice of the spherical angle. Although any angle is acceptable and will result in a safe window, some angles appear more advantageous than others. One such angle appears to be 150 degrees. Spherical windows of that angle were found to exhibit less cracking on their bearing surfaces than windows with lesser or larger spherical angles when they were pressurized to a level close to their critical pressure. The

180-degree spherical windows appeared to be next in ability to resist initiation of cracks on their bearing surfaces. In view of this, it is probably to the designer's advantage to specify 150- or 180-degree spherical angle windows wherever this is feasible.

Selection of Window Material

Besides selection of the window dimensions, great care must be taken in the choice of window material and surface finish. Since all the data generated in this report is based on grade "G" Plexiglas cast acrylic plastic, it is mandatory that prototype full-scale windows chosen for submersible service be fabricated from acrylic plastic with mechanical properties equal to, or better than, grade "G" Plexiglas (Table H-1). To determine the mechanical properties, test specimens should be taken in at least one place from each acrylic plate serving as material stock for windows. A sufficient number of test specimens should be taken to provide at least five for each of the seven distinct destructive material tests.

Table H-1. Properties of Acrylic Plastic* Recommended for Fabrication of Spherical Windows

Material Properties	Magnitude	Testing Method
Mechanical		
Tensile strength	9,000 psi minimum	ASTM D-638-64T
Flexural strength	16,000 psi minimum	ASTM D-790-66
Shear strength	9,000 psi minimum	ASTM D-732-46
Compressive strength	16,000 psi minimum	ASTM D-695-63T
Deformation under load (4,000 psi at 122°F for 24 hours)	1% maximum	ASTM D-621-64
Modulus of elasticity in compression	450,000 psi minimum	ASTM D-695-63T
Elongation under tension	3 to 6%	ASTM D-638-64T
Impact strength (Charpy unnotched)	3 ft-lb minimum	ASTM D-256-56
Deflection temperature (3.6°F/min at 264 psi on 0.250-inch-thick specimen	200°F minimum	ASTM D-648-56
Physical		
Hardness, Rockwell M	90 minimum	–
Specific gravity	1.19 ± 0.01	ASTM D-792-50
Refractive index	1.50 ± 0.01	ASTM D-542-50
Luminous transmittance	91% minimum	ASTM D-1003-52(A)
Haze	2% maximum	ASTM D-1003-52(A)

* Based on the properties of commercially available cast acrylic plates and sheets of grade "G" Plexiglas.

Selection of Fabrication Tolerances

Once the material with mechanical properties equal to grade "G" Plexiglas has been chosen, great care must be taken in the fabrication process to use such machining speeds and cutting tools that unduly large stresses are not introduced into the window at that time. The viewing surfaces of the window must be provided with an optically desirable finish, and the bearing surface of the window should have a 32-rms finish. Thorough annealing of the window must follow the machining process.

Although no special studies have been conducted on the influence of deviation in the spherical sector angle on the behavior of the spherical window, there are indications that a ± 15-minute deviation from the specified sector angle can be safely tolerated by the window. Sharp edges of the window should be beveled with a 1/32-inch radius to avoid chipping during shipping and installation.

Proof-testing of Windows

It is an accepted practice in hydrospace engineering to proof-test every component of hardware that is exposed to hydrostatic pressure. The testing either takes place on individual components, subassemblies, or complete functional assemblies. Some of the components are subjected to proof-testing several times—once when they are tested individually prior to inclusion into the habitat structure and a second time when the whole habitat structure is proof-tested.

The magnitude of proof pressure varies widely. It is never less than the maximum forecast operational pressure, but often considerably higher, in which case it is designated an overpressure proof test. The magnitude of the overpressure varies from 15% to 100% above operational pressure. It is thought that by subjecting the operational hardware to an overpressure proof test prior to the submersible's operation in the ocean, an added margin of safety for the components can be assured. Although there are many viewpoints on the subject of proof-test magnitude, they all concur on the point that some form of proof-testing is needed. This, of course, applies also to windows, as they are components of pressure hulls whose failure would lead to loss of life.

Windows may be proof-tested in a flange subassembly fastened to the end closure of an internal pressure vessel, or they may be tested when the complete habitat pressure hull assembly is proof-tested. The latter approach is more desirable so long as the proof-testing of the whole assembly takes place in an unmanned mode, inside an internal pressure

vessel, where the failure of a window will not result in the loss of life or of the habitat. This approach to proof-testing is more desirable, because the flange in which the window is located is subjected to the same hull stresses and moments that will prevail during the operational life of the window–flange assembly. Wherever such an approach to proof-testing is not feasible because of the lack of a pressure vessel sufficiently large to contain the hull of the habitat, a special jig must be utilized for the testing of windows. Although it is impossible to build a window test jig in which the flange undergoes deformations identical to those it will experience in the pressure hull, the deformation should be as nearly identical as is feasible.

The most important part of window design and subsequent proof-testing of fabricated windows is the selection of the relationship between the window's operational pressure, proof pressure, and failure pressure. Since improper relationship between these three variables may, and in many cases will, result in permanent damage to the window, it is of great importance to select a proper relationship between them. In general, the proof pressure chosen should not be so high as to permanently distort or craze the window before it actually sees operational service at lower pressure. Whether this happens or not depends to a large extent on the magnitude of the selected operational pressure in respect to the pressure at which undesirable deformation will take place. Because some of the windows for habitats may be chosen on the basis of this, or other NCEL studies published previously,[1-3] some design guidelines may be of help.

If the window dimensions are chosen as recommended on the basis of short-term data derated by a conversion factor of 12 (SF of 3), the magnitude of the proof-test pressure, p_t, must fall within the range of $p_o < p_t < p_c$, the limits being the operational and critical pressures of the window. Selecting a proof-test pressure (p_t) too close to the operational pressure (p_o) results in a proof test with inadequate overpressure margin; raising the proof-test pressure too close to the critical pressure under short-term loading (p_c) will irreversibly damage the window and thus actually lower the SF of 3 with which the windows were initially designed.

Because of the danger of irreversible damage, the maximum permissible magnitude of the proof-test pressure appears to be $1.5 \times p_o$. This magnitude of proof-test pressure appears to be sufficiently higher than operational pressure to generate confidence in the adequacy of window to withstand operational pressure. At the same time the proof-test pressure is not high enough to permanently damage the window (unless it exceeds 20,000 psi).

When such a proof test is performed, its duration should not exceed that of a single typical dive which such windows will experience in their operational life.

FLANGE

Selection of Flange Dimensions

The most important parameters that must be considered in the flange design are selection of proper conical angle for bearing surfaces of the flange, provisions for adequate window bearing surface support, correct machining tolerances, sealing of the window against external pressure, and secure retention of the window in the flange.

Any conical angle can be chosen for the window seat in the flange providing it is identical to the spherical angle chosen for the window. All of the spherical angles used in this study were found to be acceptable, however, windows with a 60-degree angle and low t/R_i ratios were found to be rather unstable on their seat in the flange and thus tended to displace unevenly under application of hydrostatic pressure. If elaborate precautions were not taken to place them squarely on the window seat in the flange or to secure them against uneven displacement by means of a sturdy retaining ring, they would rock in the flange, and fail at considerably lower pressure than they are capable of withstanding. For this reason, 60-degree conical window seat and flange assemblies are not recommended, particularly if the t/R_i ratio of the window is less than 0.275, unless the window is secured in the flange with a substantial retaining ring pressing against the high-pressure surface of the window around its circumference.

The support area of the window bearing surface on the flange must be large enough to allow for the sliding displacement of the window's edge. Since the magnitude of sliding displacement depends on the window dimensions, operational pressure, and duration of loading, the width of the bearing surface on the flange should be selected accordingly. This is possible, however, only on the basis of experimental data pertaining to the particular diving schedule that a particular window will be subjected to.

In the absence of such experimental data the selection of the proper window dimensions must either follow the criteria established for the DOL Type IV flange used in the short-term pressurization study or some other arbitrary dimensioning system.

The main feature of flange dimensioning for the DOL Type IV flange is that the width of the flange bearing surface is a function of the window's internal spherical radius, R_i, and low-pressure-face diameter, D_i. The width of the flange bearing seat used in this study was determined by the relationship $D_f = D_i - 0.2\ R_i$. Since the provision made in the DOL Type IV flange for the support of the window sliding upon the flange seat was more than adequate for short-term loading of windows to failure, it is considered an

overconservative design. This design, however, results in the low-pressure flange opening being considerably smaller than the low-pressure-face diameter of the window, thus restricting the useful size of the porthole.

To avoid undue restriction, whenever possible, a design based on the actual measured displacement of the prototype window under simulated operational dive conditions should be utilized as the basis for establishing the relationship between D_i and D_f. Utilizing this kind of approach, the D_f would be maximized and the occupants of the submersible would have the maximum possible view for the given window diameter, D_i.

Until exact data becomes available which will optimize the size of the flange opening, a flange design less conservative than the DOL Type IV but still adequate should be adopted. This less conservative flange design (Figure H-1) will perform well with windows selected on the basis of short-term data contained in this report derated by a factor of 12 (SF of 3). This design requires that $D_f = 0.9\ D_i$, regardless of what the window curvature or sector angle may be. If transparent plastic materials other than acrylics (meeting the specifications of Table H-1) or conversion factors less than 12 (SF of 3) are utilized, the suggested design relationship of $D_f = 0.9\ D_i$ should not be used.

Selection of Fabrication Tolerances

The surface finish on the flange bearing seat should be 63 rms; rougher finishes tend to restrain the sliding of the window in the flange more than necessary and thus generate larger bending moments in the spherical window. If it is feasible the bearing surface should be corrosion resistant to obviate refinishing the surface after years of service. This can be accomplished by the use of a corrosion-resistant flange insert, corrosion resistant plating, or epoxy base paints. Regardless which type, if any, of corrosion-resistant finish is used on the flange seat, liberal coverage with corrosion-retarding greases is required. Besides protecting the flange seat from corrosion the grease also aids in the sliding and in sealing the window under pressure.

Tolerances on the bearing seat angle under zero pressure should be less than ±15 minutes. The permissible change of cone-seat angle under pressure-generated stresses in the hull is presently unknown. It can be generally postulated that probably so long as the magnitude of angle distortion is less than ±30 minutes no significant effects in window performance will be detected.

Selection of Window Retainer and Seals

Since the forces generated in the window flange assembly under hydrostatic pressure tend to cock an imperfectly fitting window in its seat, particularly if it has a 60-degree spherical sector angle and low t/R_i ratio, an external restraint system should be provided. If the window is permitted to cock in its flange during application of hydrostatic pressure, it will fail at much lower pressure than it would otherwise. The initial restraint on the window is generally provided with a retainer ring situated on the high-pressure side of the window. This retainer ring, besides restraining the window from cocking in its flange, also serves as a seal gasket retainer. No mechanical restraints should be imposed on the window's displacement from the low-pressure side, as this invariably leads to premature failure of the window.

High-Pressure Seal. The sealing of spherical windows under high hydrostatic pressure relies, as in conical windows with plane surfaces, on the grease trapped between the bearing surfaces of the window and of the flange. The low-pressure seal, on the other hand, is either a neoprene gasket or an O-ring compressed by the external retainer ring. The important consideration in selecting the thickness of the gasket or O-ring is the magnitude of window displacement while it is under hydrostatic pressure. If the gasket or O-ring is sufficiently thick and well compressed by the retainer ring prior to hydrostatic loading, it will remain in contact with the window surface even when it slides upon the flange bearing surface under hydrostatic pressure. Since the displacement of most spherical windows under operational pressure (selected on the basis of a conversion factor of 12) is about 0.1 inch for those in the 4-to-6-inch-diameter range, about 0.2 inch for those in the 8-to-12-inch-diameter range, and about 0.5 inch for windows in the 20-to-30-inch-diameter range, the compression of the gasket during its installation must be at least that large, or larger. If such is the case, the external gasket will seal both under low and high pressures, making it impossible for seawater to enter between flange seat and window, and thus eliminate the major source of window seat corrosion.

Low-Pressure Seal. Preventing the entry of seawater into the space between the window and the flange seat eliminates the major, but not all sources of corrosion. Another cause of some corrosion of flange seats is condensate which runs down the interior of pressure hulls. If there is no low-pressure seal on the low-pressure face of the window, the condensate seeps into the space between the relaxing window and the flange seat when the submersible returns from the dive and is at the ocean surface or on deck. Because condensate is not seawater, its ravages are less serious, but still appreciable.

It is possible to eliminate even this source of corrosion by incorporating a low-pressure seal into the design of the window and flange system. Such a seal could take the form of a elastomeric V-shaped gasket held against the window by means of an elastic split ring that would not provide any appreciable restraint on the window displacement. This spring-loaded gasket would follow faithfully the movements of the window but still protect the flange seat under the window from influx of condensate.

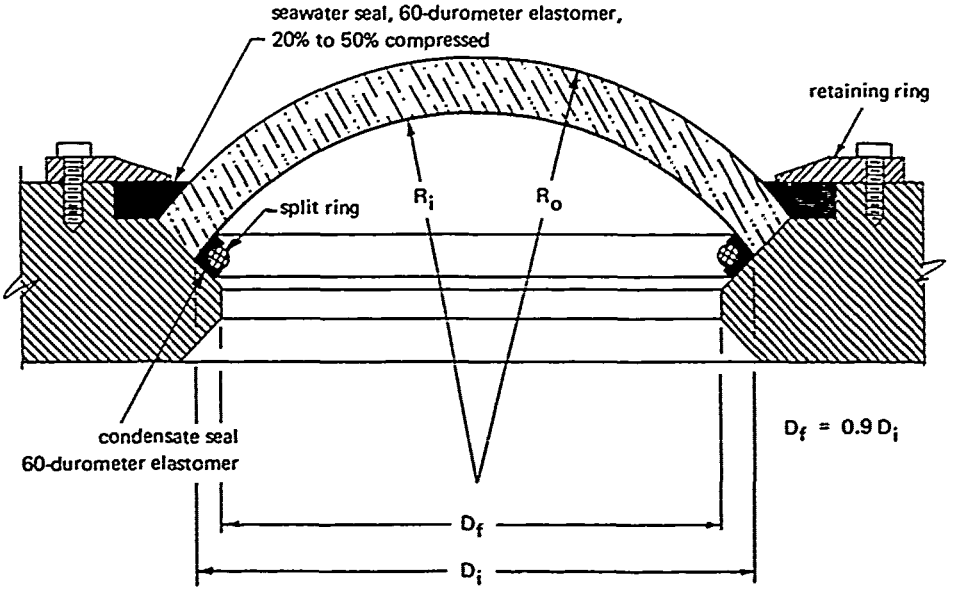

Figure H-1. Suggested configuration for spherical window and flange system for hydrospace acrylic windows.

Appendix I

TABULATED DATA FOR SHORT-TERM PRESSURIZATION TESTS OF SPHERICAL ACRYLIC WINDOWS

The experimental data generated during the short-term testing of spherical windows has been summarized in the form of graphs (Figures 28 through 57) for ready reference by the designer. However, the summarized data does not lend itself to statistical stress analysis of experimental variables recorded during the conduct of the experiment. For this reason the detailed experimental data has been included in this report as Appendix I.

Table I-1. Axial Displacement of Spherical Acrylic Windows Subjected to Short-Term Pressurization in DOL Type IV Flange

(r_i = 2.750 in., t = 0.250 in.; α = 30 degrees)

Pressure (psi)	Specimen Number 1	2	3	4	5	Maximum Value	Average Value	Minimum Value
	Axial Displacement of Center Point on Window Low-Pressure Face (in.)							
1,000	0.015	0.026	0.028	0.005	0.021	0.028	0.019	0.005
2,000	0.048	0.047	0.057	0.041	0.045	0.057	0.048	0.041
3,000	0.092	0.096	0.110	0.088	0.100	0.110	0.097	0.088
4,000								
5,000								
6,000								
7,000								
8,000								
9,000								
10,000								
11,000								
12,000								
13,000								
14,000								
15,000								
16,000								
17,000								
18,000								
19,000								
20,000								
21,000								
22,000								
23,000								
24,000								
25,000								
26,000								
27,000								
28,000								
29,000								
30,000								
	Critical Pressure (psi)							
	3,000	3,200	3,350	3,450	3,250	3,450	3,250	3,000
	Temperature (^{o}F)							
	70	70	70	71	71	71	70	70
	Pressurization Rate (psi/min)							
	667	666	684	667	688	688	674	666

Table I-2. Axial Displacement of Spherical Acrylic Windows Subjected to Short-Term Pressurization in DOL Type IV Flange

(R_i = 2.750 in., t = 0.375 in.; α = 30 degrees)

Pressure (psi)	Specimen Number					Maximum Value	Average Value	Minimum Value
	6	7	8	9	10			
	Axial Displacement of Center Point on Window Low-Pressure Face (in.)							
1,000	0.010	0.011	0.011	0.022	0.017	0.022	0.014	0.010
2,000	0.020	0.034	0.031	0.040	0.035	0.040	0.032	0.020
3,000	0.040	0.055	0.051	0.060	0.053	0.060	0.052	0.040
4,000	0.063	0.078	0.076	0.082	0.075	0.082	0.075	0.063
5,000	0.094	0.113	0.112	0.112	0.110	0.113	0.108	0.094
6,000	0.175		0.210	0.163	0.168	0.210	0.179	
7,000								
8,000								
9,000								
10,000								
11,000								
12,000								
13,000								
14,000								
15,000								
16,000								
17,000								
18,000								
19,000								
20,000								
21,000								
22,000								
23,000								
24,000								
25,000								
26,000								
27,000								
28,000								
29,000								
30,000								
	Critical Pressure (psi)							
	6,050	5,700	6,000	6,450	6,350	6,450	6,110	5,700
	Temperature (^{o}F)							
	70	71	71	70	70	71	70	70
	Pressurization Rate (psi/min)							
	665	678	668	667	667	678	669	665

Table I-3. Axial Displacement of Spherical Acrylic Windows Subjected to Short-Term Pressurization in DOL Type IV Flange

(R_i = 2.750 in.; t = 0.500 in.; α = 30 degrees)

Pressure (psi)	Specimen Number					Maximum Value	Average Value	Minimum Value
	11	12	13	14	15			
	Axial Displacement of Center Point on Window Low-Pressure Face (in.)							
1,000	0.013	0.020	0.018	0.002	0.001	0.021	0.011	0.001
2,000	0.039	0.040	0.032	0.017	0.017	0.040	0.029	0.017
3,000	0.051	0.059	0.047	0.032	0.033	0.059	0.044	0.032
4,000	0.063	0.077	0.063	0.040	0.047	0.077	0.058	0.040
5,000	0.087	0.098	0.082	0.067	0.075	0.098	0.082	0.067
6,000	0.118	0.124	0.105	0.090	0.104	0.124	0.108	0.090
7,000	0.139	0.156	0.131	0.118	0.132	0.156	0.135	0.118
8,000	0.174	0.185	0.172	0.165	0.148	0.185	0.169	0.148
9,000	0.214	0.235	0.228	0.188	0.179	0.235	0.209	0.179
10,000	0.270	0.324			0.216	0.324	0.270	0.216
11,000					0.251			
12,000					0.298			
13,000					0.395			
14,000					0.580			
15,000					0.750			
16,000								
17,000								
18,000								
19,000								
20,000								
21,000								
22,000								
23,000								
24,000								
25,000								
26,000								
27,000								
28,000								
29,000								
30,000								
	Critical Pressure (psi)							
	10,750	10,600	9,900	9,300	14,250	14,250	10,960	9,300
	Temperature (°F)							
	70	70	70	70	70	70	70	70
	Pressurization Rate (psi/min)							
	667	667	662	664	667	667	665	662

Table I-4. Axial Displacement of Spherical Acrylic Windows Subjected to Short-Term Pressurization in DOL Type IV Flange

(R_i = 2.750 in.; t = 0.625 in.; α = 30 degrees)

Pressure (psi)	Specimen Number					Maximum Value	Average Value	Minimum Value
	16	17	18	19	20			
	Axial Displacement of Center Point on Window Low-Pressure Face (in.)							
1,000	0.003	0.014	0.005	0.012	0.005	0.014	0.008	0.003
2,000	0.014	0.029	0.011	0.027	0.011	0.029	0.018	0.011
3,000	0.025	0.042	0.018	0.041	0.017	0.042	0.029	0.017
4,000	0.039	0.056	0.025	0.055	0.024	0.056	0.040	0.024
5,000	0.055	0.072	0.042	0.070	0.031	0.072	0.054	0.031
6,000	0.070	0.091	0.062	0.088	0.046	0.091	0.071	0.046
7,000	0.092	0.112	0.084	0.109	0.069	0.112	0.093	0.069
8,000	0.120	0.137	0.113	0.134	0.095	0.137	0.120	0.095
9,000	0.155	0.172	0.146	0.168	0.133	0.172	0.155	0.133
10,000	0.194	0.216	0.198	0.206	0.173	0.216	0.197	0.173
11,000	0.257	0.268	0.262	0.246	0.231	0.268	0.253	0.231
12,000	0.325	0.335	0.350	0.304	0.304	0.350	0.324	0.304
13,000	0.404	0.406	0.485	0.378	0.386	0.485	0.412	0.378
14,000	0.508	0.493	0.682	0.450	0.473	0.682	0.521	0.450
15,000		0.589		0.517	0.560			
16,000				0.613	0.740			
17,000								
18,000								
19,000								
20,000								
21,000								
22,000								
23,000								
24,000								
25,000								
26,000								
27,000								
28,000								
29,000								
30,000								
	Critical Pressure (psi)							
	14,800	15,600	14,300	16,300	15,900	16,300	15,080	14,300
	Temperature (^{o}F)							
	69	70	71	69	71	71	70	69
	Pressurization Rate (psi/min)							
	655	667	665	665	655	667	661	65.

Table I-5. Axial Displacement of Spherical Acrylic Windows Subjected to Short-Term Pressurization in DOL Type IV Flange

(R_i = 2.750 in.; t = 0.750 in.; α = 30 degrees)

Pressure (psi)	Specimen Number					Maximum Value	Average Value	Minimum Value
	21	22	23	24	25			
	Axial Displacement of Center Point on Window Low-Pressure Face (in.)							
1,000	0.002	0.001	0.015	0.001	0.009	0.015	0.006	0.001
2,000	0.016	0.011	0.028	0.012	0.020	0.028	0.017	0.011
3,000	0.028	0.019	0.040	0.025	0.031	0.040	0.029	0.019
4,000	0.042	0.030	0.052	0.040	0.045	0.052	0.042	0.030
5,000	0.055	0.044	0.066	0.055	0.058	0.066	0.056	0.044
6,000	0.071	0.059	0.082	0.075	0.075	0.082	0.072	0.059
7,000	0.091	0.073	0.098	0.094	0.092	0.098	0.090	0.073
8,000	0.105	0.094	0.116	0.116	0.111	0.116	0.108	0.094
9,000	0.128	0.115	0.135	0.141	0.128	0.141	0.129	0.115
10,000	0.154	0.137	0.156	0.167	0.144	0.167	0.152	0.137
11,000	0.182	0.160	0.179	0.192	0.166	0.192	0.176	0.160
12,000	0.212	0.190	0.197	0.212	0.184	0.212	0.199	0.184
13,000	0.234	0.227	0.214	0.243	0.205	0.243	0.225	0.205
14,000	0.271	0.267	0.234	0.262	0.227	0.271	0.252	0.227
15,000	0.308	0.310	0.252	0.286	0.253	0.310	0.282	0.252
16,000	0.342	0.360	0.270	0.310	0.280	0.360	0.312	0.270
17,000	0.393	0.419	0.293	0.339	0.312	0.419	0.351	0.293
18,000	0.440	0.481	0.318	0.365	0.344	0.481	0.390	0.318
19,000	0.489	0.535	0.341	0.396	0.375	0.535	0.427	0.341
20,000	0.536	0.594	0.365	0.424	0.401	0.594	0.464	0.365
21,000	0.587	0.644	0.387	0.461	0.438	0.644	0.503	0.387
22,000	0.695	0.685	0.419	0.485	0.466	0.695	0.550	0.419
23,000	0.765	0.723	0.532	0.525	0.512	0.765	0.611	0.512
24,000	0.787	0.760	0.590	0.570	0.537	0.787	0.645	0.537
25,000	0.823	0.797	0.660	0.640	0.577	0.823	0.700	0.577
26,000	0.836	0.826	0.698	0.689	0.614	0.836	0.732	0.614
27,000	0.851	0.843	0.758	0.742	0.652	0.851	0.769	0.652
28,000	0.890	0.879	0.820	0.808	0.715	0.890	0.822	0.715
29,000	0.925	0.918	0.906	0.890	0.810	0.925	0.890	0.810
30,000	0.960	0.945	0.915	0.905	0.898	0.960	0.925	0.898
	Critical Pressure (psi)							
	30,000*	30,000*	30,000*	30,000*	30,000*	30,000	30,000	30,000
	Temperature (°F)							
	71	68	70	71	68	71	69	68
	Pressurization Rate (psi/min)							
	532	662	650	666	666	666	635	532

* Value does not represent critical pressure, critical pressure was greater than capacity of pumping system, but failure was inevitable at pressures above 30,000 psi.

Table I-6. Axial Displacement of Spherical Acrylic Windows Subjected to Short-Term Pressurization in DOL Type IV Flange

(R_i = 2.750 in.; t = 1.000 in.; α = 30 degrees)

Pressure (psi)	Specimen Number					Maximum Value	Average Value	Minimum Value
	26	27	28	29	30			
	Axial Displacement of Center Point on Window Low-Pressure Face (in.)							
1,000	0.001	0.002	0.004	0.008	0.006	0.008	0.004	0.001
2,000	0.002	0.004	0.013	0.019	0.010	0.019	0.010	0.002
3,000	0.011	0.016	0.025	0.028	0.019	0.028	0.020	0.011
4,000	0.020	0.017	0.036	0.037	0.030	0.037	0.026	0.017
5,000	0.027	0.026	0.047	0.049	0.040	0.049	0.038	0.026
6,000	0.040	0.036	0.059	0.061	0.053	0.061	0.056	0.036
7,000	0.057	0.047	0.072	0.073	0.066	0.073	0.063	0.047
8,000	0.072	0.068	0.087	0.088	0.081	0.088	0.079	0.068
9,000	0.081	0.078	0.102	0.102	0.097	0.102	0.098	0.078
10,000	0.097	0.095	0.117	0.119	0.115	0.119	0.109	0.095
11,000	0.112	0.116	0.131	0.137	0.134	0.137	0.126	0.112
12,000	0.128	0.130	0.147	0.152	0.155	0.155	0.142	0.128
13,000	0.146	0.144	0.166	0.167	0.175	0.175	0.160	0.144
14,000	0.171	0.166	0.181	0.181	0.195	0.195	0.179	0.166
15,000	0.188	0.188	0.197	0.195	0.213	0.213	0.196	0.188
16,000	0.209	0.209	0.206	0.211	0.235	0.235	0.214	0.206
17,000	0.230	0.236	0.231	0.222	0.258	0.258	0.235	0.222
18,000	0.254	0.258	0.251	0.240	0.281	0.281	0.257	0.240
19,000	0.283	0.281	0.264	0.256	0.303	0.303	0.277	0.256
20,000	0.308	0.312	0.289	0.274	0.329	0.329	0.302	0.274
21,000	0.336	0.345	0.308	0.291	0.357	0.357	0.327	0.291
22,000	0.367	0.368	0.324	0.308	0.384	0.384	0.350	0.308
23,000	0.400	0.405	0.345	0.328	0.412	0.412	0.378	0.328
24,000	0.428	0.437	0.380	0.348	0.447	0.447	0.408	0.348
25,000	0.462	0.460	0.393	0.369	0.471	0.471	0.431	0.369
26,000	0.495	0.500	0.406					
27,000	0.528	0.534	0.427					
28,000	0.563	0.579	0.455					
29,000	0.590	0.594	0.484					
30,000	0.690	0.699	0.518					
	Critical Pressure (psi)							
	30,000*	30,000*	30,000*	30,000*	30,000*	30,000	30,000	30,000
	Temperature (°F)							
	69	70	71	67	68	71	69	67
	Pressurization Rate (psi/min)							
	665	662	640	665	663	665	659	640

* Value does not represent critical pressure; critical pressure was greater than capacity of pumping system, but failure was inevitable at pressures above 30,000 psi.

Table I-7. Axial Displacement of Spherical Acrylic Windows Subjected to Short-Term Pressurization in DOL Type IV Flange

(R_i = 2.750 in.; t = 0.250 in.; α = 60 degrees)

Pressure (psi)	Specimen Number					Maximum Value	Average Value	Minimum Value
	31	32	33	34	35			
	Axial Displacement of Center Point on Window Low-Pressure Face (in.)							
1,000	0.040	0.012	0.030	0.015	0.005	0.040	0.020	0.005
2,000	0.079	0.061	0.077		0.045	0.079	0.066	0.045
3,000								
4,000								
5,000								
6,000								
7,000								
8,000								
9,000								
10,000								
11,000								
12,000								
13,000								
14,000								
15,000								
16,000								
17,000								
18,000								
19,000								
20,000								
21,000								
22,000								
23,000								
24,000								
25,000								
26,000								
27,000								
28,000								
29,000								
30,000								
	Critical Pressure (psi)							
	2,780	2,500	2,600	1,200	2,600	2,780	2,336	2,500
	Temperature (^{o}F)							
	70	69	68	71	70	71	70	68
	Pressurization Rate (psi/min)							
	654	652	728	706	662	728	680	652

Table I-8. Axial Displacement of Spherical Acrylic Windows Subjected to Short-Term Pressurization in DOL Type IV Flange

(R_i = 2.750 in.; t = 0.500 in.; α = 60 degrees)

Pressure (psi)	Specimen Number					Maximum Value	Average Value	Minimum Value
	36	37	38	39	40			
	Axial Displacement of Center Point on Window Low-Pressure Face (in.)							
1,000	0.001	0.008	0.013	0.003	0.005	0.013	0.006	0.001
2,000	0.008	0.018	0.025	0.020	0.021	0.025	0.018	0.008
3,000	0.022	0.035	0.046	0.038	0.039	0.046	0.036	0.022
4,000	0.043	0.063	0.066	0.068	0.057	0.068	0.059	0.043
5,000	0.067	0.082	0.089	0.085	0.083	0.089	0.081	0.067
6,000	0.096	0.125	0.130	0.118	0.120	0.130	0.118	0.096
7,000	0.144		0.190	0.178	0.178	0.190	0.172	0.144
8,000	0.265							
9,000								
10,000								
11,000								
12,000								
13,000								
14,000								
15,000								
16,000								
17,0C								
18,000								
19,000								
20,000								
21,000								
22,000								
23,000								
24,000								
25,000								
26,000								
27,000								
28,000								
29,000								
30,000								
	Critical Pressure (psi)							
	8,250	6,400	7,500	7,550	7,750	8,250	7,490	7,000
	Temperature (°F)							
	69	69	70	70	70	70	70	69
	Pressurization Rate (psi/min)							
	667	661	670	662	668	670	666	661

Table I-9. Axial Displacement of Spherical Acrylic Windows Subjected to Short-Term Pressurization in DOL Type IV Flange

(R_i = 2.750 in.; t = 0.750 in.; α = 60 degrees)

Pressure (psi)	Specimen Number					Maximum Value	Average Value	Minimum Value
	41	42	43	44	45			
	Axial Displacement of Center Point on Window Low-Pressure Face (in.)							
1,000	0.001	0.002	0.029	0.001	0.000	0.029	0.007	0.000
2,000	0.011	0.013	0.041	0.033	0.001	0.041	0.020	0.001
3,000	0.025	0.031	0.054	0.046	0.011	0.054	0.033	0.011
4,000	0.036	0.048	0.068	0.060	0.026	0.068	0.046	0.036
5,000	0.050	0.063	0.082	0.074	0.041	0.082	0.062	0.041
6,000	0.066	0.078	0.100	0.090	0.058	0.100	0.078	0.058
7,000	0.081	0.094	0.118	0.100	0.076	0.118	0.094	0.076
8,000	0.100	0.109	0.138	0.128	0.098	0.139	0.115	0.100
9,000	0.135	0.138	0.164	0.154	0.123	0.164	0.143	0.123
10,000	0.157	0.169	0.191	0.190	0.151	0.191	0.172	0.151
11,000	0.193	0.222	0.228	0.220	0.187	0.229	0.210	0.187
12,000	0.241	0.264	0.281	0.272	0.250	0.281	0.262	0.241
13,000	0.319	0.358	0.358	0.354	0.334	0.359	0.345	0.258
14,000	0.545		0.645	0.720				
15,000								
16,000								
17,000								
18,000								
19,000								
20,000								
21,000								
22,000								
23,000								
24,000								
25,000								
26,000								
27,000								
28,000								
29,000								
30,000								
	Critical Pressure (psi)							
	14,200	13,800	14,050	14,050	13,500	14,200	13,920	13,500
	Temperature (°F)							
	68	70	69	69	69	70	69	68
	Pressurization Rate (psi/min)							
	670	667	667	667	669	670	668	667

Table I-10. Axial Displacement of Spherical Acrylic Windows Subjected to Short-Term Pressurization in DOL Type IV Flange

(R_i = 2.750 in.; t = 1.000 in.; α = 60 degrees)

Pressure (psi)	Specimen Number					Maximum Value	Average Value	Minimum Value
	46	47	48	49	50			
	Axial Displacement of Center Point on Window Low-Pressure Face (in.)							
1,000	0.000	0.016	0.025	0.011	0.010	0.025	0.015	0.000
2,000	0.010	0.028	0.037	0.024	0.023	0.037	0.024	0.010
3,000	0.018	0.039	0.050	0.036	0.036	0.050	0.036	0.018
4,000	0.031	0.049	0.062	0.048	0.067	0.067	0.051	0.031
5,000	0.041	0.060	0.070	0.058	0.069	0.070	0.060	0.041
6,000	0.056	0.072	–	0.071	0.076	0.076	0.069	0.056
7,000	0.072	0.083	–	0.085	0.091	0.091	0.083	0.072
8,000	0.084	0.097	0.101	0.097	0.107	0.107	0.097	0.084
9,000	0.103	0.120	0.120	0.112	0.124	0.124	0.116	0.103
10,000	0.119	0.131	0.142	0.135	0.142	0.142	0.134	0.119
11,000	0.142	0.156	0.162	0.154	0.162	0.162	0.155	0.142
12,000	0.166	0.170	0.195	0.175	0.183	0.195	0.178	0.166
13,000	0.192	0.194	0.233	0.201	0.209	0.233	0.206	0.192
14,000	0.221	0.220	0.275	0.234	0.239	0.275	0.238	0.220
15,000	0.256	0.242	0.306	0.265	0.272	0.306	0.268	0.242
16,000	0.296	0.280	0.362	0.301	0.311	0.362	0.310	0.280
17,000	0.352	0.314	0.429	0.354	0.358	0.429	0.341	0.314
18,000	0.431	0.363	0.485	0.413	0.412	0.485	0.421	0.363
19,000	0.505	0.440	0.640	0.508	0.497	0.640	0.518	0.440
20,000	0.800	0.547		0.785	0.705			
21,000	1.500							
22,000								
23,000								
24,000								
25,000								
26,000								
27,000								
28,000								
29,000								
30,000								
	Critical Pressure (psi)							
	21,200	20,800	19,400	20,750	20,980	21,200	20,626	19,400
	Temperature (°F)							
	70	69	70	70	69.8	70	70	69
	Pressurization Rate (psi/min)							
	662	665	665	668	664	668	665	662

Table I-11. Axial Displacement of Spherical Acrylic Windows Subjected to Short-Term Pressurization in DOL Type IV Flange

(R_i = 2.750 in.; t = 1.200 in.; α = 60 degrees)

Pressure (psi)	Specimen Number					Maximum Value	Average Value	Minimum Value
	51	52	53	54	55			
	Axial Displacement of Center Point on Window Low-Pressure Face (in.)							
1,000	0.007	0.007	0.009	0.008	0.002	0.009	0.007	0.002
2,000	0.017	0.017	0.020	0.015	0.004	0.020	0.015	0.004
3,000	0.027	0.025	0.030	0.024	0.013	0.030	0.024	0.013
4,000	0.036	0.034	0.040	0.034	0.022	0.040	0.033	0.022
5,000	0.046	0.043	0.051	0.044	0.032	0.051	0.045	0.032
6,000	0.057	0.055	0.062	0.056	0.042	0.062	0.054	0.042
7,000	0.069	0.067	0.073	0.067	0.054	0.073	0.066	0.054
8,000	0.081	0.080	0.087	0.080	0.066	0.087	0.079	0.066
9,000	0.095	0.094	0.100	0.093	0.079	0.100	0.092	0.079
10,000	0.108	0.109	0.115	0.106	0.093	0.115	0.106	0.093
11,000	0.126	0.125	0.131	0.122	0.109	0.131	0.123	0.109
12,000	0.143	0.141	0.147	0.140	0.126	0.147	0.140	0.126
13,000	0.161	0.160	0.167	0.159	0.146	0.167	0.159	0.146
14,000	0.181	0.180	0.187	0.180	0.165	0.187	0.179	0.165
15,000	0.203	0.202	0.210	0.202	0.188	0.210	0.201	0.188
16,000	0.226	0.225	0.232	0.221	0.209	0.232	0.223	0.209
17,000	0.252	0.251	0.259	0.246	0.237	0.259	0.249	0.237
18,000	0.277	0.275	0.287	0.274	0.261	0.287	0.275	0.261
19,000	0.304	0.306	0.315	0.299	0.293	0.315	0.303	0.293
20,000	0.338	0.335	0.345	0.321	0.326	0.346	0.333	0.321
21,000	0.376	0.375	0.377	0.362	0.376	0.377	0.373	0.362
22,000	0.413	0.413	0.409	0.401	0.418	0.418	0.411	0.401
23,000	0.473	0.460	0.461	0.447	0.486	0.486	0.465	0.447
24,000	0.538	0.532	0.525	0.503	0.550	0.550	0.530	0.503
25,000	0.605	0.610	0.629	0.595	0.633	0.633	0.614	0.595
26,000	0.704	0.725	0.720	0.693	0.753	0.753	0.719	0.693
27,000	0.833	0.839	0.830	0.844	0.904	0.904	0.850	0.830
28,000	0.988	0.995	0.956	1.032	1.280	1.280	1.050	0.956
29,000		1.188						
30,000								
	Critical Pressure (psi)							
	29,000	30,000	29,100	28,100	28,200	30,000	28,980	28,100
	Temperature (°C)							
	69	69	67	68	68	69	68	67
	Pressurization Rate (psi/min)							
	664	666	667	667	664	667	663	664

Table I-12. Axial Displacement of Spherical Acrylic Windows Subjected to Short-Term Pressurization in DOL Type IV Flange

(R_i = 2.750 in.; t = 0.250 in.; c = 90 degrees)

Pressure (psi)	Specimen Number					Maximum Value	Average Value	Minimum Value
	56	57	58	59	60			
	Axial Displacement of Center Point on Window Low-Pressure Face (in.)							
1,000	0.031	0.036	0.034	0.035	0.023	0.036	0.032	0.023
2,000	0.067	0.070	0.064	0.075	0.077	0.077	0.071	0.064
3,000		0.149						
4,000								
5,000								
6,000								
7,000								
8,000								
9,000								
10,000								
11,000								
12,000								
13,000								
14,000								
15,000								
16,000								
17,000								
18,000								
19,000								
20,000								
21,000								
22,000								
23,000								
24,000								
25,000								
26,000								
27,000								
28,000								
29,000								
30,000								
	Critical Pressure (psi)							
	2,850	3,100	2,950	2,900	2,650	3,100	2,890	2,650
	Temperature (^{o}F)							
	69	70	69	70	70	70	70	69
	Pressurization Rate (psi/min)							
	684	667	666	690	690	666	679	690

Table I-13. Axial Displacement of Spherical Acrylic Windows Subjected to Short-Term Pressurization in DOL Type IV Flange

(R_i = 2.750 in.; t = 0.500 in.; α = 90 degrees)

Pressure (psi)	Specimen Number					Maximum Value	Average Value	Minimum Value
	61	62	63	64	65			
	Axial Displacement of Center Point on Window Low-Pressure Face (in.)							
1,000	0.028	0.012	0.020	0.031	0.038	0.038	0.026	0.012
2,000	0.041	0.028	0.041	0.048	0.058	0.058	0.043	0.028
3,000	0.065	0.048	0.059	0.063	0.075	0.075	0.062	0.048
4,000	0.084	0.069	0.077	0.079	0.096	0.096	0.021	0.069
5,000	0.114	0.096	0.103	0.110	0.122	0.122	0.109	0.096
6,000	0.155	0.148	0.153	0.155	0.178	0.178	0.158	0.148
7,000	0.335							
8,000								
9,000								
10,000								
11,000								
12,000								
13,000								
14,000								
15,000								
16,000								
17,000								
18,000								
19,000								
20,000								
21,000								
22,000								
23,000								
24,000								
25,000								
26,000								
27,000								
28,000								
29,000								
30,000								
	Critical Pressure (psi)							
	7,100	6,750	6,800	7,000	6,800	7,100	6,890	6,750
	Temperature (°F)							
	69	70	71	70	70	71	70	69
	Pressurization Rate (psi/min)							
	670	667	655	652	660	670	661	652

Table I-14. Axial Displacement of Spherical Acrylic Windows Subjected to Short-Term Pressurization in DOL Type IV Flange

(R_i = 2.750 in.; t = 0.750 in.; α = 90 degrees)

Pressure (psi)	Specimen Number					Maximum Value	Average Value	Minimum Value
	66	67	68	69	70			
	Axial Displacement of Center Point on Window Low-Pressure Face (in.)							
1,000	0.020	0.004	0.001	0.011	0.005	0.001	0.008	0.000
2,000	0.033	0.015	0.003	0.023	0.029	0.032	0.023	0.003
3,000	0.049	0.030	0.014	0.036	0.041	0.049	0.034	0.014
4,000	0.059	0.044	0.027	0.050	0.055	0.059	0.047	0.027
5,000	0.075	0.058	0.041	0.064	0.069	0.075	0.061	0.041
6,000	0.096	0.075	0.057	0.080	0.086	0.096	0.079	0.057
7,000	0.110	0.095	0.079	0.100	0.105	0.110	0.098	0.079
8,000	0.135	0.120	0.107	0.125	0.131	0.135	0.124	0.107
9,000	0.169	0.150	0.150	0.159	0.166	0.169	0.159	0.150
10,000	0.231	0.208	0.207	0.213	0.220	0.223	0.216	0.207
11,000	0.350		0.400	0.370	0.362	0.400	0.371	0.335
12,000								
13,000								
14,000								
15,000								
16,000								
17,000								
18,000								
19,000								
20,000								
21,000								
22,000								
23,000								
24,000								
25,000								
26,000								
27,000								
28,000								
29,000								
30,000								
	Critical Pressure (psi)							
	11,250	11,225	11,000	11,250	11,300	11,300	11,205	11,000
	Temperature (°F)							
	70	70	71	70	69	71	70	69
	Pressurization Rate (psi/min)							
	667	667	662	661	660	667	663	660

Table I-15. Axial Displacement of Spherical Acrylic Windows Subjected to Short-Term Pressurization in DOL Type IV Flange

(R_i = 2.750 in.; t = 1.000 in.; α = 90 degrees)

Pressure (psi)	Specimen Number					Maximum Value	Average Value	Minimum Value
	71	72	73	74	75			
	Axial Displacement of Center Point on Window Low-Pressure Face (in.)							
1,000	0.010	0.003	0.017	0.005	0.020	0.011	0.011	0.000
2,000	0.022	0.025	0.029	0.007	0.036	0.036	0.024	0.007
3,000	0.037	0.048	0.039	0.009	0.038	0.048	0.034	0.009
4,000	0.048	0.050	0.049	0.011	0.055	0.055	0.043	0.011
5,000	0.061	0.051	0.061	0.027	0.073	0.073	0.055	0.027
6,000	0.077	0.074	0.073	0.037	0.075	0.077	0.067	0.037
7,000	0.089	0.096	0.090	0.047	0.092	0.096	0.083	0.047
8,000	0.106	0.098	0.104	0.061	0.109	0.109	0.096	0.061
9,000	0.116	0.122	0.126	0.078	0.127	0.127	0.114	0.078
10,000	0.137	0.146	0.149	0.098	0.145	0.149	0.135	0.098
11,000	0.162	0.170	0.169	0.122	0.163	0.170	0.157	0.122
12,000	0.208	0.196	0.203	0.151	0.199	0.208	0.191	0.151
13,000	0.240	0.248	0.230	0.189	0.235	0.248	0.208	0.189
14,000	0.295	0.300	0.279	0.237	0.290	0.300	0.280	0.279
15,000	0.412	0.398	0.363	0.347	0.368	0.412	0.378	0.347
16,000			0.650		0.650			
17,000								
18,000								
19,000								
20,000								
21,000								
22,000								
23,000								
24,000								
25,000								
26,000								
27,000								
28,000								
29,000								
30,000								
	Critical Pressure (psi)							
	15,600	15,750	16,100	16,000	16,100	16,100	15,910	15,750
	Temperature (^{o}F)							
	70	71	71	69	68	71	70	68
	Pressurization Rate (psi/min)							
	667	672	662	658	669	672	666	658

Table I-16. Axial Displacement of Spherical Acrylic Windows Subjected to Short-Term Pressurization in DOL Type IV Flange

(R_i = 2.750 in.; t = 1.200 in.; α = 90 degrees)

Pressure (psi)	Specimen Number					Maximum Value	Average Value	Minimum Value
	76	77	78	79	80			
	Axial Displacement of Center Point on Window Low-Pressure Face (in.)							
1,000	0.007	0.009	0.010	0.011	0.001	0.011	0.006	0.001
2,000	0.018	0.018	0.018	0.020	0.011	0.020	0.017	0.011
3,000	0.026	0.028	0.027	0.031	0.019	0.031	0.026	0.019
4,000	0.036	0.038	0.037	0.040	0.029	0.040	0.036	0.029
5,000	0.046	0.048	0.047	0.049	0.039	0.049	0.046	0.039
6,000	0.058	0.060	0.058	0.061	0.051	0.061	0.058	0.051
7,000	0.070	0.071	0.071	0.073	0.063	0.073	0.070	0.063
8,000	0.083	0.086	0.086	0.084	0.077	0.086	0.083	0.077
9,000	0.095	0.097	0.099	0.099	0.092	0.099	0.096	0.092
10,000	0.111	0.105	0.111	0.115	0.106	0.115	0.110	0.105
11,000	0.128	0.119	0.127	0.132	0.121	0.132	0.125	0.119
12,000	0.142	0.134	0.143	0.152	0.139	0.152	0.142	0.134
13,000	0.169	0.155	0.163	0.173	0.162	0.173	0.164	0.155
14,000	0.192	0.180	0.187	0.197	0.185	0.197	0.188	0.180
15,000	0.220	0.217	0.213	0.225	0.210	0.225	0.217	0.210
16,000	0.253	0.245	0.242	0.260	0.248	0.260	0.250	0.242
17,000	0.295	0.291	0.283	0.305	0.298	0.305	0.294	0.283
18,000	0.353	0.342	0.333	0.360	0.343	0.360	0.346	0.333
19,000	0.437	0.414	0.413	0.450	0.420	0.450	0.427	0.413
20,000	0.700	0.640	0.564	0.620	0.564	0.700	0.619	0.564
21,000								
22,000								
23,000								
24,000								
25,000								
26,000								
27,000								
28,000								
29,000								
30,000								
	Critical Pressure (psi)							
	20,100	20,200	20,300	20,520	20,650	20,650	20,350	20,100
	Temperature (^{o}F)							
	68	68	69	68	67	69	68	67
	Pressurization Rate (psi/min)							
	659	662	657	666	666	666	662	659

Table I-17. Axial Displacement of Spherical Acrylic Windows Subjected to Short-Term Pressurization in DOL Type IV Flange

(R_i = 2.750 in.; t = 0.250 in.; α = 120 degrees)

Pressure (psi)	Specimen Number					Maximum Value	Average Value	Minimum Value
	81	82	83	84	85			
	Axial Displacement of Center Point on Window Low-Pressure Face (in.)							
1,000	0.021	0.016	0.036	0.038	0.027	0.038	0.028	0.016
2,000	0.052	0.046	0.072	0.074	0.063	.74	0.061	0.046
3,000	0.070	0.070	0.095		0.093	0.095	0.082	0.070
4,000								
5,000								
6,000								
7,000								
8,000								
9,000								
10,000								
11,000								
12,000								
13,000								
14,000								
15,000								
16,000								
17,000								
18,000								
19,000								
20,000								
21,000								
22,000								
23,000								
24,000								
25,000								
26,000								
27,000								
28,000								
29,000								
30,000								
	Critical Pressure (psi)							
	3,000	3,100	3,150	2,940	3,100	2,940	3,058	3,150
	Temperature (°F)							
	70	70	70	71	71	71	70	70
	Pressurization Rate (psi/min)							
	640	673	630	667	645	.7	651	630

Table I-18. Axial Displacement of Spherical Acrylic Windows Subjected to Short-Term Pressurization in DOL Type IV Flange

(R_i = 2.750 in.; t = 0.500 in.; α = 120 degrees)

Pressure (psi)	Specimen Number					Maximum Value	Average Value	Minimum Value
	86	87	88	89	90			
	Axial Displacement of Center Point on Window Low-Pressure Face (in.)							
1,000	0.014	0.002	0.016	0.028	0.027	0.027	0.017	0.002
2,000	0.029	0.017	0.035	0.047	0.047	0.047	0.035	0.017
3,000	0.047	0.034	0.055	0.068	0.067	0.068	0.054	0.034
4,000	0.067	0.057	0.078	0.092	0.090	0.092	0.077	0.057
5,000	0.100	0.085	0.109	0.123	0.122	0.123	0.108	0.085
6,000	0.139	0.137	0.167	0.171	0.181	0.181	0.159	0.137
7,000	0.228	0.308	0.414	0.325	0.300	0.414	0.315	0.228
8,000								
9,000								
10,000								
11,000								
12,000								
13,000								
14,000								
15,000								
16,000								
17,000								
18,000								
19,000								
20,000								
21,000								
22,000								
23,000								
24,000								
25,000								
26,000								
27,000								
28,000								
29,000								
30,000								
	Critical Pressure (psi)							
	7,350	7,150	7,100	7,100	7,250	7,350	7,190	7,100
	Temperature (^{o}F)							
	68	70	69	69	68	70	69	68
	Pressurization Rate (psi/min)							
	663	669	666	665	667	669	666	663

Table I-19. Axial Displacement of Spherical Acrylic Windows Subjected to Short-Term Pressurization in DOL Type IV Flange

(R_i = 2.750 in.; t = 0.750 in.; α = 120 degrees)

Pressure (psi)	Specimen Number					Maximum Value	Average Value	Minimum Value
	91	92	93	94	95			
	Axial Displacement of Center Point on Window Low-Pressure Face (in.)							
1,000	0.002	0.028	0.026	0.010	0.001	0.028	0.013	0.001
2,000	0.003	0.038	0.041	0.026	0.002	0.041	0.022	0.002
3,000	0.026	0.039	0.056	0.040	0.018	0.056	0.036	0.018
4,000	0.050	0.056	0.071	0.055	0.033	0.071	0.053	0.033
5,000	0.051	0.076	0.088	0.072	0.050	0.088	0.067	0.050
6,000	0.074	0.094	0.108	0.092	0.068	0.108	0.087	0.068
7,000	0.097	0.124	0.131	0.114	0.090	0.114	0.111	0.090
8,000	0.120	0.141	0.161	0.144	0.119	0.144	0.137	0.119
9,000	0.165	0.187	0.205	0.194	0.165	0.205	0.183	0.165
10,000	0.250	0.270	0.295	0.294	0.245	0.295	0.271	0.245
11,000								
12,000								
13,000								
14,000								
15,000								
16,000								
17,000								
18,000								
19,000								
20,000								
21,000								
22,000								
23,000								
24,000								
25,000								
26,000								
27,000								
28,000								
29,000								
30,000								
	Critical Pressure (p *)							
	11,000	10,800	10,750	10,700	10,950	11,000	10,840	10,700
	Temperature (^{o}F)							
	70	70	70	69	70	70	70	69
	Pressurization Rate (psi/min)							
	661	666	661	660	664	666	662	660

Table I-20. Axial Displacement of Spherical Acrylic Windows Subjected to Short-Term Pressurization in DOL Type IV Flange

(R_i = 2.750 in.; t = 1.000 in.; α = 120 degrees)

Pressure (psi)	Specimen Number					Maximum Value	Average Value	Minimum Value
	96	97	98	99	100			
	Axial Displacement of Center Point on Window Low-Pressure Face (in.)							
1,000	0.001	0.015	0.013	0.015	0.002	0.015	0.013	0.001
2,000	0.002	0.025	0.025	0.028	0.017	0.028	0.019	0.002
3,000	0.015	0.040	0.036	0.041	0.029	0.041	0.032	0.015
4,000	0.024	0.054	0.048	0.054	0.042	0.054	0.044	0.024
5,000	0.035	0.064	0.062	0.067	0.057	0.067	0.057	0.035
6,000	0.046	0.081	0.076	0.081	0.071	0.081	0.071	0.046
7,000	0.065	0.098	0.091	0.100	0.087	0.100	0.088	0.065
8,000	0.076	0.115	0.108	0.115	0.103	0.115	0.103	0.076
9,000	0.103	0.139	0.130	0.135	0.123	0.139	0.126	0.103
10,000	0.119	0.162	0.152	0.157	0.144	0.162	0.147	0.119
11,000	0.146	0.196	0.180	0.186	0.170	0.196	0.176	0.146
12,000	0.183	0.232	0.221	0.225	0.205	0.232	0.213	0.183
13,000	0.240	0.299	0.280	0.288	0.253	0.299	0.272	0.240
14,000	0.328	0.420	0.375	0.410	0.330	0.420	0.353	0.328
15,000	1.000				0.495			
16,000					1.107			
17,000								
18,000								
19,000								
20,000								
21,000								
22,000								
23,000								
24,000								
25,000								
26,000								
27,000								
28,000								
29,000								
30,000								
	Critical Pressure (psi)							
	15,300	14,750	14,650	14,800	15,340	15,340	14,968	14,650
	Temperature (^{G}F)							
	69	70	68	71	68.5	71	69.3	68
	Pressurization Rate (psi/min)							
	655	665	667	665	658	667	662	555

Table I-21. Axial Displacement of Spherical Acrylic Windows Subjected to Short-Term Pressurization in DOL Type IV Flange

(R_i = 2.750 in.; t = 0.250 in.; α = 150 degrees)

Pressure (psi)	Specimen Number					Maximum Value	Average Value	Minimum Value
	101	102	103	104	105			
	Axial Displacement of Center Point on Window Low-Pressure Face (in.)							
1,000	0.018	0.034	0.021	0.034	0.033	0.034	0.028	0.018
2,000	0.049	0.063	0.053	0.064	0.060	0.064	0.058	0.049
3,000	0.077	0.087	0.084	0.100	0.090	0.100	0.088	0.077
4,000								
5,000								
6,000								
7,000								
8,000								
9,000								
10,000								
11,000								
12,000								
13,000								
14,000								
15,000								
16,000								
17,000								
18,000								
19,000								
20,000								
21,000								
22,000								
23,000								
24,000								
25,000								
26,000								
27,000								
28,000								
29,000								
30,000								
	Critical Pressure (psi)							
	3,300	3,050	3,250	3,100	3,100	3,300	3,160	3,050
	Temperature (°F)							
	69	68	68	69	70	70	69	68
	Pressurization Rate (psi/min)							
	675	660	661	641	658	675	659	641

Table I-22. Axial Displacement of Spherical Acrylic Windows Subjected to Short-Term Pressurization in DOL Type IV Flange

(R_i = 2.750 in.; t = 0.500 in.; α = 150 degrees)

Pressure (psi)	Specimen Number					Maximum Value	Average Value	Minimum Value
	106	107	108	109	110			
	Axial Displacement of Center Point on Window Low-Pressure Face (in.)							
1,000	0.015	0.001	0.020	0.034	0.017	0.034	0.017	0.001
2,000	0.024	0.007	0.037	0.052	0.038	0.052	0.033	0.007
3,000	0.040	0.020	0.054	0.070	0.057	0.070	0.048	0.020
4,000	0.073	0.039	0.075	0.089	0.082	0.089	0.071	0.039
5,000	0.100	0.056	0.100	0.117	0.109	0.117	0.096	0.056
6,000	0.151	0.120	0.141	0.158	0.148	0.158	0.144	0.120
7,000	0.238	0.188	0.191	0.209	0.215	0.238	0.212	0.188
8,000								
9,000								
10,000								
11,000								
12,000								
13,000								
14,000								
15,000								
16,000								
17,000								
18,000								
19,000								
20,000								
21,000								
22,000								
23,000								
24,000								
25,000								
26,000								
27,000								
28,000								
29,000								
30,000								
	Critical Pressure (psi)							
	7,400	7,250	7,300	7,250	7,600	7,600	7,330	7,250
	Temperature (^{o}F)							
	70	70	71	71	71	71	70.6	70
	Pressurization Rate (psi/min)							
	632	669	670	670	681	681	664.4	632

Table I-23. Axial Displacement of Spherical Acrylic Windows Subjected to Short-Term Pressurization in DOL Type IV Flange

(R_i = 2.750 in.; t = 0.750 in.; α = 150 degrees)

Pressure (psi)	Specimen Number					Maximum Value	Average Value	Minimum Value
	111	112	113	114	115			
	Axial Displacement of Center Point on Window Low-Pressure Face (in.)							
1,000	0.001	0.001	0.023	0.011	0.034	0.034	0.014	0.001
2,000	0.014	0.003	0.038	0.024	0.057	0.057	0.027	0.003
3,000	0.027	0.014	0.051	0.038	0.075	0.075	0.041	0.014
4,000	0.040	0.023	0.064	0.054	0.096	0.096	0.055	0.023
5,000	0.059	0.047	0.080	0.072	0.117	0.117	0.075	0.047
6,000	0.072	0.060	0.096	0.092	0.140	0.140	0.092	0.060
7,000	0.096	0.081	0.117	0.113	0.166	0.166	0.115	0.081
8,000	0.120	0.106	0.142	0.150	0.202	0.202	0.144	0.106
9,000	0.162	0.138	0.178	0.204	0.257	0.257	0.152	0.138
10,000	0.230	0.211	0.235	0.281	0.310	0.310	0.253	0.211
11,000	0.338	0.319	0.325	0.508	0.501	0.508	0.398	0.319
12,000								
13,000								
14,000								
15,000								
16,000								
17,000								
18,000								
19,000								
20,000								
21,000								
22,000								
23,000								
24,000								
25,000								
26,000								
27,000								
28,000								
29,000								
30,000								
	Critical Pressure (psi)							
	11,600	11,580	11,580	11,150	11,400	11,600	11,462	11,150
	Temperature (°F)							
	70	70	69	71	69.2	71	69.8	69
	Pressurization Rate (psi/min)							
	670	664	667	672	675	675	670	664

Table I-24. Axial Displacement of Spherical Acrylic Windows Subjected to Short-Term Pressurization in DOL Type IV Flange

(R_i = 2.750 in.; t = 1.000 in.; α = 150 degrees)

Pressure (psi)	Specimen Number					Maximum Value	Average Value	Minimum Value
	116	117	118	119	120			
	Axial Displacement of Center Point on Window Low-Pressure Face (in.)							
1,000	0.002	0.000	0.020	0.002	0.003	0.020	0.006	0.000
2,000	0.015	0.007	0.027	0.025	0.004	0.027	0.016	0.004
3,000	0.027	0.013	0.044	0.047	0.006	0.047	0.027	0.006
4,000	0.036	0.024	0.057	0.048	0.020	0.057	0.037	0.020
5,000	0.049	0.035	0.067	0.069	0.036	0.069	0.051	0.035
6,000	0.061	0.048	0.081	0.070	0.050	0.081	0.062	0.048
7,000	0.074	0.071	0.091	0.090	0.065	0.091	0.078	0.065
8,000	0.087	0.083	0.108	0.110	0.087	0.110	0.095	0.083
9,000	0.105	0.094	0.127	0.131	0.106	0.131	0.113	0.094
10,000	0.126	0.117	0.157	0.151	0.135	0.157	0.137	0.126
11,000	0.151	0.150	0.183	0.191	0.162	0.191	0.167	0.150
12,000	0.185	0.184	0.234	0.231	0.217	0.234	0.210	0.184
13,000	0.236	0.232	0.282	0.292	0.281	0.292	0.264	0.232
14,000	0.301	0.312	0.312	0.425	0.387	0.425	0.347	0.301
15,000	0.444	0.482			0.525			
16,000								
17,000								
18,000								
19,000								
20,000								
21,000								
22,000								
23,000								
24,000								
25,000								
26,000								
27,000								
28,000								
29,000								
30,000								
	Critical Pressure (psi)							
	15,600	15,400	14,950	14,800	15,520	15,600	15,254	14,800
	Temperature (^{o}F)							
	67	68	71	72	68	72	69.2	67
	Pressurization Rate (psi/min)							
	665	667	665	664	691	691	670.4	665

Table I-25. Axial Displacement of Spherical Acrylic Windows Subjected to Short-Term Pressurization in DOL Type IV Flange

(R_i = 2.750 in.; t = 0.250 in.; α = 180 degrees)

Pressure (psi)	Specimen Number					Maximum Value	Average Value	Minimum Value
	121	122	123	124	125			
	Axial Displacement of Center Point on Window Low-Pressure Face (in.)							
1,000	0.001	0.003	0.032	0.036	0.004	0.036	0.015	0.001
2,000	0.030	0.034	0.068	0.069	0.038	0.069	0.048	0.030
3,000		0.110			0.096			
4,000								
5,000								
6,000								
7,000								
8,000								
9,000								
10,000								
11,000								
12,000								
13,000								
14,000								
15,000								
16,000								
17,000								
18,000								
19,000								
20,000								
21,000								
22,000								
23,000								
24,000								
25,000								
26,000								
27,000								
28,000								
29,000								
30,000								
	Critical Pressure (psi)							
	3,000	3,070	2,800	2,950	3,160	3,160	2,995	2,800
	Temperature (°F)							
	70	69	70	71	71	71	70.2	69
	Pressurization Rate (psi/min)							
	664	694	674	674	706	706	682.4	664

Table I-26. Axial Displacement of Spherical Acrylic Windows Subjected to Short Term Pressurization in DOL Type IV Flange

(R_i = 2.750 in.; t = 0.500 in.; α = 180 degrees)

Pressure (psi)	Specimen Number					Maximum Value	Average Value	Minimum Value
	126	127	128	129	130			
	Axial Displacement of Center Point on Window Low-Pressure Face (in.)							
1,000	0.000	0.000	0.006	0.032	0.026	0.032	0.013	0.000
2,000	0.021	0.021	0.025	0.051	0.045	0.051	0.033	0.021
3,000	0.048	0.032	0.042	0.069	0.063	0.069	0.051	0.032
4,000	0.067	0.051	0.052	0.090	0.083	0.090	0.071	0.051
5,000	0.035	0.080	0.088	0.115	0.105	0.115	0.095	0.080
6,000	0.129	0.120	0.119	0.144	0.136	0.144	0.130	0.119
7,000	0.146	0.147	0.146	0.165	0.164	0.165	0.154	0.146
8,000								
9,000								
10,000								
11,000								
12,000								
13,000								
14,000								
15,000								
16,000								
17,000								
18,000								
19,000								
20,000								
21,000								
22,000								
23,000								
24,000								
25,000								
26,000								
27,000								
28,000								
29,000								
30,000								
	Critical Pressure (psi)							
	7,000	7,310	7,300	7,450	7,550	7,550	7,322	7,000
	Temperature (°F)							
	70	71	75	70	70	71	70	71
	Pressurization Rate (psi/min)							
	667	667	667	666	666	667	667	666

Table I-27. Axial Displacement of Spherical Acrylic Windows Subjected to Short-Term Pressurization in DOL Type IV Flange

(R_i = 2.750 in.; t = 0.750 in.; α = 180 degrees)

Pressure (psi)	Specimen Number					Maximum Value	Average Value	Minimum Value
	131	132	133	134	135			
	Axial Displacement of Center Point on Window Low-Pressure Face (in.)							
1,000	0.023	0.003	0.017	0.023	0.018	0.023	0.017	0.003
2,000	0.035	0.014	0.031	0.038	0.033	0.038	0.030	0.014
3,000	0.047	0.028	0.046	0.051	0.047	0.051	0.044	0.028
4,000	0.063	0.040	0.061	0.064	0.061	0.064	0.058	0.040
5,000	0.079	0.055	0.077	0.080	0.078	0.080	0.074	0.055
6,000	0.096	0.071	0.094	0.096	0.095	0.096	0.090	0.071
7,000	0.110	0.089	0.115	0.116	0.115	0.116	0.109	0.039
8,000	0.141	0.111	0.140	0.140	0.140	0.141	0.134	0.111
9,000	0.172	0.138	0.172	0.168	0.171	0.172	0.164	0.138
10,000	0.223	0.175	0.215	0.210	0.213	0.223	0.207	0.175
11,000	0.283	0.241	0.277	0.272	0.292	0.292	0.273	0.241
12,000		0.325		0.380				
13,000								
14,000								
15,000								
16,000								
17,000								
18,000								
19,000								
20,000								
21,000								
22,000								
23,000								
24,000								
25,000								
26,000								
27,000								
28,000								
29,000								
30,000								
	Critical Pressure (psi)							
	11,750	12,300	11,850	12,050	11,900	12,300	11,970	11,750
	Temperature (°F)							
	69	69	70	69	70	70	69	69
	Pressurization Rate (psi/min)							
	667	645	660	660	658	667	658	645

Table I-28. Axial Displacement of Spherical Acrylic Windows Subjected to Short-Term Pressurization in DOL Type IV Flange

(R_i = 2.750 in.; t = 0.750 in; α = 180 degrees)

Pressure (psi)	Specimen Number					Maximum Value	Average Value	Minimum Value
	136	137	138	139				
	Axial Displacement of Center Point on Window Low-Pressure Face (in.)							
1,000	0.000	0.010	0.002	0.008		0.010	0.005	0.000
2,000	0.000	0.026	0.012	0.024		0.026	0.016	0.000
3,000	0.002	0.040	0.025	0.035		0.040	0.025	0.002
4,000	0.022	0.052	0.039	0.048		0.052	0.040	0.022
5,000	0.034	0.066	0.052	0.061		0.066	0.053	0.034
6,000	0.051	0.081	0.066	0.075		0.081	0.068	0.051
7,000	0.070	0.098	0.082	0.091		0.098	0.085	0.070
8,000	0.089	0.115	0.098	0.108		0.115	0.103	0.089
9,000	0.104	0.140	0.120	0.128		0.140	0.123	0.104
10,000	0.132	0.162	0.146	0.152		0.162	0.148	0.132
11,000	0.169	0.198	0.178	0.181		0.198	0.182	0.169
12,000	0.209	0.245	0.220	0.254		0.254	0.232	0.209
13,000	0.296	0.308	0.285	0.283		0.308	0.293	0.283
14,000			0.410	0.350				
15,000								
16,000								
17,000								
18,000								
19,000								
20,000								
21,000								
22,000								
23,000								
24,000								
25,000								
26,000								
27,000								
28,000								
29,000								
30,000								
	Critical Pressure (psi)							
	13,900	13,850	14,100	14,200		14,200	14,012	13,850
	Temperature (^{o}F)							
	50	52	52	51		52	51	50
	Pressurization Rate (psi/min)							
	675	660	663	664		675	665	660

Table I-29. Axial Displacement of Spherical Acrylic Windows Subjected to Short-Term Pressurization in DOL Type IV Flange

(R_i = 2.750 in.; t = 1.000 in.; α = 180 degrees)

Pressure (psi)	Specimen Number					Maximum Value	Average Value	Minimum Value
	140	141	142	143	144			
	Axial Displacement of Center Point on Window Low-Pressure Face (in.)							
1,000	0.001	0.001	0.003	0.005	0.007	0.007	0.003	0.001
2,000	0.020	0.020	0.013	0.023	0.020	0.023	0.019	0.013
3,000	0.021	0.024	0.025	0.029	0.034	0.034	0.027	0.021
4,000	0.043	0.043	0.036	0.041	0.049	0.049	0.042	0.036
5,000	0.059	–	0.048	0.053	0.072	0.072	0.058	0.048
6,000	0.059	0.054	0.060	0.068	0.106	0.106	0.069	0.054
7,000	0.081	0.081	0.075	0.082	0.141	0.141	0.092	0.075
8,000	0.100	0.095	0.091	0.098	0.176	0.176	0.112	0.091
9,000	0.119	0.103	0.109	0.118	0.223	0.223	0.134	0.103
10,000	0.139	0.132	0.131	0.138	0.270	0.270	0.162	0.131
11,000	0.170	0.160	0.158	0.164	0.329	0.329	0.196	0.160
12,000	0.208	0.191	0.196	0.199	0.391	0.391	0.237	0.191
13,000	0.271	0.250	0.247	0.252	0.470	0.470	0.298	0.247
14,000	0.360	0.578	0.338	0.322	0.601	0.601	0.440	0.322
15,000	0.445		0.473	0 470				
16,000			0.850	0.746				
17,000								
18,000								
19,000								
20,000								
21,000								
22,000								
23,000								
24,000								
25,000								
26,000								
27,000								
28,000								
29,000								
30,000								
	Critical Pressure (psi)							
	15,150	15,500	16,100	16,300	15,430	16,300	15,696	15,150
	Temperature (°F)							
	70	69	71	71	71	71	70.4	69
	Pressurization Rate (psi/min)							
	696	690	663	666	686	696	680.2	663

Table I-30. Axial Displacement of Spherical Acrylic Windows Subjected to Short-Term Pressurization in DOL Type IV Flange

(R_i = 6.200 in.; t = 0.564 in.; α = 60 degrees)

Pressure (psi)	Specimen Number					Maximum Value	Average Value	Minimum Value
	145	146	147					
	Axial Displacement of Center Point on Window Low-Pressure Face (in.)							
1,000	0.056	0.030	0.033			0.056	0.040	0.030
2,000	0.133							
3,000								
4,000								
5,000								
6,000								
7,000								
8,000								
9,000								
10,000								
11,000								
12,000								
13,000								
14,000								
15,000								
16,000								
17,000								
18,000								
19,000								
20,000								
21,000								
22,000								
23,000								
24,000								
25,000								
26,000								
27,000								
28,000								
29,000								
30,000								
	Critical Pressure (psi)							
	2,200	1,200	1,600			2,200	16,000	1,200
	Temperature (^{o}F)							
	69	70	69			70	69	69
	Pressurization Rate (psi/min)							
	690	740	770			770	733	690

Table I-31. Axial Displacement of Spherical Acrylic Windows Subjected to Short-Term Pressurization in DOL Type IV Flange

(R_i = 6.200 in.; t = 1.127 in.; α = 60 degrees)

Pressure (psi)	Specimen Number					Maximum Value	Average Value	Minimum Value
	148	149	150					
	Axial Displacement of Center Point on Window Low-Pressure Face (in.)							
1,000	0.033	0.021	0.013			0.033	0.022	0.013
2,000	0.069	0.058	0.044			0.069	0.057	0.044
3,000	0.108	0.096	0.078			0.108	0.094	0.078
4,000	0.149	0.154	0.118			0.154	0.140	0.118
5,000	0.211	0.209	0.195			0.211	0.203	0.195
6,000		0.300						
7,000								
8,000								
9,000								
10,000								
11,000								
12,000								
13,000								
14,000								
15,000								
16,000								
17,000								
18,000								
19,000								
20,000								
21,000								
22,000								
23,000								
24,000								
25,000								
26,000								
27,000								
28,000								
29,000								
30,000								
	Critical Pressure (psi)							
	5,750	6,040	5,320			6,040	5,703	5,320
	Temperature (^{o}F)							
	69	69	69			69	69	69
	Pressurization Rate (psi/min)							
	660	658	662			662	660	658

Table I-32. Axial Displacement of Spherical Acrylic Windows Subjected to Short-Term Pressurization in DOL Type IV Flange

(R_i = 6.200 in.; t = 1.690 in.; α = 60 degrees)

Pressure (psi)	Specimen Number					Maximum Value	Average Value	Minimum Value
	151	152	153					
	Axial Displacement of Center Point on Window Low-Pressure Face (in.)							
1,000	0.024	0.023	0.009			0.024	0.019	0.009
2,000	0.052	0.051	0.034			0.052	0.046	0.034
3,000	0.082	0.081	0.058			0.082	0.074	0.058
4,000	0.111	0.109	0.085			0.111	0.102	0.085
5,000	0.143	0.140	0.113			0.143	0.132	0.113
6,000	0.181	0.178	0.148			0.181	0.169	0.148
7,000	0.219	0.219	0.188			0.219	0.209	0.188
8,000	0.265	0.267	0.231			0.267	0.254	0.231
9,000	0.321	0.332	0.295			0.332	0.316	0.295
10,000	0.392	0.423	0.367			0.423	0.394	0.367
11,000	0.488		0.478					
12,000			0.710					
13,000								
14,000								
15,000								
16,000								
17,000								
18,000								
19,000								
20,000								
21,000								
22,000								
23,000								
24,000								
25,000								
26,000								
27,000								
28,000								
29,000								
30,000								
	Critical Pressure (psi)							
	11,350	10,500	12,180			12,180	11,943	10,500
	Temperature (°F)							
	69	69	69			69	69	69
	Pressurization Rate (psi/min)							
	658	660	662			662	660	658

Table I-33. Axial Displacement of Spherical Acrylic Windows Subjected to Short-Term Pressurization in DOL Type IV Flange

(R_i = 6.200 in.; t = 2.254 in.; α = 60 degrees)

Pressure (psi)	Specimen Number					Maximum Value	Average Value	Minimum Value
	154	155	156					
	Axial Displacement of Center Point on Window Low-Pressure Face (in.)							
1,000	0.040	0.019	0.004			0.040	0.021	0.004
2,000	0.064	0.044	0.022			0.064	0.043	0.022
3,000	0.091	0.068	0.041			0.091	0.067	0.041
4,000	0.113	0.093	0.064			0.113	0.090	0.064
5,000	0.136	0.118	0.086			0.136	0.113	0.086
6,000	0.165	0.145	0.113			0.165	0.141	0.113
7,000	0.195	0.175	0.140			0.195	0.170	0.140
8,000	0.225	0.206	0.176			0.225	0.202	0.176
9,000	0 263	0.246	0.208			0.263	0.239	0.208
10,000	0.329	0.294	0.246			0.329	0.290	0.246
11,000	0.370	0.333	0.288			0.370	0.330	0.288
12,000	0.432	0.398	0.345			0.432	0.392	0.345
13,000	0.494	0.468	0.404			0.494	0.455	0.404
14,000	0.580	0.548	0.465			0.580	0.531	0.465
15,000	0.710	0.650	0.533			0.710	0.631	0.533
16,000	0.935	0.810	0.614			0.935	0.786	0.614
17,000		1.108	0.714					
18,000			0.834					
19,000			0.981					
20,000			1.214					
21,000			1.430					
22,000								
23,000								
24,000								
25,000								
26,000								
27,000								
28,000								
29,000								
30,000								
	Critical Pressure (psi)							
	16,750	17,300	21,920			21,920	18,657	16,750
	Temperature (°F)							
	69	69	70			70	69	69
	Pressurization Rate (psi/min)							
	650	657	669			669	659	650

Table I-34. Axial Displacement of Spherical Acrylic Windows Subjected to Short-Term Pressurization in DOL Type IV Flange

(R_i = 6.200 in.; t = 2.710 in.; α = 60 degrees)

Pressure (psi)	Specimen Number					Maximum Value	Average Value	Minimum Value
	157	158	159					
	Axial Displacement of Center Point on Window Low-Pressure Face (in.)							
1,000	0.019	0.005	0.003			0.019	0.009	0.003
2,000	0.040	0.023	0.017			0.040	0.027	0.017
3,000	0.059	0.040	0.037			0.059	0.045	0.037
4,000	0.080	0.063	0.062			0.080	0.068	0.062
5,000	0.100	0.083	0.085			0.100	0.089	0.083
6,000	0.125	0.106	0.110			0.125	0.114	0.106
7,000	0.148	0.131	0.135			0.148	0.138	0.131
8,000	0.176	0.159	0.161			0.176	0.165	0.159
9,000	0.206	0.188	0.190			0.206	0.195	0.190
10,000	0.241	0.224	0.220			0.241	0.228	0.220
11,000	0.276	0.259	0.257			0.276	0.264	0.257
12,000	0.312	0.306	0.300			0.312	0.306	0.300
13,000	0.363	0.350	0.337			0.363	0.350	0.337
14,000	0.420	0.405	0.388			0.420	0.404	0.388
15,000	0.491	0.467	0.453			0.491	0.470	0.453
16,000	0.554	0.537	0.516			0.554	0.536	0.516
17,000	0.648	0.611	0.577			0.648	0.612	0.577
18,000	0.746	0.703	0.670			0.746	0.706	0.670
19,000	0.865	0.800	0.738			0.865	0.801	0.738
20,000	0.977	0.926	0.850			0.977	0.918	0.850
21,000	1.128	1.065	0.903			1.128	1.032	0.903
22,000	1.250	1.225						
23,000	1.432	1.424						
24,000	1.608	1.650						
25,000	1.707							
26,000								
27,000								
28,000								
29,000								
30,000								
	Critical Pressure (psi)							
	25,600	24,220	25,880			25,880	25,233	24,220
	Temperature (°F)							
	71	70	69			71	70	69
	Pressurization Rate (psi/min)							
	668	666	648			668	661	648

REFERENCES

1. Naval Civil Engineering Laboratory. Technical Report R-512: Windows for external or internal hydrostatic pressure vessels, pt. I. Conical acrylic windows under short-term pressure application, by J. D. Stachiw, and K. O. Gray. Port Hueneme, Calif., Jan. 1967. (AD 646882)

2. ———. Technical Report R-527: Windows for external or internal hydrostatic pressure vessels, pt. II. Flat acrylic windows under short-term pressure application, by J. D. Stachiw, G. M. Dunn and K. O. Gray. Port Hueneme, Calif., May 1967. (AD 652343)

3. K. Tsuji, D. T. Stowell and J. D. Stachiw. "Development of a manned transparent capsule for panoramic marine observation," Journal of Hydronautics, Volume 3, Number 1, January 1959.

4. Naval Civil Engineering Laboratory. Technical Note N-755: The conversion of 16-inch projectiles to pressure vessels, by K. O. Gray and J. D. Stachiw. Port Hueneme, Calif., Aug. 1965. (AD 625950)

5. Armed Forces Supply Support Center. Military Handbook 17: Plastics for flight vehicles, pt. II. Transparent glazing materials. Washington, D. C., Aug. 1961.

DEFINITION OF TERMS

D_f	Diameter of the opening in the window flange on its low-pressure side (in.)
D_i	Diameter of the window's low-pressure face exposed to atmospheric pressure (in.)
D_o	Diameter of the window's high-pressure face exposed to hydrostatic pressure (in.)
d	Distance of eye from outside of lens
f	Focal length
M	Lateral magnification of the system
M_r	Relative magnification
m_1	Lateral magnification of spherical shell
m_2	Lateral magnification of eye, with virtual image acting as real object
n_1	Index of refraction of the lens
n_0, n_2	Indices of refraction of the media to the right and left, respectively, of the lens
p_c	Critical pressure at which explosive failure of the window takes place (psi)
p_o	Operational pressure (psi)
p_t	Proof-test pressure (psi)
R_i	Spherical radius of the concave surface on the window (in.)
R_o	Spherical radius of the convex surface on the window (in.)
s'	Erect image distance from lens
s'_e	Image distance of the eye
T	Temperature (^oF)
t	Thickness of the window (in.)
α	Spherical sector angle, included angle between the beveled surfaces of the window (deg)

Regular spherical shell window	A lens in the form of a regular spherical shell sector bounded by concentric concave and convex spherical surfaces. The edge of the lens terminates in a surface formed by the intersection of an imaginary cone and the spherical lens. The apex of that imaginary cone lies at the center of an imaginary sphere whose radius coincides with the radius of the lens convex surface
Irregular spherical shell window	This window differs from the regular spherical shell window by not having the apex of the imaginary cone lie at the center of an imaginary sphere whose radius coincides with the radius of the lens convex surface
Axial displacement	Movement of the center of window's low-pressure face measured along the axis of the cylindrical opening in the flange
Lateral displacement	Movement of the window's beveled edge along the surface of the window seat in the flange

DISTRIBUTION LIST

SNDL Code	No. of Activities	Total Copies	
–	1	20	Defense Documentation Center
FKAIC	1	10	Naval Facilities Engineering Command
FKNI	13	13	NAVFAC Engineering Field Divisions
FKN3	9	9	Public Works Centers
FA25	1	1	Public Works Center
–	15	15	RDT&E Liaison Officers at NAVFAC Engineering Field Divisions and Construction Battalion Centers
–	310	310	NCEL Special Distribution List No. 9 for Government Activities interested in reports on Deep Ocean Studies

Unclassified

Security Classification

DOCUMENT CONTROL DATA - R & D

Security classification of title, body of abstract and indexing annotation must be entered when the overall report is classified

1. ORIGINATING ACTIVITY (Corporate author) Naval Civil Engineering Laboratory Port Hueneme, California 93041	2a. REPORT SECURITY CLASSIFICATION Unclassified 2b. GROUP

3. REPORT TITLE

WINDOWS FOR EXTERNAL OR INTERNAL HYDROSTATIC PRESSURE VESSELS—PART III. Critical Pressure of Acrylic Spherical Shell Windows Under Short-Term Pressure Applications

4. DESCRIPTIVE NOTES (Type of report and inclusive dates)

Final; July 1966—August 1968

5. AUTHOR(S) (First name, middle initial, last name)

J. D. Stachiw and F. W. Brier

6. REPORT DATE	7a. TOTAL NO. OF PAGES	7b. NO. OF REFS
June 1969	147	5

8a. CONTRACT OR GRANT NO. b. PROJECT NO. YF 38.535.005.01.005 c. d.	9a. ORIGINATOR'S REPORT NUMBER(S) TR-631 9b. OTHER REPORT NO(S) (Any other numbers that may be assigned this report)

10. DISTRIBUTION STATEMENT

This document has been approved for public release and sale; its distribution is unlimited.

11. SUPPLEMENTARY NOTES	12. SPONSORING MILITARY ACTIVITY
	Naval Facilities Engineering Command Washington, D. C.

13. ABSTRACT

Model and full-scale acrylic windows in the form of spherical shell lenses with parallel convex and concave surfaces have been imploded by loading their convex surface hydrostatically at a 650-psi/min rate while their concave surface was exposed to atmospheric pressure. The thickness of the model windows varied from 0.250 to 1.200 inches and of the full-scale windows from 0.564 to 4.000 inches, while the included spherical sector angle of the lens and the bevel angle of its edge varied from 30 to 180 degrees in 30-degree increments. The low-pressure face diameters of the model windows varied from 1.423 to 5.500 inches, while those of the full-scale windows varied from 6.200 to 35.868 inches. In addition to critical pressures, displacements of the lens under hydrostatic pressure were recorded and plotted as functions of pressure.

DD FORM 1 NOV 65 1473 (PAGE 1)

S/N 0101-807-6801

Unclassified

Security Classification

14 KEY WORDS	LINK A		LINK B		LINK C	
	ROLE	WT	ROLE	WT	ROLE	WT
Windows						
Deep ocean						
Acrylic plastic						
Spherical shell						
Critical pressure tests						
Retaining flanges						
Failure modes						

Naval Civil Engineering Laboratory
WINDOWS FOR EXTERNAL OR INTERNAL HYDROSTATIC PRESSURE VESSELS—PART III. Critical Pressure of Acrylic Spherical Shell Windows Under Short-Term Pressure Applications (Final), by J. D. Stachiw and F. W. Brier

TR-631 151 p. illus June 1969 Unclassified

1. Undersea windows—Acrylic spherical shell I. YF 38.535.005.01.005

Model and full-scale acrylic windows in the form of spherical shell lenses with parallel convex and concave surfaces have been imploded by loading their convex surface hydrostatically at a 650-psi/min rate while their concave surface was exposed to atmospheric pressure. The thickness of the model windows varied from 0.250 to 1.200 inches and of the full-scale windows from 0.564 to 4.000 inches, while the included spherical sector angle of the lens and the bevel angle of its edge varied from 30 to 180 degrees in 30-degree increments. The low-pressure face diameters of the model windows varied from 1.423 to 5.500 inches, while those of the full-scale windows varied from 6.200 to 35.868 inches. In addition to critical pressures, displacements of the lens under hydrostatic pressure were recorded and plotted as functions of pressure.

Naval Civil Engineering Laboratory
WINDOWS FOR EXTERNAL OR INTERNAL HYDROSTATIC PRESSURE VESSELS—PART III. Critical Pressure of Acrylic Spherical Shell Windows Under Short-Term Pressure Applications (Final), by J. D. Stachiw and F. W. Brier

TR-631 151 p. illus June 1969 Unclassified

1. Undersea windows—Acrylic spherical shell I. YF 38.535.005.01.005

Model and full-scale acrylic windows in the form of spherical shell lenses with parallel convex and concave surfaces have been imploded by loading their convex surface hydrostatically at a 650-psi/min rate while their concave surface was exposed to atmospheric pressure. The thickness of the model windows varied from 0.250 to 1.200 inches and of the full-scale windows from 0.564 to 4.000 inches, while the included spherical sector angle of the lens and the bevel angle of its edge varied from 30 to 180 degrees in 30-degree increments. The low-pressure face diameters of the model windows varied from 1.423 to 5.500 inches, while those of the full-scale windows varied from 6.200 to 35.868 inches. In addition to critical pressures, displacements of the lens under hydrostatic pressure were recorded and plotted as functions of pressure.

Naval Civil Engineering Laboratory
WINDOWS FOR EXTERNAL OR INTERNAL HYDROSTATIC PRESSURE VESSELS—PART III. Critical Pressure of Acrylic Spherical Shell Windows Under Short-Term Pressure Applications (Final), by J. D. Stachiw and F. W. Brier

TR-631 151 p. illus June 1969 Unclassified

1. Undersea windows—Acrylic spherical shell I. YF 38.535.005.01.005

Model and full-scale acrylic windows in the form of spherical shell lenses with parallel convex and concave surfaces have been imploded by loading their convex surface hydrostatically at a 650-psi/min rate while their concave surface was exposed to atmospheric pressure. The thickness of the model windows varied from 0.250 to 1.200 inches and of the full-scale windows from 0.564 to 4.000 inches, while the included spherical sector angle of the lens and the bevel angle of its edge varied from 30 to 180 degrees in 30-degree increments. The low-pressure face diameters of the model windows varied from 1.423 to 5.500 inches, while those of the full-scale windows varied from 6.200 to 35.868 inches. In addition to critical pressures, displacements of the lens under hydrostatic pressure were recorded and plotted as functions of pressure.

Naval Civil Engineering Laboratory
WINDOWS FOR EXTERNAL OR INTERNAL HYDROSTATIC PRESSURE VESSELS—PART III. Critical Pressure of Acrylic Spherical Shell Windows Under Short-Term Pressure Applications (Final), by J. D. Stachiw and F. W. Brier

TR-631 151 p. illus June 1969 Unclassified

1. Undersea windows—Acrylic spherical shell I. YF 38.535.005.01.005

Model and full-scale acrylic windows in the form of spherical shell lenses with parallel convex and concave surfaces have been imploded by loading their convex surface hydrostatically at a 650-psi/min rate while their concave surface was exposed to atmospheric pressure. The thickness of the model windows varied from 0.250 to 1.200 inches and of the full-scale windows from 0.564 to 4.000 inches, while the included spherical sector angle of the lens and the bevel angle of its edge varied from 30 to 180 degrees in 30-degree increments. The low-pressure face diameters of the model windows varied from 1.423 to 5.500 inches, while those of the full-scale windows varied from 6.200 to 35.868 inches. In addition to critical pressures, displacements of the lens under hydrostatic pressure were recorded and plotted as functions of pressure.